I HEREBY CERTIFY THAT THIS CORRESPONDENCE IS BEING DEPOSITED WITH THE UNITED STATES POSTAL SERVICE AS FIRST CLASS MAIL IN AN ENVELOPE ADDRESSED TO: COMMISSIONER FOR PATENTS, P.O. BOX 1450, ALEXANDRIA, VA 22313-1450, ON THE DATE INDICATED BELOW.

BY: Helene Gabel Date: February 11, 2005

IN THE UNITED STATES PATENT AND TRADEMARK OFFICE

In Re Patent Application of: Jürgen Eck, *et al.*			
Conf. No.:	3271	Group Art Unit:	1644
Appln. No.:	09/347,064	Examiner:	Gerald R. Ewoldt
Filing Date:	July 02, 1999	Attorney Docket No.:	9282-5 (B 3521 US)

Title: Nucleic Acids Encoding Fusion Proteins Based on Ribosome-Inactivating Proteins of the Mistletoe *Viscum Album*

DECLARATION OF MARTIN LANGER UNDER 37 C.F.R. § 1.132

I, Martin Langer, declare and state as follows:

1. I am a citizen of the Federal Republic of Germany residing at Karlsruhe, D-76227, Lissenstrasse 5, Germany.

2. I hold a doctorate (Ph.D.) from the Institute of Biochemistry of the University Karlsruhe, Germany and a diploma in biology received from the Technical University Darmstadt, Germany.

3. I have been involved in study and research in the area of molecular biology, including research relating to the structure of enzymes, immunotoxins, mistletoe proteins, and other proteins since 1991.

4. From 1995 to 2000, I was the project and laboratory manager at B.R.A.I.N. Company of Zwingenberg, Germany, the initial assignee of the above-identified patent application. In this position at B.R.A.I.N., my research focused on the recombinant processing

of mistletoe proteins, including immunotoxins, and the characterization of the properties and structures of these proteins.

5. Since 2001, I have held the position of the head of research and development of Viscum AG, Bergisch Gladbach, Germany, the present assignee of this patent application. As head of research and development, my research focuses on research and preclinical projects involving immunotoxins and the development and proofing of biotechnological production processes of proteins up to technical scale in accordance with current good manufacturing practices (cGMP).

6. Since 1998, I have been a scientific expert of Science4Life, Germany and a scientific reviewer of peer reviewed journals in the field of immunotoxins. I am the author or co-author of numerous publications and presentations appearing in peer reviewed journals including those directed to different aspects of research of recombinant mistletoe proteins and their characterization. A list of these publications and further details of my background are set forth in my curriculum vitae, attached to this Declaration at Appendix A.

7. I am a native speaker of German. However, I am fluent in written and spoken English and frequently read, review, and study material in my field written in English, as well as correspond and work in the English language with my English-speaking colleagues in Europe and the United States.

8. Because of my background and expertise, my prior employment with B.R.A.I.N. and my present position as head of research and development of Viscum AG, I am well versed in the technology underlying the above-identified patent application, including molecular biology, cytology, and immunology.

9. Moreover, as head of research and development at Viscum AG, I am familiar with the above-identified patent application and its prosecution history.

10. I have reviewed the Office Action mailed March 11, 2004 ("March 11 O.A.") containing rejections under 35 U.S.C. § 112, first and second paragraphs.

11. I have reviewed the claims as amended by the Amendment filed simultaneously with this Declaration.

12. As at least a person of ordinary skill in the art, I present this Declaration to refute the Examiner's statements regarding the alleged deficiencies under 35 U.S.C. § 112 in this application.

13. In the March 11 O.A., the Examiner rejected claims 9, 10, 12-14, 16, 24, and 25 under 35 U.S.C. § 112, first paragraph, as containing subject matter that was not described in such a manner as to "enable" one of skill to carry out the invention as claimed. March 11 O.A. at ¶¶ 7-8. The Examiner has rejected claims 1-27 , 29, 33-37 and 47-49 under 35 U.S.C. § 112, first paragraph asserting that these claims are not supported by a written description in the specification such that a person of skill in the art would have understood that the inventors had the invention in their possession. March 11 O.A. at ¶ 9. The Examiner has rejected claims 10-14 as being indefinite. March 11 O.A. at ¶ 10. In this Declaration, I provide facts and information that demonstrate that none of these rejections should be maintained.

14. The invention includes a nucleic acid molecule that encodes a fusion protein. Spec. at, *e.g.*, 10-11. The nucleic acid is composed of several portions or modules: an effector module, a processing module, a targeting module, and, optionally, a modulator module and an affinity module. *Id.* Each of these modules is structurally defined in the specification by its function. *See, e.g.*, specification at 10, line 24; 11, lines 27-28; 12, lines 1-29 (effector module); *id.* at 10, lines 25-26; 13, lines 1-13 (processing module); *id* at 11, lines 1-3; 13, lines 15-23 (targeting module); *id.* at 17, line 21, through 21, line 22 (modulator module); and *id.* at 21, line 25, through 22, line 9; 25, lines 16-26 (affinity module).

15. Each of the effector module and the processing module is identified in the specification as being (i) a specific primary sequence (or encoded by a specific primary sequence), (ii) being a portion or fragment of one of the specific sequences, and/or (iii) hybridizing under certain conditions or being a degenerate of a molecule having one of the specific sequences or a fragment of the same.

16. Because the specification provides a primary sequence from which each of the recited fragments that may form the effector module or the processing module can be obtained, it would have been a routine matter to discern what constitutes a "fragment" using ordinary and unexceptional functionality assays, well known to a person of skill in the art at the time the priority application was filed.

17. For example, to determine whether a specific fragment of, *e.g.*, SEQ ID NO: 2, would be an effector module within the meaning of the claims, a person of skill would first identify the sequence fragment or portion of SEQ ID NO: 2 that he wished to use, based upon the sequence provided in the specification. The intracellular toxicity of the portion could be evaluated using the protocol set out in Example 6 of the specification, or other procedures, such as the XTT assay based on the degradation of a tetrazolium salt in the mitochondria of living cells (Kondo *et al.* (1994) Oncology 51, 535-539); the WST assay (also a tetrazolium salt based assay) (Hamaski *et al.* (1996) Toxicon. 34, 490-495). Furthermore, a cytotoxicity assay quantifying the total protein content of living cells could have been used to analyze the toxicity of a respective molecule (Skehan *et al.* (1990) J. Natl. Cancer Inst. 82, 1107-1112). This assay is and was at the time of filing routinely used, for example, in the National Cancer Institute (NCI)-60 cell line panel. *See, e.g.*, Staunton *et al.*, PNAS 98 (2001):10787-10792. Also of use in this regard are the MTT method (M-5655, Boehringer Mannheim, now known as Roche AG, 1983) or the method described in Scuderio *et al.* 1988, each of which is referenced in the specification. Spec. at 49, 50. Accordingly, using these art known methods, it would have been a routine matter to a person of skill in the art to ascertain whether a given fragment or portion functions to "kill or to permanently modify the vital processes of target cells," as the effector module is described. *See*, Spec. at 11.

18. With respect to the "processing module" and the "modulator molecule" recited in the claims, a similar routine evaluation using as a starting point the specific sequences provided in the application can be carried out to determine whether a given fragment possesses a recognition sequence for a protease ("processing module") or modulates the toxicity of the effector module ("modulator module"). Uptake and processing of biologics in living cells such as the processing module and the modulator module of the invention were well known and described in the literature. To monitor the mode of uptake and the processing, radiolabeling

methods using, for example, iodine^{125} can be used. *E.g.*, Finck-Barbancon *et al.* (1996) Mol. Microbiol. 22, 87-95. Using this assay, one can assess the efficacy as a modulator by measuring the radioactivity present in the cytoplasm. A similar approach using fluorescent labeled proteins, such as, Bodypy-FL (Da Poian *et al.* (1998) J. Virol. Methods 70, 45-58) could have been used to measure efficacy. In addition, numerous published examples of so-called "recognition sites" for various proteases were available at the time of the priority date of this application. *See, e.g.*, Vance *et al.* (1996) J. Biol. Chem. 271, 30811-30815 (describing a protease-sensitive site in a soluble Bci-2 protein); Jonasson *et al.* (1996) Eur. J. Biochem. 236, 656-661 (describing a protease-sensitive site in a fusion protein containing human insulin); Kwon *et al.*, (1995) PNAS. 92, 8234-8238; describing a protease-sensitive site (amino acids 247-255) in a transposase); and Lappi *et al.* (1994) J. Biol. Chem. 269, 12552-12558 (describing a fusion toxin containing the basic fibroblast growth factor linked to the type 1 RIP saporin having a protease-sensitive site in the C-terminus of bFGF).

19. The "targeting module" recited in the claims and described the specification, has a structure that is dependent on the cell one wishes to target, as would have been understood to a person of skill in the art. Examples of suitable peptide/polypeptide targeting modules are provided in the specification. However, one of ordinary skill in the art would have been well aware of the various well known and routinely used peptides/polypeptide molecules that have a targeting capacity, such as antibodies, antibody fragments, single chain antibodies, but also aptamers, antichalins, or peptides, and those described at pages 23-25 of the specification. For example, a protocol for evaluating the targeting ability of a given antibody or antibody fragment could be performed following the method of phage display that is described by Abraham *et al.* (1995) J. Immunol. Methods 183, 119-125. The binding ability of a small molecule such as, *e.g.*, a peptide or a substrate, could be measured by a similar method such as that described in Dyson *et al.* (1995) Nucl. Acids Res. 23, 1531-1535.

20. The "affinity module" recited in the claims is described as being "a peptide sequence which is characterized by a ligand binding specificity or by the presence of suitable epitopes which allows a selective purification." Spec. at 25. Ligand-substrate interactions as well as selective purification techniques were well understood at the priority date of this application, as were methods of purification using affinity chromatography. Affinity

chromatography can be performed using small molecules such as ligands on the surface of the column. Examples of purification in such a manner include the purification of lectins by using their ability to specifically bind carbohydrates, as demonstrated in, for example, Franz *et al.*, (1981), Biochem. J. 195, 481-484. Antibodies of the IgG type are often isolated by affinity chromatography using protein G or protein A as a ligand, Manil *et al.* (1986), J. Immunol. Methods 90, 25-37. Other affinity chromatography methods have been established using, *e.g.*, multi-histadine residues at the N- or C- terminus of recombinant proteins as an affinity tag. These his-tags bind to positively charged bivalent cations, such as nickel, cobalt, or copper. *See, e.g.*, Casey *et al.* (1995), J. Immunol. Methods 179, 105-116. Additionally, other affinity tags include glutathione S-transferase (GST) and strep-tag. *See, e.g.*, Ward *et al.*, (1994), Yeast 10, 441-449; Kleymann *et al.*, (1995), Biotechnology 13, 155-160.

21. Thus, in view of the information provided in the specification of this application as well as the knowledge, skill level, and information available to a person of skill in the art at the time this application was filed, such person would have found that the specification enabled the full scope of each of the claims, and moreover that sufficient information was present such that, in combination with the knowledge of a person of skill, the inventors have demonstrated that they were in possession of the invention.

22. The Examiner has stated that he considers the following terms to be indefinite, and further implies that it is necessary to define such terms in the specification as they are not art known terms:

(i) "a cell of the specific immune system;"

(ii) "a cell of the unspecific immune system; and"

(iii) "a degenerate cell of the immune system."

23. It is my understanding that under U.S. law it is not necessary to define terms that have an ordinary meaning in the art. Each of these terms is well understood in the art.

24. With respect to the (i) and (ii) above, use of these specific terms is the result of an error in translation from the German language application to the English language application.

In the German language document PCT/EP98/00009, the terms "spezifisches Immunsystem" and "unspezifisches Immunsystem" are used. Based upon my years of experience in this technology area and my research and studies carried out in both German and English, I believe that the German terms "spezifisches Immunsystem" and "unspezifisches Immunsystem" as they appear in the priority document are more properly and correctly translated into English as "acquired immune system" and "innate immune system." A person of skill in the art who is charged with the knowledge of the art of both German and English text books, the person skilled in the art would realize that in contrast to the German scientists who use the terminology "spezifisches Immunsystem" and "unspezifisches Immunsystem" consistently, in the English speaking countries the scientists rarely use the direct, less correct translations "specific immune system" and "unspecific immune system."

25. To the contrary, in the German speaking countries often the terms "spezifisches Immunsystem" and "unspezifisches Immunsystem" and, similarly, "spezifische immunitat" and unspezifische immunitat" are used in parallel. Thus, to correct the English translation of the PCT/EP98/00009 written in German language in the sense, one should rather refer to "spezifische Immunität" and "unspezifische Immunität" as it is discussed in the German translation of the American textbook Roitt *et al.*, Kurzes Lehrbuch der Immunologie (1987) G. Thieme Verlag, Stuttgart - New York (Index page 301, "Immunsystem siehe auch Immunität"). From this index one can learn that in the German literature the terms "Immunsystem" and "Immunität" are being synonymously used. Reviewing the textbook "Immunology" by Janice Kuby (3 Ed., 1997, Freeman, New York) one can see that English speaking experts also discuss innate (nonspecific) immunity as well as acquired (specific) immunity. A correct translation of these terms into the English language is therefore "acquired immunity" and "innate immunity".

26. The term "acquired immunity" is well known in the art to refer to the specific immunity, which requires the activity of a functional immune system, involving cells called lymphocytes and their products. Kuby (1997) Textbook chapter 1 "Overview of the immune system" (3rd ed. Freeman, New York) at pp. 3-24.

27. The term "innate immunity" is well known in the art to refer to the nonspecific basic resistance to disease that an individual is born with. Innate defense mechanisms provide the

first line of host defense against invading pathogens until an acquired immune response develops. See, e.g., Kuby (1997) Textbook chapter 1 "Overview of the immune system" (3rd ed. Freeman, New York) at pp. 3-24.

28. Thus, these terms are not indefinite as each one carries with it a well understood, concrete and definite meaning in the art.

29. Additionally, a person of skill in the art, upon review of the specification coupled with his knowledge of the art including the relevant lexicon would have understood the term "a degenerate cell of the immune system" to refer to a tumor cell, *i.e.*, a cell which exhibits some physical characteristics common to a normal immune cell and which may, in fact, be derived from an immune cell, but which is an abnormal, malignant cell that may develop into a tumorous disease. Examples of such immune cells are those playing a role in leukemia, such as, *e.g.*, acute lymphatic leukemia (ALL), acute myelogenous leukemia (AML), chronic lymphocytic leukemia (CLL), and chronic myelogenous leukemia (CML). *See*, additionally, Kuby (3 Ed., 1997, Freeman, New York) at pp. 573-596; Kumar (1994) J. Clin, Oncol. 12, 1710-1717.

I hereby declare that all statements herein of my own knowledge are true and that all statements made on information and belief are believed to be true; and further that these statements were made with the knowledge that false statements and the like so made are punishable by fine, imprisonment, or both, under § 1001 of Title 18 of the United States Code, and that such willful false statements may jeopardize the validity of the application or any patent issuing thereon.

Dated: February 08, 2005

Martin LANGER

REFERENCES CITED

1. Kondo *et al.* (1994). Oncology 51, 535-539.
2. Hamaski *et al.* (1996) Toxicon. 34, 490-495.
3. Skehan *et al.* (1990) J. Natl. Cancer Inst. 82, 1107-1112.
4. Staunton *et al.* PNAS 98 (2001) 10787-10792.
5. Scuderio *et al.* (1988) Cancer Res. 48, 4827-4833.
6. Finck-Barbancon *et al.* (1996) Mol. Microbiol. 22, 87-95.
7. Da Poian *et al.* (1998) J. Virol. Methods 70, 45-58.
8. Vance *et al.* (1996) J. Biol. Chem. 271, 30811-30815.
9. Jonasson *et al.* (1996) Eur. J. Biochem. 236, 656-661.
10. Kwon *et al.* (1995) PNAS 92, 8234-8238
11. Lappi *et al.* (1994) J. Biol. Chem. 269, 12552-12558.
12. Abraham *et al.* (1995) J. Immunol. Methods 183, 119-125.
13. Dyson *et al.* (1995) Nucl. Acids Res. 23, 1531, 1535.
14. Franz *et al.* (1981) Biochem. J. 195, 481-484.
15. Manil *et al.* (1986) J. Immunol. Methods 90, 25-37.
16. Casey *et al.* (1995) J. Immunol. Methods 179, 105-116.
17. Ward *et al.* (1994) Yeast 10, 441-449.
18. Kleyman *et al.* (1995) Biotechnology 13, 155-160.
19. PCT/EP98/00009
20. Roitt *et al.* (1987) Kurzes Lehrbuch der Immunologie.
21. Kuby, J. (1997) Immunology 3 Ed., 3-24; 573-596.
22. Kumar (1994) J. Clin, Oncol. 12, 1710-1717.

Curriculum vitae

Dr. Martin Langer, (Ph. D.)

Date oft birth:	11.12.1965 in Eschwege, Germany
Nationality:	German
July 1985	High School Diploma
1985 – 1986	Military Service
1986 – 1992	Study of Biology at the Technical University Darmstadt, Germany with the examination as Biologist (Diploma) Diploma Thesis in Molecular Biology and Biochemistry under supervision of Prof. Dr. H.G. Gassen
1990	Practical courses in Immunology (Prof. Dr. Kerry O. Cox) and Physiology (Dr. Marc Tester) at The Flinders University, Adelaide, Australia and the University of Adelaide, Australia
1992 – 1995	Doctorate study at the Institute of Biochemistry , Prof. Dr. Retey, of the University Karlsruhe, Germany Doctoral Thesis about molecular, biochemical, and structural explanation of mechanisms of enzymes
1995 – 2000	Project and laboratory manager at the biotech company BRAIN AG, Zwingenberg, Germany with special attention to the projects of the recombinant processing of the mistletoe proteins, of the immunotoxins and their analytical characterization
since 2001	Head of R & D of VISCUM AG, Bergisch Gladbach, Germany with special attention to R & D and pre-clinical projects on immunotoxins and to biotechnological production processes of proteins up to technical scale under cGMP

Other functions:

Since 1998	Scientific expert of Science for Life, Germany
Since 1999	Scientific reviewer of Peer Review Journal, field: immunotoxins
Since 1999	Lecturer at the University of Mannheim (FH); Topic: "Drug Development Today"
Since 1999	Member of Pharma Licensing Club (Pharma-Lizenz-Club), Germany (PLCD)

Stand: 31.08.04

M. Langer: List of Publications

Authors	Titel	Journal / Year	Volume	Pages
Blonski K., Schumacher U., Burkholder I., Edler L., Nikbakht H., Boeters I., Peters A., Kugler Ch., Horny H-P., **Langer M.**, Wilhelm-Ogunbiyi K., Witthohn K., Laack E.	Binding of recombinant mistletoe lectin (aviscumine) to resected human adenocarcinoma of the lung - a target for tumor therapy or a prognostic marker?	Lung Cancer 2004		submitted
Müthing J.,Meisen I., Kniep B., Haier J., Senninger N., Neumann U., **Langer M.**, Witthohn K., Milosevic J., Peter-Katalinic J.	Tumor associated CD75s-gangliosides and CD75s bearing glycoproteins with Neu5Acalpha2-6Galß1-4GlcNAc-residues are receptors for the anticancer drug rViscumin	FASEB J. 2004		accepted
Abuharbeid S., Apel J. Sander M. Fiedler B., **Langer M.**, Zuzarte M-L., Czubayko F. Aigner A.	Cytotoxicity of the novel anti-cancer drug rViscumin depends on HER-2 levels in SKOV-3 cells	Biochem. Biophys. Res. Commun. 2004	321	403-412
Müthing, J., Meisen, I., Bulau, P., **Langer, M.**, Witthohn, K., Lentzen, H., Neumann, U., Peter-Katalinic, J.	Mistletoe Lectin I is a sialic acid-specific lectin with strict preference to gangliosides and glycoproteins with terminal Neu5Aca2-6Galß1 4GlcNAc residues	Biochemistry 2004	43	2996-3007
Adler, M., **Langer, M.**, Witthohn, K., Eck, J., Blohm, D., Niemeyer, C.M.	Detection of rViscumin in plasma samples by immuno-PCR	Biochem. Biophys. Res. Commun. 2003	300	757-763
Müthing, J., Burg, M., Möckel, B., **Langer, M.**, Metelmann-Strupat, W., Werner, A., Neumann, U., Peter-Katalinic, J., Eck,J.	Preferential binding of the anticancer drug rViscumin (recombinant mistletoe lectin) to terminally α2-6-sialylated neolacto-series gangliosides	Glycobiology 2002	12 (8)	485-497
Lutter, P., Meyer, H.E., **Langer, M.**, Witthohn, K., Dormeyer, W., Sickmann, A., Blüggel, M.	Investigation of charge variants of rViscumin by two-dimensional gel electrophoresis and mass spectrometry	Electrophoresis 2001	22	2888-2897
Langer B., **Langer M.**, Retey J.	Methylidene-imidazolone (MIO) from histidine and phenylalanine ammonia-lyase	Adv. Protein Chem. 2001	58	175-214

M. Langer: List of Publications

Authors	Titel	Journal / Year	Volume	Pages
Schmidt, A., Möckel, B., Eck, J., **Langer, M.**, Gauert, M., Zinke, H.	Cytotoxic Activity of Recombinant bFGF-rViscum Fusion Proteins	Biochem. Biophys. Res. Commun. 2000	277	499-506
Langer, M., Möckel, B., Eck, J., Zinke, H., Lentzen, H.	Site-specific mutagenesis of mistletoe lectin: The role of RIP activity in apoptosis	Biochem. Biophys. Res. Commun. 1999	264	944-948
Eck, J., **Langer, M.**, Möckel, B., Baur, A., Rothe, M., Zinke, H., Lentzen, H.	Cloning of the mistletoe lectin gene and characterisation of the recombinant A-chain	Eur. J. Biochem. 1999	264	775-784
Eck, J., **Langer, M.**, Möckel, B., Witthohn, K., Zinke, H., Lentzen, H.	Characterisation of recombinant and plant derived mistletoe lectin and their B-chains	Eur. J. Biochem. 1999	265	788-797
Schwede T.F, Badeker M., **Langer M.**, Retey J., Schulz GE.	Homogenization and crystallization of histidine ammonia-lyase by exchange of a surface cysteine residue	Protein Eng. 1999	12	151-153
Möckel, B., Eck, J., **Langer, M.**, Zinke, H., Lentzen, H.	Induction of apoptosis in human blood cells by natural and recombinant mistletoe lectin	COST 98: Effects of antinutrients on the nutritional value of legume diets. , eds: Bardocz, Pfüller, Puztai, 1998	Vol. 5	94-101
Langer, M., Eck, J., Möckel, B., Zinke, H.	Fluorescence analysis of the interaction between RIP II molecules and its specific ligands	COST 98: Effects of antinutrients on the nutritional value of legume diets. eds. Bardocz, Pfüller, Puztai, 1998	Vol. 5	48-54
Zinke, H., Eck, J., **Langer, M.**, Möckel, B., Lentzen, H.	Molecular cloning of Viscum album ML gene: characterization of the gene and expression products	COST 98: Effects of antinutrients on the nutritional value of legume diets. eds.Bardocz, Pfüller, Puztai, 1998	Vol. 5	40-47
Möckel, B., Schwarz, T., Zinke, H., Eck, J., **Langer, M.**, Lentzen, H.	Effects of Mistletoe Lectin I on Human Blood Cell Lines and Peripheral Blood Cells. Cytotoxicity, apoptosis and induction of cytokines	Drug Res. 1997	47	1145-1151
Langer, M., Rothe, M., Eck, J., Möckel, B., Zinke, H.	A Nonradioactive Assay for Ribosome-Inactivating Proteins	Anal. Biochem. 1996	243	150-153

M. Langer: List of Publications

Authors	Titel	Journal / Year	Volume	Pages
Langer M., Lieber A., Retey J.	Histidine ammonia-lyase mutant S143C is posttranslationally converted into fully active wild-type enzyme.	Biochemistry 1994	33	14034-14038
Langer M., Reck G., Reed J., Retey J.	Identification of serine-143 as the most likely precursor of dehydroalanine in the active site of histidine ammonia-lyase. A study of the overexpressed enzyme by site-directed mutagenesis	Biochemistry 1994	33	6462-6467

M. Langer: Poster / Oral Presentations on Congresses

Authors	Titel	Congress	Place	Date
Witthohn, K., Müthing, J., **Langer, M.**, Burg, M., Peter-Katalinic, J., Eck, J., Lentzen, H.	alpha2-6-sialylated neolacto-series gangliosides Serve as Receptors for rViscumin	26th German Cancer Congress	Berlin	27.02.-01.03.2004
Heuck, F., **Langer, M.**, Kleber, A., Gauert, M., Purr, I., Borchmann, P., Pogge von Strandmann, E., Engert, A.	Development of a new anti-CD30 immunotoxin based on a recombinant mistletoe lectin, which is deleted in the vascular leak syndrome motives	Jahrestagung der Deutschen Gesellschaft für Hämatologie u. Onkologie (DGHO)	Basel/CH	05.-08.10.2003
Kleber, A., Back, R., Gauert, M., Krohn, M., **Langer, M.**, Eck,J.	Development of GnRH-targeted fusiontoxins containing mistletoe lectin A-chain	7th Biotherapy of Cancer Meeting	München	10.-13.09.2003
Langer, M., Möckel, B., Wilhelm-Ogunbiyi, K., Witthohn, K., Lentzen, H.	Antitumor Activity of rViscumin in vitro and in vivo	Novel Approaches forthe Discovery of Anticancer Agents (CESAR - Central European Society for Anticancer Drug Research)	Freiburg	18.-21. Juni 2003
Langer, M., Korn, B., Eck, J., Möckel, B., Poustka, A., Zinke, H., Lentzen, H.	Characterisation of Novel Drugs by Transcriptional Profiling	14th EORTC--NCI-AACR Conference	Frankfurt/M.	19.-22. November 2002
Müthing, J., Burg, M., Möckel, B., **Langer, M.**, Peter-Katalinic, J., Eck, J., Lentzen, H.	alpha-6-Sialylated Neolacto-series Gangliosides Serve as Receptors for rViscumin	14th EORTC--NCI-AACR Conference	Frankfurt/M.	19.-22. November 2002
Schöffski, P., Campone, M., Riggert, S., Mali, S., Govaerts, A.-S., Wilhelm-Ogunbiyi, K., **Langer, M.**, Fumoleau, P., Twelves, C.	Pharmacokinetics of the Intravenous Administration of rViscumin in Patients with Solid Tumours - First Results from EORTC Phase I Study 16002	14th EORTC--NCI-AACR Conference	Frankfurt/M.	19.-22. November 2002
Möckel, B., Wilhelm-Ogunbiyi, **M. Langer**, H. Zinke, H. Lentzen	rViscumin - the first recombinant plant-derived protein in drug development	The Twentieth International Lectin Meeting - INTERLEC 20	Kopenhagen / DK	20.-25.05.2002
Langer, M., Witthohn, K., Berlin, J., Möckel, B., Eck, J., Zinke, H., Lentzen, H.	New Analytical Methods to Describe the Quality of the Active Substance aViscumine manufactured under GMP	4th World Meeting on Pharmaceutics, Biopharmaceutics, Pharmaceutical Technology	Florenz/I	08.-11.April 2002

M. Langer: Poster / Oral Presentations on Congresses

Authors	Titel	Congress	Place	Date
Möckel, B., Wilhelm-Ogunbiyi, K., Burger, A., **Langer, M.**, Zinke, H., Fiebig, H.H., Lentzen, H.	Preclinical and Clinical Development of the Novel Anticancer Agent rViscumin	25th German Cancer Congress	Berlin	10.-14. März 2002
Adler, M., Niemeyer, Ch., Witthohn, K., **Langer, M.**, Blohm, D.	Hochsensitiver Nachweis des Antitumor-Wirkstoffs rViscumin in Blutserum mit der Immuno-PCR Methode	Medizinische Forschung und Gesundheitswissenschaften Symposium der Univ. Bremen	Bremen	30.11.-02. November 2001
Wilhelm-Ogunbiyi, K., Möckel, B., Burger, A., **Langer, M.**, Zinke, H., Fiebig, H.H., Lentzen, H.	rViscumin, a novel anticancer agent - preclinical and clinical development status	Biological Therapy of Cancer 6th International Symposium	München	12.-15. September 2001
Langer, M., Möckel, B., Schmidt, A., Eck, J., Gauert, M., Zinke, H., Lentzen, H.	Cytotoxic Activity of Recombinant bFGF-rViscumin Fusion Proteins	Biological Therapy of Cancer 6th International Symposium	München	12.-15. September 2001
Möckel, B., Burger, A. Schultz, R.J., Wilhelm-Ogunbiyi, K., **Langer, M.**, Zinke, H., Fiebig, H.H., Lentzen, H.	Assessing the cancerostatic potency of rViscumin towards human tumor xenografts and cell lines	Biological Therapy of Cancer 6th International Symposium	München	12.-15. September 2001
Langer, M., Möckel, B., Krohn, M., Eck, J., Zinke, H., Lentzen, H.	rViscumin: Triggering of MAPK-pathways in target cells and induction of apoptosis is correlated to enzymatic RIP-activity	Aktuelle Entwicklungen in der Naturstofforschung 13. Irseer Naturstofftage der DECHEMA e. V.	Kaufbeuren	28.Februar - 02. März 2001
Möckel, B., Korn, B., Eck, J., **Langer, M.**, Pousta, A., Zinke, H., Lentzen, H.	Characterisation of novel drugs by transcriptonal profiling	Statusseminar Chiptechnologien: Vom Genom zum Proteom, DECHEMA e. V.	Frankfurt am Main	22.-23. Januar 2001
Möckel, B., Burger, A.M., Sausville, E., Schultz, R.J., Wilhelm-Ogunbiyi, K., **Langer, M.**, Eck, J., Zinke, H., Fiebig, H.H., Lentzen, H.	Antitumor Activity of rViscumin in vitro and in vivo	11th AACR-NCI-EORTC Conference	Amsterdam, NL	07.-10. November 2000

M. Langer: Poster / Oral Presentations on Congresses

Authors	Titel	Congress	Place	Date
Hostanska, K., Möckel, B., **Langer, M.**, Eck, J., Saller, R. Zinke, H., Lentzen, H.	Immunostimulating activity of rViscumin in vitro	11th AACR-NCI-EORTC Conference	Amsterdam, NL	07.-10. November 2000
Langer, M., Möckel, B., Krohn, M., Eck, J., Zinke, H., Lentzen, H.	rViscumin: Triggering of MAPK-pathways in target cells and induction of apoptosis is correlated to enzymatic RIP-activity	11th AACR-NCI-EORTC Conference	Amsterdam, NL	07.-10. November 2000
Möckel, B., Burger, A., Hostanska, K., Mengs, U., Krohn, M., **Langer, M.**, Eck, J., Zinke, H., Fiebig, H.H., Lentzen, H.	Mode of action and in vivo antitumor activity of rViscumin	International Symposium Oncology, New Aspects	Schliersee	18.-20. Oktober 2000
Lutter, P., Meyer, H.E., **Langer, M.**, Witthohn, K., Blüggel, M.	Investigation of rViscumin (recombinant mistletoe lectin) in two-dimensional gel electrophoresis by mass spectroscopy	International Proteome and Proteomics Symposium	Siena, I	04.-07. September 2000
Möckel, B., Burger, A., Katzenmaier, A., **Langer, M.**, Eck, J., Zinke, H., Fiebig, H. H., Lentzen, H.	Apoptosis induction and cytotoxic activity towards cancer cells of recombinant Mistletoe lectin (rViscumin) in vitro	Biotechnology 2000, 11th World Congress on Biotechnology	Berlin	03.-08. September 2000
Krohn, M., Möckel, B., Katzenmaier, A., Eck, J., **Langer, M.**, Zinke, H., Lentzen, H.	Mode of action of rML: triggering of specific signalling pathways is probably due to intracellular ribosome-inactivation	Biotechnology 2000, 11 th World Congress on Biotechnology	Berlin	03.-08. September 2000
Langer, M., Möckel, B., Eck, J., Zinke, H., Lentzen, H.	Genetic engineering of rViscumin (rML): the role of RIP activity in apoptosis	Biotechnology 2000, 11th World Congress on Biotechnology	Berlin	03.-08. September 2000
Adler, M., Miemeyer, Ch.M., Witthohn, K., **Langer, M.**, Blohm, D.	Detection of Subattomol Amounts of rViscumin in Serum by Immuno-PCR	Biotechnology 2000, 11th World Congress on Biotechnology	Berlin	03.-08. September 2000
Langer, M., Möckel, B., Eck, J., Zinke, H., Lentzen, H.	Both biochemical activities of rViscumin are a prerequisite for its cytotoxic action	91st AACR Conference	San Francisco, USA	01.-05. April 2000

M. Langer: Poster / Oral Presentations on Congresses

Authors	Titel	Congress	Place	Date
Möckel, B., Burger, A.M., Hostanska, K., **Langer, M.**, Eck, J., Zinke, H. Fiebig, H.H., Lentzen, H.	rViscumin: in vitro effects and mode of action of a novel anticancer agent	91st AACR Conference	San Francisco, USA	01.-05. April 2000
Langer, M., Möckel, B., Eck, J., Zinke, H., Lentzen, H.	Cloning, recombinant expression and biochemical characterization of rViscumin	10th AACR-NCI-EORTC Conference	Washington, DC USA	16.-19. November 1999
Gauert, M., Eck, J., **Langer, M.**, Zinke, H., Lentzen, H.	Plasmid Stability of the pT7 RNA Polymerase Expression system in E. coli BL21 during Fermentation	Gesellschaft für Biochemie und Molekularbiologie	Rauschholz-hausen, Marburg	02.-04. November 1999
Möckel, B., Krohn, M., Katzenmeier, A., Eck, J., **Langer, M.**, Zinke, H., Lentzen, H.	Mode of action of rML: triggering of specific signalling pathways is probably due to intracellular ribosome-inactivation	5th Biological Therapy of Cancer Conference	München	27.-30. Oktober 1999
Langer, M., Möckel, B., Eck, J., Zinke, H., Lentzen, H.	Assessing the biochemical properties of Mistletoe lectin by means of genetic engineering	5th Biological Therapy of Cancer Conference	München	27.-30. Oktober 1999
Möckel, B., Katzenmeier, A., Krohn, M., Eck, J., **Langer, M.**, Zinke, H., Lentzen, H.	Stress pathways and apoptosis cascades induced by recombinant mistletoe lectin	Deutsche Krebsgesellschaft, Arbeitskreis experimentelle Krebsforschung	Heidelberg	24.-26. März 1999
Katzenmeier, A., Krohn, M., Möckel, B., Eck, J., **Langer, M.**, Zinke, H., Lentzen, H.	The potential anticancer drug rML - a cytotoxic agent and profiteer of cellular signalling cascades.	Advances in Gene Technology: Signal Transdruction and Therapeutic Strategies	Miami, USA	6.-10. Februar 1999
Schmidt, A., Möckel, B., Eck, J., **Langer, M.**, Gauert, M., Zinke, H.	Cytotoxicity Activity of a Basic Fibroblast Growth Factor-Mistletoe Lectin A-Chain Fusion Protein	Gesellschaft für Biochemie und Molekularbiologie	Rauischholz-hausen, Marburg	11.-13. November 1998
Langer, M., Rothe, M., Eck, J., Möckel, B., Zinke, H.	A Nonradioactive Assay for Ribosome-Inactivating Proteins.	Gesellschaft für Biochemie und Molekularbiologie	Rauischholz-hausen, Marburg	11.-13. November 1998
Möckel, B., Zinke, H., Eck, J., **Langer, M.**, Lentzen, H.	Induction of apoptosis by recombinant mistletoe lectin	Deutsche Gesellschaft für Immunologie, Biozentrum	Frankfurt am Main	04.-07. März 1998

M. Langer: Poster / Oral Presentations on Congresses

Authors	Titel	Congress	Place	Date
Langer, M., Zinke, H., Eck, J., Möckel, B., Lentzen, H.	Cloning of the active principle of Mistletoe: The contribution of mistletoe lectin single chains to biological functions	Biological Therapy of Cancer 4th International Symposium	München	11.-14. Juni 1997
Möckel, B., Schwarz, T., Eck, J., **Langer, M.**, Zinke, H., Lentzen, H.	Apoptosis and cytokine release are biological responses mediated by recombinant mistletoe lectin in vitro	Biological Therapy of Cancer 4th International Symposium	München	11.-14. Juni 1997
Möckel, B., Schwarz, T., Eck, J., **Langer, M.**, Zinke, H., Lentzen, H.	Effect of mistletoe lectin on human blood cells: correlation between cytotoxicity induction of apoptosis and cytokine induction	2. International Congress on Phytomedicine	München	11.-14. September 1996
Zinke, H., Eck, J., **Langer, M.**, Möckel, B., Baur, A., Lentzen, H.	Molecular cloning of Viscum album L. gene for ML-1 and characterization of the recombinant protein.	2. International Congress on Phytomedicine	München	11.-14. September 1996

Original Paper

Oncology 1994;51:533–539

High-Sensitivity Antitumor Drug Sensitivity Testing

'atsuhei Kondo
:imio Wada
Aiyako Kawashima
'oshitaka Sato
Aasaji Yamauchi

)epartment of Surgery, Tokai Central
lospital, Kakamigahara, Japan

ey Words
ntitumor drug sensitivity testing
uccinic dehydrogenase inhibition
test
TT assay

Abstract

For antitumor drug sensitivity testing we have been performing the succinic dehydrogenase inhibition test using 3-(4,5-dimethylthiazol-2-yl)-2,5-diphenyltetrazolium bromide (MTT). A new tetrazolium salt 2,3-bis(2-methoxy-4-nitro-5-sulfophenyl)-5-[(phenyl-amino) carbonyl]-2H-tetrazolium hydroxide (XTT) has been synthesized recently, and we have been conducting basic studies using it. We were able to obtain a high degree of sensitivity by adding phenazine methosulfate as a promoter in this assay. In these assays, there was a positive correlation between absorbance and cell count and XTT assay was more sensitive than MTT assay. In XTT assay, the production of formazan increases with reaction time over a protracted period of time, we assessed the possibility of performing assays with fewer cells than MTT was used. The results using cancer cell lines showed that when reacted for a longer time (6 h), it was possible to perform adequate assays using this method with 5,000 cells per well, and it will be useful when the amount of biopsy specimen is limited. We also evaluated the inhibition index of each of the drugs, comparing it with the MTT assay.

Introduction

Remarkable advances have been made in the chemoerapy of malignant neoplasms in recent years, but with me exceptions the results have been very inadequate. loreover, although tumor sensitivity to antitumor drugs nds, to some extent, to depend on the organ in which the mor arises, it is unrelated to the histological picture, and ug efficacy varies widely even in tumors classified into e same histological category in the same organ. Consequently, when conducting chemotherapy it is essential to lect and employ effective drugs, and to increase clinical ficacy, while at the same time avoiding ineffective drugs hich are of no avail. To achieve this goal, a variety of antitumor drug sensitivity tests are currently being evaluated [1–3]. One such test, the succinic dehydrogenase inhibition (SDI) test [4, 5], utilizes a reaction in which tetrazolium salts are reduced to formazans by succinic dehydrogenase within living cancer cells. The method permits quantitative determination of the efficacy of antitumor drugs. Kondo [5] used 2,3,5-triphenyl tetrazolium chloride (TTC) as the tetrazolium salt, but after the highly sensitive 3-(4,5-dimethylthiazol-2-yl)-2,5-diphenyltetrazolium bromide (MTT) was later synthesized. Saito et al. [6] and Mosmann [7] described the SDI method using MTT, and intense evaluations are currently in progress [8–11]. Recently, the new tetrazolium salt 2,3-bis(2-methoxy-4-nitro-5-sulfophenyl)-5-[(phenyl-amino) car-

T. Kondo, MD
Department of Surgery
Tokai Central Hospital, Higashijima, Sohara
Kakamigahara-City, 504 (Japan)

0030–2414/94/0516–0535
$8.00/0

REF. 1

bonyl]-2H-tetrazolium hydroxide (XTT) was synthesized [12] and a method using XTT was reported [13].

In this study we performed the SDI test using XTT in experimental tumors and made basic comparisons with the method using MTT. We also made an experimental assessment of the possibility of performing assays with smaller numbers of cells, taking advantage of the special characteristics of XTT, and report our findings here.

Materials and Methods

Cell Lines

Human stomach cancer cell lines NUGC 4, SC-1-NU, MK 28 and large intestine cancer cell lines SW 1222, Colo 320, SW 1083, Colo 26 were obtained from the 2nd Department of Surgery, Nagoya University. These cell lines grown as monolayers in RPMI-1640 with 20% FCS were trypsinized with 0.25% trypsin and harvested before use. The viable cell count was obtained by the trypan blue exclusion method and adjusted to known cell counts by RPMI-1640 with 10% FCS.

Chemicals and Drugs

MTT and PMS were obtained from Sigma Pharmaceutical, XTT was obtained from Polysciences. Mitomycin C (MMC), fluorouracil (5FU) (Kyowa Hakko), cisplatin (CDDP; Bristol Meyers Squibb Co.) were freshly prepared in RPMI-1640 supplemented with 10% fetal calf serum (FCS) at the beginning of each experiment.

Drug Sensitivity Test

Both MTT and XTT assays were performed by suspending the cells in RPMI-1640 + 20% FCS, pouring 100 µl each into the wells of a 96-well culture plate adding the antitumor agents (100 µl), and culturing in an incubator at 37 °C for 48 h.

After culturing in MTT assay [11], antitumor agents were washed out with PBS. 20 µl of MTT reagent (MTT 4 mg/ml + 0.1 *M* sodium succinic acid) was added and incubation was performed for 3 h at 37 °C. Then formazan formed was extracted with 150 µl of dimethyl sulfoxide and measured at a wavelength of 540 nm with ELISA reader calculating the inhibition index (II).

In XTT assay, XTT reagent (XTT 1 mg/ml + PMS 0.025 m*M*) was added and incubation was performed. Table 1 shows the enhancement of the metabolic reduction of XTT in the presence of PMS. The addition of 0.01 or 0.025 m*M* PMS resulted in a marked increase in measured absorbance, and in due consideration of increase of background absorbance 0.025 m*M* PMS was adopted. The XTT formazan formed was measured at a wavelength of 450 nm and II was calculated. Gibco RPMI-1640 with HEPES buffer + Gibco FCS was used as the medium.

In both assays, to establish antitumor drug sensitivity, the II was calculated versus the control using the following formula:

$$II = a - p/a - m \times 100\%$$

where a = cells with no antitumor drug added + tetrazolium salt, p = cells with antitumor drug added + tetrazolium salt, m = background.

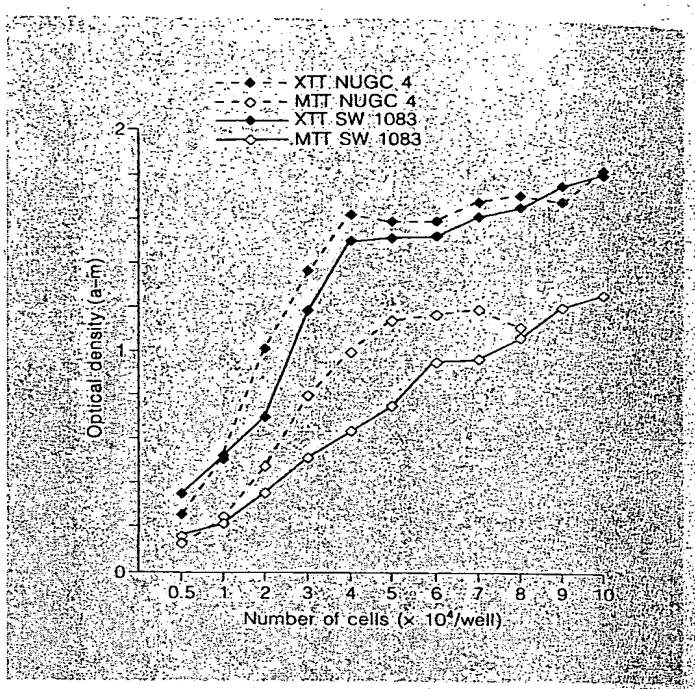

Fig. 1. Absorbance in XTT assay and MTT assay with various numbers of cells.

Table 1. Absorbance of XTT assay in the presence of various concentrations of PMS

Concentration of PMS, m*M*	Cell line		Background
	NUGC4	SW1083	
0.000	0.149	0.083	0.216
0.010	0.217	0.304	0.217
0.025	0.321	0.530	0.231
0.050	0.713	0.991	0.278

Results

Relationship between Absorbance and Cell Count

When NUGC4 and SW1083 were used and the MTT and XTT assays were performed using different numbers of cells, there was a positive correlation between absorbance (a – m) and cell count as shown in figure 1. In addition, the XTT assay appeared to be more sensitive than the MTT assay and capable of being performed even when there were few cells.

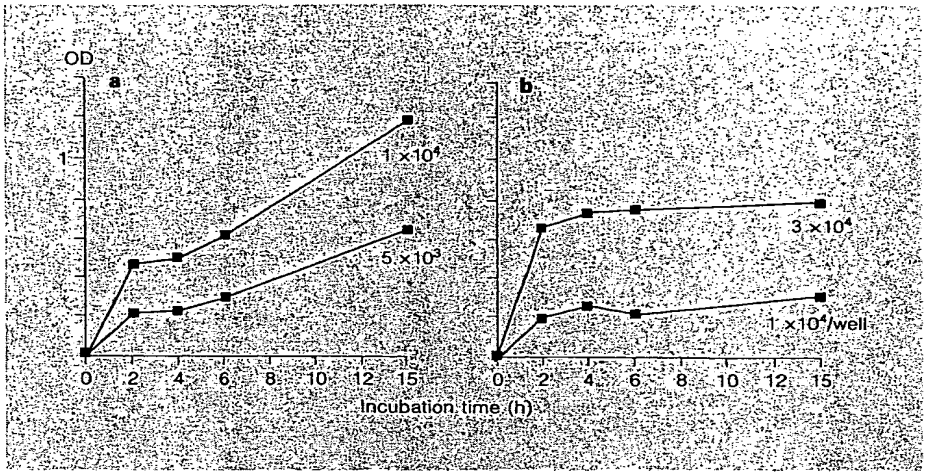

Fig. 2. Relationship between reaction time and absorbance in the XTT (**a**) and MTT (**b**) assay, with various cell numbers (NUGC 4).

Table 2. Absorbance after 3 or 6 h of incubation with various tumor cell counts in the XTT assay

Cell line	Number of cells/well				
	500	1,000	3,000	5,000	10,000
3-hour incubation					
S-180	–	–	–	+	+
NUGC 4	–	+	+	+	+
SW 1222	–	+	+	+	+
Colo3320	–	+	+	+	+
SC-1-NU	–	–	+	+	+
SW 1083	+	+	+	+	+
Colo3	–	–	+	+	+
Colo26	+	+	+	+	+
MKW 28	–	–	+	+	+
MM 48	–	–	–	+	+
6-hour incubation					
S-180	–	–	–	+	+
NUGC 4	+	+	+	+	+
SW 1222	–	+	+	+	+
Colo3320	–	+	+	+	+
SC-1-NU	–	+	+	+	+
SW 1083	+	+	+	+	+
Colo3	–	–	+	+	+
Colo26	+	+	+	+	+
MM 48	–	+	+	+	+

+: OD ≥ 0.1; –: OD <0.1.

Relationship between Reaction Time and Absorbance of XTT and MTT Assays

The absorbance of the MTT and XTT assays over time in different numbers of cells is shown in figure 2. When the reaction time was increased from 0 to 15 h, the XTT assay was more sensitive than the MTT assay and absorbance increased with reaction time and continued to increase. In the MTT assay it plateaued after 3–4 h, i.e., the same value was obtained as in the MTT assay by longer incubation in the XTT assay with fewer cells.

Changes in Absorbance in Tumor Cell Lines with Various Cell Counts

When we performed the XTT assay after incubation of 3 and 6 h with various kinds of tumor cells, sarcoma 180, gastric cancer cell lines (NUGC 4, MKW 28, MM 48) and colon cancer cell lines (SW 1222, Colo 320, SW 1083, Colo 3, Colo 26), in cell numbers of 500–10,000/well, the optical density was over 0.10 with more than 5,000 cells in all cell lines (table 2).

Based on the above, we are able to perform the XTT assay by using at least 5,000 cells/well and incubating with XTT for 6 h.

Inhibition Index Correlations in SDI Tests Using MTT and XTT

The correlation of the II in the MTT and XTT assays with various concentrations of compounds, MMC, CDDP or 5FU (0.01–100 μg/ml), was investigated. There were positive correlations in both assays with NUGC 4, in the MTT assay 20,000 cells/well and 10,000 cells/well in the XTT assay (fig. 3).

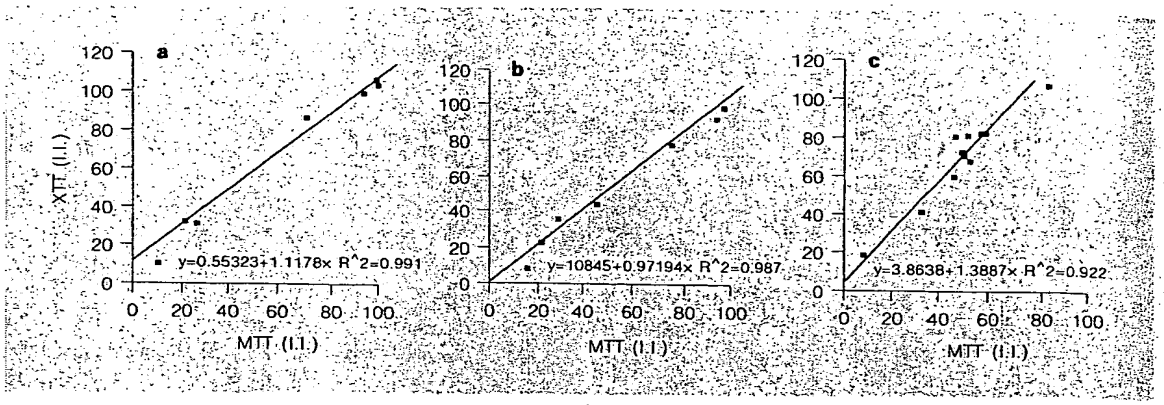

Fig. 3. Relationship between the II of the XTT assay and MTT assay, with various concentrations of MMC (**a**), CDDP (**b**), and 5FU (**c**).

Discussion

TTC was used by Lakon [14] to sort out viable seeds, and later it was applied to tissue slices by Black and Kleiner [15]. In order to evaluate sensitivity to antitumor drugs quantitatively, however, Kondo et al. [4] reactivated tumor cell suspensions and reported it as the SDI test. This test consists of exposing tumor cells to antitumor drugs for a fixed period of time and then measuring cell activity enzymatically. It is convenient to perform, has good reproducibility, results can be obtained rapidly, and response rate is high compared with other brief-culture antitumor drug sensitivity tests. This test has also been reported to be useful clinically [16]. Although MTT is currently being widely used as the tetrazolium salt for determining enzyme activity, extremely high sensitivity was later reported when PMS was added to the newly synthesized compound XTT, and in the present study we compared this with the MTT assay, using tumor cell lines.

Both XTT and MTT are water-soluble. Although the formazan of MTT is not ionized, the formazan of XTT has a bivalent negative ion and is water-soluble. Thus, when the SDI test is performed using XTT, the centrifugation step and the formazan extraction step using DMSO etc. required when MTT is used, are unneccessary. However, the production of formazan continues to increase even after 15 h when XTT is used in the SDI test, but plateaus after 3–4 h when MTT is used. Thus in case of MTT, measurements are made with approximately 50×10^3 cells/well, whereas in the case of XTT, by incubating for 6 h, it becomes possible to measure with only 5×10^3 cells/well, making the XTT assay more sensitive. We have investigated the optical density of the XTT assay with various gastrointestinal cancer cell lines and we know that we can obtain enough absorbance with more than 5,000 cells in almost all cell lines.

In clinical cases the amount of tissue which can be sampled is often limited, and a sensitive test permitting assays with as little tissue as possible is desirable. From this standpoint the SDI test using XTT appears to be a useful sensitivity test and the result is parallel to the MTT assay. Sensitivity testing methods employing tetrazolium salts require a solution to the problems of cell sampling, normal cell admixtures, and since these are problems shared with other sensitivity tests, it will be necessary to proceed with additional studies in the future.

As far as the relationship to clinical efficacy is concerned, there have been reports claiming that correlations exist equivalent to the degree observed among the results of the SDI test [5, 17, 18]. According to reviews of the literature comparing clinical efficacy with the results of various sensitivity tests to date [19, 20], 60–69% of those determined to be efficacious on the basis of sensitivity testing were also efficacious clinically, and 91–97% of those which lacked efficacy when tested were also ineffective clinically. This indicates that many problems remain in sensitivity testing at the present time, but while it is hard to accurately predict the usefulness of antitumor drugs, it is possible to predict lack of efficacy and exclude absurd drugs in almost every case, if we use the most effective drugs. Consequently, sensitivity testing appears to be a technique deserving wide clinical application as a prerequisite to cancer chemotherapy.

References

1 Hamburger AW, Salmon SE: Primary bioassay of human tumor stem cells. Science 1977;197: 461–463.

2 Bogden AE, Cobb WR, LePage DJ, Haskell PM, Gulkin TA; Ward A, Kelton DE, Esber HJ: Chemotherapy responsiveness of human tumors as first transplant generation xenografts in the normal mouse: Six-day subrenal capsule assay. Cancer 1981;48:10–20.

3 Skehan P, Storeng R, Scudiero D, Monks A, McMahon J, Vistica D, Warren JT, Bokesch H, Kenney S, Boyd MR: New colorimetric cytotoxicity assays for anticancer-drug screening. J Natl Cancer Inst 1990;82:1107–1112.

4 Kondo T, Imamura T, Ichihashi H: In vitro test for sensitivity of tumor to carcinostatic agents. Gann 1966;57:113–121.

5 Kondo T: Prediction of response of tumor and host to cancer chemotherapy. Natl Cancer Inst Monogr 1971;34:251–256.

6 Saito K, Sasada H, Natsuno T, Mitsuhashi S: A fine sensitivity test of anticancer agents by the modification of SDI test. J Jpn Cancer Chemother 1980;7:1952–1958.

7 Mosmann T: Rapid colorimetric assay for cellular growth and survival: Application to proliferation and cytotoxicity assays. J Immunol Methods 1983;65:55–63.

8 Twentyman PR, Luscombe M: A study of some variables in a tetrazolium dye (MMT) based assay for cell growth and chemosensitivity. Br J Cancer 1987;56:279–285.

9 Carmichael J, Degraff WG, Gazdar AF, Minna JD, Mitchell JB: Evaluation of a tetrazolium-based semiautomated colorimetric assay: Assessment of chemosensitivity testing. Cancer Res 1987;47:936–942.

10 Campling BG, Pym J, Baker HM, Cole SPC, Lam YM: Chemosensitivity testing of small cell lung cancer using the MTT assay. Br J Cancer 1991;63:75–83.

11 Yamauchi M, Satta T, Ito A, Kondo T, Takagi H: A feasibility study of the SDI test for the evaluation of gastrointestinal cancer sensitivity to anticancer drugs. J Surg Oncol 1991;47:253–260.

12 Paull KD, Shoemaker RH, Boyd MR, Parsons JL, Risbood PA, Barbera WA, Sharma MN, Baker DC, Hand E, Scudiero DA, Monks A, Alley MC, Grote M: The synthesis of XTT; a new tetrazolium reagent that is bioreducible to a water soluble formazan. J Heterocyclic Chem 1988;25:911–914.

13 Scudiero DA, Shoemaker RH, Paull KD, Monks A, Tierney S, Nofziger TH, Currens MJ, Semiff D, Boyd MR: Evaluation of a soluble tetrazolium/formazan assay for cell growth and drug sensitivity in culture using human and other tumor cell lines. Cancer Res 1988;48: 4827–4833.

14 Lakon G: Das Schwinden der Keimfähigkeit der Samen, insbesondere der Getreidefrüchte. Beitr Dtsch Bot Ges 1942;60:299–305.

15 Black MM, Kleiner IS: The use of tetrazolium chloride for the study of respiration of tissue slices. Science 1949;110:660–661.

16 Kondo T (ed): Determination Sensitivity to Anticancer Agents and Its Clinical Application – SDI test, SRCA –. Tokyo, Cancer and Chemother Publ Inc, 1991.

17 Hongo T, Fujii Y, Igarashi Y: An in vitro chemosensitivity test for the screening of anticancer agents in childhood leukemia. Cancer 1990; 65:1263–1272.

18 Furukawa T, Kubota T, Suto A, Takahara T, Yamaguchi H, Takeuchi T, Kase S, Kodaira S, Ishibiki K, Kitajima M: Clinical usefulness of chemosensitivity testing using the MTT assay. J Surg Oncol 1991;48:188–193.

19 Weisenthal LM, Lippman ME: Clonogenic and nonclonogenic in vitro chemosensitivity assays. Cancer Treat Rep 1985;69:615–632.

20 Phillips RM, Bibby MC, Double JA: A critical appraisal of the predictive value of in vitro chemosensitivity assays (review). J Natl Cancer Inst 1990;82:1457–1468.

Pergamon

0041-0101(95)00151-4

Toxicon, Vol. 34, No. 4, pp. 490–495, 1996

Printed in Great Britain
0041-0101/96 $15.00 + 0.00

A BIOLOGICAL METHOD FOR THE QUANTITATIVE MEASUREMENT OF TETRODOTOXIN (TTX): TISSUE CULTURE BIOASSAY IN COMBINATION WITH A WATER-SOLUBLE TETRAZOLIUM SALT

KOJI HAMASAKI[1], KAZUHIRO KOGURE[2] and KOUICHI OHWADA[2]

[1]Department of Bioengineering, Faculty of Engineering, Soka University, 1-236, Tangi, Hachioji, Tokyo 192, Japan and [2]Ocean Research Institute, University of Tokyo, Minamidai, Nakano-ku, Tokyo 164, Japan

(*Received* 22 *May* 1995; *accepted* 23 *November* 1995)

K. Hamasaki, K. Kogure and K. Ohwada. A biological method for the quantitative measurement of tetrodotoxin (TTX): tissue culture bioassay in combination with a water-soluble tetrazolium salt. *Toxicon* **34**, 490–495, 1996.—A tissue culture bioassay, using the mouse neuroblastoma cell line (Neuro2A), was improved to provide a simple and sensitive bioassay for TTX or sodium channel-blocking toxins (SCB). The water-soluble tetrazolium salt, 2-(4-iodophenyl)-3-(4-nitrophenyl)-5-(2,4-disulfophenyl)-2H-tetrazolium, monosodium salt (WST-1), was applied to replace the time-consuming and subjective cell-counting procedure of the cells with automatic measurement, using a microplate reader. It was also confirmed that this method is directly applicable to bacterial culture supernatants, with the precaution of possible interference. Copyright © 1996 Elsevier Science Ltd.

A tissue culture bioassay (TCBA) using the mouse neuroblastoma cell line, Neuro 2A (ATCC, CCL 131), is a sensitive method for the quantitative measurement of sodium channel-blocking toxins such as TTX, saxitoxin (STX) and related compounds (Kogure *et al.*, 1988a). TTX is originally produced by bacteria and subsequently distributed widely in various marine organisms (Noguchi *et al.*, 1986; Yasumoto *et al.*, 1986). STX and related toxins are originally produced by dinoflagellates and accumulated in shellfish through ingestion of these dinoflagellates during their blooms (Schantz, 1986). Both toxins occasionally cause severe poisoning through consumption of marine fishery products. It is important that the distribution of these toxins in marine environment is closely monitored. Most environmental work on these toxins relies on the mouse bioassay system because of its ease of use, low cost and short time course (Egmond, 1993). However, this method is not sensitive enough for laboratory use and, in view of ethical considerations, alternative methods should be adopted.

REF. 2

TCBA has been used for the low-level detection of TTX in marine environment (Kogure *et al.*, 1988b; Do *et al.*, 1993). If its objectivity and ease of use were improved, it could be a candidate for an alternative method. In this assay, the relative abundance of living cells in the presence of a toxin sample and two chemicals, veratridine and ouabain, which enhance the persistent influx of sodium ions into the cell, is used for the estimation of the toxin concentration in the sample. Because it depends solely on morphological change to distinguish dead cells from living cells, the original method is time-consuming and subjective. Recently, cell staining and subsequent absorbence measurement by microplate reader were introduced to simplify the counting process (Gallacher and Birkbeck, 1992; Jellett *et al.*, 1992). Although these improvements made the cell-counting procedure easier and more objective, the results are still likely to be affected by personal skill in the washing steps for removal of free dye and dead cells. Manger *et al.* (1993) reported the use of the tetrazolium salt 3-(4,5-dimethyl-2-thiazolyl)-2,5-diphenyl-2H tetrazolium bromide (MTT) as an indicator of living cells. This approach seems promising because it permits the omission of a washing step and simplifies the counting process. However, a solubilization step is still required before the measurement of absorbence, as the formazan dye crystal generated from MTT is not readily soluble in water.

In this study, we describe an improved and simplified method using a water-soluble tetrazolium salt, 2-(4-iodophenyl)-3-(4-nitrophenyl)-5-(2,4-disulfophenyl)-2H-tetrazolium, monosodium salt (WST-1) which permits direct measurement without the solubilization step. Additionally, the interfering effect of a bacterial culture supernatant in the assay was checked to validate the applicability for the simple measurement of TTX produced by bacteria.

Mouse neuroblastoma cells (Neuro2A) were grown in RPMI1640 medium supplemented with 10% fetal bovine serum and 1% antibiotic antimycotic solution (Sigma) in an air atmosphere at 37°C. Cells were removed from the culture surface by trypsinization and resuspended in the culture medium. TCBA was conducted following the method described by Kogure *et al.* (1988a). The final concentrations of veratridine and ouabain were 0.05 mM and 1.0 mM, respectively. Each plate received serial concentrations of TTX to obtain the standard dose–response curve. A cell-counting kit (Dojindo) was used for the WST-1 assay. WST-1 was dissolved in a solution of 1-methoxy-5-methylphenazinium methylsulfate (1-methoxy PMS), which mediates and accelerates the reduction of WST-1 (Ishiyama *et al.*, 1993). Mixed solution was filter-sterilized and added to each well 20–24 hr after TTX, veratridine and ouabain exposure. After the incubation at 37°C, absorbence was measured at 405 nm using a microplate reader with reference wavelength at 595 nm. The absorbence increased in proportion to incubation time after the addition of WST-1, and an incubation time of 4 hr was used in this study. Shorter incubation times may be possible depending on the cell number and other assay conditions.

The resulting TTX dose–response relation was sigmoidal (Fig. 1A). Probit analysis was carried out using probit paper (Sokal and Rohlf, 1981). The transformed data showed a good regression against TTX concentration (Fig. 1B). The regression equation can be used for quantitative measurement of TTX. The dose–response curve is similar to the curve of $^{22}Na^+$ uptake inhibition previously reported by Catterall and Nirenberg (1973). This suggests that WST-1 reduction responds to the inhibitory effect of TTX against Na^+ influx caused by veratridine and ouabain. In electrophysiological experiments using the squid giant axon and skeletal muscle fiber of the frog, both TTX and STX showed similar sigmoidal dose–response relations (Kao, 1986). Comparing our results with those of the previous reports on modified TCBA, the dose–response curve differs slightly between TTX

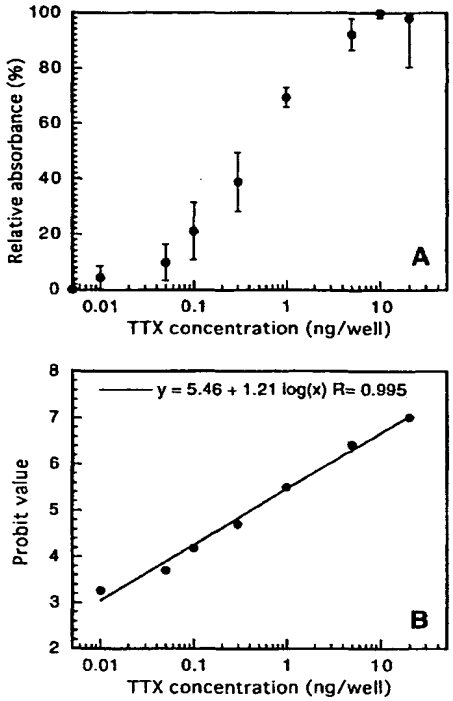

Fig. 1. (A) The dose–response curve was established, with cell response expressed as relative absorbence value, calculated from the following formula:100 × (AB − MIN)/(MAX − MIN). AB = absorbence at each concentration of TTX; MAX = maximum absorbence at each concentration of TTX; and MIN = minimum absorbence at each concentration of TTX. Each point represents the mean and S.D. of four replicates. (B) Regression line of dose–response after probit transformation.

and STX (Gallacher and Birkbeck, 1992; Jellett *et al.*, 1992; Manger *et al.*, 1993). The curve of STX reached a plateau at a lower concentration and was described in a narrower range of concentration than TTX. Responses of the Neuro2A cell to TTX and STX might be different. As for the comparison between MTT and WST-1, almost identical dose–response curves were obtained in our additional experiments. Three kinds of solvents are available to solubilize formazan generated from MTT (acid isopropanol, dimethyl sulfoxide and sodium dodecyl sulfate). The solubilization of MTT is not only laborious, but also includes the risk of exposing laboratory personnel to potentially hazardous solutions. Alternative tetrazolium reagents such as WST-1 are reduced to a water-soluble formazan product. This reagent allows direct readings of absorbence, eliminating a solubilization step and further shortening the assay procedure.

Escherichia coli K-12 (IAM 1264) culture supernatant supplemented with a known amount of TTX was used to check the applicability of the WST-1-TCBA method to the measurement of TTX produced by bacteria. In previous work, TTX production was not detected in this strain (Simidu *et al.*, 1987). The supernatant was divided into fractions, and these fractions were supplemented with serial concentrations of TTX. When the dose–response curves of TTX with and without *E. coli* supernatant were compared, the

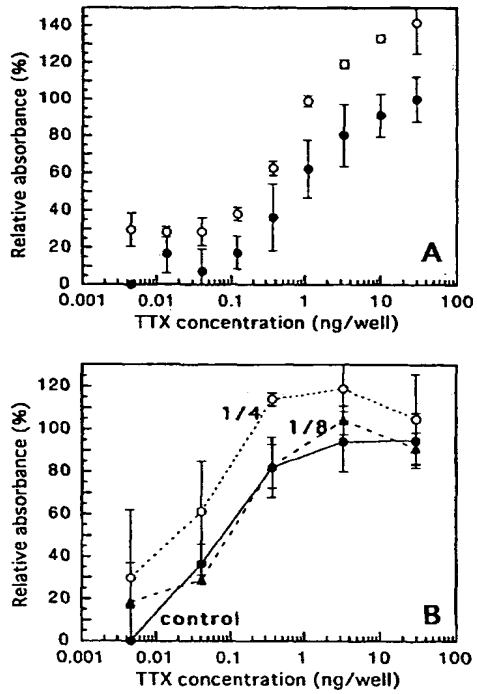

Fig. 2. The dose–response curve in the presence or absence of *E. coli* culture supernatant. *E. coli* was cultured in modified L medium (ML medium) containing 0.5% polypeptone, 0.1% yeast extract, 0.2% NaCl, 0.2% KCl, 0.4% $MgSO_4 7H_2O$ and 50 mM Tris–HCl in distilled water at pH 7.5–7.6 and incubated at 20°C with shaking. After centrifugation at 7000 × *g* for 20 min, the cell-free supernatant was obtained. The supernatant was divided into small fractions, and these fractions were supplemented with serial concentrations of TTX. (A) Dose–response curve of TTX (○) contained in the supernatant; (●) without supernatant. (B) Dose–response curve of TTX (○) contained in the 1/4 diluted supernatant; (▲) 1/8 diluted supernatant; (●) without supernatant.

curve of TTX with supernatant gave 12–39% higher absorbence at all dilution steps (Fig. 2A). *Escherichia coli* supernatant seemed to accelerate formazan formation. In general, WST-1 is metabolized less efficiently than MTT, so that electron-coupling agents such as 1-methoxy PMS are necessary to enhance cellular reduction of WST-1. The addition of electron-coupling agents makes the assay system more complex and possibly susceptible to interference by matrix constituents. This effect was observed in 1/4 diluted supernatant, but not in 1/8 diluted supernatant (Fig. 2B). Therefore, the interfering effect of bacterial culture supernatant causing overestimation in the assay would be avoidable by sample dilution. Such accelerating effects might vary with bacterial species. In our additional check on this effect, it was also seen in the supernatants of *Alteromonas tetraodonis* (GFC) and *Vibrio alginolyticus* (NCMB1903) but not in *Bacillus subtilis* (IFO3134). For these species, such an interference effect was also avoidable by dilution. Furthermore, it is recommended that non-specific reduction in the sample be checked in the absence of ouabain and veratridine as a control. Net toxin concentration should be calculated by correcting the data with the control value.

Intrinsically, identification of TTX is impossible only by TCBA because this method is not specific for TTX but detects any kind of SCB toxin or antagonist of veratridine. However, this remains a useful assay for biochemical studies on a particular bacterium which has been already confirmed as a TTX producer. In the future, combination with immunological methods using anti-STX or anti-TTX antibody will lead to rapid and even specific detection of toxin-producing bacteria (Chu and Fan, 1985; Kaufman *et al.*, 1991; Raybould *et al.*, 1992).

WST-1-TCBA is simple, owing to the omission of both washing and solubilizing steps. The dose of TTX producing half-maximal cell protection in our method (6.6 nM) was lower than that obtained by another modified method (Gallacher and Birkbeck, 1992). The sensitivity is about 100 times higher than that of the mouse bioassay and several times higher than that of the original TCBA. Once samples are loaded in the tissue culture plate with two chemicals, measurement with a microplate reader provides quantitative data. This enables rapid and sensitive analysis of large numbers of samples. TCBA is promising as a substitute method for the mouse bioassay, and in the future more work should be directed to comparing these two methods and to revealing the inhibitory effects of natural samples in the assay.

Acknowledgements—We thank the staff of Physiology of Marine Organisms Division in Ocean Research Institute, University of Tokyo, for providing the use of their facilities. This work was supported in part by a Grant-in-Aid for Scientific Research from the Ministry of Education, Science, and Culture of Japan. K. Hamasaki acknowledges the support of Research Fellowships of the Japan Society for the Promotion of Science for Young Scientists.

REFERENCES

Catterall, W. A. and Nirenberg, M. (1973) Sodium uptake associated with activation of action potential ionophores of cultured neuroblastoma and muscle cells. *Proc. natn. Acad. Sci. U.S.A.* **70**, 3759–3763.

Chu, F. S. and Fan, T. S. (1985) Indirect enzyme-linked immunosorbent assay for saxitoxin in shellfish. *J. Ass. off. analyt. Chem.* **68**, 13–16.

Do, H. K., Hamasaki, K., Ohwada, K., Shimidu, U., Noguchi, T., Shida, Y. and Kogure, K. (1993) Presence of tetrodotoxin and tetrodotoxin-producing bacteria in freshwater sediment. *Appl. environ. Microbiol.* **59**, 3934–3937.

Egmond, H. P. (1993) Paralytic and diarrhoeic shellfish poisons: occurrence in Europe, toxicity, analysis and regulation. *J. Nat. Toxins* **2**, 41–83.

Gallacher, S. and Birkbeck, T. H. (1992) A tissue culture assay for direct detection of sodium channel blocking toxins in bacterial culture supernates. *FEMS Microbiol. Lett.* **92**, 101–108.

Ishiyama, M., Shiga, M., Sasamoto, K., Mizuguchi, M. and He, P. (1993) A new sulfonated tetrazolium salt that produces a highly water-soluble formazan dye. *Chem. pharm. Bull.* **41**, 1118–1122.

Jellett, J. F., Marks, L. J., Stewart, J. E., Dorey, M. L., Watson-Wright, W. and Lawrence, J. F. (1992) Paralytic shellfish poison (saxitoxin family) bioassays: automated endpoint determination and standardization of the *in vitro* tissue culture bioassay, and comparison with the standard mouse bioassay. *Toxicon* **30**, 1143–1156.

Kaufman, B., Wright, D. C., Ballou, W. R. and Monheit, D. (1991) Protection against tetrodotoxin and saxitoxin intoxification by a cross-protective rabbit anti-tetrodotoxin antiserum. *Toxicon* **29**, 581–587.

Kao, C. Y. (1986) Structure–activity relations of tetrodotoxin, saxitoxin, and analogues. In: *Tetrodotoxin, Saxitoxin and the Molecular Biology of the Sodium Channel*, pp. 52–67 (Kao, C. Y. and Levinson, S. R., Eds). New York: NY Academy of Science.

Kogure, K., Tampline, M. L., Simidu, U. and Colwell, R. R. (1988) A tissue culture assay for tetrodotoxin, saxitoxin and related toxins. *Toxicon* **26**, 191–197.

Kogure, K., Do, H. K., Thuesen, E. V., Nanba, K., Ohwada, K. and Simidu, U. (1988) Accumulation of tetrodotoxin in marine sediment. *Mar. Ecol. Prog. Ser.* **45**, 303–305.

Manger, R. L., Leja, L. S., Lee, S. Y., Hungerford, J. M. and Wekell, M. M. (1993) Tetrazolium-based cell bioassay for neurotoxins active on voltage-sensitive sodium channels: semiautomated assay for saxitoxins, brevetoxins, and ciguatoxins. *Analyt. Biochem.* **214**, 190–194.

Noguchi, T., Joen, J. K., Arakawa, O., Sugita, H., Deguchi, Y., Shida, Y. and Hashimoto, K. (1986) Occurrence of tetrodotoxin and anhydrotetrodotoxin in *Vibrio* sp. isolated from the intestine of a xanthid crab *Atergatlis floridus*. *J. Biochem.* **99**, 311–314.

Raybould, T. J. G., Bignami, G. S., Inouye, L. K., Simpson, S. B., Byrnes, J. B., Grothaus, P. G. and Vann, D. C. (1992) A monoclonal antibody-based immunoassay for detecting tetrodotoxin in biological samples. *J. clin. Lab. Anal.* **6**, 65–72.

Schantz, E. J. (1986) Chemistry and biochemistry of saxitoxin and related toxins. In: *Tetrodotoxin, Saxitoxin and the Molecular Biology of the Sodium Channel*, pp. 15–23 (Kao, C. Y. and Levinson, S. R., Eds). New York: NY Academy of Science.

Simidu, U., Noguchi, T., Hwang, D. F., Shida, Y. and Hashimoto, K. (1987) Marine bacteria which produce tetrodotoxin. *Appl. environ. Microbiol.* **53**, 1714–1715.

Sokal, R. R. and Rohlf, F. J. (1981) Examination of residuals and transformations in regression. In: *Biometry*, 2nd Edn, pp. 539–546. New York: F. W. Freeman.

Yasumoto, T., Yasumura, D., Yotsu, M., Michishita, T., Endo, A. and Kotaki, Y. (1986) Bacterial production of tetrodotoxin and anhydrotetrodotoxin. *Agric. biol. Chem.* **50**, 793–795.

ARTICLES

New Colorimetric Cytotoxicity Assay for Anticancer-Drug Screening

Philip Skehan, Ritsa Storeng, Dominic Scudiero, Anne Monks, James McMahon, David Vistica, Jonathan T. Warren, Heidi Bokesch, Susan Kenney, Michael R. Boyd*

We have developed a rapid, sensitive, and inexpensive method for measuring the cellular protein content of adherent and suspension cultures in 96-well microtiter plates. The method is suitable for ordinary laboratory purposes and for very large-scale applications, such as the National Cancer Institute's disease-oriented in vitro anticancer-drug discovery screen, which requires the use of several million culture wells per year. Cultures fixed with trichloroacetic acid were stained for 30 minutes with 0.4% (wt/vol) sulforhodamine B (SRB) dissolved in 1% acetic acid. Unbound dye was removed by four washes with 1% acetic acid, and protein-bound dye was extracted with 10 m*M* unbuffered Tris base [tris (hydroxymethyl)aminomethane] for determination of optical density in a computer-interfaced, 96-well microtiter plate reader. The SRB assay results were linear with the number of cells and with values for cellular protein measured by both the Lowry and Bradford assays at densities ranging from sparse subconfluence to multilayered supraconfluence. The signal-to-noise ratio at 564 nm was approximately 1.5 with 1,000 cells per well. The sensitivity of the SRB assay compared favorably with sensitivities of several fluorescence assays and was superior to those of both the Lowry and Bradford assays and to those of 20 other visible dyes. The SRB assay provides a colorimetric end point that is nondestructive, indefinitely stable, and visible to the naked eye. It provides a sensitive measure of drug-induced cytotoxicity, is useful in quantitating clonogenicity, and is well suited to high-volume, automated drug screening. SRB fluoresces strongly with laser excitation at 488 nm and can be measured quantitatively at the single-cell level by static fluorescence cytometry. [J Natl Cancer Inst 82:1107–1112, 1990]

The recent emergence of computer-interfaced fiber-optic readers for 96-well microtiter plates has provided the basis for rapid in vitro cytotoxicity analysis that is particularly well suited to preclinical drug discovery and development. Although a variety of spectrophotometric methods are available for the analysis of large numbers of cells, few possess the sensitivity required by the semi-micro dimensions of microtiter plates. Fewer still are suitable for the very high volume of samples involved in large-scale drug screens, such as the disease-oriented in vitro anticancer-drug discovery project of the National Cancer Institute (NCI). This project tests 10,000 or more samples each year in a manner that requires the analysis of several million individual wells (*1*).

We compared the abilities of 21 histological dyes to measure cell density and drug cytotoxicity in 96-well microtiter plates. The dyes bind electrostatically to macromolecular counterions in cells fixed with trichloroacetic acid (TCA) (*2–4*), which allows their binding and solubilization to be controlled by variations in pH (*2*). In one pH range, the dyes bind stoichiometrically to target macromolecular counterions, whereas in another, they can be quantitatively extracted for measurement of optical density (*2*).

Thirteen of the dyes stained well enough to provide an adequate basis for assay of cytotoxicity in 96-well plates. Optimized protocols were developed for the seven best dyes. Four of these were anionic protein stains with sulfonic or sulfinic groups that bind electrostatically to protein basic amino acid residues under mildly acidic conditions (*2–5*). These dyes can be quantitatively extracted from cells and solubilized for optical density measurement by weak bases (*2*). The other three dyes were cationic dyes that bind electrostatically to macromolecular negative fixed charges (*3,4*). Under mildly basic conditions, these dyes bind to proteins, RNA, DNA, and glycosaminoglycans, serving as gen-

Received September 5, 1989; revised December 11, 1989; accepted March 15, 1990.

P. Skehan, R. Storeng, J. McMahon, D. Vistica, J. T. Warren, S. Kenney (Developmental Therapeutics Program, Division of Cancer Treatment), D. Scudiero, A. Monks, H. Bokesch (Program Resources, Inc.), National Cancer Institute, Frederick Cancer Research Facility, Frederick, MD.

M. R. Boyd, Developmental Therapeutics Program, Division of Cancer Treatment, National Cancer Institute, Bethesda, MD.

* *Correspondence to:* Philip Skehan, M.D., Developmental Therapeutics Program, Division of Cancer Treatment, Bldg. 560, Rm. 3260, National Cancer Institute, Frederick Cancer Research Facility, Frederick, MD 21701.

REF 2

eral biomass stains (*4*). They can be extracted from cells with a weak acid.

Materials and Methods

Cells

We performed preliminary experiments with the human A-2780 ovarian, HT-29 colon, and UO-31 renal tumor cell lines to identify the most promising dyes, which were subsequently examined in detail with some or all of the cell lines currently used in the NCI's in vitro anticancer-drug screen (*6*).

Stock cultures were grown in T-75 flasks containing 50 mL of RPMI-1640 medium with glutamine, bicarbonate, and 5% fetal calf serum. Medium was changed at 48-hour intervals. Cells were dissociated with 0.25% trypsin and 3 m*M* 1,2-cyclohexanediaminetetraacetic acid in NKT buffer (137 m*M* NaCl, 5.4 m*M* KCl, and 10 m*M* Tris; pH 7.4). Experimental cultures were plated in microtiter plates (Costar, Cambridge, MA) containing 0.2 mL of growth medium per well at densities of 1,000–200,000 cells per well.

Dyes

Dyes were purchased from Sigma Chemical Co., St. Louis, MO. Preliminary studies were conducted with each of these 21 dyes to determine whether each stained cells more intensely at acidic, neutral, or basic pH (*2*). The anionic dyes bromophenol blue, chromotrope 2R, Coomassie brilliant blue, naphthol yellow S, orange G, and sulforhodamine B (SRB) were dissolved in 1% acetic acid for cell staining and extracted from cells with 10 m*M* unbuffered Tris base [tris(hydroxymethyl)aminomethane]. The cationic dyes acridine orange, azure A, azure B, azure C, cresyl violet acetate, methyl green, methylene blue, phenosafranin, safranin O, thionin, and toluidine blue O were dissolved in unbuffered 10 m*M* Tris base to stain cells and were resolubilized for measurement of optical density with either 1% or 10% acetic acid. The cationic dyes ethidium bromide, propidium iodide, and pyronin B were dissolved in water for staining. Although these are excellent fluorescent dyes (*7*), their staining intensity was poor at visible wavelengths. Crystal violet was dissolved in 10% ethanol and 90% water at a neutral pH; its staining intensity varied considerably from one cell line to another. The absorption maximum of each dye in its solubilizing solution was determined with a DU-70 scanning spectrophotometer (Beckman Instruments, Inc., Fullerton, CA).

Cell Fixation

Washing cultures with buffer prior to fixation to remove serum protein commonly caused cell detachment and loss. To avoid this potential problem, cultures were fixed with TCA before washing. Cells attached to the plastic substratum were fixed by gently layering 50 μL of cold 50% TCA (4 °C) on top of the growth medium in each well to produce a final TCA concentration of 10%. The cultures were incubated at 4 °C for 1 hour and then washed five times with tap water to remove TCA, growth medium, and low-molecular-weight metabolites, and serum protein. Plates were air dried and then stored until use. Background optical densities were measured in wells incubated with growth medium without cells.

Cells in suspension were allowed to settle out of solution. When these cells were physically resting on the bottom of the wells, 50 μL of cold 80% TCA (4 °C) was gently layered on top of the overlying growth medium. The cultures were left undisturbed for 5 minutes and then refrigerated at 4 °C for an additional hour of fixation. This procedure led to the attachment of single cell suspensions to the plastic substratum, provided that cells were in contact with it when the fixative was applied. This method was as effective in promoting cell attachment as were cytospinning and using the macromolecular adhesive Cell-Tak (Biopolymers, Farmington, CT). However, it did not adequately attach cells that grew as floating aggregates rather than as single cell suspensions. Small cell lung carcinoma lines were particularly unsuited to this method of fixation.

Following fixation, suspension cultures were processed with procedures identical to those used for cultures of cells attached to the plastic substratum. After cells were stained and washed, individual wells were checked for cell detachment (clear spots or regions in the normally homogeneous pink carpet of cells), a potentially important source of artifact with cell suspensions. Although 80% TCA caused cells from suspensions to adhere to the plastic substratum, this attachment was extremely sensitive to movement, and very gentle handling of both the cells and the TCA was required. The efficiency of this attachment varied with cell type: cells from some cell lines were well attached by this method, while others were not.

Organic solvents such as ethanol and methanol were not suitable fixatives for the dye assays. When mixed with growth medium, these solvents generated intense interfacial shearing forces, which could be seen by phase-contrast microscopy to rip cells from the substratum, lysing many in the process. These shearing forces represented a major source of fixation artifacts and were not diminished by prior aspiration of the growth medium. Aqueous fixatives did not produce this effect. TCA and perchloric acid both gave extremely rapid fixation, and no morphological artifacts were observable by phase-contrast microscopy. Formaldehyde was less satisfactory. It caused the formation of extensive plasma membrane blebs with a concomitant loss of cytoplasmic protein. Glutaraldehyde was unsuitable for the purposes of this study, because of its ability to interfere with dye–protein interactions by reacting with and masking the positive fixed charges of protein amino groups (*8*). In addition, formaldehyde also caused the loss of nuclear structure in some cell lines.

Background Levels

Background levels of SRB staining were sensitive to the length of TCA fixation and serum concentration. Cultures could be left in TCA for several hours with little increase in background optical density (OD), which was typically about 0.035 OD units at 520 nm for 96-well plates. When cells were left in TCA overnight, the background OD doubled. Similarly, the background OD of medium containing 10% fetal calf serum was twice that of medium containing 5% fetal calf serum.

Optimized Staining Protocols

An optimized protocol (*2*) was developed for each of the dyes examined in detail. A plateau staining time was determined from the binding kinetics of a 2% dye solution. Optimal destaining was

achieved by determining the number of washes necessary to remove unbound dye without desorbing cell-associated stain. A supramaximal dye concentration that fully saturated cellular binding sites was determined by dose–response analysis of heavily confluent multilayers.

SRB Assay

TCA-fixed cells were stained for 30 minutes with 0.4% (wt/vol) SRB dissolved in 1% acetic acid. At the end of the staining period, SRB was removed and cultures were quickly rinsed four times with 1% acetic acid to remove unbound dye. The acetic acid was poured directly into the culture wells from a beaker. This procedure permitted rinsing to be performed quickly so that desorption of protein-bound dye did not occur. Residual wash solution was removed by sharply flicking plates over a sink, which ensured the complete removal of rinsing solution. Because of the strong capillary action in 96-well plates, draining by gravity alone often failed to remove the rinse solution when plates were simply inverted. After being rinsed, the cultures were air dried until no standing moisture was visible. Bound dye was solubilized with 10 m*M* unbuffered Tris base (pH 10.5) for 5 minutes on a gyratory shaker.

OD was read in either a UVmax microtiter plate reader (Molecular Devices, Menlo Park, CA) or a Beckman DU-70 spectrophotometer. For maximum sensitivity, OD was measured at 564 nm. Because readings were linear with dye concentrations only below 1.8 OD units, however, suboptimal wavelengths were generally used, so that all samples in an experiment remained within the linear OD range. With most cell lines, wavelengths of approximately 490–530 nm worked well for this purpose.

Optical Density Linearity

Curves of OD versus dye concentration were generally linear to 1.5–2.0 OD units. When the linearity range was exceeded, it was necessary either to dilute an aliquot and reread its OD or to use a suboptimal wavelength as a filter to reduce OD and extend the working range of dye concentrations that fell within the limits of linearity. This second method was generally more convenient but had the disadvantage of reducing resolution at low cell density. The problem was averted by reading samples at two separate wavelengths, then converting one to another with a least-squares linear regression equation determined over the range of OD values that were linear for both wavelengths.

Culture Cell Protein Analysis

Cell protein was measured by the Oyama and Eagle modification of the Lowry method, with bovine serum albumin used as a standard (*9*). The contents of individual wells were digested with 0.5 *M* NaOH. Aliquots of the digest were diluted with 0.5 *M* NaOH to a final volume of 0.4 mL and mixed with 2 mL of Lowry C solution. To this mixture was added 0.2 mL of Folin–Ciocalteu's phenol reagent (Sigma Chemical Co.) diluted 5:4 with distilled water. Color was allowed to develop for 30 minutes, and OD was measured at 660 nm.

Cell protein was also measured by the Bradford Coomassie brilliant blue dye method (*10*) using Pierce protein assay reagent (Pierce Chemical Co., Rockford, IL). The contents of individual wells were digested with 0.1 mL of 0.5 *M* NaOH. The digest was mixed with 4 volumes of 0.5 *M* NaOH and 5 volumes of Pierce reagent and agitated on a gyratory shaker for 5 minutes. Absorbance was then measured at 595 nm. A calibration curve was constructed, with bovine serum albumin used as a standard.

Results

Comparison of Dyes

Of the 21 dyes tested, 13 stained TCA-fixed cultures sufficiently well to provide the basis for a quantitative assay of cell number and drug cytotoxicity in a 96-well plate. These dyes were acridine orange, azure A, azure B, bromophenol blue, chromotrope 2R, cresyl violet acetate, methylene blue, orange G, phenosafranin, safranin O, SRB, thionin, and toluidine blue O. Four of these dyes were protein stains, while the remainder were general macromolecular biomass stains (*2–5*). The other eight dyes either stained too lightly to be useful or stained different cell lines with widely varying intensity. These dyes were azure C, Coomassie brilliant blue, crystal violet, ethidium bromide, methyl green, naphthol yellow S, propidium iodide, and pyronin B.

The most intensely staining dyes were bromophenol blue and SRB, both of which are protein stains. They were closely followed by thionin, azure A, and toluidine blue O, which are thiazin quinone–imine cationic biomass stains.

There was no clear advantage to any one of these dyes at high cell densities. All commonly produced OD values for confluent cultures that exceeded their linearity limits. At low cell densities, however, SRB was distinctly superior in signal-to-noise ratio (table 1). Results were quantitative at densities above 2,500 cells

Table 1. Optimal staining protocols for selected dyes*

Dye	Concentration (%)	Staining solution†	Minimum stain time (min)	No. of washes	Solubilizing solution†	Optimal wavelength (nm)	Signal-to-noise ratio at 5,000 cells per well	Resolution ($\times 10^3$ cells per well)
SRB	0.4	AcOH	15	4	Tris	564	4.83	1-2
ORG	1.5	AcOH	5	3	Tris	478	2.46	2-3
BPB	1.0	AcOH	20	4	Tris	590	1.92	3-4
CTR	0.25	AcOH	30	3	Tris	508	2.03	4-5
TNN	0.3	Tris	10	4	AcOH	594	1.56	>5
AZRA	0.25	Tris	30	4	AcOH	628	1.18	>10
TBO	0.2	Tris	10	3	AcOH	626	1.16	>10

*Ratios were determined for human HT-29 colon adenocarcinoma cells. ORG = orange G, BPB = bromophenol blue, CTR = chromotrope 2R, TNN = thionin, AZRA = azure A, TBO = toluidine blue, AcOH = acetic acid.
†Solutions were either 1% acetic acid or 10 m*M* unbuffered Tris base.

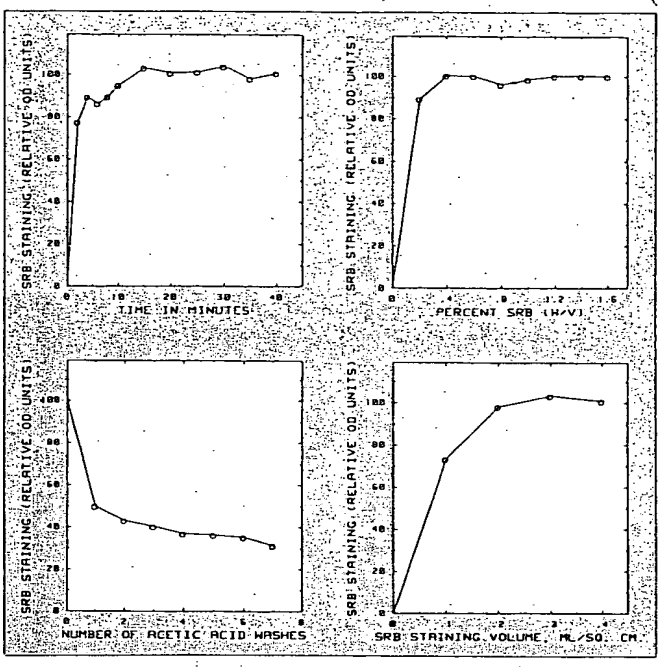

Figure 1. Optimization of SRB assay parameters for HT-29 colon adenocarcinoma cells in 96-well microtiter plates. SRB binding was determined as a function of time (upper left), dye concentration (upper right), number of destaining washes (lower left), and dye volume per unit area of cell culture (lower right). Cells were heavily confluent for optimizing dye volume per unit area and nearly confluent in the other experiments. Optical densities were measured with a UVmax plate reader at the wavelength setting (550, 520, or 490 nm) that provided the greatest sensitivity while remaining below the limit of linearity of 1.8 OD units.

per well and semiquantitative at 1,000 cells per well. Most of the other dyes examined had limits of resolution of 5,000–10,000 cells per well.

As a group, the protein stains tended to provide slightly better resolution than the biomass stains. Thus, two of the organosulfonic protein stains, chromotrope 2R and orange G, while not staining as intensely as some of the other dyes, had signal-to-noise ratios that were among the best at low cell densities (table 1). Their lower staining intensity was offset by the fact that they could be measured at their optimal wavelengths. This gave them an effective sensitivity nearly equal to that of SRB and bromophenol blue and superior to that of thionin, all of which had to be measured at suboptimal wavelengths to ensure that their measured OD values were within the range of linearity.

Optimized Protocols

Optimized protocols were developed for several of the dyes that provided better resolution (table 1). Data for SRB are shown in figure 1. SRB optimizations performed for more than 60 human tumor cell lines gave optimized protocols that were essentially identical. However, optimized parameters did change slightly from one commercial lot of SRB to the next. It is therefore advisable that the staining protocol be individually reoptimized for each new lot of dye.

A threefold increase in sensitivity was achieved by measuring SRB fluorometrically. SRB fluoresced strongly with laser excitation at 488 nm and could be quantitated at the single-cell level by static fluorescence cytometry.

SRB Calibration

Linearity of the SRB assay with cell number was evaluated by plating twofold serial dilutions of rapidly adhering cells (human H-23 lung cancer, SK-MEL-28 and UACC-62 melanoma, and SKOV-3 ovarian cancer cell lines). Cultures were fixed with TCA as soon as attachment was completed. The SRB assay was linear with the number of cells at densities ranging from 1% to more than 200% of confluence (fig. 2). Least-squares linear correlation coefficients for the SRB–cell number relationship in the four cell lines were 0.9999, 0.9998, 0.9989, and 0.9998, respectively. For non-drug-treated HT-29 colon adenocarcinoma cells, regression analysis showed an average correlation coefficient of 0.9727 for the SRB and Bradford assays. For 37 drugs producing 135 data points on the decreasing portions of their dose–response curves, the correlation coefficient for the SRB and Lowry assays with HT-29 cells was 0.9855 (fig. 3). All correlations were statistically significant at $P < .001$.

From the best-fit parameters of the least-squares analyses, the cell protein determination by the Lowry assay was equal to

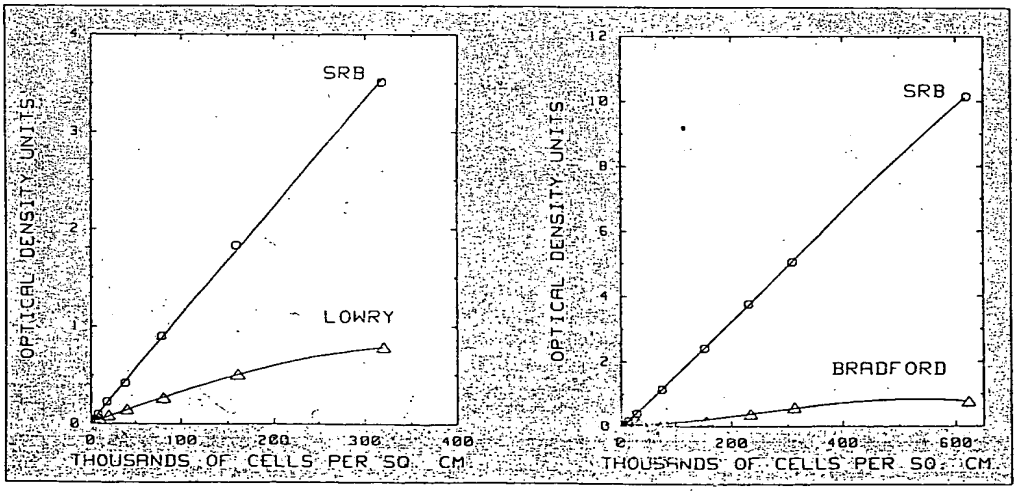

Figure 2. Calibration of the SRB, Lowry, and Bradford assays vs. number of cells. Cells were plated at densities of 25,000–600,000 cells per square centimeter in 96-well microtiter plates with a surface area of 0.32 cm^2. This corresponds to a density range of approximately 1%–200% of confluence. Cultures were fixed with TCA as soon as cells were attached. Growth during this period was negligible.

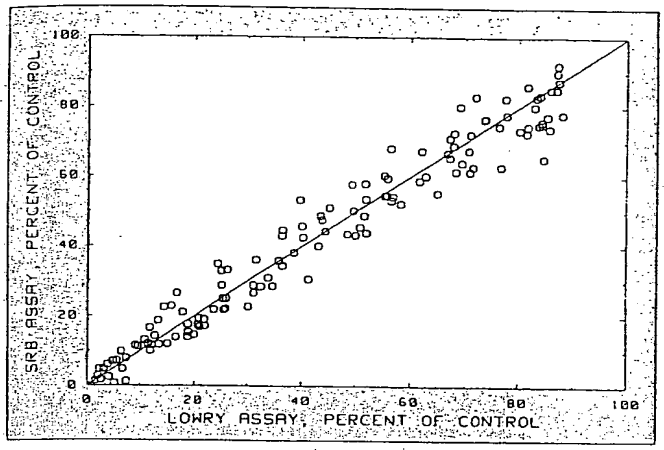

Figure 3. Comparison of the SRB and Lowry assays in evaluating drug-induced cytotoxicity. HT-29 colon adenocarcinoma cells were incubated for 48 hr with six concentrations of each of 37 clinical and experimental anticancer drugs. At the end of the incubation period, replicate cultures were separately evaluted by the SRB and Lowry assays. Each measurement was performed in triplicate. The data represent the 137 points that fell on descending arms of the Lowry dose–response curves. The least-squares correlation coefficient for the SRB–Lowry regression was 0.9855 ($P < .001$). Drugs included doxorubicin, 6-azauridine, colchicine, chromomycin A_3, cytarabine, ellipticine, erythromycin, fluorouracil, homoharringtonine, mercaptopurine, methotrexate, mitomycin, podophyllotoxin, vinblastine, and vincristine.

(137.6 × SRB OD_{520} units) + 1.615, while the cell protein determination by the Bradford assay was equal to (7.386 × SRB OD_{520} units) + 0.549, in micrograms of bovine serum albumin equivalents. (OD_{520} = OD at 520 nm.)

SRB Assay

The SRB assay provided a rapid and sensitive method for measuring the drug-induced cytotoxicity in both attached and suspension cultures in 96-well microtiter plates. Representative dose–response curves for fluorouracil and cisplatin are shown in fig. 4. SRB staining was also of use in assays of colony formation and colony extinction, permitting colony counts to be compared with the cell protein content of the same cultures (data not shown).

Discussion

SRB is a bright pink aminoxanthene dye with two sulfonic groups (*3*). Its histochemistry is similar to that of related dyes, such as Coomassie brilliant blue, bromophenol blue, and naphthol yellow S, which are used widely as protein stains (*2–5*). Under mildly acidic conditions, SRB binds to protein basic amino acid residues in TCA-fixed cells to provide a sensitive index of cellular protein content that is linear over a cell density range of at least 2 orders of magnitude (fig. 2).

Of the dyes examined in the present study, SRB provided the best combination of staining intensity and signal-to-noise ratio (table 1). Its sensitivity is comparable to the sensitivities of some fluorescent dyes (*11,12*) and superior to those of conventional visible dyes (*2,8,10,13–16*; fig. 2). The 100-fold range of linearity of the SRB assay far exceeds that of the Lowry and Bradford assays, eliminating the need for time-consuming and error-prone dilutions of samples with high-protein contents.

Color development in the SRB assay is rapid, stable, and visible. The OD of SRB can be measured over a broad range of visible wavelengths in either spectrophotometers or 96-well plate readers.

With a properly optimized protocol, SRB staining reaches a true and stable end point that does not have to be measured within any fixed period of time. When air dried, both TCA-fixed and SRB-stained samples can be stored indefinitely without deterioration. Tris-solubilized SRB is also stable for extended periods, provided that evaporation does not occur.

The SRB staining method is nondestructive in the sense that it is not necessary to digest samples. This allows cultures from which dye has been extracted to be restained and saved for future reference. The Tris extraction solution, however, does cause some deterioration in the morphology of samples fixed in 5% or 10% TCA or air dried for short periods of time. This deterioration is accompanied by the solubilization and loss of some cell protein. These effects can be reduced by extending fixation, storing air-dried samples for several weeks prior to Tris extraction, and minimizing the time of sample exposure to Tris.

Although the SRB assay was originally developed for cells attached to a plastic substratum, a variation of the method with an elevated TCA concentration was adequate for a number of cell lines in suspension culture, including the murine P388 lymphoma and the human CCRF-CEM, K562, MOLT-4, HL-60, and RPMI-8226 leukemia lines. This modified method was also useful for cell lines with weakly adherent monolayer cells or with adherent cultures that shed floating cells or small aggregates into the surrounding growth medium.

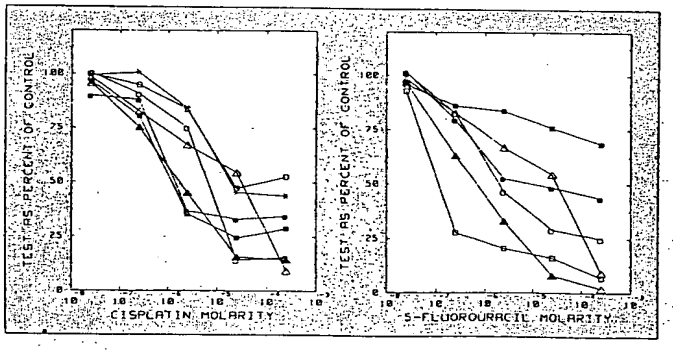

Figure 4. Cytotoxicity analysis in 96-well microtiter plates using the SRB assay to identify human tumor cell lines differentially sensitive to cisplatin and fluorouracil. Cell lines used in the cisplatin experiment were SF-268 central nervous system (CNS) cancer (■), HT-29 colon adenocarcinoma (○), RPMI-8226 leukemia (*), M19-MEL melanoma (△), H-460 non-small cell lung cancer (▲), OVCAR-4 ovarian cancer (●), and CAKI-1 renal cancer (□). Cell lines used in the fluorouracil experiment were XF-498 CNS cancer (■), HCT-116 colon cancer (▲), MOLT-4 leukemia (○), SK-MEL-5 melanoma (△), H-460 non-small cell lung cancer (□), and OVCAR-8 ovarian cancer (●). Cultures were preincubated in growth medium for 24 hr to permit recovery from trypsinization and then incubated for an additional 48 hr with control medium or test solution in growth medium. The H-460, HCT-116, and HT-29 cell lines were plated at 5,000 cells per well; the CAKI-1, M19-MEL, OVCAR-4, OVCAR-8, and SK-MEL-5 cell lines at 10,000 cells per well; the SF-268 cell line at 15,000 cells per well; the RPMI-8226 and XF-498 cell lines at 20,000 cells per well; and the MOLT-4 cell line at 30,000 cells per well.

The SRB assay provides a sensitive method for measuring drug cytotoxicity in culture. In a pilot study of the NCI's in vitro anticancer-drug discovery project, the SRB assay was used to examine the differential sensitivities of 60 human tumor cell lines to more than 1,000 test compounds (*1,6,17,18*). The method appears to offer several advantages over the MTT and XTT assays (*19,20*) for very large-scale drug screening.[1] The SRB assay was simpler, faster, and more sensitive than the MTT assay, provided better linearity with cell number, permitted the use of saturating dye concentrations, was less sensitive to environmental fluctuations, was independent of intermediary metabolism, and provided a fixed end point that did not require a time-sensitive measurement of initial reaction velocity (*21,22*).

References

(*1*) BOYD MR: Status of the NCI preclinical antitumor drug discovery screen; implications for selection of new agents for clinical trial. *In* Cancer Principles and Practice of Oncology Updates (DeVita VT Jr, Hellman S, Rosenberg SA, eds). Philadelphia: Lippincott, 1990

(*2*) SKEHAN P, FRIEDMAN SJ: A rapid Naphthol Yellow S method for measuring the cellular protein content of anchorage cultures. In Vitro 21:288–290, 1985

(*3*) LILLIE RD: H.J. Conn's Biological Stains, 9th ed. Baltimore: Williams & Wilkins, 1977

(*4*) KIERNAN JA: Histological & Histochemical Methods: Theory & Practice. Oxford: Pergamon Press, 1981

(*5*) FLORES R: A rapid and reproducible assay for quantitative estimation of proteins using bromophenol blue. Anal Biochem 89:605–611, 1978

(*6*) STINSON SF, ALLEY MC, KENNEY S, ET AL: Morphologic characterization of human carcinoma cell lines. Proc Am Assoc Cancer Res 30:613, 1989

(*7*) CRISSMAN HA, MULLANEY PF, STEINKAMP JA: Methods and applications of flow systems for analysis and sorting of mammalian cells. Methods Cell Biol 9:179–246, 1975

(*8*) SKEHAN P: The mechanisms of glutaraldehyde-fixed sarcoma 180 ascites cell aggregation. J Membrane Biol 24:87–106, 1975

(*9*) OYAMA VI, EAGLE H: Measurement of cell growth in tissue culture with a phenol reagent (Folin-Ciocalteu). Proc Soc Exp Biol Med 91:305–307, 1956

(*10*) BRADFORD M: A rapid and sensitive method for the quantitation of microgram quantities of protein utilizing the principles of protein-dye binding. Anal Biochem 72:248–254, 1976

(*11*) VAN LAMBALGEN R, LELIEVELD P: The PIT method: An automated in vitro technique for drug toxicity testing. Invest New Drugs 5:161–165, 1987

(*12*) MCCAFFREY TA, AGARWAL LA, WEKSLER BB: A rapid fluorometric DNA assay for the measurement of cell density and proliferation in vitro. In Vitro 24:247–252, 1988

(*13*) MOSMANN T: Rapid colorimetric assay for cellular growth and survival: Application to proliferation and cytotoxicity assays. J Immunol Methods 65:55–63, 1983

(*14*) FINLAY GJ, BAGULEY BL, WILSON WR: A semiautomated microculture method for investigating growth inhibitory effects of cytotoxic compounds on exponentially growing carcinoma cells. Anal Biochem 139:272–277, 1984

(*15*) LANDEGREN U: Measurement of cell numbers by means of the endogenous enzyme hexosaminidase. Applications to detection of lymphokines and cell surface antigens. J Immunol Methods 67:379–388, 1984

(*16*) EVERITT E, WOHLFART C: Spectrophotometric quantitation of anchorage-dependent cell number using extraction of Naphthol Blue-Black-stained cellular protein. Anal Biochem 162:122–129, 1987

(*17*) MONKS A, SCUDIERO D, SKEHAN P, ET AL: Implementation of a pilot scale, high flux anticancer drug screen utilizing disease-oriented panels of human tumor cell lines in culture. Proc Am Assoc Cancer Res 30:607, 1989

(*18*) SKEHAN P, STORENG R, SCUDIERO D, ET AL: Evaluation of colorimetric biomass stains for assaying in vitro drug effects upon human tumor cell lines. Proc Am Assoc Cancer Res 30:612, 1989

(*19*) ALLEY MC, SCUDIERO DA, MONKS A, ET AL: Feasibility of drug screening with panels of human tumor cell lines using a microculture tetrazolium assay. Cancer Res 48:589–601, 1988

(*20*) SCUDIERO DA, SHOEMAKER RH, PAULL KD, ET AL: Evaluation of a soluble tetrazolium/formazan assay for cell growth and drug sensitivity in culture using human and other tumor cell lines. Cancer Res 48:4827–4833, 1988

(*21*) VISTICA DT, SKEHAN P, SCUDIERO D, ET AL: Tetrazolium-based assays for cellular viability: A critical examination of parameters which affect formazan production. Proc Am Assoc Cancer Res 30:612, 1989

(*22*) RUBINSTEIN LV, PAULL KD, SHOEMAKER RH, ET AL: Correlation of screening data generated with a tetrazolium assay (MTT) versus a protein assay (SRB) against a broad panel of human tumor cell lines. Proc Am Assoc Cancer Res 30:607, 1989

[1]MTT = 3-(4,5-dimethylthiazol-2-yl)-2,5-diphenyltetrazolium bromide. XTT = 2,3-bis[2-methoxy-4-nitro-5-sulfophenyl]-5-[(phenylamino)carbonyl]-2H-tetrazolium hydroxide.

Chemosensitivity prediction by transcriptional profiling

Jane E. Staunton*, Donna K. Slonim*†, Hilary A. Coller*‡, Pablo Tamayo*, Michael J. Angelo*, Johnny Park*, Uwe Scherf§, Jae K. Lee§, William O. Reinhold§, John N. Weinstein§, Jill P. Mesirov*, Eric S. Lander*¶‖, and Todd R. Golub*‖**

*Whitehead/Massachusetts Institute of Technology Center for Genome Research, Cambridge, MA 02139; §Laboratory of Molecular Pharmacology, Division of Basic Sciences, Building 37/5D-02, National Cancer Institute, National Institutes of Health, Bethesda, MD 20892; ¶Department of Biology, Massachusetts Institute of Technology, Cambridge, MA 02139; and **Dana-Farber Cancer Institute and Harvard Medical School, Boston, MA 02115

Contributed by Eric S. Lander, July 17, 2001

In an effort to develop a genomics-based approach to the prediction of drug response, we have developed an algorithm for classification of cell line chemosensitivity based on gene expression profiles alone. Using oligonucleotide microarrays, the expression levels of 6,817 genes were measured in a panel of 60 human cancer cell lines (the NCI-60) for which the chemosensitivity profiles of thousands of chemical compounds have been determined. We sought to determine whether the gene expression signatures of untreated cells were sufficient for the prediction of chemosensitivity. Gene expression-based classifiers of sensitivity or resistance for 232 compounds were generated and then evaluated on independent sets of data. The classifiers were designed to be independent of the cells' tissue of origin. The accuracy of chemosensitivity prediction was considerably better than would be expected by chance. Eighty-eight of 232 expression-based classifiers performed accurately (with $P < 0.05$) on an independent test set, whereas only 12 of the 232 would be expected to do so by chance. These results suggest that at least for a subset of compounds genomic approaches to chemosensitivity prediction are feasible.

A long-term goal of pharmacogenomics research is the accurate prediction of patient response to drugs, as it would facilitate the individualization of patient treatment. Such an approach is particularly needed in cancer therapy, where commonly used agents are ineffective in many patients, and where side effects are common, given the nonspecific mechanism of action of most chemotherapeutic drugs. Previous efforts to use genetic information to predict drug sensitivity primarily have focused on individual genes that have broad effects, such as multidrug resistance genes *mdr1* and *mrp1* (1). Here we describe a predictive methodology that seeks to tap more complex genetic contributions to drug sensitivity. The recent development of DNA microarrays, which permit the simultaneous measurement of the expression levels of thousands of genes, raises the possibility of an unbiased, genomewide approach to the genetic basis of drug response.

Prediction of chemosensitivity in the clinic is particularly challenging because drug responses reflect not only properties intrinsic to the target cell, but also host metabolic properties. By modeling this approach in cultured cells, we limited our study to cell-intrinsic properties that are exposed in culture. A panel of 60 such cancer cell lines has been used extensively by the National Cancer Institute's Developmental Therapeutics Program, and the merits and limitations of their use as screening tools for drug development have been described (2–5). These cell lines have been analyzed for their sensitivity to a broad range of chemical compounds and thus offer an extensive database for the testing of our methodology.

We investigated the feasibility of chemosensitivity prediction by using oligonucleotide microarrays to measure the expression levels of 6,817 genes in each of the 60 cell lines in the NCI-60 panel. The data can be found at www.genome.wi.mit.edu/MPR/NC160/NC160.html. We then asked whether patterns of gene expression were sufficient to predict sensitivity or resistance of the cell lines to 232 chemical compounds. To maintain statistical rigor, the data set was divided into two groups—a training set, which was used to develop a gene expression-based chemosensitivity classifier, and a test set, on which we evaluated the accuracy of the classifier. When compared with random prediction, a significant number of the expression-based classifiers performed accurately, indicating that the response of cancer cell lines to drugs is indeed predictable.

Materials and Methods

Compound Selection. The 60 cell lines were previously assayed for their sensitivity to a variety of compounds as a part of the Developmental Therapeutics Program at the National Cancer Institute, as described (refs. 2 and 3; see also: http://dtp.nci.nih.gov). Briefly, each cell line was exposed to each compound for 48 h, and growth inhibition was assessed by the sulforhodamine B assay for cellular protein. The concentration of compound required for 50% growth inhibition was scored as the GI_{50}. For each compound, $\log_{10}(GI_{50})$ values were normalized across the 60 cell lines. Cell lines with $\log_{10}(GI_{50})$ at least 0.8 SDs above the mean were defined as resistant to the compound, whereas those with $\log_{10}(GI_{50})$ at least 0.8 SDs below the mean were defined as sensitive. Cell lines with $\log_{10}(GI_{50})$ within 0.8 SDs of the mean were considered to be intermediate and were eliminated from analysis. Prediction analysis was performed for compounds that had a minimum of 30 sensitive and resistant lines, with at least 10 each sensitive and resistant. To avoid choosing drug compounds with narrow dynamic ranges of drug responses, which are essentially sensitive or resistant to most of the 60 cell lines, we also required that the 1.6-SD window around the mean GI_{50} correspond to at least 1 order of magnitude in raw GI_{50} values. Of 5,084 compounds evaluated, 232 met these criteria. Importantly, gene expression data were not used in any way in compound selection.

Training and Test Set Selection. For each selected compound, a set of training cell lines was chosen in the following manner. Within each tissue type (e.g., breast cancer; see *Results*), the most sensitive and most resistant cell line were chosen. If a tissue type lacked either sensitive or resistant cell lines according to the

Abbreviation: GI_{50}, 50% growth inhibition.

†Present address: Genetics Institute, 35 Cambridge Park Drive, Cambridge, MA 02140.

‡Present address: Fred Hutchinson Cancer Research Center A3-100, 1100 Fairview Avenue North, Seattle, WA 98109.

‖To whom reprint requests may be addressed. E-mail: lander@wi.mit.edu or golub@genome.wi.mit.edu.

The publication costs of this article were defrayed in part by page charge payment. This article must therefore be hereby marked "*advertisement*" in accordance with 18 U.S.C. §1734 solely to indicate this fact.

REF. 4

criteria above, it was not used in training. All sensitive or resistant cell lines not selected for training were reserved as a test set for final evaluation of the classifier.

Gene Expression Data. RNA was isolated as described (6). Poly(A) selected RNA (1.5 μg) from each cell line was used to prepare biotinylated cRNA targets as described (7); details are provided at www.genome.wi.mit.edu/MPR. Targets were hybridized to Affymetrix (Santa Clara, CA) high-density Hu6800 arrays, washed, stained with phycoerythrin-conjugated streptavidin (Molecular Probes), and signal-amplified with biotinylated anti-streptavidin antibody (Vector Laboratories). Expression values (average difference units) were calculated by using Affymetrix GENECHIP software. An expression level of 100 units was assigned to measurements <100.

An earlier version of the gene expression data was generated by hybridizing the biotinylated targets to an earlier-generation, low-density Affymetrix HU6800 four-chip set (HU6800 subA, subB, subC, subD). These data were analyzed by Butte *et al.* (13), using relevance networks, and are available at http://www.genome.wi.mit.edu/MPR. However, all analyses described in this article were performed on the data from the newer, higher density arrays.

Weighted Voting Classification. We used a weighted voting scheme to classify each cell line as sensitive or resistant on the basis of gene expression data. In this scheme, a set of marker genes "vote" on the class of each cell line (8). For each compound being classified, genes were excluded if they varied by less than 5-fold and 500 units across training cell lines, and by less than 2-fold across each pair of training cell lines of a single tissue type. The remaining genes on the microarray were ranked according to the correlation between their expression level and the sensitivity and resistance profile of the training cell lines. We used a measure of correlation, $P(g,c)$, as described (8). Let $[\mu 1(g), \sigma 1(g)]$ and $[\mu 2(g), \sigma 2(g)]$ denote the means and SDs of the expression levels of gene g for the samples in class 1 and class 2, respectively. Let $P(g,c) = [\mu 1(g) - \mu 2(g)]/[\sigma 1(g) + \sigma 2(g)]$, which reflects the difference between the class means relative to the variance within the classes. Large values of $P(g,c)$ indicate strong correlation between gene expression and class distinction, whereas the sign of $P(g,c)$ indicates whether higher expression correlates with class 1 or class 2. The vote for each gene can be expressed as the weighted difference between the normalized log expression in the cell line to be classified and the average of the sensitive and resistance class mean expression levels, where weighting is determined by the correlation $P(g,c)$ from the training set. The class of the cell line is determined by the sum of votes for all marker genes used in a classifier. In previous work (8), classification was subjected to a confidence (prediction strength) threshold; no such threshold was used here.

Optimizing Classifiers by Cross-Validation. Classifiers with 1–200 marker genes were used for training set cross-validation to determine the number of marker genes that best classify each compound. For each classifier, cross-validation was performed with the entire training set: one cell line was removed, the classifier was trained on the remaining cell lines and then tested for its ability to classify the withheld cell line. This procedure was repeated for each cell line in the training set. Cross-validation accuracy rates are available at www.genome.wi.mit.edu/MPR/NC160/NC160.html.

Evaluating Classifier Accuracy. The model that was most accurate in cross-validation was chosen as the optimized classifier for that compound. In the case of multiple models that scored identically, the model with the larger number of genes was chosen. The training set-optimized classifier for each compound was then used to classify test cell lines. Performance was measured as the average of the accuracy of classifying sensitive cell lines and the accuracy of classifying resistant cell lines. As a control, 1,000 iterations of a simulation were run to classify the same 232 test sets by random coin flip. The distributions from observed and random results were compared by using the Kolmogorov–Smirnov test (9), which is a test for whether two sets of data are drawn from different distributions (see www.genome.wi.mit.edu/MPR/NC160/NC160.html for details).

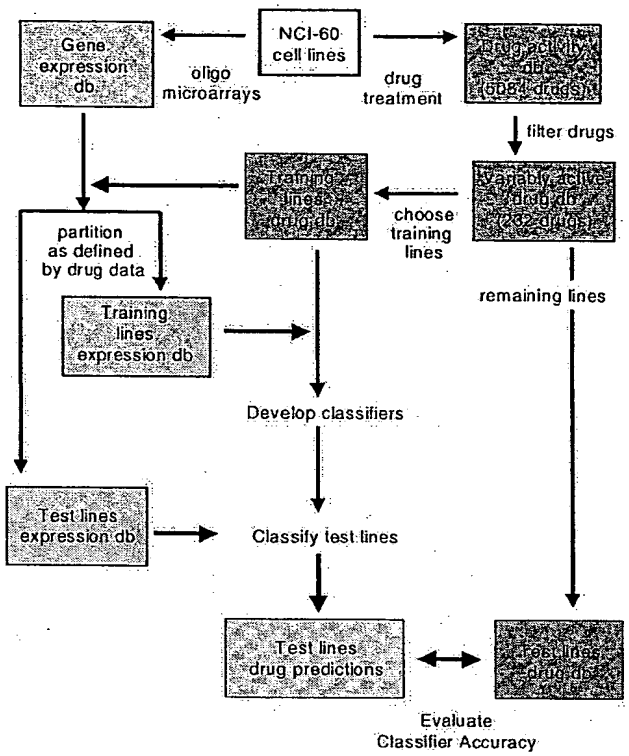

Fig. 1. General scheme for classification of compound sensitivity in cell lines by using gene expression data.

For computing the significance of individual classifier performance, we computed the probability of the observed prediction accuracy occurring by chance if such predictions were the result of a fair coin flip. Consider a compound with n cell lines in the test set, and a classifier that predicts j of the n cell lines correctly. Because training introduces no class bias, the probability of doing at least this well by chance, Pr(j correct predictions), is the same as Pr($\geq j$ heads of n fair coin flips), which can be represented as

$$\sum_{i=j}^{n} \binom{n}{i} \left(\frac{1}{2}\right)^{(n-i)} \left(\frac{1}{2}\right)^{i} = \left(\frac{1}{2}\right)^{n} \sum_{i=j}^{n} \binom{n}{i}.$$

Results

Our classification scheme is outlined in Fig. 1. We approached chemosensitivity prediction as a binary classification problem, and thus for each compound, two classes of cell lines were defined: sensitive and resistant. The majority of the 5,084 compounds demonstrated relatively uniform growth inhibitory activities (GI_{50}) across the 60 cancer cell lines, but we restricted

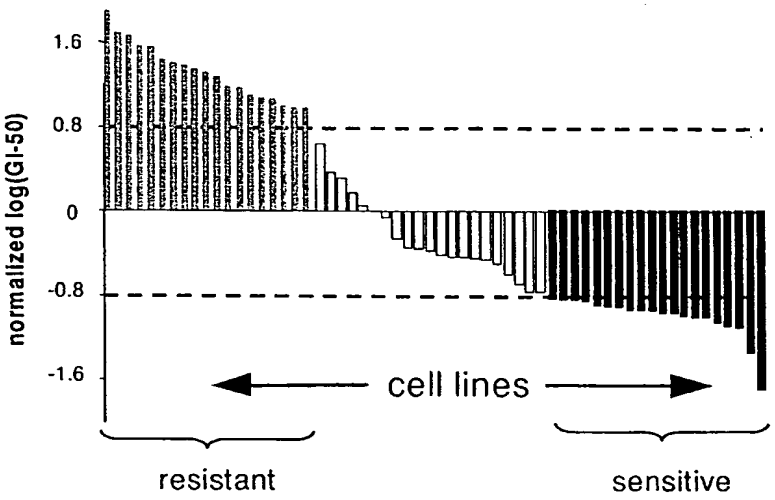

Fig. 2. Example of compound (NSC 749; Azaguanine) with bimodal distribution of growth inhibition. For each compound, log(GI_{50}) values were normalized across the 60 cell lines, and cell lines with log(GI_{50}) within 0.8 SDs of the mean are eliminated from analysis; remaining cell lines were defined as sensitive or resistant to the compound. Compounds with at least 30 cell lines outside the 1.6-SD window, and for which the window represents at least 1 order of magnitude in raw GI_{50} data were analyzed further. A total of 232 compounds met these criteria.

our analysis to compounds that included a balance of sensitive and resistant lines (see *Materials and Methods* and Fig. 2). A total of 232 compounds met these criteria (see www.genome.wi.mit.edu/MPR/NC160/NC160.html for complete list of compounds and cell lines).

For each of the 232 compounds, the sensitive and resistant cell lines were divided into a training set and a test set, again by using only drug sensitivity data to make these assignments. One approach would be to select a set of cell lines at random for training and use the remaining lines as a test set. The problem with this approach is that the cell lines in the NCI-60 panel are derived from nine broad categories of tissue of origin (lung, breast, colon, kidney, bone marrow, melanocyte, central nervous system, prostate, and ovary). Sensitivity to some drugs correlates with tissue of origin, and thus one runs the risk of developing classifiers that simply classify according to tissue type, rather than according to drug sensitivity *per se*. To circumvent this problem, we designed "tissue-aware" training sets. Each training set included one sensitive and one resistant cell line from each of multiple tissue types. A tissue type was used in training only if it included both sensitive and resistant cell lines for the compound, and thus the 232 training sets contained variable numbers of cell lines (6 to 18). For each compound, the remaining cell lines (16 to 35) were reserved as a test set that was used to independently evaluate prediction accuracy. All reported prediction accuracies are for test set samples only.

To create a gene expression database, RNA was extracted from the 60 cell lines before any drug treatment. These RNAs were then analyzed on oligonucleotide microarrays containing probes for 6,817 known human genes. The genes were not selected to be particularly informative for the present experiments, but rather they represent the named human genes identified in GenBank at the time the array was designed. The expression levels of the 6,817 genes in each of the 60 cell lines are available at www.genome.wi.mit.edu/MPR/NC160/NC160.html.

To build and train classifiers, we used both drug sensitivity data and gene expression data. The GI_{50} profile of each training set was used as a template for marker gene selection. Each gene was ranked according to the correlation in the training set between its expression level and the sensitivity-resistance class distinction (see *Materials and Methods*). Classification (sensitive vs. resistant) was performed by using a weighted voting algorithm, in which correlated genes "vote" on whether a cell line is predicted to be sensitive or resistant (8). The vote for each gene is a function of its expression in the cell line to be classified and the degree to which its expression is correlated with sensitivity or resistance in the training set (see *Materials and Methods*). Classifiers with up to 200 correlated genes were tested through cross-validation by holding back one cell line, training on the remaining lines, predicting the class of the withheld line, and repeating this cycle for each cell line in the training set. For each compound, the classifier model that was most accurate in training set cross-validation was selected as the optimized classifier for that compound, and it was evaluated without further modification on the independent test set. Each optimized classifier contained between five and 200 genes, with an average of 68 genes per classifier (all classifier genes and weights are available at www.genome.wi.mit.edu/MPR/NC160/NC160.html). This process of cross-validation diminishes the problem of overfitting during selection of the optimal classifier, a particular problem when dealing with small number of cases and large numbers of variables.

Each classifier, optimized on a training set, was evaluated on a test set of cell lines that had not participated in training. The distribution of accuracies from expression-based classification was compared with the distribution obtained from random classification of the same 232 test sets (Fig. 3). The difference between the two distributions is highly significant, as indicated by the Kolmogorov–Smirnov test ($P \leq 10^{-24}$) (9, 10), with the expression-based distribution clearly skewed toward higher accuracy.

The significance of each classifier's performance was assessed by determining the probability of obtaining the observed accuracy rate by chance if each classification was the result of a fair coin toss (see *Materials and Methods*). A total of 88 of 232 (38%) expression-based classifiers performed accurately with a significance of $P \leq 0.05$, whereas only 12 such classifiers (5% of 232) would be expected to do so by chance. The statistically significant classifiers had a median accuracy of 75% (range 64% to 92%). This result indicates that for a substantial subset of compounds gene expression data were sufficient for accurate prediction of chemosensitivity.

The compounds whose chemosensitivity was highly predictable spanned multiple structural categories, the majority functioning through unknown mechanisms of action. We observed

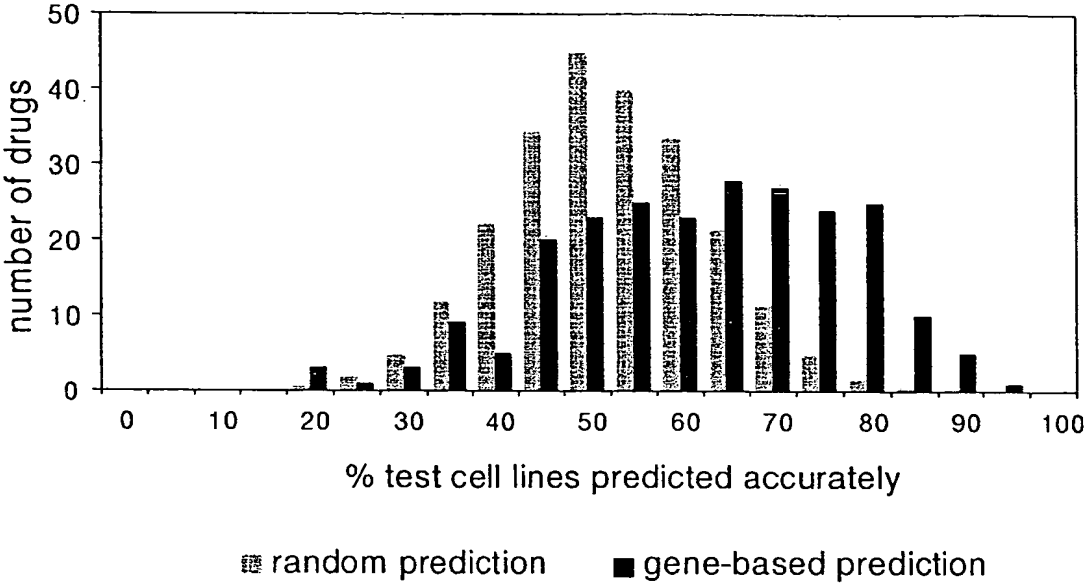

Fig. 3. Distribution of classification accuracies for 232 compounds. Percent accuracy for each compound is the average accuracy for classification of sensitive and resistant test cell lines. The control distribution represents results obtained from random classification (1,000 iterations) of the 232 test sets.

no obvious connection between mechanism of drug action and classifier accuracy. No obvious relationship was seen between prediction accuracy and number of genes used or number of cell lines used for training (data not shown).

In addition to yielding accurate predictors of chemosensitivity, the gene expression data generated herein provide potential insights into mechanisms of drug resistance. In general, the gene expression correlates of drug sensitivity were complex, and their biological significance not easily interpretable (all lists of genes and weights are available at www.genome.wi.mit.edu/MPR/NC160/NC160.html). Our method required variable expression across multiple pairs of training cell lines, which explains some notable absences, such as *mdr1*, whose expression level surpassed our detection threshold (100 average difference units) in only three cell lines. However, anecdotal relationships between correlated marker genes and known mechanisms of drug action suggest that marker genes may provide insights into mechanisms of drug action—or of sensitivity or resistance—for compounds with unknown mechanism of action.

For example, the 120-gene classifier for cytochalasin D (NSC 209835) classified 20 cell lines with accuracy of 80% (significant at a threshold of $P < 0.0013$). The marker genes for the cytochalasin D classifier included 29 genes (24%) related to the cytoskeleton or extracellular matrix (ECM). This set is enriched relative to the ≈5% known cytoskeletal/ECM genes on the entire array (data not shown). The top 30 cytochalasin D marker genes are shown in Fig. 4, along with the expression level of each gene across the 20 cell lines (a classifier built on only 30 genes similarly yields 80% accuracy). Cytochalasin D binds to actin and induces dimers that interfere with polymerization, thus disrupting cytoskeletal integrity (11), but it has not been previously suspected that the expression pattern of cytoskeletal genes in untreated cells would be predictive of cytochalasin D sensitivity. Interestingly, an excess of cytoskeletal/ECM genes also was observed for a number of other classifiers, including ones for compounds that are not thought to act through cytoskeletal components. For example, the 100-gene classifier for the antifolate, NSC 633713 is highly accurate (87.5% accuracy; significant at a threshold of $P < 0.0003$) and includes 21 (21%) cytoskeletal/ECM genes. It is possible that cytoskeletal signatures may reflect cellular components that influence sensitivity to a variety of compounds rather than functioning as direct targets of compound activity.

Discussion

Implicit in the goal of personalized medicine is the notion that an individual patient's response to drugs should be predictable. However, experimental data supporting the genetic basis of differential drug response are limited. We report here a systematic approach for gene expression-based prediction of chemosensitivity. We have applied this methodology to the prediction of cytotoxicity for 232 compounds in 60 cell lines by using the gene expression profiles of untreated cells. The NCI-60 panel has been used extensively in drug evaluation efforts at the National Cancer Institute, and more recently, it has been studied at the gene expression level by using an alternative approach to gene expression profiling (cDNA microarrays) (6, 12). Those and other studies (13) clearly demonstrate that biological correlates of gene expression are identifiable. In the present study, we explored whether such gene-drug correlates are sufficiently robust to permit development of a chemosensitivity classifier built exclusively on gene expression data.

A particular challenge in such an effort is the small size of the data set. DNA microarrays allow for the measurement of thousands of genes, yet most experiments contain relatively few samples. The NCI-60 panel contains a total of 60 cell lines, but only 2–9 cell lines represent each tissue type (e.g., kidney, colon). When analyzing small data sets, one runs the risk of overfitting a model to the data. This can result in overestimating the classifier's accuracy. We addressed this problem in two ways. First, we used a leave-one-out cross-validation procedure to build the prediction models. Second, we divided the data set into two parts: a training set on which chemosensitivity predictors were developed, and a test set, on which they were evaluated.

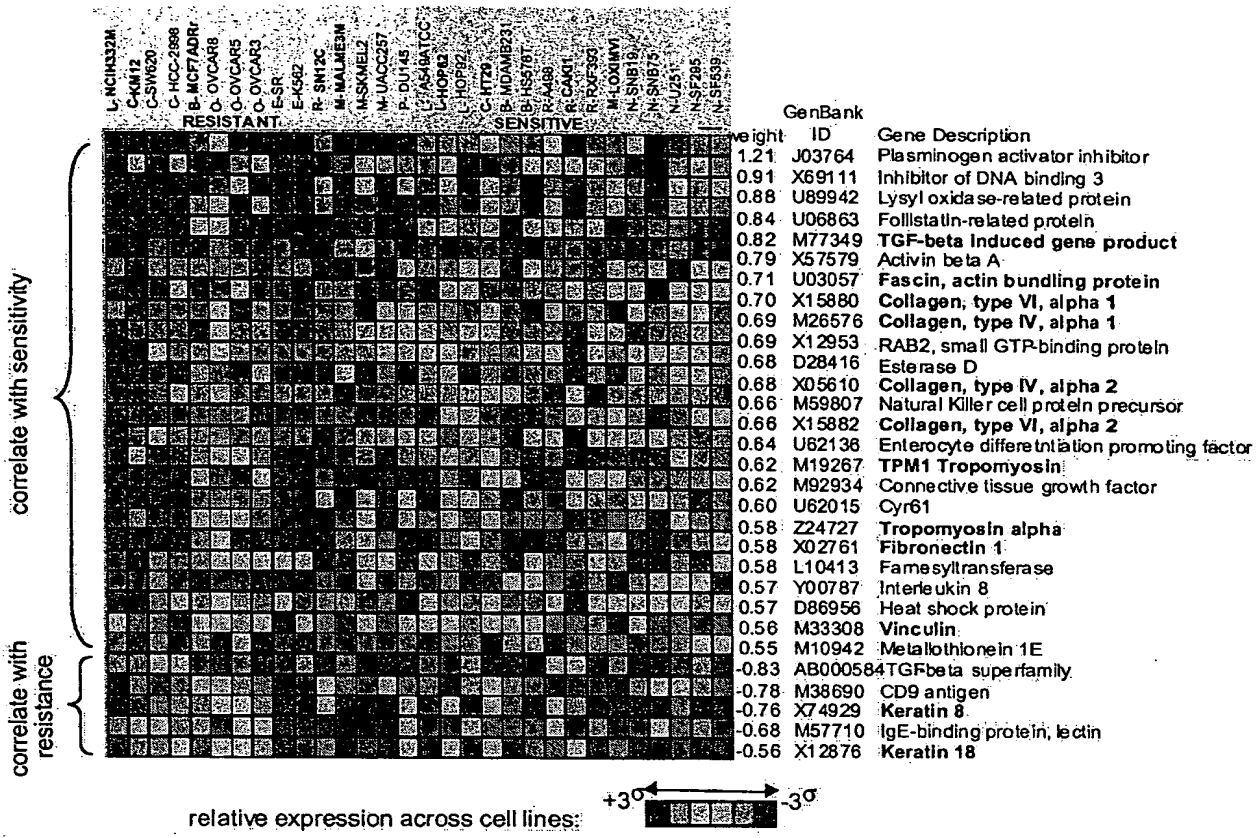

Fig. 4. Top 30 classifier genes for cytochalasin D (NSC-209835). The red and blue matrix represents the normalized expression patterns for each gene across the cell lines (brightest red indicates highest relative expression, darkest blue indicate, lowest relative expression). (*Top*) The sensitive and resistant cell lines are shown. Tissue of origin for each cell line is indicated as follows: L, lung (nonsmall cell); C, colon; B, breast; O, ovarian; E, leukemia; R, renal; M, melanoma; P, prostate; N, central nervous system. Lines used as training sets are shown in bold. The list at right shows the weighting factor [measure of correlation; weights were computed by using negative log(GI_{50}) values and thus a positive value correlates with sensitivity], the GenBank accession number, and the gene name. Genes whose products are known to have cytoskeletal and/or extracellular matrix functions are shown in bold.

One disadvantage to this approach is that it further reduces the size of the data set used to generate the model, and therefore accuracy can be potentially compromised. A particular goal of this study was thus to determine whether a data set of only 60 diverse cell lines would be sufficiently large to generate accurate, statistically significant chemosensitivity classifiers.

Given the above limitations, the observed accuracies are quite remarkable. Classification accuracy was far greater than one would expect by chance alone, with approximately one-third of the evaluated compounds being predictable with statistical significance ($P < 0.05$). These results suggest that, for at least some compounds, chemosensitivity is predictable by using only the gene expression patterns of untreated cells. The results further suggest that the identification of such patterns is feasible in data sets of only modest size.

The training sets were specifically designed to identify gene expression correlates of chemosensitivity within a tissue type, so as to reduce the confounding problem of chemosensitivity-tissue type correlations. However, such correlations may not be entirely avoided by the method. The selection of extreme cell lines within a given tissue type (i.e., those with the highest and lowest GI_{50}s) for the training of the classifier leaves open the possibility that the training samples are atypical in their lack of chemosensitivity-tissue type correlation. For example, the classification of cytochalasin D sensitivity (Fig. 4) is in part correlated with tissue type in that the ovarian cancer cell lines tend to be resistant, whereas the central nervous system (CNS) cell lines are sensitive. Notably, neither ovarian nor CNS cell lines were used to train the classifier.

For some compounds, gene-based classification was no more accurate than random classification. There are several possible explanations for this. First, we measured the expression level of only 6,817 genes, estimated to represent roughly one-fifth of the human genome (14). It is possible that if the entire genome were analyzed, the number of compounds with predictable chemosensitivity would increase. It is also conceivable that alternative gene selection or machine learning algorithms would be more successful. Second, we limited ourselves to a binary classification scheme, whereas a multiclass or continuous definition of sensitivity may be more appropriate for some compounds. It is likely that larger data set would be required for such efforts. Finally, for some compounds, chemosensitivity may be governed by mechanisms that are not readily revealed at the transcriptional level, such as posttranscriptional regulation, posttranslational modification, proteasome function, or protein–protein interactions. The ability to increase prediction accuracy by capturing

such information by using proteomic approaches, for example, remains to be determined.

To achieve the goal of personalized medicine, chemosensitivity prediction must be extended beyond cell line models to include the analysis of primary patient material, and the prediction of intermediate levels of chemosensitivity that were not addressed in our experiments. Although few clinical studies have been reported to date, early indications are that clinically relevant gene expression patterns can be extracted from tumor samples (8, 12, 15, 16). However, the current study demonstrates the potential for screening samples for genetic determinants of drug sensitivity and, thus, suggests that the goal of individualizing patient treatment plans based on genetic features of a tumor may indeed be feasible.

We thank current and former members of the Whitehead/Massachusetts Institute of Technology Center for Genome Research for helpful discussions and reviewers for comments on the manuscript. We are especially grateful to Nathan Siemers for scientific input and Julian Fowler for the web-page implementation. This work was supported in part by Affymetrix, Millennium Pharmaceuticals, and Bristol-Myers Squibb (to E.S.L.), and by grants from the National Cancer Institute and National Cancer Institute Intramural Breast Cancer Think Tank (to U.S., J.N.W., J.K.L., and W.O.R.).

1. Sonneveld, P. (2000) *J. Intern. Med.* **247**, 521–534.
2. Grever, M. R., Schepartz, S. A. & Chabner, B. A. (1992) *Semin. Oncol.* **19**, 622–638.
3. Stinson, S. F., Alley, M. C., Kopp, W. C., Fiebig, H. H., Mullendore, L. A., Pittman, A. F., Kenney, S., Keller, J. & Boyd, M. R. (1992) *Anticancer Res.* **12**, 1035–1053.
4. Monks, A., Scudiero, D. A., Johnson, G. S., Paull, K. D. & Sausville, E. A. (1997) *Anticancer Drug Des.* **12**, 533–541.
5. Weinstein, J. N., Myers, T. G., O'Connor, P. M., Friend, S. H., Fornace, A. J., Jr., Kohn, K. W., Fojo, T., Bates, S. E., Rubinstein, L. V., Anderson, N. L., *et al.* (1997) *Science* **275**, 343–349.
6. Scherf, U., Ross, D. T., Waltham, M., Smith, L. H., Lee, J. K., Tanabe, L., Kohn, K. W., Reinhold, W. C., Myers, T. G., Andrews, D. T., *et al.* (2000) *Nat. Gent.* **24**, 236–244.
7. Lockhart, D., Dong, H., Byrne, M., Follettie, M., Gallo, M., Chee, M., Mittmann, M., Wang, C., Kobayashi, M., Horton, H. & El, B. (1996) *Nat. Biotechnol.* **14**, 1675–1680.
8. Golub, T. R., Slonim, D. K., Tamayo, P., Huard, C., Gaasenbeek, M., Mesirov, J. P., Coller, H., Loh, M. L., Downing, J. R., Caligiuri, M. A., *et al.* (1999) *Science* **286**, 531–537.
9. Press, W. H., Teukolsky, S. A., Vetterling, W. T. & Flannery, B. P. (1992) *Numerical Recipes in C: The Art of Scientific Computing* (Cambridge Univ. Press, Cambridge, U.K.), 2nd Ed.
10. Zar, J. H. (1999) *Biostatistical Analysis* (Prentice–Hall, Upper Saddle, NJ).
11. Goddette, D. W. & Frieden, C. (1986) *J. Biol. Chem.* **261**, 15974–15980.
12. Ross, D. T., Scherf, U., Eisen, M. B., Perou, C. M., Rees, C., Spellman, P., Iyer, V., Jeffrey, S. S., Van de Rijn, M., Waltham, M., *et al.* (2000) *Nat. Genet.* **24**, 227–235.
13. Butte, A., Tamayo, P., Slonim, D., Golub, T. R. & Kohane, I. S. (2000) *Proc. Natl. Acad. Sci. USA* **97**, 12182–12186. (First Published October 10, 2000; 10.1073/pnas.220392197)
14. International Human Genome Sequencing Consortium (2001) *Nature (London)* **409**, 860–921.
15. Alizadeh, A. A., Eisen, M. B., Davis, R. E., Ma, C., Lossos, I. S., Rosenwald, A., Boldrick, J. C., Sabet, H., Tran, T., Yu, X., *et al.* (2000) *Nature (London)* **403**, 503–511.
16. Bittner, B., Meltzer, P., Chen, Y., Jiang, Y., Seftor, E., Hendrix, M., Radmacher, M., Simon, R., Yakhini, Z., Ben-Dor, A., *et al.* (2000) *Nature (London)* **406**, 536–540.

[CANCER RESEARCH 48, 4827–4833, September 1, 1988]

Evaluation of a Soluble Tetrazolium/Formazan Assay for Cell Growth and Drug Sensitivity in Culture Using Human and Other Tumor Cell Lines[1]

Dominic A. Scudiero,[2] Robert H. Shoemaker, Kenneth D. Paull, Anne Monks, Siobhan Tierney, Thomas H. Nofziger, Michael J. Currens, Donna Seniff, and Michael R. Boyd

Program Resources, Inc., National Cancer Institute-Frederick Cancer Research Facility, Frederick, Maryland 21701 [D. A. S., A. M., S. T., M. C., T. N., D. S.], and Developmental Therapeutics Program, Division of Cancer Treatment, National Cancer Institute, Bethesda, Maryland 20892 [R. S., K. P., M. B.]

ABSTRACT

We have previously described the application of an automated microculture tetrazolium assay (MTA) involving dimethyl sulfoxide solubilization of cellular-generated 3-(4,5-dimethylthiazol-2-yl)-2,5-diphenyltetrazolium bromide (MTT)-formazan to the *in vitro* assessment of drug effects on cell growth (M. C. Alley *et al.*, Proc. Am. Assoc. Cancer Res., *27*:389, 1986; M. C. Alley *et al.*, Cancer Res. *48*: 589–601, 1988). There are several inherent disadvantages of this assay, including the safety hazard of personnel exposure to large quantities of dimethyl sulfoxide, the deleterious effects of this solvent on laboratory equipment, and the inefficient metabolism of MTT by some human cell lines. Recognition of these limitations prompted development of possible alternative MTAs utilizing a different tetrazolium reagent, 2,3-bis(2-methoxy-4-nitro-5-sulfophenyl)-5-[(phenylamino)carbonyl]-2*H*-tetrazolium hydroxide (XTT), which is metabolically reduced in viable cells to a water-soluble formazan product. This reagent allows direct absorbance readings, therefore eliminating a solubilization step and shortening the microculture growth assay procedure. Most human tumor cell lines examined metabolized XTT less efficiently than MTT; however, the addition of phenazine methosulfate (PMS) markedly enhanced cellular reduction of XTT. In the presence of PMS, the XTT reagent yielded usable absorbance values for growth and drug sensitivity evaluations with a variety of cell lines. Depending on the metabolic reductive capacity of a given cell line, the optimal conditions for a 4-h XTT incubation assay were 50 μg of XTT and 0.15 to 0.4 μg of PMS per well. Drug profiles obtained with representative human tumor cell lines for several standard compounds utilizing the XTT-PMS methodology were similar to the profiles obtained with MTT. Addition of PMS appeared to have little effect on the metabolism of MTT. The new XTT reagent thus provides for a simplified, *in vitro* cell growth assay with possible applicability to a variety of problems in cellular pharmacology and biology. However, the MTA using the XTT reagent still shares many of the limitations and potential pitfalls of MTT or other tetrazolium-based assays.

INTRODUCTION

The metabolic reduction of soluble tetrazolium salts to insoluble colored formazans has been exploited for many years for histochemical localization of enzyme activities (1, 2). In one of the earliest efforts to develop a practical *in vitro* drug sensitivity test, Black and Speer (3) utilized a tetrazolium/formazan method to assess inhibition of dehydrogenase activity by cancer chemotherapeutic drugs in slices of excised tissue. As an *in situ* vital staining process this phenomenon has also been used for identifying viable colonies of mammalian cells in soft agar culture (4) and for facilitating *in vitro* drug sensitivity assays with human tumor cell populations in primary culture (5). Mosmann (6) described a tetrazolium-based assay which allowed rapid measurement of growth of lymphoid cell populations and their response to lymphokines. Recent reports from our laboratories (7, 8) and others (9, 10) have described modifications of Mosmann's procedure for *in vitro* assay of tumor cell response to chemotherapeutic agents. We have found that this MTA[3] approach allows reproducible estimates of drug sensitivity in a variety of human and other tumor cell lines. Moreover, because of its microscale and potential for automation, the MTA is one of several assays under consideration by the National Cancer Institute for potential application to a large-scale antitumor drug-screening program (7, 8).

The previously described MTA (7, 8) requires DMSO solubilization of MTT-formazan generated by cellular reduction of the MTT tetrazolium reagent. This step is not only laborious, but also may risk exposure of laboratory personnel to large quantities of potentially hazardous solutions in DMSO. Frequent DMSO exposure also produces deleterious effects upon some laboratory equipment. Therefore, to allow the investigation of a simplified MTA and to address potential problems associated with solvent handling, a series of new tetrazolium salts have been developed which, upon metabolic reduction by viable cells, yield aqueous-soluble formazans (11). In this paper we describe the development of one such tetrazolium salt (XTT) and its application to the MTA.

MATERIALS AND METHODS

Cell Lines and Culture. Cell lines (Table 1) were maintained as stocks in RPMI 1640 (Quality Biological, Gaithersburg, MD) supplemented with 10% fetal bovine serum (Sterile Systems, Logan, UT) and 2 mM L-glutamine (Central Medium Laboratory, NCI-FCRF). Cell cultures were passaged once or twice weekly using trypsin-EDTA (Central Medium Laboratory, NCI-FCRF) to detach the cells from their culture flasks.

Drugs. All experimental agents were obtained from the Drug Synthesis and Chemistry Branch, Developmental Therapeutics Program, DCT, NCI. Crystalline stock materials were stored at −70°C and solubilized in 100% DMSO. Compounds were diluted into complete medium (RPMI 1640 plus fetal bovine serum) plus 0.5% DMSO before addition to cell cultures.

MTT-Microculture Tetrazolium Assay. Cellular growth in the presence or absence of experimental agents was determined using the previously described MTT-microculture tetrazolium assay (7, 8). Briefly, rapidly growing cells were harvested, counted, and inoculated at the appropriate concentrations (100-μl volume) into 96-well microtiter plates using a multichannel pipet. After 24 h, drugs were applied (100-μl volume) to triplicate culture wells, and cultures were incubated for 6 days at 37°C. MTT (Sigma, St. Louis, MO) was prepared at 5 mg/ml in PBS (Dulbecco and Vogt formulation, without calcium and magnesium; Quality Biological, Gaithersburg, MD) and stored at 4°C. On Day 7, MTT was diluted 1 to 5 in medium without serum (in the MTA described in Refs. 7 and 8, MTT was diluted in complete medium containing 10% fetal bovine serum), and 50 μl were added to microculture wells. After 4-h incubation at 37°C, 250 μl were removed from

Received 7/10/87; revised 1/6/88; accepted 5/17/88.

The costs of publication of this article were defrayed in part by the payment of page charges. This article must therefore be hereby marked *advertisement* in accordance with 18 U.S.C. Section 1734 solely to indicate this fact.

[1] Supported by NCI Contract N01-CO-23910 with Program Resources, Inc.

[2] To whom requests for reprints should be addressed, at Building 539, National Cancer Institute-Frederick Cancer Research Facility, Frederick, MD 21701.

[3] The abbreviations used are: MTA, microculture tetrazolium assay; DMSO, dimethyl sulfoxide; MEN, menadione; MTT, 3-(4,5-dimethylthiazol-2-yl)-2,5-diphenyltetrazolium bromide; PBS, phosphate-buffered saline; PMS, phenazine methosulfate; XTT, 2,3-bis(2-methoxy-4-nitro-5-sulfophenyl)-5-[(phenylamino)carbonyl]-2*H*-tetrazolium hydroxide, inner salt, sodium salt; IC_{50}, 50% inhibitory concentration; NCI, National Cancer Institute; FCRF, Frederick Cancer Research Facility; DCT, Division of Cancer Treatment.

REF. 5

Table 1 *Cell strains used in this study*

Cell line	Origin	Source	MTT/XTT absorbance[a] with the following PMS concentrations[b]				
			MTT, 0.0 mM	XTT 0.0 mM	XTT 0.001 mM	XTT 0.01 mM	XTT 0.0250 mM
H23	Lung adenocarcinoma	a[c]	1.176	0.105	0.115	0.492	1.224
H322	Lung bronchioloalveolar carcinoma	a[c]	0.738	0.242	0.256	0.561	1.337
H324	Lung adenocarcinoma	a[c]	0.492	0.031	0.052	0.710	1.110
H358	Lung bronchioloalveolar carcinoma	a[c]	0.545	0.077	0.081	0.266	0.637
H460	Lung large cell carcinoma	a[c]	2.580	0.288	0.342	1.688	2.830
A549	Lung adenocarcinoma	b[d]	2.700	0.233	0.356	2.360	2.804
LOX	Malignant melanoma	c[e]	1.030	0.201	0.266	1.489	2.279
HT-29	Colon adenocarcinoma	b[d]	1.914	0.201	0.196	1.014	1.555
MCF-7	Breast adenocarcinoma	d[f]	1.110	0.086	0.093	0.374	0.828
CCD-19 LU	Lung fibroblast	b[d]	0.356	0.109	0.120	0.369	1.090
MCR-5	Lung fibroblast	b[d]	0.326	0.186	0.211	0.300	0.695
W138	Lung fibroblast	b[d]	0.257	0.045	0.092	0.317	0.747
P388	Murine leukemia	e[g]	0.674	0.101	0.174	0.426	1.262
	Background (n = 13)		0.023 ± 0.006[h]	0.175 ± 0.031	0.186 ± 0.057	0.204 ± 0.034	0.250 ± 0.015

[a] Data represent average absorbance minus background from triplicate wells. Cells were inoculated at 1250 cells/well. Culture duration was for 7 days, and MTT or XTT incubation for 4 h at 37°C.
[b] PMS concentration: 0.001 mM = 0.015 μg/well; 0.01 mM = 0.15 μg/well; 0.025 mM = 0.38 μg/well.
[c] Supplied by Dr. A. Gazdar, Navy Medical Oncology Branch, Division of Cancer Treatment, NCI, Bethesda, MD.
[d] Obtained from the American Type Culture Collection, Rockville, MD.
[e] Supplied by Dr. O. Fodstad, Norwegian Radium Hospital, Oslo, Norway.
[f] Supplied by Dr. K. Cowan, Clinical Pharmacology Branch, Division of Cancer Treatment, NCI, Bethesda, MD.
[g] Supplied by the NCI, DCT Tumor Repository, NCI-FCRF, Frederick, MD.
[h] Mean ± SD of 39 triplicate well background measurements.

each well, and 150 μl of 100% DMSO were added to solubilize the MTT-formazan product. After thorough mixing with a mechanical plate mixer, absorbance at 540 nm was measured with a Dynatech Model MR 600 microplate reader.

XTT-Microculture Tetrazolium Assay. The new tetrazolium reagent (XTT) was designed to yield a suitably colored, aqueous-soluble, nontoxic formazan upon metabolic reduction by viable cells. The chemical structures of MTT, XTT, and their respective formazan reduction products are shown in Fig. 1. The presence of two sulfonic acid groups in XTT is the key to its aqueous solubility in both the tetrazolium ion form and the formazan form. XTT has a single net negative charge at physiological pH, and bioreduction of the central positively charged tetrazolium nucleus increases the net charge to two. The corresponding reduction of MTT reduces the net positive charge to zero, and thus the MTT formazan is quite insoluble. For the present investigations, XTT was obtained by a synthetic procedure described elsewhere (11). The XTT reagent is now available from at least one commercial supplier (Polysciences, Warrington, PA).

The XTT-assay methodology was essentially the same as that described using the MTT reagent with the following modifications: XTT was prepared at 1 mg/ml in prewarmed (37°C) medium without serum. PMS (Sigma, St. Louis, MO; Catalogue No. P9625) was prepared at 5 mM (1.53 mg/ml) in PBS. The 5 mM PMS solution was stable at 4°C for at least 3 mo. MEN (Sigma; Catalogue No. M5625) was prepared at 10 mM (1.72 mg/ml) in acetone. MEN was prepared fresh immediately before use. Fresh XTT and PMS were mixed together at the appropriate concentrations. For a 0.025 mM PMS-XTT solution, 25 μl of the stock 5 mM PMS were added per 5 ml of XTT (1 mg/ml). Fifty μl of this mixture (final concentration, 50 μg of XTT and 0.38 μg of PMS per well) were added to each well on Day 7 after cell inoculation. For experiments designed to examine various PMS concentrations, 5 mM PMS was diluted in PBS before addition to the 1-mg/ml solution of XTT. After an appropriate incubation at 37°C (4 h unless otherwise indicated), the plates were mixed on a mechanical plate shaker, and absorbance at 450 nm was measured with the Dynatech Model MR 600. Absorption spectra of tetrazolium reagents, formazan products, and cellular-generated formazans were measured with a Beckman Model MVI scanning spectrophotometer.

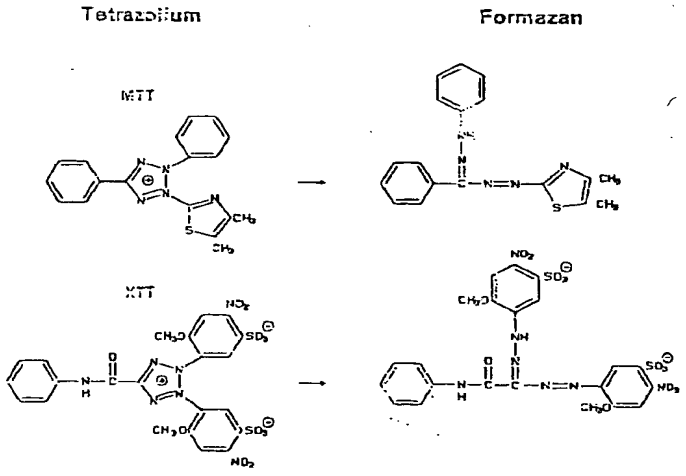

Fig. 1. Structures of MTT and XTT tetrazolium and formazan.

RESULTS

Metabolic Reduction of XTT by Human Cells. To determine the suitability of the new XTT reagent for a microculture growth inhibition methodology, we investigated the ability of several human tumor cell lines to reduce XTT to a measurable aqueous-soluble formazan product. Table 2 shows typical MTT and XTT metabolism data for different cell inoculation densities. Two human lung tumor cell lines were incubated for different times with MTT (only 4-h data shown) or XTT, and the absorbances were measured. Cell line A549 reduced MTT far more efficiently than H322, illustrating two extremes of cellular metabolic ability. Neither cell line was able to efficiently reduce XTT during the 4-h incubation time, thus making obligatory longer incubation times for the generation of a substantial absorbance. These data also indicated that the formazan product resulting from the cellular reduction of XTT was not toxic to human tumor cells over the 96-h period of this experiment. The absorbance continued to increase, and microscopic examination of cultures confirmed that cells remained viable in the presence of the XTT-formazan. Table 1 compares absorbance measurements with MTT and XTT for several cell lines. In all cases the metabolic reduction of the tetrazolium was substantially less for XTT than for MTT (Table 1). Table 1 also

Table 2 *Metabolism of MTT or XTT*

Cell line	Cell density[a]	MTT/XTT absorbance[b] at the following metabolism time[c]					
		MTT, 4 h	XTT				
			4 h	8 h	24 h	48 h	96 h
A549	10	0.15	0.02	0.02	0.07	0.22	0.35
	20	0.28	0.03	0.08	0.18	0.40	0.52
	39	0.55	0.07	0.07	0.32	0.59	0.65
	78	0.95	0.14	0.14	0.44	0.85	0.97
	156	1.39	0.15	0.12	0.53	0.82	1.20
	312	1.61	0.20	0.14	0.55	0.85	1.21
	625	1.68	0.16	0.14	0.54	0.83	1.46
	1,250	1.62	0.17	0.18	0.52	0.82	1.43
	2,500	1.71	0.16	0.19	0.50	0.80	1.92
	5,000	1.62	0.18	0.27	0.52	0.82	1.85
	10,000	1.75	0.18	0.32	0.54	0.86	1.97
H322	10	0.00	0.00	0.00	0.02	0.01	0.03
	20	0.00	0.01	0.00	0.02	0.02	0.04
	39	0.00	0.01	0.01	0.02	0.04	0.06
	78	0.01	0.02	0.02	0.05	0.09	0.13
	156	0.02	0.03	0.04	0.11	0.18	0.30
	312	0.04	0.06	0.09	0.21	0.35	0.45
	625	0.25	0.09	0.15	0.34	0.41	0.63
	1,250	0.48	0.15	0.22	0.48	0.53	0.74
	2,500	0.65	0.17	0.27	0.55	0.63	0.89
	5,000	0.78	0.17	0.26	0.52	0.68	0.93
	10,000	0.86	0.15	0.23	0.48	0.65	0.91

[a] The inoculation cell density: cells inoculated/well.
[b] Data represent average absorbances minus background from triplicate wells. Culture duration was for 7 days.
[c] Plates were incubated at 37°C in 5% CO_2 for the indicated time.

illustrates the marked enhancement of the metabolic reduction of XTT in the presence of the electron-coupling agent, phenazine methosulfate (1). The addition of 0.01 or 0.025 mM PMS (0.15 or 0.38 μg/well) resulted in a marked increase in measured absorbance, and absorbance measurements generally were equal to or greater than those obtained for MTT. One complication of the addition of PMS was an increase of background absorbance (no cells in the well) with increasing concentrations of added PMS (Table 1). With the conventional MTA the liquid medium is aspirated from the assay well prior to solubilization of the formazan product. This step results in lower background absorbance with MTT in comparison to XTT, since with the soluble XTT derivative, the aspiration step is deleted. Background absorbances at PMS concentrations equal or less than 0.38 μg/well are nevertheless acceptable, since control absorbances are at least 3.5-fold greater than background at the optimal PMS concentration.

On occasion, we have observed crystal formation in microculture wells containing PMS and XTT, sometimes resulting in diminished absorbance measurements for some cell lines. The presence of such crystals in a given microplate renders the data difficult to interpret and compromises the reproducibility and validity of an experiment. In addition to high-pressure liquid chromatography and mass spectroscopy analysis of crystals, we initiated studies to examine the potential role of several experimental variables in crystal formation: pH; temperature; cell density; and incubation time. Presently we conclude that PMS is necessary for crystal formation, and that an alkaline pH (which can occur if plates are removed from their CO_2 environment for too long a time) exacerbates the problem. We do not yet have an experimental solution to this occasional interference by crystal formation; thus, until this problem is resolved, careful microscopic examination of individual microculture wells is necessary to ensure the absence of crystal formation in a given experiment. All data presented in this paper result from experiments in which crystal formation was not observed. In addition, we are examining the utility of other electron-coupling agents as a substitute for PMS in an XTT-MTA. In initial experiments, one such agent, menadione (1), has proved promising, resulting in both a manageable background and large enough absorbance values for several cell lines tested (Table 3). After careful microscopic observation, we have yet to observe crystal formation in experiments utilizing XTT in combination with menadione; however, since our total experience with menadione is thus far more limited than with PMS, we cannot yet conclude that crystal formation is totally eliminated with this alternative electron-coupling reagent.

To evaluate the relationship between measured absorbance and viable cell number at the time of tetrazolium addition, cells were plated, allowed to attach for 1 h, and incubated with MTT or XTT plus PMS for 4 h (Fig. 2). At optimal PMS plus XTT conditions (as with MTT), absorbances peak and plateau at different inoculation densities depending on the cell line being studied. From such data (Fig. 2) a range of cell densities which give rise to a detectable and relatively linear range of absorbance values can be determined for each cell line at a given assay duration. An extensive discussion of the effects of inoculation density and culture duration is given in Ref. 8.

XTT-metabolism data for the murine leukemia cell line, P388, are also given in Table 1. The conventional MTA requires the use of a centrifugation step prior to medium aspiration for P388 and other suspension cell lines. Use of the XTT reagent eliminates the need for centrifugation of suspension cell lines. XTT has proved useful for other suspension cultures, including human leukemia cell lines (data not shown).

The absorbance values obtained with two human cell lines as a function of PMS concentration are given in Fig. 3. From data such as these, we have determined that all of the cell lines examined thus far yield adequately quantifiable absorbance measurements when incubated with XTT plus 0.01 to 0.025 mM PMS. Some of the cell lines which metabolized MTT less efficiently also required a larger PMS concentration to yield adequate absorbance values. The addition of PMS had little qualitative or quantitative effect on the MTT response of the cell lines tested (Fig. 3).

Spectral Characteristics of XTT Tetrazolium/Formazan. Spectral analysis of the MTT and XTT/formazan products derived from A549 cells in culture is shown in Fig. 4. Although the absorbance spectrum of XTT is rather different than for MTT, the addition of PMS resulted in little qualitative difference in either spectrum. The absorbance maxima for cellular-generated, DMSO-solubilized MTT-formazan and aqueous-soluble XTT/formazan are 560 and 475 nm, respectively. XTT/formazan can be easily discriminated from the background or from the unreacted XTT tetrazolium reagent.

Application of XTT to Drug Sensitivity Assays. To determine the suitability of the XTT assay for large-scale drug screening, we utilized XTT microculture methodology to generate drug sensitivity profiles for some representative standard compounds and experimental agents. Figs. 5 and 6 show drug profiles generated for Adriamycin-treated H324 cells using both the MTT and XTT reagents. The profiles were very similar for both reagents supplemented with 0.005 to 0.01 mM PMS. Lower PMS concentrations resulted in very low XTT absorbance measurements precluding accurate drug treatment analysis. The drug profiles using MTT were virtually identical for all PMS concentrations studied. Treatment of human tumor cell lines with several other experimental compounds resulted in comparable IC_{50} values (drug concentrations resulting in a 50% inhibition of growth) for either the MTT or XTT methodology (Table 4). Analysis of the data in Table 4 using the Spearman

Table 3 *Comparison of menadione and phenazine methosulfate in the XTT-MTA*

	MTT/XTT absorbance at the following PMS/MEN concentration[b]						
		XTT					
Cell line	MTT, 0	0.01 mM PMS	0.025 mM PMS	0.01 mM MEN	0.05 mM MEN	0.10 mM MEN	0.20 mM MEN
A549	1.947	1.433	2.110	1.065	1.107	3.057	2.973
LOX	1.026	0.403	1.514	1.059	0.789	0.740	1.573
H322	0.535	0.409	0.802	0.651	0.937	1.151	1.312
H460	2.124	1.721	2.427	0.987	1.241	2.763	3.210
MCF-7	1.443	0.553	0.737	0.459	1.434	1.299	1.551
HT-29	1.464	1.084	1.411	0.300	0.953	1.519	2.553
H23	1.042	0.423	1.241	0.217	0.472	1.121	1.324
Background ($n = 7$)	0.022 ± 0.006[c]	0.210 ± 0.010	0.191 ± 0.011	0.187 ± 0.014	0.120 ± 0.044	0.126 ± 0.038	0.109 ± 0.021

[a] Data represent average absorbance minus background from triplicate wells. Cells were inoculated at 1250 cells/well, culture duration was 7 days, and MTT or XTT metabolism was for 4 h at 37°C.

[b] PMS concentration: 0.01 mM = 0.15 μg/well; 0.025 mM = 0.38 μg/well. MEN concentration: 0.01 mM = 0.086 μg/well; 0.05 mM = 0.43 μg/well; 0.10 mM = 0.86 μg/well; 0.20 mM = 1.72 μg/well.

[c] Mean ± SD of 21 well background measurements.

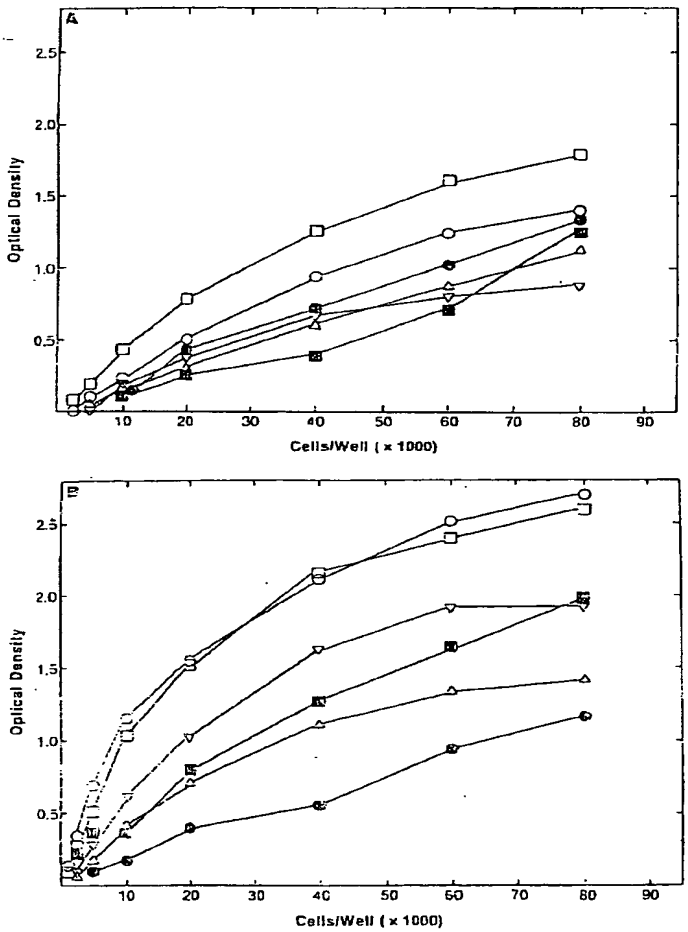

Fig. 2. Absorbance measurement as a function of viable cell density: MTT (*A*) and XTT (*B*). Viable cells were plated at the indicated cell density, allowed to attach for 1 h, and incubated with MTT or XTT plus 0.025 mM PMS (0.38 μg/well) for 4 h. A549 (○), H460 (□), MCF-7 (△), H322 (▽), LOX (●), HT-29 (■).

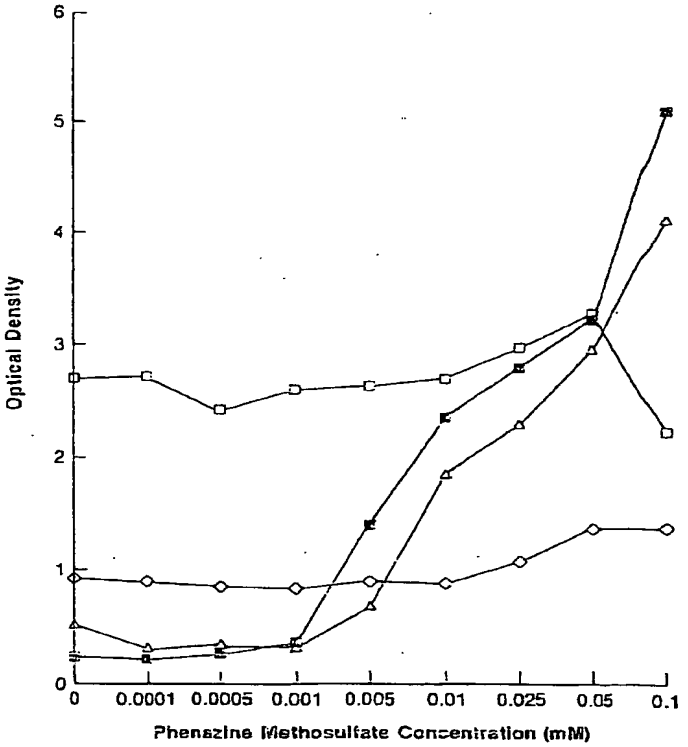

Fig. 3. Absorbance measurement as a function of PMS concentration. The PMS concentration indicated on the *abscissa* is the concentration of PMS in the XTT-PMS solution added to microculture wells. Culture duration, 7 days. A549 MTT (□), A549 XTT (■), LOX MTT (○), LOX XTT (△).

rank-order correlation method revealed a highly significant association between IC_{50}'s derived from MTT and XTT assays ($r = 0.76$, $P = 0.0001$).

DISCUSSION

In exploring the suitability of a new microculture methodology for large-scale drug screening in the NCI/DCT drug-screening program, we initially developed a useful assay based on the reduction of MTT tetrazolium salt to a formazan product which could be easily and quickly measured in a multiwell scanning spectrophotometer system (7, 8). In this paper, we describe the evaluation of a different tetrazolium reagent which is metabolically reduced by human cells to an aqueous-soluble formazan product. Several design criteria for the new tetrazolium reagent were considered: bioreducibility of the tetrazolium; usable spectrum of the formazan product; low cellular toxicity of both the tetrazolium and formazan; and the aqueous solubility of the tetrazolium and formazan. Certain critical assay modifications were required before the new XTT reagent would approach these requirements. The XTT reagent alone proved unsuitable

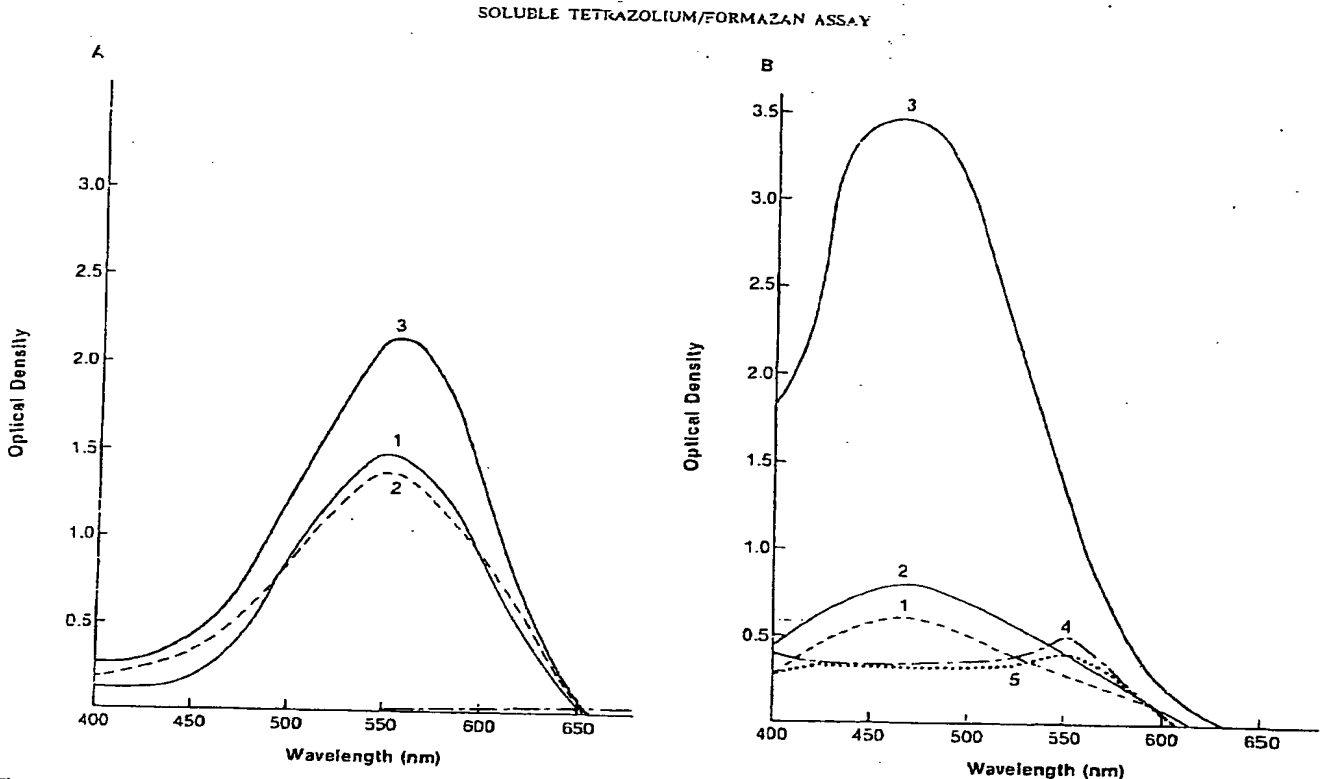

Fig. 4. Absorption spectra of MTT (*A*) and XTT (*B*) formazan products derived from cultured A549 cells (1000-cells/well inoculation, 7-day culture duration, 4-h incubation). Formazan products after incubation with the tetrazolium reagents plus: 0 mM (*1*) 0.001 mM (0.5 μg/well) (*2*), and 0.025 mM (0.38 μg/well) PMS (*3*). Nonreduced XTT tetrazolium (*4*). Background (absence of cells), tetrazolium plus 0.025 mM (0.38 μg/well) PMS (*5*).

for direct incorporation into the MTA; during a 4-h incubation, none of the human cell lines tested was able to sufficiently metabolize XTT to yield a formazan absorbance significantly greater than background. However, supplementation of the XTT incubation mixtures with the electron-coupling agent PMS resulted in adequate absorbance levels. Depending upon the metabolic capacity of a given cell line, the optimal conditions for a 4-h XTT incubation assay are 50 μg of XTT and 0.15 to 0.4 μg of PMS per well.

Fig. 2 illustrates that cellular reduction of XTT resulted in a formazan product which was not itself toxic to the cells under the assay conditions used. Cells retained the capacity to metabolize XTT for at least 96 h without evidence of toxicity. However, since metabolism times of 6 hr or less are required for our high-flux assay applications, and since the addition of XTT terminates the assay, the viability of cells after 24 h or more XTT metabolism times is not immediately relevant to the present usage. The longer incubation times resulted in both elevated absorbance measurements and increased background absorbances. XTT metabolism times of 2 to 6 h proved a suitable compromise between background and cell-generated absorbance.

The new XTT reagent used with PMS allowed application of the MTA to additional cell lines with various growth characteristics previously difficult to accommodate with the MTT-based MTA. For example, the XTT reagent greatly enhanced the usefulness of the MTA for the evaluation of cell growth and inhibition of human fibroblast cell lines (Table 2). Fibroblast cell lines are generally inefficient at metabolism of the MTT tetrazolium reagent; however, usable absorbances were obtained with XTT plus PMS. Also, the use of XTT eliminates a centrifugation step from the MTA methodology for nonadherent cell cultures. The XTT-MTA has proved usable for several suspension cell lines, including P388 and human leukemia cell lines. The XTT reagent may have an advantage for other applications of the MTA for cell growth measurements (*e.g.*, for potential antiviral compounds) where the aspiration step required by the MTT-MTA would be undesirable for either technical or safety reasons. It is beyond the scope of this paper to consider other potential uses of the XTT methodology; *e.g.*, to multicell aggregates and spheroids, however, these potential applications would appear both feasible and straightforward.

The initial experiments designed to assess the utility of the XTT-MTA in drug sensitivity assays indicate that, with certain compromises, XTT can be substituted for MTT to give comparable sensitivity and accuracy. Drug profiles obtained utilizing XTT are similar to the MTT profiles for a variety of human tumor cell lines and several experimental compounds. More extensive XTT-MTA experiments utilizing a panel of 48 human tumor cell lines treated with a wide variety of experimental drugs are under way to further explore the applicability of the XTT reagent to large-scale drug screening.[4] Results of these experiments will be detailed separately.

Even though the XTT-MTA offers several advantages over other *in vitro* assay systems, several inherent shortcomings must be considered. XTT, along with other tetrazolium approaches, depends on cellular reductive capacity, including the activity of mitochondrial dehydrogenases. The assays depend on a correlation between tetrazolium enzymatic reduction (reflected by absorbance measurements) and some associated culture characteristic such as cell number (6, 8, 9) or cell protein (8, 12). This assumption requires that cellular reductive capacity is

[4] A. Monks *et al.*, unpublished results.

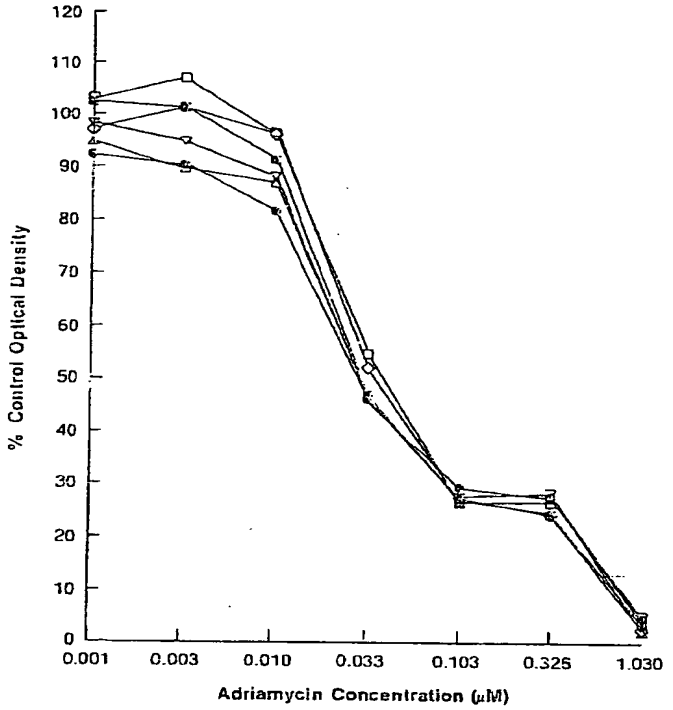

Fig. 5. Dose-response curves for Adriamycin-treated H324 cells (1000-cells/well inoculation, 7-day culture duration, 6-day Adriamycin treatment, 4-h incubation with MTT plus various PMS concentrations). *Points*, mean values from a single experiment calculated from triplicate wells subtracting background. Zero mM (□), 0.001 mM (■), 0.001 mM (○), 0.01 mM (△), 0.025 mM (●), and 0.10 mM PMS (▽). The PMS concentrations are the concentrations of PMS in the XTT-PMS solution added to microculture wells.

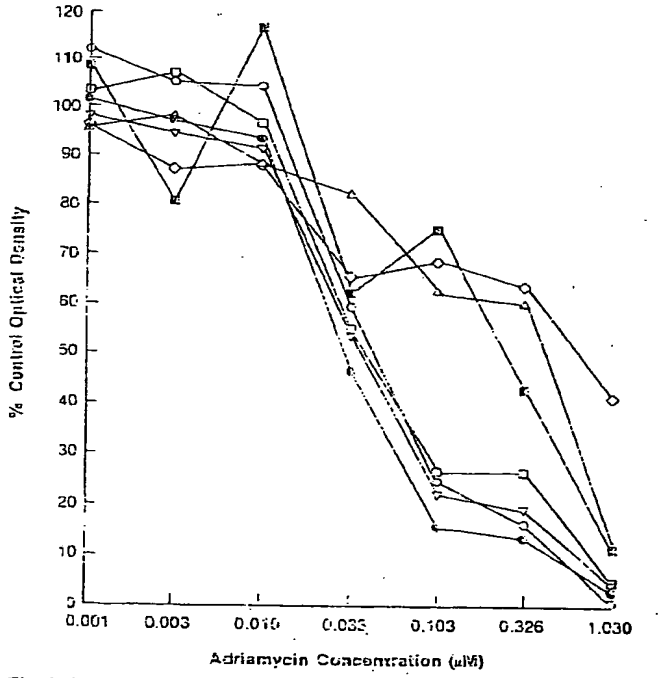

Fig. 6. Dose-response curves for Adriamycin-treated H324 cells (same experimental conditions as in Fig. 5). MTT, 0 mM PMS (□); XTT, 0 mM (■), 0.0001 mM (○), 0.001 mM (△), 0.01 mM (●), 0.025 mM (▽), 0.10 mM PMS (○).

Table 4 *Comparison of IC_{50}s for MTT and XTT*

Compound	Cell line	MTT	XTT
ADRI[b]	A549	1.92×10^{8}	2.28×10^{9}
	H125	2.94×10^{8}	6.39×10^{8}
	H322	5.10×10^{8}	4.84×10^{8}
	LOX	1.03×10^{8}	6.70×10^{9}
	HT-29	2.39×10^{8}	4.38×10^{8}
	MCF-7	1.97×10^{8}	1.77×10^{8}
$HgCl_2$	A549	2.15×10^{5}	2.16×10^{5}
	H125	1.35×10^{5}	1.93×10^{5}
	H322	1.54×10^{5}	1.52×10^{5}
	LOX	5.88×10^{7}	5.22×10^{7}
	HT-29	1.77×10^{5}	1.92×10^{5}
	MCF-7	1.81×10^{5}	1.94×10^{5}
BLEO	A549	5.98×10^{8}	8.74×10^{8}
	H125	2.61×10^{9}	1.30×10^{8}
	H322	1.01×10^{8}	1.80×10^{8}
	LOX	6.35×10^{9}	1.76×10^{9}
	HT-29	5.79×10^{8}	1.88×10^{7}
	MCF-7	5.56×10^{7}	9.31×10^{7}
MIT-C	A549	1.98×10^{9}	7.35×10^{8}
	H125	7.35×10^{8}	1.12×10^{7}
	H322	2.43×10^{8}	1.53×10^{8}
	LOX	3.75×10^{8}	1.53×10^{8}
	HT-29	4.17×10^{8}	8.19×10^{8}
	MCF-7	2.70×10^{8}	2.97×10^{8}
BCNU	A549	4.30×10^{5}	4.46×10^{5}
	H125	2.36×10^{5}	4.20×10^{5}
	H322	3.12×10^{5}	2.45×10^{5}
	LOX	1.30×10^{5}	4.76×10^{6}
	HT-29	4.27×10^{5}	7.94×10^{5}
	MCF-7	3.74×10^{5}	4.49×10^{5}
ACT-D	A549	2.73×10^{9}	2.78×10^{8}
	H125	2.63×10^{9}	3.03×10^{9}
	H322	2.42×10^{8}	1.60×10^{8}
	LOX	2.29×10^{8}	1.75×10^{9}
	HT-29	1.39×10^{8}	7.97×10^{9}
	MCF-7	1.43×10^{8}	1.36×10^{8}
5-FU	A549	1.45×10^{6}	2.02×10^{6}
	H125	5.36×10^{7}	2.73×10^{7}
	H322	6.24×10^{7}	1.67×10^{6}
	LOX	2.29×10^{6}	1.75×10^{6}
	HT-29	1.24×10^{6}	3.36×10^{7}
	MCF-7	7.69×10^{7}	7.15×10^{7}

[a] IC_{50} values calculated from seven concentration-dose responses. Cell inoculation densities: 1000 cells/well for all cell lines except H322 (2000 cells/well). MTA: 7-day culture duration, 6-day drug treatment, 4-h incubation with MTT or XTT plus 0.01 mM (0.15 μg/well) PMS.

[b] ADRI, Adriamycin; BLEO, bleomycin; MIT-C, mitomycin C; BCNU, 1,3-bis(2-chloroethyl)-1-nitrosourea; ACT-D, actinomycin D; 5-FU, 5-fluorouracil.

constitutive and remains relatively constant throughout the time duration of an experiment. However, any regulation of the cellular metabolic machinery resulting in different enzyme activity at any time will render this assumption invalid. Thus, changes of reductive capacity resulting from enzymatic regulation, pH, cellular ion concentration (*e.g.*, sodium, calcium, potassium), cell cycle variation, or other environmental factors may affect the final absorbance reading. For example, Mosman (6) has reported that mitogen-stimulated mouse spleen cells produce more MTT-formazan than do resting cells. Perturbations of these factors by experimental test compounds may further exacerbate this variability. In addition, the XTT-MTA has several unique shortcomings which must be considered before adaption of this assay for generalized drug testing. The present requirements for the addition of an electron-coupling agent increase the complexity of the cellular reduction environment (1, 13) potentially resulting in greater variability and a lack of reproducibility. PMS sometimes can cause nonspecific deposition of formazan (13), and Pearse (1) recommends that intermediate electron acceptors be avoided except to demonstrate activities which cannot otherwise be revealed. The occasional appearance of crystal formation, as yet not completely understood, is a potential interference requiring microscopic surveillance of each individual microwell. Whereas this problem may be less significant for other applications (*e.g.*, antiviral), it

may nevertheless preclude adaption of the XTT methodology to more complex drug-screening paradigms (*e.g.*, involving large cell line panels). Substitution of a different electron transport agent for PMS in the XTT-MTA may eliminate the crystal problem; however, additional work is required to better characterize the menadione-XTT system. In addition, the relatively elevated background levels characteristic of XTT plus PMS result in the inability to utilize this method for some cell lines that exhibit poor metabolic capacity and also decrease the reliability and reproducibility of drug sensitivity measurements at drug concentrations resulting in growth inhibition greater than 80% of control values. At these levels of growth inhibition, the relatively large background absorbances generated by XTT plus PMS (or manadione) in growth medium (Tables 1 and 3) can result in signal/noise ratios of less than one.

While safety and efficiency considerations argue for the possible advantage of the XTT over the MTT-based assay for applications to high-flux drug sensitivity screens, nevertheless, there remain serious problems with the XTT-based MTA, as well as tetrazolium assays in general. Such questions should continue to be of major concern and consideration for adaption of any particular assay protocol for general usage in anticancer, antiviral, or other drug-screening programs. However, the present investigation demonstrates the feasibility of a microculture methodology utilizing a water soluble tetrazolium/formazan reagent, suggesting the inherent advantages in the development of additional reagents which might not require the use of electron-coupling agents. In addition, our present cell line panels of human tumor cell lines (8) would provide a useful resource for studying the biological activity and suitability of such new materials.

ACKNOWLEDGMENTS

The authors express their appreciation to all additional staff members of the *In Vitro* Cell Line Screening Program for technical assistance in cell line characterizations and assay development. They also thank Dr. Philip Skehan, Dr. David Vistica, and Dr. James McMahon for helpful discussion and commentary on the manuscript and Marthena Finney-frock for help with manuscript preparation.

REFERENCES

1. Pearse, A. G. E. Principles of oxidoreductase histochemistry. *In:* Histochemistry, Theoretical and Applied. Ed. 3, Chap. 20. Edinburgh: Churchill Livingston, 1972.
2. Altman, F. P. Tetrazolium salts and formazans. Prog. Histochem. Cytochem., *9:* 1–56, 1977.
3. Black, M. M., and Speer, F. D. Effects of cancer chemotherapeutic agents on dehydrogenase activity of human cancer tissue *in vitro*. Am. J. Clin. Pathol., *23:* 218–227, 1953.
4. Schaeffer, W. I., and Friend, K. Efficient detection of soft-agar grown colonies using a tetrazolium salt. Cancer Lett., *1:* 275–279, 1976.
5. Alley, M. C., and Lieber, M. M. Improved optical detection of colony enlargement and drug cytotoxicity in primary soft agar cultures of human solid tumour cells. Br. J. Cancer, *49:* 225–233, 1984.
6. Mosmann, T. Rapid colorimetric assay for cellular growth and survival: application to proliferation and cytotoxicity assays. J. Immunol. Methods, *65:* 55–63, 1983.
7. Alley, M. C., Scudiero, D. A., Monks, A., Czerwinski, M., Shoemaker, R. H., and Boyd, M. R. Validation of an automated microculture tetrazolium assay (MTA) to assess growth and drug sensitivity of human tumor cell lines. Proc. Am. Assoc. Cancer Res., *27:* 389, 1986.
8. Alley, M. C., Scudiero, D. A., Monks, A., Hursey, M. L., Czerwinski, M. J., Fine, D. L., Abbott, B. J., Mayo, J. G., Shoemaker, R. H., and Boyd, M. R. Feasibility of drug screening with panels of human tumor cell lines using a microculture tetrazolium assay. Cancer Res., *48:* 589–601, 1988.
9. Carmichael, J., DeGraff, W. G., Gazdar, A. F., Minna, J. D., and Mitchell, J. B. Evaluation of a tetrazolium-based semiautomated colorimetric assay: assessment of chemosensitivity testing. Cancer Res., *47:* 936–942, 1987.
10. Cole, S. P. C. Rapid chemosensitivity testing of human lung tumor cell lines. Cancer Chemother. Pharmacol., *17:* 259–263, 1986.
11. Paull, K. D., Shoemaker, R. H., Boyd, M. R., Parsons, J. L., Risbood, P. A., Barbera, W. A., Sharma, M. N., Baker, D., Hand, E., Scudiero, D. A., Monks, A., and Grote, M. The synthesis of XTT: a new tetrazolium reagent bioreducible to a water-soluble formazan. J. Heterocyclic Chem., in press, 1988.
12. Finlay, G. J., Wilson, W. R., and Baguley, B. C. Comparison of *in vitro* activity of cytotoxic drugs towards human carcinoma and leukemia cell lines. Eur. J. Cancer Clin. Oncol., *22:* 655–662, 1986.
13. Kiernan, J. A. Oxidoreductases. *In:* Histological and Histochemical Methods, Theory, and Practice, Chap. 16. New York: Pergamon Press, 1981.

Molecular Microbiology (1996) 22(1), 87–95

Preferential processing of the S1 subunit of pertussis toxin that is bound to eukaryotic cells

Viviane Finck-Barbançon and Joseph T. Barbieri*
Department of Microbiology, Medical College of Wisconsin, 8701 Watertown Plank Road, Milwaukee, Wisconsin 53226, Wisconsin, USA.

Summary

Labelled [^{125}I]-pertussis toxin was prepared and used to measure the association of pertussis toxin (PT) to eukaryotic cells. PT was radioiodinated by the lactoperoxidase method which preferentially radioiodinated the S1 subunit. PT was radioiodinated at a high specific activity and possessed the same cytotoxicity as native PT as demonstrated by the ability to cluster Chinese hamster ovary (CHO) cells. Cell association of [^{125}I]-PT was not inhibited by excess non-radiolabelled PT, which indicated that the initial interaction between PT and CHO cells involved a large number of low-affinity receptors. At 37°C, the S1 within cell-associated PT was preferentially processed to an S1 with a lower apparent molecular weight (termed S1p). This processing was inhibited by the addition of unlabelled PT, indicating that the processing event was saturable and specific. S1 processing occurred in CHO, Madin–Darby canine kidney (MDCK) cells, and pig kidney (LLC-PK1) cells. A pulse-chase experiment showed that, at 37°C but not at 22°C, essentially all of the cell-associated S1 was processed within 3 h of a chase. Reagents that were previously shown to inhibit the ability of PT to ADP-ribosylate G_i proteins in intact CHO cells also inhibited the preferential processing of S1 within cell-associated PT, in the order of efficiency: 22°C > chloroquine > nocodazole > brefeldin A. This indicates that S1 processing requires an early endosomal function.

Introduction

Pertussis toxin (PT) is one of the major virulence factors of *Bordetella pertussis* (Weiss and Hewlett, 1986), the aetiologic agent of whooping cough. PT is a member of the family of bacterial ADP-ribosylating toxins (bARES) which possess A:B structure–function organization (Gill, 1978; Tamura *et al.*, 1982). The 'A' subunit, S1, expresses ADP-ribosyltransferase activity, while the 'B' subunit, B-oligomer (composed of five non-covalently-bound subunits organized in a molar ratio of 1:1:2:1 for S2:S3:S4:S5) binds to susceptible cells and delivers S1 to intracellular target proteins (Tamura *et al.*, 1983). The subset of heterotrimeric GTP-binding proteins that are ADP-ribosylated by PT include G_i, G_o, and G_t (Ui, 1990).

B. pertussis secretes PT as a proenzyme which is cytotoxic when assayed in animals or cultured cells, but requires activation for expression of ADP-ribosyltransferase activity *in vitro* (Tamura *et al.*, 1982). *In vitro* activation of ADP-ribosyltransferase activity requires both the reduction of the disulphide bond (C41 and C201) within S1 and ATP (for reviews, see Kaslow and Burns, 1992; Krueger and Barbieri, 1993). ATP stimulates a conformational change within S1 of the holotoxin which reduces the affinity of S1 for B-oligomer without concomitant dissociation of S1. The conformation of S1 within ATP-activated holotoxin appears to be identical to free S1 (Krueger and Barbieri, 1993).

In addition to the plasma membrane, functional heterotrimeric G_i proteins exist in several intracellular compartments of the eukaryotic cell. Stow *et al.* (1991) identified PT-sensitive G_{i2} within the plasma membrane and G_{i3} within the Golgi of LLC-PK1 cells. Although the mechanism utilized by PT to ADP-ribosylate intracellular G_i proteins remains unclear, recent studies (Xu and Barbieri, 1995; 1996) showed that in intact CHO cells, both G_{i2} and G_{i3} were ADP-ribosylated by PT, and agents that blocked intracellular trafficking also inhibited ADP-ribosylation. These data implicated an endosomal pathway that included a Golgi function for the ADP-ribosylation of G_i proteins by PT (Xu and Barbieri, 1995; 1996). The inability to produce radiolabelled PT which retained cytotoxicity has impaired the ability to directly characterize the delivery of PT to its intracellular targets. In this study, we describe the preparation of radioiodinated PT at high specific activity and report the preferential processing of the S1 subunit of cell-associated PT.

Results

Radioiodination of PT

PT was radioiodinated by lactoperoxidase to a specific activity of 1.2–1.5 mol of ^{125}I per mole of PT (approx. 5–8 × 10^7 counts per minute (c.p.m.) μg^{-1} of PT). ^{125}I was

Received 4 April, 1996; revised 18 July, 1996; accepted 26 July, 1996. *For correspondence. E-mail toxin@post.its.mcw.edu; Tel. (414) 4568412; Fax (414) 2668522.

preferentially incorporated into the S1 subunit, with ≈0.7–0.8 mol of ^{125}I per mole of S1. The amount of radioiodine incorporated into each subunit expressed as a percentage of the total (determined from seven independent labelling experiments) was: S1, 54; S2, 10; S3, 10; S4, 13; S5, 13. [^{125}I]-PT possessed a potency for the clustering of CHO cells identical to that of native PT (data not shown), which indicated that radioiodination did not interfere with biological activity. [^{125}I]-PT was stable for >10 d during storage at 4°C as determined by SDS–PAGE.

Binding of [^{125}I]-PT to CHO cells

Upon incubation at three temperatures, the amount of [^{125}I]-PT bound to CHO cells increased with time (Fig. 1). The absolute amount of [^{125}I]-PT bound was greater at 4°C and 37°C than at 22°C. Addition of non-radiolabelled PT at a 1000-fold excess with respect to [^{125}I]-PT did not reduce the amount of cell-associated [^{125}I]-PT (Table 1). At 4°C, the amount of PT bound to CHO cells showed a dose response with respect to the amount of added [^{125}I]-PT, with the amount of bound PT representing approx. 0.03% of [^{125}I]-PT added (Fig. 1, insert). Together, these data suggest that the cellular receptor for PT is present at high numbers, but possesses low affinity for the toxin.

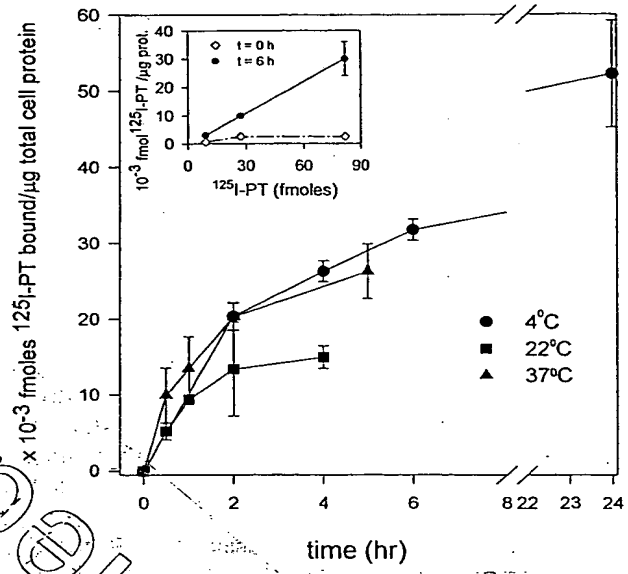

Fig. 1. Binding of [^{125}I]-PT to CHO cells at 4°C, 22°C, and 37°C. CHO cell monolayers, in 24-well plates, were incubated with [^{125}I]-PT (0.05 pmoles) for various time periods at 4°C, room temperature (22°C), and 37°C. Cells were rinsed four times with cold D-PBS and lysed in 300 µl of 0.1 N NaOH. Cell-associated [^{125}I]-PT was expressed as x 10^{-3} fmoles of [^{125}I]-PT bound per microgram of total cell protein. A representative experiment performed in duplicate is shown. The insert shows the binding of [^{125}I]-PT to CHO cells as a function of [^{125}I]-PT. [^{125}I]-PT (between 0.01 and 0.08 pmoles) was added to CHO cells at 4°C and, at 0 h or 6 h, the amount of cell-associated PT was determined.

Table 1. Association of [^{125}I]-PT to CHO cells.[a]

Inhibitor	4°C[b]	22°C[c]	37°C[d]
No inhibitor	71.5 ± 1	10.3 ± 1	30.0 ± 0.7
Unlabelled PT (0.5 µM)	72.7 ± 9	22.0 ± 2.7	43.1 ± 3.9

a. Confluent lawns of CHO cells were assayed for the cell association of [^{125}I]-PT as described in the *Experimental procedures*, using 0.1 pmoles of [^{125}I]-PT. Experiments were performed twice, in duplicate, and are expressed as x10^{-3} fmoles of bound [^{125}I]-PT per µg of total cell protein.
b. Experiment performed at 4°C for 18 h.
c. Experiment performed at 22°C for 2 h.
d. Experiment performed at 37°C for 2 h.

Physical state of cell-associated [^{125}I]-PT

The physical state of CHO cell-associated [^{125}I]-PT was determined following incubations at 4°C, 22°C, or 37°C (Fig. 2). After 2 h at 37°C, SDS–PAGE analysis of CHO cell-associated [^{125}I]-PT showed the preferential processing of the S1 subunit of the holotoxin. Processed S1, termed S1p, migrated with the same relative mobility as the S2 subunit. Based upon the previously determined trypsin and chymotrypsin sites of S1 within holotoxin (Krueger *et al.*, 1991), and the migration of deletion peptides of S1 (Krueger and Barbieri, 1994), S1p migrated at an apparent molecular weight consistent with its cleavage between residues 205 and 214. In contrast, no preferential processing of cell-associated [^{125}I]-PT was detected upon incubation at 4°C or 22°C (Fig. 2). As observed with CHO cells, S1 was also preferentially processed within cell-associated PT in LLC-PK1 and MDCK cells (Fig. 3). With respect to CHO cells, the amount of cell-associated PT was three- to 1.8-fold greater per microgram of LLC-PK1 and MDCK cell protein, respectively. With all three cell lines, S1 processing to cell-associated [^{125}I]-PT was detected within approx. 30 min after the addition of [^{125}I]-PT and accumulated over the time-course (Fig. 3). The [^{125}I]-PT in the culture medium showed no detectable S1 processing (Fig. 3). These data indicate that the processing of S1 occurs after cell association and, as processing is not detected within cell-associated holotoxin during incubation at 4°C, processing does not occur on the cell surface. Cell-associated B oligomer (measured as cell-associated S3) did not show detectable processing over the time-courses (Fig. 3).

Kinetics of S1 processing within cell-associated [^{125}I]-PT

A pulse-chase experiment (Fig. 4) was performed to evaluate the kinetics of S1 processing within cell-associated

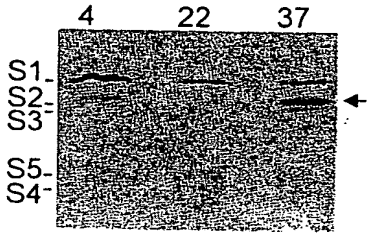

Fig. 2. Processing of [^{125}I]-PT by CHO cells. CHO cell monolayers, in 12-well plates were incubated with [^{125}I]-PT (0.2 pmoles) at 4°C for 18 h or at 22°C and 37°C for 2 h (incubation temperatures are indicated above the respective lane), washed, lysed, and analysed by SDS–PAGE under reducing conditions. The gel was dried and subjected to autoradiography. Migration of the subunits of PT are indicated to the left of the panel; the arrow indicates S1p.

holotoxin. CHO cells were incubated with [^{125}I]-PT for 30 min at 22°C and washed to remove unbound PT (pulse). Cells were then incubated (chase) at either 22°C or 37°C and assayed by SDS–PAGE to characterize the cell-associated holotoxin. During the 37°C chase, there was a steady decrease in the amount of cell-associated S1, with essentially all of the cell-associated S1 being chased to S1p. Within the first hour of the chase approx. 50% of the S1 was processed to S1p. The amount of cell-associated B-oligomer (represented by the S3 subunit) decreased, but without detectable degradation (Fig. 4). Analysis of the culture media during the chase period showed the accumulation of both TCA-soluble and TCA-insoluble material (data not shown). The TCA-soluble material may represent PT that has been internalized and subsequently degraded and exported. The TCA-insoluble material is unprocessed PT, determined by gel electrophoresis, which probably represents PT that was released from the cell surface prior to internalization. During the 22°C chase there was also a decrease in the amount of cell-associated S1, but little S1 was processed to S1p. Within the first hour of the chase < 5% of the S1 was processed to S1p (Fig. 4). The observation that, at 37°C, essentially all of the S1 was processed indicated that processing represented the fate of the majority of cell-associated PT. The lack of S1 processing at 22°C was consistent with the processing event representing the physiological pathway for PT, as previous studies had shown that at 22°C PT did not ADP-ribosylate G_i proteins in intact CHO cells (Xu and Barbieri, 1995).

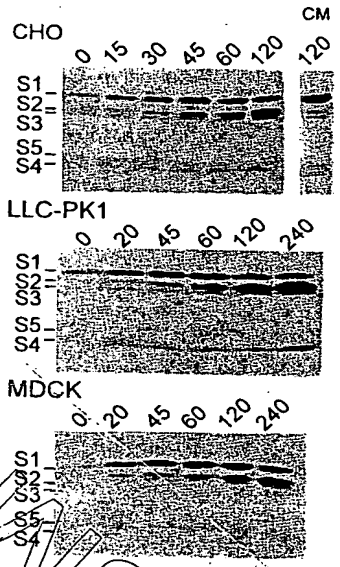

Fig. 3. Kinetics of PT processing in CHO, LLC-PK1 and MDCK cells. Cell monolayers, in 12-well plates, were incubated at 37°C with [^{125}I]-PT (0.1 pmoles) for the times (min) indicated. The culture media (CM) and cell-associated material from CHO (upper panel), LLC-PK (middle panel) and MDCK (lower panel) were subjected to SDS–PAGE followed by autoradiography. Migration of the subunits of PT are indicated to the left of the panel.

Pronase sensitivity of cell-associated [^{125}I]-PT

The conversion of a toxin from a protease-sensitive form to a protease-resistant form has been used to implicate toxin internalization within a cell (Dorland *et al.*, 1979). Initial experiments defined conditions that degraded cell-surface-bound [^{125}I]-PT. Cell-surface-bound [^{125}I]-PT was prepared by exposing CHO cells to [^{125}I]-PT at 4°C, followed by washing cells to remove unbound PT. Cell-surface-bound PT was exposed to pronase followed by analysis with SDS–PAGE. These experiments showed that low concentrations of pronase preferentially cleaved S1 of cell-surface-bound PT. Relative to its electrophoretic migration, this preferential cleavage of S1 was estimated to occur between residues 205–214 (Fig. 5). Greater amounts of pronase completely cleaved S1 through this nicked form and into lower-molecular-weight fragments (Fig. 5). Pronase concentrations above 4 mg ml^{-1} damaged the integrity of the CHO cells and were not used in this analysis. In contrast to the pronase sensitivity of PT bound to cells at 4°C, after an incubation at 37°C, a detectable amount of S1 was resistant to pronase. The percentage of pronase-resistant S1 within cell-associated PT increased with increasing incubation time at 37°C (Table 2). These data were consistent with the internalization of S1 during incubations at 37°C.

Inhibitors of intracellular trafficking influence the formation of S1p within cell-associated PT

Studies were performed to localize the processing of S1, by determining whether reagents that had been shown to inhibit PT from ADP-ribosylating G_i proteins in intact cells (Xu and Barbieri, 1995; 1996) also influenced the processing of S1 within cell-associated PT. The concentrations of

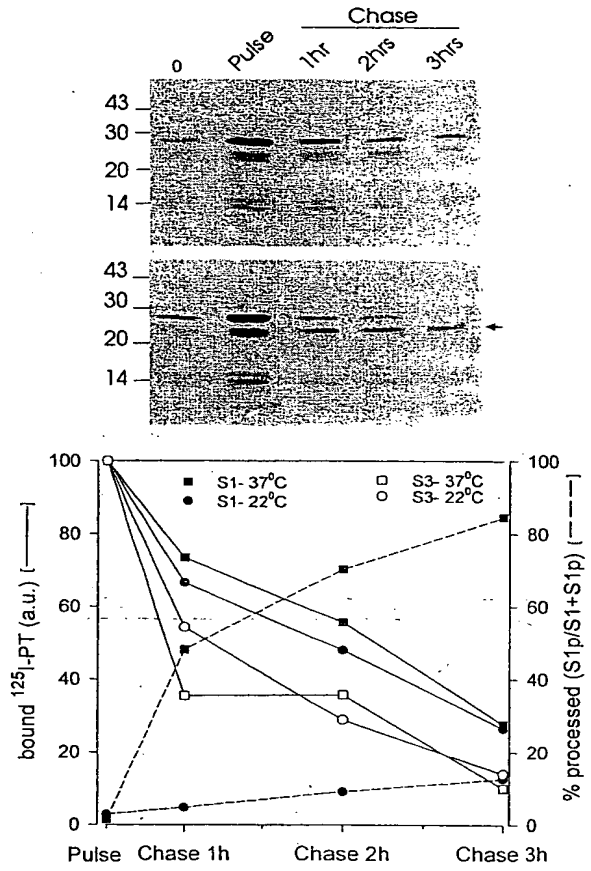

Fig. 4. A. Pulse chase of cell-associated [^{125}I]-PT. CHO cell monolayers, in 12-well plates, were incubated with [^{125}I]-PT (0.1 pmoles) at 22°C for 30 min, after which cells were washed to remove unbound toxin (Pulse). Cells were then incubated for an additional 1, 2, or 3 h (Chase) at either 22°C (upper panel) or 37°C (lower panel), after which cells were washed, and then resuspended in SDS–PAGE sample buffer. Cell-associated material was subjected to SDS–PAGE followed by autoradiography. Migration of molecular weight markers (kDa) are indicated to the left of the panel, the arrow on the right indicates S1p.
B. Quantification of S1 processing. The autoradiograph was quantified by densitometry to determine the total cell-associated material, the total number of units of cell-associated S1 (S1 + S1p), and S1p. S1p was calculated by subtracting the unit value of S3 from the unit value of S2, because S1p migrated with the same relative mobility as S2. This calculation was made after determining that on a molar basis, S2 and S3 are radiolabelled to the same extent (see the *Results*).

inhibitors used were previously shown to be optimal for inhibiting the *in vivo* ADP-ribosylation of G_i proteins by PT. Chloroquine reduced the amount of S1 processed by threefold, while nocodazole and brefeldin A produced progressively smaller effects on the amount of S1 processed, respectively (Table 3). This suggested that S1 processing required an early endosome function, and that later events in the intracellular trafficking pathway, such as late endosome or Golgi function, did not contribute to the processing event. In addition, an inhibitor of the cytosolic enzyme calpain (Croall and DeMartino, 1991) did not affect the processing of S1p, which was consistent with an endosomal function for S1 processing (data not shown). Also, addition of unlabelled PT did not inhibit the amount of PT that was cell associated, but did inhibit the processing event, indicating that S1 processing was saturable and specific. Figure 6 is a schematic diagram of the ADP-ribosylation of G_i proteins by PT, which includes a temporal assignment for the processing of S1 within holotoxin.

Discussion

Early models predicted that PT entered eukaryotic cells via the binding of the S2–S4 and S3–S4 dimers of the B oligomer to carbohydrate moieties of cell-surface proteins (Kaslow and Burns, 1992). In these models, subsequent to binding to the cell surface, the S1 subunit was translocated across the plasma membrane, released from the B-oligomer, reduced by cellular glutathione, and then ADP-ribosylated PT-sensitive G proteins. This model was supported by *in vitro* experiments which showed that in the presence of detergents, such as 3-((3-cholamidopropyl)dimethylammonio)-1-propane-sulphonate (CHAPS), ATP stimulated the release of S1 from the holotoxin (Burns and Manclark, 1986; Kaslow *et al.*, 1987), and S1 had greater affinity for lipid bilayers than B oligomer (Hausman and Burns, 1992). Other studies were also consistent with the delivery of PT to the cytosol by direct translocation across the plasma membrane (Montecucco *et al.*, 1986). Although the physical association of S1 with the holotoxin *in vivo* has not been resolved, recent studies suggest that PT requires a functional endocytic mechanism to ADP-ribosylate PT-sensitive G_i proteins in intact CHO cells (Xu and Barbieri, 1995, 1996). Consistent with the involvement of endocytic movement of PT within the cell, PT-sensitive G_i proteins of the G_{i3} subtype that are associated with the Golgi of LLC-PK1 cells were identified (Stow *et al.*, 1991).

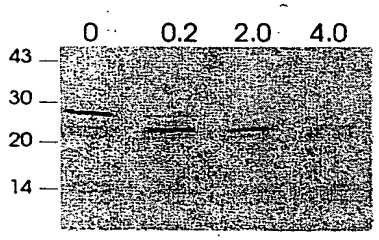

Fig. 5. Pronase digestion of surface-exposed (at 4°C, cell-associated) [^{125}I]-PT. CHO cell monolayers, in 12-well plates, were incubated with [^{125}I]-PT (0.1 pmoles) at 4°C. After 18 h, the monolayer was washed and incubated alone or with 0.2, 2.0, or 4.0 mg ml^{-1} of pronase for 1 h at 4°C. Newborn-calf serum (NCS, 50%, final concentration) and 20 mM EDTA were added and the cells were scraped, washed with D-PBS, and subjected to SDS–PAGE, followed by autoradiography. Molecular weight markers are indicated to the left of the panel (in kDa). Pronase concentrations are indicated above each lane.

Table 2. Sensitivity of S1 within cell-associated [^{125}I]-PT to extracellular pronase.[a]

Incubation temperature	Cell-associated S1 (Arbitrary Units) total	pronase resistant
4°C (overnight)	100	0
37°C (30 min)		
Experiment 1	100	23
Experiment 2	100	18
37°C (120 min)		
Experiment 1	100	54
Experiment 2	100	48

a. CHO cell monolayers, in 12-well plates, were incubated with [^{125}I]-PT (0.1 pmoles) either at 4°C overnight or at 37°C for 30 or 120 min. Cells were washed and 0.5 ml of 4 mg ml^{-1} of pronase in D-PBS was added for 1 h at 4°C, after which 0.5 ml of NCS with EDTA (20 mM, final concentration) was added to inhibit pronase. Cells were pelleted and washed in ice-cold D-PBS containing 20 mM EDTA, and suspended in sample buffer. Samples were subjected to SDS–PAGE followed by autoradiography. Autoradiographs were quantified with an optical imaging system (AMBIS).

To extend our understanding of the movement of PT within cells, we have produced radioiodinated PT which retains biological activity. Armstrong and Peppler (1987) reported a protocol to radioiodinate PT at high specific activity by the chloramine-T method, but with low recovery of radiolabelled PT. In the present study, lactoperoxidase was used to radiolabel PT at a high specific activity, and the radiolabelled PT could be purified by gel-filtration chromatography with good recovery. [^{125}I]-PT prepared by lactoperoxidase retained biological activity as assayed by the ability to cluster CHO cells. Analysis by SDS–PAGE showed that lactoperoxidase preferentially radiolabelled the S1 subunit of the holotoxin. This preferential radiolabelling of S1, along with radiolabelling in the presence of NAD and NeuNAcI(2-6)GalJ1-4Glc (6′SL), may be responsible for retention of the cytotoxic activity of [^{125}I]-PT.

The observation that the amount of [^{125}I]-PT bound to CHO cells was proportional to the amount of toxin added, together with the observation that the addition of unlabelled PT did not compete with [^{125}I]-PT for cell binding, indicated that the cell receptor for PT was present in high copy number and that this receptor possessed a low affinity for PT. Although the identity of the PT cell receptor in CHO cells has not been resolved, to date, both glycolipids (Hausman and Burns, 1993) and a glycoprotein (Brennan *et al.*, 1988) have been implicated as candidate cell receptors. Difficulties in detecting competitive binding of other toxins to their cell receptor have been described, including that of exotoxin A (Manhart *et al.*, 1984), which was subsequently shown to bind to low-density lipoprotein-receptor-related protein (LRP)/α2

Table 3. Effect of inhibitors of cell trafficking on the processing of PT by CHO cells.[a]

Inhibitor		Experiment 1 (arbitrary units)	Per cent S1 processed[b]	Experiment 2 (arbitrary units)	Per cent S1 processed
None	S1[b]	36	ND	52	ND
	S1p[c]	22	38	50	49
Unlabelled PT	S1	ND	ND	96	ND
	S1p	ND	ND	4	4
22°C	S1	ND	ND	78	ND
	S1p	ND	ND	5	6
Chloroquine	S1	52	ND	85	ND
	S1p	8	13	22	21
Nocodazole	S1	43	ND	ND	ND
	S1p	11	20	ND	ND
Brefeldin A	S1	38	ND	68	ND
	S1p	16	30	51	43

a. CHO cell monolayers, in 12-well plates, were incubated with brefeldin A (2 μg ml^{-1}), chloroquine (100 μM), nocodazole (50 μg ml^{-1}), or unlabelled PT (33 pmoles) for 30 min at 37°C prior to addition of [^{125}I]-PT (0.1 pmoles) in 0.75 ml of temperature-equilibrated (at 37° or 22°C) complete media. After 2 h, cells were washed in ice-cold D-PBS, lysed in SDS sample buffer, boiled for 10 min, and analysed by SDS–PAGE under reducing conditions, followed by autoradiography. Autoradiographs were quantified by optical densitometry.
b. Per cent S1 processed = S1p/(S1 + S1p) × 100.
c. S1p was calculated by subtracting the unit value of S3 from the unit value of S2, because S1p migrated at the same position as S2. This calculation was made after determining that, on a molar basis, S2 and S3 are radiolabelled to the same extent (see the *Results*).
ND, not determined.

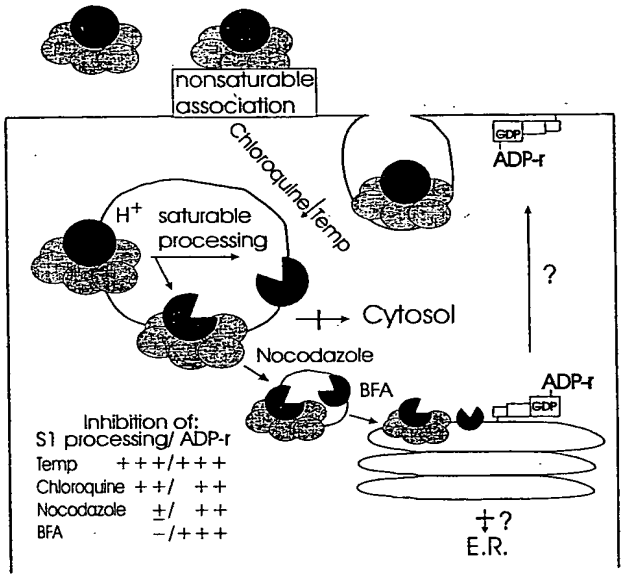

Fig. 6. Model for the entry of PT into CHO cells. This schematic diagram illustrates the mechanism of entry of PT into CHO cells, which results in the *in vivo* ADP-ribosylation of G_i proteins by PT and the *in vivo* processing of the S1 subunit of PT. The table (lower left) defines the ability of several reagents to inhibit either *in vivo* ADP-ribosylation or S1 processing. This varies from no inhibition (−), to essentially complete inhibition (+++).

macroglobulin (Kounnas *et al.*, 1992). Although unlabelled PT did not reduce the amount of [^{125}I]-PT bound to cells, unlabelled PT did inhibit the processing of S1 within cell-associated PT. This is consistent with S1 processing being a saturable and specific event of the intoxication pathway of PT which occurs subsequent to cell association.

Several lines of evidence are consistent with the suggestion that S1 processing follows the physiological pathway that PT utilizes for the ADP-ribosylation of G_i proteins in intact cells: (i) time-course experiments allowed the detection of S1 processing within cell-associated PT as early as 30 min after the addition of [^{125}I]-PT to cells (Fig. 3). This precedes the earliest detection of PT catalysed ADP-ribosylation of G_i proteins in intact CHO cells (Xu and Barbieri, 1995); (ii) both a reduced temperature and chloroquine, which inhibited the preferential processing of S1 within cell-associated PT, also inhibited the ability of PT to ADP-ribosylate G_i proteins in intact CHO cells (Xu and Barbieri, 1995; 1996); and (iii) the preferential processing of S1 was observed in the three cell lines tested. It should be noted that the presence of a large number of low-affinity receptors for PT may mask the detection of high-affinity PT receptors that may be present on the cell surface.

S1 processing appears to require an early-endosomal event, as processing was inhibited more efficiently by low temperature and chloroquine than by reagents that inhibited later trafficking functions, such as nocodazole and brefeldin A. The observation that brefeldin A inhibited the ADP-ribosylation of G_i proteins by PT (Xu and Barbieri, 1995) but not S1 processing suggests that the brefeldin A-sensitive step occurs subsequent to S1 processing. Together, these data indicate that S1 processing is necessary but not sufficient for the *in vivo* ADP-ribosylation of G_i proteins by PT. Also, earlier studies showed that protease (trypsin and chymotrypsin) treatment of PT did not affect the intoxication kinetics of cells (Krueger *et al.*, 1991). This suggests that proteolysis is not a rate-limiting step in the intoxication process.

The observed preferential processing of S1 within cell-associated PT at 37°C appears to represent cleavage within its protease-sensitive loop, which comprises residues between 210 and 220. This protease-sensitive loop within S1 has been described in both biochemical (Peppler *et al.*, 1985; Krueger *et al.*, 1991) and structural (Stein *et al.*, 1994a) studies. An inhibitor of the cytoplasmic protease calpain did not protect the loop from cleavage. Also, the data in this study did not implicate furin as the processing protease, as S1 lacks the furin-recognition site (R-X-X-R) and S1 was not processed at the cell surface, as has been observed for the protective antigen of anthrax toxin (Klimpel *et al.*, 1992; Steiner *et al.*, 1992). The lack of observed processing of S1 at room temperature could be explained by either a slower rate of endocytosis or a reduced rate of endosomal fusion (Morris, 1990 and Olsnes *et al.*, 1993).

The amount of processing of S1 within cell-associated PT was greater than reported for cholera toxin (CT) and exotoxin A (ETA), where only a small percentage of cell-associated CT and ETA was processed (Fishman, 1990; Orlandi *et al.*, 1993; Ogata *et al.*, 1990). Proteolysis appears to be a common event in the intoxication process of bacterial and plant toxins, although its requirement for the expression of cytotoxicity appears to vary (reviewed in Gordon and Leppla, 1994). Leppla and co-workers reported that the proteolytic cleavage of protective antigen to a 63 kDa fragment was required to allow binding of either oedema factor or lethal factor (Singh *et al.*, 1989; Leppla, 1991), while proteolysis was required for the expression of cytotoxicity by ETA (Ogata *et al.*, 1990; 1992). In contrast, cleavage of the A subunit of native Shiga-like toxin (SLT-IIv) and a Shiga-His(R247H/R250H) mutant did not correlate with the cytotoxicity of the respective strains, which suggested that cleavage at these Arg residues was not required for toxicity (Samuel and Gordon, 1994). Alternate cleavage of the Shiga-His(R248H/R251H) mutant occurred at a later transport stage than native toxin (Garred *et al.*, 1995). Cieplak and co-workers (Grant *et al.*, 1994) reported that *Escherichia coli* heat-labile enterotoxin (LT) that was mutated at Arg-192 retained cytotoxicity,

which suggested that proteolytic cleavage at this residue was not an absolute requirement for cytotoxicity.

Endocytosis is inhibited at 4°C (discussed in Morris, 1990), such that PT remained accessible to extracellular pronase. Incubation of [^{125}I]-PT bound to CHO cells at 4°C with varied concentrations of pronase showed that S1 was preferentially nicked within the holotoxin at low concentrations of pronase. The relative size of the nicked S1 was consistent with cleavage within the protease-sensitive loop of S1, between amino acids 205 and 214 (Krueger *et al.*, 1991; Stein *et al.*, 1994b). Accessibility of this protease-sensitive site suggests that cell-bound PT is orientated such that the protease-sensitive loop of S1 is exposed to the culture medium rather than buried within the cell membrane.

Experimental procedures

Materials

6′SL was from Oxford Glyco Systems; chloroquine, nocodazole, brefeldin A, and calpain inhibitor were from Sigma; and lactoperoxidase and pronase were from Calbiochem. PT was a generous gift from Rino Rappuoli (IRIA, Sienna, Italy) and was also purchased from List Biological. ^{125}I (IMS-30) was from Amersham.

Cell culture

CHO-K1 cells were obtained from ATCC (CCL61) and cultivated in Ham's F12 medium (Gibco, BRL) supplemented with 10% newborn-calf serum, 10% sodium bicarbonate, 50 μg ml^{-1} of streptomycin, and 50 U ml^{-1} of penicillin (complete media). LLC-PK1 (CRL-1392) and MDCK cells (CCL-34) were obtained from ATCC and cultivated in Dulbecco's Minimum Eagle Medium (Gibco, BRL) supplemented with 10% fetal-calf serum, sodium bicarbonate, and streptomycin–penicillin.

Radioiodination of PT

PT was iodinated using lactoperoxidase as described by Roth (1975) with some modifications. Labelling mixtures contained (in 150 μl): 0.1 M sodium acetate buffer, pH 5.6, 1 mCi of carrier-free sodium ^{125}I, 13 pmoles of PT, 200 μM NAD, 10 mM 6′SL, and 0.12 μg of lactoperoxidase. The reaction was started with the addition of hydrogen peroxide (0.0001%, final concentration). After 30 s, the reaction was stopped by adding 100 μl of a tyrosine-saturated solution containing 0.02% sodium azide. The labelling mixture was subjected to gel-filtration P-100 chromatography (a 3 ml column equilibrated in 25 mM Tris-HCl (pH 7.6), 300 mM NaCl, and 0.3% bovine serum albumin (BSA) to separate [^{125}I]-PT from free ^{125}I (Krueger and Barbieri, 1993). Fractions (120 μl) were collected, assayed for ^{125}I by K-counting, and the first radioactive peak, which contained [^{125}I]-PT, was pooled. The ratio of ^{125}I bound to each subunit of PT was determined, using a radio-analytical imaging system (AMBIS). Bands corresponding to [^{125}I]-PT were cut from the gel and counted in a K-counter to determine specific activities.

CHO cell cytotoxicity assay

The assay was performed essentially as described by Hewlett *et al.* (1983). The labelling mixture, which contained [^{125}I]-PT, was serially diluted (threefold) with 25 mM Tris (pH 7.6) containing 0.1% BSA, and 10 μl of each dilution was added to a well (24-well tissue-culture plate) containing 5×10^4 of freshly dispensed CHO cells in 1 ml of complete media. After 24 h at 37°C, cells were examined microscopically to determine the extent of cell-clustering morphology. The amount of cell clustering was compared to unlabelled PT (positive control) and labelling mixture without PT (negative control).

Association of [^{125}I]-PT to CHO cells

Binding assay. CHO cells were seeded in a 24-well tissue-culture plate. At confluency, lawns were overlayed with 0.5 ml of fresh complete media. Fifteen minutes prior to addition of [^{125}I]-PT (0.05 pmoles), the indicated inhibitor (as 10× stocks in 250 mM HEPES, pH 7.0) or unlabelled 0.5 μM PT was added; the sample was assayed in duplicate. Incubations were performed at the indicated temperatures and times. Monolayers were rinsed four times with 2 ml of cold Dulbecco's phosphate buffered saline (D-PBS, Gibco), dissolved in 300 μl of 0.1 N NaOH, and cell-associated [^{125}I]-PT was measured in a K-counter. An aliquot (50 μl) of the dissolved monolayer was also assayed for protein, using the BCA protein assay (Pierce) to normalize the amount of cell-associated [^{125}I]-PT to protein in the monolayer. The value of [^{125}I]-PT bound to the monolayer following a zero-time incubation was subtracted from the reported values (Table 1).

Cell association of [^{125}I]-PT to cells. CHO, LLC-PK1 or MDCK cells were seeded in 12-well plates. At confluency, 0.75 ml of fresh temperature-equilibrated media was added, followed by the addition of [^{125}I]-PT (see figure legends). Incubations were performed at the indicated temperatures and times. An aliquot of spent medium was obtained and the monolayer was then washed four times with 3 ml of cold D-PBS and scraped off the plate in SDS sample buffer without β-mercaptoethanol, and boiled. Aliquots were counted and subjected either to a BCA protein assay or SDS–PAGE in the presence of β-mercaptoethanol.

Effect of inhibitors of cell trafficking on the association of [^{125}I]-PT to CHO cells. CHO cells (12-well plates) were incubated for 30 min at 37°C with the indicated inhibitor, as described in Table 3, in 0.75 ml of fresh temperature-equilibrated media prior to the addition of [^{125}I]-PT. After a 2 h incubation at 37°C or at room temperature (RT), cells were washed and treated as described above.

Pulse-chase analysis of cell-associated [^{125}I]-PT

CHO cell monolayers (12-well plates) were incubated with [^{125}I]-PT (0.1 pmoles) at 22°C for 30 min and then washed to remove unbound toxin (pulse). Cells were then incubated for

an additional 1, 2, or 3 h (chase) at either 22°C or 37°C after which time cells were washed, and then resuspended in SDS–PAGE sample buffer and boiled. Cell-associated [^{125}I]-PT was assayed by SDS–PAGE followed by autoradiography of the dried gel.

Pronase treatment of cell-associated [^{125}I]-PT

CHO cells, grown to confluency in 12-well plates, were incubated with 0.1 pmoles of [^{125}I]-PT in 0.75 ml of fresh media for the indicated temperatures and times. At the appropriate time, cells were washed four times with cold D-PBS, and then incubated alone or with 0.2–4 mg of pronase per millilitre of D-PBS for 1 h at 4°C. The digestion was stopped with 20 mM EDTA in 50% newborn-calf serum. Control samples were treated with 20 mM EDTA in 50% newborn-calf serum prior to pronase. Cells were transferred to microfuge tubes and centrifuged at 8160 × *g* for 1 min at 4°C. Undisturbed pellets were washed in D-PBS containing 20 mM EDTA, centrifuged for 30 s, suspended in 90 µl of sample buffer containing 10 mM EDTA, and boiled for 10 min. Aliquots were subjected to SDS–PAGE under reducing conditions, followed by autoradiography. Autoradiographs were quantified by an optical imaging system (AMBIS). Cell-associated PT was determined after a zero-time incubation and subtracted from the values determined after 30 and 120 min.

Acknowledgements

This research was supported by Public Health Service grants AI-RO1-30162 and AI-KO4-01087 to J.T.B. from the National Institutes of Health. V.F.B. is a postdoctoral fellow supported by the International Human Frontier Science Program.

References

Armstrong, G.D., and Peppler, M.S. (1987) Maintenance of biological activity of pertussis toxin radioiodinated while bound to fetuin–agarose. *Infect Immun* **55:** 1294–1299.

Brennan, M.J., David, J.L., Kenimer, J.G., and Manclark, C.R. (1988) Lectin-like binding of pertussis toxin to a 165 kilodalton Chinese hamster ovary cell glycoprotein. *J Biol Chem* **263:** 4895–4899.

Burns, D.L., and Manclark, C.R. (1986) Adenine nucleotides promote dissociation of pertussis toxin subunits. *J Biol Chem* **261:** 4324–4327.

Croall, D.E., and DeMartino, G.N. (1991) Calcium-activated neutral protease (calpain) system: structure, function, and regulation. *Physiol Rev* **71:** 813–847.

Dorland, R.B., Middlebrook, J.L., and Leppla, S.H. (1979) Receptor-mediated internalization and degradation of diphtheria toxin by monkey kidney cells. *J Biol Chem* **254:** 11337–11342.

Fishman, P.H. (1990) Mechanism of action of cholera toxin. In *ADP-Ribosylating Toxins and G-proteins: Insights into Signal Transduction.* Moss, J., and Vaughan, M. (eds). Washington, DC: American Society for Microbiology, pp. 127–140

Garred, O., Dubinina, E., Holm, P.K., Olsnes, S., van Deurs, B., Kozlov, J.V., and Sandvig, K. (1995) Role of processing and intracellular transport for optimal toxicity of Shiga toxin and toxin mutants. *Exp Cell Res* **218:** 39–49.

Gill, D.M. (1978) Seven toxic peptides that cross cell membranes. In *Bacterial Toxins and Cell Membranes.* Jeljaszewic, J., and Wadstrom, T. (eds). Orlando, Florida, USA: Academic Press, pp. 291–332.

Gordon, V.M., and Leppla, S.H. (1994) Proteolytic activation of bacterial toxins: role of bacterial and host cell proteases. *Infect Immun* **62:** 333–340.

Grant, C.C.R., Messer, R.J., and Cieplak, Jr, W. (1994) Role of trypsin-like cleavage at arginine 192 in the enzymatic and cytotonic activities of *Escherichia coli* heat-labile enterotoxin. *Infect Immun* **62:** 4270–4278.

Hausman, S.Z., and Burns, D.L. (1992) Interaction of pertussis toxin with cells and model membranes. *J Biol Chem* **267:** 13735–13739.

Hausman, S.Z., and Burns, D.L. (1993) Binding of pertussis toxin to lipid vesicles containing glycolipids. *Infect Immun* **61:** 335–337.

Hewlett, E.L., Sauer, K.T., Myers, G.A., Cowell, J.L., and Guerrant, R.L. (1983) Induction of a novel morphological response in Chinese hamster ovary cells by pertussis toxin. *Infect Immun* **40:** 1198–1203.

Kaslow, H.R., and Burns, D.L. (1992) Pertussis toxin and target eukaryotic cells: binding, entry, and activation. *FASEB J* **6:** 2684–2690.

Kaslow, H.R., Lim, L.-K., Moss, J., and Lesikar, D.D. (1987) Structure-activity analysis of the activation of pertussis toxin. *Biochemistry* **26:** 123–127.

Klimpel, K.R., Molloy, S.S., Thomas, G., and Leppla, S.H. (1992) Anthrax toxin protective antigen is activated by a cell surface protease with the sequence specificity and catalytic properties of furin. *Proc Natl Acad Sci USA* **89:** 10277–10281.

Kounnas, M.Z., Morris, R.E., Thompson, M.R., Fitzgerald, D.J., Strickland, D.K., and Saelinger, C.B. (1992) The alpha 2-macroglobulin receptor/low density lipoprotein receptor-related protein binds and internalizes *Pseudomonas* exotoxin A. *J Biol Chem* **267:** 12420–12423.

Krueger, K.M., and Barbieri, J.T. (1993) Molecular characterization of the *in vitro* activation of pertussis toxin by ATP. *J Biol Chem* **268:** 12570–12578.

Krueger, K.M., and Barbieri, J.T. (1994) Assignment of functional domains involved in ADP-ribosylation and B-oligomer binding within the carboxyl terminus of the S1 subunit of pertussis toxin. *Infect Immun* **62:** 2071–2078.

Krueger, K.M., Mende-Mueller, L.M., and Barbieri, J.T. (1991) Protease treatment of pertussis toxin identifies the preferential cleavage of the S1 subunit. *J Biol Chem* **266:** 8122–8128.

Leppla, S.H. (1991) The anthrax toxin complex. In *Sourcebook of Bacterial Proteins Toxins.* Alouf, J.E., and Freer, J.H. (ed.). London, UK: Academic Press, pp. 277–302.

Manhart, M.D., Morris, R.E., Bonventre, P.F., Leppla, S.H., and Saelinger, C.B. (1984) Evidence for *Pseudomonas* exotoxin A receptors on plasma membrane of toxin-sensitive LM fibroblasts. *Infect Immun* **45:** 596–603.

Montecucco, C., Tomasi, M., Schiavo, G., and Rappuoli, R. (1986) Hydrophobic photolabelling of pertussis toxin subunits interacting with lipids. *FEBS Lett* **194:** 301–304.

Morris, R.E. (1990) Interaction between *Pseudomonas*

exotoxin A and mouse LM fibroblast cells. In *Trafficking of Bacterial Toxins*. Saelinger, C.B. (ed.). Boca Raton, Florida, USA: CRC Press Inc., pp. 50–66.

Ogata, M., Chaudhary, V.K., Pastan, I., and Fitzgerald, D.J. (1990) Processing of *Pseudomonas* exotoxin by a cellular protease results in the generation of a 37 000 Da toxin fragment that is translocated to the cytosol. *J Biol Chem* **265:** 20678–20685.

Ogata, M., Fryling, C.M., Pastan, I., and Fitzgerald, D.J. (1992) Cell-mediated cleavage of *Pseudomonas* exotoxin between Arg279 and Gly280 generates the enzymatically active fragment which translocates to the cytosol *J Biol Chem* **267:** 25396–25401.

Olsnes, S., van Deurs, B., Sandvig, K. (1993) Protein toxins acting on intracellular targets: cellular uptake and translocation to the cytosol. *Med Microbiol Immunol* **182:** 51–61.

Orlandi, P.A., Curran, P.K., and Fishman, P.H. (1993) Brefeldin A blocks the response of cultured cells to cholera toxin. Implications for intracellular trafficking in toxin action. *J Biol Chem* **268:** 12010–12016.

Peppler, M.S., Judd, R.C., and Munoz, J.J. (1985) Effect of proteolytic enzymes, storage and reduction on the structure and biological activity of pertussigen, a toxin from *Bordetella pertussis*. *Dev Biol Stand* **61:** 75–87.

Roth, J. (1975) Methods for assessing immunologic and biologic properties of iodinated peptide hormones. *Meth Enzymol* **37:** 223–233.

Samuel, J.E., and Gordon, V.M. (1994) Evidence that proteolytic separation of Shiga-like toxin type IIv A subunit into A1 and A2 subunits is not required for toxin activity. *J Biol Chem* **269:** 4853–4859.

Singh, Y., Chaudhary, V.K., and Leppla, S.H. (1989) A deleted variant of *Bacillus anthracis* protective antigen is non-toxic and blocks anthrax toxin action *in vivo*. *J Biol Chem* **264:** 19103–19107.

Stein, P.E., Boodhoo, A., Armstrong, G.D., Heerze, L.D., Cockle, S.A., Klein, M.H., and Read, R.J. (1994a) Structure of a pertussis toxin–sugar complex as a model for receptor binding. *Structural Biol* **1:** 591–596.

Stein, P.E., Boodhoo, A., Armstrong, G.D., Cockle, S.A., Klein, M.H., and Read, R.J. (1994b) The crystal structure of pertussis toxin. *Structure* **2:** 45–57.

Steiner, D.F., Smeckens, S.P., Ohagi, S., and Chan, S.J. (1992) The new enzymology of precursor processing endoproteases. *J Biol Chem* **267:** 23435–23438.

Stow, J.L., de Almeida, J.B., Narula, N., Holtzman, E.J., Ercolani, L., and Ausiello, D.A. (1991) A heterotrimeric G protein, G alpha i-3, on Golgi membranes regulates the secretion of a heparin sulfate proteoglycan in LLC-PK1 epithelial cells. *J Cell Biol* **114:** 1113–1124.

Tamura, M., Nogimori, K., Murai, S., Yajima, M., Ito, K., Katada, T., and Ui, M. (1982) Subunit structure of islet-activating protein, pertussis toxin, in conformity with the A-B model. *Biochemistry* **21:** 5516–5522.

Tamura, M., Nogimori, K., Yajima, M., Ase, K., and Ui, M. (1983) A role of the B-oligomer moiety of islet-activating protein, pertussis toxin, in development of the biological effects on intact cells. *J Biol Chem* **258:** 6756–6761.

Ui, M. (1990) Pertussis toxin as a valuable probe for G-protein involvement in signal transduction. In *ADP-Ribosylating Toxins and G-proteins: Insights into Signal Transduction*. Moss, J., and Vaughan, M. (eds). Washington, DC: American Society for Microbiology, pp. 45–66.

Weiss, A.A., and Hewlett, E.L. (1986) Virulence factors of *Bordetella pertussis*. *Annu Rev Microbiol* **40:** 661–686.

Xu, Y., and Barbieri, J.T. (1995) Pertussis toxin-mediated ADP-ribosylation of target proteins in Chinese hamster ovary cells involves a vesicle trafficking mechanism. *Infect Immun* **63:** 825–832.

Xu, Y., and Barbieri, J.T. (1996) Pertussis toxin-catalyzed ADP-ribosylation of Gi-2 and Gi-3 in CHO cells is modulated by inhibitors of intracellular trafficking. *Infect Immun* **64:** 593–599.

ELSEVIER

Journal of Virological Methods 70 (1998) 45–58

Journal of Virological Methods

Kinetics of intracellular viral disassembly and processing probed by Bodipy fluorescence dequenching

Andrea T. Da Poian *, André M. O. Gomes, Tatiana Coelho-Sampaio

Departamento de Bioquímica Médica, Instituto de Ciências Biomédicas, Universidade Federal do Rio de Janeiro, 21941-590, Rio de Janeiro, RJ, Brazil

Received 10 June 1997; received in revised form 18 September 1997; accepted 19 September 1997

Abstract

A novel method is described for the study of viral disassembly and processing in live cells. Vesicular stomatitis virus (VSV) was labelled with the fluorescent probe Bodipy-FL and the resulting conjugate was 97.6% self-quenched due to fluorescence resonance energy transfer between neighbouring Bodipy molecules. In vitro experiments showed a four-fold increase in Bodipy fluorescence after extraction of VSV G protein from the virus envelope with Triton X-100 or β-octylglucoside. Bodipy-labelled virus retained its capacity to mediate fusion of viral membrane with phosphatidylserine liposomes. Incubation of Bodipy-VSV with proteases in the presence of detergent promoted a total fluorescence enhancement of ca. 20 fold, showing that the conjugate fluorescence was also sensitive to proteolysis. Fluorescence microscopy and flow cytometry experiments with macrophages incubated with Bodipy-VSV revealed that intracellular relaxation of fluorescence self-quenching resulted from a combination of viral disassembly due to pH-induced membrane fusion and viral protein degradation inside the endosomes. When macrophages were incubated simultaneously with ammonium chloride and protease inhibitors, the increase in fluorescence was abolished completely due to inhibition of both endosomal acidification and proteolysis. In addition, experiments carried out in the presence of protease inhibitors alone allowed, for the first time, isolated observation of G protein-mediated fusion of viral envelope with the endosomal membrane in living cells. The results indicate that this methodology may find wide application for further studies of viral infection. © 1998 Elsevier Science B.V.

Keywords: Virus; Disassembly; Fluorescence dequenching

1. Introduction

The entry of viruses into animal cells is a complex process not completely understood. Enveloped viruses are internalised either via direct

* Corresponding author. Tel.: + 55 21 2705988; fax: + 55 21 2708647; e-mail: dapoian@bioqmed.ufrj.br

PII S0166-0934(97)00166-3

REF. 7

fusion of their envelope with the host plasma membrane (Choppin and Compans, 1975) or via receptor-mediated endocytosis (Helenius et al., 1980; Matlin et al., 1982a,b; Schlegel et al., 1982; Marsh and Helenius, 1989; Lanzrein et al., 1994). In the latter case, the endosome-encased virus must escape from the endosomal compartment in order to gain access to the cytosol and eventually to the cell nucleus. It has been postulated that the endosomal environment, characterised by an acidic pH, leads to conformational changes of viral spike glycoproteins, which mediate fusion of the viral envelope with the membrane of the endosome, thus allowing extrusion of the nucleocapsid into the cytosol (White et al., 1981; Gaudin et al., 1995; Hernandez et al., 1996).

Despite the relative wealth of current knowledge regarding the infection process for enveloped viruses, in situ experimental observations of virus fusion with endosomes are still lacking. To date, membrane fusion has been investigated by testing the ability of isolated viruses to promote fusion of model cells or liposomes (White et al., 1981; Blumenthal et al., 1987; Pal et al., 1988). The disassembly of an enveloped virus in an intact cell was studied. Disassembly here is understood as the loss of integrity of viral structure without chemical modification, as induced by membrane fusion, by fusion-induced uncoating of viral nucleic acid with full dissociation of viral proteins or, in the case of in vitro studies, by artificial detergent solubilisation of the virus envelope.

In order to assess intracellular viral disassembly the rhabdovirus vesicular stomatitis virus (VSV) was labelled with the unique fluorescent probe Bodipy-FL (Fig. 1). VSV is composed of a negative-sense RNA, tightly encased by the nucleoprotein (N protein), and a lipidic envelope, which presents a type I spike glycoprotein (G protein) and a peripheral matrix protein (M protein) aligning on the inner surface of the membrane (Wagner, 1987). The fluorescent probe Bodipy-FL presents highly superimposed absorption and emission spectra. Thus, in a heavily labelled Bodipy-VSV conjugate, in which probe molecules are in close proximity, Bodipy fluorescence is self-quenched due to fluorescence resonance energy transfer (FRET). As neighbouring Bodipy molecules become physically separated, such as in the dissociation of protein subunits upon VSV disassembly, relaxation of self-quenching occurs, leading to increase in fluorescence.

It should be noted, however, that an increase in fluorescence intensity of Bodipy-VSV, besides reporting viral disassembly, may also reflect proteolytic degradation of viral proteins if more than one probe molecule is attached to a single viral polypeptide chain. In order to address this issue, an investigation of the proteolytic processing of Bodipy-VSV was carried out. Thus, for in vitro characterisation of the conjugate, detergents were used to induce VSV disassembly and proteases to promote proteolysis. In addition, for in situ studies macrophages were used, in which both viral disassembly and proteolysis are expected to occur. Distinction between fluorescence increase due to disassembly or proteolysis was made by using specific inhibitors of either process. The results showed that the Bodipy-VSV conjugate is a sensitive probe to report virus disassembly and processing in live cells, and it is suggested that this approach may find future applications in in situ studies of the mechanisms of viral infection.

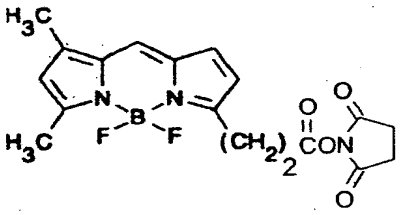

Fig. 1. Structure of the succinimidyl ester of Bodipy-FL.

2. Materials and methods

2.1. Reagents

Cell culture reagents, pepstatin A, leupeptin, phenylmethylsulfonyl fluoride (PMSF), ammonium chloride, bovine brain phosphatidylserine and proteinase K were purchased from Sigma (St. Louis, MO). Fetal bovine serum (FBS) was provided by Cultilab (Campinas, SP, Brazil). The amino reactive succinimidyl ester derivative of

Bodipy-FL was from Molecular Probes (Eugene, OR). All other reagents employed in this study were of analytical grade.

2.2. Cell culture

Macrophages from the lineage J774 were kindly provided by Dr. Pedro Persechini (Universidade Federal do Rio de Janeiro, Brazil). Cells were grown in monolayers on 24-well plates at 37°C in a CO_2 incubator, using Dulbecco's modified Eagle's medium (DMEM) supplemented with 10% FBS, 1% Eagle's minimum essential medium non-essential amino acids, gentamicyn-ampicillin antibiotics and buffered with sodium bicarbonate. Two days before use for flow cytometry experiments, cells were harvested from stock culture flasks by gentle pippeting, diluted to 5×10^4 cells/ml and transferred to 96-well plates (200 μl/well). For microscopy experiments, cells were dropped onto coverslips, incubated for 1 h to allow attachment to the glass surface, placed in petri dishes containing 10 ml supplemented DMEM and used 3–4 days later.

2.3. Virus propagation and purification

VSV type Indiana was kindly supplied by Dr. Carlos F.S. Bonafé (Unicamp, Brazil). Virus was propagated in monolayers of baby hamster kidney cells (BHK21) for 16 h on a roller apparatus placed in a CO_2 incubator (37°C) and purified as described by Da Poian et al. (1996).

2.4. Virus labelling

VSV was labelled with the succinimidyl ester (SE) derivative of Bodipy-FL (Fig. 1), which reacts with unionised aliphatic amines provided predominantly by lysine residues at pH 8.0. A purified viral sample, diluted to 100 μg protein/ml in 40 mM phosphate buffer (pH 8.0), was incubated with a freshly dissolved solution of Bodipy-FL SE in dimethylformamide to give a final probe concentration of 7.3 μM in 1% dimethylformamide. Labelling proceeded for 72 h at 4°C, under constant stirring. Free probe was removed by extensive dialysis against 50 mM Tris–HCl buffer, pH 7.5. Labelled virus was kept at 4°C, protected from the light.

2.5. Fluorescence microscopy

Fluorescence microscopy was carried out using a Zeiss Axioskop microscope equipped with a short mercury arc lamp (Osram HBO 50 W; Osram, Berlin). Bodipy fluorescence was observed by setting the instrument for detection of fluorescein fluorescence (Zeiss 487909 filter set). Images were collected with a Star I camera system (Photometrics, Tucson, AZ) consisting of a cooled camera head, a charge-coupled device, a camera controller and a cooling liquid circulation unit (LC200), using processing software provided by the manufacturer.

Macrophages attached to coverslips were pulsed in a petri dish containing 2 ml of complete DMEM with 16 μg/ml Bodipy-VSV. After 10 min at 37°C, pulsing medium was removed, coverslips were washed 3 times with Bodipy-free DMEM, and the petri dish was returned to 37°C. At the desired chase times, individual coverslips were removed from the dish and placed in 4% paraformaldehyde for fixation. Observation fields were selected using transmitted light to minimise photo-bleaching of the sample. Time exposures were 0.2 s for transmitted light and 5 s for fluorescence pictures. The same scale of intensities was used in all pictures. Images were processed on a personal computer equipped with a GPIB interface (NI-488.2, National Instruments).

2.6. Fluorescence measurements on Bodipy-VSV

Fluorescence intensity and light scattering measurements were recorded using ISS GREG 200 or ISS K2 spectrofluorometers (ISS, Champaign, IL). Fluorescence intensity was measured using excitation and emission wavelengths of 490 and 510 nm, respectively. Bodipy-VSV was diluted to 2 μg/ml in 50 mM Tris–HCl buffer, pH 7.5, and a baseline was recorded for 5 min. Detergents or proteases were added at the indicated concentrations and fluorescence was recorded at

37°C. Light scattering was measured at 90° in the spectrofluorometer by selecting the same wavelength for both excitation and emission monochromators (370 nm).

2.7. Polyacrylamide gel electrophoresis of labelled virus

Approximately 30 μg of purified labelled virus was solubilised in electrophoresis sample buffer (200 mM Tris, 1% sodium dodecyl sulphate (SDS), 2% β-mercaptoethanol and 3 M urea, pH 6.8). The sample was boiled for 2 min and run on a 15% polyacrylamide gel, protected from light. For photography, the gel was transilluminated with UV light (254 nm) and transmitted light was rejected using a 3-69 Corning filter (cut-off at 525 nm).

2.8. Preparation of liposomes

Phosphatidylserine (PS) dissolved in chloroform was evaporated under nitrogen and the lipid film formed was resuspended in 10 mM Tris, 10 mM sodium acetate buffer, pH 5.0 or 7.3, to produce a final concentration of 1 mM. The suspension was vortexed vigorously for 5 min. Small unilamellar vesicles were formed by sonicating the turbid suspension using a Branson Sonifier (Sonic Power Company, Danbury, CT) equipped with a titanium microtip probe. Sonication was performed in an ice bath, alternating cycles of 30 s at 50% full power, with 60 s resting intervals until a transparent solution was obtained (approximately 10 cycles).

2.9. Isolation of G protein from labelled virus

VSV G protein was isolated according to Mathieu et al. (1996). Purified labelled virus in 50 mM Tris–HCl (pH 7.5) was incubated with 60 mM octylglucoside at room temperature for 1 h. Nucleocapsids were removed by centrifugation at 43 000 rpm for 90 min in a Beckman 50 Ti rotor. The supernatant was dialysed against deionised water to remove detergent.

2.10. Flow cytometry

Flow cytometry was carried out using a Coulter EPICS-Elite ESP instrument (Miami, FL). Bodipy fluorescence measurements were made by setting the instrument for detection of fluorescein fluorescence, i.e. excitation was obtained with an argon ion laser (488 nm) and emission was collected through a combination of a 525 nm bandpass and a 550 cut-off filter. For each data point, 10 000 cells were analysed for size and granularity using, respectively, refraction index and 90° light scattering. A cell population corresponding to the majority of live cells was gated and fluorescence analysis performed exclusively for this population. Typically, 80% of cells analysed were included in the gate. The data presented correspond to the percentage of fluorescent cells or to the centers of mass of the distributions of fluorescence in the population defined in the gate.

In a typical experiment, cells attached to 96-well plates were pulsed for 10 min with 10 μg/ml Bodipy-VSV, washed three times with virus-free medium and incubated in virus free medium for variable times. Immediately before analysis, cells were removed from the wells by vigorous pipetting and transferred to cytometry tubes. When protease inhibitors or ammonium chloride were used, a pre-incubation step of 15 min was included before pulsing, and inhibitors were present throughout the experiment.

3. Results

3.1. Dequenching of Bodipy-VSV fluorescence in intact macrophages

The highly substituted Bodipy-VSV conjugate used throughout was analysed in order to determine its labelling stoichiometry, as well as to define the degree of self-quenching due to fluorescence homotransfer. The stoichiometry of labelling was calculated by dividing the number of equivalents of Bodipy in the conjugate, measured using $\epsilon_{502} = 77\,000\ M^{-1}/cm$, by the total number of VSV units, estimated using a proteic molecular mass of 198 MDa (Thomas et al., 1985). The

Bodipy:VSV labelling ratio thus obtained was 15 000 Bodipy molecules per virus. This corresponds to a stoichiometry of three probes per polypeptide chain, supposing an even distribution of the 15 000 probe equivalents among the 4800 viral subunits (Thomas et al., 1985). In addition, considering that G, M and N proteins present between 21 and 30 lysine residues each (Rose and Gallione, 1981; Gallione et al., 1981), we expect that approximately 10% of the lysine residues in viral subunits would be bound to the probe. The degree of self-quenching was calculated by comparing the fluorescence intensities obtained for free and for VSV-bound Bodipy at identical OD_{502}, which revealed that the Bodipy-VSV conjugate was 97.6% self-quenched due to FRET.

Considering this high level of self-quenching, it would be expected that a substantial increase in fluorescence would occur upon VSV disassembly (loss of integrity of viral envelope) and/or upon its proteolytic degradation. Fluorescence changes of Bodipy-VSV due to disassembly and/or processing in live macrophages were monitored by fluorescence microscopy (Fig. 2). J774 macrophages adhered onto coverslips were pulsed with labelled virus for 10 min, washed to remove non-internalised conjugate and observed on the fluorescence microscope at different times. At time zero, i.e. immediately after washing, a relatively low level of intracellular fluorescence was observed (Fig. 2A IV). Cell-associated fluorescence was clearly concentrated in internal compartments of the macrophage, compatible with an endosomal localisation of Bodipy-VSV. 1 and 2 h after washing, a progressive increase in intracellular fluorescence was evident (Fig. 2A V and VI). This time-dependent fluorescence enhancement precisely reflected the kinetics of Bodipy fluorescence dequenching, since the removal of Bodipy-labelled VSV from the incubation medium (washing step) ensured that fluorescence would not increase due to continuous uptake, nor would it decrease due to a concentration effect. The fluorescence intensities of the images were analysed quantitatively as histograms, representing the distributions of intensities per image pixel. The average fluorescence intensities of the images were expressed by quantifying the centres of mass of these distributions. Values were calculated either for entire images or for individual cells randomly selected from different images (Fig. 2B and C, respectively), yielding comparable increases in intracellular fluorescence intensities.

3.2. In vitro characterisation of virus disassembly

The results shown in Fig. 2 demonstrate that the fluorescence of Bodipy-VSV was dequenched progressively following internalisation into macrophages. However, in vitro characterisation of Bodipy-VSV was necessary to investigate whether the conjugate was sensitive to the two processes which could lead to fluorescence dequenching, namely viral disassembly and proteolytic degradation. In vitro characterisation of VSV disassembly was carried out by taking advantage of the previous observation that G protein can be solubilised selectively from the viral membrane by treatment of purified virus with non-ionic detergents such as Triton X-100 (Bishop et al., 1975) or β-D-octylglucoside (Petri and Wagner, 1979). The fluorescence emission of untreated labelled virus was very low, while spectra obtained after incubation of the sample with 1% Triton X-100 or 60 mM octylglucoside presented a four–five-fold increase in fluorescence emission at 510 nm (Fig. 3A). Stepwise addition of increasing concentrations of either detergent resulted in a gradual increase in Bodipy fluorescence (Fig. 3B). The detergent concentration which promoted half-maximal fluorescence increase was 0.01% for Triton and 18 mM for octylglucoside.

VSV G protein exists predominantly as a trimer of identical subunits in the virions and in infected cells (Dubovi and Wagner, 1977; Kreis and Lodish, 1986; Doms et al., 1987). Since the protein is obtained in trimeric form when it is solubilised from the virions either with octylglucoside (Lyles et al., 1990) or with Triton X-100 (Wilcox et al., 1992), the increase in Bodipy fluorescence observed in Fig. 3B corresponded to release of trimers from the virus. Panel C in Fig. 3 shows that stepwise addition of Triton decreased the intensity of light scattering of the sample, compatible with a decrease in hydrody-

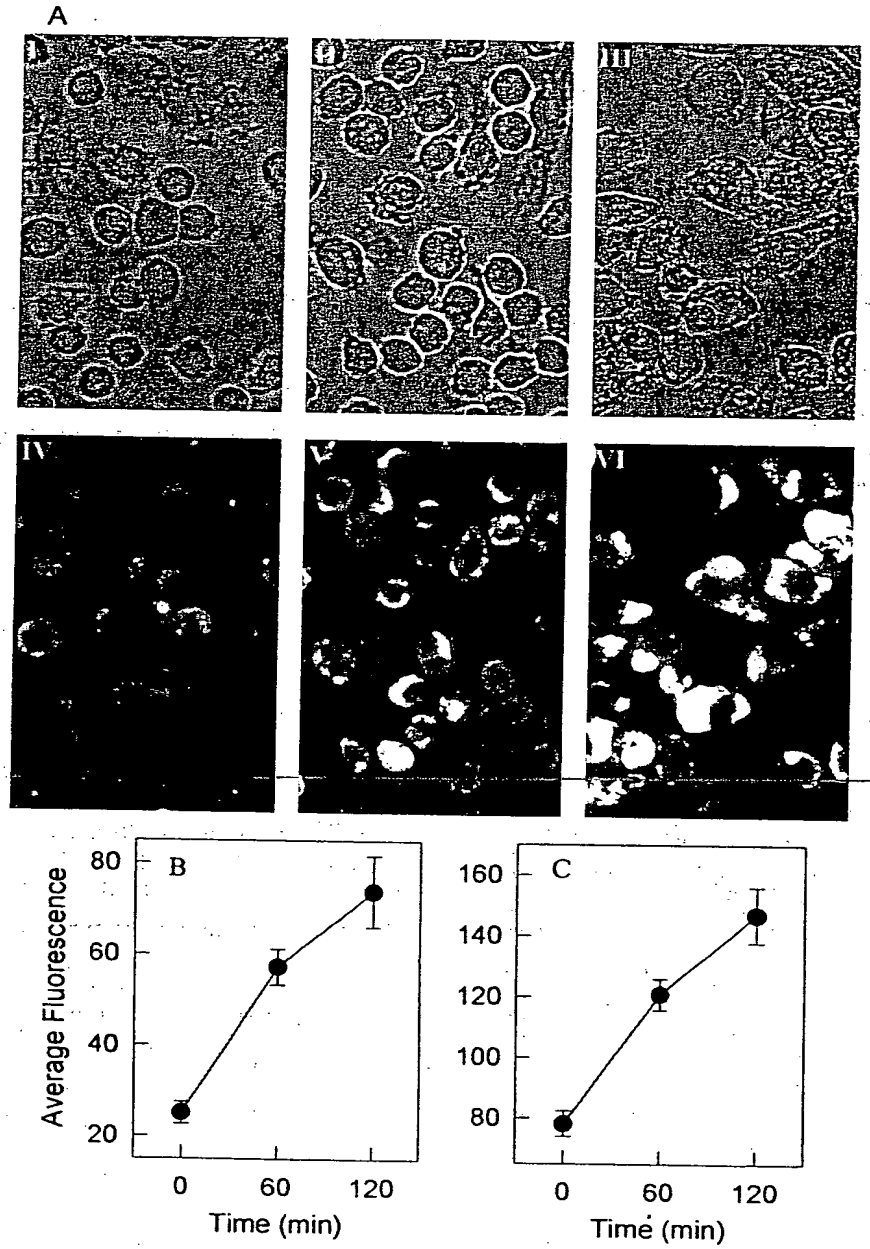

Fig. 2. Fluorescence dequenching of Bodipy-VSV in macrophages. J774 macrophages adhered to glass coverslips were pulsed with 16 μg/ml Bodipy-VSV for 10 min, washed with virus-free DMEM and incubated for different times at 37°C. Intracellular fluorescence was observed in the fluorescence microscope immediately, 60 or 120 min after washing (panel A, frames IV, V and VI, respectively). Corresponding transmitted light micrographs are also shown (panel A, frames I, II and III). The centers of mass of the distributions of fluorescence intensities per image pixel were analysed for different fields ($n = 6$) at the indicated time after washing (panel B). Alternatively, fluorescence distributions were analysed for individual cells ($n = 20$), randomly chosen in different fields (panel C).

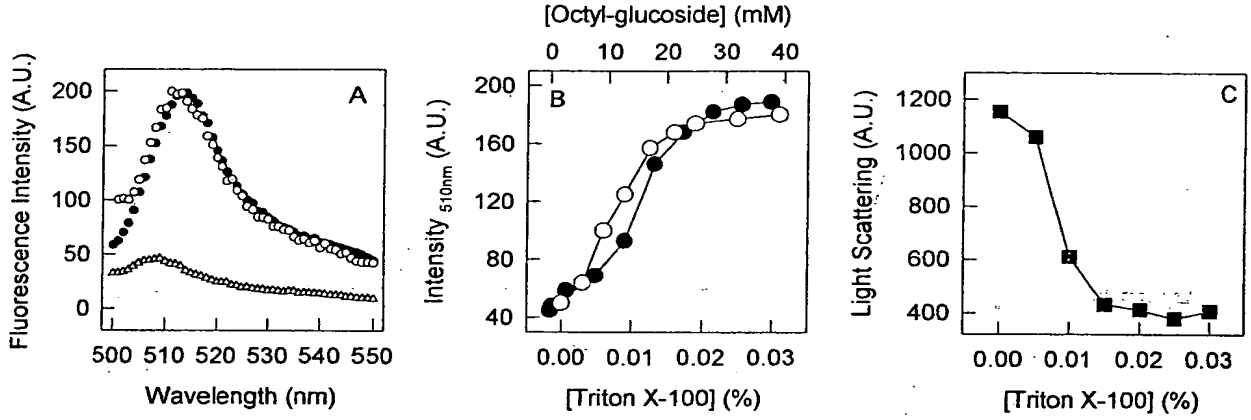

Fig. 3. Effect of detergents on the fluorescence of isolated Bodipy-VSV. (A) Fluorescence emission spectra of 2 μg/ml Bodipy-VSV were recorded in buffer (△), in the presence of 1% Triton X-100 (○) or in the presence of 60 mM octylglucoside (●). Excitation wavelength was 490 nm. (B) Effects of Triton X-100 (○) and octylglucoside (●) on Bodipy-VSV fluorescence. Excitation and emission wavelengths were 490 and 510 nm, respectively. (C) Effect of Triton X-100 on light scattering measured at 370 nm.

namic radius of VSV upon virus disassembly. A maximal decrease in light scattering of approximately 70% was observed at 0.03% Triton, while 0.01% Triton promoted half-maximal effect.

Due to the hydrophobic nature of Bodipy, one possibility that was examined was whether, instead of labelling viral proteins, the probe could partition into the lipid moiety of the viral membrane during the labelling procedure. If this were the case, the fluorescence increase induced by detergents could be determined exclusively by the release of membrane-associated Bodipy molecules. In order to demonstrate that in the Bodipy-VSV conjugate Bodipy was bound covalently to the protein moiety of VSV, SDS–PAGE analysis of the solubilised virus was undertaken (Fig. 4). The fluorescence pattern on a non-stained gel showed that Bodipy was bound to protein bands corresponding to the three major VSV protein components, namely G, N and M proteins. It should be noted that the overall fluorescence intensities observed in individual polypeptide bands did not directly reflect the extent of labelling, since fluorescence emission depended not only on the number of probe molecules bound to each protein but also on the extent of energy transfer between them.

3.3. pH-induced membrane fusion mediated by isolated Bodipy-VSV

In order to investigate whether VSV retained the capacity of mediating membrane fusion after extensive labelling with Bodipy, the ability of Bodipy-labelled VSV to induce fusion of viral membrane with PS liposomes (Fig. 5) was exam-

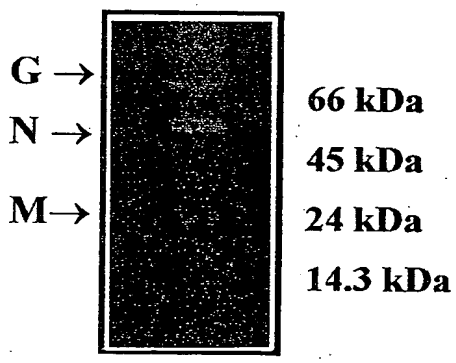

Fig. 4. SDS–PAGE of the Bodipy-VSV conjugate. Bodipy-VSV solubilised in electrophoresis sample buffer was examined on SDS–PAGE, using a 15% polyacrylamide gel. The gel was transilluminated with UV-light (254 nm) and photographed through a 3-69 Corning filter (cut-off at 525 nm). Positions of G, N and M proteins, as well as of molecular weight markers are indicated.

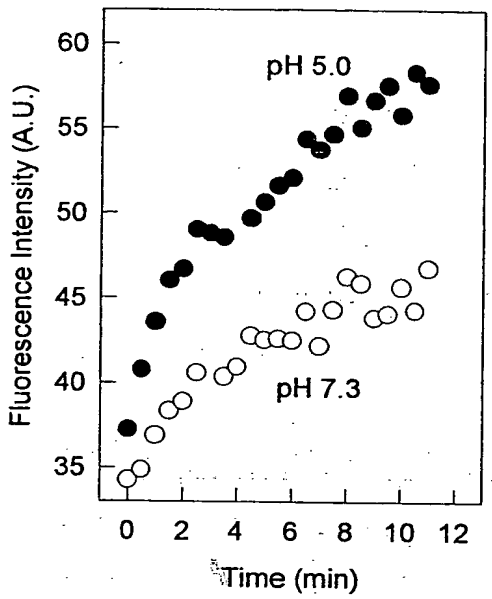

Fig. 5. VSV-mediated membrane fusion probed by Bodipy fluorescence dequenching. Fluorescence intensity of Bodipy-labelled VSV (2 μg/ml) at 510 nm was recorded, following addition of phosphatidylserine liposomes (625 μg/ml). The experiment was performed in 50 mM Tris, 10 mM sodium acetate buffer either at pH 7.3, (○) or at pH 5.0 (●). Excitation wavelength was 490 nm.

ined. Bodipy-VSV was incubated with PS vesicles at pH 5.0 and this interaction resulted in 70% increase in Bodipy fluorescence (Fig. 5, closed circles). However, when the same experiment was repeated at pH 7.3, a 28% increase in fluorescence was observed (Fig. 5, open circles). The fluorescence intensity reached a plateau after about 10 min of incubation at 37°C. The kinetics of fusion reported now were similar to that described by Pal et al. (1988), indicating that Bodipy-VSV fluorescence dequenching may also be used to follow separation between G proteins as a consequence of membrane fusion.

3.4. Proteolytic degradation of Bodipy-VSV

The kinetics of in vitro degradation of Bodipy-VSV are shown in Fig. 6A. Addition of 0.03% Triton to the native virus immediately led to a four-fold increase in Bodipy fluorescence. Further

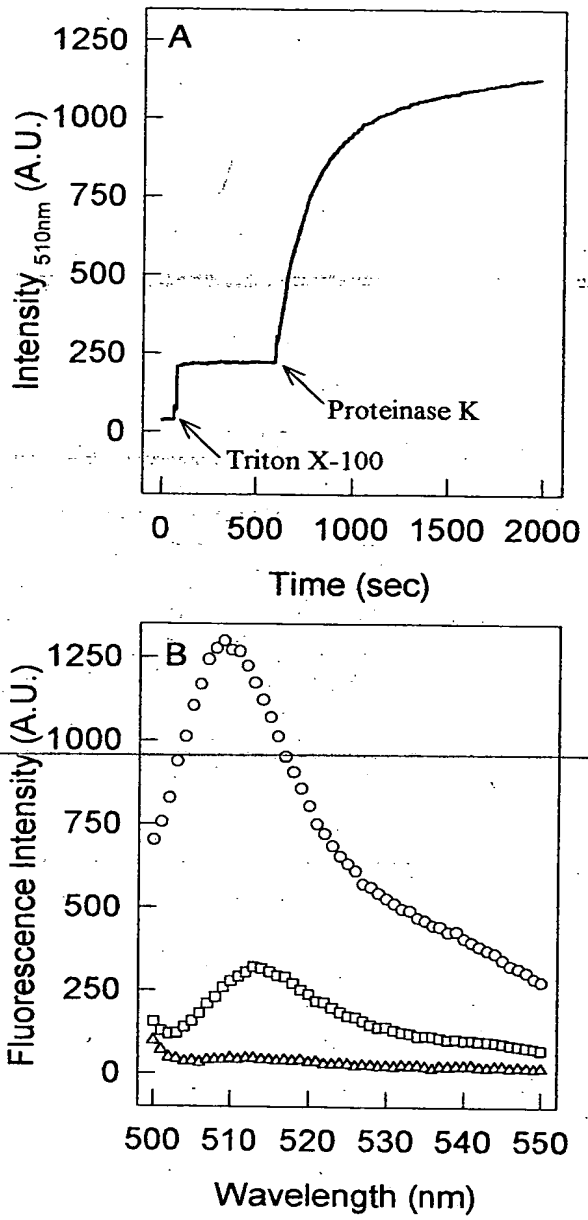

Fig. 6. Proteolytic degradation of Bodipy-VSV. (A) Fluorescence emission at 510 nm of a 2 μg/ml Bodipy-VSV sample was measured over time, at 37°C. Arrows indicate addition of 0.03% Triton X-100 or 500 μg/ml Proteinase K. (B) Fluorescence emission spectra were recorded prior to additions (△), after addition of Triton X-100 (□) and after incubation with Proteinase K for 30 min (○). Excitation wavelength was 490 nm.

addition of proteinase K promoted an additional four–six-fold increase in fluorescence intensity of the sample. Bodipy fluorescence emission spectra in each condition are shown in Fig. 6B. When the protease was added before detergent treatment, a ten-fold increase in fluorescence was observed. Addition of 0.03% Triton after proteolysis promoted a further increase of two-fold (not shown). Thus, increase in fluorescence obtained was approximately 20 fold whether the protease was added before or after incubation with Triton.

In order to compare the dependence of detergent- or protease-induced dequenching on the stoichiometry of labelling of Bodipy-VSV, in vitro studies were carried out using a different conjugate, in which the labelling ratio was reduced to 5000:1, as compared the 15000:1 ratio used throughout this work. In this conjugate, Bodipy fluorescence was 92.4% quenched and addition of Triton followed by addition of proteinase K led to fluorescence increases of five and three-fold, respectively (not shown). This result shows that a three-fold decrease in the labelling stoichiometry did not lead to loss of sensitivity of the conjugate to either disassembly or proteolysis.

3.5. Disassembly and proteolysis of Bodipy-VSV in live cells

In the previous sections Bodipy-VSV indicated both viral disassembly and degradation in vitro and to undergo fluorescence dequenching inside macrophages. In order to identify and quantify VSV disassembly and processing in live cells, Bodipy fluorescence dequenching in J774 macrophages was investigated, using flow cytometry. Macrophages were pulsed with Bodipy-VSV for a fixed time, washed and cell-associated fluorescence was measured at increasing times (Fig. 7, filled circles). Within 2 h, the percentage of fluorescent-labelled cells had gradually increased from 5 to 25% (circles, in panel A), which corresponded to an approximately two-fold increase in the average fluorescence intensity of the cell population (circles, in panel B). Between 2 and 3 h the fluorescence intensity remained constant. Thus, the kinetics measured by flow cytometry in live cells was compatible with the kinetics observed in fluorescence microscopy experiments.

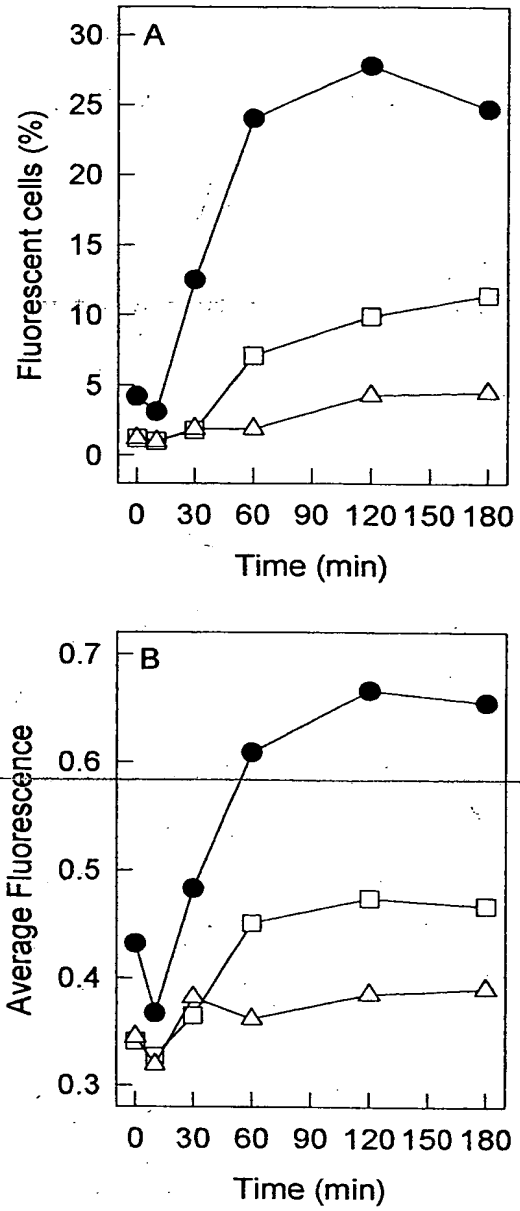

Fig. 7. Disassembly and proteolytic degradation of Bodipy-VSV in macrophages. Macrophages were pulsed for 10 min with 10 μg/ml Bodipy-VSV. After washing, cells were incubated for the time periods indicated in the abscissa and analysed by flow cytometry. Panel A shows the percentage of fluorescent cells obtained in a control experiment (●), in the presence of a mixture of protease inhibitors (□) or in the presence of both protease inhibitors and ammonium chloride (△). Panel B depicts results from the same experiment expressed as centers of mass of the fluorescence distributions.

The observed increase in cell-associated fluorescence might result from dissociation of the virus structure, proteolysis of labelled viral proteins, or a combination of both processes. To investigate the origin of fluorescence dequenching in macrophages, we have carried out experiments were carried out using ammonium chloride and inhibitors of three different types of cell proteases. When ammonium chloride and inhibitors were present simultaneously throughout the experiment, the increase in cellular fluorescence was abolished completely (Fig. 7, triangles). However, when only protease inhibitors were used, a significant increase in cell fluorescence was detected, although significantly lower than the fluorescence increase observed in control cells (Fig. 7, squares). In the presence of protease inhibitors alone (in the absence of ammonium chloride), acidification of endosomal compartments occurs normally. Thus, the significant fluorescence increase observed in this condition corresponded to an effect induced by acidification but independent of proteolysis. This probably reflects viral disassembly, or, more precisely, the separation of G protein molecules as a consequence of membrane fusion.

To confirm that the increase in fluorescence of cells incubated with protease inhibitors alone resulted from G protein dissociation and not from its denaturation or to residual activity of endosomal proteases, G protein was isolated from labelled virus and used for experiments similar to those described for the whole virus. In vitro proteolytic degradation of isolated G protein (with proteinase K) promoted a three-fold increase in Bodipy fluorescence (Fig. 8A). The initial fluorescence intensity of G protein before proteolytic degradation was higher than that observed for intact virus at the same concentration (compare triangles and squares in Fig. 8B). This difference is compatible with the more effective self-quench-

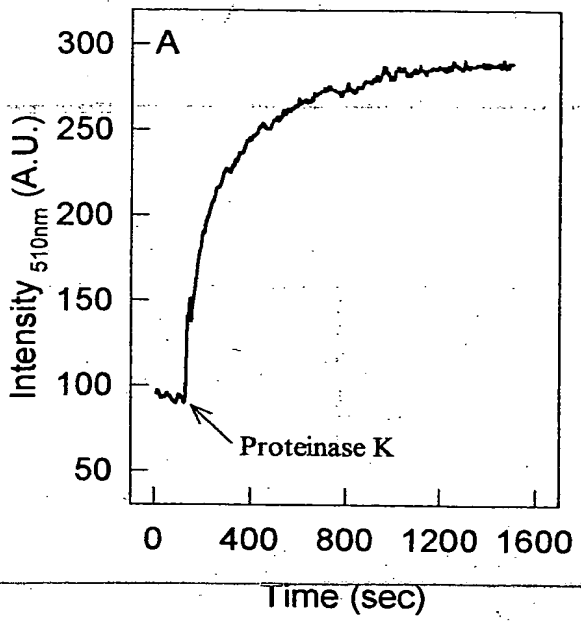

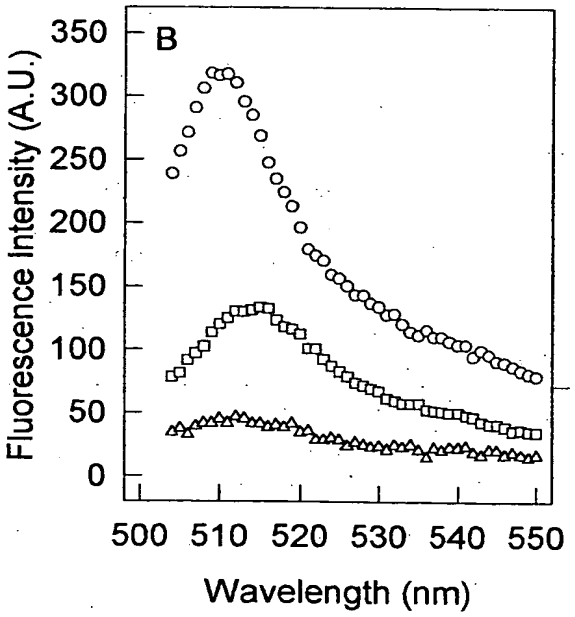

Fig. 8. Proteolysis of isolated Bodipy-labelled G protein detected by fluorescence dequenching. G protein was isolated from purified labelled virus (total protein concentration of 100 μg/ml) and diluted 50-fold before the experiment. (A) Bodipy fluorescence emission of isolated labelled G protein incubated at 37°C was measured at a fixed emission wavelength (510 nm). The arrow indicates addition of 500 μg/ml Proteinase K. (B) Fluorescence emission spectra were recorded for the purified labelled virus (2 μg/ml) (△) and for isolated G protein before (□) and after incubation with 500 μg/ml Proteinase K at 37°C for 30 min (○). Excitation wavelength was 490 nm.

ing expected to occur in the whole virus. When isolated G protein was incubated with 0.03% Triton, a small fluorescence increase (20%) was observed (not shown). This fluorescence increase can possibly be explained by the previous report that isolated G protein, after solubilisation with Triton and dialysis, forms small aggregates (Petri and Wagner, 1979). Addition of high detergent concentrations probably induced dissociation of G protein aggregates, leading to this modest increase in fluorescence. Similar aggregates have been observed for the isolated envelope glycoprotein of Semliki forest virus (Helenius et al., 1977) and Friend leukaemia virus (Schneider et al., 1979), as well as for the neuraminidase glycoprotein of influenza virus (Laver and Valentine, 1969).

Degradation of isolated G protein by macrophages was also followed by flow cytometry. The kinetics of degradation was measured in control cells, as well as in cells incubated in the presence of protease inhibitors, or in the presence of protease inhibitors plus ammonium chloride (Fig. 9A). Differently from observed with whole virus, no increase in intracellular fluorescence could be detected either in the presence of protease inhibitors or in the presence of protease inhibitors plus ammonium chloride (Fig. 9A). This result confirmed that the increase in intracellular fluorescence after internalisation of intact Bodipy-VSV observed in the presence of protease inhibitors (Fig. 7, squares) was due to virus disassembly in the endosomes. As an additional control to confirm that complete inhibition of protein degradation occurred in cells incubated with protease inhibitors in the absence of ammonium chloride, the same type of experiment was repeated, using a highly substituted Bodipy-BSA conjugate (Fig. 9B). Similarly to the result found for G protein, no significant intracellular fluorescence enhancements were observed for cells treated with protease inhibitors alone or combined with ammonium chloride.

4. Discussion

We have shown that Bodipy-VSV is a sensitive probe to study VSV disassembly and processing in live macrophages. The sensitivity of the conjugate to viral disassembly was due to fluorescence homotransfer between different viral proteins,

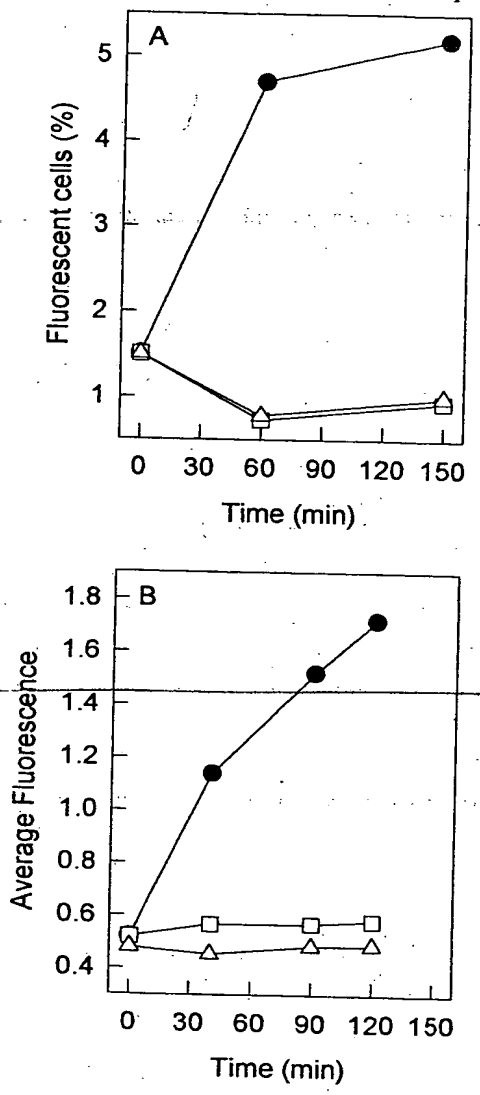

Fig. 9. Degradation of Bodipy-G protein by macrophages. Macrophages were pulsed for 30 min with 3 μg/ml Bodipy-labelled G protein. After washing, cells were chased for the time periods indicated in the abscissa and analysed by flow cytometry. Panel A shows the percentage of fluorescent cells obtained in the absence of additions (●), in the presence of a mixture of protease inhibitors (□) or in the presence of both protease inhibitors and ammonium chloride (△). Panel B shows a similar experiment performed for Bodipy-BSA at a final concentration of 20 μg/ml.

whereas sensitivity to proteolytic processing originated from energy transfer between Bodipy molecules localised in a single polypeptide chain.

In vitro studies showed that treatment of Bodipy-VSV with Triton or octylglucoside led to dequenching of Bodipy fluorescence. It has been shown previously that non-ionic detergents solubilise G protein from native virions but do not promote extraction of M and N proteins (Newcomb and Brown, 1981). In the conditions used above, i.e. 60 mM octylglucoside or 1% Triton at low ionic strength, only G protein and lipids are solubilised, leaving insoluble structures called 'skeletons', which contain viral RNA complexed with N and M proteins (Cartwright et al., 1970; Newcomb and Brown, 1981). Therefore, although N and M proteins were also labelled in the Bodipy-VSV conjugate (Fig. 4), the detergent-induced increase in fluorescence measured in vitro corresponded exclusively to relaxation of self-quenching occurring between Bodipy-labelled G proteins or between G proteins and 'skeleton' N and M proteins.

In situ studies showed that the increase in fluorescence observed in macrophages resulted from two additive effects, one sensitive to protease inhibitors plus ammonium chloride and another inhibited by ammonium chloride alone. The latter component was identified as corresponding to relaxation of self-quenching between neighbouring G proteins upon fusion of VSV envelope with the endosomal membrane, a process known to depend on pH acidification (Matlin et al., 1982b). Since N and M proteins were also labelled with Bodipy, it is possible that their dissociation following membrane fusion also contributed to the observed fluorescence dequenching. It is not known whether the VSV nucleocapsid evades the endosomes to the cytosol while still preserving its RNA-N protein assembly or whether the nucleic acid becomes fully uncoated after fusion. Experiments with Semliki Forest virus (SFV) have shown that uncoating depends on the interaction of virus capsid protein and the 60S ribosomal subunits (Singh and Helenius, 1992), which suggests that the nucleocapsid structure might be preserved in infected cells until SFV nucleocapsid encounters a ribosome. However, in the case of influenza virus, the proton channel M2 protein promotes internal acidification of the virus, priming the nucleocapsid for dissociation upon penetration into the cytosol (Helenius, 1992). Selective labelling of VSV N protein with Bodipy may be employed in the future to elucidate the uncoating step of VSV infection.

Bodipy-VSV has also been shown to be a sensitive probe for monitoring proteolytic degradation by endosomal proteases. In situ studies on viral processing are particularly interesting because endosomes of fibroblasts, which are model VSV hosts, have been shown to possess constitutive proteases (Roederer et al., 1987; Schaudies et al., 1987). Thus, some extent of degradation of viral proteins may occur during infection of viruses internalised by endocytosis. This phenomenon can be easily detected in target cells using the methodology described here. Densely labelled protein conjugates, such as self-quenched fluorescein-BSA, have previously been used to study proteolytic cleavage, which was accompanied by significant increases in fluorescence intensity (Voss et al., 1996). Exogenous proteinase K and chymotrypsin promoted an approximately 28-fold increase in fluorescence emission of FITC-BSA, whereas digestion with trypsin resulted in a 14-fold increase (Voss et al., 1996). Proteolysis of Bodipy-labelled BSA also led to fluorescence enhancements of similar magnitude (Reis, R.C.M., Sorgine, M.H.F. and Coelho-Sampaio, T., unpublished results).

The present study deals with the intracellular fate of VSV in macrophages. Although other cells of the immune system, such as T lymphocytes, can be infected by VSV, macrophages are not natural targets for VSV infection (Whitton and Oldstone, 1996). For this reason, this study did not focus on the investigation of either the mechanism or the kinetics of VSV internalisation by macrophages. However, as a widely distributed antigen-presenting cell (APC), macrophages can internalise VSV, participating in the general immune response against the virus. The short-lived generation of antibodies against VSV is known to be predominantly helper T-cell independent (Charan and Zinkernagel, 1986). However, long-lived

production of IgG is dependent on the presence of helper T-cells and, hence, on antigen presentation by APC (Leist et al., 1987). Thus, internalisation of virus by macrophages and presentation to helper T-cells take part in the development of a humoral response against VSV.

The cytotoxic T-cell-mediated response against VSV plays a major role in the elimination of VSV infection. Participation of APC-activated CD4+ T-cells in the cytotoxic response against different viruses has been shown to vary largely depending on virus type and on the spectrum of cytokine production associated with different viruses (Doherty et al., 1992). In this regard, the involvement of CD4+ T-cells has been demonstrated in the case of chronic infection by lymphocytic choriomeningitis virus (Matloubian et al., 1994). In the case of VSV, CD4+ cytotoxic T cells have been shown to mediate lysis of APCs presenting soluble G protein fragments in the context of MHC II, which has been postulated to mediate the spread of viral pathogenicity in infected tissues (Browning et al., 1990). In this case, recognition by T cells has been demonstrated to be strictly dependent on proteolytic degradation of soluble G protein in acidic vacuoles in the APC.

In conclusion, the results demonstrate the feasibility and interest in employing viral particles densely labelled with Bodipy to examine in real-time the intracellular disassembly and processing of VSV. Similar studies using other viruses and target cells are possible and will contribute to the understanding of the mechanisms of viral infection. In this regard, we have recently observed that VSV labelled 5000:1 with Bodipy was able to infect fibroblats with efficiency similar to that of unlabelled virus and that the kinetics of disassembly could be clearly followed through Bodipy fluorescence dequenching (Da Poian, A.T., Coelho-Sampaio, T., unpublished results).

Acknowledgements

We thank Dr. Sérgio T. Ferreira for use of his laboratory facilities, for suggestions and for critical reading of this manuscript. We also thank Dr. Jerson L. Silva for use of the tissue culture facility and the fluorescence microscope. The authors are indebted to Drs. Ana Beatriz F. Pacheco and Maria Lucia Bianconi for their expert help. Flow cytometry measurements were performed at the Flow Cytometry Facility at the Institute of Biophysics Carlos Chagas Filho (Federal University of Rio de Janeiro), with the valuable assistance of Carlos B. Daniel.

This work was supported by grants from the Brazilian agencies Fundação de Amparo à Pesquisa do Estado do Rio de Janeiro (FAPERJ) and Conselho Nacional de Desenvolvimento Científico e Tecnológico (CNPq) (TCS and ATDP), and Fundação Universitaria Jose Bonifacio (FUJB) (ATDP).

References

Bishop, D.H.L., Repik, P., Obijeski, J.F., Moore, N.F., Wagner, R.R., 1975. Restitution of infectivity to spikeless vesicular stomatitis virus by solubilized viral components. J. Virol. 16, 75–84.

Blumenthal, R., Bali-Puri, A., Walter, A., Covell, D., Eidelman, O., 1987. pH-dependent fusion of vesicular stomatitis virus with Vero cells. J. Biol. Chem. 262, 13614–13619.

Browning, M., Reiss, C.S., Huang, A.S., 1990. The soluble viral glycoprotein of vesicular stomatitis virus efficiently sensitizes target cells for lysis by CD4+ lymphocytes. J. Virol. 64, 3810–3816.

Cartwright, B., Smale, C.J., Brown, F., 1970. Dissection of vesicular stomatitis virus into the infective ribonucleoprotein and immunizing components. J. Gen. Virol. 7, 19–32.

Charan, S., Zinkernagel, R.M., 1986. Antibody mediated suppression of secondary IgM response in nude mice against vesicular stomatitis virus. J. Imunol. 136, 3057–3061.

Choppin, P.W., Compans, R.W., 1975. Replication of paramyxoviruses. Compr. Virol. 4, 94–178.

Da Poian, A.T., Gomes, A.M.O., Oliveira, R.J.N., Silva, J.L., 1996. Migration of vesicular stomatitis virus glycoprotein to the nucleus of infected cells. Proc. Natl. Acad. Sci. U.S.A. 93, 8268–8273.

Doherty, P.C., Allan, W., Eichelberger, M., Carding, S.R., 1992. Roles of $\alpha\beta$ and $\gamma\delta$ T cell subsets in viral immunity. Annu. Rev. Immunol. 10, 123–151.

Doms, R.W., Keller, D.S., Helenius, A., Balch, W.E., 1987. Role of adenosine triphosphate in regulating the assembly and transport of vesicular stomatitis virus G protein trimers. J. Cell Biol. 105, 1957–1969.

Dubovi, E.J., Wagner, R.R., 1977. Spatial relationships of the proteins of vesicular stomatitis virus: induction of reversible oligomers by cleavable protein cross-linkers and oxidation. J. Virol. 22, 500–509.

Gallione, C.J., Greene, J.R., Iverson, L.E., Rose, J.K., 1981. Nucleotide sequences of the mRNA's encoding the vesicular stomatitis virus N and NS proteins. J. Virol. 39, 529–535.

Gaudin, Y., Ruigrok, R.W.H., Brunner, J., 1995. Low-pH induced conformational changes in viral fusion proteins: implications for the fusion mechanism. J. Gen. Virol. 76, 1541–1556.

Helenius, A., 1992. Unpacking the incoming influenza virus. Cell 69, 577–578.

Helenius, A., Fries, E., Kartenbeck, J., 1977. Reconstitution of Semliki forest virus membrane. J. Cell Biol. 75, 866–880.

Helenius, A., Marsh, M., White, J., 1980. The entry of viruses into animal cells. Trends Biochem. Sci. 5, 104–106.

Hernandez, L.D., Hoffman, L.R., Wolfsberg, T.G., White, J.M., 1996. Virus–cell and cell–cell fusion. Annu. Rev. Cell Dev. Biol. 12, 627–661.

Kreis, T.E., Lodish, H.F., 1986. Oligomerization is essential for transport of vesicular stomatitis virus glycoprotein to the cell surface. Cell 46, 929–937.

Lanzrein, M., Schlegel, A., Kempf, C., 1994. Entry and uncoating of enveloped viruses. Biochem. J. 302, 313–320.

Laver, W.G., Valentine, R.C., 1969. Morphology of the isolated hemagglutinin and neuraminidase subunits of influenza virus. Virology 38, 105–119.

Leist, T.P., Cobbold, S.P., Waldmann, H., Aguet, M., Zinkernagel, R.M., 1987. Functional analysis of T lymphocyte subsets in antiviral host defense. J. Immunol. 138, 2278–2281.

Lyles, D.S., Varela, V.A., Parce, J.W., 1990. Dynamic nature of the quaternary structure of the vesicular stomatitis virus envelope glycoprotein. Biochemistry 29, 2442–2449.

Marsh, M., Helenius, A., 1989. Virus entry into animal cells. Adv. Virus Res. 36, 107–151.

Mathieu, M.E., Grigera, P.R., Helenius, A., Wagner, R.R., 1996. Folding, unfolding and refolding of the vesicular stomatitis virus glycoprotein. Biochemistry 35, 4084–4093.

Matlin, K.S., Reggio, H., Helenius, A., Simons, K., 1982a. Infectious entry pathway of influenza virus in a canine kidney cell line. J. Cell Biol. 91, 601–613.

Matlin, K.S., Reggio, H., Helenius, A., Simons, K., 1982b. Pathway of vesicular stomatitis virus entry leading to infection. J. Mol. Biol. 156, 609–631.

Matloubian, M., Conception, R.J., Ahmed, R., 1994. CD4+ T cells are required to sustain CD8+ cytotoxic T-cell responses during chronic viral infection. J. Virol. 68, 8056–8063.

Newcomb, W.W., Brown, J.C., 1981. Role of the vesicular stomatitis virus matrix protein in maintaining the viral nucleocapsid in the condensed form found in native virions. J. Virol. 39, 295–299.

Pal, R., Barenholz, Y., Wagner, R.R., 1988. Pyrene phospholipids as biological fluorescent probes for studying fusion of virus membranes with liposomes. Biochemistry 27, 30–36.

Petri, W.A., Wagner, R.R., 1979. Reconstitution into liposomes of the glycoprotein of vesicular stomatitis virus by detergent dialysis. J. Biol. Chem. 254, 4313–4316.

Roederer, M., Bowser, R., Murphy, R.F., 1987. Kinetics and temperature dependence of exposure of endocytosed material to proteolytic enzymes and low pH: Evidence for a maturation model for the formation of lysosomes. J. Cell. Phys. 131, 200–209.

Rose, J.K., Gallione, C.J., 1981. Nucleotide sequences of the mRNA's encoding the vesicular stomatitis virus G and M proteins determined from cDNA clones containing the complete coding regions. J. Virol. 39, 519–528.

Schaudies, R.P., Gorman, R.M., Savage, C.R. Jr., Poretz, R.D., 1987. Proteolytic processing of epidermal growth factor within endosomes. Bioch. Biophys. Res. Commun. 143, 710–715.

Schlegel, R., Dickson, R.B., Willingham, M.C., Pastan, I.H., 1982. Amantadine and dansylcadaverine inhibit vesicular stomatitis virus uptake and receptor-mediated endocytosis of α_2-macroglobulin. Proc. Natl. Acad. Sci. U.S.A. 79, 2291–2295.

Schneider, J., Schwarz, H., Hunsmann, G., 1979. Rosettes from Friend leukemia virus envelope: preparation and physicochemical and partial biological characterization. J. Virol. 29, 624–632.

Singh, I., Helenius, A., 1992. Role of ribosome's in Semliki forest virus nucleocapsid uncoating. J. Virol. 66, 7049–7058.

Thomas, D., Newcomb, W.W., Brown, J.C., Wall, J.S., Hainfeld, J.F., Trus, B.L., Steven, A.C., 1985. Mass and molecular composition of vesicular stomatitis virus: a scanning transmission electron microscopy analysis. J. Virol. 54, 598–607.

Voss, E.W. Jr., Workman, C.J., Mummert, M.E., 1996. Detection of protease activity using a fluorescence-enhancement globular substrate. Biotechniques 20, 286–291.

Wagner, R.R., 1987. Rhabdovirus biology and infection. An overview. In: Wagner, R.R. (Ed.), The Rhabdoviruses. Plenum, New York, pp. 9–74.

White, J., Matlin, K., Helenius, A., 1981. Cell fusion by Semliki Forest virus, influenza and vesicular stomatitis virus. J. Cell Biol. 89, 674–679.

Whitton, J.L., Oldstone, M.B.A., 1996. Immune response to viruses. In: Fields, B.N., Knipe, D.M., Howley, P.M., Chanock, R.M., Melnick, J.L., Monath, T.P., Roizman, B., Straus S.E. (Eds), Fields Virology. 3rd edn. Lippincott–Raven, Philadelphia, PA, pp. 345–374.

Wilcox, M.D., McKenzie, M.O., Parce, J.W., Lyles, D.S., 1992. Subunit interactions of vesicular stomatitis virus envelope glycoprotein influenced by detergent micelles and lipid bilayers. Biochemistry 31, 10458–10464.

THE JOURNAL OF BIOLOGICAL CHEMISTRY

Vol. 271, No. 48, Issue of November 29, pp. 30811–30815, 1996
Printed in U.S.A.

Recombinant Mouse Bcl-$2_{(1-203)}$

TWO DOMAINS CONNECTED BY A LONG PROTEASE-SENSITIVE LINKER*

(Received for publication, June 11, 1996, and in revised form, August 6, 1996)

Barbara A. Vance‡, Charles M. Zacharchuk§, and David M. Segal‡¶

From the ‡Experimental Immunology Branch and §Laboratory of Immune Cell Biology, NCI, National Institutes of Health, Bethesda, Maryland 20892-1360

Bcl-2 is a cytoplasmic integral membrane protein with potent anti-apoptotic activity but whose mechanism of action is poorly understood. The purpose of this paper was to obtain large amounts of soluble Bcl-2 protein for structural and functional studies. Mouse Bcl-$2_{(1-203)}$ (missing the COOH-terminal hydrophobic tail) was produced in bacterial inclusion bodies, solubilized in guanidine, and refolded by dialysis. The resulting protein was monomeric in nondenaturing solution and was active in protecting mouse T hybridoma cells from glucocorticoid-induced apoptosis. Refolded Bcl-$2_{(1-203)}$ showed no tendency to homodimerize by gel filtration or analytical ultracentrifugation. Limited proteolysis experiments identified a region between the BH3 and BH4 homology domains of Bcl-$2_{(1-203)}$ which was extremely susceptible to digestion by several common proteases, but not by a cell extract known to contain CPP-32-like (interleukin-1β-converting enzyme family) protease activity. The protease-sensitive sites were located within a 50-residue stretch that contained most of the nonconserved and proline residues of Bcl-$2_{(1-203)}$. Trypsin-cleaved Bcl-$2_{(1-203)}$ eluted in the same position as the undigested protein on gel filtration in nondenaturing solution, indicating that the two portions of the molecule connected by the protease-sensitive region associate stably and noncovalently. The solution properties of Bcl-$2_{(1-203)}$ suggest that it consists of two noncovalently associated domains connected by a long protease-sensitive linker and that its structure is similar to that of Bcl-x_L, which has been determined by x-ray and NMR analysis.

Bcl-2 was first detected as a t(14:18) chromosomal translocation in follicular B cell lymphomas/leukemias (1) which placed the Bcl-2 gene under the control of the Ig heavy chain promoter, resulting in its overproduction. Subsequent work indicated that overexpression of Bcl-2 prolonged cell survival (2) and inhibited programmed cell death induced by multiple, diverse stimuli including growth factor withdrawal, glucocorticoids, and γ-irradiation (3, 4). Bcl-2 is an intracellular transmembrane protein and was the first member described of a new family of structurally related proteins which now includes Bax, Bak, Bcl-x, ced-9, Mcl-1, A1, NR13, Bad, and Bik, all of which either promote or inhibit programmed cell death (5, 6). A number of studies have identified four domains that are highly conserved among Bcl-2 family members and which are required for Bcl-2 function. From the NH_2 terminus, these Bcl-2 homology regions are designated BH4, BH3, BH1, and BH2 (see Fig. 6). Mutational analyses of Bcl-2 have shown that amino acid residues within BH4, BH1, and BH2 are required for its anti-apoptotic activity (7–9). In addition, immunoprecipitation or yeast two-hybrid experiments have demonstrated that Bcl-2 forms homodimers using residues within BH4, BH1, and BH2 (9–11). Bcl-2 also heterodimerizes with the pro-apoptotic protein Bax, resulting in enhanced cell survival (9, 12). Heterodimerization involves residues from BH1 and BH2 in Bcl-2 (9) and residues from BH3 in Bax (13) and the related protein, Bak (14).

Recently, the x-ray and NMR structures of the cytoplasmic portion of Bcl-x_L, a molecule sharing 35% amino acid sequence identity with Bcl-2, have been published (15). The structure consists of seven associated α-helices and a long flexible region that connects the first and second helices. The first helix (α1) comprises most of BH4, whereas the remaining helices lie in the COOH-terminal part of the molecule which contains BH1, BH2, and BH3. The flexible domain corresponds to a region of the Bcl-x_L and Bcl-2 molecules which exhibits the greatest variability in amino acid sequence between molecules from different species and Bcl-2 family members. Unlike the BH1–4 regions, the flexible domain can be deleted without loss of anti-apoptotic activity (7, 15).

Since most previous studies have focused on Bcl-2 rather than Bcl-x, it is important to establish that Bcl-2 and Bcl-x have similar structures. Previous work showed that mouse Bcl-2 truncated at residue 203 (approximately 12 residues NH_2-terminal of the transmembrane portion) retained biologic activity (8, 16). In the current paper we have produced recombinant mouse Bcl-$2_{(1-203)}$ in bacteria. We show that refolded Bcl-$2_{(1-203)}$ is active, contains a long, protease-sensitive portion that corresponds to the Bcl-2 variable region, and that the NH_2- and COOH-terminal portions remain noncovalently associated following digestion. Our data indicate that Bcl-2 and Bcl-x have similar structures.

MATERIALS AND METHODS

Cloning of Bcl-$2_{(1-203)}$—DNA encoding Bcl-$2_{(1-203)}$ was prepared by polymerase chain reaction amplification of a plasmid containing a full-length murine Bcl-2 cDNA (a kind gift from Dr. Jeff Huth, NIDDK, Bethesda, MD) using 5′ primer CTTGCAGAAGGAGATATACATATGGCGCAAGCCGGGAGAACA and 3′ primer GTTAGCAGCCCTCGAGTTATTACATGCTGGGGCCATATA. The polymerase chain reaction product was cloned directly into pCR™II with an Invitrogen (San Diego, CA) TA cloning kit. The insert encoding Bcl-$2_{(1-203)}$ was removed by digestion with *NdeI* and *XhoI* and subcloned into *NdeI*/*XhoI* sites of pET21a (Novagen, Madison, WI). Sequence analysis using the dideoxy chain termination procedure confirmed that the insert contained the correct Bcl-$2_{(1-203)}$ sequence. The BL21(DE3) strain of *Escherichia coli* was transformed with the pET21aBcl-$2_{(1-203)}$ plasmid for protein expression.

Induction and Purification of Bcl-$2_{(1-203)}$ Protein—Transformed bacteria were grown to an OD_{600} of 0.4–0.8 and induced with isopropyl-β-

* The costs of publication of this article were defrayed in part by the payment of page charges. This article must therefore be hereby marked "*advertisement*" in accordance with 18 U.S.C. Section 1734 solely to indicate this fact.

¶ To whom correspondence should be addressed: Bldg. 10, Rm. 4B17, NIH, 9000 Rockville Pike, Bethesda, MD 20892-1360. Tel.: 301-496-4746; Fax: 301-496-0887.

REF. 8

D-thiogalactoside (Calbiochem) as described (17). The bacteria were pelleted and resuspended in 20 ml of 5 × TE (1 × TE = 0.01 M Tris, 1 mM EDTA, pH 7.5) for each 500 ml of culture. Chicken egg white lysozyme (Sigma Chemical Co.) was added to a final concentration of 0.1 mg/ml, and the bacteria were incubated 1 h at 30 °C and then frozen at −20 °C. After thawing, purified inclusion bodies were prepared by washing (17). The purified inclusion bodies were stored at −70 °C.

Refolding of Bcl-$2_{(1-203)}$—Purified inclusion bodies containing Bcl-$2_{(1-203)}$ protein were solubilized in 6 M guanidine HCl, 10 mM dithiothreitol and diluted to 0.5 mg/ml in the same solvent. This solution was dialyzed at 4 °C against 10 volumes of TE containing 0.4 M arginine, 1 mM dithiothreitol for 24 h with two solution changes. The dialyzed protein was concentrated with Centriprep 10 concentrators (Amicon, Beverly, MA) and fractionated on a 100 × 2.6-cm Sephacryl S-200 preparative gel filtration column in the same solvent (Pharmacia Biotech Inc.). The peak corresponding to monomeric Bcl-$2_{(1-203)}$ was collected, concentrated, and stored at 4 °C. In later experiments, the guanidine-solubilized protein was dialyzed twice against 10 volumes of TE containing 0.4 M arginine and twice against 10 volumes of borate-buffered saline (BBS[1]; 0.15 M NaCl, 0.01 M sodium borate, pH 8.5) at 4 °C, centrifuged for 10 min at 32,000 × *g*, and the supernatant concentrated. Protein prepared in this way was as homogeneous as Bcl-$2_{(1-203)}$ that had been purified by gel filtration.

Transient Transfection Death Assay—The transient transfection death assay was performed as described previously (18) except that refolded Bcl-2 protein instead of a Bcl-2 plasmid expression vector was electroporated into cells. Bovine serum albumin or Bcl-$2_{(1-203)}$ refolded protein (approximately 1 mg/ml) was dialyzed against RPMI 1640 with 20 mM HEPES. 2B4.11 cells were pelleted and resuspended in the protein solution to which 5 μg of cytomegalovirus β-galactosidase reporter and 10 μg of pCIFas (expression vector for human Fas) DNA were added per cuvette. Following electroporation, the cells were cultured in medium or treated with dexamethasone or anti-Fas monoclonal antibody CH11 (Kamiya, Thousand Oaks, CA). The transfected cells were incubated overnight and assayed for β-galactosidase as described (18).

Gel Filtration, SDS-Polyacrylamide Gel Electrophoresis (PAGE), and Protein Concentration—Gel electrophoresis was done with a Pharmacia PhastSystem®. Homogeneous 20% gels and pH 3–9 gels were used for SDS-PAGE and isoelectric focusing (IEF), respectively. All gels shown in this study were stained with Coomassie Brilliant Blue. Analytical gel filtration was done using an HR 10/30 Superdex 75 column in BBS on a Pharmacia FPLC® unit. Protein concentration was determined using a calculated E_{280} of 1.7 for a 1 mg/ml solution (19).

NH_2-terminal Protein Sequencing—NH_2-terminal protein sequencing was done by Patricia Spinella, Protein Expression Laboratory, NIH, using an Applied Biosystems Protein Sequencer. Trypsin-digested Bcl-$2_{(1-203)}$ was run on a 13% SDS-polyacrylamide gel, transferred to a polyvinylidene disulfide membrane, and individual bands were sequenced.

Jurkat Cell Extracts—Detergent extracts from anti-Fas-treated apoptotic Jurkat cells were a gift from Dr. Ming-Lei Wu, NCI. They were prepared essentially as described (20) and hydrolyzed the fluorogenic substrate ZDEVD-AFC (which measures CPP-32-like interleukin-1β-converting enzyme family proteolytic activity) at a 1:250 dilution.

Analytical Ultracentrifugation—Molecular weights were determined by equilibrium sedimentation by David Millar (NIDDK) using a Beckman XL-A analytical ultracentrifuge. Bcl-$2_{(1-203)}$ was dialyzed against BBS and loaded into centrifuge cells at concentrations of 0.44, 0.27, and 0.13 mg/ml. Equilibrium runs were done for 48 h at 5 °C at a rotor speed of 12,000 rpm. Data were analyzed using Beckman software.

RESULTS

Expression and Folding of Bcl-$2_{(1-203)}$ Protein—Mouse Bcl-$2_{(1-203)}$, a 22.5-kDa protein that lacks the membrane-spanning region, was produced in *E. coli* as insoluble inclusion bodies. Fig. 1*A* shows that induced bacteria produced large amounts of a 25-kDa protein that was easily purified by washing the inclusion bodies. After solubilization in guanidine and dialysis, the resulting protein eluted on gel filtration in nondenaturing solution as a single peak with an M_r of 22,000 (Fig. 1*B*). Column-purified Bcl-$2_{(1-203)}$ gave a single band by SDS-PAGE

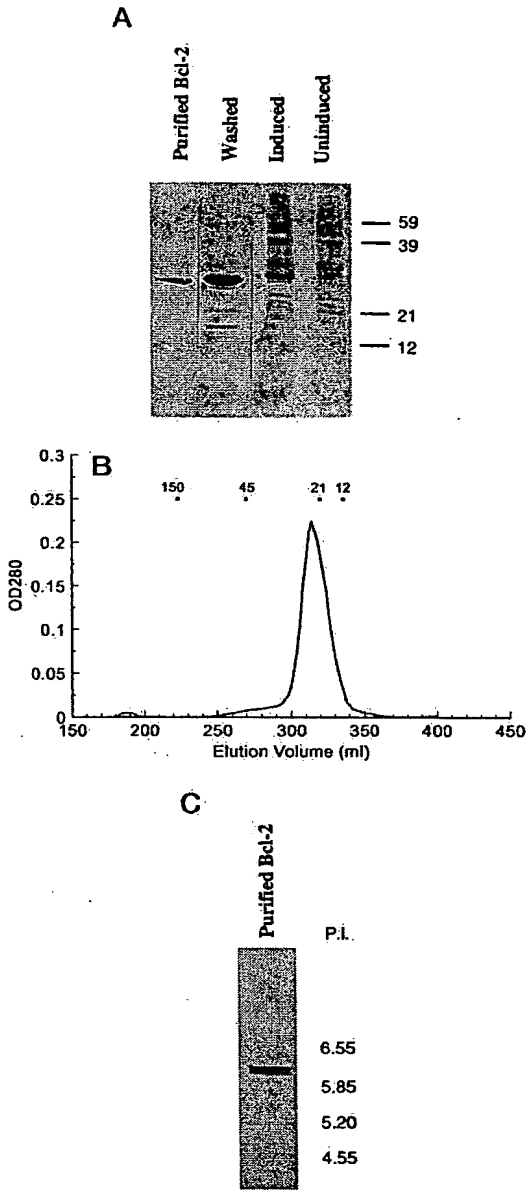

FIG. 1. **Expression and folding of Bcl-$2_{(1-203)}$ protein.** *Panel A*, SDS-PAGE of uninduced or induced bacterial lysates, washed inclusion bodies, and refolded, gel-purified Bcl-$2_{(1-203)}$. The anomalously low migration rate of Bcl-$2_{(1-203)}$ relative to the standards is probably due to its lack of disulfide bonds. *Panel B*, preparative gel filtration of Bcl-$2_{(1-203)}$ after solubilization in guanidine, dialysis, and concentration. *Panel C*, IEF of purified, refolded Bcl-$2_{(1-203)}$. The sample was applied near the high pH end of the IEF gel.

(Fig. 1*A*) and two very closely spaced bands by IEF near the predicted isoelectric point of 6.05 (Fig. 1*C*). The IEF results revealed minor heterogeneity, perhaps due to partial deamidation of Asn or Gln residues. NH_2-terminal sequence analysis confirmed that the refolded protein was indeed Bcl-2 (see Fig. 6). Bcl-$2_{(1-203)}$ protein was soluble at 1–2 mg/ml in physiological buffers but precipitated at higher concentrations; typical yields were 5–10 mg of refolded Bcl-$2_{(1-203)}$/liter of bacteria. Since misfolded proteins tend to aggregate in nondenaturing solvents (21) and precipitate on IEF gels, these data suggest

[1] The abbreviations used are: BBS, borate-buffered saline; PAGE, polyacrylamide gel electrophoresis; IEF, isoelectric focusing.

TABLE I
Bcl-2$_{(1-203)}$ inhibits apoptosis

Bovine serum albumin (control) and Bcl-2$_{(1-203)}$ proteins (approximately 1 mg/ml) were electroporated into 2B4.11 T hybridoma cells along with a plasmid encoding β-galactosidase. Cells were then treated with dexamethasone (Dex) or anti-Fas monoclonal antibody (mAb) as indicated, and the numbers of viable, transfected cells were determined by β-galactosidase expression. Cytotoxicity is expressed as the percentage decrease of β-galactosidase signal in samples treated with programmed cell death inducer relative to the untreated controls. Two representative experiments are shown.

Programmed cell death inducer	% Cytotoxicity	
	BSA	Bcl-2
Experiment 1		
Dex (10 nM)	34	−8
Dex (100 nM)	56	18
Anti-Fas mAb (5 ng/ml)	46	41
Experiment 2		
Dex (10 nM)	33	16
Dex (100 nM)	57	26
Anti-Fas mAb (5 ng/ml)	28	22

that Bcl-2$_{(1-203)}$ was folded correctly.

Recombinant Bcl-2 Protein Is Active—Overexpression of Bcl-2 or Bcl-2$_{(1-203)}$ inhibits dexamethasone-induced, but not Fas-mediated, apoptosis in the mouse T cell hybridoma 2B4.11 (Ref. 18 and data not shown). To determine if the bacterially expressed and refolded Bcl-2$_{(1-203)}$ protein was functionally active, 2B4 cells were electroporated with either bovine serum albumin or Bcl-2$_{(1-203)}$ protein (Table I). A plasmid expressing β-galactosidase was cotransfected to provide a measure of viable, transfected cells (18). The refolded Bcl-2$_{(1-203)}$ protein inhibited dexamethasone-induced death, at two different concentrations, but did not block anti-Fas-induced death. Thus, the bacterially produced Bcl-2$_{(1-203)}$ protein showed qualitatively the same anti-apoptotic activity as the transfected full-length Bcl-2 gene.

Bcl-2$_{(1-203)}$ Does Not Self-associate—Because Bcl-2 has been reported to homodimerize (9, 10), we asked whether recombinant Bcl-2$_{(1-203)}$ would form aggregates in solution. Initial studies using size exclusion chromatography at different Bcl-2$_{(1-203)}$ concentrations failed to reveal stable self-association. Analytical equilibrium ultracentrifugation was therefore used as a more sensitive probe of aggregation. At equilibrium, the mass distribution data were best fit by a single species with a molecular mass of 23 kDa, with less than 3% aggregate, over the full concentration range tested (Fig. 2). The highest concentration of Bcl-2$_{(1-203)}$ in the centrifuge cell exceeded 0.5 mg/ml (22 μM). At this concentration we would have detected self-association if the K_d had been 200 μM or less.

Limited Proteolysis of Bcl-2$_{(1-203)}$—We next probed the structure of Bcl-2$_{(1-203)}$ by limited proteolysis using three relatively nonspecific proteases. When Bcl-2$_{(1-203)}$ was incubated with trypsin, chymotrypsin, or papain, discrete bands were produced by each of the proteases at low protease:Bcl-2 ratios (Fig. 3). Trypsin digestion at a weight ratio as low as 1:6,400 gave two major fragments migrating at about 15 and 10 kDa. Chymotrypsin also produced two bands, one larger than the 15-kDa tryptic fragment, and one smaller than the 10-kDa peptide. Finally, papain produced a 12-kDa band and a larger fragment that disappeared rapidly. The fact that very low concentrations of three different proteases each produced one or two large fragments suggests that Bcl-2$_{(1-203)}$ contains one or more regions that are highly exposed, with the remaining regions being protected from proteolytic attack. In view of its high susceptibility to cleavage by common proteases, Bcl-2$_{(1-203)}$ was also tested with extracts from Jurkat cells that contained CPP-32-like (interleukin-1β-converting enzyme family) protease activity. After a 30-min incubation at 37 °C, undiluted cell extract did not cleave Bcl-2$_{(1-203)}$ (data not shown).

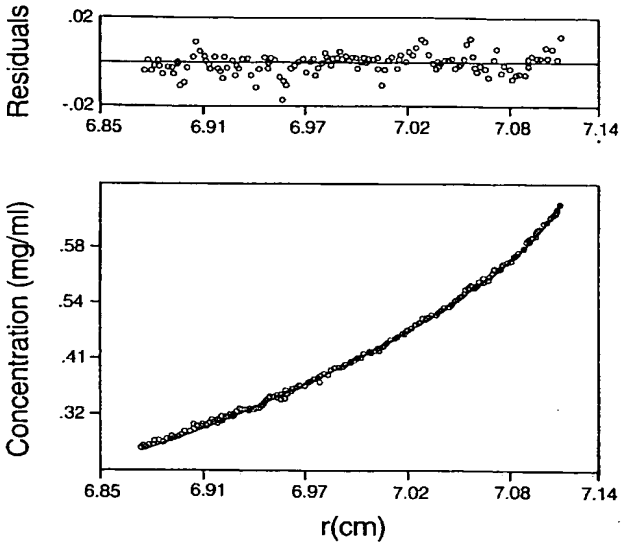

FIG. 2. **Ultracentrifugal analysis of Bcl-2$_{(1-203)}$ at 5 °C.** Equilibrium mass distribution data (points) are best fit to a model (line) in which 97% of the protein has a molecular mass of 23 kDa, and 3% has a molecular mass of 130 kDa. Residuals of the fit are shown in the *upper panel*.

Time Course of Digestion and Noncovalent Association of Tryptic Fragments—Bcl-2$_{(1-203)}$ was digested with trypsin for various times, and the reaction products were examined by SDS-PAGE and size exclusion chromatography. SDS-PAGE (Fig. 4B) showed that by 10 min, most of the Bcl-2$_{(1-203)}$ was digested into the two major fragments described above. Both bands appeared simultaneously, suggesting that they were produced by a single cleavage of the intact Bcl-2 molecule. In contrast, these same samples, when analyzed by gel filtration in nondenaturing solution (Fig. 4A) showed little evidence of fragmentation into peptides of the size observed by SDS-PAGE, indicating that the two tryptic peptides remained associated by noncovalent interactions. To confirm this, Bcl-2$_{(1-203)}$ was digested with trypsin, fractionated by gel filtration, and analyzed by SDS-PAGE (Fig. 5). Two gel filtration peaks were analyzed. The fraction (Fig. 5A, peak B) eluting at 21 kDa (the same position as intact, monomeric Bcl-2$_{(1-203)}$) consisted of cleaved protein (Fig. 5B, *lane 4*), clearly demonstrating that the tryptic fragments associated noncovalently. The high molecular weight fraction (Fig. 5A, peak A), probably consisted of aggregated low molecular weight peptides since no large fragments were seen by SDS-PAGE with either Coomassie (Fig. 5B, *lane 3*) or silver (not shown) staining.

Location of Protease-sensitive Sites—To identify the protease-sensitive sites of Bcl-2$_{(1-203)}$, three tryptic fragments were NH_2-terminally sequenced (Fig. 6). Fragment 2, the 15-kDa band, was produced by cleavage at Arg^{68} and fragment 3, the 10-kDa band, had the same NH_2-terminal sequence as intact Bcl-2$_{(1-203)}$. Thus it is likely that cleavage at Arg_{68} produced fragments 2 and 3. Fragment 1 was a very faint band that migrated at the same rate as the high molecular weight chymotryptic fragment. It arose by cleavage at Phe^{49} and was probably due to contaminating chymotrypsin in our trypsin preparation. In view of the fact that Bcl-2$_{(1-203)}$ contains potential trypsin and chymotrypsin sites throughout the molecule, it is clear that residues 49 and 68 were particularly susceptible to proteolytic attack.

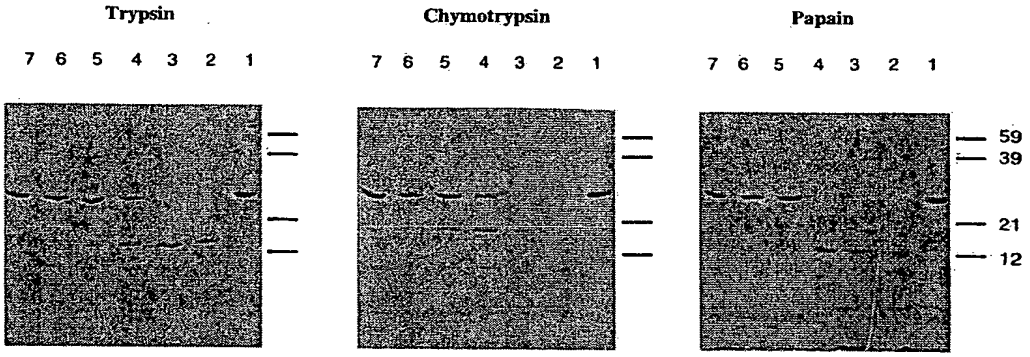

FIG. 3. **Proteolytic digestion of Bcl-$2_{(1-203)}$.** Refolded Bcl-$2_{(1-203)}$ was incubated in the absence (*lanes 1*) or presence (*lanes 2–7*) of the indicated protease for 20 min at 37 °C. Weight ratios of protease to Bcl-2: *lanes 2*, 1:100; *lanes 3*, 1:400; *lanes 4*, 1:1,600; *lanes 5*, 1:6,400; *lanes 6*, 1:25,600; *lanes 7*, 1:102,400. Reactions were terminated by the addition of SDS loading buffer and boiling.

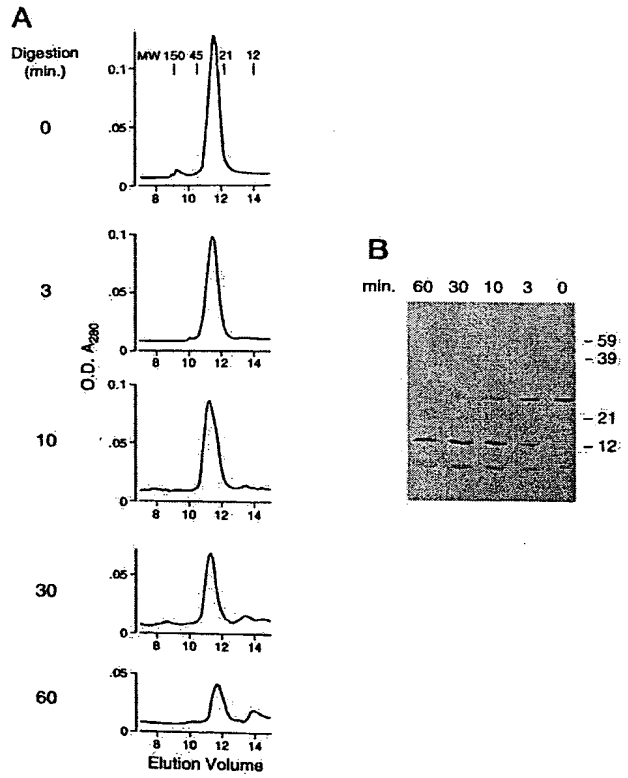

FIG. 4. **Time course of digestion of Bcl-$2_{(1-203)}$.** *Panel A*, Bcl-$2_{(1-203)}$ samples were digested with a 1:1,600 trypsin:Bcl-2 weight ratio for the indicated times at 37 °C, and reactions were terminated by the addition of soybean trypsin inhibitor. Equivalent amounts of digest were applied to a Superdex 75 column in BBS and analyzed by fast protein liquid chromatography. *Panel B*, SDS-PAGE of the samples shown in *panel A*.

DISCUSSION

Refolded mouse Bcl-$2_{(1-203)}$ is a biologically active protein that is soluble and monomeric in nondenaturing solution. By contrast, misfolded proteins almost invariably aggregate in solution (21) and lack biological activity. It is highly likely, therefore, that the recombinant Bcl-$2_{(1-203)}$ used in this study was folded correctly. Bacterially produced mouse Bcl-$2_{(1-203)}$ has thus provided a source of soluble protein suitable for probing the structure and function of the Bcl-2 cytoplasmic domain.

Previous reports showed that Bcl-2 homodimerizes in mammalian cells or in yeast two-hybrid systems (9–11); in contrast, Bcl-x_L fails to homodimerize (22). It is therefore not surprising that recombinant Bcl-x_L does not dimerize either in solution or in the crystal (15). However, the failure of recombinant mouse Bcl-$2_{(1-203)}$ to self-associate even at relatively high protein concentrations appears to be inconsistent with previous results. One reason for this inconsistency could be that residues COOH-terminal to 203 are required for homodimerization. Hanada *et al.* (10) showed by yeast two-hybrid analysis that residues between 196 and 218 in human Bcl-2 (193–215 in the mouse) are necessary for homodimerization, but whether residues between 203 and 215 are required for self-association is not known. Another reason might be that bacterially produced Bcl-2 lacks post-translational modifications, present in yeast or mammalian cells, which are required for homodimerization. Bcl-2 can be phosphorylated (23–25), but other modifications are also possible.

The most striking feature of the Bcl-$2_{(1-203)}$ molecule is its extraordinary susceptibility to a variety of proteases. Trypsin, chymotrypsin, and papain all rapidly produced one or two well defined fragments at low protease:Bcl-2 ratios, even though multiple potential cleavage sites were present throughout the molecule. The sites cleaved by trypsin and chymotrypsin were located within a region of Bcl-2 which is highly variable in amino acid sequence between species and between Bcl-2 and Bcl-x (*shaded* residues in Fig. 6). The Bcl-2 variable region is also rich in the helix-breaking residue, proline, which varies from 20 to 24% in the variable regions of mouse, chicken, and human Bcl-2 compared with 3–4% in the conserved regions. Interestingly, this region also contains very few aspartate residues, the cleavage site for interleukin-1β-converting enzyme family proteases, which may explain why Bcl-$2_{(1-203)}$ was not susceptible to proteolysis by the Jurkat cell extracts.

The exquisite sensitivity of the Bcl-2 variable region to proteolysis is readily understood from the Bcl-x_L NMR and x-ray results (15), assuming that Bcl-2 and Bcl-x_L have similar structures. Both NMR and x-ray analyses indicate that the Bcl-x_L variable region is highly mobile, flexible, and exposed to solvent. The conserved regions, on the other hand, are rigid, compact, and mostly inaccessible to solvent. It is therefore not surprising that the variable region exhibits a high preferential susceptibility to proteolytic attack. In Bcl-x_L, the two portions of the molecule which are joined by the variable loop form a globular structure consisting of seven interacting α-helices with the helix in the NH_2-terminal portion (BH4), making extensive hydrophobic contacts with helices in the COOH-terminal region (15). Our observation that the cleaved Bcl-2 molecule behaves as it were the undigested, monomeric protein in nondenaturing solution demonstrates that the two halves of

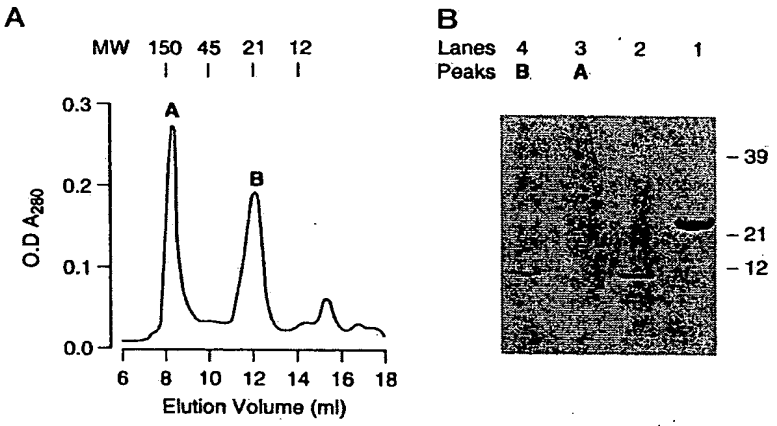

FIG. 5. **Digested Bcl-$2_{(1-203)}$ behaves as monomeric protein in nondenaturing solution.** *Panel A*, Bcl-$2_{(1-203)}$ (0.5 mg) was digested 15 min at 37 °C with a 1:1,600 weight ratio of trypsin to Bcl-2, and the reaction was terminated with soybean trypsin inhibitor. After sitting overnight at 4 °C, the sample was fractionated by size exclusion chromatography on a 10/30 Superdex 75 column in BBS. Two fractions, fraction A corresponding to highly aggregated material and fraction B corresponding to monomeric Bcl-$2_{(1-203)}$, were collected and concentrated. *Panel B*, SDS-PAGE analysis of undigested Bcl-$2_{(1-203)}$ (*lane 1*), digested Bcl-$2_{(1-203)}$ prior to fractionation (*lane 2*), peak A (*lane 3*), and peak B (*lane 4*). Peak A probably consisted of small peptides that aggregated on standing but dissociated in SDS and ran off the gel.

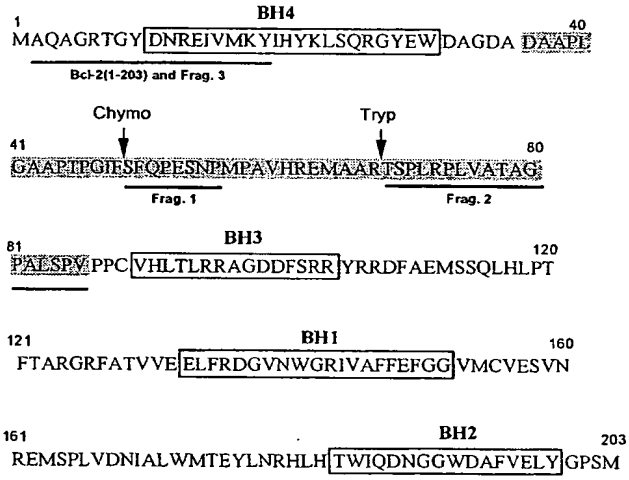

FIG. 6. **Amino acid sequence of murine Bcl-$2_{(1-203)}$.** *Underlined* areas represent experimentally determined NH_2-terminal sequences from Bcl-$2_{(1-203)}$ protein or from tryptic fragments isolated by SDS-PAGE. *Arrows* indicate chymotrypsin (*Chymo*) and trypsin (*Tryp*) sites based on NH_2-terminal sequences of the fragments. Homology domains BH1-BH4 (from Ref. 13) are *boxed*, and the variable region is *shaded*.

the Bcl-2 molecule associate with high affinity, as might be expected from the x-ray structure of Bcl-x_L. Thus, the biochemical analysis of Bcl-$2_{(1-203)}$ indicates that it most likely has the same general structure as Bcl-x_L.

A long variable region has been preserved in Bcl-2 and Bcl-x of all species, suggesting that it has an important function. However, in transfection experiments, this region is not required for anti-apoptotic activity (7, 15). One possibility is that the variable region may serve as a site for proteolytic attack or other modification *in vivo*, to control Bcl-2 function or turnover. We were unable to detect degradation of Bcl-$2_{(1-203)}$ by interleukin-1β-converting enzyme family proteases, but other proteolytic activities would be expected to cleave Bcl-2 rapidly. Cleaved Bcl-2 could lose its ability to neutralize death-promoting members of the Bcl-2 family, thus leading to apoptosis. Another possible function of the variable region might be to serve as a long, flexible linker that would allow the BH4 region of one molecule to interact with either another Bcl-2 molecule or with other Bcl-2 family members, even when Bcl-2 family members were present at low densities. For this to happen, however, the stable association between BH4 and the COOH-terminal region within a molecule would have to be disrupted. Regulation of the internal association between these regions, perhaps by post-translational modification, might therefore be an important aspect of Bcl-2 structure and function.

Acknowledgments—We thank Drs. Pierre Henkart and John Ashwell for thoughtful suggestions concerning the manuscript. We are also grateful to Dr. Jeff Huth for providing the mouse Bcl-2 clone, Dr. Ming-Lei Wu for the Jurkat cell extract, Pat Spinella for determining the NH_2-terminal sequences, and David Millar for the analytical ultracentrifugation analysis.

Note Added in Proof—A recent paper by Strack *et al.* (Strack, P. R., Frey, M. W., Rizzo, C. J., Cordova, B., George, H. J., Meade, R., Ho, S. P., Corman, J., Tritch, R., and Korant, B. D. (1996) *Proc. Natl. Acad. Sci. U. S. A.* **93**, 9571–9576) demonstrated that Bcl-2 is cleaved by HIV protease subsequent to apoptosis.

REFERENCES

1. Tsujimoto, Y., Cossman, J., Jaffe, E., and Croce, C. M. (1985) *Science* **228**, 1440–1443
2. Vaux, D. L., Cory, S., and Adams, J. M. (1988) *Nature* **335**, 440–442
3. Reed, J. C. (1994) *J. Cell Biol.* **124**, 1–6
4. Hockenbery, D. M. (1995) *Bioessays* **17**, 631–638
5. Yin, X. M., Oltvai, Z. N., Veis-Novack, D. J., Linette, G. P., and Korsmeyer, S. J. (1994) *Cold Spring Harbor Symp. Quant. Biol.* **59**, 387–393
6. Boise, L. H., Gottschalk, A. R., Quintans, J., and Thompson, C. B. (1995) *Curr. Top. Microbiol. Immunol.* **200**, 107–121
7. Hunter, J. J., Bond, B. L., and Parslow, T. G. (1996) *Mol. Cell. Biol.* **16**, 877–883
8. Borner, C., Martinou, I., Mattmann, C., Irmler, M., Schaerer, E., Martinou, J. C., and Tschopp, J. (1994) *J. Cell Biol.* **126**, 1059–1068
9. Yin, X.-M., Oltvai, Z. N., and Korsmeyer, S. J. (1994) *Nature* **369**, 321–323
10. Hanada, M., Aimé-Sempé, C., Sato, T., and Reed, J. C. (1995) *J. Biol. Chem.* **270**, 11962–11969
11. Sato, T., Hanada, M., Bodrug, S., Irie, S., Iwama, N., Boise, L. H., Thompson, C. B., Golemis, E., Fong, L., and Wang, H. G. (1994) *Proc. Natl. Acad. Sci. U. S. A.* **91**, 9238–9242
12. Oltvai, Z. N., Milliman, C. L., and Korsmeyer, S. J. (1993) *Cell* **74**, 609–619
13. Zha, H., Aimé-Sempé, C., Sato, T., and Reed, J. C. (1996) *J. Biol. Chem.* **271**, 7440–7444
14. Chittenden, T., Flemington, C., Houghton, A. B., Ebb, R. G., Gallo, G. J., Elangovan, B., Chinnadurai, G., and Lutz, R. J. (1995) *EMBO J.* **14**, 5589–5596
15. Muchmore, S. W., Sattler, M., Liang, H., Meadows, R. P., Harlan, J. E., Yoon, H. S., Nettesheim, D., Chang, B. S., Thompson, C. B., Wong, S., Ng, S., and Fesik, S. W. (1996) *Nature* **381**, 335–341
16. Borner, C., Olivier, R., Martinou, I., Mattmann, C., Tschopp, J., and Martinou, J. C. (1994) *Biochem. Cell Biol.* **72**, 463–469
17. Kurucz, I., Jost, C. R., George, A. J. T., Andrew, S. M., and Segal, D. M. (1993) *Proc. Natl. Acad. Sci. U. S. A.* **90**, 3830–3834
18. Memon, S. A., Moreno, M. B., Petrak, D., and Zacharchuk, C. M. (1995) *J. Immunol.* **155**, 4644–4652
19. Mach, H., Middaugh, C. R., and Lewis, R. V. (1992) *Anal. Biochem.* **200**, 74–80
20. Schlegel, J., Peters, I., and Orrenius, S. (1995) *FEBS Lett.* **364**, 139–142
21. Jaenicke, R. (1987) *Prog. Biophys. Mol. Biol.* **49**, 117–237
22. Sedlak, T. W., Oltvai, Z. N., Yang, E., Wang, K., Boise, L. H., Thompson, C. B., and Korsmeyer, S. J. (1995) *Proc. Natl. Acad. Sci. U. S. A.* **92**, 7834–7838
23. Haldar, S., Jena, N., and Croce, C. M. (1995) *Proc. Natl. Acad. Sci. U. S. A.* **92**, 4507–4511
24. Haldar, S., Chintapalli, J., and Croce, C. M. (1996) *Cancer Res.* **56**, 1253–1255
25. Chen, C.-Y., and Faller, D. V. (1996) *J. Biol. Chem.* **271**, 2376–2379

Eur. J. Biochem. 236, 656–661 (1996)

Single-step trypsin cleavage of a fusion protein to obtain human insulin and its C peptide

Per JONASSON, Joakim NILSSON, Elisabet SAMUELSSON, Tomas MOKS, Stefan STÅHL and Mathias UHLÉN
Department of Biochemistry and Biotechnology, Royal Institute of Technology (KTH), Stockholm, Sweden

(Received 12 October 1995) – EJB 95 1663/2

The kinetics for trypsin cleavage of different fusion proteins, consisting of human proinsulin and two IgG-binding domains (ZZ), were investigated. To achieve simultaneous removal of the fusion tag and processing of proinsulin to insulin and free C peptide, three versions of the ZZ-proinsulin fusion protein were generated, having different trypsin-sensitive cleavage sites, Arg, Lys-Arg or Lys. The ZZ-proinsulin fusion proteins which accumulated as inclusion bodies in *Escherichia coli* cells were solubilized, refolded and purified by IgG affinity chromatography. The yield of ZZ-proinsulin monomers exceeded 90%. The kinetics for the trypsin cleavage revealed unexpected differences when comparing the three linkers and it was found that the single arginine linker was most efficiently processed. Characterization of the cleavage products by reverse-phase chromatography, mass spectrometry and N-terminal sequencing verified that human insulin and C peptide were generated. The results demonstrate that high yields of native insulin, C peptide and affinity tag can be achieved by simultaneous cleavage of a fusion protein at three different trypsin-sensitive sites in a single step. The implications for production and recovery of various recombinant proteins are discussed.

Keywords: fusion protein; proinsulin; staphylococcal protein A; affinity chromatography; refolding.

When setting up a scheme for a recombinant protein production, genetic design of the gene product can be utilized to dramatically simplify the recovery. The strategy of splicing the target gene to a gene encoding a fusion partner, 'tag', with affinity for a certain ligand, has been used extensively for more than a decade to enable affinity purification of recombinant products (Uhlén et al., 1983, 1992; Nygren et al., 1994). However, gene fusion technology employed to engineer proteins to facilitate the downstream processing has not been widely used for the production of recombinant proteins on an industrial scale (Nygren et al., 1994). The main reason for this is probably due to the fact that gene fusion strategies introduce an additional problem into the downstream processing, since a site-specific cleavage is required to remove the fusion tag. A vast number of cleavage methods, both chemical and enzymic, have been investigated for this purpose (Nygren et al., 1994). Chemical cleavage methods have generally a rather low specificity and the relatively harsh cleavage conditions can cause chemical modifications of the released products (Nygren et al., 1994). Some of the enzymic methods offer significantly higher cleavage specificities together with high efficiency, e.g. H64A subtilisin, IgA protease and factor Xa (Uhlén et al., 1992; Nygren et al., 1994), but these enzymes have the drawback of being quite expensive. Trypsin, which cleaves C-terminally of basic amino acid residues, has been used for a long time to cleave fusion proteins (Kemmler et al., 1971; Wang et al., 1989). Despite expected low specificity, trypsin has been shown to be useful for specific cleavage of fusion proteins, leaving basic residues within folded protein domains uncleaved (Wang et al., 1989). Trypsin has the additional advantages of being inexpensive and readily available.

In the human pancreas, insulin is produced as its precursor proinsulin. For recombinant insulin production in *Escherichia coli* or yeast, proinsulin has been utilized as a precursor molecule (Frank et al., 1981; Williams et al., 1982; Cousens et al., 1987). Proinsulin consists of a B chain which has its carboxyl terminus linked to the A chain by a connecting C peptide. Renewed interest in proinsulin production is partly due to the fact that several studies indicate that the C peptide also has a clinical relevance (Johansson et al., 1992, 1993). In patients with type-1 diabetes, who lack endogenous C peptide, administration of the peptide improves renal function, stimulates muscle and glucose utilization and improves blood-retinal barrier function (Johansson et al., 1992, 1993). Novel insulin processes should thus preferably enable recovery also of the C peptide.

Proinsulin has been processed to native insulin, composed of cysteine-bridged A and B chains, and free C peptide by treatment with trypsin and carboxypeptidase B (Kemmler et al., 1971; Frank et al., 1981; Cousens et al., 1987). Carboxypeptidase B digests the carboxylterminal basic residues (Kemmler et al., 1971) resulting from trypsin cleavage. Fusions of different extensions to proinsulin have proven to be advantageous for production in *E. coli* both in terms of expression levels (Guo et al., 1984; Kang and Yoon, 1991, 1994) and to confer stability to proteolysis (Shen, 1984; Murby et al., 1991; Kang and Yoon, 1994). However, the fusion tail strategy has, as mentioned above, introduced an additional unit operation since the fusion partners need to be cleaved off enzymically or chemically to release proinsulin (Shen, 1984).

Here, we have investigated the production of proinsulin as a fusion to the IgG-binding domains (ZZ) derived from staphylococcal protein A (Nilsson et al., 1987). Three variants of ZZ-proinsulin were constructed, having different trypsin cleavage

Correspondence to M. Uhlén, Department of Biochemistry and Biotechnology, Royal Institute of Technology (KTH), S-100 44 Stockholm, Sweden
Fax: +46 8 245452.
Enzymes. Trypsin (EC 3.4.21.4); carboxypeptidase B (EC 3.4.17.12).

REF. 9

sites engineered at the junction between ZZ and proinsulin. The cleavage kinetics for these three variants have been evaluated in order to develop an integrated scheme for the processing of the ZZ-proinsulin fusion to enable recovery of native insulin and its C peptide.

MATERIALS AND METHODS

Bacterial strains and plasmids. *E. coli* RRIΔM15 (Rüther, 1982) cells were used as host for subcloning and gene expression. Plasmids pUC19 (Yanisch-Perron et al., 1985) and pTrpBB (Öberg et al., 1994) were used as vectors for subcloning. Plasmid pEZZ318 (Löwenadler et al., 1987) was used as a source for the ZZ fragment, plasmid pKK223-3 (Pharmacia Biotech) as source for the *E. coli* ribosomal terminator *rrnB* (Brosius and Holy, 1984) and pRIT37 (Murby et al., 1991) as source for the human proinsulin gene.

DNA constructions. Restriction enzymes, T4 DNA ligase and *Taq* DNA polymerase were purchased from Boehringer Mannheim and used as recommended. The oligonucleotides used were synthesized on a Gene Assembler Plus (Pharmacia Biotech). PCR was performed according to a standard protocol (Hultman et al., 1989). Solid-phase DNA sequencing was performed as described by Hultman and coworkers (1989) using an automated laser fluorescence (A. L. F.™) system (Pharmacia Biotech). A vector for intracellular expression of ZZ fusion proteins (Nilsson et al., 1987) was constructed by insertion of an *Fsp*I–*Eco*RI restriction fragment from pEZZ318, containing the ZZ-encoding gene fragment, into pTrpBB previously digested with the same enzymes, resulting in pTrpZZ. A transcription terminator sequence was obtained from pKK223-3 using a standard PCR amplification protocol (Hultman et al., 1989) and the oligonucleotides HEAN-19, 5′-CCC CCT GCA GCT CGA GCG CCT TTA ACC TGT TTT GGC GGA TG-3′ and HEAN-20, 5′-CCC CAA GCT TAG AGT TTG TAG AAA CGC-3′. The restriction sites introduced by PCR were digested with *Pst*I and *Hin*dIII, followed by insertion into pTrpZZ, previously digested with the same enzymes. The resulting expression vector pTrpZZT1T2 encodes an affinity handle consisting of a *trp* operon-derived leader sequence (eight amino acids), the six amino-terminal amino acids from the E domain of staphylococcal protein A, a cloning rest sequence (five amino acids) followed by the 116-residue IgG-binding ZZ domains, under control of the *E. coli* trp promoter. In addition, the plasmid carries the gene for kanamycin resistance. The oligonucleotide primers used for the three different PCR amplifications of the proinsulin gene from pRIT37 were JOPE-1, 5′-TTG AAT TCA GCA CGT TTT GTA AAC CAA CAC CTG TGC GGC-3′, JOPE-2, 5′-TTG AAT TCA GCA AAA CGT TTT GTA AAC CAA CAC CTG TGC GGC-3′and JOPE-3, 5′-TTG AAT TCA GCA AAA TTT GTA AAC CAA CAC CTG TGC GGC-3′ as the three different upstream primers, all annealing with the first 24 bases of the proinsulin gene, and JOPE-4, 5′-CC GGA TCC TTA GTT GCA GTA GTT CTC CAG CTG G-3′ as downstream primer, annealing with the last 25 bases of the proinsulin gene. The first three primers were used to introduce an upstream *Eco*RI site and codons for arginine, lysine-arginine or lysine residues, respectively, at the 5′ end of the proinsulin gene. The downstream primer (JOPE-4) was designed to introduce a downstream *Bam*HI restriction site. The PCR fragments encoding R-proinsulin, KR-proinsulin and K-proinsulin, were digested with *Eco*RI and *Bam*HI restriction enzymes, ligated into similarly digested pUC19, and thereafter sequenced. Verified proinsulin constructs were digested with *Eco*RI and *Sal*I and inserted into the similarly restricted expression vector pTrpZZT1T2, resulting in pTrpZZ-R-proinsulin, pTrpZZ-KR-proinsulin and pTrpZZ-K-proinsulin. These plasmids encodes fusion proteins consisting of the IgG-binding ZZ affinity handle fused to human proinsulin with arginine, lysine-arginine or lysine residues, respectively, between ZZ and the proinsulin gene.

Cultivation and recovery of inclusion bodies. *E. coli* cells harbouring pTrpZZ-R-proinsulin, pTrpZZ-KR-proinsulin and pTrpZZ-K-proinsulin were grown overnight at 37°C in shake-flasks containing 20 ml Tryptic Soy Broth (30 g/l, Difco) supplemented with yeast extract (5 g/l, Difco) and kanamycin monosulfate (50 mg/l). The overnight cultures were diluted 25-fold to 500 ml in baffled shake-flasks having the same type of media and grown at 37°C. Gene expression was induced at mid-log phase ($A_{600\,nm} \approx 1$) by the addition of 2-indole acrylic acid to 25 μg/ml. Cells were harvested 4 hours after induction, by centrifugation at approximately 6000 *g* for 10 min. Cells were resuspended in 5% of the culture volume in 50 mM Tris/HCl, pH 8.0, 200 mM NaCl, 0.05% Tween 20, 1 mM EDTA (buffer A), lysed by sonication and centrifuged at approximately 7500 *g*. The pellets, containing inclusion bodies, were washed twice with 5% of the culture volume in 50 mM Tris/HCl, pH 8.0, supplemented with 5 mM $MgSO_4$.

Solubilization, refolding and protein purification. The inclusion bodies, containing ZZ-R-proinsulin, ZZ-KR-proinsulin and ZZ-K-proinsulin were solubilized and converted to their hexasulfonate derivatives by sulfitolysis (Cole, 1967), essentially as described by Frank and coworkers (1981), by adding 10% of the culture volume of a solution containing 8 M urea, 0.8 M Na_2SO_3 and 0.3 M $Na_2S_4O_6 \cdot 2\,H_2O$ (Cousens et al., 1987). The pH was adjusted to 7.5 with HAc and the mixtures incubated under gentle stirring for 6 hours at 37°C. After dilution 1:1.5 with water and subsequent centrifugation at 30000 *g* for 20 min, the supernatants were dialysed three times (Spectra/Por 1 membrane, MWCO 6-8000, Spectrum Medical Industries Inc.) against 10 culture volumes of 10 mM Tris/HCl, pH 8. Dialysed protein solution was supplemented with 1 M glycine/NaOH, pH 10.5, to a final concentration of 0.1 M glycine/NaOH. In addition, 2-mercaptoethanol was added (≈18 mol/mol fusion protein; Frank et al., 1981). This mixture was incubated overnight under gentle stirring at 4°C, at ZZ-proinsulin hexasulfonate concentrations of approximately 0.1 mg/ml. After pH adjustment to 8 with HAc, a 1:2 dilution with water and centrifugation at 30000 *g* for 20 min, the supernatants containing refolded fusion proteins were applied to columns containing 5 ml IgG-Sepharose (Pharmacia Biotech) and purified according to a standard procedure (Ståhl et al., 1989). Eluted proteins in 0.5 M HAc, pH 3.2, were lyophilized. The fusion proteins were dissolved in 5 ml 2 M guanidine hydrochloride, pH 8, and separated by size-exclusion chromatography on a 16/60 XK column (Pharmacia Biotech) containing 120 ml Superdex 75 prep grade (Pharmacia Biotech). The buffer used was 200 mM ammonium acetate, pH 8.0, containing 15% (by vol.) acetonitrile. The flow rate was 1 ml/min and the absorbance was measured at 280 nm. The fusion protein monomers were collected and lyophilized.

Cleavage of the proinsulin fusion proteins. The different lyophilized monomeric ZZ-proinsulin fusion proteins were dissolved in 100 mM Tris/H_3PO_4, pH 7.5, containing 0.1% (by vol.) Tween 20 to protein concentrations of 2 mg/ml. Trypsin (sequencing grade, Boehringer Mannheim) and carboxypeptidase B (Boehringer Mannheim) were added to trypsin/fusion protein ratios of 1:2000 (by mass) and carboxypeptidase B/fusion protein ratios of 1:1000 (by mass). After 5, 15 and 30 min, samples were removed from the cleavage mixtures and the digestions stopped by decreasing the pH to 3 by adding HAc. A sample after 60 min, from the cleavage of the ZZ-K-proinsulin,

was also taken. Acetonitrile to 20% (by vol.) was added in order to stabilize the cleavage products.

Protein analyses. SDS/PAGE was performed on a homogeneous 12% gel (BioRad Inc.) and Coomassie brilliant blue R-350 (Pharmacia Biotech) was used for staining. The homogeneity of the IgG-affinity purified proinsulin fusion proteins was analyzed by size-exclusion chromatography on a Superdex 75 PC 3.2/10 column (Pharmacia Biotech) using the SMART™ system (Pharmacia Biotech). The buffer was 200 mM sodium phosphate, pH 7.2, containing 15% (by vol.) acetonitrile. The flow rate used was 100 µl/min and the absorbance was measured at 214 nm. Samples were taken from the cleavage mixtures and analyzed by size-exclusion chromatography in the same way as described above. Cleavage products after complete digestion (R 30 min, KR 30 min and K 60 min) were analyzed by reverse-phase chromatography on a µRPC C2/C18 SC 2.1/10 column using the SMART™ system. Elution was performed using a gradient of 31–36% acetonitrile containing 0.1% (by vol.) trifluoroacetic acid for 12 min at 25°C. The flow rate was 100 µl/min and the absorbance was measured at 214 nm. To determine the IgG-binding components in the cleavage mixtures, IgG-Sepharose was added and incubated for 2 min with gentle mixing. The IgG-Sepharose was removed by centrifugation and the supernatant was analyzed by RPC on the SMART™ system as described above. Internal standards, human insulin (Hoechst AG, Germany) and C peptide fragment 3–33 (Sigma), were used both in the size-exclusion chromatography and the RPC analyses. Proteins for N-terminal sequencing and mass determinations were isolated by RPC as described above. N-terminal sequencing was performed on a HP-G1000A (Hewlett Packard) sequencer and protein mass determinations were carried out using a JEOL SX102 mass spectrometer (JEOL) equipped with an electrospray unit.

Protein quantification. To calculate the absorption coefficient, IgG-affinity-purified monomeric ZZ-KR-proinsulin fusion protein was lyophilized and the mass determined on an analytical balance. The lyophilized proinsulin fusion protein was dissolved in 0.5 M HAc, pH 3.2, and the absorbance at 280 nm was measured. The calculated absorption coefficient (0.34 cm²/mg) was used for spectrophotometrical concentration determinations of proinsulin fusion proteins in solution. Quantification of proinsulin fusion proteins in whole cell lysates, in lyophilized material and in insoluble material was performed by SDS/PAGE analysis on the PhastSystem™ (Pharmacia Biotech) using 8–25% polyacrylamide gradient gels and comparison to weighed ZZ-KR-proinsulin fusion protein samples.

RESULTS

Design of fusion proteins. Three different expression vectors were constructed encoding the fusion proteins ZZ-R-proinsulin, ZZ-KR-proinsulin and ZZ-K-proinsulin. The junctions between ZZ and proinsulin were engineered to contain single or double basic amino acids (Fig. 1) to potentially allow trypsin cleavage at a rate similar to the processing of proinsulin to insulin and C peptide; the removal of the fusion tag should then be integrated into the proinsulin processing step. All three fusion proteins have a theoretical molecular mass of 25 kDa and consist of the two synthetic ZZ domains derived from staphylococcal protein A (Nilsson et al., 1987) and human proinsulin (Fig. 1). The ZZ fusion tail was selected as fusion partner because, (a) ZZ-fusions can be produced at high expression levels in *E. coli* (Hansson et al., 1994; Moks et al., 1987), (b) ZZ fusions allow efficient recovery by IgG-affinity chromatography (Moks et al., 1987) also after solubilization of inclusion bodies (Murby et al., 1994), and

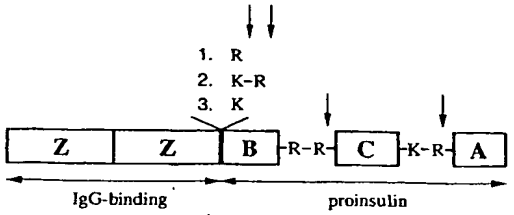

Fig. 1. Schematic presentation of the three variants of the ZZ-proinsulin fusion proteins. Three different trypsin-sensitive cleavage linkers, Arg, Lys-Arg or Lys, were engineered between the ZZ fusion partner and proinsulin. The trypsin-sensitive processing sites flanking the C peptide of proinsulin are also indicated. Arrows indicate expected trypsin-cleavage sites.

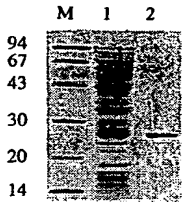

Fig. 2. Analyses of ZZ-R-proinsulin. Reduced SDS/PAGE analysis of a ZZ-R-proinsulin cultivation. Lane 1, total cell protein from an *E. coli* cultivation harbouring the construct encoding ZZ-R-proinsulin. Lane 2, ZZ-R-proinsulin after a single-step affinity purification on IgG-Sepharose. Lane M, marker proteins with molecular masses (in kilodaltons) indicated on the left. Coomassie brilliant blue was used for staining.

(c) the solubilizing properties of ZZ have earlier been shown to facilitate the *in vitro* product refolding at high protein concentrations (Samuelsson et al., 1994). Furthermore, ZZ contains no cysteine residues that could cause formation of unwanted disulfide bridges and the acidic properties of ZZ have earlier demonstrated to be useful for recovery by ion-exchange chromatography (Hansson et al., 1994).

Protein production. The three different fusion proteins, ZZ-R-proinsulin, ZZ-KR-proinsulin and ZZ-K-proinsulin (Fig. 1) were expressed intracellularly in *E. coli* and were found to accumulate as inclusion bodies. SDS/PAGE analysis of total cell lysates indicated that the ZZ-proinsulin fusions constituted major products of the total cell proteins (Fig. 2, lane 1; data not shown). After cell disruption, the inclusion bodies containing the ZZ-proinsulin fusions were washed. The expression levels were similar for the shake-flask cultivations of the three variants of ZZ-proinsulin, being approximately 200 mg/l culture as determined by SDS/PAGE analysis (data not shown).

Solubilization, refolding and affinity purification. The ZZ-proinsulin fusion proteins were solubilized and subjected to oxidative sulfitolysis (Cole, 1967; Frank et al., 1981; Cousens et al., 1987). Since the ZZ fusion partner contains no cysteine residues, only the proinsulin will be sulfonated. Renaturation of the ZZ-proinsulin hexasulfonate derivatives was performed at an approximate protein concentration of 0.1 mg/ml. The renatured ZZ-proinsulin material was affinity purified on IgG-Sepharose (Moks et al., 1987; Ståhl et al., 1989); SDS/PAGE analysis demonstrated electrophoretically pure material without degradation products (Fig. 2, lane 2). To determine the amount of multimeric forms of ZZ-proinsulin, a sample of the IgG-affinity purified material was analyzed by size-exclusion chromatography (data not shown). Integration of the peak areas on the chromatogram

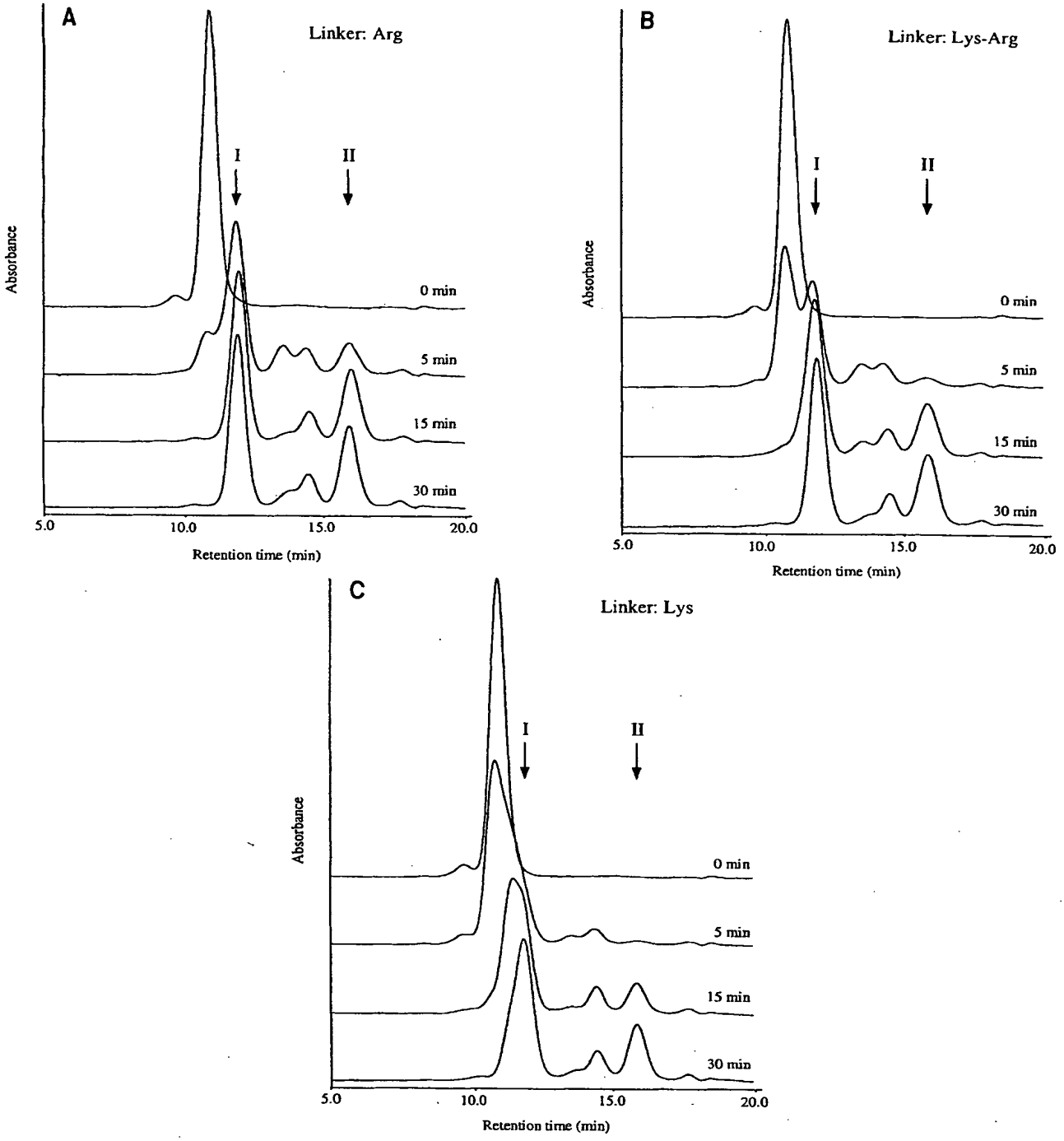

Fig. 3. Kinetic analysis of the trypsin cleavage of the three variants of ZZ-proinsulin. Size-exclusion chromatography analysis of trypsin/carboxypeptidase B digestion of (A) ZZ-R-proinsulin, (B) ZZ-KR-proinsulin and (C) ZZ-K-proinsulin. The three ZZ-proinsulin variants were digested for 0 (top curve), 5, 15 and 30 min (bottom curve). The sizes of peaks I and II were found to correspond to the sizes of ZZ and human insulin, respectively. Note, that the C peptide is too small for the separation range.

indicated that approximately 90% of ZZ-proinsulin was recovered in the monomeric form. Again, the results were the same for all three ZZ-proinsulin fusions (data not shown).

Trypsin cleavage of the fusion proteins and analysis of the cleavage mixtures. An evaluation of the cleavage kinetics of the three different trypsin cleavage linkers in ZZ-proinsulin was performed. Monomeric fractions of the three fusion proteins, ZZ-R-proinsulin, ZZ-KR-proinsulin and ZZ-K-proinsulin, were subjected to trypsin/carboxypeptidase B treatment for 5, 15 and 30 min, respectively, and the cleavage material was analyzed by size-exclusion chromatography (Fig. 3). Uncleaved ZZ-proinsulin could easily be separated from ZZ (Fig. 3, peak I) and insulin (Fig. 3, peak II). The linker showing the fastest cleavage kinetics was the arginine linker which was completely cleaved after 15 min (Fig. 3A). The lysine-arginine linker was cleaved

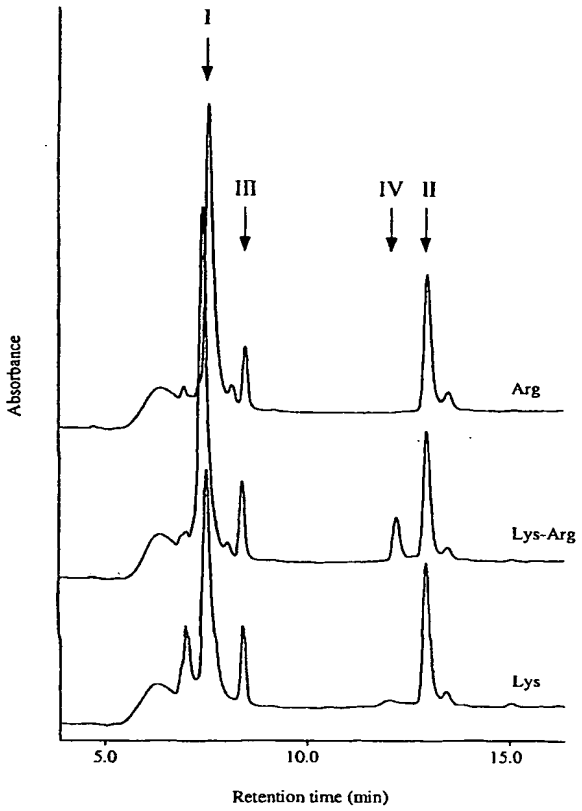

Fig. 4. Characterization of cleavage products from the cleaved ZZ-proinsulin variants. Reverse-phase chromatography analysis of ZZ-R-proinsulin (top curve), ZZ-KR-proinsulin (middle curve) and ZZ-K-proinsulin (bottom curve), digested with trypsin and carboxypeptidase B for 30 min (ZZ-R-proinsulin and ZZ-KR-proinsulin) or 60 min (ZZ-K-proinsulin).

slightly slower but was completely processed after 30 min (Fig. 3B). The lysine linker demonstrated the slowest cleavage kinetics and was not completely cleaved after 30 min (Fig. 3C).

In order to identify the products after trypsin/carboxypeptidase B cleavage of the ZZ-proinsulin variants, reverse-phase chromathography separations were performed. The two fusions, ZZ-R-proinsulin and ZZ-KR-proinsulin, were cleaved for 30 min, and ZZ-K-proinsulin was cleaved for 60 min prior to reverse-phase chromatography analysis (Fig. 4). Human insulin and C peptide internal standards showed that peaks II and III corresponded to human insulin and C peptide, respectively (data not shown). Peaks II–IV were also collected and further analyzed by amino-terminal sequencing and mass spectrometry (Table 1). The indications from the reverse-phase chromatography analysis for peaks II and III were corroborated by these analyses, giving molecular masses and amino-terminal amino acids corresponding to the expected results (Table 1). Peak IV, collected after cleavage and reverse-phase chromatography of ZZ-KR-proinsulin, was found to be insulin carrying an amino-terminal arginine residue on the B chain (Table 1). This demonstrates that the lysine-arginine linker found in ZZ-KR-proinsulin was, to a large extent, processed by trypsin between the lysine and arginine residues, thus leaving the amino-terminal arginine residue on the B chain.

In order to identify the IgG binding portion ZZ in the cleavage mixture, cleaved ZZ-KR-proinsulin was incubated with IgG-Sepharose. The supernatant was analyzed by reverse-phase chromatography and compared with a sample not treated with IgG-Sepharose (data not shown). This comparison verified that peak I in the cleavage mixtures corresponded to ZZ, since this peak disappeared after IgG treatment (data not shown). Furthermore, these results showed that the fusion partner is resistant to the trypsin cleavage, despite the presence of internal dibasic amino acids. This analysis thus suggests that a passage of a completely processed cleavage mixture over an IgG-Sepharose column would yield pure human insulin and C peptide.

Table 1. Characterization of cleavage products resulting from trypsin/carboxypeptidase B digestion. X, unspecified amino acid. The experimental molecular mass was determined by electrospray mass spectrometry. Peak IV was collected from the cleavage of ZZ-KR-proinsulin.

Peak	Amino-terminal amino acids		Molecular mass	
	expected	sequenced	calculated	experimental
			Da	
II	FVNQHL and GIVEQ	FVNQHL and GIVEQ	5807.7	5808.3
III	EAEDLQV	XAXXLQV	3020.3	3019.8
IV		RFVNQ and GIVXQ	5963.9	5964.6

DISCUSSION

Three different trypsin-sensitive sites, introduced between ZZ and proinsulin, were investigated with respect to their cleavage efficiency, through the production of ZZ-R-proinsulin, ZZ-KR-proinsulin and ZZ-K-proinsulin. All three variants were found to be expressed at high levels and, after solubilization from inclusion bodies and subsequent renaturation, could be efficiently purified using affinity chromatography. No proteolytic degradation of the ZZ-proinsulin fusions could be detected. Upon treatment with trypsin and carboxypeptidase B, ZZ-R-proinsulin containing the single arginine residue linker was completely cleaved after 15 min, resulting in released human insulin and C peptide. The trypsin digestion was demonstrated to be unexpectedly specific, cleaving only at the junctions between ZZ and proinsulin and at the trypsin-sensitive sites flanking the C peptide. Basic and dibasic amino acid residues within the proinsulin and the ZZ tag, were not found to be accessible for trypsin after the refolding procedure. Trypsin, which is used extensively for trypsin digests of denatured proteins, can thus be used for highly specific cleavage of fusion proteins after renaturation of the expressed recombinant gene products. Since the affinity tag was resistant to trypsin cleavage, it could be efficiently removed by affinity chromatography.

These results suggest that an integrated large-scale process could be designed from this laboratory-scale set up. Such a process would include the following unit operations: fermentation; cell disruption and harvest of inclusion bodies; solubilization and renaturation; IgG-affinity chromatography; enzymic processing; IgG affinity chromatography to remove the affinity tag or, alternatively, preparative reverse-phase chromatography. All individual steps are straightforward with documented high yields, suggesting a good overall yield for such a process. Intracellular production of inclusion bodies is an attractive alternative due to recent advances in industrial-scale *in vitro* renaturation of recombinant proteins from intracellular precipitates (Rudolph, 1995). Alternatively, it may be possible to utilize recently described expanded bed technology (Hansson et al., 1994) to obtain an even more condensed downstream processing scheme.

In conclusion, the described results demonstrate that trypsin cleavage can be used for efficient and specific cleavage of fusion

proteins. The use of a trypsin-resistant affinity tag in combination with an efficient renaturation scheme gives high yields of both native human insulin and its C peptide.

This work was financed by support from the Protein Engineering Program funded by the Swedish National Board for Industrial and Technical Development (NUTEK). We thank Drs Maria Murby and Anders Hedrum for help with vector constructions and Drs Per Persson and Anders Karlström (Pharmacia Biopharmaceuticals, Stockholm, Sweden) for mass spectrometry analysis and amino-terminal sequencing, respectively.

REFERENCES

Brosius, J. & Holy, A. (1984) Regulation of ribosomal RNA promotors with a synthetic *lac* operator, *Proc. Natl Acad. Sci. USA 81*, 6929–6933.

Cole, R. D. (1967) Sulfitolysis, *Methods Enzymol. 11*, 206–208.

Cousens, L. S., Shuster, J. R., Gallegos, C., Ku, L., Stempien, M. M., Urdea, M. S., Sanchez-Pescador, R., Taylor, A. & Tekamp-Olson, P. (1987) High level expression of proinsulin in the yeast, *Saccharomyces cerevisiae*, *Gene (Amst.) 61*, 265–275.

Frank, B. H., Pettee, J. M., Zimmerman, R. E. & Burck, P. J. (1981) The production of human proinsulin and its transformation to human insulin and C peptide, in *Peptides: synthesis, structure and function, proceedings of the seventh american peptide symposium* (Rich, D. H. & Gross, E., eds) pp. 729–738, Pierce Chemical Company, Rockford, IL.

Guo, L.-H., Stepién, P. P., Tso, J. Y., Brousseau, R., Narang, S., Thomas, D. Y. & Wu, R. (1984) Synthesis of human insulin gene. Construction of expression vectors for fused proinsulin production in *Escherichia coli*, *Gene (Amst.) 29*, 251–254.

Hansson, M., Ståhl, S., Hjorth, R., Uhlén, M. & Moks, T. (1994) Single-step recovery of a secreted recombinant protein by expanded bed adsorption, *Biotechnology 12*, 285–288.

Hultman, T., Ståhl, S., Hornes, E. & Uhlén, M. (1989) Direct solid phase sequencing of genomic and plasmid DNA using magnetic beads as solid support, *Nucleic Acids Res. 17*, 4937–4946.

Johansson, B.-L., Sjöberg, S. & Wahren, J. (1992) The influence of human C peptide on renal function and glucose utilization in type 1 (insulin-dependent) diabetic patients, *Diabetologia 35*, 121–128.

Johansson, B.-L., Kernell, A., Sjöberg, S. & Wahren, J. (1993) Influence of combined C peptide and insulin administration on renal function and metabolic control in diabetes type 1, *J. Clin. Endocrinol. Metab. 77*, 976–981.

Kang, Y. & Yoon, J.-W. (1991) Development of a high-expression vector (pYK10-9) of human proinsulin gene, *Biotechnol. Lett. 13*, 755–760.

Kang, Y. & Yoon, J.-W. (1994) Effect of modification of connecting peptide of proinsulin on its export, *J. Biotechnol. 36*, 45–54.

Kemmler, W., Peterson, J. D. & Steiner, D. F. (1971) Studies on the conversion of proinsulin to insulin, *J. Biol. Chem. 246*, 6786–6791.

Löwenadler, B., Jansson, B., Paleus, S., Holmgren, E., Nilsson, B., Moks, T., Palm, G., Josephson, S., Philipson, L. & Uhlén, M. (1987) A gene fusion system for generating antibodies against short peptides, *Gene (Amst.) 58*, 87–97.

Moks, T., Abrahmsén, L., Österlöf, B., Josephson, S., Östling, M., Enfors, S.-O., Persson, I., Nilsson, B. & Uhlén, M. (1987) Large-scale affinity purification of human insulin-like growth factor I from culture medium of *Escherichia coli*, *Biotechnology 5*, 379–382.

Murby, M., Cedergren, L., Nilsson, J., Nygren, P.-Å., Hammarberg, B., Nilsson, B., Enfors, S.-O. & Uhlén, M. (1991) Stabilization of recombinant proteins from proteolytic degradation in *Escherichia coli* using a dual affinity fusion strategy, *Biotechnol. Appl. Biochem. 14*, 336–346.

Murby, M., Nguyen, T. N., Binz, H., Uhlén, M. & Ståhl, S. (1994) Production and recovery of recombinant proteins of low solubility, in *Separations for biotechnology* (Pyle, D. L., ed.) vol. 3, pp. 336–344, Boockcraft Ltd, Bath.

Nilsson, B., Moks, T., Jansson, B., Abrahmsén, L., Elmblad, A., Holmgren, E., Henrichson, C., Jones, T. A. & Uhlén, M. (1987) A synthetic IgG-binding domain based on staphylococcal protein A, *Prot. Eng. 1*, 107–113.

Nygren, P.-Å., Ståhl, S. & Uhlén, M. (1994) Engineering proteins to facilitate bioprocessing, *Trends Biotechnol. 12*, 184–188.

Öberg, U., Rundström, G., Grönlund, H., Uhlén, M. & Nygren, P.-Å. (1994) Intracellular production and renaturation from inclusion bodies of a scFv fragment fused to a serum albumin binding affinity tail, in *Proc. 6th Eur. Congr. Biotechnol.* (Alberghina, L., Frontali, L. & Sensi, P., eds) pp. 179–182, Elsevier Science B. V., Amsterdam, The Netherlands.

Rudolph, R. (1995) Successful protein folding on an industrial scale, in *Principles and practice of protein folding* (Cleland, J. L. & Craik, C. S., eds) pp. 283–298, John Wiley and Sons Inc., New York.

Rüther, U. (1982) pUR 250 allows rapid chemical sequencing of both DNA strands of inserts, *Nucleic Acids Res. 10*, 5765–5772.

Samuelsson, E., Moks, T., Nilsson, B. & Uhlén, M. (1994) Enhanced *in vitro* refolding of insulin-like growth factor I using a solubilizing fusion partner, *Biochemistry 33*, 4207–4211.

Shen, S.-H. (1984) Multiple joined genes prevent product degradation in *Escherichia coli*, *Proc. Natl Acad. Sci. USA 81*, 4627–4631.

Ståhl, S., Sjölander, A., Nygren, P.-Å., Berzins, K., Perlmann, P. & Uhlén, M. (1989) A dual expression system for the generation, analysis and purification of antibodies to a repeated sequence of the *Plasmodium falciparum* antigen Pf155/RESA, *J. Immunol. Meth. 124*, 43–52.

Uhlén, M., Nilsson, B., Guss, B., Lindberg, M., Gatenbeck, S. & Philipson, L. (1983) Gene fusion vectors based on staphylococcal protein A, *Gene (Amst.) 23*, 369–378.

Uhlén, M., Forsberg, G., Moks, T., Hartmanis, M. & Nilsson, B. (1992) Fusion proteins in biotechnology, *Curr. Opin. Biotechnol. 3*, 363–369.

Wang, M., Scott, W. A., Rao, R., Udey, J., Conner, G. E. & Brew, K. (1989) Recombinant bovine α-lactalbumin obtained by limited proteolysis of a fusion protein expressed at high levels in *Escherichia coli*, *J. Biol. Chem. 264*, 21116–21121.

Williams, D. C., Van Frank, R. M., Muth, W. L. & Burnett, J. P. (1982) Cytoplasmic inclusion bodies in *Escherichia coli* producing biosynthetic human insulin proteins, *Science 215*, 687–689.

Yanisch-Perron, C., Vieira, J. & Messing, J. (1985) Improved M13 phage cloning vectors and host strains: nucleotide sequences of M13mp18 and pUC19 vectors, *Gene (Amst.) 33*, 103–119.

Proc. Natl. Acad. Sci. USA
Vol. 92, pp. 8234–8238, August 1995
Biochemistry

Structural domains of IS*10* transposase and reconstitution of transposition activity from proteolytic fragments lacking an interdomain linker

(transposition/Tn*10*/limited proteolysis/DNA binding)

DOUGLAS KWON, RONALD M. CHALMERS, AND NANCY KLECKNER*

Department of Molecular and Cellular Biology, Harvard University, 7 Divinity Avenue, Cambridge, MA 02138

Contributed by Nancy Kleckner, June 1, 1995

ABSTRACT **All of the DNA cleavage and strand transfer events required for transposition of insertion sequence IS*10* are carried out by a 46-kDa IS*10*-encoded transposase protein. Limited proteolysis demonstrates that transposase has two principal structural domains, a 28-kDa N-terminal domain (N$\alpha\beta$; aa 1–246) and a 17-kDa C-terminal domain (C; aa 256–402). The two domains are connected by a 1-kDa proteolytic-sensitive linker region (aa 247–255). The N-terminal domain N$\alpha\beta$ can be further subdivided into domains Nα and Nβ by a weaker protease-sensitive site located 6 kDa (53 aa) from the N terminus. The Nβ and N$\alpha\beta$ fragments are capable of nonspecific DNA binding as determined by Southwestern blot analysis. None of the fragments alone is capable of carrying out the first step of transposition, assembly of a synaptic complex containing a pair of transposon ends. Remarkably, complete transposition activity can be reconstituted by mixing fragment N$\alpha\beta$ and fragment C, with or without the intervening linker region. We infer that the structural integrity of transposase during the transitions involved in the chemical steps of the transposition reaction is maintained independent of the linker, presumably by direct contacts between and among the principal domains. Reconstitution of activity in the absence of the linker region is puzzling, however, because mutations that block strand transfer or affect insertion specificity alter linker region residues. Additional reconstitution experiments demonstrate that the Nα region is dispensable for formation of a synaptic complex but is required for complexes to undergo cleavage.**

Tn*10* is a composite bacterial transposon consisting of a tetracycline-resistance determinant flanked by two nearly identical IS*10* insertion elements, designated IS*10*-Left and IS*10*-Right (for review, see ref. 1). Only IS*10*-Right encodes a functional IS*10* transposase protein. This transposase mediates all of the DNA cleavage and strand transfer events required for transposition of either Tn*10* or IS*10*. Transposition occurs via a nonreplicative mechanism in which the transposon is first excised from the donor molecule by a pair of flush double-strand breaks made precisely at the ends of the element. The free 3′-hydroxyl groups at the transposon ends are then joined to the target at 5′-phosphates located 9 bp apart on opposite strands (2–4). These chemical steps all occur within the context of a stable synaptic complex between transposon ends (5).

IS*10* transposase has 402 aa and shares regions of sequence similarity with other insertion element transposases of the IS*4* family (6). Organizational information about the protein has been obtained primarily from genetic approaches, which have defined two regions in IS*10* transposase known as Patch I (aa 102–167) and Patch II (aa 243–264) (7). Patch I and Patch II are broadly defined by the positions of mutations that specifically block transposition between the excision and strand transfer (integration) steps, referred to as SOS$^+$Tnsp$^-$ (7). Two mutations that confer altered target specificity also occur in these regions, one in Patch I and one in Patch II (8). It has been suggested that these two regions of the protein interact (9).

We describe herein a physical investigation of IS*10* transposase structure and function. Limited proteolysis shows that transposase protein is organized into two principal domains separated by an exposed linker region that corresponds to a predicted flexible loop. The N-terminal domain (N$\alpha\beta$) is further divisible by more extensive proteolysis into two subdomains (Nα and Nβ). Southwestern blot analysis demonstrates that the full N-terminal domain N$\alpha\beta$ and subdomain Nβ are both capable of nonspecific DNA binding. Mixtures of purified domains N$\alpha\beta$ and C catalyze normal transposition reactions irrespective of the presence of the linker region. If the most N-terminal segment (Nα) is missing, however, the only activity detected is the assembly of abnormal synaptic complexes.

MATERIALS AND METHODS

Enzymatic Digestion of Transposase. IS*10* transposase (0.8 mg/ml) was purified as described (10). The purified protein solubilized in buffer A (25 mM Tes, pH 7.5/2 mM EDTA/10 mM dithiothreitol/25 mM Triton X-100/1.5 M NaCl) was treated on ice with trypsin (Boehringer) or chymotrypsin (Boehringer) at a protein/protease ratio of 500:1 (wt/wt) for various times. Proteolysis was stopped with phenylmethylsulfonyl fluoride added to 1 mM. The proteolytic fragments were then separated by SDS/PAGE on 12.5% gels and visualized by Coomassie blue staining.

Protein Sequence Analysis. Purified transposase was digested as above and proteolytic fragments were separated by SDS/PAGE on 12.5% gels and electroblotted onto a poly(vinyldiene difluoride) membrane (Bio-Rad) in 25 mM Tris/190 mM glycine/20% (vol/vol) methanol. Membranes were then stained with 0.2% Ponceau S in 1% acetic acid to visualize bands. The desired bands were then excised and the N-terminal amino acid sequence was determined by automated Edman degradation performed at the Harvard Microchemistry Facility.

Southwestern Blot DNA Binding Analysis. Purified IS*10* transposase was digested with trypsin as described above. Proteolytic fragments were then separated by SDS/PAGE on 12.5% gels and electroblotted onto nitrocellulose in 25 mM Tris/190 mM glycine. The membrane was then washed once in blocking buffer [5% (wt/vol) dry milk/10 mM Tris·HCl, pH 7.5/150 mM NaCl] for 1 h at room temperature and then

The publication costs of this article were defrayed in part by page charge payment. This article must therefore be hereby marked "*advertisement*" in accordance with 18 U.S.C. §1734 solely to indicate this fact.

Abbreviations: IHF, integration host factor; PEC, paired ends complex.

*To whom reprint requests should be addressed.

REF. 10

several times in buffer B (25 mM Tes, pH 7.5/2 mM EDTA/10 mM dithiothreitol) for 6 h all at 4°C. The membrane was then placed in renaturation buffer [25 mM Tes, pH 7.5/2 mM EDTA/10 mM dithiothreitol/2 M NaCl/bovine serum albumin (1 mg/ml)/50% (vol/vol) glycerol] for 2 h. Membranes were incubated overnight at room temperature in 20 mM Tris·HCl, pH 7.5/10 mM dithiothreitol/50 mM KCl/15% glycerol with 0.5 nM nonspecific radiolabeled DNA. The nonspecific DNA fragment was a 147-bp *Msp* I fragment cut from pBR322 which was labeled by end-filling with avian myeloblastosis virus reverse transcriptase (Promega). After DNA binding, membranes were washed in several changes of buffer B for 4 h at room temperature and visualized by autoradiography.

Peptide Purification. A C_{18} reversed-phase chromatography column (Vydac, Hesperia, CA, 4.6 mm × 25 cm) was used to purify tryptic proteolytic fragments generated from two point mutants of IS*10* transposases (obtained from S. Bolland, this laboratory) that are completely catalytically inactive. N-terminal proteolytic fragments were purified from a tryptic digest of the EA292 mutant and C-terminal proteolytic fragments were purified from the DA161 mutant. Purified mutant transposase was digested with trypsin as above and bound to the column equilibrated in 0.1% trifluoroacetic acid. Fragments were eluted by using a gradient of 0–70% (vol/vol) acetonitrile in 0.1% trifluoroacetic acid, over 90 min at a flow rate of 1 ml/min. Fractions were collected and assayed for the presence of various proteolytic fragments by SDS/PAGE followed by silver staining.

Reconstitution of Activity and Short Linear Fragment Assay. Transposition was assayed as described (5) with the radiolabeled 136-bp *Sal* I–*Bgl* II fragment from pNK1935. This fragment contained the 23-bp transposase binding site, an adjacent integration host factor (IHF) recognition site, and additional flanking sequences (11). Fragments were radiolabeled by end-filling with avian myeloblastosis virus reverse transcriptase. Both termini of the fragment were labeled, but the end containing the flanking DNA was labeled ≈1.4 times more efficiently than the other end.

For reconstitution experiments, proteolytic fragments were mixed and incubated on ice for 30 min. The mixture was then used in the same manner as purified transposase. Protein concentrations for reconstitution reactions were approximately the same as those performed with whole transposase. Strand transfer was assayed with a supercoiled target plasmid as described (5).

RESULTS

Trypsin Digestion Products. The domain structure of the 46-kDa transposase was investigated by limited proteolysis of the purified protein. A time course of trypsin digestion is shown in Fig. 1. At early time points (<30 min), digestion yields five major proteolytic products with masses of 40, 29, 28, 18, and 17 kDa. At intermediate time points (30–60 min), a 22-kDa species appears with traces of a 23-kDa species. At late time points (≥120 min), the larger species progressively disappear and most of the protein is present in the 17-kDa species and in a group of species of ≈21 kDa.

Five of the major products were mapped within the transposase protein. The first five N-terminal residues from each of the fragments were determined by automated Edman degradation (Fig. 1). The 28-kDa fragment produced by trypsin digestion (T28) contains the N terminus of the protein; T40 and T22 both begin at residue 54; T18 and T17 begin at residues 247 and 256, respectively. T18 also contains a minor contaminant (≈10%) whose N terminus is 3 residues away at position 244. All of these sites occur after Lys or Arg residues, as expected from the digestion specificity of trypsin.

From these data and the relative mobilities of the proteolytic fragments in SDS/PAGE, the five major tryptic digestion products can be deduced to have arisen as follows: Single cleavages at two nearby positions, residues 246 and 255, yield two complementary pairs of products. A single cleavage after residue 246 yields T28 (aa 1–246) and T18 (aa 247–402); a single cleavage after residue 255 yields T17 (aa 256–402) and, as deduced from its molecular weight, T29 (aa 1–255). Cleavage at residue 246 appears to be faster than at residue 255, since the abundance of the T28/T18 pair is greater than the T29/T17 pair at early times in the digestion. A single cleavage after residue 53 produces T40 (aa 54–402). This same cleavage in combination with cleavages at either position 246 or 255 yields T22 (aa 54–246) and T23 (aa 54–255), respectively.

Inferred Domain Structure of Transposase. The observed array of tryptic digest products shows that transposase is organized into two principal domains, a 28-kDa N-terminal portion (N$\alpha\beta$) and a 17-kDa C-terminal portion (C), which are connected by a protease-sensitive linker region of ≈9 residues. The N-terminal domain is further divisible into a proximal segment of 6 kDa (Nα) and the remainder (Nβ; 22 kDa).

This interpretation is further supported by analysis with other proteases. Digestion of transposase by chymotrypsin yields an array of digestion products very similar to that

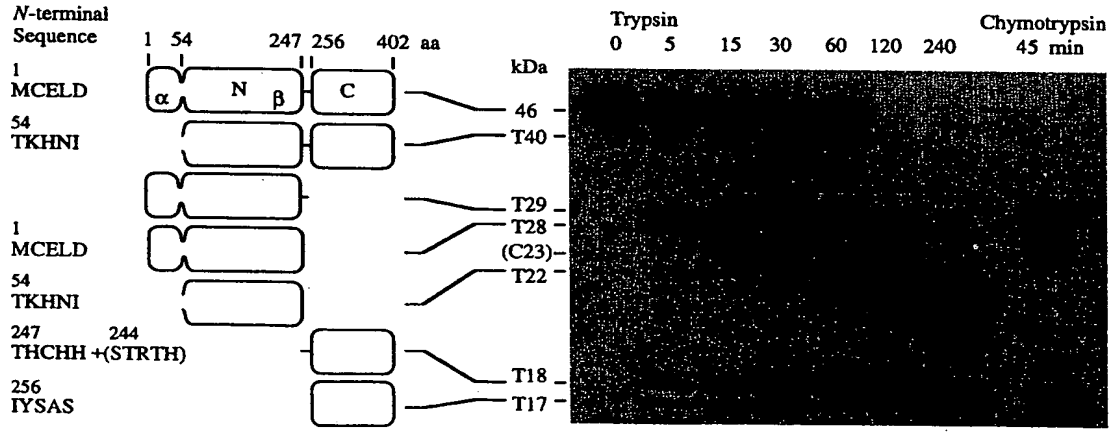

FIG. 1. Limited proteolysis of IS*10* transposase and the N-terminal sequences of fragments. At various times, proteolysis with trypsin or chymotrypsin was stopped and reaction products were analyzed by SDS/PAGE and Coomassie blue staining. The N-terminal amino acids of five major fragments generated by tryptic digestion were determined. The regions of the transposase molecule from which each fragment was derived were found by alignment with the gene sequence of IS*10* transposase, and this information was used to determine the domain structure. The primary sequence of T18 was found to have a minor contaminant (≈10%) that was offset by 3 aa.

obtained with trypsin (Fig. 1). At early stages of digestion, two major species are present that correspond to T29 and T17. These products probably result from cleavage near residue 255. Digestion with elastase, V8 protease, and proteinase K also identifies protease-sensitive site(s) within or very close to the proposed linker region (data not shown).

The linker region probably extends from residues 233 to 255 with the greatest proteolytic sensitivity at residues 244–255. Tryptic cleavages have been detected after residues 243, 246, and 255, which are all of the predicted preferred cleavage positions within this 11-aa segment (aa 244–255). In addition, Chou–Fasman analysis of secondary structure for this area of transposase predicts the presence of a turn extending over the larger segment (aa 233–255). In this larger region, there are five other closely spaced preferred tryptic cleavage sites; cleavage at these positions could account for the further degradation of T22 at late times (Fig. 1).

The N-Terminal Domain Exhibits Nonspecific DNA Binding. The ability of individual domains of transposase to bind DNA was assayed by Southwestern blot analysis with a nonspecific DNA fragment of 147 bp from pBR322 as probe (Fig. 2). A mixture of proteolytic fragments, generated by limited trypsin digestion, was separated by SDS/PAGE and transferred to a nitrocellulose membrane. After treatment with a solution of blocking reagent to prevent binding of the probe to the charged membrane, transposase was given the opportunity to renature by incubation under conditions known to allow full recovery of activity of the undigested protein in solution after SDS treatment. Whole transposase, T40, T28, and T22 bind the nonspecific DNA probe under these conditions, but not if the renaturation incubation is short or omitted. In all cases, binding decreases uniformly as salt concentration is increased from 0 to 100 mM KCl (data not shown). The two C-terminal fragments T17 and T18 exhibited no detectable binding (Fig. 2).

The same pattern of DNA binding was obtained in Southwestern blot analysis performed with a labeled fragment containing the outside end of Tn*10* (data not shown).

Transposase Activity Is Reconstituted from Mixtures of Proteolytic Fragments. The activities of individual domains were examined after they were purified by C_{18} reverse-phase chromatography (Fig. 3). The fragments chosen included the two C-terminal fragments, T17 and T18, which differ with respect to the presence or absence of the linker region, and two N-terminal fragments, T28 and T22; these latter two lack the linker region but contain or lack the proximal 6-kDa domain Nα, respectively.

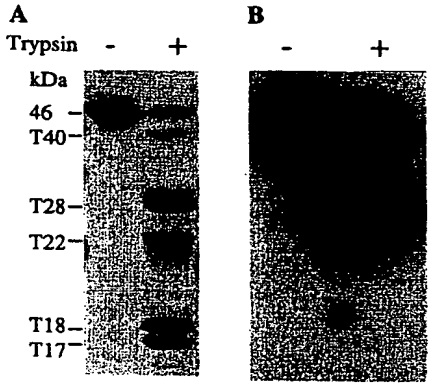

FIG. 2. Southwestern blot analysis of DNA binding. Whole transposase and trypsin-treated transposase were electrophoresed in an SDS/polyacrylamide gel. They were then stained with Coomassie blue or transferred to nitrocellulose to assay for DNA binding. (*A*) Coomassie blue staining of whole and trypsin-treated transposase. (*B*) Southwestern blot probed with nonspecific DNA from pBR322. DNA binding reactions were in 50 mM KCl.

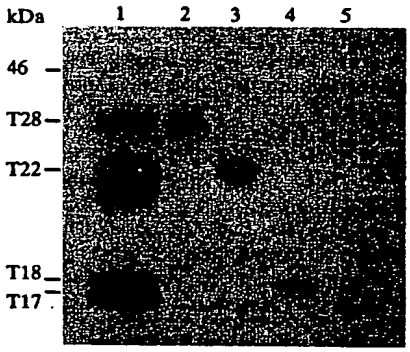

FIG. 3. Silver-stained gel of C_{18} purification of tryptic fragments. Lanes: 1, trypsin-treated transposase; 2 and 3, T28 and T22 purified from tryptic digestion of EA292 mutant transposase; 4 and 5, T18 and T17 purified from tryptic digestion of DA161 transposase.

Purified fragments were assayed singly or in appropriate mixtures for their ability to carry out defined steps of the transposition reaction. To further ensure that no full-length active transposase was present in these preparations, fragments corresponding to N-terminal and C-terminal domains were purified from mutant transposases in which the complementary portions of the proteins (C- and N-terminal regions, respectively) carried point mutations that confer a complete block to the chemical steps of the reaction (catalysis minus; S. Bolland, personal communication). In these experiments, proteolytic fragments were present at concentrations that were close to that of wild-type transposase in control reactions.

The Tn*10*/IS*10* transposition reaction involves assembly of a synaptic complex containing a pair of transposon ends, successive double-strand cleavages at the two ends within each complex, and finally, strand transfer of the two ends to target DNA (5). All of these events can be assayed by using purified transposase and short linear DNA fragments containing the outside end of IS*10*, which are radiolabeled to permit monitoring of the reaction (Fig. 4 and ref. 5). A stable synaptic complex containing transposase and a pair of substrate fragments forms rapidly in the absence of divalent cations. Upon addition of Mg^{2+}, these complexes undergo cleavage at the two component transposon ends with concomitant release of flanking DNA. If supercoiled target DNA is added to the reaction with Mg^{2+}, the two ends undergo strand transfer to the target after cleavage. All reactions include IHF protein, which is an essential accessory component in this system.

The first two stages of the transposition reaction are monitored by gel retardation of protein–DNA complexes; uncleaved paired ends complex (PEC) and double end break complex migrate with distinct characteristic mobilities (Fig. 4 *A* and *B*). Strand transfer in the short linear fragment assay is monitored by analysis of DNA after removal of proteins. Joining of the two labeled end fragments within a single complex to a target DNA molecule linearizes that molecule; joining of one labeled end fragment (single end strand transfer) yields a nicked circular species.

In this assay, the four purified fragments individually exhibit neither PEC formation (Fig. 4*A*) nor cleavage (data not shown). All four possible combinations of N- and C-terminal fragments were, however, capable of forming a PEC (Fig. 4*A*).

The full-length N-terminal fragment T28 (domain N$\alpha\beta$) in combination with either of the two C-terminal fragments (T18 or T17) appears to be very nearly normal not only with respect to formation of PECs but also in the ability of such complexes to proceed through the chemical steps of transposition (Fig. 4). Both types of reconstituted PECs exhibit the mobility and

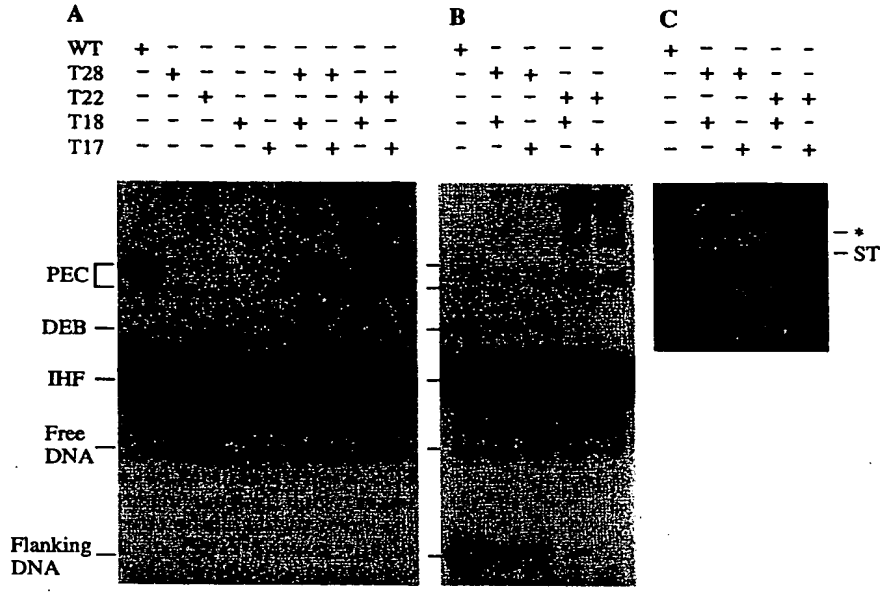

FIG. 4. Transposition activities of digested transposase. Purified proteolytic fragments were renatured and used in the short linear fragment assay. (*A*) The reaction without Mg^{2+} shows that none of the fragments alone are capable of forming complex and that complex formation can be reconstituted by mixing fragments. (*B*) After the addition of Mg^{2+}, only complexes with T28, which contains domain Nα, are capable of cleavage. Note that radioactive label was incorporated more efficiently at the end containing the flanking DNA. (*C*) T28 complexes go on to do strand transfer in the presence of a supercoiled target. WT, whole transposase (aa 1–402); T28, N$\alpha\beta$ (aa 1–246); T22, Nβ (aa 54–246); T18, C + linker (aa 247–402); T17, C − linker (aa 256–402); PEC, paired ends complex; DEB, double end break complex; IHF, IHF–DNA complex; free DNA, unbound DNA fragment; flanking DNA, cleaved flanking DNA; ST, linear strand transfer product; *, the strand transfer product that retained supercoiling because the synaptic complex was not completely dissociated.

discreteness characteristic of native complexes (Fig. 4*A*). These complexes are also capable of undergoing efficient cleavage irrespective of the presence or absence of the linker region in the C-terminal partner (Fig. 4*B*). In both cases, the level of PEC and cleavage products is consistently similar over several trials to that observed for the native reaction. Finally, after cleavage, both reconstituted reactions yield strand transfer products (Fig. 4*C*). Reactions containing T18 are reproducibly more efficient than reactions containing T17; in the experiment shown, the efficiency of strand transfer per precleavage complex is 51% of the native level for the T28–T18 complexes and 27% for the T28–T17 complexes.

T22, the shorter N-terminal fragment that lacks the 6-kDa Nα domain, in combination with either of the C-terminal fragments is capable of giving rise to precleavage complexes in the absence of Mg^{2+} (Fig. 4*A*). These complexes are, however, abnormal. The precleavage complexes formed in these two fragment mixtures migrate faster and are less discrete than native complexes. Furthermore, upon addition of Mg^{2+}, these complexes fail to give rise to any cleavage products (Fig. 4*B*). Nor do they give strand-transfer in reactions where Mg^{2+} and target DNA are both added (Fig. 4*C*).

DISCUSSION

The domain structure of IS*10* transposase deduced from the analysis presented above is summarized in Fig. 5*A*. The protein is organized into two principal domains that are connected by a short linker region that probably corresponds to an exposed loop. The N-terminal domain is further subdivided into short proximal and longer distal segments.

Patch I and Patch II are two regions genetically defined by the positions of SOS^+Tnsp^- mutants (7). The N-terminal domain, Nβ, contains Patch I while Patch II is in the linker region and the C-terminal domain C. The experiments presented here suggest that Patch II (aa 243–264) is composed of two distinguishable regions that we shall define as Patch IIA (aa 243–255) and Patch IIB (aa 256–264). The linker region (aa 247–255) corresponds to Patch IIA and is thought to be a flexible loop as determined by secondary structure predictions and proteolytic sensitivity. Patch IIB appears to have a more ordered structure. Interestingly, the SOS^+Tnsp^- mutations in Patch IIA generally confer more severe transposition defects than those in Patch IIB (7).

The complete N-terminal domain N$\alpha\beta$ and its distal subdomain Nβ are both capable of nonspecific DNA binding. Neither specific DNA binding nor synaptic complex formation was detected with any of the isolated domains alone. In contrast, full transposition activity can be reconstituted by mixing a fragment containing the complete N-terminal domain with C-terminal fragments that either contain or lack the linker region. The presence of the linker region appears to be irrelevant for synaptic complex formation and cleavage but to be slightly beneficial for strand transfer (Fig. 4).

Current genetic evidence suggests that the two principal structural domains of transposase are functionally interdependent. Most importantly, the active site of the protein appears to be formed from residues within both domains. IS element transposases of the IS*4* family have amino acid sequence similarity within three segments, two within the Nβ domain and the third within domain C (Fig. 5 and ref. 6). Moreover, acidic residues at which mutations completely abolish catalysis occur within these three segments (S. Bolland, personal communication). The observations presented here fully support this view. Thus, they suggest that formation of a synaptic complex and, quite possibly, specific interaction of transposase with transposon ends require communication between the N- and C-terminal portions of the protein either within a single molecule or between two molecules.

The dispensability of the linker region further demonstrates that the structural integrity of transposase and of the transposase synaptic complex during the transitions involved in the

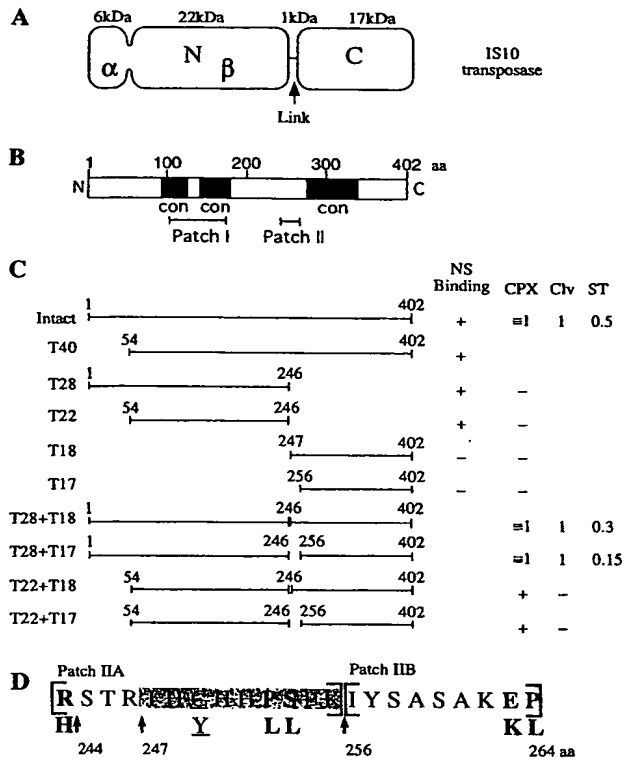

FIG. 5. Summary of transposase and activities measured. (*A*) Domain structure of IS*10* transposase. (*B*) Line representation of the protein with regions previously defined by homology with members of the IS*4* family (con) and genetic analysis (Patches I and II). (*C*) Measurement of the activities of transposase, proteolytic fragments, and mixtures of fragments. Strand transfer efficiency was calculated by taking the ratio of radioactive label present in the strand transfer product to the label present in the cleaved flanking DNA band (correcting for the different labeling efficiencies at each of the ends). NS, nonspecific; CPX, complex; Clv, cleavage; ST, strand transfer. (*D*) Sequence of Patch II and the location of mutants. Arrows represent detected trypic cleavage sites. The shaded box indicates the linker region that is deleted in the reconstitution experiment by using the purified proteolytic fragments. Although these residues are dispensable for complete transposition activity, three mutations have been mapped within this region: two $SOS^+/Tnsp^-$ mutations (boldface type) and one altered target specificity mutation (underlined).

chemical steps of transposition is maintained independent of this connector. Other proteins have been shown to retain biochemical function in the absence of covalent integrity of the polypeptide chain [e.g., β-galactosidase (12)].

The linker region is generally dispensable for the transposition reaction. This finding is particularly intriguing because the linker region corresponds to sites at which mutations affecting transposition have been identified (Fig. 5*D*). More specifically, the PL252 and SL253 mutations block the transposition reaction after excision but prior to strand transfer, and the CY249 mutation reduces site specificity of transposon insertion (7, 8).

After excision, the synaptic complex undergoes a transition from one conformation to another, which permits it first to undergo a stable noncovalent interaction with target DNA and then strand transfer (5). Based on the results presented here, we can propose one specific model that can account for the effects of both genetic and physical changes in the interdomainal linker region. We propose that the linker region must move for target capture and/or strand transfer to occur; once the linker segment has moved, it has a modest positive effect in promoting strand transfer. According to this model, SOS^+Tnsp^- mutations block strand transfer by keeping the linker region from moving properly after cleavage. Deletion of the linker region has no effect on the transition *per se*, but the slightly positive effect of the linker on strand transfer is eliminated. The altered target specificity mutations strengthen the linker region interaction that promotes strand transfer, thus, rendering the reaction less dependent upon effective target capture.

We thank S. Bolland and J. Sakai for helpful discussion. This research was funded by a grant to N.K. from the National Institutes of Health (RO1 GM25326). D.K. was also supported in part by a Ford Foundation grant for undergraduate research.

1. Kleckner, N. (1989) in *Mobile DNA*, eds. Berg, D. E. & Howe, M. M. (Am. Soc. Microbiol., Washington, DC), pp. 225–267.
2. Bender, J. & Kleckner, N. (1986) *Cell* **45**, 801–815.
3. Benjamin, H. & Kleckner, N. (1992) *Proc. Natl. Acad. Sci. USA* **89**, 4648–4652.
4. Morisato, D. & Kleckner, N. (1984) *Cell* **39**, 181–190.
5. Sakai, J., Chalmers, R. M. & Kleckner, N. (1995) *EMBO J.*, in press.
6. Mahillion, J., Seurinck, J., Van Rompuy, L., Delcour, J. & Zabeau, M. (1985) *EMBO J.* **4**, 3895–3899.
7. Haniford, D. B., Chelouche, A. R. & Kleckner, N. (1989) *Cell* **59**, 385–394.
8. Bender, J. & Kleckner, N. (1992) *EMBO J.* **11**, 741–750.
9. Junop, M. S., Chelouche, A. R. & Haniford, D. (1994) *Genetics* **137**, 343–352.
10. Chalmers, R. M. & Kleckner, N. (1994) *J. Biol. Chem.* **269**, 8029–8035.
11. Husiman, O., Herrada, P. R., Signon, L. & Kleckner, N. (1989) *EMBO J.* **8**, 2101–2109.
12. Ullman, A., Jacob, F. & Monod, J. (1968) *J. Mol. Biol.* **32**, 1–13.

THE JOURNAL OF BIOLOGICAL CHEMISTRY

Vol. 269, No. 17, Issue of April 29, pp. 12552–12558, 1994
Printed in U.S.A.

Expression and Activities of a Recombinant Basic Fibroblast Growth Factor-Saporin Fusion Protein*

(Received for publication, November 29, 1993, and in revised form, January 31, 1994)

Douglas A. Lappi‡, Wenbin Ying‡, Isabel Barthelemy‡§, Darlene Martineau‡, Ignacio Prieto‡§, Luca Benatti¶, Marco Soria‖, and Andrew Baird‡

From the ‡Department of Molecular and Cellular Growth Biology, The Whittier Institute for Diabetes and Endocrinology, La Jolla, California 92037, the ¶Farmitalia Carlo Erba, Via Papa Giovanni XXIII 23, 20014 Nerviano, Italy, and the ‖Dipartimento di Biotecnologia, Istituto Scientifico S. Raffaele, I-20132 Milano, Italy

A fusion protein containing the full-length sequences of the mitogen, basic fibroblast growth factor (FGF-2), and the ribosome-inactivating protein, saporin (SAP), has been expressed in *E. coli*. As expected, it binds with high affinity to heparin-Sepharose like FGF-2 and can displace the binding of radiolabeled FGF-2 to its high affinity receptor. In contrast, the fusion protein only has much lower ribosome-inactivating activity than free saporin, although full ribosome-inactivating protein activity can be generated by proteolytic removal of the FGF-2 moiety. Cytotoxicity experiments with B16-F10 mouse melanoma cells establish that the fusion protein is active as a chemical conjugate against these intact cells. Presumably these cells have the ability to activate the SAP component of the fusion protein through an intracellular metabolism of the fusion protein. Because we also show the fusion protein has tumor growth inhibition properties and antimetastatic activity in *in vivo* models of melanoma, the findings support the hypothesis that FGF-based ligand-mediated cytotoxicity can serve to target cytotoxic agents *in vivo*.

The chemical conjugation of basic fibroblast growth factor (FGF-2)[1] with saporin (SAP) creates a molecule that is an extremely potent cytocidal agent for cells that express cell surface high affinity FGF receptors. This molecule (FGF-SAP) has been used to eliminate contaminating FGF receptor-bearing cells from mixed cell populations (1, 2), in tumor models to inhibit solid tumor growth (3), in the inhibition of corneal re-epithelialization (4), and to inhibit smooth muscle cell proliferation in experimental models of restenosis (5, 6).

Over the course of the last few years, fusion proteins containing bacterial toxins and ligands (7–9) or antibody fragments (10) have led to a second generation of mitotoxins and immunotoxins. These recombinant proteins provide numerous advantages. First and foremost, proteins can be purified that are chemically homogeneous. Their structures can be engineered to enhance potency or to modulate their effects (11). In some instances, for example, the ligand moiety is modified to enhance its binding to high affinity receptors (12). In others, the toxin moiety is engineered for increased stability (13, 14), decreased intrinsic toxicity (15), or to enhance its translocation into the cellular cytoplasm after internalization (16).

In a recent study, we reported the expression of one of the four isoforms of saporin, a ribosome-inactivating protein isolated from the plant *Saponaria officinalis* in *Escherichia coli* (17). Saporin is a type 1 ribosome-inactivating protein that has been used in many applications as the targeted toxin moiety of chemically conjugated immunotoxins (18, 19) and mitotoxins (20). Recently, for example, SAP chemical conjugates have been evaluated in clinical trials as anti-tumor agents (21, 22) and in the development of experimental models of Alzheimer's disease (23). Because the expression of saporin in *E. coli* produces a recombinant protein with the full intrinsic ability to inhibit protein synthesis (17), we constructed a cDNA encoding a fusion protein of FGF-2 and SAP. It was cloned into the pET11 expression system (24) and the expressed molecule (rFGF-SAP) was characterized.

EXPERIMENTAL PROCEDURES

Reagents—Restriction and modification enzymes were purchased from Life Technologies, Inc., Stratagene (La Jolla, CA), and New England Biolabs (Beverly, MA). Native SAP, chemically conjugated FGF-SAP, and rabbit polyclonal antisera to SAP and FGF-2 were prepared as described previously (25, 26). The pET System Induction Control was purchased from Novagen (Madison, WI). pFC80, containing the FGF-2 coding sequence (27), was a kind gift of Dr. Paolo Sarmientos of Farmitalia Carlo Erba (Milan, Italy). The SAP coding sequence Seq3 is described in Barthelemy *et al.* (17).

Plasmid Construction—An *Nco*I restriction site was introduced into the sequence of the SAP Seq3 by site-directed mutagenesis using the Amersham Corp. *in vitro* mutagenesis system 2.71. Oligonucleotides were synthesized using a 380B automatic DNA synthesizer (Applied Biosystems, Foster City, CA). The oligonucleotide used for creation of this site was CAA CAA CTG CCA TGG TCA CAT C replacing the original SAP gene sequence CAA CAA CTG ATG CGG TCA CAT C. The resulting phage has the *Nco*I site located at the beginning of the mature SAP coding sequence and is termed mpNG4. The stop codon of the FGF-2 coding sequence in the pFC80 plasmid was also removed by site-directed mutagenesis. The FGF-2 sequence was isolated as a *Hga*I-*Sal*I fragment and after filling its protruding ends, it was cloned in the *Sma*I site of M13mp18. An insert in the origin of replication minus direction was mutagenized using the Amersham Corp. kit with the sequence GCT AAG AGC GCC ATG GAG A to replace the naturally occurring GCT AAG AGC TGA CCA TGG AGA. The resulting M13 replicative form was cut with *Nco*I and *Sac*I to yield a fragment containing FGF-2 coding sequence with the stop codon replaced. An *Eco*RI-*Nco*I fragment from mpNG4 was ligated to a *Nco*I-*Sac*I fragment from FGFM13. The resulting fragment was inserted into M13mp18 opened with *Eco*RI and *Sac*I to create mpFGFSAP. mpFGFSAP was digested with *Xba*I and *Eco*RI, and the resulting fragment that contains the

* This work was funded by the Whittier/Erbamont Angiogenesis Project, National Institutes of Health Grant DK18811, the Associazione Italiana per le Ricerca sul Cancro (AIRC), and the Italian AIDS Program. The costs of publication of this article were defrayed in part by the payment of page charges. This article must therefore be hereby marked "*advertisement*" in accordance with 18 U.S.C. Section 1734 solely to indicate this fact.

This paper is dedicated to the memory of our colleague, Gianpaolo Nitti.

§ Present address: Antibioticos Farma, S. A., C/Antonio Lopez 109, Madrid, 28026 Spain.

[1] The abbreviations used are: FGF-2, basic fibroblast growth factor; SAP, saporin; FGF, fibroblast growth factor; rFGF-SAP, recombinant basic fibroblast growth factor-saporin fusion protein; RIP, ribosome-inactivating protein; IL-4, interleukin 4; IL-6, interleukin 6; TGFα, transforming growth factor α; ELISA, enzyme-linked immunosorbent assay.

REF. 11

rFGF-SAP coding sequence was isolated and ligated into pET11a pretreated with *Eco*RI and *Xba*I. The resulting plasmid (pT7-FS) contains a λ cII ribosome binding site from the pFC80 plasmid which replaces the ribosome binding site of the pET vector. It was transformed into host strain BL21(DE3)pLysS according to manufacturer's instructions.

Purification of Recombinant FGF-SAP (rFGF-SAP)—4 liters of LB broth containing carbenicillin (Sigma, 50 μg/ml) and chloramphenicol (Sigma, 50 μg/ml) were inoculated with plasmid-containing bacterial cells from a culture grown to 1 OD_{600} (1:100 dilution). Cells were grown at 28 °C in an incubator shaker to an OD_{600} of 0.5. Isopropyl-1-thio-β-D-galactopyranoside (Sigma) was added to a final concentration of 0.2 mM and growth continued to OD_{600} of 1.2 at which time cells were centrifuged. The pellet was resuspended in 10 mM Tris, 0.6 M NaCl, pH 7.4. The solution was frozen and thawed five times and sonicated for 2 min. The suspension was centrifuged; the supernatant was saved and the pellet was resuspended for further analysis and saved. The supernatant was applied to a HiTrap heparin-Sepharose column (Pharmacia, Uppsala, Sweden) equilibrated with 0.15 M NaCl in 10 mM Tris, pH 7.4 (buffer A), and washed with equilibration buffer, 0.6 M NaCl in buffer A, 1.0 M NaCl in buffer A, and finally eluted with 2 M NaCl in buffer A. The column fractions were analyzed by SDS-gel electrophoresis, Western blotting with anti-saporin antibodies, and the sandwich ELISA described below. Peak fractions of the 2 M elution were pooled and diluted 10-fold with 10 mM sodium phosphate, pH 7.5, and applied to a Mono S 5/5 column (Pharmacia) equilibrated with the same. A 30-min gradient at 1 ml/min was run. SDS-gel electrophoresis and the sandwich ELISA were used for analysis. Peak fractions were pooled and dialyzed *versus* 10 mM sodium phosphate, 0.15 M NaCl, pH 7.4, and stored. Yield of purified rFGF-SAP was 460 μg/liter of fermentation broth. For sequencing rFGF-SAP, an aliquot of the Mono S pool was dialyzed against water and the protein sequenced as described (28). Recovery from the first cycle was 53%. For sequencing of the tryptic fragment, material was purified by reverse phase chromatography before sequencing.

Sandwich ELISA for FGF-SAP—Wells of a 96-well plate (Costar) were coated with an antibody to FGF-2 (26) that was diluted 1:400 in 50 mM carbonate/bicarbonate buffer, pH 9.6. The plate was incubated overnight at 4 °C. The wells were washed with washing buffer (0.15 M NaCl, 10 mM Tris, 0.05% Tween 20, pH 8.0). 50 μl of column fractions or standard, diluted in dilution buffer (washing buffer with 0.1% bovine serum albumin), were added in duplicate. Chemically conjugated FGF-SAP was used as the standard. The plate was incubated for 1 h at 37 °C. The wells were washed three times with washing buffer. 50 μl of a rabbit anti-SAP antiserum (25) that had been linked to horseradish peroxidase was diluted 1:100 and added to each well and for 1 h at 37 °C. The wells were washed four times, and 50 μl of freshly prepared o-phenylenediamine substrate was added to each well. The plate was incubated at 37 °C for 2–10 min, depending on the rate of color development. 50 μl of 4.5 M H_2SO_4 was added to stop color formation. The optical density at 492 nm was measured, and unknown values were interpolated from the standard curve values.

Sodium Dodecyl Sulfate (SDS)-Gel Electrophoresis and Western Blotting—SDS-gel electrophoresis was performed on a PhastSystem using 20% gels (Pharmacia). Western blotting was accomplished by transfer of the electrophoresed protein to nitrocellulose using the PhastTransfer system (Pharmacia), as described by the manufacturer. The antisera to SAP and FGF-2 were used at a 1:1000 dilution. Horseradish peroxidase-labeled anti-IgG was used as the second antibody as described (29).

In Vitro Assays of Cytotoxic Activity—The ribosome-inactivating protein (RIP) activity of recombinant FGF-SAP was compared with the RIP activity of chemically conjugated FGF-SAP and the RIP activity of native SAP, in an *in vitro* assay measuring cell-free protein synthesis. Immediately before assay, both the chemically conjugated and recombinant FGF-SAP molecules were reduced by treatment with 50 mM dithiothreitol for 1 h at 37 °C. Samples were diluted in PBS, and 5 μl of sample was added on ice to 35 μl of a nuclease-treated rabbit reticulocyte lysate (Promega, Madison, WI), and 10 μl of a reaction mixture containing 0.5 μg of Brome mosaic virus RNA, 1 μl of a 1 mM amino acid mixture minus leucine, 5 μCi of tritiated leucine, and 3 μl of water. Assay tubes were incubated 1 h in a 30 °C water bath. The reaction was stopped by transferring the tubes to ice, and 5 μl of the assay mixture was added in triplicate to 75 μl of 1 N sodium hydroxide, 2.5% hydrogen peroxide in the wells of a Millititer HA 96-well filtration plate (Millipore, Bedford, MA). When the red color had bleached from the samples, 300 μl of ice-cold 25% trichloroacetic acid were added to each well and the plate left on ice for another 30 min. The plate was placed on a Millipore vacuum holder attached to a vacuum source and the liquid vacuumed through. The wells were washed three times with 300 μl of ice-cold 8% trichloroacetic acid. After drying, the filter paper circles were punched out of the 96-well plate and counted by liquid scintillation techniques.

Cytotoxicity experiments were performed with the Promega CellTiter 96 Cell Proliferation/Cytotoxicity Assay using human (SK-Mel-28, ATCC HTB72) and mouse (B16-F10) melanoma cell lines. The procedure was optimized for 1500 cells plated per well.

In Vivo Assay of Cytotoxic Activity—Both a solid tumor and metastatic model of melanoma were examined. In the solid tumor model, on day 0, 5×10^5 B16-F10 cells were injected subcutaneously in the flanks of each C57BL/6 mouse. By day 3, tumors were visible on all mice. The mice in Group C were given two injections at the LD_{10} (105 μg/kg), one on day 3, the other on day 7. Mice in Group D were injected on days 3, 6, and 9 with 26 μg/kg. Tumor size was evaluated on days 5 and 10. Saporin treatment was done on day 3 at 82 μg/kg, a dose equimolar to the LD_{10}. Mice in the "no treatment" category were injected with Dulbecco's PBS at day 3. The mice were sacrificed on day 10, and the tumors were removed and weighed. The mean tumor weights and mean tumor volumes (tumor volume = $ab^2/2$, where a is equal to the larger dimension measured and b is equal to the smaller dimension) were determined for each group, and statistical comparisons of the various treatment groups were performed using Student's t test.

For the metastatic model, on day 0 of the experiment, B16-F10 cells (5×10^5 in 0.1 ml of Dulbecco's PBS) were injected via the tail vein into the circulation of C57BL/6 mice. On day 1, the mice were randomly divided into two groups and treated as follows: 12 mice were injected via the tail vein with 105 μg/kg rFGF-SAP, and 10 mice were injected as above with Dulbecco's PBS. On day 7, the mice were sacrificed, and the number of nodules on the lungs were counted using a dissecting microscope.

RESULTS

Expression of rFGF-SAP as a Fusion Protein—Our first attempts to express and characterize a rFGF-SAP fusion protein from *E. coli* (30) resulted in the expression of a protein that had none of the binding properties of FGF-2, SAP's cell-free protein synthesis inhibition activity, or cytotoxicity to cells expressing the FGF-2 receptors. Because of these negative results, we revised our strategy and used the entire coding sequences of both saporin and FGF-2. New restriction sites were introduced by site-directed mutagenesis, and we used the pET expression system, which provides tight control of gene induction (24). This new construct is described in Fig. 1. An *Nco*I restriction site was introduced 5′ to the SAP encoding sequence, leaving the *Eco*RI site derived from the genomic sequence intact. After removal of the stop signal in the FGF-2 sequence, it was ligated to SAP, resulting in a sequence encoding for the entire FGF-2 protein, an intervening 2-amino acid linker peptide (Ala-Met), and the entire SAP sequence. After excision from M13, the DNA was inserted into pET11a for expression.

Purification of the Expressed Fusion Protein—The induction of cells containing the plasmid pT7-FS results in the appearance of a 45-kDa protein detectable by Western blotting with anti-SAP and anti-bFGF antisera. Purification is straightforward by virtue of the heparin affinity of FGF-2. rFGF-SAP elutes from heparin-Sepharose with 2 M NaCl just as native and recombinant FGF-2. This clearly indicates that the heparin affinity of FGF-2, one of its biochemical characteristics (31, 32), is retained in the fusion protein. The final step of purification was Mono S chromatography. Exploiting the strong positive charge of both FGF-2 (pI 9.6) and SAP (pI 10.5) yields an essentially pure protein, as judged by SDS-gel electrophoresis and sandwich ELISA.

As shown in Fig. 2, SDS gels were either stained with Coomassie Blue, or the proteins were transferred to nitrocellulose and blotted with anti-SAP or anti-FGF-2 antisera. Both antisera reveal a band at molecular weight approximately 43,000, which is slightly lower than the sum of the molecular weights of SAP (30,000) and FGF-2 (18,000). The basic isoelectric points of the two proteins result in a faster migration and its appearance as a doublet. As expected, there is no rFGF-SAP in the fermentations of noninduced bacteria, establishing that there

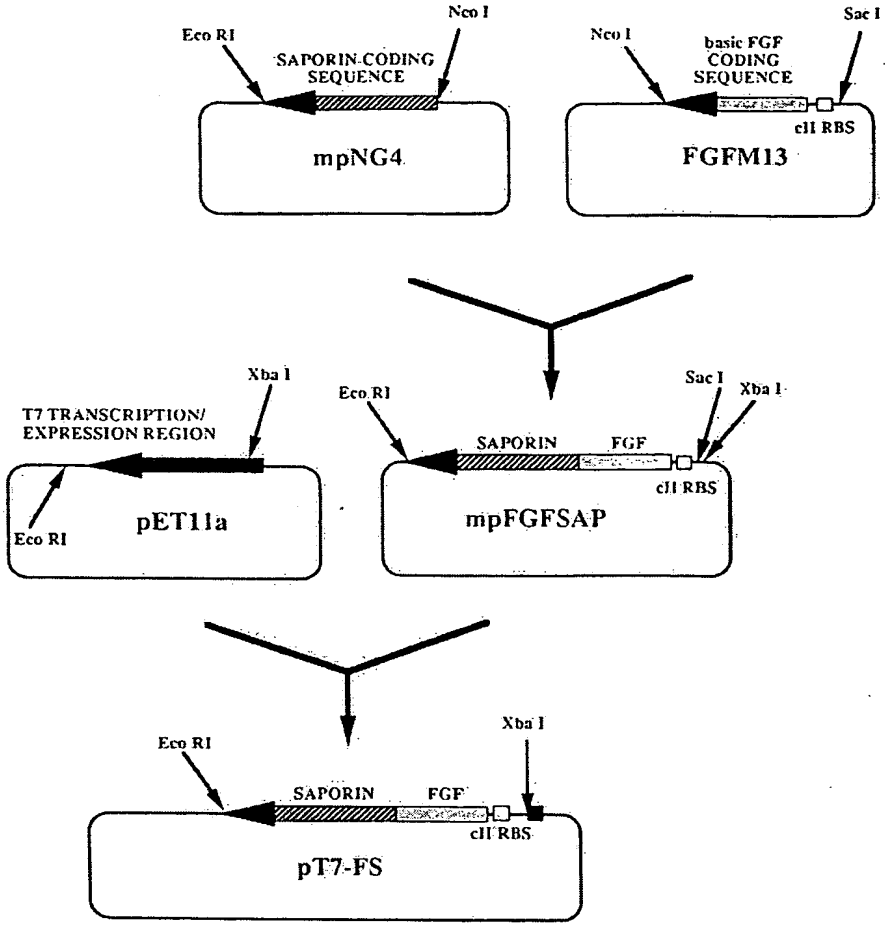

FIG. 1. **Schematic of the construction of the rFGF-SAP fusion protein expression plasmid.** An *Nco*I restriction site was introduced into the 5' end of the saporin coding sequence as described under "Experimental Procedures." An *Eco*RI site remained from the native genomic DNA. A stop signal in the FGF-2 coding sequence was removed by site-directed mutagenesis. An *Eco*RI-*Nco*I fragment from mpNG4, containing the SAP coding sequence, was ligated to a *Nco*I-*Sac*I fragment, containing the FGF-2 coding sequence, from FGFM13. The resulting fragment was inserted into M13mp18 opened with *Eco*RI and *Sac*I to create mpFGFSAP. This fusion protein sequence, containing the entire coding sequence for FGF-2 and saporin, with a 2-amino acid spacer (Ala-Met), was excised from mpFGFSAP with *Eco*RI and *Xba*I and inserted by ligation into the pET11a vector that had been cut with the same restriction enzymes. The resulting plasmid pT7-FS was used for expression of rFGF-SAP.

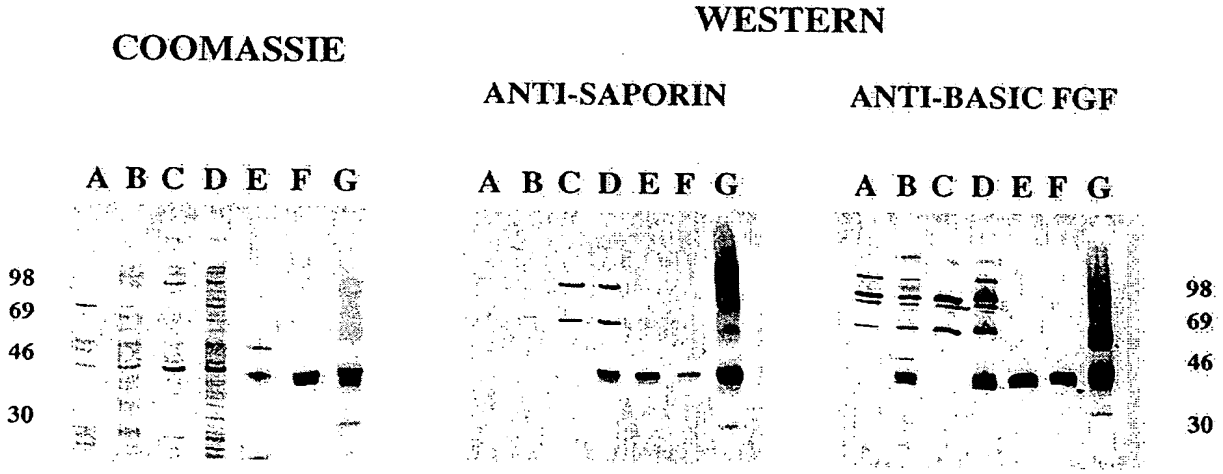

FIG. 2. **SDS-gel electrophoresis analysis of rFGF-SAP production and purification.** Samples were electrophoresed with a PhastSystem (Pharmacia) in 12% PhastGels according to the manufacturer's instructions. Gels were either stained with Coomassie Blue or transferred to nitrocellulose by the PhastTransfer system and used in Western blotting with anti-saporin or anti-FGF-2 antisera. Lanes are the same for all three methods. See "Experimental Procedures" for details of the preparations. *Lane A*, resuspended pellet of extract of uninduced bacteria (0.5 μl); lane B, resuspended pellet of extract of induced bacteria (0.5 μl); *lane C*, supernatant of extract of uninduced bacteria (0.5 μl); *lane D*, supernatant of extract of induced bacteria (0.5 μl); *lane E*, pool of heparin-Sepharose chromatography peak fractions (1.1 μg for Coomassie staining, 11 ng for Westerns); *lane F*, pool of Mono S 5/5 chromatography peak fractions (750 ng for Coomassie staining, 7.5 ng for Westerns); *lane G*, FGF-SAP chemical conjugate (2.5 μg for Coomassie staining, 25 ng for Westerns). Molecular weight standards are given on the ends and correspond to the molecular weight in thousands. *Lanes A–F* are under reducing conditions; *lane G* is without reducing agent.

is tight control of rFGF-SAP expression in this expression system. Although some rFGF-SAP is also present in the pellet of the induced extract, no attempt was made to characterize this material. No immunoreactivity was detected in extracts of bacteria containing the pET11 plasmid without the rFGF-SAP coding sequence. Gas phase sequence analysis of the purified

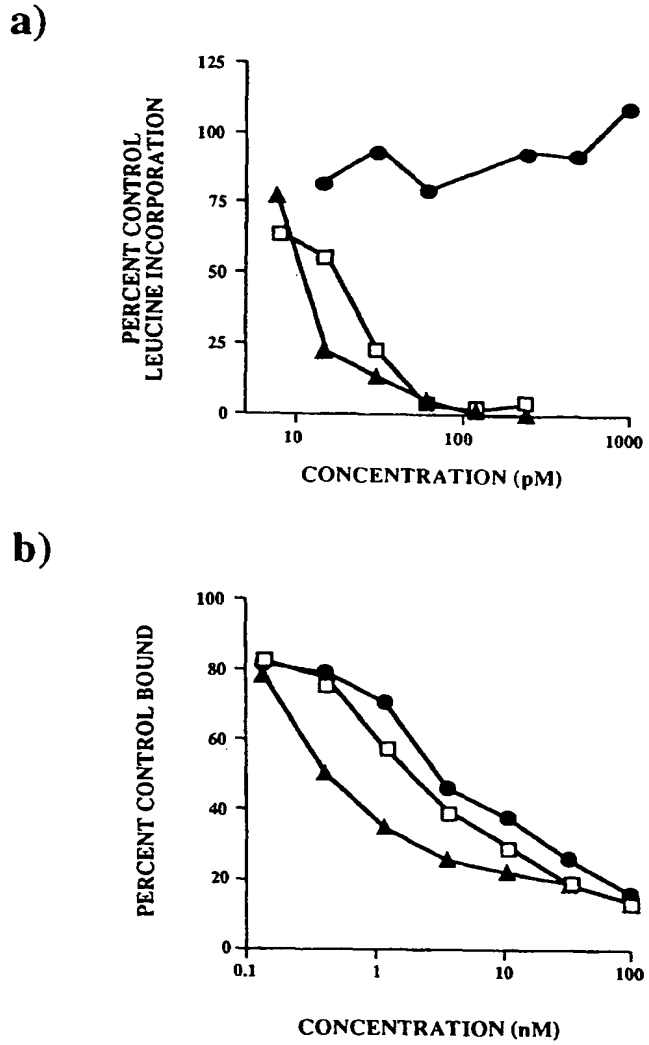

FIG. 3. *a*, inhibition of cell-free protein synthesis by rFGF-SAP, chemically conjugated FGF-SAP, and unconjugated SAP. Leucine incorporation was used as a measure of protein synthesis. Experimentation was done as described under "Experimental Procedures." Results indicate that the SAP moiety of rFGF-SAP is less active than free SAP or chemically conjugated FGF-SAP. ▲, SAP; □, chemically conjugated FGF-SAP; ●, rFGF-SAP. *b*, receptor binding by FGF-2, rFGF-SAP, and chemically conjugated FGF-SAP. The capacity of rFGF-SAP to recognize FGF receptors was examined in baby hamster kidney cells by the method of Moscatelli (61). Briefly, cells were grown to subconfluence and incubated at 4 °C for 2 h with radioiodinated FGF-2 in the presence of unlabeled FGF-2 (▲), chemically conjugated FGF-SAP (□), or rFGF-SAP (●). The cells were then washed twice with PBS and twice with 2 M NaCl. Binding to high affinity receptor was determined by counting the membrane fraction that was solubilized with 0.5% Triton X-100 in PBS.

protein revealed that the expressed protein has its NH_2-terminal methionine removed and begins with alanine, the second amino acid of the FGF-2 (1–155) sequence (33). Approximately 10% of the sample contains a protein whose amino terminus begins at the second alanine.

In Vitro Activities of the Fusion Protein—The ability of FGF-SAP to inhibit protein synthesis was determined using rabbit reticulocyte lysates in a cell-free system which measures leucine incorporation into acid-precipitatable material (Fig. 3*a*). Surprisingly, the RIP activity of the fusion protein is significantly less than the RIP activity of chemically conjugated

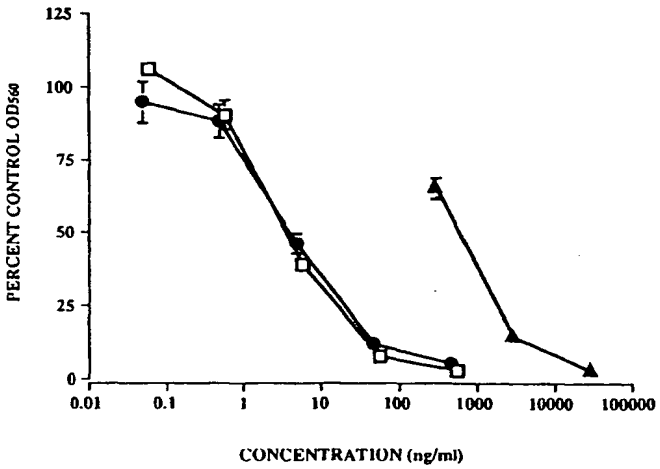

FIG. 4. **Cytotoxicity of rFGF-SAP to melanoma cells expressing the FGF-2 receptor.** Incorporation and conversion of the dye 3-(4,5-dimethyl thiagol-2-yl)-2,5-diphenyl tetrazolium bromide was used as a measure of living cells. Results indicate that rFGF-SAP has a similar cytotoxicity to B16-F10 melanoma cells as chemically conjugated FGF-SAP. □, chemically conjugated FGF-SAP; ●, rFGF-SAP; ▲, nonconjugated SAP.

FGF-SAP or SAP alone. In contrast, the fusion protein's ability to compete with radioiodinated FGF-2 for FGF receptors, while somewhat less than FGF-2, is quite similar to the chemically conjugated FGF-SAP (Fig. 3*b*).

The cytotoxicity of rFGF-SAP was examined using B16-F10 cells, a subclone of a mouse melanoma which is widely used in anti-tumor screening procedures (34–38). These cells have been shown to be very sensitive to the chemical conjugate FGF-SAP, both *in vitro* and *in vivo*.[2] As shown in Fig. 4, the chemical conjugate and the recombinant fusion protein have very similar cytotoxicity profiles *in vitro*. Similar results were seen with SK-MEL-28 cells, another melanomo cell line. The cytotoxicity is competed by free FGF-2, indicating that it is mediated through FGF receptors (data not shown). SAP alone is 100 times less cytotoxic to these cells than its targeted counterpart. This is particularly surprising in light of the results in the cell-free system described above, showing the SAP component of the fusion protein is less effective than SAP alone. We therefore examined whether its activity could be generated by degradation of the fusion protein.

Generation of Biologically Active SAP from rFGF-SAP—The full RIP activity of SAP can be detected from the fusion protein after proteolysis. Because saporin is protease-resistant (39, 40) and FGF-2 is not (41), we treated rFGF-SAP overnight at 37 °C with either chymotrypsin, trypsin, or cathepsin B. With chymotrypsin and trypsin, there was a complete and quantitative degradation of the 45-kDa fusion protein to a protein with a molecular weight similar to that expected for SAP. The protein was identified as SAP by Western blotting (Fig. 5*a*). Sequence analysis of the purified trypsin-treated material showed that it had been cleaved after the last lysine (Lys^{154}) of FGF-2; this would leave 3 amino acids in addition to the NH_2 terminus of SAP. When assayed, it has RIP activity equivalent to that of native saporin (Fig. 5*b*). Because FGF-2 is rapidly degraded in target cells by cleavage at its COOH terminus shortly after internalization (41), we reasoned that the degradation of rFGF-SAP in B16-F10 and SK-Mel-28 cells activates the saporin moiety of the fusion protein to yield a molecule having full cytotoxicity.

[2] W. Ying, D. Martineau, J. Beitz, D. A. Lappi, and A. Baird, submitted for publication.

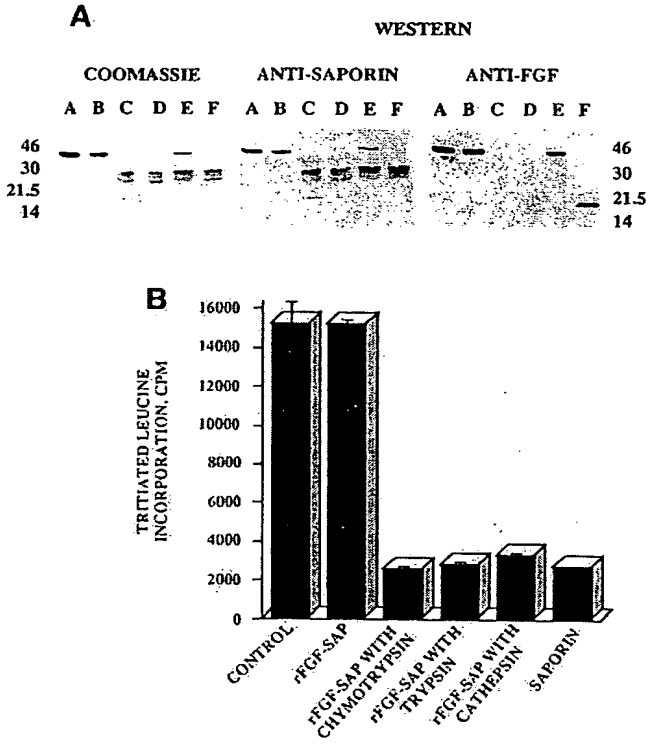

FIG. 5. **Proteolytic digestion of rFGF-SAP.** 50-μg quantities of rFGF-SAP and 31 μg of SAP were incubated with 100-fold less (by weight) quantities of chymotrypsin, trypsin, or cathepsin B (Sigma) overnight at 37 °C. Samples were then removed and assayed for ribosome-inactivating protein activity or electrophoresed and stained with Coomassie stain or transferred to nitrocellulose and immunostained with anti-FGF-2 or anti-saporin. *a*, Coomassie staining and Western blotting of protease-treated rFGF-SAP. *Lane A*, rFGF-SAP, no protease, no 37 °C incubation overnight; *lane B*, rFGF-SAP, no protease, incubation at 37 °C overnight; *lane C*, rFGF-SAP, treated with chymotrypsin at 37 °C overnight; *lane D*, rFGF-SAP, treated with trypsin at 37 °C overnight; *lane E*, rFGF-SAP, treated with cathepsin B at 37 °C overnight; *lane F*, saporin standard (Coomassie and anti-saporin Western), FGF-2 (anti-FGF-2 Western). The double band of SAP is presumably a result of its high isoelectric point (10.5). This behavior is described in Lappi *et al.* (25). *b*, protein synthesis inhibition activity of protease-treated rFGF-SAP. Inhibition of protein synthesis by a rabbit reticulocyte lysate system is measured as described under "Experimental Procedures." Samples were assayed at a final concentration of 45 pM. *Error bars* denote standard deviation. This saporin standard was incubated overnight at 37 °C without protease addition and is similar to untreated saporin standard and saporin that had been incubated with protease (data not shown). Samples containing proteases were assayed without removal of proteases; separate assays showed no effect of proteolytic enzymes at the same dilution on leucine incorporation.

In Vivo Activity of the Fusion Protein—We tested the activities of the rFGF-SAP in both a solid tumor and a metastatic model of melanoma with B16-F10 cells in order to demonstrate its activity *in vivo*. In the solid tumor model, two different dosage regimens were used, one receiving two treatments (Group C) and the other receiving three (Group D), as described under "Experimental Procedures." For both groups, by day 5, there was a significant reduction in tumor volume (not shown) that increased in significance by day 10 (Fig. 6). For Group C, the mean tumor volume of the treated mice on day 10 was 28% that of the nontreated mice ($p < 0.0005$) and for Group D, the mean tumor size on day 10 was 29% of the mean tumor volume of the nontreated mice ($p < 0.001$). Tumor weight measurements gave similar results (no treatment: Group C, $p < 0.001$; no treatment: Group D, $p < 0.005$).

In the metastatic model, cells are injected in the tail vein of

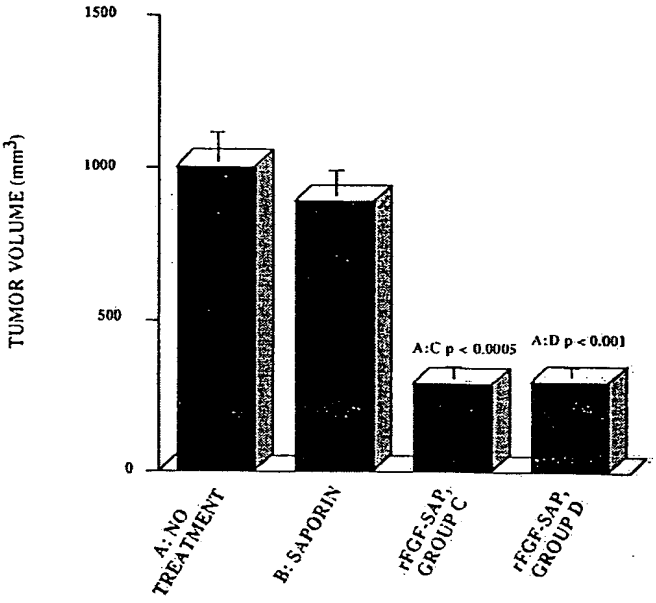

FIG. 6. ***In vivo* anti-tumor activity of rFGF-SAP.** C57BL/6 mice were injected subcutaneously with B16-F10 melanoma cells. 3 days later when the tumors were visible, the mice were treated with Dulbecco's PBS (nontreated), saporin (82 μg/kg), for Group C (rFGF-SAP at 105 μg/kg at days 5 and 7), or for Group D (rFGF-SAP at 26 μg/kg at days 3, 6, and 9). On day 10, these measurements of tumor volumes were recorded. *Numbers* above the *bars* for Groups C and D represent the probabilities from two-tail paired *t* tests.

mice on day 0, and within 7 days, colonies of B16-F10 cells form in the lung. Because these colonies are black and on the lung surface, the extent of metastases can be quantitated by counting colonies under a dissecting microscope. The day after injecting cells, the mice were treated with a single intravenous dose (105 μg/kg) of rFGF-SAP. The mean number of colonies on the lungs of the vehicle-treated mice is 165 ± 23 (±S.E.). The mean number of colonies on the lungs of the animals treated with rFGF-SAP is 49 ± 14 ($p < 0.001$), a 70% reduction of the number of colonies in control animals. Treatment with the same dose of the chemically conjugated FGF-SAP resulted in a 60% decrease in the number of colonies in control animals ($p < 0.002$). Like its chemical conjugate counterpart, recombinant FGF-SAP possesses potent *in vivo* activity in this metastatic melanoma model system.

DISCUSSION

There are a number of ways in which the chemical heterogeneity of conjugated proteins can be minimized. For example, we have recently addressed this problem in FGF-SAP by performing site-directed mutagenesis of FGF-2, selectively removing reactive cysteines, and conjugating the protein to monoderivatized saporin. The reaction produces a chemical conjugate that appears as a single band in nonreducing sodium dodecyl sulfate-gel electrophoresis and has the same intrinsic activities of the wild type (unmutagenized) chemical conjugate (42). Because purified saporin preparations contain at least four isoforms of the protein that differ by several amino acids (17, 43, 44), there is still considerable heterogeneity in this material. For these reasons, we expressed the gene encoding one of these isoforms ligated to a cDNA encoding FGF-2. We show here that the resulting recombinant fusion protein is expressed as a single chain that retains the ability of FGF-2 to bind immobilized heparin, but that it also has greatly reduced ribosome-inactivating protein activity. When evaluated against an FGF receptor-bearing cell type B16-F10, however, the re-

combinant material has cytotoxicity that is comparable with the chemical conjugate. This strongly implies that the saporin moiety of the fusion protein is activated during or after internalization, since cytotoxicity requires the inhibition of protein synthesis. One possible explanation of the data indicating inactivity in the cell-free system, but activity against some whole cells, is that the FGF-2 moiety of the fusion protein is cleaved from NH_2-terminal of the saporin moiety by lysosomal proteases after internalization. Saporin activity, previously inhibited by the NH_2-terminal extension, is then activated and has full intrinsic ribosome-inactivating activity. Indeed, proteolysis *in vitro* demonstrates that the degradation of rFGF-SAP activates the saporin moiety of the fusion protein. Because Walicke and Baird (41) have shown that the initial processing of FGF-2 after internalization occurs at a point seven amino acids from the carboxyl terminus of FGF-2, it is possible that cleavage at this point could activate saporin. This metabolism and activation could then mediate its cytotoxic actions on cells in culture and explain the observation that rFGF-SAP is also active as a single intravenous injection to inhibit tumor growth in a model of melanoma metastases. Whether cleavage at points that would leave longer residual portions of FGF-2 would still be active is under investigation. Preliminary results indicate that another SAP fusion protein, constructed with the amino-terminal fragment (ATF) of human urokinase plasminogen activator (45), also requires that the ATF moiety, situated likewise at the NH_2-terminal of SAP, be removed to obtain protein synthesis inhibition activity. Thus the inhibitory activity of the FGF-2 moiety is not peculiar to the FGF-2 sequence or molecular size.

O'Hare *et al.* (46) have reported a ricin A chain fusion protein with staphylococcal protein A at the NH_2 terminus that is 30-fold less active in cell-free protein synthesis inhibition. This molecule was inactive against target cells. When the protease-sensitive linker was cleaved by trypsin, leaving a disulfide linkage between the two chains, the molecule became cytotoxic. In some cell types (*i.e.* B16-F10, SK-Mel-28, and K562), the rFGF-SAP and chemically conjugated FGF-SAP are equipotent. With baby hamster kidney cells and PA-1 ovarian carcinoma cells, the recombinant material is greater than 100-fold less cytotoxic (results not shown). These cells express high levels of FGF receptors (3, 47), but are perhaps less able to remove the SAP moiety from the FGF-2 moiety. Because they are very sensitive to the chemical conjugate FGF-SAP, it is clear that SAP, internalized by FGF-2, is able to inhibit protein synthesis in these cells. The mechanisms for the differences in these cell types are under investigation, but may be related, as in the ricin A chain fusion protein, to release of the free RIP.

Fusion proteins to target toxins have now been created using bacterial toxins like diphtheria toxin (48) and *Pseudomonas aeruginosa* exotoxin (15) and type II ribosome-inactivating protein, ricin A chain (46). For example, Chaudhary *et al.* (49) expressed a recombinant immunotoxin that targeted *Pseudomonas* exotoxin by its fusion to two antibody-variable domains. Selective killing of human immunodeficiency virus-infected cells has also been reported when the targeting agent is to CD4 (50). This has led several investigators to examine the feasibility of directing bacterial toxins to cells with growth factors. Accordingly, these mitotoxins have been engineered with interleukin-2 to abolish cell mediated immunity *in vivo* (51), to mitigate adjuvant-induced arthritis in rats (52), and enhance cardiac allograft survival in mice (53). Similar reagents have been designed using IL-4 (54), IL-6 (55), and TGFα (56). Each has shown significant activity *in vitro*, and TGFα-PE40 has been extensively evaluated in bladder cancer (57). More recently, Pastan and his co-workers (60) have also produced a fusion protein between acidic FGF (FGF-1) and *Pseudomonas* exotoxin. This construct has been shown to be cytotoxic *in vitro* for proliferating rat smooth muscle cells (58), endothelial cells (59), and several tumor cell types (60). As in the case of FGF-2, inhibition studies established that this mitotoxin exerts its action through high affinity FGF receptors (60).

The studies described here are a natural extension of our previous studies reporting the cloning, characterization, expression, and activity of recombinant SAP (17). The availability of a plant-derived type 1 RIP for the design of mitotoxins offers several advantages over similar approaches with bacterial toxins or type II RIPs. First, because they have no high affinity cell surface binding domain, they need not be engineered to decrease endogenous toxicity. Second, molecules of the saporin family are extremely resistant to proteolysis. Moreover, from the results shown here, the fusion protein has the characteristics of a prodrug: it requires activation, presumably intracellular, to generate full SAP activity. It should be reasonable to anticipate the engineering of a form of fusion protein that has even greater specificity by including cell-specific activation sequences within the fusion protein. Under these circumstances, increased target cell specificity could be conferred beyond that generated by the ligand's high affinity receptor expression at the cell surface. Finally, the demonstration that plant-derived type I RIPs can be targeted by a ligand moiety of fusion proteins to kill cells *in vivo* supports the feasibility of replacing SAP with mutagenized forms of the RIP or with other cytotoxic enzymes that might overcome the issues of immunogenicity, toxicity, and activity of all protein based experimental models.

Acknowledgments—We acknowledge the excellent scientific contributions of Antonella del Vecchio, Michael Ong, Roland Schroeder, and Dr. Nicholas Ling. We especially acknowledge the discussions and encouragement of Professor Roger Guillemin. We are grateful to Annemarie Putze for manuscript preparation.

REFERENCES

1. Beattie, G. M., Lappi, D. A., Baird, A., and Hayek, A. (1990) *Diabetes* **39**, 1002–1005
2. Beattie, G. M., Lappi, D. A., Baird, A., and Hayek, A. (1991) *J. Clin. Endocrinol. Metab.* **73**, 93–98
3. Beitz, J. G., Davol, P., Clark, J. W., Kato, J., Medina, M., Frackelton, A. R., Jr., Lappi, D. A., Baird, A., and Calabresi, P. (1992) *Cancer Res.* **52**, 227–230
4. David, T., Tassin, J., Lappi, D. A., Baird, A., and Courtois, Y. (1992) *J. Cell. Physiol.* **153**, 483–490
5. Lindner, V., Lappi, D. A., Baird, A., Majack, R. A., and Reidy, M. A. (1991) *Circ. Res.* **68**, 106–113
6. Casscells, W., Lappi, D. A., Olwin, B. B., Wai, C., Siegman, M., Speir, E. H., Sasse, J., and Baird, A. (1992) *Proc. Natl. Acad. Sci. U. S. A.* **89**, 7159–7163
7. Murphy, J. R., Bishai, W., Williams, D., Bacha, P., Borowski, M., Parker, K., Boyd, J., Waters, C., and Strom, T. B. (1987) *Biochem. Soc. Symp.* **53**, 9–23
8. Murphy, J. R., Bishai, W., Borowski, M., Miyanohara, A., Boyd, J., and Nagle, S. (1986) *Genetics* **83**, 8258–8262
9. Lorberboum-Galski, H., Kozak, R. W., Waldmann, T. A., Bailon, P., Fitzgerald, D. J., and Pastan, I. (1988) *J. Biol. Chem.* **263**, 18650–18656
10. Kreitman, R. J., Chaudhary, V. K., Waldmann, T., Willingham, M. C., Fitzgerald, D. J., and Pastan, I. (1990) *Proc. Natl. Acad. Sci. U. S. A.* **87**, 8291–8295
11. Kiyokawa, T., Williams, D. P., Snider, C. E., Waters, C. A., Nichols, J. C., Strom, T. B., and Murphy, J. R. (1991) *Ann. N. Y. Acad. Sci.* **636**, 331–339
12. Jean, L.-F. L., Waters, C. A., Keemy, D., and Murphy, J. R. (1993) *Protein Eng.* **6**, 305–311
13. Kasturi, S., Kihara, A., FitzGerald, D., and Pastan, I. (1992) *J. Biol. Chem.* **267**, 23427–23433
14. Brinkmann, U., Pai, L. H., Fitzgerald, D. J., and Pastan, I. (1992) *Proc. Natl. Acad. Sci. U. S. A.* **89**, 3065–3069
15. Pastan, I., and FitzGerald, D. (1989) *J. Biol. Chem.* **264**, 15157–15160
16. VanderSpek, J. C., Mindell, J. A., Finkelstein, A., and Murphy, J. R. (1993) *J. Biol. Chem.* **268**, 12077–12082
17. Barthelemy, I., Martineau, D., Ong, M., Matsunami, R., Ling, N., Benatti, L., Cavallaro, U., Soria, M., and Lappi, D. A. (1993) *J. Biol. Chem.* **268**, 6541–6548
18. Oeltmann, T. N., and Frankel, A. E. (1991) *FASEB J.* **5**, 2334–2337
19. Uckun, F. M., and Frankel, A. (1993) *Leukemia (Baltimore)* **7**, 341–348
20. Lappi, D. A., and Baird, A. (1991) *Prog. Growth Factor Res.* **2**, 223–236
21. Bonardi, M. A., Bell, A., French, R. R., Gromo, G., Hamblin, T., Modena, D., Tutt, D., and Glennie, M. J. (1992) *Int. J. Cancer* **7**, (suppl.) 73–77
22. Falini, B., Bolognesi, A., Flenghi, L., Tazzari, P. L., Broe, M. K., Stein, H., Durkop, H., Aversa, F., Corneli, P., Pizzolo, G., Barbabietola, G., Sabattini, E., Pileri, S., Martelli, M. F., and Stirpe, F. (1992) *Lancet* **339**, 1195–1196
23. Wiley, R. G., Oeltmann, T. N., and Lappi, D. A. (1991) *Brain Res.* **562**, 149–153
24. Studier, W., Rosenberg, A. H., Dunn, J. J., and Dubendorf, J. W. (1990) *Methods Enzymol.* **185**, 60–89
25. Lappi, D. A., Esch, F. S., Barbieri, L., Stirpe, F., and Soria, M. (1985) *Biochem.*

Biophys. Res. Commun. **129**, 934–942
26. Lappi, D. A., Martineau, D., and Baird, A. (1989) *Biochem. Biophys. Res. Commun.* **160**, 917–923
27. Isacchi, A., Statuto, M., Chiesa, R., Bergonzoni, L., Rusnati, M., Sarmientos, P., Ragnotti, G., and Presta, M. (1991) *Proc. Natl. Acad. Sci. U. S. A.* **88**, 2628–2632
28. Esch, F. (1992) *Anal. Biochem.* **136**, 39–47
29. Davis, L., Dibner, M., and Battey, J. F. (1986) *Basic Methods in Molecular Biology*, Elsevier Science Publishing Co., New York
30. Prieto, I., Lappi, D. A., Ong, M., Matsunami, R., Benatti, L., Villares, R., Soria, M., Sarmientos, P., and Baird, A. (1991) *Ann. N. Y. Acad. Sci.* **638**, 434–437
31. Baird, A., and Ling, N. (1987) *Biochem. Biophys. Res. Commun.* **142**, 428–435
32. Vlodavsky, I., Fuks, Z., Ishai-Michaeli, R., Bashkin, P., Levi, E., Korner, G., Bar-Shavit, R., and Klagsbrun, M. (1991) *J. Cell. Biochem.* **45**, 167–176
33. Abraham, J. A., Whang, J. L., Tumolo, A., Mergia, A., Friedman, J., Gospodarowicz, D., and Fiddes, J. C. (1986) *EMBO J.* **5**, 2523–2528
34. Santoro, M. G., Philpott, G. W., and Jaffe, B. M. (1977) *Cancer Res.* **37**, 3774–3779
35. Hill, G. J., and Littlejohn, K. (1971) *J. Surg. Oncol.* **3**, 1–7
36. Goldin, A., Venditti, J. M., and Geran, R. (1985) *Invest. New Drugs* **3**, 3–21
37. Murata, J., Saiki, I., Nishimura, S., Nishi, N., Tokura, S., and Azuma, I. (1989) *Jpn. J. Cancer Res.* **80**, 866–872
38. Griswold, D. P., Jr. (1972) *Cancer Chemother. Rep.* **3**, 315–324
39. Stirpe, F., Gasperi-Campani, A., Barbieri, L., Falasca, A., Abbondanza, A., and Stevens, W. A. (1983) *Biochem. J.* **216**, 617–625
40. Soria, M., Benatti, L., Ceriotti, A., Lappi, D. A., Lorenzetti, R., Nitti, G., and Solinas, M. (1992) *Targeted Diagn. Ther.* **7**, 193–212
41. Walicke, P. A., and Baird, A. (1991) *J. Neurosci.* **11**, 2249–2258
42. Lappi, D. A., Matsunami, R., Martineau, D., and Baird, A. (1993) *Anal. Biochem.* **212**, 446–451
43. Barra, D., Maras, B., Schininà, E., Angelaccio, S., and Bossa, F. (1991) *Biotechnol. Appl. Biochem.* **13**, 48–53
44. Maras, B., Ippoliti, R., DeLuca, E., Lendaro, E., Bellelli, A., Barra, D., Bossa, F., and Brunori, M. (1990) *Biochem. Int.* **21**, 831–838
45. Stoppelli, M. P., Corti, A., Soffientini, A., Cassani, G., Blasi, F., and Assoian, R. K. (1985) *Proc. Natl. Acad. Sci. U. S. A.* **82**, 4939–4943
46. O'Hare, M., Brown, A. N., Hussain, K., Gebhardt, A., Watson, G., Roberts, L. M., Vitetta, E. S., Thorpe, P. E., and Lord, J. M. (1990) *FEBS Lett.* **273**, 200–204
47. Lappi, D. A., Maher, P. A., Martineau, D., and Baird, A. (1991) *J. Cell. Physiol.* **147**, 17–26
48. Bacha, P., Williams, D. P., Waters, C., Williams, J. M., Murphy, J. R., and Strom, T. B. (1988) *J. Exp. Med.* **167**, 612–622
49. Chaudhary, V. K., Queen, C., Junghans, R. P., Waldmann, T. A., Fitzgerald, D. J., and Pastan, I. (1989) *Nature* **339**, 394–397
50. Chaudhary, V. K., Mizukami, T., Fuerst, T. R., Fitzgerald, D. J., Moss, B., Pastan, I., and Berger, E. A. (1988) *Nature* **335**, 369–372
51. Kelley, V. E., Bacha, P., Pankewycz, O., Nichols, J. C., Murphy, J. R., and Strom, T. B. (1989) *Proc. Natl. Acad. Sci. U. S. A.* **85**, 3980–3984
52. Case, J. P., Lorberboum-Galski, H., Lafyatis, R., FitzGerald, D., Wilder, R., and Pastan, I. (1989) *Proc. Natl. Acad. Sci. U. S. A.* **86**, 287–291
53. Lorberboum-Galski, H., Barrett, L. V., Kirkman, R. L., Ogata, M., Willingham, M. C., Fitzgerald, D. J., and Pastan, I. (1989) *Proc. Natl. Acad. Sci. U. S. A.* **86**, 1008–1012
54. Ogata, M., Chaudhary, V. K., Fitzgerald, D. J., and Pastan, I. (1989) *Proc. Natl. Acad. Sci. U. S. A.* **86**, 4215–4219
55. Siegall, C. B., Chaudhary, V. J., Fitzgerald, D. J., and Pastan, I. (1988) *Proc. Natl. Acad. Sci. U. S. A.* **85**, 9738–9742
56. Siegall, C. B., Xu, Y.-H., Chaudhary, V. K., Adhya, S., Fitzgerald, D., and Pastan, I. (1989) *FASEB J.* **3**, 2647–2652
57. Theuer, C. P., Fitzgerald, D. J., and Pastan, I. (1993) *J. Urol.* **149**, 1626–1632
58. Biro, S., Siegall, C. B., Fu, Y.-M., Speir, E., Pastan, I., and Epstein, S. E. (1992) *Circ. Res.* **71**, 640–645
59. Merwin, J. R., Lynch, M. J., Madri, J. A., Pastan, I., and Siegall, C. B. (1992) *Cancer Res.* **52**, 4995–5001
60. Siegall, C. B., Epstein, S., Speir, E., Hla, T., Forough, R., Maciag, T., Fitzgerald, D. J., and Pastan, I. (1991) *FASEB J.* **5**, 2843–2849
61. Moscatelli, D. (1987) *J. Cell. Physiol.* **131**, 123–130

ELSEVIER

Journal of Immunological Methods 183 (1995) 119–125

JOURNAL OF IMMUNOLOGICAL METHODS

Screening and kinetic analysis of recombinant anti-CEA antibody fragments

Ralph Abraham *, Sarah Buxbaum, John Link, Rodger Smith, Colleen Venti, Michael Darsley

IGEN, Inc., 1530 East Jefferson Street, Rockville, MD 20852, USA

Abstract

Four different carcinoembryonic antigen (CEA)-binding antibody fragments were prepared using the genes of the variable regions of the T84 epitope-specific antibody 7F7 and phage display techniques. The genes were successfully cloned and expressed in the pCANTAB5 phage display vector to investigate the kinetic binding parameters of each synthesized construct. Single chain fragments, Fab fragments, and two diabodies were purified and compared in their CEA-binding properties with the parent IgG using surface plasmon resonance detection. The on-rates for all these molecules were in the same order of magnitude (about 1×10^5 M^{-1} s^{-1}) whereas major differences were detected in the off-rates. IgG and diabodies had slow off-rates due to bivalent binding, while single chain and Fab fragments dissociated rather fast. We also present a method for the immobilization of large amounts of CEA on CM5 sensorchips. These high density surfaces can be used for observing mass transport limited binding of CEA-specific molecules and are convenient tools for screening and quality control.

Keywords: Recombinant; Fragment; sFv; Fab; Diabody; Phage display; Carcinoembryonic antigen; BIAcore; Surface plasmon resonance; Screening; Mass transport limited binding; (Antibody)

1. Introduction

In immunodiagnostics and immunotherapy, recombinant antibody fragments are being investigated as alternatives or adjuncts to whole immunoglobulins (Owens and Young, 1994). In order to change or generate desired specificities and kinetic parameters of antigen binding molecules, recombinant antibody fragments are the preferred starting material for molecular engineers. New binding species are generated by manipulating antibody gene repertoires from naive or immunized donors. These constructs are expressed as fragments containing the variable regions in a variety of contexts (Hoogenboom et al., 1992). In therapeutic applications, small molecules such as single chain and Fab fragments or diabodies (Holliger et al., 1993) are now being investigated to try to overcome the limitations with whole immunoglobulins such as antigenicity and poor immunolocalization (Adair, 1992). In the diagnostic field, mostly whole antibody or enzymatically produced fragments are used but fine specificities and kinetic binding properties of

* Corresponding author. Tel.: (301) 984-8000; Fax: (301) 230-0158.

SSDI 0022-1759(95)00039-9

REF. 12

the antibodies frequently limit the performance of immunoassays. We and other groups are using the techniques of antibody engineering to overcome these limitations.

In this study, we chose three different molecular species derived from the CEA-binding antibody 7F7 for evaluation of kinetic binding properties. sFv, Fab, and diabody were cloned into the pCANTAB5 phage display vector and expressed in *E. coli*. Clones were screened in an electrochemiluminescence-based immunoassay (Blackburn et al., 1991) or by mass transport limited binding on high density CEA surfaces in a biosensor system using surface plasmon resonance detection (BIAcore system, Karlsson et al., 1993). For this purpose we coupled large amounts of CEA to sensorchips via periodate-oxidized carbohydrate residues on the antigen (aldehyde coupling). After purification of the CEA-binding fragments the kinetic behaviour was evaluated in the BIAcore system (Malmqvist, 1993). We describe the differences in binding properties between sFv, Fab, two diabody constructs and parent IgG and the use of the BIAcore system for screening and characterization of the engineered molecules.

2. Materials and methods

2.1. Cloning and purification of antibody sFv and Fab fragments

The 7F7 mAb fragments used in this study were cloned and purified as described previously (Darsley et al., 1994). Briefly, the heavy and light chain genes of the variable region were amplified by PCR from cDNA derived from the hybridoma cell line CEA129.7F7. The 7F7 mAb has specificity for the 'T84' epitope of CEA as shown by its ability to inhibit the binding of the mAb M207 (Medix, Foster City, CA) to purified CEA. The PCR product was cloned into the pCANTAB5 phage display vector and expressed as sFv or Fab in the *E. coli* strain HB2151. After screening the bacterial cell culture supernatants from several 96 well microtiter plates in the electrochemiluminescence-based Origen immunoassay as described by Darsley et al. (1995), clones with the highest expression level were grown on a 1.5 liters scale. Fab and sFv were purified by immobilized metal affinity chromatography (IMAC, Invitrogen ProBond resin) and size exclusion chromatography on a Superdex 75 column (Pharmacia). Purity was checked by SDS-PAGE and analytical size exclusion chromatography. The protein concentration was determined in a micro BCA assay (Bio-Rad).

2.2. Cloning and purification of diabodies

Messenger RNA was isolated from CEA129.7F7 using the 'Micro Fast-Track' kit (InVitrogen, San Diego, CA) according to the manufacturers' protocol. cDNA was synthesized and the segments encoding variable regions of the antibody heavy and light chains were amplified by the polymerase chain reaction (PCR) using specific primers. PCR of the heavy chain fragments utilized a set of 10 different 5'VH specific primers (combined into five pairs) in combination with a single JH specific primer. For the light chain, five different 5'VK primers were used in combination with a set of four JK specific primers. The 3'JH primer and 5'VK primers were modified to contained complimentary end sequences which will encode the $(Gly)_2$ or $(Gly)_4Ser$ linker segments in the final diabody construct (2-linker and 5-linker diabody, respectively). This short region of complementarity allows the specific linking of the VH and VK gene segments in frame using a splice overlap extension PCR reaction. During the linking PCR reaction step the outside PCR primers used contained restriction site tails to allow subsequent cloning of the diabody PCR product into the phage display vector, pCANTAB5 (Pharmacia, Piscataway NJ) as described in the Pharmacia users manual and by Hoogenboom et al. (1991). After ligation and transformation into the *E. coli* strain HB2151, individual transformants were grown in 96 well plates and the expression of diabody was induced by growing overnight at 30° C in 2 × YT + AMP with 1 mM IPTG. Supernatants were cleared by centrifugation in the culture plate for 20 min at 2000 rpm in a Sorval RT6000D centrifuge at 4° C and screened

for soluble diabody by mass transport limited binding to a high density CEA sensorchip surface in the BIAcore system as described below. Diabodies were purified from 1L HB2151 cultures grown at 23° C for 4 h after induction with 1 mM IPTG. The cell pellets were sonicated 3 × for 10 s on ice. After centrifugation diabodies were purified from the supernatants and characterized as described above for sFv and Fab.

2.3. Amine coupling of CEA to CM5 sensorchip surface

Lyophilized CEA (Scripps) was dissolved to 5 mg/ml in PBS and diluted 1/50 in 10 mM acetate/citrate pH 4.5. At a flow rate of 5 μl/min of HBS/p20 (10 mM Hepes, 150 mM NaCl, 3.4 mM EDTA, 0.05% p20 (Biosensor), pH 7.4) the following samples were injected sequentially on CM5 sensorchip surfaces:

- 1 × or 3 × 35 μl NHS/EDC mixture from Biosensor amine coupling kit;
- 1 × or 2 × 35 μl CEA (100 μg/ml);
- 35 μl 1 M ethanolamine pH 8.5 from Biosensor amine coupling kit.

2.4. Aldehyde coupling of CEA to CM5 sensorchip surface

For this procedure we followed the recommendations for aldehyde coupling provided by Biosensor in the BIAcore Users Manual. To 300 μg CEA (Scripps) dissolved in 60 μl PBS, pH 7.4, 240 μl 100 mM sodium acetate pH 5.5 (buffer A) were added. The oxidation of CEA was started by adding 6 μl freshly prepared 50 mM sodium metaperiodate in buffer A (final concentration 1 mM). After 20 min incubation on ice 0.2 ml of buffer A were added and the reaction was stopped by desalting the mixture on a NAP-5 column (Pharmacia) into 1 ml 10 mM sodium acetate pH 4.0 (buffer B). The absorbance at 280 nm was determined (OD_{280} = 0.084) and the product was stored at 4° C. Aliquots of this sample were used for immobilization on CM5 sensorchip surfaces. At a flow rate of 5 μl/min of HBS/p20 the following samples were injected sequentially on CM5 sensorchip surfaces:

- 15 μl NHS/EDC mixture from Biosensor amine coupling kit;
- 35 μl hydrazine at 0.2 mM, 1 mM, or 5 mM;
- 35 μl 1 M ethanolamine pH 8.5 from Biosensor amine coupling kit;
- 35 μl oxidized CEA undiluted or diluted 1/5 or 1/25 in buffer B;
- 40 μl 0.1 M sodium cyanoborohydride in buffer B at 2 μl/min;
- 3 × 4 μl 10 mM HCl.

2.5. Determination of kinetic binding parameters by BIAcore

Serial dilutions of 7F7 IgG and fragments (30–1000 nM) in HBS/p20 were bound to CEA surfaces prepared by the aldehyde or amine coupling method with an antigen density of 900–2600 RU at a flow rate of 5 μl/min. Kinetic binding parameters were calculated with the BIAevaluation software version 1 (Biosensor).

2.6. Mass transport limited binding experiments

For screening purposes 4 μl aliquots of diabody samples were injected on high density CEA surfaces (6000–12000 RU oxidized CEA) at a flow rate of 5 μl/min using the above described HBS/p20 buffer. The total amounts of diabody bound in RU were determined from sensorgrams. The mass transport limited binding characteristics of sFv, Fab, 2-linker diabody and IgG were evaluated by injecting 35 μl of serial dilutions of samples in HBS/p20 at a flow rate of 5 μl/min on high density CEA surfaces (8000–12000 RU oxidized CEA). The slopes of mass transport limited binding determined from sensorgrams for time intervals between 15 and 100 s of injection start were plotted against the sample concentration.

3. Results

In this study we have generated a range of CEA-binding molecules of different structure. Using the cDNA synthesized from a hybridoma cell line expressing the CEA-specific 7F7 IgG,

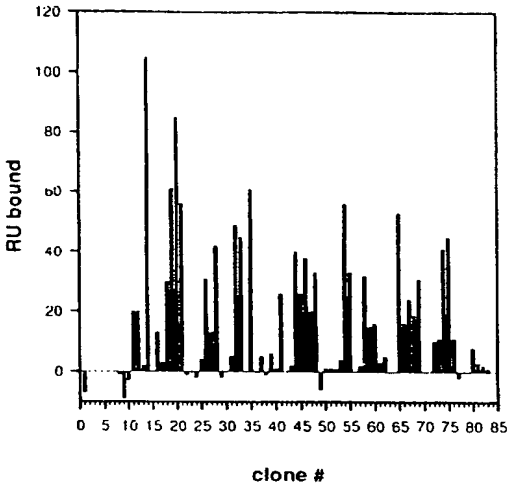

Fig. 1. Screening of 2-linker diabody clones. 4×μl of cell culture supernatant were injected on to a high density CEA surface (about 12000 RU CEA bound). The total amount of RU diabody bound is plotted against the number of the clone.

the variable regions were successfully cloned and expressed in *E. coli*. All four different forms of CEA-binding molecules (sFv, Fab, and two diabody molecules with different linker regions) were cloned and expressed in the pCANTAB5 vector, which also encodes a poly-histidine affinity label for purification (Skerra et al., 1991). Clones expressing the desired molecules were identified from cell culture supernatants using an electrochemiluminescence-based immunoassay (sFv and Fab, see Darsley et al., 1995) or by mass transport limited binding to a high density CEA surface (diabody, Fig. 1). All fragments were released from HB2151 *E. coli* cell pellets by sonication. They were purified by IMAC and size exclusion chromatography. The protein yields for sFv and diabody were about 100 μg, whereas for Fab we obtained 400 μg per liter of cell culture. Purity of the preparations was checked by analytical size exclusion chromatography and SDS-PAGE (purity > 95%). After determination of the protein concentration with a Micro BCA Assay using BSA as a standard the kinetic binding parameters of the samples were analyzed in the BIAcore system (see below).

CEA was immobilized on CM5 sensorchips

Table 1
Amine coupling of CEA

# of EDC/NHS injections	Buffer	# of CEA injections	RU CEA bound
1	pH 4.0	1	712
3	pH 4.0	1	890
1	pH 4.5	1	1117
3	pH 4.5	2	2341

All injections are 35 μl at a flow rate of 5 μl/min using HBS/p20 as eluent. [CEA] is 100 μg/ml in 10 mM citrate in all experiments.

using the amine and aldehyde coupling methods. Table 1 summarizes the experiments performed to immobilize CEA via its amino groups. In order to increase the sensitivity of CEA sensorchips for screening a large number of samples and to carry out mass transport binding studies we oxidized the carbohydrate residues of CEA with sodium metaperiodate. The oxidized material was linked via its aldehyde groups to amino groups previously introduced to the CM5 sensorchip surface. Fig. 2 shows how different concentrations of hydrazine and oxidized CEA influence the amount of antigen coupled to a sensorchip surface. With the aldehyde coupling method it was possible to immobilize between 1400 and 12000 RU of CEA.

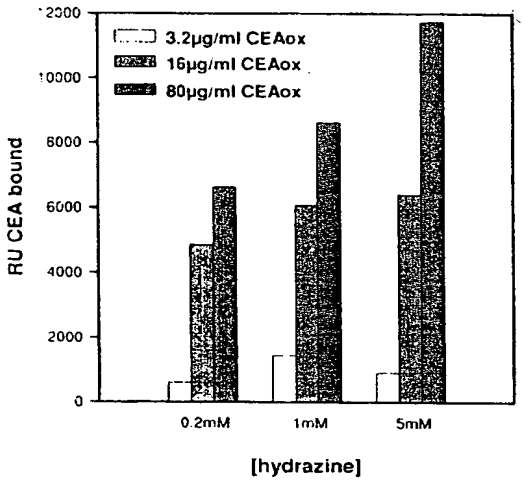

Fig. 2. Immobilization of periodate-oxidized CEA on CM5 sensorchips pretreated with EDC/NHS and various concentrations of hydrazine.

Surfaces with more than 6000 RU CEA were used for studying mass transport limited binding and screening of diabody clones.

The kinetic binding parameters of the CEA-binding proteins were evaluated on surfaces with CEA densities of 900–2600 RU. Maximum binding was observed to be about 1000 RU for each sample. The apparent binding kinetic parameters calculated with the BIAevaluation software version 1 are summarized in Table 2. Whereas the on-rate k_{on} only shows minor differences between the molecules (from 4×10^4 M^{-1} s^{-1} for 2-linker diabody to 1×10^5 M^{-1} s^{-1} for Fab) very large difference are found for the off-rate k_{off}. The rates differ by a factor of 200. The sFv molecule dissociates very fast at a rate of 9.4×10^{-4} s^{-1} and IgG shows the slowest k_{off} of 4.9×10^{-6} s^{-1}. The diabodies both have off-rates comparable to those observed for IgGs indicating an avidity effect caused by the bivalent binding to the CEA surface but they still dissociate about ten times faster than 7F7 IgG.

The preparation of high density CEA surfaces on CM5 sensorchips permitted us to conveniently screen diabody clones directly from bacterial cell culture supernatants. Injecting 4 μl of supernatant from a 96 well microtiter plate was sufficient to identify clones expressing CEA-binding diabody (Fig. 1). One or two plates can be screened in an overnight run in the BIAcore system. The clone with the highest expression level, i.e., the highest RU bound was selected, grown on a 1 liter scale, purified with a yield of 100 μg and characterized as described above.

Mass transport limited binding rates for sFv, Fab, 2-linker diabody and IgG were determined by injecting various concentrations of sample on high density CEA surfaces. After reading the slopes from the sensorgrams at time intervals of 15–100 s after injection the binding rates were plotted against sample concentration as shown in Fig. 3. The monovalent Fab fragment exhibited the fastest mass transport limited binding rate (slope of Fab standard curve b[1] = 1.044), whereas the bivalent diabody was found to bind at approximately half the rate (slope of diabody standard curve b[1] = 0.484).

Table 2
Apparent kinetic constants of CEA binding molecules derived from 7F7 IgG

Form	k_{on}	k_{off}	K_D (nM)
sFv	1.11×10^5	9.44×10^{-4}	8.5
Fab	1.19×10^5	4.09×10^{-4}	3.4
Diabody 2L	3.62×10^4	7.42×10^{-5}	2.1
Diabody 5L	7.61×10^4	5.72×10^{-5}	0.75
IgG	9.54×10^4	4.90×10^{-6}	0.051

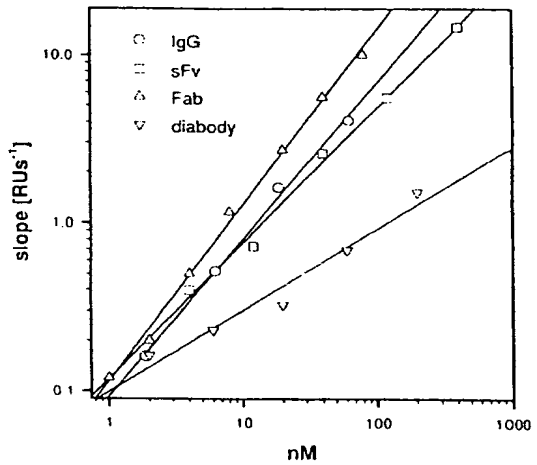

Fig. 3. Mass transport limited binding of CEA-specific fragments and IgG to high density CEA surfaces prepared by aldehyde coupling. The slope of the standard curves for the samples are 0.932 (IgG), 1.044 (Fab), 0.484 (2-linker diabody), and 0.806 (sFv).

4. Discussion

Four different forms of recombinant antibody fragments directed against the T84 epitope of CEA were generated by phage display techniques (Hoogenboom et al., 1991). The sFv fragment consists of the variable regions of the heavy and light chain covalently linked by the 15 amino acid long bridge $[(Gly)_4Ser]_3$; in the Fab fragment whole light chain and the Fd fragment of the heavy chain form a non-covalent complex (Orum et al., 1993). Two diabody molecules were prepared to investigate the influence on binding kinetics of the length of the amino acid linker

[$(Gly)_2$ or $(Gly)_4Ser$] between the variable regions of heavy and light chain. All fragments were successfully expressed in HB2151 *E. coli* cells using the pCANTAB5 phage display vector with final protein yields ranging from 100 to 400 μg/l. Material purified by immobilized metal affinity chromatography and size exclusion chromatography was subjected to kinetic analysis using the BIAcore system, which is based on surface plasmon resonance detection (Malmqvist, 1993). The apparent kinetic binding constants of the fragments were compared with the parent 7F7 IgG and are shown in Table 2. Only minor differences were found in the on-rates which ranged from 4×10^4 M^{-1} s^{-1} for the 2-linker diabody to 1.1×10^5 M^{-1} s^{-1} for sFv and Fab but large differences were detected in the off-rates. The sFv fragment dissociates very fast from the CEA surface with 9.4×10^{-4} s^{-1} while, at the other extreme, the parent IgG shows a very slow dissociation rate of 4.8×10^{-6} s^{-1}. This off-rate in fact becomes almost undetectable with the BIAcore system. The off-rates of the diabodies are comparable to those of immunoglobulins. With $6–7 \times 10^{-5}$ s^{-1} for the 5-linker and 2-linker diabodies respectively both molecules apparently bind bivalently, thus taking advantage of the avidity effect. Their avidities are in the nanomolar range. We therefore conclude that these types of construct might be interesting candidates for immunodiagnostic applications. We are currently trying to improve the kinetic parameters of these fragments by chain-shuffling and other mutagenesis techniques (Marks et al., 1992).

In order to identify and characterize the synthesized CEA-specific fragments by surface plasmon resonance detection in the BIAcore system we have coupled various amounts of CEA to CM5 sensorchip surfaces. CEA has a molecular weight of approximately 180 kDa and is heavily glycosylated (Bates et al., 1992). Due to its low p*I* the amine coupling method only yielded surfaces suitable for kinetic analyses (Table 1). In order to observe mass transport limited binding, surfaces with much higher CEA densities had to be prepared. The carbohydrate residues were oxidized with sodium metaperiodate and CEA was linked via the generated aldehyde groups to pretreated sensorchip surfaces. The variation of oxidized CEA and hydrazine concentrations in the immobilization procedure proved to be an excellent tool to influence the amount of CEA coupled (Fig. 2). The chemistry of the immobilization method had no influence on the apparent kinetic binding parameters for all molecules tested.

The high density CEA surfaces with 6000–12000 RU of CEA bound (6–12 ng/mm^2) were successfully used for screening clones expressing diabody by mass transport limited binding (Fig. 1). At that stage we used the amount of diabody bound after a 4 μl injection to identify good expressors. After the purification of all the molecules described above it was possible to establish standard curves of mass transport limited binding for three of the fragments (sFv, Fab, 2-linker diabody) and the IgG. Different concentrations of these molecules were injected on CEA surfaces and mass transport limited binding rates were determined (Fig. 3). The CEA density had no influence on the binding rates. Mass transport limited binding rates are dependent on the concentration, molecular weight, and the diffusion coefficient of the molecules and are with some limitations independent of kinetic binding properties (Karlsson et al., 1993). The diffusion coefficient for spherical macromolecules is inversely proportional to the cube root of the molecular weight. The slopes of the observed standard curves in Fig. 3 display a dependency on concentration, molecular weight and, apparently, valency. Theoretically the mass transport limited binding rates for IgG and diabody should have been twice as high. Most notably the slope for the diabody is about 50% of that of the Fab although both molecules have the same molecular weight. Since other factors such as the shape of the molecules and the viscosity of the hydrogel forming the binding matrix on the sensorchip (Karlsson et al., 1994) also influence the mass transport binding properties of macromolecules, the exact theoretical rates are difficult to determine. In addition the question has to be raised about the 'gold-standard' to which samples are to be compared. Although the proteins tested in the mass transport limited binding experiments displayed at least 95% purity there is still the possibility

that for example the IgG or diabody preparations contain inactive material. Nevertheless the standard curves obtained with the purified molecules (Fig. 3) will now allow us to calculate approximate concentrations of sFv, Fab, diabody, or IgG specific for the 7F7 defined epitope in unpurified samples by mass transport limited binding to high density CEA surfaces prepared by the aldehyde method presented in this paper. This will make it easier to screen larger numbers of new clones for improved kinetic binding properties using the BIAcore system.

References

Adair, J.R. (1992) Engineering antibodies for therapy. Immunol. Rev. 130, 5.

Bates, P.A., Luo, J. and Sternberg, M.J.E. (1992) A predicted three-dimensional structure for the carcinoembryonic antigen (CEA). FEBS Lett. 301, 207.

Blackburn, G.F., Shah, H.P., Kenten, J.H., Leland, J., Kamin, R.A., Link, J., Peterman, J., Powell, M.J., Shah, A. and Talley, D.B. (1991) Electrochemiluminescence detection for development of immunoassays and DNA probe assays for clinical diagnostics. Clin. Chem. 37, 1534.

Darsley, M., Abraham, R., Buxbaum, S., Kadey, S., Link, J. and Smith, R. (1994) Application of electrochemiluminescence-based immunoassays in antibody engineering. Submitted.

Holliger, P., Prospero, T. and Winter, G. (1993) Diabodies - Small Bivalent and Bispecific Antibody Fragments. Proc. Natl. Acad. Sci. USA 90, 6444.

Hoogenboom, H.R., Griffiths, A.D., Johnson, K.S., Chiswell, D.J., Hudson, P. and Winter, G. (1991) Multi-subunit proteins on the surface of filamentous phage, methodologies for displaying antibody (Fab) heavy and light chains. Nucleic Acids Res. 19, 4133.

Hoogenboom, H.R., Marks, J.D., Griffiths, A.D. and Winter, G. (1992) Building Antibodies from Their Genes. Immunol. Rev. 130, 41.

Karlsson, R., Fagerstam, L., Nilshans, H. and Persson, B. (1993) Analysis of active antibody concentration – Separation of affinity and concentration parameters. J. Immunol. Methods 166, 75.

Karlsson, R., Roos, H., Fägerstam, L. and Persson, B. (1994) Kinetic and concentration analysis using BIA technology. Methods Companion Methods Enzymol. 6, 97.

Malmqvist, M. (1993) Surface plasmon resonance for detection and measurement of antibody-antigen affinity and kinetics. Curr. Opin. Immunol. 5, 282.

Marks, J.D., Griffiths, A.D., Malmqvist, M., Clackson, T.P., Bye, J.M. and Winter, G. (1992) Bypassing immunization – Building high affinity human antibodies by chain shuffling. Bio/Technology 10, 779.

Orum, H., Andersen, P.S., Oster, A., Johansen, L.K., Riise, E., Bjornvad, M., Svendsen, I. and Engberg, J. (1993) Efficient method for constructing comprehensive murine Fab antibody libraries displayed on phage. Nucleic Acids Res. 21, 4491.

Owens, R.J. and Young, R.J. (1994) The genetic engineering of monoclonal antibodies. J. Immunol. Methods 168, 149.

Skerra, A., Pfitzinger, I. and Plückthun, A. (1991) The functional expression of antibody Fv fragments in *Escherichia coli*: Improved vectors and a generally applicable purification technique. Bio/Technology 9, 273.

Nucleic Acids Research, 1995, Vol. 23, No. 9 1531–1535

Direct measurement via phage titre of the dissociation constants in solution of fusion phage–substrate complexes

Michael R. Dyson, Volker Germaschewski and Kenneth Murray*

Institute of Cell and Molecular Biology, University of Edinburgh, King's Buildings, Mayfield Road, Edinburgh EH9 3JR, UK

Received January 5, 1995; Revised and Accepted March 13, 1995

ABSTRACT

Studies of interactions between filamentous fusion phage particles and protein or nucleic acid molecules have gained increasing importance with recent successes of screening techniques based upon random phage display libraries (biopanning). Since a number of different phage are usually obtained by biopanning, it is useful to compare quantitatively the binding affinities of individual phage for the substrate used for selection. A procedure is described for determination of relative dissociation constants (K_d^{Rel}) between filamentous phage carrying peptide fusions to the coat protein gpIII and substrates in solution. This novel method is based on the measurement of phage titres. Phage selected from a random fusion phage library for binding to a monoclonal antibody or a viral structural protein exhibited K_d^{Rel} values in the nanomolar and micromolar ranges for their respective substrates, thus validating the method over a wide range of binding affinities.

INTRODUCTION

Libraries of phage displaying random peptide sequences are being used increasingly to identify sequences that interact specifically with a particular protein or nucleic acid. In some instances the substrate used for screening the library has been a monoclonal antibody and the system has been used for epitope mapping (1). The method can give very high resolution, defining the specific amino acids involved in binding the antibody (2). However, the power of the random approach lies in the discovery of amino acid sequences that bind to proteins or specific nucleic acid sequences about which little or nothing is known of potential binding sites (3–8). In such cases, ligands isolated from the library frequently show little or no primary sequence motifs of any known proteins. These so-called mimotope sequences presumably resemble the structure of a potential binding site and therefore bind the protein (9).

To identify mimotopes as specific ligands and subsequently compare them with other sequences in terms of affinity for the substrate used in screening it is necessary to examine the interaction quantitatively as well as qualitatively. The method described here provides direct comparison of the binding affinity of different phage for a substrate in solution without the need to synthesize peptides. That the assay is performed in solution is crucial, since the conformation of a protein can change on binding to a solid phase, with a resulting change of binding affinity (10).

We have used two groups of phage that were isolated from a random phage display library by screening with: (i) a monoclonal antibody specific for the PreS1 domain of the surface antigen of hepatitis B virus (HBV); (ii) a structural protein from the nucleocapsid of HBV, to determine the relative dissociation constants (K_d^{Rel}) for the interactions between the phage particles and their target proteins in solution. All phage were previously identified as specific ligands for the proteins used for screening the library and the selection procedures have been described elsewhere (2,8). The essential features of the method are that the substrate is incubated with the phage in solution until equilibrium is reached and the amount of unbound phage remaining in solution is then determined by adsorption on a solid phase coated with the substrate. The adsorbed phage are then eluted from the solid phase and titred, representing a value proportional to the free phage in the solution of the reactants at equilibrium. The titration of infective units (plaque forming units, p.f.u.) thereby offers a sensitivity that could not be achieved with most other techniques, as, in principle, one free phage particle can be detected. Scatchard plots of such results from a series of reactions at a range of protein concentrations deliver K_d^{Rel} values.

MATERIALS AND METHODS

Phage particles and proteins

Phage particles B1–B4 are specific for the HBV core antigen particle (HBcAg) and were isolated from a random hexapeptide phage display library (11) by three rounds of biopanning against HBcAg adsorbed on nitrocellulose discs (8). HBcAg was expressed in *Escherichia coli* (12). Phage particles E2-16, E2-17, E4-2 and E4-4 are specific for the monoclonal antibody MA18/7, directed against the PreS1 protein domain of HBV surface antigen (13), and originated from rounds two and four of a

* To whom correspondence should be addressed

biopanning procedure using the same random hexapeptide phage display library and MA18/7-coated wells of an ELISA plate (2).

Large scale preparation of phage particles

Phage particles were purified from the supernatant of 500 ml overnight cultures of infected *E.coli* K91Kan cells by polyethylene glycol precipitation and CsCl gradient centrifugation, as described by Smith and Scott (14).

Determination of phage titre as plaque forming units (p.f.u.)

Phage solutions were diluted serially in TBS (0.05 M Tris–HCl, pH 7.5, 0.15 M NaCl) containing gelatin (1 g/l) and aliquots of these dilutions (100 µl) were added to a suspension of K91Kan cells (400 µl) at OD_{600} 0.2 (1/10 dilution). Melted soft agar (3 ml) was then poured into the tubes containing the suspension of phage and host cells and the mixture poured on agar plates containing kanamycin (100 µl). The plates were incubated overnight at 37°C and plaques counted the following day.

Phage binding assay on solid phase

U-shaped wells of 'high capacity' polystyrene strip plates (#2585; Costar) were coated with protein [20 µg/ml HBcAg in 25 mM potassium phosphate, pH 7.5, 150 mM NaCl (PBS) or 1 µg/ml MA18/7 in 0.2 M ammonium bicarbonate buffer, pH 9.6; volume 200 µl] overnight at room temperature, washed three times with TBS and blocked for 2 h at room temperature by adding TBS containing bovine serum albumin (BSA) (200 µl, 10 mg/ml). After three further washes with TBS, wells were filled with various concentrations of purified phage particles diluted in TBS buffer containing 0.2 mg/ml BSA, 0.02% NaN_3 (10^7–10^{10} p.f.u./200 µl) and incubated for 1 h at 6°C. After 1 h the phage solutions were removed from the wells and the plates were then washed 10 times with TBS containing 0.2 mg/ml BSA and bound phage eluted by incubation with elution buffer (200 µl, 0.1 M HCl, titrated to pH 2.2 by addition of solid glycine) for 10 min. Eluates were neutralized with 40 µl 1 M Tris–HCl, pH 9.5, and the phage titres determined. Triplicate measurements were made at each phage concentration.

For time course experiments five identical sets of plates were prepared with coating conditions as above and the input phage concentrations were kept constant (200 µl, 10^8 p.f.u./well). Each plate represented a point on a time course with incubation times of 10, 31, 100, 316 and 1000 min (corresponding to half-log intervals). After each incubation period the relevant plate was treated as described above and the bound phage eluted and titred.

Phage binding assay in solution

This procedure was adapted from Friguet *et al.* (15). First, the proteins (HBcAg or MAb) were incubated in solution with the purified phage particles until equilibrium was reached (18 h). In the case of binding of phage B1 to HBcAg this was attained as follows. The antigen at various concentrations (0.32–10 µM) was mixed with a constant amount of phage (10^9 p.f.u./ml) in TBS containing 0.2 mg/ml BSA, 0.02% NaN_3. After 18 h at 6°C, an aliquot (100 µl) of each mixture was transferred to the wells of a U-shaped, polystyrene, radioimmunoassay strip plate that had been coated with HBcAg as described above. After 1 h at 6°C the wells were washed 10 times with TBS supplemented with 0.2 mg/ml BSA. Bound phage were then eluted, neutralized and titred as described above; all assays were performed in triplicate. In the case of binding phage B2 and B3 to HBcAg, the antigen concentration was varied from 1.58 to 50 µM and for phage B4 the antigen concentrations were varied from 0.63 to 20 µM. The binding assay between monoclonal antibody MA18/7 and phage was performed in the same way, except that the antibody concentration was varied from 0.32 to 30 nM and the solid phase was coated with MA18/7 as described.

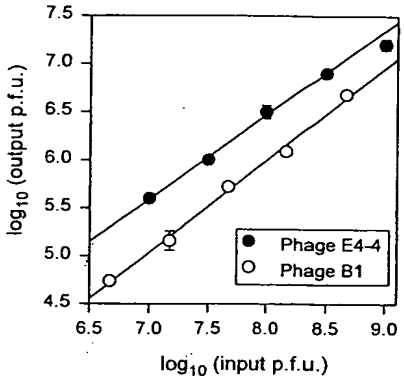

Figure 1. Linear relationship between input and output p.f.u. from wells coated with HBcAg or monoclonal antibody. Varying input concentrations of either phage B1 (○) or phage E4-4 (●) were incubated for 1 h on polystyrene wells coated with either HBcAg or MA18/7 respectively and the number of bound phage (output) determined by titrating eluted p.f.u. Assays were performed in triplicate and error bars represent the deviation from the mean.

RESULTS

The method for determination of relative dissociation constants between fusion phage and substrate molecules in solution is based upon that used for the measurement of affinity constants in solution between antigens and antibodies (15). A constant concentration of fusion phage was incubated with varying concentrations of substrate until equilibrium was reached. The number of free phage can be quantitated by incubating the mixture in microtitre plates coated with antigen or antibody, washing the wells, eluting the phage bound to the wells with glycine–HCl buffer, pH 2.2, and quantitating the phage in the eluate by titration of p.f.u.. To show that the phage concentration in the eluate reflected the free phage concentration in the reaction mixture, varying concentrations of phage (input) were incubated in microtitre wells coated with antigen or antibody for 1 h, the wells were washed and bound phage eluted (output) and titred. The output p.f.u. was directly proportional to input p.f.u. over a two log range for fusion phage B1 and E4-4 (Fig. 1), which differ greatly in their binding affinities (Table 1). The standard error involved in measuring phage titre varied between 5 and 10%.

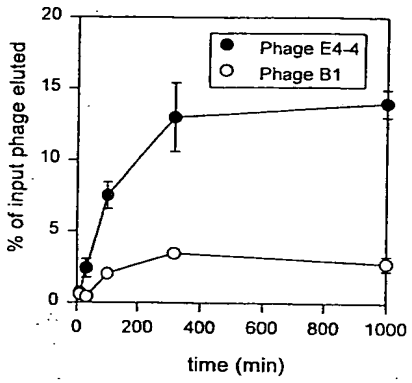

Figure 2. Time course of phage binding to substrate-coated solid phase. Fusion phage (10^8 p.f.u.) E4-4 (●) or B1 (○) were incubated on polystyrene wells coated with either MA18/7 or HBcAg respectively for different periods of time and bound phage determined by titrating eluted p.f.u. Points represent the average of three assays and error bars the deviation from the mean.

Table 1. Relative dissociation constants and characteristics of phage analysed

Phage	gpIII fusion[a]	Specificity	$K_d^{Rel\ b}$	$K_d^{Rel\ c}$
B1	LLGRMK	HBcAg	0.15 ± 0.01 μM	0.17 ± 0.01 μM
B2	YLLRFR	HBcAg	1.4 ± 0.1 μM	1.5 ± 0.1 μM
B3	LLGRLK	HBcAg	1.1 ± 0.1 μM	1.1 ± 0.1 μM
B4	LLGRFK	HBcAg	0.56 ± 0.02 μM	0.64 ± 0.03 μM
E4-2	*PDPGFN*	MA18/7	0.17 ± 0.02 μM	0.2 nM
E4-4	*QLDPGF*	MA18/7	0.25 ± 0.02 nM	0.2 nM
E2-16	*LDPVFR*	MA18/7	0.10 ± 0.01 nM	nd[d]
E2-17	*DPAFND*	MA18/7	0.22 ± 0.01 nM	nd[d]

[a]Italic indicates matching amino acids with the sequence of the PreS1 antigen.
[b]Relative dissociation constants calculated by linear regression of Scatchard plots (Fig. 3).
[c]Relative dissociation constants calculated by curve fitting to a hyperbolic function (2,8).
[d]Not determined.

Figure 2 shows a time course experiment in which a constant concentration of fusion phage (10^8 p.f.u.) was incubated with substrate-coated wells for different time periods. A plateau was reached after 5 h, with ~14% of phage E4-4 bound to MA18/7-coated wells and ~4% of phage B1 captured by HBcAg-coated wells. These results presumably reflect the differing strengths of binding in the two cases.

The linear relationship between input phage titre and output of phage eluted from ligand-coated wells allows the determination of free phage concentration at equilibrium, provided that the total phage concentration is known. Indeed, if the total phage concentration (p_t) is incubated with the binding substrate at any given concentration, the free phage concentration (p), is related to the p.f.u. measured in the eluate by the following equation:

$$p/p_t = \text{p.f.u.}/\text{p.f.u.}_o \quad (1)$$

where p.f.u.$_o$ is the titre measured for the (eluted) phage in the absence of antigen. This will only be true if the equilibrium in the liquid phase is undisturbed during exposure of the mixture to the coated wells. It is unlikely that this will result in significant perturbation of the equilibrium in solution, since the number of phage binding to the solid phase under the experimental conditions used (i.e. quantity and accessibility of the protein substrate coated on the wells and time of incubation of the mixtures in the wells) represents <5% of the total free phage concentration (Figs 1 and 2). To verify this, fusion phage B1 and E4-4 were incubated at various concentrations (in triplicate) for 1 h with substrate-coated wells (HBcAg and MA18/7 respectively) and the contents of each well were then transferred to another coated well and again incubated for the same time. The bound phage in the two sets of wells were quantitated as described previously and found to be identical, within 95% standard error limits. This linear relationship between input and output p.f.u. from HBcAg-coated wells was also demonstrated for fusion phage B2, B3 and B4 (data not shown).

Since Equation 1 was shown to be valid and if one phage particle binds one antigen particle or antibody molecule, the concentrations of bound phage (x) and of free antigen or antibody (a) at equilibrium can be calculated from the mass conservation equations:

$$x = p_t - p \quad (2)$$

$$a = a_o - x \quad (3)$$

where a_o is the total concentration of antigen and p_t and p represent the total and free phage concentrations respectively. At equilibrium, x, a and p_t are related to the dissociation constant K_d by the Scatchard equation (16):

$$x/a = [p_t - x]/K_d \quad (4)$$

Equation 4 can be rearranged to give:

$$x/p_t\,a = (1/K_d) - (x/K_d\,p_t) \quad (5)$$

The gradient of a plot of $x/p_t a$ against x/p_t is therefore equal to $-1/K_d$. Figure 3 shows Scatchard plots for phage B1–4 binding to truncated HBcAg (Fig. 3A) and phage E2-16, E2-17, E4-2 and E4-4 binding to MA18/7 (Fig. 3B). K_d^{Rel} values were calculated from linear regressions of the plots and show the order of affinity of the hexapeptides displayed on the phage for the ligands against which they were selected (Table 1).

Once the linearity of the input to output ratio (Fig. 1) has been confirmed, up to five dissociation constants may be conveniently determined over a 2 day period, including data analysis. For ease of handling of larger numbers of plates, an image analyser may be used for counting plaques.

DISCUSSION

The method described here for measuring relative dissociation constants between fusion phage and ligands in solution should be generally applicable and enables direct comparison of the binding abilities of individual phage clones. However, dissociation constants obtained in this way should be regarded as *relative* values, since the presence of up to five copies of the gpIII fusion protein of the filamentous phage complicates matters. This could enable a single phage particle to simultaneously bind one molecule or particle on the solid phase and another molecule in solution or

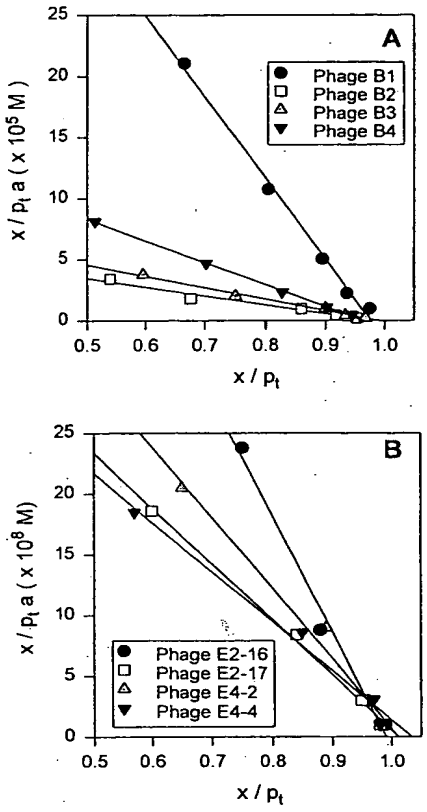

Figure 3. Scatchard plots for fusion phage bound to HBcAg (**A**) or monoclonal antibody MA18/7 (**B**). x is the concentration of bound phage, p_t is the total phage concentration and a is the free substrate concentration. Measurements were as described in the Materials and Method. Points represent the average of three results.

a single phage particle could bind to the ligand (particulary in the case of the HBcAg particle) via multiple interactions, thus enhancing the affinity. Further, since HBcAg and MA18/7 were present in large excess over the fusion phage, a single phage could bind more than one protein molecule or particle unless steric hindrance played a role.

However, these factors should remain constant when comparing individual fusion phage clones selected for a given substrate or a given phage clone for different ligands and the method described for measuring K_d^{Rel} is valid because two essential criteria have been fulfilled. First, and most importantly, input and output phage titres are linearly related (Fig. 1), although the high affinity of phage E4-4 for the MAb apparently leads to saturation with inputs higher than $10^{8.5}$ p.f.u. This linear relationship between input and output phage concentrations has been observed in all cases that have been studied, which include examples that differ by four orders of magnitude in their apparent K_d values. Secondly, in both cases <5% of free phage were bound to the wells during the 1 h incubation period used in the experiment (Fig. 2). Thus with both high and moderate affinity interactions it is unlikely that the equilibrium between the reactants in solution is significantly disturbed during this phase of the assay.

Compared with the high affinity interactions of phage E2-16, E2-17, E4-2 and E4-4 with the monoclonal antibody, the relative dissociation constants measured for the interactions of phage B1–4 with HBcAg represent moderate binding affinities (Table 1). This validates the method over a wide range (four orders of magnitude) of binding constants for reactions between phage and proteins. The K_d^{Rel} values (Table 1), calculated by linear regression of the Scatchard plots (Fig. 3), are very similar to those obtained by a curve fitting calculation using the same data (2,8). The slight differences are probably attributable to the additional constraint introduced into the curve fitting that $p = p_t$ at zero antigen or antibody concentration.

Surface plasmon resonance has been used to evaluate the binding of fusion phage clones to a monoclonal antibody (17), but it did not appear possible to determine the rates of association or dissociation. Measurement of phage titre offers greater sensitivity compared with refractive index changes at the surface of the sensor chip. For example, phage concentrations greater than 10^{11} p.f.u./ml were required to observe a signal above background in the surface plasmon resonance experiments, whereas here concentrations of 10^9 p.f.u./ml were employed and, in principle, this could be much lower. Additionally the determination of phage titres involves minimum expense.

The procedure described here for calculating relative dissociation constants between fusion phage and substrates in solution should find wide application in the growing field of selection of peptide ligands to complex macromolecules and assemblies by the use of phage display libraries (3,8,18). After the selection process has been completed and amplified phage clones sequenced, it is necessary to confirm that the selected phage bind to their substrate in solution and to compare relative binding affinities between the various phage clones. The procedure described here achieves both these objectives. Further, the choice of synthetic peptides for competition studies is facilitated by comparing binding affinities for the same ligand of fusion phage with varying amino acids in their displayed peptide sequences. Although examples do exist where the gpIII protein context contribute significantly to the binding affinity of the fusion phage for the substrate (19), it is expected that the relative order of binding of a set of fusion phage will be similar to that of the free peptides. In addition, for the examples discussed here the free peptides were synthesized and found to bind the selected substrates (2,8). The method may also find use in studying structure–function relationships where whole protein domains, such as human growth hormone (20), zinc finger domains (7,21) or antibodies (22), have been expressed on filamentous phage. Therefore, it should be possible to rank affinity variants in the phage-associated form without the need to purify free domains.

ACKNOWLEDGEMENTS

We thank Prof. G. Smith for the fusion phage library and Prof. W. Gerlich for the gift of Mab MA18/7. VG is currently supported by the Roseanne Campbell Trust for Hepatitis Research, Edinburgh. The work was also supported in part by Biogen Inc., Cambridge, MA, USA.

REFERENCES

1 Lane,D.P. and Stephen,C.W. (1993) *Curr. Opin. Immunol.*, **5**, 268–271.
2 Germaschewski,V. and Murray,K. (1995) *J. Med. Virol.*, **45**, 300–305.
3 Blond-Elguindi,S., Cwirla,S.E., Dower,W.J., Lipshutz,R.J., Sprang,S.R., Sambrook,J.F. and Gething,M.J.H. (1993) *Cell*, **75**, 717–728.
4 Dedman,J.R., Kaetzel,M.A., Chan,H.C., Nelson,D.J. and Jamieson,G.A. (1993) *J. Biol. Chem.*, **268**, 23025–23030.

5 Hammer,J., Valsasnini,P., Tolba,K., Bolin,D., Higelin,J., Takacs,B. and Sinigaglia,F. (1993) *Cell*, **74**, 197–203.
6 Koivunen,E., Gay,D.A. and Ruoslahti,E. (1993) *J. Biol. Chem.*, **268**, 20205–20210.
7 Rebar,E.J. and Pabo,C.O. (1994) *Science*, **263**, 671–673.
8 Dyson,M.R. and Murray,K. (1995) *Proc. Natl. Acad. Sci. USA*, **92**, 2194–2198.
9 Clackson,T. and Wells,J.A. (1994) *Trends Biotechnol.*, **12**, 173–184.
10 Friguet,B., Djavadi-Ohaniance,L. and Goldberg,M.E. (1984) *Mol. Immunol.*, **21**, 673–677.
11 Scott,J.K. and Smith,G.P. (1990) *Science*, **249**, 386–390.
12 Stahl,S.J. and Murray,K. (1989) *Proc. Natl. Acad. Sci. USA*, **86**, 6283–6287.
13 Heermann,K.H., Goldmann,U., Schwartz,W., Seyffarth,T., Baumgarten,H. and Gerlich,W.H. (1984) *J. Virol.*, **52**, 396–402.
14 Smith,G.P. and Scott,J.K. (1993) *Methods Enzymol.*, **217**, 228–257.
15 Friguet,B., Chaffotte,A.F., Djavadi-Ohaniance,L. and Goldberg,M.E. (1985) *J. Immunol. Methods*, **77**, 305–319.
16 Scatchard,G. (1947) *Annls NY Acad. Sci.*, **51**, 660–672.
17 Lasonder,E., Schellekens,G.A. and Welling,G.W. (1994) *Nucleic Acids Res.*, **22**. 545–546.
18 Balass,M., Heldman,Y., Cabilly,S., Givol,D., Katchalski-Katzir,E. and Fuchs,S. (1993) *Proc. Natl. Acad. Sci. USA*, **90**, 10638–10642.
19 Felici,F., Luzzago,A., Folgori,A. and Cortese,R. (1993) *Gene*, **128**, 21–27.
20 Lowman,H.B., Bass,S.H., Simpson,N. and Wells,J.A. (1991) *Biochemistry*, **30**, 10832–10944.
21 Choo,Y., Sanchez-Garcia,I. and Klug,A. (1994) *Nature*, **372**, 642–645.
22 McCafferty,J., Griffiths,A.D., Winter,G. and Chiswell,D.J. (1990) *Nature*, **348**, 552–554.

Biochem. J. (1981) **195**, 481–484
Printed in Great Britain

Isolation and properties of three lectins from mistletoe (*Viscum album* L.)

Hartmut FRANZ, Peter ZISKA and Annemarie KINDT
Staatliches Institut für Immunpräparate und Nährmedien, 1120 Berlin-Weissensee, German Democratic Republic

(*Received 21 November 1980/Accepted 16 January 1981*)

Three lectins have been isolated from an extract of mistletoe (*Viscum album*) by affinity chromatography on partially hydrolysed Sepharose and human immunoglobulin–Sepharose. The lectins differ in molecular weight and sugar specificity (lectin I, mol.wt. 115000, D-galactose-specific; lectin II, mol.wt. 60000, both D-galactose- and *N*-acetyl-D-galactosamine-specific; lectin III, mol.wt. 50000, *N*-acetyl-D-galactosamine-specific). All three lectins react with human erythrocytes without specificity for the A, B and O blood groups. In contrast with abrin and ricin the mistletoe lectins cannot be divided into 'toxins' and 'haemagglutinins'.

Since ancient times the toxic seeds of jequirity (*Abrus precatorius*; Leguminosae) and castor bean (*Ricinus communis*; Euphorbiaceae) have been used in folk medicine for the treatment of different diseases. It is now known that both plants contain toxic lectins with D-galactose specificity. Likewise, preparations from mistletoe (*Viscum album*; Loranthaceae) have been used therapeutically for thousands of years, and this plant also has a toxic lectin with galactose specificity.

A comparison of the well-investigated castor-bean and jequirity lectins ricin and abrin with the lectin(s) of mistletoe seemed worthwhile. After having investigated the possibilities of purification of mistletoe lectin(s) by use of affinity chromatography (Franz *et al.*, 1977; Ziska *et al.*, 1978), we now report the isolation and identification of three different lectins from mistletoe and discuss possible relationships between the lectins of the three plants.

Materials and methods

The lectins were isolated from ground plant material from mistletoe grown on the locust tree (*Robinia pseudoacacia*) by using affinity chromatography. Lectin I was isolated using acid-treated agarose as carrier (Ziska *et al.*, 1978). The non-adsorbed material was applied to a column (2.6 cm × 30 cm) of immunoglobulin–Sepharose and the column was washed with 0.15 M-NaCl. The affinity adsorbent had been prepared by coupling human immunoglobulin, mainly immunoglobulin G, to CNBr-activated Sepharose 4B (20 mg/ml of gel).

Lectin II was eluted with 0.2 M-D-galactose in 0.15 M-NaCl. The fractions containing the haemagglutinating protein were pooled, dialysed against water and freeze-dried. After the lectin II had been displaced from the column, lectin III was eluted with 0.2 M-glycine/HCl buffer, pH 2.6. The fractions containing active material were pooled and neutralized with Na_2CO_3. The neutral solution was put on a column (1.5 cm × 30 cm) of Sepharose–*N*-(6-aminohexanoyl)-β-D-galactosamine (Gordon *et al.*, 1972). The column was washed and the lectin III was eluted with glycine/HCl buffer, pH 2.6. The haemagglutinating proteins were pooled, dialysed against water and freeze-dried. Haemagglutinating activity was determined in a 1% suspension of washed human erythrocytes by using the microtitrator of Takatsy (1967). Haemagglutination-inhibition tests were performed as follows: to 0.05 ml of a 2-fold serial dilution of carbohydrate, 0.025 ml of lectin solution with a haemagglutinating activity of 4 units was added. After incubation at 37°C for 1 h, 0.025 ml of a 2% human erythrocyte suspension was added. After 2 h at 37°C the degree of agglutination was estimated. Stock solutions of 0.2 M-carbohydrate in 0.15 M-NaCl were prepared. T.l.c. for determination of the molecular weight was performed with Sephadex G-200 (Superfine grade). Proteins with known molecular weights were used as markers [cytochrome *c* (12400), chymotrypsinogen (25700), ovalbumin (45000) and bovine serum albumin (68000)].

For polyacrylamide-gel disc electrophoresis the method of Maurer (1968) was used; 7.5% polyacrylamide gels were used in a 35 mM-β-alanine/acetic acid buffer of pH 4.3. The molecular weights of the lectin chains were obtained in 10%-polyacrylamide gels in the presence of 1% sodium

0306-3275/81/050481-04$01.50/1

REF. 14

dodecyl sulphate. The lectins were treated with 1% sodium dodecyl sulphate and 1% β-mercaptoethanol (Weber & Osborn, 1969). Staining was performed with Coomassie Brilliant Blue R250 (for proteins) and periodic acid/Schiff reagent (for glycoproteins; Fairbanks *et al.*, 1971).

Anti-(lectin I) serum was prepared as follows. The purified lectin I was treated with 1% formaldehyde in 0.1 M-phosphate buffer, pH 7.5, for 3 days at 37°C, and excess formaldehyde was removed by dialysis against 0.85% NaCl solution. Immunization of a rabbit was initiated by subcutaneous injection of 0.5 mg of protein in complete Freund's adjuvant, followed by 0.5 mg booster doses with Freund's incomplete adjuvant intracutaneously every week. The antiserum used was obtained 6 weeks after the first immunization.

Results

By using affinity chromatography with different carriers we have been able to isolate three lectins from crude extracts of mistletoe. The isolation, properties and chemical modification of D-galactosyl-specific lectin I was published previously (Ziska *et al.*, 1978, 1979). Only lectin I is bound by partially-hydrolysed Sepharose. After separation of the lectin I, the extract contains two lectins, which are adsorbed by the carbohydrate moieties of the immobilized immunoglobulins (immunoglobulins G, A or M). Lectin II can be eluted from this column by 0.2 M-D-galactose solution. Lectin III cannot be eluted with 0.5 M-D-galactose solution, but with 0.2 M-glycine/HCl buffer, pH 2.6. For further purification the solution of lectin III is applied to a column of Sepharose–*N*-(6-aminohexanoyl)-β-D-galactosamine and then eluted with glycine/HCl buffer (Scheme 1).

Lectins I and II each give a single band on disc electrophoresis, and lectin III shows a major band and three faint bands (Fig. 1). After reduction with 2-mercaptoethanol, each of the lectins shows two bands in polyacrylamide-gel electrophoresis in the presence of 0.1% sodium dodecyl sulphate. Disc electrophoresis of mixtures of lectins I and II, and I and III showed that they are not identical (Fig. 2).

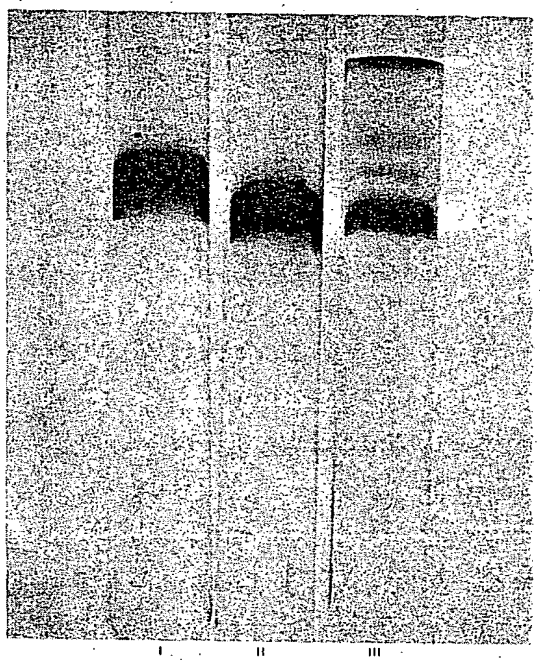

Fig. 1. *7.5%-Polyacrylamide-gel electrophoresis (pH 4.3) of mistletoe lectins I, II and III*

Electrophoresis was performed at 4 mA per tube for 2.5 h. The gels were stained with Coomassie Brilliant Blue R250.

Mistletoe (100 g) mixed with 750 ml of 0.15 M-NaCl
↓ → Discard precipitate
Acid-treated Sepharose column
↓ → Elute with 0.2 M-D-galactose: **lectin I**
Effluent
↓
Immunoglobulin–Sepharose column
↓
Elute with 0.2 M-D-galactose: **lectin II**
↓
Elute with glycine/HCl, pH 2.6
↓
Neutralized
↓
Sepharose&*N*-(6-aminohexanoyl)-β-D-galactosamine column
↓
Elute with glycine/HCl, pH 2.6: **lectin III**

Scheme 1. *Flow sheet for the isolation of mistletoe lectins I, II and III*

Thus lectin I, in agreement with Luther *et al.* (1980), consists of two identical non-covalently bound subunits.

Lectins II and III and also the subunit of lectin I contain two chains linked by a disulphide bridge. Each of them show two bands on polyacrylamide-gel electrophoresis after reduction with 2-mercaptoethanol. The lectins differ in their molecular weights (Table 1). All three lectins agglutinated human erythrocytes with similar potency, but when tested against erythrocytes from other species, marked differences in potency were observed (Table 2). The sugar specificities of the three lectins were different (Table 3). Agglutination of human erythrocytes by lectin I was strongly inhibited by D-galactose and α- and β-methyl galactosides. Lectin II was inhibited with both *N*-acetyl-D-galactosamine and the galactosides, whereas lectin III was inhibited strongly only by *N*-acetyl-D-galactosamine.

All the six chains of the three lectins are different. However, lectins II and III cross-react with anti-(lectin I) antibody in radial immunodiffusion. Lectins I, II and III are stained by periodate/Schiff reagent.

Four of the chains of the three lectins can be separated, but there could be up to six different chains present. No mitogenic effect could be demonstrated on guinea-pig lymph-node cells, since the cells were killed within 6h by lectin I at a concentration of 25–80 μg/ml (10^6 cells) (Scherbaum *et al.*, 1978). Lectin I inhibits protein synthesis in a lysate of rabbit reticulocytes with an ID_{50} (concentration giving 50% inhibition) of 2.6 μg/ml. This effect is enhanced (ID_{50} 0.21 μg/ml) if the lectin is first reduced with 2-mercaptoethanol. The lectin also inhibits protein synthesis by BL8L cells in culture. The ID_{50} is 7ng/ml and the potency

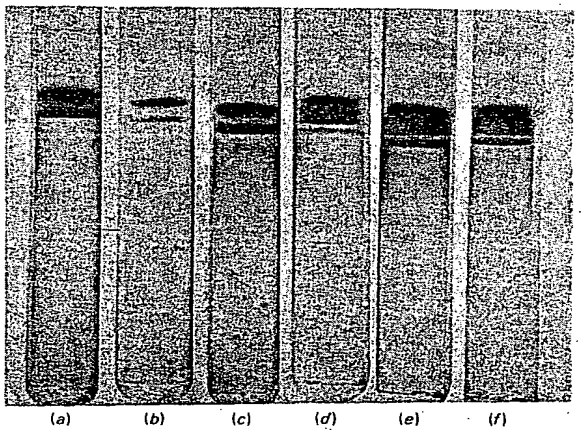

Fig. 2. *Chains of mistletoe lectins produced by β-mercaptoethanol treatment and analysed on sodium dodecyl sulphate/polyacrylamide gels*

The conditions are described in detail in the Materials and methods section. (*a*) lectin I; (*b*) lectin II; (*c*) lectin III; (*d*) mixture of lectins I and II; (*e*) mixture of lectins I and III; (*f*) mixture of lectins I, II and III.

Table 2. *Haemagglutination titres*

All lectin solutions used were diluted to a titre of 1:32 and made to react against human erythrocytes of group A.

Source of erythrocytes	Mistletoe lectin ...	Titre I	II	III
Human		1:32	1:32	1:32
Goat		1:2	0	1:32
Sheep		0	0	1:2
Rabbit		1:32	1:64	1:2
Mouse		1:8	1:16	1:16
Dog		1:32	1:16	1:8
Cow		1:8	0	0
Horse		0	1:4	1:4
Pig		1:32	1:32	1:8
Guinea pig		1:16	1:64	1:32

Table 3. *Inhibition by sugars*

The inhibition concentrations are expressed as μmol of carbohydrate/ml needed for complete inhibition of 4 haemagglutination units.

Sugar	Lectin ...	Concentration I	II	III
D-Galactose		12	12	200
N-Acetyl-D-galactosamine		200	6	3
Methyl α-D-galactoside		12	6	200
Methyl β-D-galactoside		6	3	50

Table 1. *Some properties of the mistletoe lectins*

Lectin	Mol.wt.	Carbohydrate specificity	Blood-group specificity	No. of chains	Mol.wts. of chains
I	115000	D-Galactose	None	4	34000 and 29000
II	60000	D-Galactose/*N*-acetyl-D-galactosamine	None	2	32000 and27000
III	50000	*N*-Acetyl-D-galactosamine	None	2	30000 and 25000

decreased after reduction of the lectin (Stirpe *et al.*, 1980).

Discussion

Crude mistletoe extract contains three lectins with different molecular weights and differences in specificity. Disc electrophoresis showed that lectins II and III are not simple monomers of lectin I.

All three of the isolated lectins agglutinate human erythrocytes and react with immunoglobulins. A single mistletoe lectin described by Luther *et al.* (1980) may not be homogenous, because they used glutaraldehyde-fixed erythrocytes for the isolation of the lectin. Neither crude mistletoe extract nor solutions of purified lectins I, II and III show any specificity for human blood groups. Therefore all three lectins from mistletoe bind to human erythrocytes. These results are in contrast with the findings of Luther *et al.* (1973), who detected a B-blood-group specificity in mistletoe extracts. Immobilized immunoglobulins are useful for the affinity chromatography of mistletoe lectins (Franz *et al.*, 1977). When applied in conjunction with partially hydrolysed Sepharose, it is possible to fractionate the three lectins. Insolubilization of the immunoglobulins can be achieved in three ways: (1) cross-linking with glutaraldehyde; (2) heat aggregation; (3) fixation on CNBr-activated Sepharose. Pretreatment with neuraminidase is not necessary for the immunoglobulin to bind the lectins.

Lectin I from mistletoe was shown previously to be highly toxic (Stirpe *et al.*, 1980). Preliminary results indicate that lectins II and III are also toxic. The mistletoe lectins, like those from *Abrus precatorius* and *Ricinus communis*, comprise species with either two (lectins II and III) or four (lectin I) chains. It has yet to be determined whether the different chains of the three mistletoe lectins functionally correspond to the A- and B-chains of abrin and ricin (Olsnes & Pihl, 1976). It is clear, however, that the mistletoe lectins cannot be classified as either toxic or haemagglutinating species.

Viscotoxins, toxic peptides comprising 46 amino acids, extracted from mistletoe, have been investigated by Samuelsson (1973). It would be interesting to see whether the primary sequences described for the viscotoxins also appear in the mistletoe lectins.

References

Fairbanks, G., Steck, T. L. & Wallach, F. H. (1971) *Biochemistry* **10**, 2606–2617

Franz, H., Haustein, B., Luther, P., Kuropka, U. & Kindt, A. (1977) *Acta Biol. Med. Germ.* **36**, 113–117

Gordon, J. A., Blumberg, S., Lis, H. & Sharon, N. (1972) *Methods Enzymol* **28**, 365–368

Luther, P., Prokop, O. & Köhler, W. (1973) *Z. Immunitaetsforsch. Exp. Klin. Immunol.* **146**, 29–35

Luther, P., Theise, H., Chatterjee, B., Karduck, D. & Uhlenbruck, G. (1980) *Int. J. Biochem.* **11**, 429–435

Maurer, H. R. (1968) *Disk Elektrophorese*, De Gruyter, Berlin

Olsnes, S. & Pihl, A. (1976) in *Receptors and Recognition*, series B, vol. 1 (Cuatrecasas, P., ed.), pp. 129–173 Chapman and Hall, London

Samuelsson, G. (1973) *Syst. Zool.* **22**, 566–569

Scherbaum, I., Drössler, K., Ziska, P. & Franz, H. (1978) *Allerg. Immunol.* **24**, 208–211

Stirpe, F., Legg, R. F., Onyon, L. J., Ziska, P. & Franz, H. (1980) *Biochem. J.* in the press

Takatsy, K. (1967) *Symp. Ser. Immunobiol. Stand.* **4**, 275–280

Weber, K. & Osborn, M. (1969) *J. Biol. Chem.* **244**, 4406–4412

Ziska, P., Franz, H. & Kindt, A. (1978) *Experientia* **34**, 123–124

Ziska, P., Eifler, R. & Franz, H. (1979) *Acta Biol. Med. Germ.* **38**, 1361–1363

Journal of Immunological Methods, 90 (1986) 25–37
Elsevier

JIM 03921

Evaluation of protocols for purification of mouse monoclonal antibodies

Yield and purity in two-dimensional gel electrophoresis

Luc Manil [1,*], Philippe Motté [1], Patrick Pernas [1], Frédéric Troalen [1], Claude Bohuon [2] and Dominique Bellet [1]

[1] *Unité d'Immunochimie, and* [2] *Département de Biologie Clinique, Institut Gustave-Roussy, F 94805 Villejuif, France*

(Received 29 August 1985, accepted 13 January 1986)

Protocols for purification of mouse monoclonal antibodies (MAbs) from nude mice ascites were investigated in order to assess the yield and to compare the purified products in two-dimensional gel electrophoresis (2DGE). Three MAbs (one IgG2 and two IgG1), selected for their differing behaviours towards protein A, were purified by ammonium sulphate precipitation and/or gel filtration, anion exchange (DEAE), hydroxylapatite and affinity (protein A) chromatography, or by a combination of these methods. Protein A constantly provided the highest purity whatever the IgG subclass. The best results in terms of yields and purity were a function of the optimization of the protein A protocol. In our study, they were obtained in a 3 h protocol (IgG2), a 16 h protocol with discontinuous pH gradient method (IgG1 with sufficiently high affinity for protein A) or a multi-step protocol involving DEAE and protein A (IgG1 with low affinity for protein A). DEAE chromatography alone provided a slightly better yield, but only moderate purity. Hydroxylapatite chromatography appeared to be less potent in terms of yield, purity and day-to-day reproducibility. Salt precipitation and gel filtration enabled only relative enrichment of the MAb solution. Some degradation products of both heavy and light chains clearly appeared in the 2DGE patterns of antibodies purified by different protocols, and seem to be partly related to the elution pH and to the duration of the purification procedure. Finally, this work highlights considerable heterogeneity not only between two different MAbs of the IgG1 subclass but also within a monoclonal population of immunoglobulins.

Key words: *Monoclonal antibody; Immunoglobulin IgG purification; Protein A; Hydroxylapatite; Anion exchange; Two-dimensional gel electrophoresis*

Introduction

Over the past decade, hybridoma technology has led to the production of highly specific monoclonal antibodies (MAbs) directed against a single epitope (Köhler and Milstein, 1975). After cloning, antibody-producing cells are allowed to grow either in vitro or, more commonly, in the mouse peritoneal cavity. Next, a purification procedure is required to obtain from either cell supernatants or ascitic fluids a sufficiently pure MAb for further use.

Several methods of purification from ascitic fluids have been proposed: the most frequently described protocols involve salt precipitation (Na_2SO_4, $(NH_4)_2SO_4$), anion exchange chro-

* To whom correspondence should be addressed.

matography (DEAE) (Godin, 1980) and affinity chromatography (protein A) (Ey et al., 1978). Polyethylene glycol (PEG) or ethanol precipitation, gel filtration (Phillips et al., 1984), HPLC (Burchiel et al., 1984) and more recently cation exchange chromatography (Carlsson et al., 1985) or hydroxylapatite chromatography (Stanker et al., 1985) have been also proposed. The advantages of each method are to be compared in terms of yield, cost, ease of use, rapidity and purity. For some applications, the nature and the level of impurities is not critical, and relatively crude purification protocols are sufficient. In contrast, such applications as labelling of the MAb require highly purified products. For in vivo applications (immunoimagery and targeting), the use of contamination-free MAbs is important to decrease non-specific background (Kennel et al., 1983) and to avoid generation of host antibodies against irrelevant compounds.

The aim of this work was to compare several easily performed one-step or multi-step purification protocols, paying special attention to yield and impurity patterns. We have studied protein A, DEAE, hydroxylapatite, and gel filtration chromatography as well as salt precipitation used alone or in combination. For control of purity, we have chosen two-dimensional gel electrophoresis (2DGE (O'Farrell, 1975)) with silver staining as an analytical tool because of its high resolution and sensitivity.

The conclusions drawn in our study may be extended to most MAbs and provide both qualitative and quantitative information which should be useful in the final selection of purification protocols.

Materials and methods

Production of monoclonal antibodies (MAbs)

Three mouse monoclonal antibodies directed against human α-fetoprotein (AFP) were used. They were produced in our laboratory and are referred to as AF01, AF04 and AF08.

The immunization protocol chosen for generation of AF01 involved 5 AFP injections into BALB/c mice, as described previously (Bellet et al., 1984). For AF04, the protocol involved five injections: 15 μg s.c. in FCA (day 1), 15 μg i.p. in FIA (day 98), 50 μg i.p. in FCA (day 118), 15 μg i.p. in NaCl (day 119) and 50 μg i.v. in NaCl (day 120). AF08 was produced after immunization with only two injections: 15 μg s.c. in FCA at day 1 and 15 μg i.v. in NaCl at day 160.

Cell fusions were performed 3–4 days after the last injection by incubating $2–3 \times 10^6$ NS1 mouse myeloma cells with $2–3 \times 10^7$ mouse spleen cells in 40% polyethylene glycol (MW 1000) except for AF01, where 5×10^6 Sp2/0-Ag14 mouse myeloma cells were incubated with 5×10^7 spleen cells. Hybridoma supernatants were screened for anti-AFP activity in a radioimmunoassay using ^{125}I-labelled AFP (^{125}I-AFP) and precipitation by polyethylene glycol (MW 6000).

Anti-AFP antibody-producing cells were cloned twice by limiting dilution, and ascitic fluids were produced by i.p. inoculation of nude mice with $5–10 \times 10^5$ hybridoma cells.

Purification and characterization of MAbs

(A) Precipitation by ammonium sulphate. The ascitic fluids were filtered on Whatman (Maidstone, England) filters and precipitated by dropwise addition of an equal volume of a saturated solution of ammonium sulphate at 4°C. After 1 h of continuous stirring, the resulting pellet was separated by centrifugation ($15\,000 \times g$, 30 min) and dissolved in distilled water (1 : 5 of the initial ascites volume).

(B) Gel filtration chromatography. The filtered ascites of AF04 (on 0.45 μm Millex-HA filters, Millipore, Molsheim, France) was directly purified on a 16 × 700 mm Sephacryl S200 (Pharmacia) column equilibrated with 0.1 M, pH 7.4 sodium phosphate buffer (flow rate 10 ml/h).

(C) Ion exchange chromatography (DEAE). The filtered ascites were dialyzed overnight at 4°C against 0.01 M, pH 8.0 Tris-HCl buffer and applied to a 40 ml DEAE-Sephacel column (Pharmacia, Uppsala, Sweden) equilibrated with the same buffer.

The elution was performed overnight at 4°C using a 300 ml NaCl linear gradient (0–0.3 M in pH 8.0, 0.01 M Tris HCl buffer) (flow rate 30 ml/h).

(D) Protein A (prot. A) affinity chromatography. Three protocols using prot. A-Sepharose 4B (Pharmacia) were tested.

Protocol 1: this method, called *fast batch purification*, involved filtration of up to 7 ml of ascitic fluid on 0.45 μm Millex-HA filters and chromatography on a 5 ml prot. A-Sepharose column. This column was first washed with 0.05 M, pH 2.2 sodium citrate buffer and equilibrated with 0.1 M, pH 8.5 sodium phosphate buffer (PB). After application of the sample, the column was incubated for 1 h at 4°C and thereafter washed with 50 ml of PB (flow rate 50 ml/h). The prot. A-bound proteins were then eluted by 20 ml of pH 5 sodium phosphate buffer. Such a protocol allowed a 3 h purification. Regeneration of the column was performed by successive elution of 50 ml of 0.05 M pH 2.2 sodium citrate buffer and 50 ml of pH 8.5 phosphate starting buffer.

Protocol 2: this *standard protocol* involved ammonium sulphate precipitation (up to 30 ml of ascites) as described above and overnight dialysis at 4°C against 0.1 M, pH 8.5 phosphate buffer. Next, the sample was applied to a 10 ml Sepharose 4B-prot. A column equilibrated with the same buffer and the flow rate was adjusted to 10 ml/h. Elution was performed at 25 ml/h using a discontinuous pH gradient, according to Ey et al. (1978), with steps at pH 8.5, 5.8, 4.5, 3.5 and 2.2. An automatic Ultrograd gradient mixer (LKB, Orsay, France) was used for this purpose.

Protocol 3: a third method combining salt precipitation, DEAE and prot. A chromatographies was used to purify IgG1 antibody displaying a low affinity for prot. A (AF04). The ascites were precipitated by ammonium sulphate and chromatographed on DEAE as described above. The antibody-containing fractions, detected by immunoreactivity measurements, were collected, concentrated and dialyzed against 0.1 M, pH 8.5 phosphate buffer. The sample was then further purified by prot. A as described in protocol 2.

Protocol 3b: the homogeneity of the protocol 3-purified AF04 was assessed by a further prot. A purification using the same discontinuous pH gradient as in protocol 2.

(E) Hydroxylapatite chromatography. Hydroxylapatite chromatography was performed according to Stanker et al. (1985) with several modifications; 1–30 ml of ascitic fluid, previously filtered on 0.45 μm Millex-HA filters (Millipore), were applied at 4°C to a 16 × 200 mm column containing HTP DNA grade hydroxylapatite (Bio-Rad) equilibrated with 0.01 M, pH 6.8 sodium phosphate buffer (buffer HA). The bound proteins were then eluted with 500 ml of 0–0.3 M linear or discontinuous NaCl gradient (pH 6.8) at 4°C. The flow rate was adjusted with a peristaltic pump at 30 ml/h and 5 ml fractions were collected. Columns were regenerated by washing with 150 ml of 0.5 M, pH 6.8 sodium phosphate buffer, followed by 150 ml of 1 N NaCl and then equilibrated with the buffer HA.

(F) Storage of the MAbs. Except for the fast batch purification, all chromatographies were continuously monitored by 280 nm transmission measurement. Fractions corresponding to the sections of the 280 nm profile were collected, pooled and concentrated in ultrafiltration cells fitted with a XM50 membrane (Amicon). Their volume and protein concentration were determined (Bio-Rad Prot-Assay). Antibodies were kept frozen at −20°C, either concentrated in pH 7 saline solutions (> 1 mg/ml) or diluted in protein-containing buffers.

(G) Characterization of the MAbs. Anti-AFP MAb class and subclass were found to be either IgG2 (AF01) or IgG1 (AF04 and AF08), as determined by double-antibody RIA with ^{125}I-AFP and goat antiserum specific for mouse IgM, IgA, IgG1, IgG2ab, IgG3 (Nordic, Tilburg, The Netherlands).

Affinity constants of the anti-AFP MAbs were determined with a double-antibody RIA technique by measuring the binding of ^{125}I-AFP in the presence of increasing amounts of AFP and calculated by Scatchard plot analysis (Scatchard, 1949). Affinity constants of AF01, AF04 and AF08 are 1.6×10^{10} M^{-1}, 0.8×10^{10} M^{-1} and 1.1×10^{10} M^{-1}, respectively.

Two-dimensional gel electrophoresis

The samples (0.5–3 mg protein/ml) were diluted with an equal volume of a mixture composed of 9 M urea, 4% NP40, 5% glycerol, 10 mM dithiothreitol and 2% ampholytes (Ampholines 3.5–10, LKB, Orsay, France), and incubated for 2 h at 25°C. Next, 15 μl of analyzed solution were applied to prefocused gels. Isoelectric focusing was performed for 14 000 V × h on 1 mm diameter cylindrical gels containing 4% acrylamide, 2%

NP40, 9 M urea and 2% of a mixture of ampholytes 3.5–10 (LKB), 3–10 (Serva, France) and 3–10 (Pharmacia) at a ratio of 2:2:1, respectively. Focused gels, equilibrated in the migration buffer for 5 min at 25°C, were laid on top of the 1 mm thick second-dimension resolving gel. This latter contained 13.5% acrylamide, and separation was performed at 20°C according to Laemmli (1970) in a Sebia SM2 device, as previously described (Motté et al., 1984). The gels were finally fixed and silver-stained according to a recent modification (Blangardin et al., 1984) of Oakley's procedure (Oakley et al., 1980).

Immunoreactivity measurements

Liquid phase radioimmunoassay (RIA). RIA was performed by incubating overnight at 20°C, 100 μl of ^{125}I-labelled AFP (10^4 cpm/100 μl) (Commissariat à l'Energie Atomique, Saclay, France) with 100 μl of various dilutions of antibodies in PBS (Na_2HPO_4 0.01 M, NaCl 0.15 M, pH 7.4). The antibody-antigen complex was precipitated by 1 ml of 20% PEG 6000 (w/v in PBS) in the presence of 100 μl of 1:3 diluted normal human serum (NHS) in PBS. After mixing and centrifugation, the radioactivity of the resulting pellets was measured in a gamma-counter.

Expression of the immunoreactivity results. Protein quantities were always expressed relative to 1 ml of the involved ascites. Immunoreactivity was determined by RIA on samples whose protein concentration was adjusted to 10^5 ng/ml and thereafter serially diluted up to 1 ng/ml. Then, the concentration of proteins displaying 50% of maximum specific binding of radiolabelled antigen was graphically determined. The inverse of this value was defined as the specific anti-AFP activity (ml/mg).

Results

Reference 2DGE maps

Normal mouse serum was subjected to 2DGE in order to obtain reference patterns of mouse proteins. Spot identification was performed by comparison with previously published human serum 2DGE maps (Anderson and Anderson, 1977; Felgenhauer and Hagedorn, 1980; Tracy et al., 1982). As illustrated in Fig. 1*A*, many mouse proteins exhibited migration profiles similar to human ones. The typical protein content of mouse

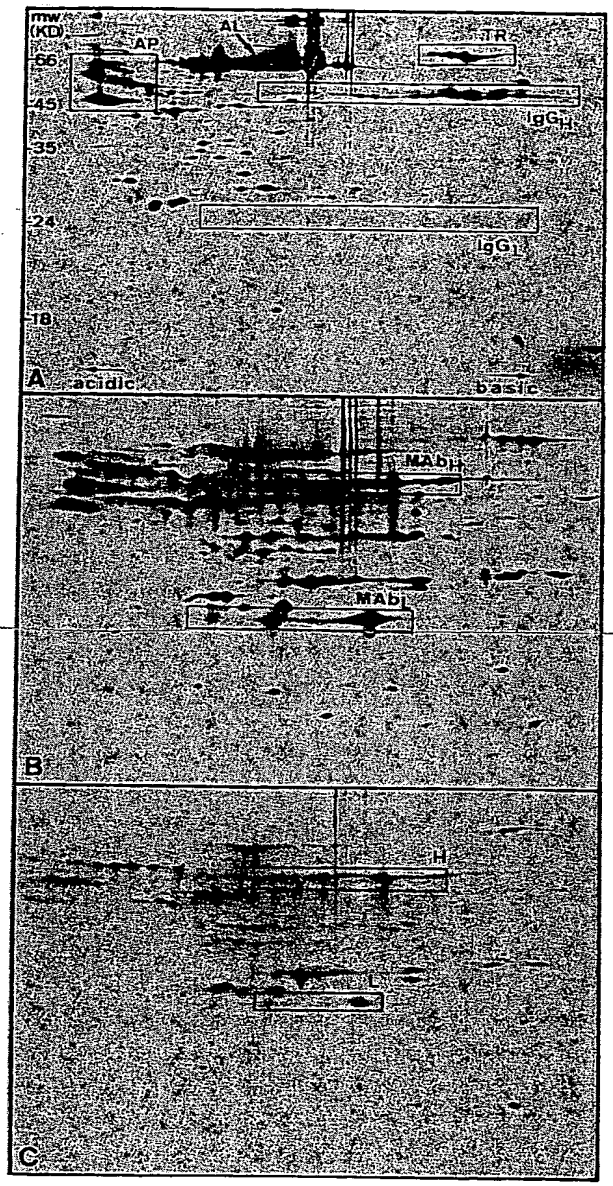

Fig. 1. 2DGE patterns of normal mouse serum (*A*), AF04 crude ascites (*B*) and salt-precipitated AF04 (*C*). Some proteins were identified and highlighted with boxes or arrows. Namely, albumin (AL), transferrin (TR), alpha-acidic proteins (AP), IgG heavy chains (IgG_H), IgG light chains (IgG_L), AF04 MAb heavy (MAb_H,H) and light (MAb_L,L) chains. Protein amounts applied: 20 μg (*A*), 20 μg (*B*) and 17 μg (*C*).

ascites is shown in Fig. 1*B*. Both heavy and light chains of the monoclonal antibody secreted by the injected hybridoma were clearly seen as major proteins of the ascitic fluid. As previously described (Pearson and Anderson, 1983), the heavy- and light-chain electrophoretogram is typical for a given MAb and each chain constantly exhibits about 3–8 subpopulations with different isoelectric points (pHi).

Ammonium sulphate precipitation

Salt precipitation of the ascites was performed before prot. A purification (protocol 2). More than 90% immunoreactivity was recovered in the pellet (Tables I, II and III). A typical pattern of the $(NH_4)_2SO_4$-precipitated fraction of ascites fluid (AF04) is shown in Fig. 1*C*: in fact, this technique led to an enrichment of the MAb rather than to real purification. High molecular weight and acidic proteins seem to be removed preferentially from the ascites by this method.

Reference purification method: prot. A chromatography (standard protocol)

The results of immunoreactivity and yield are presented in Tables I (AF01), II (AF08) and III (AF04).

Using sulphate-precipitated ascites and elution from prot. A with a discontinuous pH gradient (protocol 2), the elution of AF01, an IgG2, was not expected at a pH higher than 4.5 (Ey et al., 1978). In fact, the main fraction (44%) of the immunoreactive material was released at pH 5.8, as shown in Table I. Moreover, a longer elution time at this pH enhanced this ratio, but did not lead to complete elution of the bound monoclonal antibody (results not shown). This observation suggested heterogeneity in behaviour towards prot. A in the MAb population. Most of remaining immunoreactivity was eluted at pH 4.5 (25%).

Results obtained with AF08 (IgG1) demonstrated that the bound fraction of the MAb was partly released at pH 8.5 (24%) whereas 68% were

TABLE I

PURIFICATION AND YIELD OF AF01 MOUSE MONOCLONAL ANTIBODY USING VARIOUS PURIFICATION PROCEDURES

	Fractions	Specific anti-AFP activity [a] A	Factor of purification $B = A/A_1$	Protein mg/ml ascites C	Yield % protein $D = C/C_1$	Yield % activity $E = D \times B$
Crude ascites		33 000 (A_1)	1.0	28.0 (C_1)	100.0	100.0
Ammonium sulphate	Precipitate	65 000	2.0	12.8	46	90
	Supernatant	1 300	0.04	12.8	46	2
Hydroxylapatite	1: 0 mM Cl^-	90	< 0.01	9.5	34	< 0.1
	2: 50	1 600	0.05	3.2	11	0.6
	3: 220	154 000	4.7	2.9	10	47
DEAE	1: 60 mM Cl^-	175 000	5.4	4.2	15	81
	2: 90	13 000	0.4	0.4	1.4	0.6
	3: 140	7 000	0.2	1.3	4.6	1.1
	4: 160	20 000	0.6	11.5	4.1	2.4
Prot. A batch	Unbound pH 8.5	100	< 0.01	23.3	83	< 0.1
	Eluate pH 5.0	290 000	8.8	3.0	11	94
Prot. A protocol 2	1: pH 8.5	1 000	0.03	9.0	32	1.0
	2: pH 5.8	320 000	9.5	1.3	4.6	44
	3: pH 4.5	250 000	7.7	0.9	3.2	25
	4: pH 3.5	53 000	1.6	0.1	0.4	0.6

[a] Specific anti-AFP activity is defined as the dilution of a solution containing 1 mg protein per ml required to attain 50% of maximum specific binding of radiolabelled antigen.

TABLE II
PURIFICATION AND YIELD OF AF08 MOUSE MONOCLONAL ANTIBODY USING VARIOUS PURIFICATION PROCEDURES

	Fraction	Specific anti-AFP activity A	Factor of purification $B = A/A_1$	Protein mg/ml ascites C	Yield % protein $D = C/C_1$	Yield % activity $E = D \times B$
Crude ascites		46 700 (A_1)	1.0	26.0 (C_1)	100.0	100.0
Ammonium sulphate	Precipitate	70 000	1.5	16.1	62	93
	Supernatant	2 100	0.04	10.0	38	1.5
Hydroxylapatite	1: 0 mM Cl^-	230	< 0.01	10.5	40	0.2
	2: 170	130 000	2.8	5.8	22	62
Prot. A batch	Unbound pH 8.5	26 100	0.6	13.0	50	28
	Eluate pH 5.0	187 000	4.0	4.0	15	62
Prot. A protocol 2	1: pH 8.5	500	0.01	6.5	25	0.3
	2: pH 8.5	121 000	2.6	2.4	9.2	24
	3: pH 5.8	210 000	4.5	3.9	15	68
	4: pH 4.5	600	0.01	0.1	0.1	< 0.01

TABLE III
PURIFICATION AND YIELD OF AF04 MOUSE MONOCLONAL ANTIBODY USING VARIOUS PURIFICATION PROCEDURES

	Fraction	Specific anti-AFP activity A	Factor of purification $B = A/A_1$	Protein mg/ml ascites C	Yield % protein $D = C/C_1$	Yield % activity $E = D \times B$
Crude ascites		60 000 (A_1)	1.0	39 (C_1)	100.0	100.0
Ammonium sulphate	Precipitate	99 000	1.65	22.3	57.1	94.0
	Supernatant	780	0.01	14.7	37.7	0.5
Gel filtration	1	1 800	0.03	2.4	6.1	0.2
	2	93 000	1.5	3.6	9.2	14.2
	3	70 000	1.2	24.9	63.8	75.2
	4	1 700	0.03	2.5	6.4	0.2
	5	3 300	0.05	1.3	3.3	0.2
Hydroxylapatite	1: 0 mM Cl^-	600	0.01	10.4	26.7	0
	2: 170	230 000	3.8	5.7	14.6	55.6
	3: 250	107 000	1.8	3.1	7.9	14.4
DEAE	1: 45 mM Cl^-	120	< 0.01	2.2	5.6	0
	2: 80	204 000	3.4	9.7	24.9	84.0
	3: 150	3 900	0.06	18.5	47.4	3.1
Prot. A batch	Unbound pH 8.5	62 000	1.0	32.0	82.8	85.0
	Eluate pH 5.0	260 000	4.3	0.2	0.6	2.8
Prot. A protocol 2	1: pH 8.5	108 000	1.08	15.2	38.0	70.1
	2: pH 5.8	280 000	4.7	0.2	0.7	3.1
	3: pH 4.5	60 000	1.0	0.1	< 0.01	1.0
Prot. A protocol 3	1: pH 8.5	9 200	0.15	1.6	4.1	0.7
	2: pH 8.5	275 000	4.5	4.8	12.3	55.3
	3: pH 5.8	245 000	4.1	0.6	1.4	5.9
Prot. A protocol 3b	1: pH 8.5	255 000	4.3	4.2	10.8	45.4
	2: pH 5.8	270 000	4.5	0.6	1.5	0.9

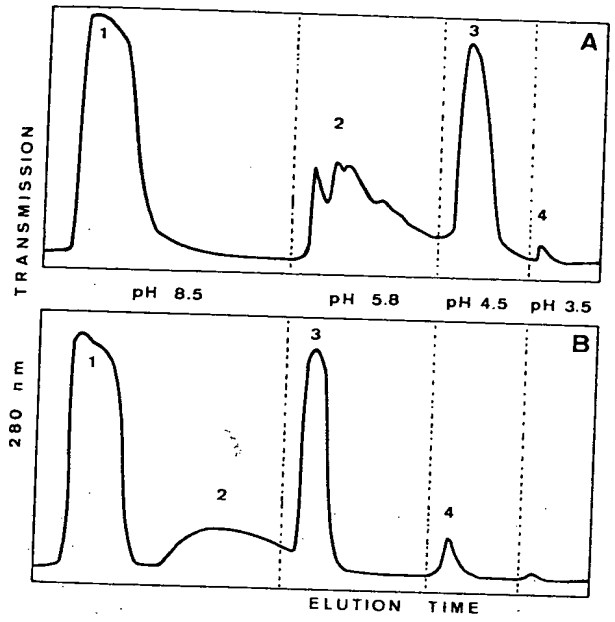

Fig. 2. 280 nm transmission chromatograms of prot. A standard protocol. An automatic gradient mixer was used. *A*: AF01 (30 ml of salt precipitated ascites); *B*: AF08 (20 ml of salt-precipitated ascites). Fraction numbers according to Tables I (AF01) and II (AF08).

eluted at pH 5.8 (Table II). Typical elution profiles are shown in Figs. 2*A* (AF01) and *B* (AF08).

For AF04, this protocol resulted in the recovery of only 3% purified antibody in the pH 5.8 fraction. About 70% of involved MAb was released at pH 8.5. In fact, the 280 nm transmission profiles (Fig. 5*A*) constantly displayed two overlapping peaks at pH 8.5, suggesting the presence of at least two subpopulations of proteins with different affinity for prot. A. Attempts to improve the separation of these two fractions by increasing the pH of the elution buffer (up to 9.2) were unsuccessful.

The 2DGE patterns of the most highly purified fractions of these prot. A purifications are pre-

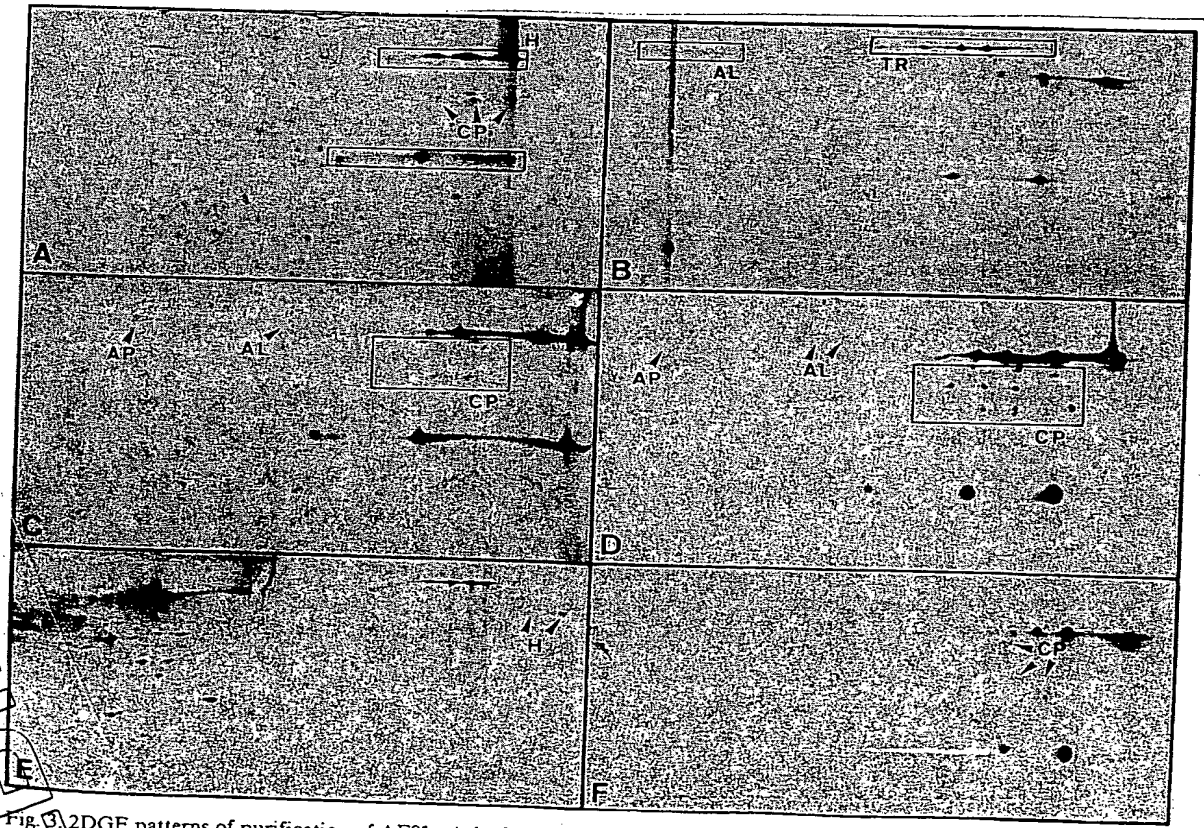

Fig. 3. 2DGE patterns of purification of AF01. *A*: hydroxylapatite chromatography (fraction 3); *B*: DEAE chromatography (fraction 1); *C* and *D*: prot. A, standard protocol, elution fractions pH 5.8 and 4.5 respectively. *E* and *F*: prot. A, fast batch purification, unbound fraction at pH 8.5, and pH 5.0 eluate, respectively. Protein amounts applied to the gels: 6 μg (*B*, *F*); 7 μg (*A*); 8 μg (*C*, *D*); 12 μg (*E*). Fraction numbers as in Table I. Co-purified proteins (CP) as described in results. Other abbreviations as in Fig. 1.

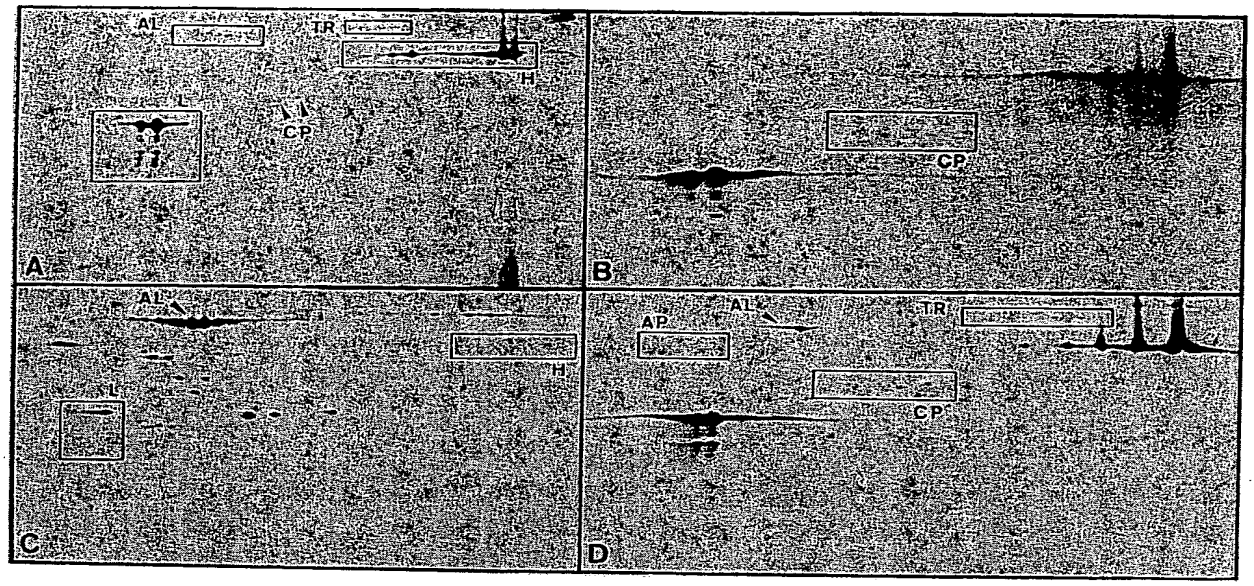

Fig. 4. 2DGE patterns of purifications of AF08. *A*: hydroxylapatite (fraction 2); *B*: prot. A, standard protocol, elution fraction at pH 5.8 (CP as in Fig. 3); *C* and *D*: prot. A, fast batch purification, unbound fraction (pH 8.5) and pH 5.0 eluate, respectively. Protein amounts applied: 7 μg (*A, B, C, D*). Fraction numbers as in Table II.

sented in Figs. 3*C* and *D* (AF01), 4*B* (AF08) and 7*H* (AF04). As expected, highly purified antibodies were obtained from prot. A purifications. Purified AF08 antibody released at pH 8.5 (fraction 2, pattern not shown) appeared to be more contaminated by mouse proteins than fraction 3 (pH 5.8, Fig. 4*B*). In other respects, small amounts of 30–45 kDa compounds were detected in the electrophoretograms of highly purified MAbs. These spots were designated as co-purified proteins (CP). Their pattern was fairly constant when the same ascites batch was used as a source of monoclonal antibody, but could vary from one ascites batch to another. However, the pHi of these CP strikingly differed for each MAb, suggesting a close relationship between these compounds and the antibody. This result might be partly due to degradation of the MAb. Indeed, in the case of AF01, a higher ratio of these proteins was observed in the fraction eluted at pH 4.5 than in the fraction released at pH 5.8 (Fig. 3*C* and *D*).

Finally, this prot. A standard protocol resulted in highly purified products but in a low yield for some but not all MAbs of the IgG1 subclass.

Using this method as a reference, the three MAbs were then separately studied in order to select protocols able to either enhance the yield and the rapidity of purification or reduce the cost of both basic material and products without loss of purity.

AF01: the example of an IgG2

The rapid prot. A batch protocol was particularly interesting to test for AF01: the results shown in Table II indicate almost complete binding of the antibody at pH 8.5 and an excellent recovery in the pH 5.0 eluate (94% immunoreactivity). The 2DGE patterns of both pH 8.5 and pH 5.0 fractions (Fig. 3*E* and *F*) confirmed these results. Indeed, only trace amounts of AF01 heavy chains were detected in the fraction eluted at pH 8.5 (Fig. 3*E*). In contrast, the 2DGE of the pH 5.0 eluate displayed a very pure AF01 pattern that differed only slightly from that obtained with the pH 4.5 fraction eluted during the prot. A standard protocol (Fig. 3*D* and 3*F*). However, contaminating proteins (CP) of 30–45 kDa seemed to be present in greater amounts in the latter. DEAE chromatography produced less purified antibodies (albumin and transferrin are clearly observed in Fig. 3*B*), but there was no evidence of marked denaturation. Hydroxylapatite-purified AF01 was

more contaminated (Fig. 3*A*). Moreover, 280 nm profiles were only weakly reproducible day-to-day, as was the ratio of irrelevant proteins (Fig. 3*A*).

Thus, prot. A fast batch purification appeared to be the most efficient method for purification of AF01 MAb in terms of yield, purity and rapidity.

AF08: an IgG1 with a good affinity for prot. A

For this MAb, the 2 prot. A purification protocols provided a similar recovery of purified antibody. However, both 2DGE analysis and immunoreactivity measurements of the batch-purified samples showed that a large proportion of AF08 (28%) did not bind to prot. A (Fig. 4*C*) at pH 8.5. Moreover, the fraction eluted at pH 5.0 was more contaminated (Fig. 4*D*), by transferrin, albumin and alpha-acidic proteins, in comparison to the prot. A standard protocol (Fig. 4*B*). For hydroxylapatite, the conclusions drawn from data obtained with AF01 could be extended to AF08: the yield was relatively good (62% of immunoreactivity), but purity was only moderate (Fig. 4*A*). Thus, prot. A standard protocol provided the highest yield and purity for AF08 MAb.

From an examination of all the AF08 2DGE patterns, it was noted that the IgG light chains of this MAb constantly displayed considerable heterogeneity in their molecular weight range whatever the purification protocol used.

AF04: an IgG1 with a weak affinity for prot. A

As expected, the batch protocol did not improve the yield of purified AF04 when compared to standard protocol. Moreover, the 2DGE patterns showed a sizable proportion of unpurified antibody in the pH 8.5 unbound fraction (Fig. 7*E*) and an increased contamination of the pH 5.0 eluate (Fig. 7*G*).

For this antibody, we attempted to improve the yield while maintaining purity. As shown in Table III, DEAE chromatography yielded 9.7 mg purified MAb per ml of crude ascites, which corresponded to the recovery of 84% of initial immunoreactivity. As shown in Fig. 7*E*, many proteins were co-purified with the MAb. It was striking that the isoelectric point of the contaminating proteins and AF04 heavy and light chains were in the same pHi range. This ion-exchange purified fraction was then submitted to further prot. A

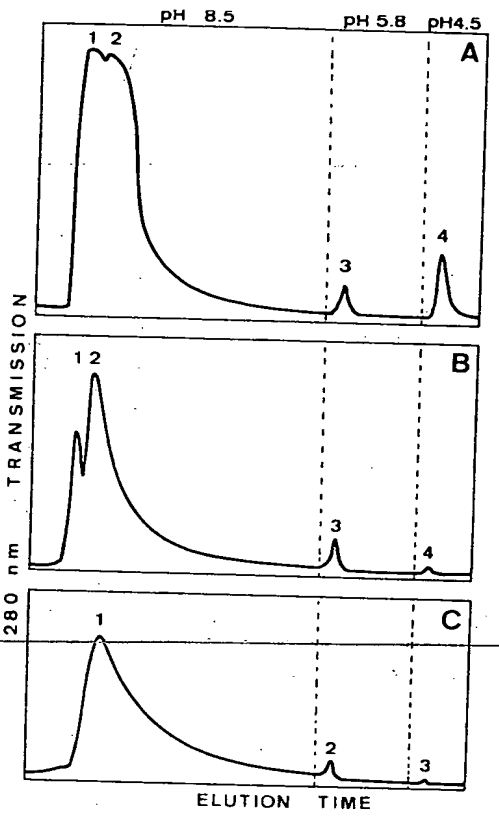

Fig. 5. Purification of AF04 by prot. A with discontinuous pH gradient (protocol 2): 280 nm transmission profiles. *A*: prot. A purification of AF04 after ammonium sulphate precipitation and dialysis against 0.1 M pH 8.5 phosphate. Only about 3% of antibody was found in pH 5.8 fraction. *B*: purification on prot. A of the purest fraction obtained by DEAE chromatography (profile not shown); 55.3% of the MAb present in ascites was recovered in the second pH 8.5 peak. *C*: the second pH 8.5 fraction of Fig. 5*B* was further purified on prot. A (protocol 3b). Only one peak was seen at pH 8.5.

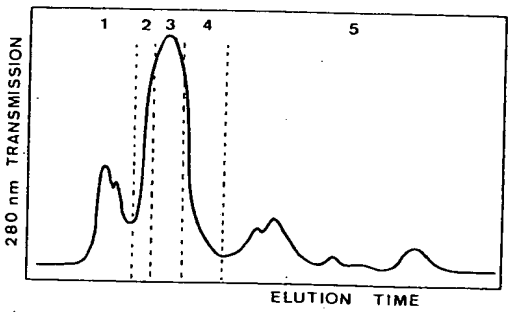

Fig. 6. Sephacryl S200 gel filtration chromatography: 280 nm transmission profile. As demonstrated by RIA, most of the immunoreactivity was found in fractions 2 (highest specific activity) and 3.

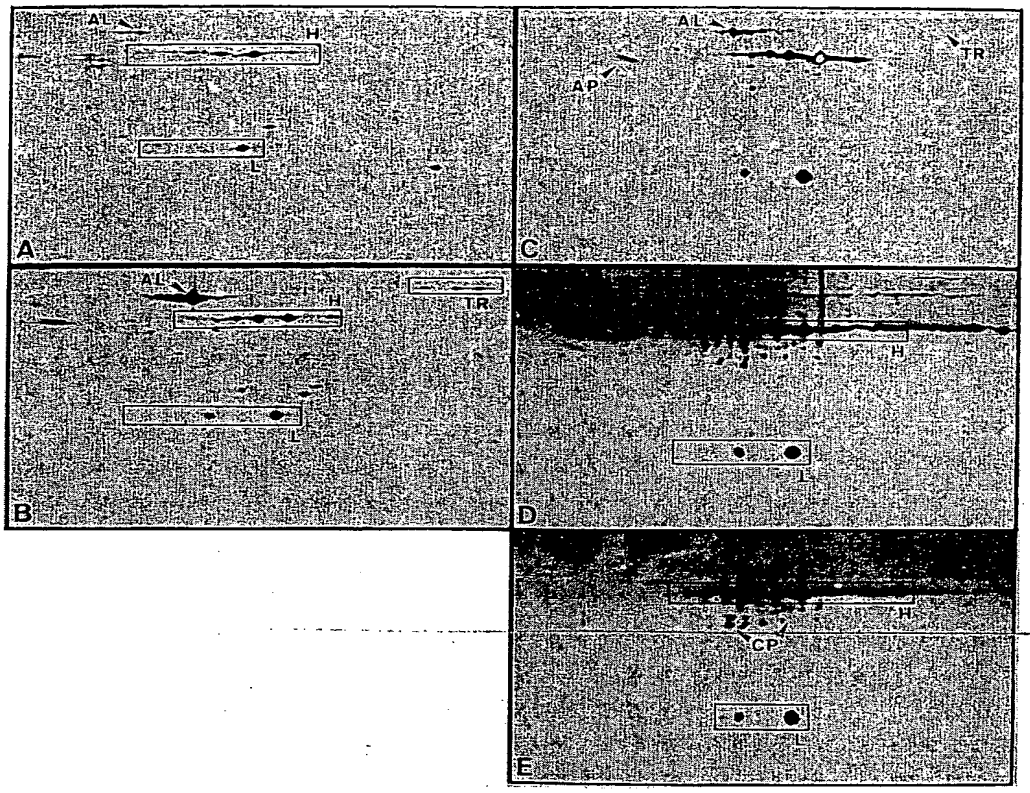

purification. The elution profile (Fig. 5*B*) showed two peaks eluted at pH 8.5. The antibody was recovered in the second pH 8.5 peak which contained 55% of original immunoreactivity of ascites and yielded 4.8 mg per ml (Table III). The first pH 8.5 peak corresponded to 1.6 mg proteins per ml of ascites, but contained less than 1% of immunoreactivity. As analyzed by 2DGE, peak 1 exhibited only minor amounts of AF04 MAb (Fig. 7*I*) whereas a number of other proteins was present. Antibody in peak 2 appeared to be almost contamination-free (Fig. 7*J*). In an attempt to assess the purity of this fraction, a 4-fold higher amount of protein was submitted to 2DGE (Fig. 7*K*). Artefacts due to partial precipitation of the IgG chains in the focusing gel were clearly observed, but none of the proteins detected in peak 1 were visible on electrophoretograms corresponding to peak 2. However, some spots were seen in the 30–50 kDa area of the gel (CP). In other respects, additional spots (Fig. 7*K*) corresponding to IgG light chains, appeared in this pattern. Comparison of patterns 7*E*, 7*I* and 7*J* clearly demonstrated the usefulness of prot. A purification to remove DEAE-co-purified impurities. No differences could be observed in the 2DGE pattern between peaks 2 and 3 obtained from protocol 3 (Fig. 5*B*), and peak 1 obtained from protocol 3b (Fig. 5*C*) (data not shown).

The results obtained by hydroxylapatite purification of AF04 were not strikingly different from those described for AF01 and AF08. Two overlapping peaks were eluted at 170 and 250 mM NaCl and yielded 55.6% and 14.4% immunoreactivity, respectively. 2DGE analysis of peak 2 (Fig. 7*C*) indicated that numerous irrelevant proteins were present. Peak 3 (fig. 7*D*) exhibited striking contamination. Results were not improved by using either a discontinuous NaCl gradient or a phosphate gradient at room temperature, as described by Stanker et al. (1985) (results not shown). Moreover, this technique was poorly reproducible even

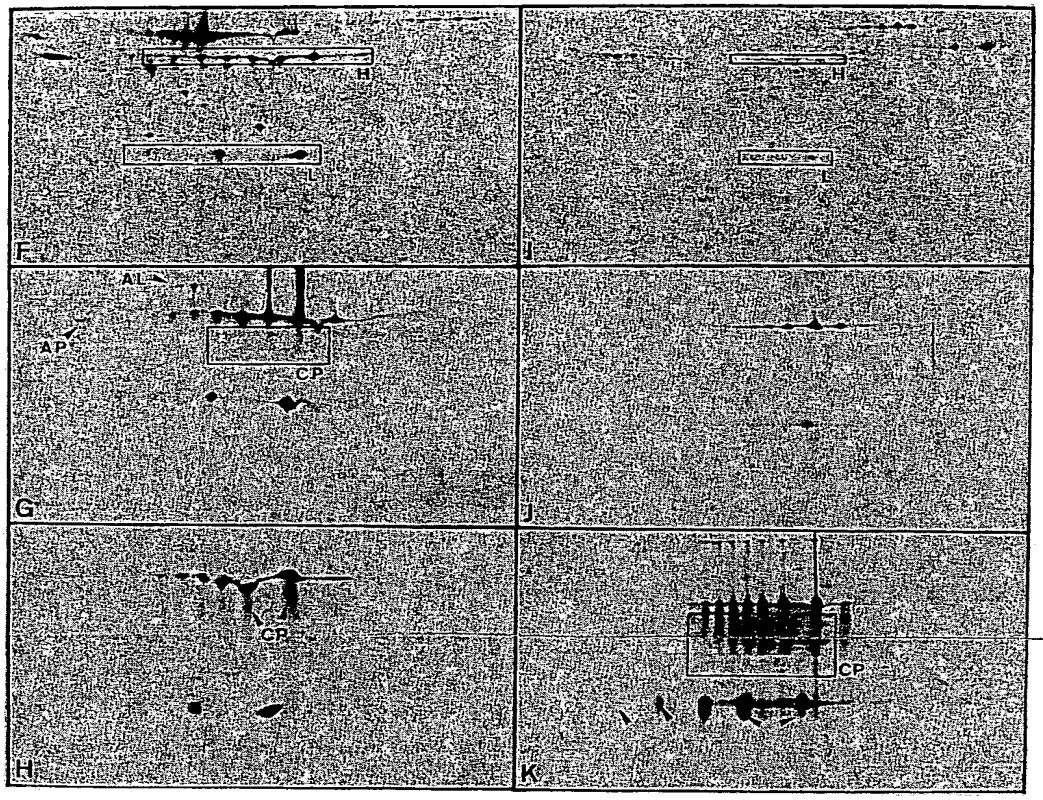

Fig. 7. 2DGE patterns of purification of AF04. *A*: Sephacryl S200 gel filtration, fraction 2; *B*: idem, pooled fractions 2 , 3 and 4; *C* and *D*: hydroxylapatite chromatography, peaks 2 and 3, respectively; *E*: DEAE chromatography, fraction 2: *F* and *G*: prot. A batch purification (protocol 1), unbound fraction at pH 8.5 and eluate at pH 5.0, respectively; *H*: prot. A standard protocol, pH 5.8 eluate; DEAE and prot. A purifications (protocol 3): pH 8.5 fraction 1 (*I*), fraction 2 (*J* and *K*). Other abbreviations as in Fig. 1. Protein amounts applied: 7 μg (*A, B, C, D, E, F, G*), 9μg (*H*), 5 μg (*I, J*), 20 μg (*K*).

after dialysis of ascites against the starting buffer. Overall, hydroxylapatite chromatography resulted in highly diluted and poorly purified antibodies.

Gel filtration was carried out on AF04-filtered ascites. The chromatogram is shown in Fig. 6. Fractions were pooled on the basis of their 280 nm profiles and their immunoreactivity. Fractions 2 and 3 yielded 14.2% and 75.2% of immunoreactivity (patterns in Figs. 7*A* and 7*B*). Sephacryl S200 gel filtration resulted in either low yield and moderate purity (fraction 2 alone), or improved yield but lower purity of the MAb (pooled fractions 2–4).

Discussion

For analysis of a mixture of proteins such as ascitic fluids, 2DGE with silver staining is one of the most powerful analytical tools. This method was thus selected to control the quality of purified MAbs. Solubilization of the samples in a urea-NP40 buffer and equilibrium focusing permit the detection of most of the IgG MAb heavy and light chains. For IgG molecules with a pHi higher than 8, SDS solubilization (Blangardin et al., 1984) and/or non-equilibrium pH gel electrofocusing (O'Farrell et al., 1977) could be a prerequisite to 2DGE analysis. Because of the similarities in the migration of human and murine serum proteins, most of the major spots could be easily identified. It appeared that the contaminating proteins frequently found with purified MAb were albumin, transferrin and alpha-acidic proteins.

2DGE also demonstrated the presence of the so-called 'co-purified proteins' (CP). The pattern of these proteins detected in the 30–50 kDa range

of purified fractions of the 3 MAbs seemed to be related to each antibody. During prot. A purifications, these CP appeared in higher amounts when a long-duration protocol was used (Figs. 3*D* and *F* for AF01) and/or when low pH buffers were employed for the elution of bound MAb (Figs. 3*C* and *D*). However, hydroxylapatite (Figs. 7*C* and *D*, and 4*A*) or DEAE (Fig. 7*E*) chromatography might also result in the appearance of these CP. In fact, although the presence of CP in crude ascites might not be excluded, it is more likely that they resulted from degradation of the MAb during purification.

In addition to impurities, electrophoretograms highlighted dramatic molecular weight heterogeneity of AF08 light chains (Fig. 4). In fact, whatever the ascites batch and the purification protocol used, rows of vertically aligned spots were visible on the gels in the light chains area. Artefacts due to solubilization of samples were unlikely to have resulted in such molecular weight variations since AF01 and AF04 never displayed this pattern. Rather, commonly observed 2DGE artefacts are probably charge shifts due to partial carbamylation of proteins (Pearson and Anderson, 1983). The molecular weight shifts observed in AF08 patterns may be partly explained by removal of neutral sugars or by partial degradation of the light chains 'in vivo' and/or inside a defined ascitic fluid. This heterogeneity could also be a characteristic of the antibody molecules secreted by AF08 hybridoma, e.g., a variation in kinetics of glycosylation.

For a comparison of purification methods of MAbs, two parameters, yield and purity, were particularly considered. In terms of purity, the best results were constantly obtained with protocols involving prot. A. Concerning the yield, the efficiency was closely dependent on the optimization of the protocol. For IgG2 like AF01, the rapid batch protocol provided the best yield and purity, whereas standard protocols resulted in both the appearance of higher amounts of degradation products and a lower yield. For AF08 (IgG1 with good affinity for prot. A), about 30% of recovered antibody was not bound to prot. A in the batch protocol which, furthermore, provided more contaminated purified antibody. In this case the standard protocol remained the most efficient method. In contrast, IgG1 with very low affinity for prot. A such as AF04 could not be efficiently purified by prot. A alone, whatever the protocol used. Then, a prior step with DEAE-chromatography was performed and this permitted the removal of most ascitic proteins. In a following prot. A step, the actual interaction of AF04 with prot. A at pH 8.5 allowed a separation from residual impurities. This heterogeneous behaviour towards prot. A inside the IgG1 subclass strengthens the hypothesis that IgG1 may comprise several subclasses (Stanislawski and Mitard, 1976; Villemez et al., 1984).

For all tested MAbs, DEAE-chromatography alone appeared to be less potent than prot. A for the production of very pure antibodies but possibly resulted in a slightly better yield.

All the other methods tested were found to be less efficient.

Practically, we propose a logical process to optimize the purification protocol of a MAb, without previous knowledge of IgG subclass. The prot. A standard protocol should be performed in order to determine the proportion of MAb released at each pH value and to measure the yield of purified antibody. If the bound fraction at pH 8.5 is sufficiently high, the 3 h long batch protocol should be carried out. If most of the immunoreactivity is found in the pH 8.5 unbound fraction, DEAE chromatography should be performed before the prot. A standard protocol.

Finally, it is noteworthy that optimization of the purification procedure for a MAb which bound weakly to protein A (AF04) permitted a 30-fold enhancement of the yield with no loss in purity.

Acknowledgements

We are grateful to L. Fougeat, J.P. Laborde, P. Gauchet, C. Logé and C. Chimchirian for technical assistance. We wish to thank Dr. C. Gosse for continuous help and Dr. J.J. Madjar and Dr. J.M. Bidart for fruitful discussions.

This work was supported in part by Grant CRC 8414 from the 'Institut Gustave-Roussy', Villejuif, France.

LM is a recipient of a research fellowship from the 'Fondation pour la Recherche Médicale', Paris.

PM is a recipient of a research fellowship from the 'Association pour la Recherche sur le Cancer', Villejuif.

References

Anderson, L. and N.G. Anderson, 1977, Proc. Natl. Acad. Sci. U.S.A. 74, 5421.

Bellet, D.H., J.R. Wands, K.J. Isselbacher and C. Bohuon, 1984, Proc. Natl. Acad. Sci. U.S.A. 81, 3869.

Blangardin, P., P. Deviller, K. Kindbeiter and J.J. Madjar, 1984, Clin. Chem. 30, 2021.

Burchiel, S.W., J.R. Billman and T.R. Alber, 1984, J. Immunol. Methods 69, 33.

Carlsson, M., A. Hedin, M. Inganäs, B. Härfast and F. Blomberg, 1985, J. Immunol. Methods 79, 89.

Ey, P.L., S.J. Prowse and C.R. Jenkin, 1978, Immunochemistry 15, 429.

Felgenhauer, K. and D. Hagedorn, 1980, Clin. Chim. Acta 100, 121.

Goding, J.W., 1980, J. Immunol. Methods 39, 285.

Kennel, S.J., L.J. Foote, P.K. Lankford, M. Johnson, T. Mitchell and G.R. Slawsky, 1983, Hybridoma 2, 297.

Köhler, G. and C. Milstein, 1975, Nature 256, 495.

Laemmli, U.K., 1970, Nature 227, 680.

Motté, Ph., J.M. Bidart, J.C. Delarue, E. Comoy, P. Moingeon and C. Bohuon, 1984, Clin. Chem. 30, 1947.

Oakley, B.R., D.R. Kirsch and N.R. Morris, 1980, Anal. Biochem. 105, 361.

O'Farrell, P.H., 1975, J. Biol. Chem. 250, 4007.

O'Farrell, P.Z., H.M. Goodman and P.H. O'Farrell, 1977, Cell 12, 1133.

Pearson, T.W. and N.L. Anderson, 1983, Methods Enzymol. 92, 196.

Phillips, A.P., K.L. Martin and W.H. Horton, 1984, J. Immunol. Methods 74, 385.

Scatchard, G., 1949, Ann. N.Y. Acad. Sci. 51, 660.

Stanislawski, M. and M. Mitard, 1976, Immunochemistry 13, 979.

Stanker, L.H., M. Vanderlaan and H. Juarez-Salinas, 1985, J. Immunol. Methods 76, 157.

Tracy, R.P., R.M. Currie and D.S. Young, 1982, Clin. Chem. 28, 890.

Villemez, C.L., M.A. Russell and P.L. Carlo, 1984, Mol. Immunol. 21, 993.

Willard, K.E., C.S. Giometti, N.L. Anderson, et al., 1979, Anal. Biochem. 100, 289.

ELSEVIER

Journal of Immunological Methods 179 (1995) 105–116

JOURNAL OF IMMUNOLOGICAL METHODS

Purification of bacterially expressed single chain Fv antibodies for clinical applications using metal chelate chromatography

J.L. Casey [a,*], P.A. Keep [a], K.A. Chester [a], L. Robson [a], R.E. Hawkins [b], R.H.J. Begent [a]

[a] *Cancer Research Campaign Laboratories, Department of Clinical Oncology, Royal Free Hospital Medical School, Rowland Hill Street, London NW3 2PF, UK*

[b] *MRC Centre, Hills Road, Cambridge CB2 2QH, UK*

Received 18 July 1994; revised 1 October 1994; accepted 26 October 1994

Abstract

A new procedure is described for the purification of an anti-carcinoembryonic antigen (CEA) single chain Fv (scFv), referred to as MFE-23, from bacterial supernatant. A simple insertion of a hexa-histidine tail fused at the C-terminus (MFE-23 His) provides an affinity tag which selectively binds to transition metal ions immobilised on an iminodiacetic acid (IDA) derivitised solid phase matrix. This method proved to be superior to standard CEA antigen affinity chromatography in the following ways. (1) A higher yield was produced (10 mg/l as opposed to 2.2 mg/l of bacterial supernatant). The latter figure was largely affected by the limited availability (size of the column) of immobilised CEA antigen. (2) Scale-up was relatively simple and less costly. (3) The risk of tumour derived antigen leaching from the column is eliminated. Results showed that immobilised Cu^{2+} ions were more effective than Ni^{2+} and Zn^{2+} ions in retaining the His tagged product giving a 90% pure product on elution. Clinical grade material was generated using size exclusion chromatography to remove aggregated material, and Detoxi gel to remove bacterial endotoxins. Validation assays to measure DNA, copper and endotoxins were performed to assess the levels of contaminants. MFE-23 His retained 84% antigen binding after 6 months storage at 4°C and > 75% after radiolabelling. Further experiments confirmed that the His tail did not affect biodistribution and tumour localisation in nude mice bearing human colorectal tumour xenografts.

Keywords: Chromatography, metal chelate; Phage derived single chain Fv; Tumor targeting

Abbreviations: Mabs, monoclonal antibodies; scFv, single chain Fv; IMAC, immobilised metal affinity chromatography; CEA, carcinoembryonic antigen; IDA, iminodiacetic acid; NTA, nitrilotriacetic acid; PBS, phosphate buffered saline; SDS PAGE, sodium dodecyl sulphate polyacrylamide gel electrophoresis; LAL, Limulus amoebocyte lysate; OD, optical density; DIG, digoxigenin; TLC, thin-layer chromatography; SOP, standard operating procedure; %ID, % injected dose per gram.

* Corresponding author. Tel.: (071) 794-0500; Fax: (071) 794-3341.

SSDI 0022-1759(94)00278-9

REF. 16

1. Introduction

The use of monoclonal antibodies (Mabs) and their fragments is now well established for therapeutic and diagnostic antigen specific targeting of colorectal cancer (Begent and Pedley, 1990). However, the ability to deliver therapeutic doses of radiation to tumours has been limited by the retention of radiolabelled Mabs in normal organs and the slow clearance from the circulation resulting in bone marrow toxicity (Begent et al., 1989). Furthermore, whole antibody or enzyme digested fragments have poor diffusion characteristics, slowly penetrating through tumour masses after extravasation (Boxer et al., 1992). The recent development of genetically engineered single chain Fv (scFv) molecules which consist of only the antibody variable regions held together by a flexible linker to increase stability (Huston et al., 1993) have the potential to alleviate some of these problems. Studies have shown that scFvs with their smaller size (27 kDa) penetrate tumours more rapidly and evenly than do larger fragments and intact Mabs. They may also clear from the circulation within hours of administration (Yokota et al., 1992). In addition smaller size molecules lacking constant regions, have the potential to reduce the host immune response to antibody, the production of which is a major limiting factor to repeating antibody therapy (Ledermann et al., 1988).

The advent of phage technology has permitted the generation of a large number of new scFvs which can be selected for desired characteristics. For example high affinity scFvs can be selected from large libraries for potential clinical use (Hawkins et al., 1992). ScFvs can be expressed in soluble form in mammalian cells or alternatively in *Escherichia coli* (*E. coli*). Since the fermentation of bacteria is both rapid and inexpensive, it could form the basis for an improved method of production in clinical studies (Chester et al., 1994a). It is therefore essential that purification systems adapt to handling large volumes of bacterial extracts and validation studies are performed to ensure removal of contaminants by the various chromatographic steps.

Traditionally, Mabs and antibody fragments have been purified using immunoaffinity or ion exchange chromatography. Anti-CEA antibodies can be purified using antigen affinity columns, which are highly specific but consist of tumour derived antigen which tends to leach out during elution of antibody. Clearly, this is undesirable when purifying clinical grade material. In addition it is often impractical and costly to scale-up antigen columns to handle large volumes of material. Ion exchange chromatography overcomes some of these problems, but has other disadvantages such as low selectivity and instability at low ionic strengths leading to precipitation of protein during the procedure.

Recombinant DNA technology enables insertion of specific sequences or genes by fusion to the protein of interest; which can provide 'affinity handles' designed to bind specific matrices enabling the selective purification of the protein of interest. Examples of affinity tail fusion proteins include protein A, β-galactosidase and maltose binding protein (reviewed by Narayanan, 1994). However, problems encountered when using these particular affinity tags include the incorrect folding of recombinant molecules masking the ligand binding site, and the requirement to cleave off the fusion protein and repurify the parent protein. c-*myc* oncoprotein fusion tags have been widely used (including this study) to ease the detection of recombinant proteins via an anti-c-*myc* antibody. However, for the preparation of clinical products the use of oncogene derived determinants such as c-*myc* is not desirable.

An improved purification process applicable to scFvs has been developed by genetically engineering sequences of amino acid tails or tags away from the antigen binding site by insertion at the N- or C-terminus. In a study carried out by Skerra et al. (1991) it was reported that the addition of a five amino acid polyhistidine tail proved to be a stable product which could be purified by immobilised metal ion affinity chromatography (IMAC) making the use of its high affinity for transition metal ions.

In this study we have inserted an amino acid tail consisting of six consecutive histidine amino acid residues (6 × His) at the C terminus of an anti-CEA scFv antibody. The native scFv contains

only two naturally occurring histidine residues and hence the histidine addition provides a tail which can be used to selectively purify the scFv by IMAC.

IMAC is a powerful affinity chromatography method introduced by Porath et al. (1975). It exploits the interaction between proteins and transition metal ions immobilised on a support derivitised by IDA, *N,N,N'*-tris-(carboxymethyl)-ethylenediamine or nitrilotriacetic acid (NTA) groups. The exposure of certain amino acids including cysteine, tryptophan and predominantly the imidazole ring of histidine on the surface of proteins is required for the absorption to transition metal ions immobilised on the support (Arnold, 1991). Proteins with a high affinity for given metal ions bind through open coordination sites and are retained on the column whilst other proteins without a high affinity for immobilised metal ion elute from the column during the wash. IMAC has advantages over conventional affinity chromatography in that relatively mild elution conditions are employed to disrupt protein binding. Either metal binding ligands such as imidazole can be used to compete for metal coordination sites thereby displacing the protein, or a reduction in pH can be used to protonate the histidine residues releasing the product. Strong chelators such as EDTA at the end of elution are used to strip metal ions from the column. IMAC has wide applications. It has been used to purify many biological materials including interferons (Hochuli, 1988), α-feto-protein (Itami et al., 1987) and MHC class II molecules (Nag et al., 1994) with a range of metal ions including Ni^{2+}, Zn^{2+}, Fe^{2+}, and Co^{2+}. IMAC has also been exploited as an analytical tool to study exposure of certain amino acid residues on the surface of the proteins (Hemdam et al., 1989). More recently histidine tails have been engineered into many recombinant proteins to facilitate this purification technique, for example the isolation of histidine tagged peptides from complex mixtures (Yip et al., 1989). In this paper we explore the use of IMAC to prepare clinical grade anti CEA scFv antibodies with the aid of a hexahistidine C-terminal tail.

2. Materials and methods

The preparation of clinical grade material requires particular precautions which are not necessary in the preparation of laboratory products. The clinical grade scFv produced here was in accordance with the guidelines specified in the Cancer Research Campaign control operation manual for recombinant products (Begent et al., 1993). A summary of the guidelines for the quality and safety of clinical products include:

(1) designated sterile work areas and equipment which will prevent contamination of the purified product;
(2) full details of product development including expression systems and DNA sequencing;
(3) preparation of a clinical seed lot including testing for homogeneity and reactivity on storage;
(4) purification details and reproducibility;
(5) final product characterisation including contamination levels, potency, biological activity and toxicity.

Standard operating procedures (SOPs) have been drawn up for each individual stage of the production process outlined above. As full details and records are beyond the scope of this paper, here we have emphasised only the new purification technique and finished product characterisation.

2.1. Single chain Fv

MFE-23 is a high affinity scFv antibody (K_d = 2.529 nmol/l SD ± 1.3) which was selected from a pIIEN phagemid library generated by immunising BALB/c mice with carcinoembryonic antigen (CEA). It has been shown to selectively localise in nude mice human colorectal tumour xenografts (Chester et al., 1994b).

2.2. Subcloning and expression of the polyhistidine tail

The gene encoding MFE-23 was subcloned into a pUC 119 expression vector to contain 6 × His at the C-terminus (Fig. 1, MFE-23 His

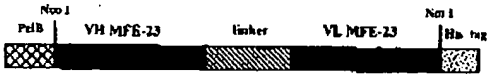

HIS TAG...

H H H H H H * *
VL.....CATCACCATCATCACCATTAATAA

Fig. 1. Schematic representation of MFE-23 subcloned for expression containing the gene for 6×His at the C terminus. For antibody expression the vector (Hawkins et al., 1994) contains a Pel B signal sequence which directs scFv into the bacterial periplasm, from here the scFv is released into the supernatant (Pluckthun, 1990). * Denotes stop codon.

vector). The construct was transfected into *E. coli* TG1 cells using electroporation and plated onto 2×TY agar containing 100 μg/ml ampicillin and 1% glucose. An individual colony was used to produce a seed lot in accordance with safety guidelines (Begent et al., 1993) and DNA sequencing was employed to confirm identity. For expression, seed lot aliquots were cultured in 2×TY medium containing 100 μg/ml ampicillin and 1% glucose at 37°C shaking for 16–20 h. Cells were grown until a cell density of 0.9 at an optical density (OD) 600 nm was achcived. Production of scFv was promoted by the addition of 1 mM isopropyl β-D-thiogalactoside and the temperature reduced to 30°C for a further 16 h. Cells were pelleted at 11300×*g* and the supernatant containing the MFE-23 His was passed through 0.45 μm followed by 0.2 μm 1 litre Nalgene disposible filters (Fisons, Loughborough, UK).

2.3. Concentration and dialysis of MFE-23 His supernatant

The bacterial supernatant was concentrated using an Amicon CH2 ultrafiltration system (Amicon. Stonehouse, Glocestershire, U.K) incorporating a RA2000 reservoir and S1Y10 spiral cartridge with a molecular weight cut off of 10 kDa. To sterilise the ultrafiltration system for the clinical grade material it was washed in Hospec neutral detergent followed by 0.1 M sodium hydroxide and pyrogen free water (Baxter, Norfolk, UK) to neutrilise. MFE-23 His culture supernatant (1–4 litres) was concentrated to 200–300 ml and pressure dialysed against sterile phosphate buffered saline pH 7.2 (Dulbecco's PBS, Sigma, Poole, UK). The crude MFE-23 His was centrifuged at 6300×*g* for 20 min at 4°C and re-filtered using 0.45 μm and 0.2 μm Nalgene filters to sterilise and remove any large protein aggregates which may have formed during the concentration steps.

2.4. Purification

IMAC purification was optimised on a small scale using non sterile conditions. Clinical purification procedures were performed under rigorous conditions, using sterile glassware, disposables and chemicals. All buffers were made with pyrogen free water. Imidazole solutions were buffered with Dulbecco's sterile PBS containing 1 M sodium chloride (NaCl) to supress ionic interactions, thereby improving selectivity of the metal for the histidine ligands (Sulkowski, 1985).

2.5. IMAC

A 10×2.5 cm Econocolumn (Bio-Rad, Hemel Hempsted, UK) was packed with 40 ml chelating Sepharose fast flow (Pharmacia Biotech. St Albans, UK) and equilibrated under gravity with 100 ml water. Metal ions (100 ml) were loaded as 0.1 M copper sulphate, zinc chloride or nickel chloride (Sigma) in water and washed through with the same volume of equilibrium buffer (PBS/1 M NaCl). NaCl was added to the concentrated dialysed supernatant to a final concentration of 1 molar to prevent leaching of metal ions from the column (Sulkowski, 1985). Up to 300 ml supernatant was loaded and the unbound material collected. Competitive elution was carried out using an imidazole gradient of 40, 60, 80, 100 and 120 mM, collecting 250 ml batchwise of bound product at each step. The column was regenerated by stripping metal ions with 100 ml of 50 mM EDTA and re-equilibrated with several column volumes of water.

All fractions were dialysed into PBS to remove salt, eluting agents and any metal ions which may have leached from the column. The fractions

were then pooled and concentrated using stirred cell ultrafiltration and a PM10 membrane (Amicon) for SDS PAGE analysis. To increase recovery of clinical material all dialysed fractions excluding the 120 mM imidazole fraction were subsequently pooled and reapplied to the column.

2.6. Gel filtration

The IMAC purified material was further purified by size exclusion to remove aggregates and metal ions. The concentrated, dialysed 0.22 μm sterile filtered (Gelman, Northampton, UK) 120 mM imidazole fraction was applied to a 350 ml Sephacryl S-100 (Pharmacia Biotech) column (XK 16/100, Pharmacia Biotech). Fractions were measured at $OD_{280\ nm}$, relevant fractions were pooled and concentrated, using stirred cell ultrafiltration and stored at 4°C.

2.7. Affinity chromatography

2 litres of MFE-23 His which had been concentrated and dialysed in PBS (400 ml) was purified using a 6 ml cyanogen bromide activated Sepharose 4B (Pharmacia Biotech) affinity column coupled to CEA (8 mg). CEA was obtained from a patient's colorectal tumour liver metastasis by extraction using perchloric acid (Keep et al., 1978). One column pass of 30 ml supernatant per run was performed.

2.8. Bacterial endotoxin removal

A 10 × 2.5 cm Econocolumn (Bio-Rad) was packed under gravity with 10 ml of Detoxi gel (Pierce Warriner, Chester, UK) and equilibriated with sterile PBS. 10 ml of the concentrated purified product was loaded, carefully mixed with the gel and incubated overnight at room temperature in a sealed column. The product was eluted by washing with 30 ml PBS.

2.9. Final product testing

Samples at each purification stage were analysed for endotoxin levels using Limulus ameobocyte lysate (LAL) gel clot vials (Atlas Bioscan, Bognor Regis, UK) according to the manufacturers' recommended instructions; a further aliquot (three times the patient dose) was tested by injection into rabbits (Safepharm Laboratories, Derby, UK). Bacterial supernatant containing MFE-23 His, semi-purified MFE-23 His and the final product were tested for the presence of bacterial DNA using the Digoxigenin (DIG) DNA labelling and detection assay (Boehringer Mannheim, Lewes, UK). A probe was constructed using a mixture of equal proportions of MFE-23 plasmid DNA and total bacterial DNA. DIG labelled DNA probes were detected after hybridisation to target samples by enzyme-linked immunoassay using an anti-DIG alkaline phosphatase conjugate. The probe was sensitive to 12 pg of DNA. The final product was also assayed for Cu^{2+} content and compared with earlier purification stages, using flame photometry (Trace Element Laboratory, University of Surrey). An aliquot was also protein sequenced using amino acid analysis by the CRC protein sequencing facility (University College of London); to confirm homogeneity of the final product and cleavage of the pelB leader sequence in the periplasm. Stability of the antibody was assessed by storing aliquots at 4°C and −70°C and subsequently analysing samples at certain time intervals using a Superose 12 HR 10/30 (Pharmacia) FPLC column. Fig. 5 illustrates the trace for MFE-23 His stored at −70°C for 6 months. Retention of antigen binding following 6 months storage at 4°C was measured by applying a known amount of purified antibody to the CEA affinity column (refer to section 2.7) and quantitating the % bound (specific activity). These values were compared by applying a known amount of MFE-23 His previously purified using the same column.

2.10. Iodination of MFE-23 His

Radiolabelling of MFE-23 His with iodine-125 (^{125}I) was performed using the chloramine T method (Greenwood and Hunter, 1963). Typically 67–250 μg of purified product in 0.5 ml was radiolabelled to give specific activities of 167–481 MBq/μg.

Table 1
Bacterial endotoxin and copper removal in each chromatographic step

Purification step	Endotoxin EU/ml	Cu^{2+} μmol/l
Supernatant	50000	–
Cu^{2-} chelate column eluate:		
pre dialysis (120 mM fraction)	–	75
post dialysis (120 mM fraction)	750	8
Gel filtration S-100 eluate	25	3.4
Detoxi gel eluate (final product)	< 2.5	–

2.11. Analysis of radiolabelled product

Thin layer chromatography (TLC) was performed to measure % ^{125}I incorporation. Antigen binding was also assessed by applying a dilution of the radiolabel to a CEA coupled Sepharose 4B (1 mg CEA; 1 ml column volume). The unbound fraction was washed through with 2 column volumes of PBS and the bound fraction with the same volume of 3 M ammonium thiocyanate. A control scFv B1.8 which is not specific for CEA and MFE-23 containing a c-*myc* tag (MFE-23 *myc*) were tested as a comparison. The unbound and bound fractions were analysed for ^{125}I activity using a gamma counter. Stability assessments were carried out by applying a sample of the radiolabel and unlabelled product to a 15% SDS PAGE minigel. The ^{125}I-MFE-23 His was visualised by autoradiography and the unlabelled product by Coomassie blue staining. ^{125}I-MFE-23 His was also applied to a 100 ml Sephacryl S-100 column (115 × 1 cm). 1.5 ml fractions were collected and counted for ^{125}I activity.

2.12. In vivo xenograft experiment

Tumour localisation and biodistribution of ^{125}I-MFE-23 His was carried out in TO nude mice bearing LS174T human tumour xenografts. MFE-23 *myc* which had been previously characterised, affinity assessed and shown to localise in human tumour xenografts (Chester et al., 1994b) was included as a comparison. Radiolabelled antibody was administered into the tail vein of mice, when the tumours were approximately 0.5 g in weight. Each mouse received 5 μg/10 μCi of ^{125}I-labelled antibody and four mice from each group were killed 24 h later. Tissues and blood samples were removed, weighed, digested in 7 M potassium hydroxide for 24 h and assessed for activity using a gamma counter.

3. Results

3.1. Optimising IMAC

Ni^{2+}, Zn^{2+} and Cu^{2+} were compared for efficacy as metal ions for IMAC solid support. SDS PAGE electrophoresis (Figs. 2A–2C) showed that in general the majority of non specific proteins were washed through the column in the unbound fraction. Further impurities were eluted by competing with low concentrations of imidazole 10–40 mM (data not shown). Increasing the concentration of imidazole to compete for metal binding

Table 2
Specific activity of MFE-23 His purified using IMAC (a–c) and CEA antigen affinity chromatography (d)

Antibody applied to column (mg)	Unbound (mg)	Bound (mg)	Specific activity (%)
(a) 2	0.35	0.76	69
(b) 1	0.23	0.68	75
(c) 0.5	0.09	0.40	81
(d) 1	0.10	0.83	89

The specific activities were based on antibody levels recovered, as some losses occurred on dialysis and concentration steps. The mean % bound specific activity for the IMAC purified material (a–c) is 75%.

sites results in elution of His tagged product. This stepwise imidazole gradient was useful for comparing the efficiency of antibody binding to Ni^{2+}, Zn^{2+} and Cu^{2+} immobilised metal ions and the level at which pure product eluted from the column. Any remaining product eluted when the column was stripped with EDTA. Fig. 2A illustrates that impurities were present in all imidazole elution and EDTA fractions when the column was primed with Ni^{2+}. There was also visible leaching of Ni^{2+} on imidazole elution reflecting the weak binding affinity of Ni^{2+} to the column. In contrast, when the column was primed with Zn^{2+} the imidazole gradient was more effective in producing pure product (Fig. 2B) than when Ni^{2+} was used. However the 80–120 mM imidazole and EDTA fractions contained some remaining impurities (Fig. 2B a–d). The best elution profile was produced by priming the column with Cu^{2+} ions, pure product eluted at 60–120 mM imidazole and EDTA fractions (Fig. 2C a–e). Although pure product also eluted in the EDTA fraction this could not be further processed for clinical use due to the presence of high levels of copper ions which were difficult to remove even after extensive dialysis. This fraction was dialysed and reapplied to the column. Considering these results, copper was selected as the immobilised metal ion for clinical production of MFE-23 His. To ease handling large volumes of the clinical batch a step gradient of 40 and 120 mM imidazole concentrations was employed as illustrated in Fig. 3. Impurities were separated by eluting with 250 ml 40 mM imidazole (b) from pure product at 120 mM imidazole (250 ml) (c) in a single chromatographic step.

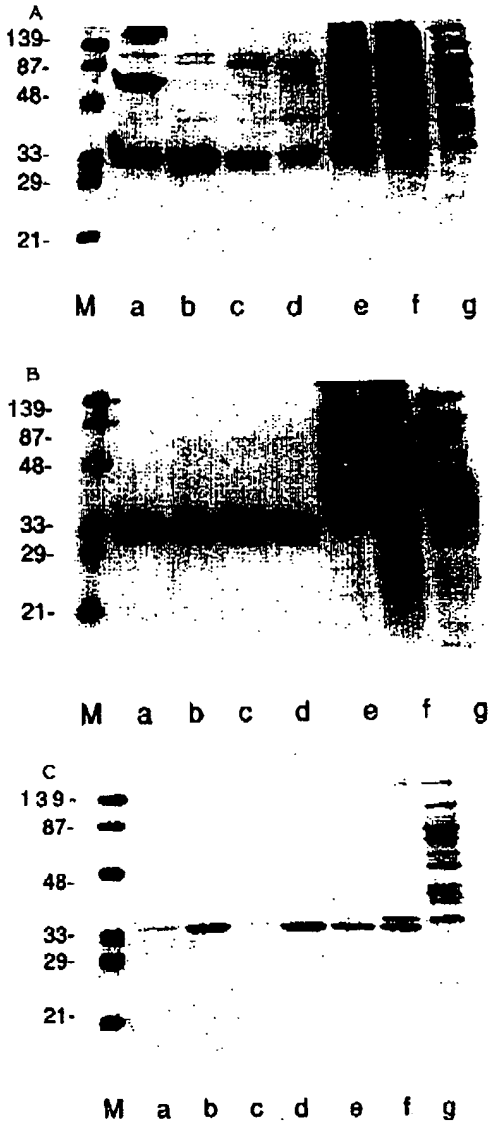

Fig. 2. SDS PAGE analysis of (*A*) Ni^{2+}, (*B*) Zn^{2+} and (*C*) Cu^{2+} primed IMAC column fractions. (a) EDTA fraction; (b) 120 mM imidazole fraction; (c) 100 mM imidazole fraction; (d) 80 mM imidazole fraction; (e) 60 mM imidazole fraction; (f) 40 mM imidazole fraction; (g) unbound wash through. M = low molecular weight markers (Bio-Rad). Gels were stained with coomassie brilliant blue R250.

3.2. Purity and yield

Gel filtration of the clinical grade MFE-23 His revealed that 90% of the product was in monomer form after one purification step. Large molecular

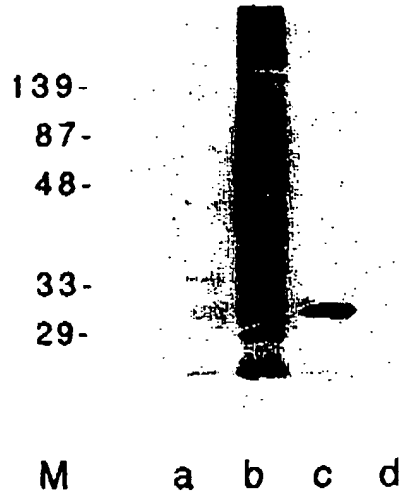

Fig. 3. SDS PAGE analysis of optimised Cu^{2+} chelate column fractions. a: unbound wash through; b: 40 mM imidazole fraction; c: 120 mM imidazole fraction; d: EDTA fraction. M = low molecular weight markers.

weight material was effectively separated from the product shown in Fig. 4. The final product yield of the clinical batch was approximately 10 mg/l of supernatant at $OD_{280\ nm}$ using the extinction coefficient of 0.7. The affinity purified material produced a 2.2 mg/l yield with a single pass through the column.

3.3. Final product evaluation

The contamination levels of clinical grade MFE-23 His with bacterial endotoxins and copper at each chromatographic step are shown in Table 1. The results showed that Detoxi gel was effective in removing at least one log scale of bacterial endotoxins from the purified scFv with no decrease in yield. The final product was also confirmed as non pyrogenic by in vivo rabbit testing. The extent of ligand leaching was also monitored by Cu^{2+} analysis. Copper levels were largely reduced after extensively dialysing and very low levels are present in the final product. DNA was not detected (sensitivity of assay = 12 pg) in the final purified product. Protein sequencing of the first 15 N-terminal amino acids of the protein showed consistency with the DNA sequence. This also confirms that the pel B leader has been cleaved in the periplasm. Stability assessments at 4°C and −70°C up to 6 months showed one peak on FPLC analysis consistent with the molecular weight of scFv and no evi-

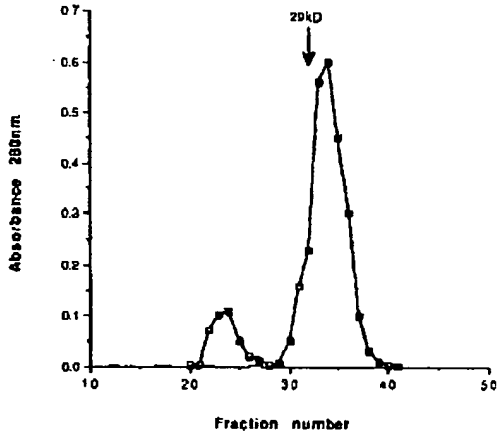

Fig. 4. Gel filtration elution profile for MFE-23 His on S-100. The smaller peak consists of large molecular weight material which can be separated from MFE-23 His at 27 kDa. The column has been calibrated with the molecular weight marker carbonic anhydrase 29 kDa.

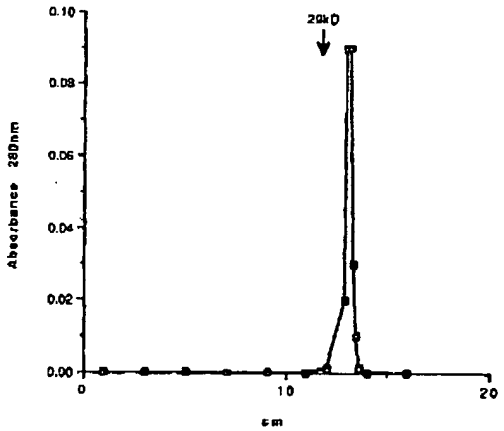

Fig. 5. Superose 12 HR 10/30 trace of MFE-23 His stored at −70°C for 6 months. A single peak at 13.3 cm is consistent with the molecular weight of scFv at 27 kDa. The column has been calibrated with the molecular weight marker carbonic anhydrase 29 kDa.

dence of aggregation. Fig. 5 illustrates the trace for 6 months storage at −70°C. Retention of antigen binding on 6 months storage at 4°C is shown in Table 2. This indicates that an average value of 75% binding was achieved.

3.4. Radiolabelled MFE-23 His

When the radiolabelled product was tested for % incorporation using TLC analysis the results demonstrated that 95–99% of the iodine-125 was bound to the antibody. Retention of antigen binding was assessed after radiolabelling by measuring the binding to antigen. A sample of radiolabelled clinical MFE-23 His batch was applied to the CEA column. Of the total number of counts recovered (1710 cpm), 435 cpm (25%) washed through in the unbound fraction and 1275 cpm (75%) eluted in the bound fraction. The unbound fraction was subsequently reapplied to the column and a further 58% of total counts loaded was recovered in the bound fraction. Samples of diluted radiolabelled MFE-23 *myc* and B1.8 were also applied to the CEA column. For MFE-23 *myc* 56% (23023 cpm) of total counts recovered (40901 cpm) bound to the column and 17878 cpm (43%) washed through in the unbound. For the non-specific control antibody B1.8 only 10% (1301 cpm) of the total recovered counts (12717 cpm) bound to the column and 89% (11416 cpm) was contained in the unbound fraction. Figs. 6 and 7 illustrate the stability of radiolabelled product by SDS PAGE and gel filtration, revealing that it was monomeric, intact and unaggregated.

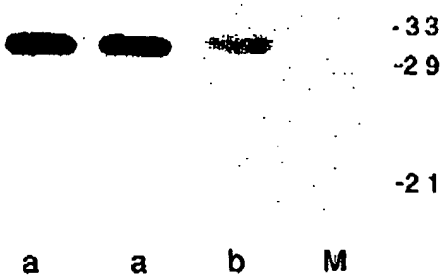

Fig. 6. SDS PAGE gel (15%) analysis of (a) iodinated MFE-23 His, autoradiograph; (b) unlabelled MFE-23 His, Immunoblot. M = molecular weight markers (Bio-Rad).

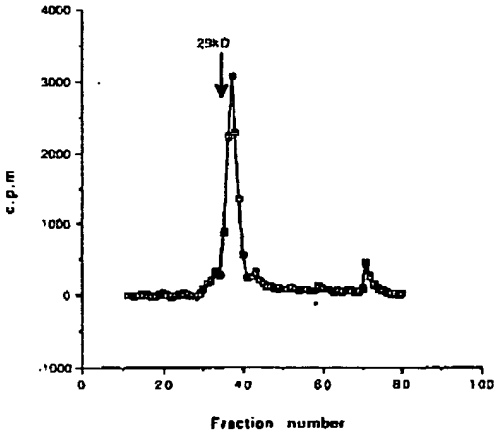

Fig. 7. S-100 gel filtration profile of radiolabelled MFE-23 His. The smaller peak consists of free iodine and the larger peak of labelled product. c.p.m. = counts per minute of ^{125}I.

3.5. In vivo studies

^{125}I-MFE-23 His localised in tumour selectively giving a therapeutic tumour to blood ratio of 22:1 (Fig. 8). MFE-23 *myc* produced similar results with a tumour to blood ratio of 9:1. The

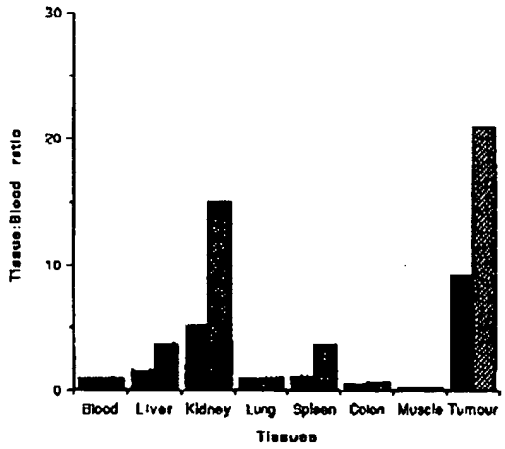

Fig. 8. Biodistribution of ^{125}I-MFE-23 myc (black) and ^{125}I-MFE-23 His (hatched) 24 h after injection, expressed as tissue: blood ratios.

uptake of MFE-23 His in normal tissues was also comparable to the previously characterised MFE-23 *myc*, except for high levels in the kidney, which is the main clearance pathway of the antibody.

4. Discussion

This paper describes in detail the procedure used to process and purify a phage derived scFv containing a 6 × His tail. This purification system eliminates the harsh conditions required to elute antibody from antigen affinity columns. IMAC's mild elution conditions and ease of regeneration make this system an attractive alternative to standard affinity chromatography methods and already a large number of recombinant proteins have been purified using this method (Linder et al., 1992). The good yields achieved with MFE-23 His purification eliminated the need to carry out periplasmic extraction. The latter is known to release proteolytic enzymes which makes the purification and removal of contaminants more difficult. The yields were also superior (10 mg/l) to those achieved when MFE-23 His was purified using a CEA antigen affinity column (2.2 mg/l). However, since only one column pass was performed through the CEA antigen column, the yield would be expected to be higher if the unbound fraction was re-applied to the column. A larger antigen column would also produce higher yields.

The overall effectiveness of IMAC relies on: (1) the affinity of metal ions for the resin and (2) the ability to permit reversible interactions between immobilised metal ions and protein. The relative metal ion capacity for the IDA resin follows the order $Cu^{2+} > Ni^{2+} > Zn^{2+}$ (Porath et al., 1975). Metals will coordinate 4–6 ligands. IDA has 3 chelating sites (QIA express, 1992), the His tagged protein binds to remaining coordination sites unoccupied by the metal ions to form a complex between the chelate with its bound metal ion and the protein. The high stability of copper ions for the IDA matrix contributes to the strength of MFE-23 His retention. This is reflected by the purity and high concentration of imidazole required to elute the product, compared to Ni^{2+} and Zn^{2+} primed columns.

Recent advances include the development of a new NTA adsorbent which has four chelating sites for Ni^{2+} with greater stability and affinity ($K_d = 10^{-13}$) than IDA resins (Hochuli et al., 1987). It has a particulary strong affinity for neighbouring histidine residues with minimal metal ion leaching. This new chelating ligand may produce even better yields of MFE-23 His.

An essential feature in the purification of antibodies to clinical grade, is the removal of pyrogenic contaminants (Begent et al., 1993; Hochstein, 1987). Endotoxin contamination is a recurrent problem in the preparation of therapeutic agents for parenteral use in humans. Detoxi gel (polymyxin crosslinked to 6% agarose) proved to be successful in removing sufficient quantities of the lipopolysaccaride component of gram negative bacterial cell walls (endotoxins) to within regulatory acceptable levels with no detrimental effects on the antibody. Another possible major contaminant is bacterial DNA. As there were no detectable levels in the final product there was no requirement for any additional purification. Takacs and Girard (1991) designed a dot blot analysis to quantitate *E. coli* protein levels by overlaying with an anti-*E. coli* antiserum obtained from immunising rabbits. This semi-quantitative technique would be a useful approach to measure effective removal of host proteins in clinical grade material at each chromatographic stage. It is also important to establish levels of affinity ligand leaching. The levels of Cu^{2+}, < 2 nM per patient dose, were well below the recommended level given routinely in intravenous nutrition (5–10 μM/day). The histidine tail and the purification process did not appear to interfere with the avidity of the antibody.

The specific activity or % binding to antigen of IMAC and CEA antigen purified material were also asssessed in this study. Good retention of antigen binding on storage has been achieved. This assessment also revealed the efficiency of the column for antibody which has previously been purified using the same column. By re-applying a small aliquot of the CEA purified material to the column one would expect 100% to

bind. However, only 89% binding was acheived, (overloading of the column was eliminated due to the small amount loaded and larger amounts of antibody have been purified on one column pass using the same column). If we now take into consideration the efficiency of the column, the % binding to antigen of MFE-23 His purified using IMAC increases from 75% to 84% ($\frac{75}{89} \times 100$). CEA antigen binding of His and c-*myc* scFvs was also maintained after radiolabelling compared to the control scFv. CEA binding of antibody preparations was found to be dependent on the total number of counts loaded. A larger dilution factor (lower number of counts) produced a relatively higher % of counts bound, approximately a 40 fold higher level of the *myc* tagged antibody was applied to the column, of which 56% of the total recovered counts eluted in the bound fraction compared to 75% of recovered counts for the His tagged product. The CEA column (1 ml) containing 1 mg of antigen was obviously saturated by the dilution factor of antibody used here. This was demonstrated by re-applying the unbound fraction of the MFE-23 His sample and measuring the % bound (refer to section 3.4). However, it was clearly shown in the results that the non specific antibody B1.8 did not bind to CEA and the clinical material maintained > 75% binding to antigen after radiolabelling. The data descibed here demonstrates no adverse effects of IMAC purified MFE-23 His binding to antigen on storage and radiolabelling; therefore, no attempt was made to remove the Histidine tag after purification, although this is possible using enzymatic or chemical methods (Hochuli et al., 1988).

In vivo distribution data revealed on average slightly improved localisation in nude mice human tumour xenografts of the His tagged product. Although it appears that there are higher levels of MFE-23 His in the tumour, the ratios depended on the average % injected dose per gram (%ID/g) measured. At this time point (24 h post injection), tumour levels were variable in each individual mouse: MFE-23 *myc* range 0.87–3.3%, $n = 4$, SD = 1.32 and for MFE-23 His range 0.5–2.98%, $n = 4$, SD = 1.35. However, overall the tumour %ID/g ranges were comparable for both products. There were no adverse effects which altered the biodistribution to normal tissues and therefore we can conclude that the histidine tail does not adversely affect the biodistribution in the nude mouse model.

The major drawback to the therapeutic use of scFvs is retention by the kidney (Huston et al., 1993). This is partly due to dehalogenation of iodine from the antibody and also because of the small size (27 kDa) which is below the threshold of 50 kDa for renal clearance. This is also a common finding with most, if not all single-chain antibodies. However, biodistribution data shows only 0.7%ID remains in the kidney 48 h post injection (data not shown) due to rapid clearance of the antibody. This rapid clearance makes MFE-23 His an attractive imaging agent.

Recent experiments have been performed using scFv labelled with iodine-123 which has a half life of 12.3 h and is suitable as an imaging agent. Characterisation of ^{123}I-MFE-23-His proved to be consistent in the data described here and a patient imaging trial is now in progress.

In conclusion, we have developed a potentially universal method for purifying recombinant phage antibodies for therapeutic use which complies with the safety data legislation regarding antibody purity as required by the Cancer Reasearch Campaign Phase I Trials Committee.

Acknowledgements

The authors whould like to thank Dr. R.B. Pedley, J.A. Boden and R. Boden for carrying out the in vivo experiments, Dr. B. Coles for protein sequencing and Dr M.J. Verhaar for technical assistance. This work is supported by the Cancer Research Campaign.

References

Arnold, F.H. (1991) Metal-affinity separations: A new dimension in protein processing. Bio/Technology 9, 151.

Begent, R.H.J. and Pedley, R.B. (1990) Antibody targeted therapy in cancer: comparison of murine and clinical studies. Cancer Treatment Rev. 17, 373.

Begent, R.H.J., Lederman, J.A., Green, A.J., Bagshawe, K.D., Riggs, S.J., Searle, F., Keep, P.A., Adam, T., Dale, R.G.

and Glaser, M.G. (1989) Antibody distribution and dosimetry in patients receiving radiolabelled antibody therapy for colorectal cancer. Br. J. Cancer 60, 406.

Begent, R.H.J., Chester, K.A., Connors, T., Crowther, D., Fox, B., Griffiths, E., Hince, T.A., Lederman, J.A., McVie, J.G., Minor, P., Secher, D.S., Schwartsmann, G., Thorpe, R., Wilbin, C. and Zwierzina, H. (1993) Cancer Research Campaign Operation Manual for control recommendations for products derived from recombinant DNA technology prepared for investigational administration to patients with cancer in phase I trials. Eur. J. Cancer 29A, 1907.

Boxer, G.M., Begent, R.H.J., Kelly, A.M., Southall, P.J., Blair, S.B., Theodorou, N.A., Dawson, P.M. and Lederman, J.A. (1992) Factors influencing variability of localisation of antibodies to CEA in patients with colorectal carcinoma: implications to radioimmunotherapy. Br. J. Cancer 65, 825.

Chester, K.A., Robson, L., Keep, P.A., Pedley, R.B., Boden, J.A., Boxer, G.M., Hawkins, R.E. and Begent, R.H.J. (1994a) Production and tumour binding characterisation of a chimeric anti-CEA fab expressed in Escherichia coli. Int. J. Cancer 57, 67.

Chester, K.A., Begent, R.H.J., Robson, L., Keep, P.A., Pedley, R.B., Boden, J.A., Boxer, G.M., Green, A., Winter, G., Cochet, O. and Hawkins, R.E. (1994b) Phage libraries for generation of clinically useful antibodies. Lancet 343, 455.

Greenwood, F.C. and Hunter, W.M. (1963) The preparation of ^{131}I-labelled human growth hormone of high specific radioactivity. Biochem. J. 89, 114.

Hawkins, R.E., Russell, S.J. and Winter, G. (1992) Selection of phage antibodies by binding affinity : mimicing affinity maturation. J. Mol. Biol. 226, 889.

Hawkins, R.E., Zhu, D., Ovecka, M., Winter, G., Hamblin, T.J., Long, A. and Stevenson., F. K. (1994) Idiotypic vaccination against human B-cell lymphoma. Rescue of variable region gene sequences from biopsy material for assembly as single-chain Fv personal vaccines. Blood 83, 3279.

Hemdam, E.S., Zhao, Y.J., Sulkowski, E. and Porath, J. (1989) Surface topography of histidine residues: A facile probe by immobilised metal ion affinity chromatography. Proc. Natl. Acad. Sci. USA 86, 1811.

Hochstein, H.D., (1987) The LAL test versus the rabbit pyrogen test for endotoxin detection. PharmTechnol. June, 124.

Hochuli, E. (1988) Large scale chromatography of recombinant proteins. J. Chromatogr. 444, 293.

Hochuli, E., Dobeli, H. and Schacher, A. (1987) New metal chelate absorbent for proteins and peptides containing neighbouring histidine residues. J. Chromatogr. 411, 177.

Hochuli, E., Bannwarth, W., Dobeli, H., Gentz, R. and Stuber, D. (1988) Genetic approach to facilitate purification of recombinant proteins with a novel metal chelate absorbent. Bio/Technology 6, 1321.

Huston, J.S., McCartney, J., Tai, M.S., Mottola-Hartshorn, C., Jin, D., Warren, F., Keck, P. and Oppermann, H. (1993) Medical applications of single-chain antibodies. Int. Rev. Immunol. 10, 195.

Itami, T., Ema, M., Sakamoto, J. and Kawasaki, H. (1987) Microheterogeneity of rat alpha fetoprotein on a copper chelate column. J. Chromatogr. 417, 168.

Keep, P.A., Leake, B.A. and Rogers, G.T. (1978) Extraction of CEA from tumour tissue, foetal colon and patients sera, and the effect of perchloric acid. Br. J. Cancer 37, 171.

Lederman, J.A., Begent, R.H.J., Bagshawe, K.D., Riggs, S.J., Searle, F., Glaser, M.G., Green, A.J. and Dale, R.G. (1988) Repeated antitumour antibody therapy in man with suppression of the host response by cyclosporin A. Br. J. Cancer 58, 654.

Linder, P., Guth, B., Wulfgang, C., Krebber, C., Steipe, B., Muller, F. and Pluckthun, A. (1992) Purification of native proteins from the cytoplasm and periplasm of Escherichia coli using IMAC and histidine tails: A comparison of proteins and protocols. Methods: A companion to Methods Enzymol. 4, 41.

Nag, B., Mukku, P.V., Arinulli, S., Kendric, T., Deshpande, S.V. and Sharma, S.D. (1994) Separation of complexes of major histocompatibility class II molecules and known antigenic peptide by metal chelate affinity chromatography. J. Immunol. Methods 142, 105.

Narayanan, S.R. (1994) Preparative affinity chromatography of proteins. J. Chromatogr. 658, 237.

Pluckthun, A. (1990) Antibodies from *Escherichia coli*. Nature 347, 497.

Porath, J., Carlsson, J., Olsson, I. and Belfrage, G. (1975) Metal chelate affinity chromatography, a new approach to protein fractionation. Nature 258, 598.

QIA express (1992) Information booklet. Qiagen, Hilden, Germany.

Skerra, A., Pfitzinger, I. and Pluckthun, A. (1991) The functional expression of antibody Fv fragments in *Escherichia coli*: Improved vectors and a generally applicable purification technique. Bio/Technology 9, 273.

Sulkowski, E. (1985) Purification of proteins by IMAC. Trends Biotechnol. 3, 1.

Takacs, B.J. and Girard, M.F. (1991) Preparation of clinical grade proteins produced by recombinant DNA technologies. J. Chromatogr. 143, 231.

Yip, T.T., Nakagawa, Y. and Porath, Y. (1989) Evaluation of the interaction of peptides with Cu(II), Ni(II) and Zn(II) by high performance immobilised metal ion affinity chromatography. Anal. Biochem. 168, 75.

Yokota, T. Milenic, D.E., Whitlow, M. and Schlom, J. (1992) Rapid tumour penetration of single-chain Fv and comparison with other immunoglobulin forms. Cancer Res. 52, 3402.

YEAST VOL. 10: 441–449 (1994)

Vectors for Cu^{2+}-inducible Production of Glutathione *S*-Transferase-Fusion Proteins for Single-step Purification from Yeast

ALISTER C. WARD*†, LAURA A. CASTELLI*, IAN G. MACREADIE* AND AHMED A. AZAD*

**Biomolecular Research Institute, 343 Royal Parade, Parkville, Victoria 3052, Australia*
†*Russell Grimwade School of Biochemistry, University of Melbourne, Parkville, Victoria 3052, Australia*

Received 29 June 1993; accepted 14 October 1993

We describe six new yeast episomal vectors which encode glutathione *S*-transferase (GST) affinity tags. These allow for the production of GST-fusion proteins in *Saccharomyces cerevisiae* under the control of the *CUP1* promoter. Affinity chromatography with glutathione–Sepharose permits convenient purification of the fusion protein from a yeast lysate. The presence of a protease cleavage site facilitates subsequent removal of the GST tag. The expression and single-step purification of both GST and a functional GST–metallothionein fusion from yeast are shown as an example of the application of these vectors.

KEY WORDS — *Saccharomyces cerevisiae*; *CUP1*; Cu^{2+}-regulated; yeast expression; affinity purification; glutathione *S*-transferase; metallothionein.

INTRODUCTION

Protein purification from cell lysates can be greatly enhanced by the addition of affinity tags. Smith and Johnson (1988) have previously engineered the gene encoding glutathione *S*-transferase (GST) from *Schistosoma japonicum* as a tag for recombinant proteins expressed in *Escherichia coli*. The pGEX vectors which they developed also carry sequences encoding a protease recognition site located between the GST and a multiple cloning site (MCS). Fusion proteins can be rapidly affinity-purified using immobilized glutathione, and the protein of interest can be subsequently cleaved from the GST using a specific protease, thrombin or Factor Xa.

The pYEULC series of vectors have been used for the production of foreign proteins in the yeast *S. cerevisiae* (Macreadie *et al.*, 1991, 1992, 1993). The presence of the *CUP1* cassette in these plasmids allows Cu^{2+}-regulated expression of foreign proteins, while the 2 μm origin of replication gives medium to high copy number in yeast. Two selectable markers, *URA3* and *leu2-d* (Macreadie *et al.*, 1991), provide flexible strain selection. However, these vectors do not allow easy purification of recombinant proteins. We report here the construction of expression vectors which direct synthesis of recombinant GST-fusion proteins in *S. cerevisiae* from a pYEULC-based plasmid. These combine the advantages of the pYEULC series of vectors with the purification capabilities of the pGEX vectors and provide a convenient alternative for large-scale protein production.

Address correspondence to: Alister C. Ward, Biomolecular Research Institute, 343 Royal Parade, Parkville, Victoria 3052, Australia.

CCC 0749–503X/94/040441–09

MATERIALS AND METHODS

Cloning of GST for expression in yeast

Sequences encoding GST, the protease recognition site and the MCS were obtained from plasmids pGEX-2T and pGEX-3X (Smith and Johnson, 1988) using the polymerase chain reaction (PCR), with the oligonucleotide pair W104 [5′ GTGAGATCT*ATG*ACCAAGTTACCTATAC] and W105 [5′ CAGTCAGTCACGATGAATTCC], and a GeneAmp kit (Perkin Elmer-Cetus). The *Bgl*II and *Eco*RI sites used for cloning are underlined on the respective primer sequence, while the GST start codon is italicized. Standard PCR protocols were employed (Erlich, 1989),

REF. 17

using the following conditions: 94°C/1 min, 47°C/2 min, 72°C/2·5 min for three cycles; 94°C/1 min, 55°C/1 min, 72°C/2·5 min for 28 cycles; 72°C/10 min. The products were purified using GeneClean [Bio101], cleaved with *Bgl*II and *Eco*RI and cloned into the *Bam*HI-*Eco*RI sites of pYEULCBX (Macreadie *et al.*, 1993) to produce pYEULCGT and pYEULCGX respectively (Figure 1). During the construction of pYEULCGT, a plasmid clone was isolated which contained a deletion of the thrombin cleavage site. This plasmid was designated pYEULCGN.

To introduce an amino acid linker after the thrombin cleavage site in pYEULCGT, the oligonucleotides T1 [5′ GATCTGGTTCCGCGTG] and T2 [5′ GATCCACGCGGAACCA] were annealed and inserted into the *Bam*HI site. A clone was identified with the insert orientated with a *Bam*HI site at the 3′ end of insertion—this plasmid was called pYEULCGL. The *Hin*dIII-*Bam*HI fragments of pYEULCGT and pYEULCGL were then cloned into pYEULCBX to yield pYEULCGS and pYEULCGK respectively.

The *E. coli* strain MC1066, genotype Δ(*lacI-POZYA*) *leuB6 trpC9830 pyrF74*::Tn(Km^r) (Casadaban *et al.*, 1983) was utilized for the maintenance and construction of shuttle plasmids. All constructs were confirmed by nucleotide sequence analysis. The complete nucleotide sequence of plasmid pYEULCGT (7805 bp) has been deposited at GenBank (accession no. L19873).

Yeast transformations

S. cerevisiae strains DY150 (*MAT***a** *ura3-52 leu 2-3, 112 trp1-1 ade2-1 his 3-11 can 1-100*) and BZ31-1-7Ba (*MAT***a** *ura3-52 ade8-18 trp1-289 arg4-16 cup1*^{s}) were used as host strains for these studies. Yeast were transformed by electroporation (Becker and Guarente, 1991). Transformants were initially selected on synthetic minimal medium (0·67% Difco yeast nitrogen base without amino acids, 2% dextrose), containing all required supplements except uracil, solidified with 1·5% agar. In subsequent culturing of transformants both leucine and uracil were omitted. Yeast transformants were authenticated by back-transformation of their plasmid DNA into *E. coli* (Ward, 1990) and subsequent molecular analysis.

Copper-inducible expression of GST and GST-fusions in yeast

For induced expression of GST and GST-fusions yeast transformants were grown for 18 h in minimal synthetic medium containing histidine, adenine and tryptophan (20 μg/ml). The cells were then pelletted (3000 *g*, 5 min), resuspended in the same medium and grown for a further 2 h to restore log phase growth. Expression was induced by the addition of $CuSO_4$ to 0·5 mM and the cultures were maintained for 2 h before harvest (3000 *g*, 5 min).

Single-step affinity purification of GST and GST–metallothionein (MT)

Cells were disrupted using a Braun-MSK homogenizer with 0·45–0·50 mm glass beads as described (Macreadie *et al.*, 1993), spun at 3000 *g* for 5 min to remove the beads and unbroken cells and the supernatant further fractionated by centrifugation at 12 000 *g* for 15 min. The 12 000 *g* supernatant was applied to glutathione–Sepharose and affinity purification performed as previously described (Smith and Johnson, 1988), except standard phosphate-buffered saline (PBS) was used instead of mouse tonicity-PBS and all solutions contained 1 mM-dithiothreitol to decrease aggregation.

Protein analysis and Western blotting

Cell fractions were run on sodium dodecyl sulphate–10–20% polyacrylamide gels (SDS–PAGE; Laemmli, 1970; Novex), which were either stained with Coomassie Brilliant Blue or electrophoretically transferred to nitrocellulose (Towbin *et al.*, 1979). Western blots were probed with either rabbit anti-GST antisera, previously pre-absorbed with an acetone powder (Harlow and Lane, 1988) derived from DY150 [pYEULCBX], or with unadsorbed rabbit anti-MT. Antibody-bound protein was visualized by the use of alkaline phosphatase-conjugated goat anti-rabbit Ig antibody (BioRad), and subsequent development as described by the manufacturer.

Analysis of copper ion resistance

Minimal synthetic medium as described above but solidified with 2% Phytagar (Gibco-BRL) was used for the analysis of copper resistance. Cells, previously grown in the absence of copper ions were pipetted onto plates containing a series of copper ion concentrations. Growth was scored after 4–5 days at 30°C.

Copper analysis

The copper content of affinity-purified protein was determined using a Perkin-Elmer absorption

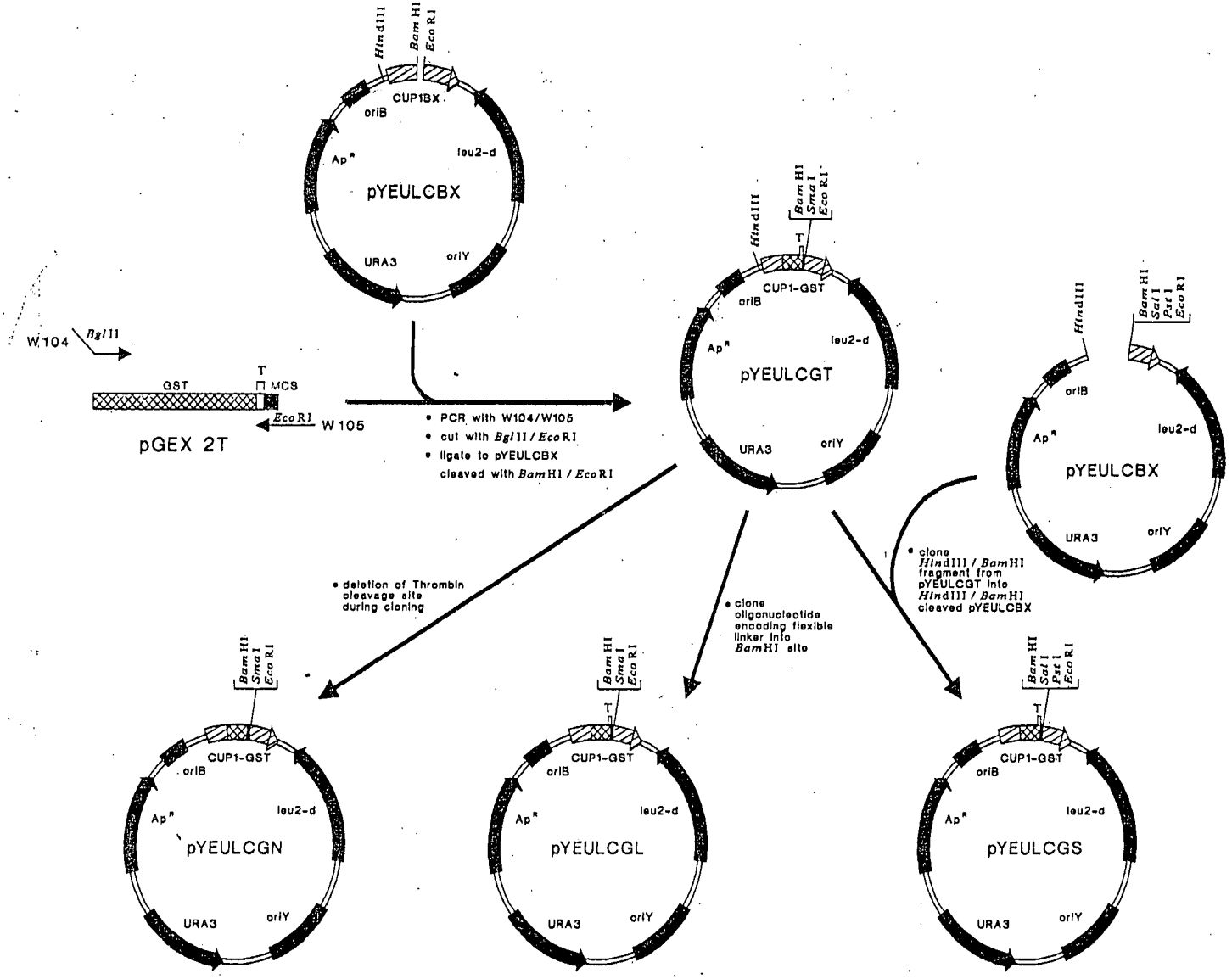

Figure 1. Construction of the pYEULCG series of GST-fusion vectors. Relevant unique restriction sites are shown. Bacterial and yeast origins of replication are denoted as *oriB* and *oriY* respectively. Selection of plasmids in *E. coli* is mediated by the β-lactamase gene (Ap^R), while in yeast selection is achieved using either *URA3* or *leu-2d*. *CUP1* (denoted with a single hatch) contains promoter elements for Cu^{2+}-regulated expression while GST (shown with a cross hatch) encodes glutathione *S*-transferase. Sequences encoding GST and thrombin cleavage site (T) and including the multiple cloning site were amplified by PCR from pGEX-2T and inserted into pYEULCBX to create pYEULCGT. The same strategy was used with pGEX-3X to construct pYEULCGX (not shown). A deletion event during cloning produced pYEULCGN. Cloning of oligonucleotides encoding an amino acid linker into the *Bam*HI site of pYEULCGT yielded pYEULCGL. Finally the *Hin*dIII-*Bam*HI fragment from pYEULCGT replaced the equivalent fragment in pYEULCBX to give pYEULCGS. Plasmid pYEULCGK was produced using the same approach with the *Hin*dIII-*Bam*HI fragment from pYEULCGX (not shown).

spectrophotometer at the University of Utah Medical Center.

RESULTS

Construction of the pYEULCG vectors

Sequences encoding GST, a protease cleavage site and MCS from pGEX-2T and pGEX-3X were amplified using PCR and cloned into pYEULCBX (Macreadie *et al.*, 1992) to produce pYEULCGT and pYEULCGX respectively (Figure 1). A deletion of the thrombin cleavage site during cloning yielded the plasmid pYEULCGN. The vectors pYEULCGN, pYEULCGT and pYEULCGX are essentially equivalent to the *E. coli* vectors pGEX-1N, pGEX-2T and pGEX-3X respectively and have the same utility for cloning (Figure 2). This permits identical cloning strategies to be used for producing GST-fusions in both yeast and *E. coli*.

Further variation was made to pYEULCGT by inserting a pair of oligonucleotides encoding an amino acid linker (Gly-Ser-Ala-Cys) between the thrombin cleavage site and the MCS to give the plasmid pYEULCGL (Figure 2). The addition of a linker has been shown to be important in instances where protease cleavage is inefficient (Guan and Dixon, 1991).

Additional derivatives of pYEULCGT and pYEULCGL were constructed by moving the *Hin*dIII-*Bam*HI fragment of each into pYEULCBX, producing pYEULCGS and pYEULCGK. These latter two vectors have identical cloning sites to pYEULCBX thereby assisting the cloning of fragments for production of both non-fused and GST-fused proteins in yeast.

Expression of GST and GST-fusions in S. cerevisiae

The plasmids pYEULCGT and pYEULCGS contain a stop codon immediately after the MCS and so should produce a protein of ca. 26 kDa, comparable to native GST (Smith *et al.*, 1986). However, the reading frames of pYEULCGX, pYEULCGL and pYEULCGK direct production of GST-fusion proteins which are translated for 61 codons past the Ser codon shown in Figure 2, and so encode proteins of ca. 32 kDa, while the pYEULCGN reading frame allows translation of a further 51 amino acids of metallothionein after the Asn residue in Figure 2 to produce a GST–MT fusion protein of 31 kDa.

The pYEULCG vectors and pYEULCBX were transformed into DY150 by electroporation and transformants subjected to Cu^{2+}-induction. Lysates of induced cultures were subjected to SDS–PAGE, transferred to nitrocellulose and probed with anti-GST antisera (data not shown). The anti-GST detected a predominant protein band in each of the pYEULCG transformants whose size varied according to the construct as expected. No reaction was seen in the pYEULCBX transformants.

Affinity-purification of GST-fusions from yeast

In order to examine affinity purification of GST-fusions from yeast, DY150 transformants harboring pYEULCGT and pYEULCGN were induced with Cu^{2+}. Cells were disrupted with glass beads and the 12 000 *g* supernatant was applied to glutathione–Sepharose and washed extensively as described in Materials and Methods. The pooled glutathione-elution and the 12 000 *g* supernatant and pellet were subjected to SDS–PAGE and Western blot analysis. Figure 3 shows that both GST and GST–MT were predominantly in the 12 000 *g* supernatant and so are produced as soluble proteins in yeast. The products eluted from the glutathione–Sepharose can be seen as single bands after Coomassie staining. The corresponding bands on Western blots react with anti-GST, while the GST–MT also reacts with anti-MT. This indicates that not only is this method of affinity purification applicable to yeast, but it has the advantage of high purity after a single chromatography step, unlike equivalent *E. coli* expression where contaminants and breakdown products are a major problem (A.C.W., unpublished observations). The lack of proteolytic cleavage appears to be protein independent and required no addition of protease inhibitors during cell disruption except 1 mM-EDTA and low temperature (data not shown). The effect of yeast strain on this phenomenon was not investigated. Yields of purified fusion protein are of the order 0·5–6·0 mg/l.

Production of functional GST–MT by pYEULCGN

The pYEULCGN vector provides an example of GST fused to MT, a protein that normally functions in copper sequestration and copper resistance in yeast (reviewed in Thiele, 1992). It was of interest, therefore, to examine the properties of the expressed GST–MT fusion protein.

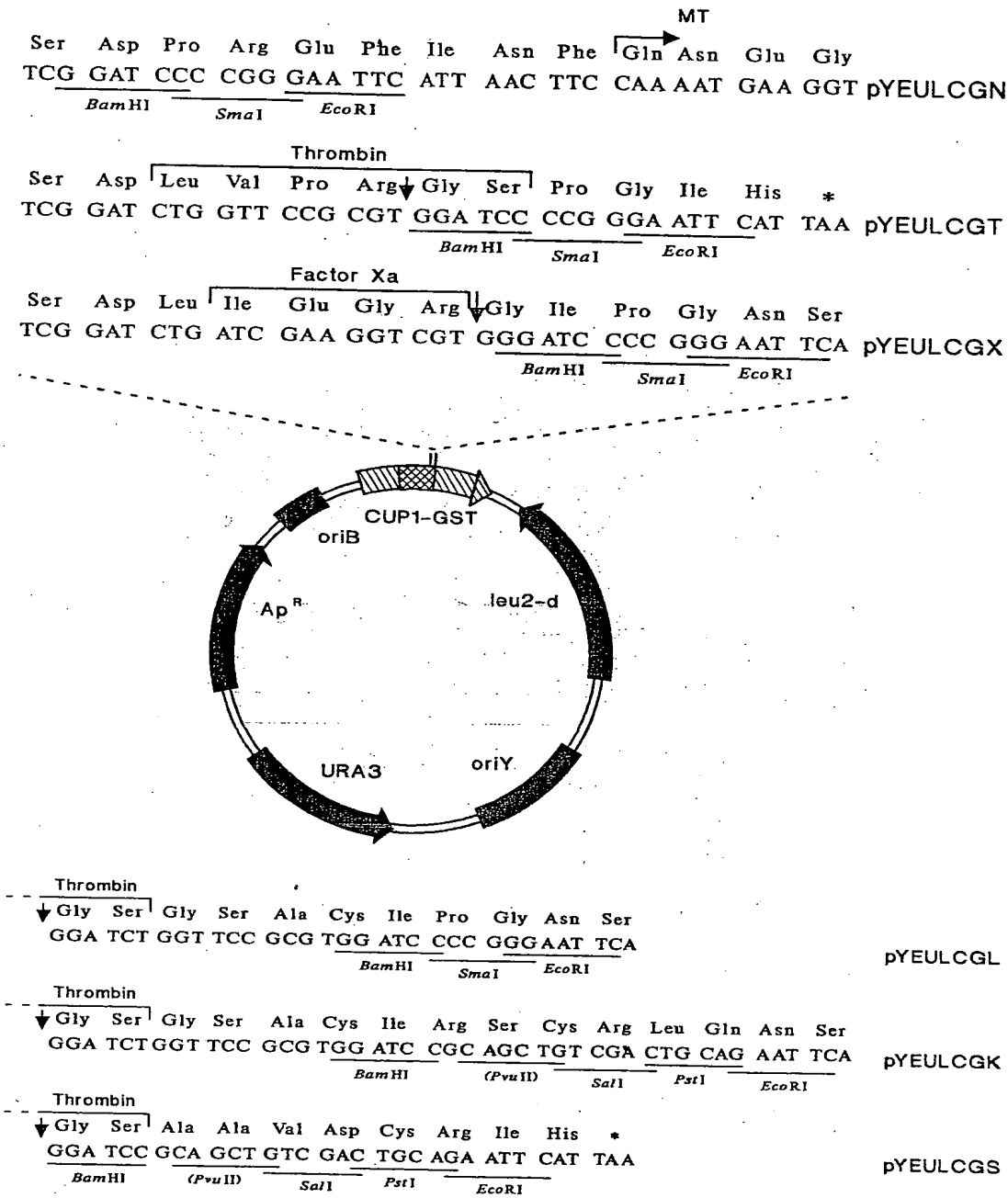

Figure 2. The pYEULCG series of vectors. Nucleotide sequences around the MCS with corresponding translation products are shown. Restriction enzyme sites are shown in italics with non-unique sites in parentheses. Protease recognition sites are bracketted and corresponding cleavage sites are indicated with an arrow; asterisks indicate stop codons. The start of the MT sequence encoded by pYEULCGN is shown.

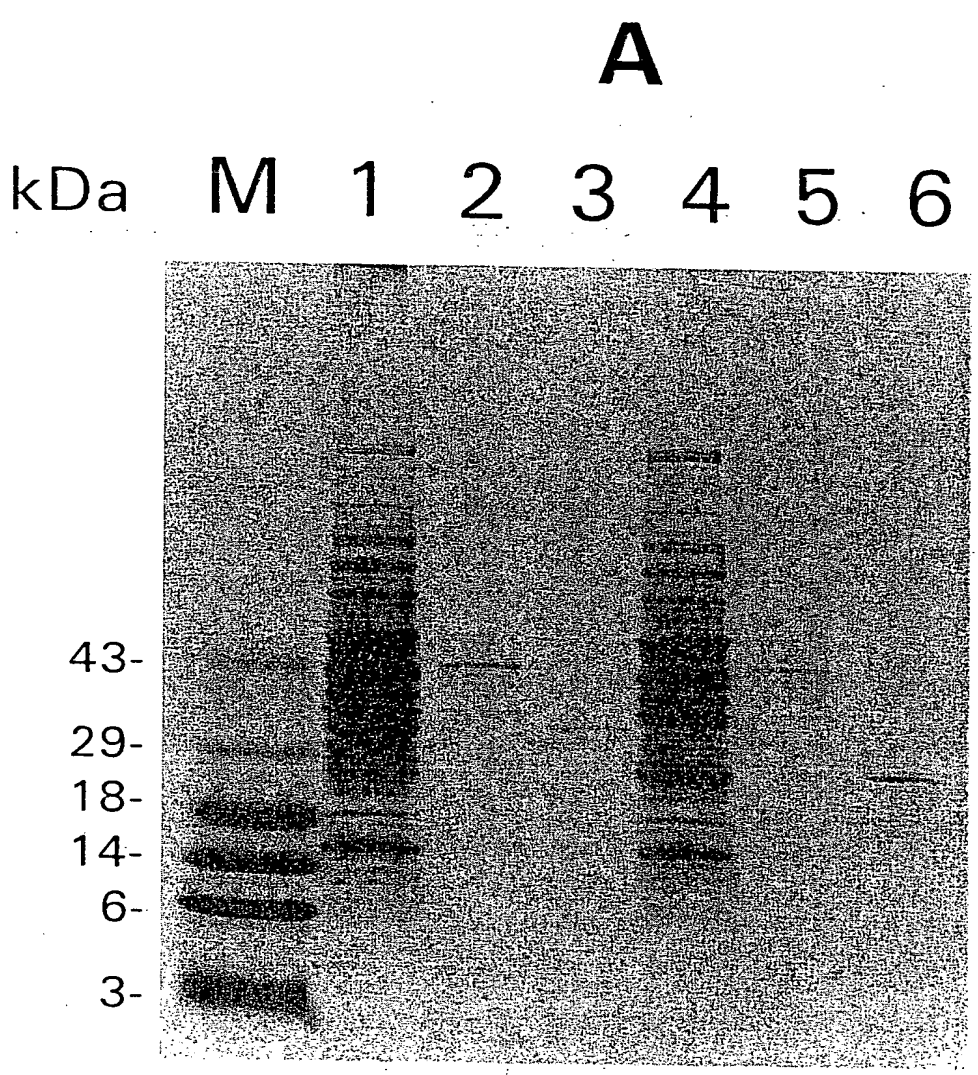

Figure 3(a).

For this study we utilized the strain BZ31-1-7Ba, which is copper sensitive, having only a single copy of the *CUP1* gene. We compared transformants harbouring pYEULCGN with transformants containing pYEULCB (Macreadie *et al.*, 1991), which encodes an active MT with a small N-terminal extension, pYEULCBX (Macreadie *et al.*, 1992), which has the MT start codon mutated so that no MT is produced, pYEULCGT, which encodes GST, and the strain without a plasmid. Table 1 compares the copper-resistance of these strains and shows that the GST–MT encoded by pYEULCGN does confer resistance to copper compared to the non-MT-producing controls. Thus the MT fused to GST is functional at sequestering copper ions, even though the N-terminal GST-fusion is large. It is apparent that there is a slightly lower level of Cu^{2+}-resistance relative to pYEULCB which may be due to steric hindrance or incorrect folding caused by the GST. Alternatively, it may be caused by decreased translational efficiency of the GST–MT fusion, since the MT encoded by pYEULCB uses the native MT start codon, while the GST–MT of pYEULCGN uses

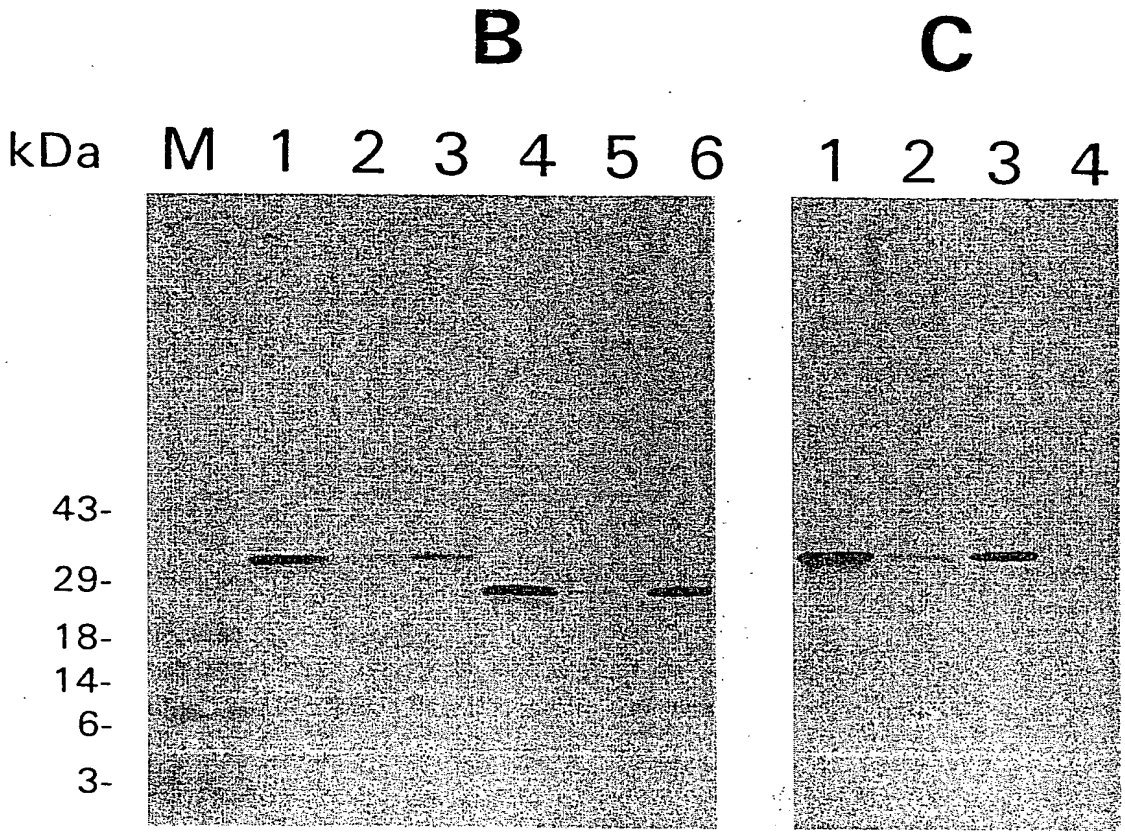

Figure 3(b) and (c).

Figure 3. Single-step purification of GST and GST–MT proteins from yeast using glutathione–Sepharose affinity chromatography as described in Materials and Methods. Equivalent amounts of the 12 000 *g* supernatants and pellets, and a sample of the eluted protein were analysed in triplicate by SDS–PAGE. One gel was stained with Coomassie blue-R250 (A) while the others were blotted to nitrocellulose for probing with rabbit anti-GST (B) or anti-MT (C). Samples are: lane M, molecular weight markers (BRL), lanes 1 and 2, 12 000 *g* supernatant and pellet respectively of induced DY150 (pYEULCGN); lane 3, affinity-purified GST–MT; lanes 4 and 5, 12 000 *g* supernatant and pellet respectively of induced DY150 (pYEULCGT); lane 6, affinity-purified GST.

an introduced ATG downstream of the native start codon, and the MT is a much smaller protein. Other possible influences, such as differences in protein or mRNA turnover rates, cannot be ruled out.

Atomic absorption spectrophotometry on the affinity-purified proteins detected Cu(I) bound to GST–MT (6·4 ± 3·9 Cu/molecule) but not to GST (≤0·2 Cu/molecule). This compares to the 7–8 Cu/molecule estimated to be bound when all sites are occupied on native MT (Winge *et al.*, 1985). This suggests that Cu^{2+}-resistance is due to direct binding of Cu^{2+} to the MT of the GST–MT fusion.

DISCUSSION

We have constructed new *E. coli–S. cerevisiae* shuttle vectors for Cu^{2+}-regulated expression of foreign proteins as GST-fusions to facilitate purification of recombinant proteins by affinity chromatography. The primary vectors, pYEULCGN, pYEULCGT and pYEULCGX, provide equivalent cloning strategies to those for the *E. coli* pGEX counterparts, allowing genes to be conveniently cloned and expressed in parallel in both systems. The vector pYEULCGL offers a further modification for applications where more efficient

Table 1. Growth of *S. cerevisiae* strain BZ31-1-7Ba and transformants on plates containing $CuSO_4$

Plasmid	Plasmid-encoded Cu^{2+}-induced product	Copper concentration (mM) 0·00	0·10	0·20	0·50	1·00	1·50
None	None	++	++	−	−	−	−
pYEULCBX	None	++	++	+/−	−	−	−
pYEULCB	MT	++	++	++	++	+	−
pYEULCGN	GST–MT	++	++	++	+	−	−

− No growth; +/− scanty growth; + partial growth; ++ maximal growth.

cleavage is required. In addition, the vectors pYEULCGS and pYEULCGK provide the same cloning capacity as the pYEULCBX vector, facilitating expression of recombinant proteins in a non-fused or a GST-fused conformation depending on the choice of vector.

We have shown the production of a functional GST–MT fusion as an example of the applications of these plasmids. The GST–MT protein provided protection from Cu^{2+}-toxicity in a sensitive yeast strain, and was shown to bind copper ions. Affinity-chromatography with glutathione–Sepharose has allowed single-step purification of the GST–MT fusion protein. In addition the use of such GST-fusions has wide potential for use in analysing protein–protein interactions both *in vitro* and in the yeast cell environment. These vectors therefore provide an attractive adjunct to the current pYEULC series of vectors and provide an alternative to *E. coli* production of GST-fusions.

After the primary submission of this manuscript, Mitchell *et al.* (1993) published details of two vectors for expression of GST-fusion proteins in yeast. In addition, they showed that one such fusion, GST-Ras2p, undergoes correct post-translational modification, which further increases the attractiveness of using yeast GST-fusions for the expression of eukaryotic proteins. The vectors described in this report, however, present an attractive alterative to those of Mitchell *et al.* (1993), since they are more convenient for cloning, providing all three reading frames for cloning and completely compatible sites to the widely used pGEX vectors. Also, the use of a different promoter offers increased flexibility, for example, in co-expression studies for determining protein–protein interactions.

ACKNOWLEDGEMENTS

A.C.W. acknowledges receipt of an Australian Postgraduate Research Award. We are indebted to Lisa Raschke for synthesis of oligonucleotides, Professor Dennis Winge for the anti-MT antibody and the atomic absorption spectrophotometry data, Kathy Davern for the anti-GST antibody, and Drs Casadaban, Stillman, Welch and Fogel for strains used in this study. We also respectfully thank John Bentley and Dr Paul Vaughan of the CSIRO Division of Biomolecular Engineering for critical reading of the manuscript.

NOTE ADDED IN PROOF

These vectors are available from AMRAD Operations Pty. Ltd., Private Bag 6, Kew, Victoria 3101, Australia (fax +613 853 0607).

REFERENCES

Becker, D. M. and Guarente, L. (1991). High efficiency transformation of yeast by electroporation. *Meth. Enzymol.* **194**, 182–187.

Casadaban, M. J., Martinez-Arias, A., Shapira, S. K. and Chou, J. (1983). β-galactosidase gene fusions for analyzing gene expression in *Escherichia coli* and yeast. *Meth. Enzymol.* **100**, 293–308.

Erlich, H. A. (1989). *PCR Technology; Principles and Applications for DNA Amplification.* Stockton Press, New York.

Guan, K. L. and Dixon, J. E. (1991). Eukaryotic proteins expressed in *Escherichia coli*: an improved thrombin cleavage and purification procedure of fusion proteins with glutathione *S*-transferase. *Anal. Biochem.* **192**, 262–267.

Harlow, E. and Lane, D. (1988). *Antibodies: A Laboratory Manual*. Cold Spring Harbor Laboratory Press, Cold Spring Harbor Laboratory, New York.

Laemmli, U. K. (1970). Cleavage of structural proteins during assembly of the head of bacteriophage T4. *Nature* **227,** 680–685.

Macreadie, I. G., Horaitis, O., Verkuylen, A. J. and Savin, K. W. (1991). Improved shuttle vectors for cloning and high-level Cu^{2+}-mediated expression of foreign proteins in yeast. *Gene* **104,** 107–111.

Macreadie, I. G., Failla, P., Horaitis, O. and Azad, A. A. (1992). Production of HIV-1 Vpu with pYEULCBX, a convenient vector for the production of non-fused proteins in yeast. *Biotechnol. Letts.* **14,** 639–642.

Macreadie, I. G., Ward, A. C., Failla, P., Grgacic, E., McPhee, D. and Azad, A. A. (1993). Expression of HIV-1 *nef* in yeast: The 27 kDa protein is myristylated and fractionates with the nucleus. *Yeast* **9,** 565–573.

Mitchell, D. A., Marshall, T. K. and Deschenes, R. J. (1993). Vectors for the inducible overexpression of glutathione S-transferase fusion proteins in yeast. *Yeast* **9,** 715–723.

Smith, D. B., Davern, K. M., Board, P. G., Tiu, W. U., Garcia, E. G. and Mitchell, G. F. (1986). M_r 26000 antigen of *Schistosoma japonicum* recognised by resistant WEHI 129/J mice is a parasite glutathione *S*-transferase. *Proc. Natl. Acad. Sci. USA* **83,** 8703–8707.

Smith, D. B. and Johnson, K. D. (1988). Single-step purification of polypeptides expressed in *Escherichia coli* as fusions with glutathione *S*-transferase. *Gene* **67,** 31–40.

Thiele, D. J. (1992). Metal-regulated transcription in eukaryotes. *Nucl. Acids. Res.* **20,** 1183–1191.

Towbin, H., Staehelin, T. and Gordon, J. (1979). Electrophoretic transfer of proteins from acrylamide gels to nitrocellulose sheets: procedure and some applications. *Proc. Natl. Acad. Sci. USA* **76,** 4350–4354.

Ward, A. C. (1990). Single-step purification of shuttle vectors from yeast for high frequency back-transformation into *E. coli*. *Nucl. Acids Res.* **18,** 5319.

Winge, D. R., Nielson, R. B., Gray, W. R. and Hamer, D. (1985). Yeast metallothionein: sequence and metal binding properties. *J. Biol. Chem.* **26,** 14461–14470.

Engineered Fv Fragments as a Tool for the One-Step Purification of Integral Multisubunit Membrane Protein Complexes

Gerald Kleymann, Christian Ostermeier, Bernd Ludwig[1], Arne Skerra and Hartmut Michel*

Max-Planck-Institut für Biophysik, Abteilung Molekulare Membranbiologie, Heinrich-Hoffmann-Straße 7, D-60528 Frankfurt, Germany.
[1]Biozentrum N 200, Molekulare Genetik, Marie-Curie-Straße 9, D-60439 Frankfurt. *Corresponding author.

The preparation of pure and homogeneous membrane proteins or membrane protein complexes is time consuming, and the yields are frequently insufficient for structural studies. To circumvent these problems we established an indirect immunoaffinity chromatography method based on engineered Fv fragments. cDNAs encoding the variable domains of hybridoma-derived antibodies raised against various membrane proteins were cloned and expressed in *Escherichia coli*. The Fv fragments were engineered to serve as bifunctional adaptor molecules. The Fv fragment binds to the epitope of the membrane protein, while the *Strep tag* affinity peptide, which was fused to the carboxy-terminus of the V_H chain, immobilizes the antigen-Fv complex on a streptavidin sepharose column. The usefulness of this technique is illustrated with membrane protein complexes from *Paracoccus denitrificans*, namely, the cytochrome c oxidase (EC 1.9.3.1), the ubiquinol:cytochrome c oxidoreductase (EC 1.10.2.2), and subcomplexes or individual subunits thereof. These membrane proteins were purified simply by combining the crude *P. denitrificans* membrane preparation with the *E. coli* periplasmic cell fraction containing the corresponding Fv fragment, followed by solubilization and streptavidin affinity chromatography. Pure and highly active membrane protein complexes were eluted in the Fv-bound form using diaminobiotin for mild competitive displacement of the *Strep tag*. The affinity column could thus be reused under continuous operation for several months. Five to 10 mg of membrane protein complexes could be obtained without any detectable impurities within five hours.

Received 9 September 1994; accepted 24 October 1994.

Membrane protein complexes such as the ubiquinol:cytochrome c oxidoreductase (EC 1.10.2.2, also known as cytochrome bc_1 complex or complex III) and the cytochrome c oxidase (EC 1.9.3.1, also known as cytochrome aa_3 or complex IV) have, until now, been purified using classical biochemical tools like ion-exchange chromatography or molecular sieve chromatography[1-3].

Other membrane proteins are only available in minute quantities from natural sources or even when produced with the help of homologous and heterologous expressions systems[4]. As a consequence, extremely high purification factors are required to obtain a homogeneous protein preparation. Unfortunately, the performance of conventional purification methods on the basis of properties like charge, size, hydrophobicity etc. becomes worse in the presence of detergents. Therefore many scientists favor the use of affinity chromatography based on fusion proteins[5], ligands[6] or antibodies. Numerous proteins have been purified by immunoaffinity chromatography using monoclonal[7,8] or polyclonal[9,10] antibodies. The antibody or its fragments[11] were either covalently coupled to activated matrices[12,13] or trapped by immobilized Protein A[14] or G[14,15]. Immunoglobulins were also chemically activated and crosslinked to solid supports or biotinylated[16] and immobilized on streptavidin matrices[17]. Although immunoaffinity columns[8] usually offer purification factors of 100–10,000, their widespread use is limited by the lack of elution protocols for the recovery of native protein due to the strong interaction between antibody and antigen. Elution of a whole antigen-antibody complex has only been possible in a few cases[13,38]. Bearing in mind the key features of the antibody molecule, namely the combination of antigen specificity with functional coupling to other systems, novel bifunctional Fv adaptor molecule were created.

In this paper, we describe the cloning, production and use of engineered Fv fragments for the one-step immunoaffinity purification of multisubunit integral membrane protein complexes. The concept introduced here is based on the production of functional antibody Fv fragments in *E. coli*[18] (for review see ref. 19) and on the *Strep tag*[20] affinity peptide. We demonstrate the potential of this method for two membrane protein complexes and several subunits or subcomplexes depending on the stability of the membrane protein and the nature of detergent used.

Results

Vector construction for Fv expression. pASK68 (Fig. 1) was designed as a cloning and expression vector for the bacterial production of Fv fragments displaying the *Strep tag*[20] at the C-

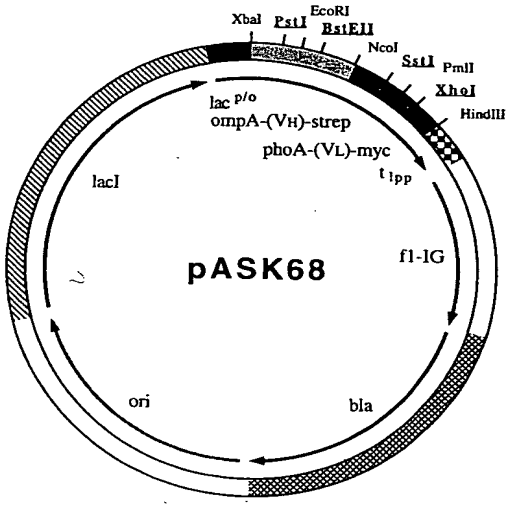

FIGURE 1. Schematic representation of plasmid pASK68, a cloning and expression vector for the bacterial production of Fv fragments. The unique restriction sites used for cloning of the Ig variable domain genes are printed in bold and underlined. See results and Figure 2 for additional details.

REF. 18

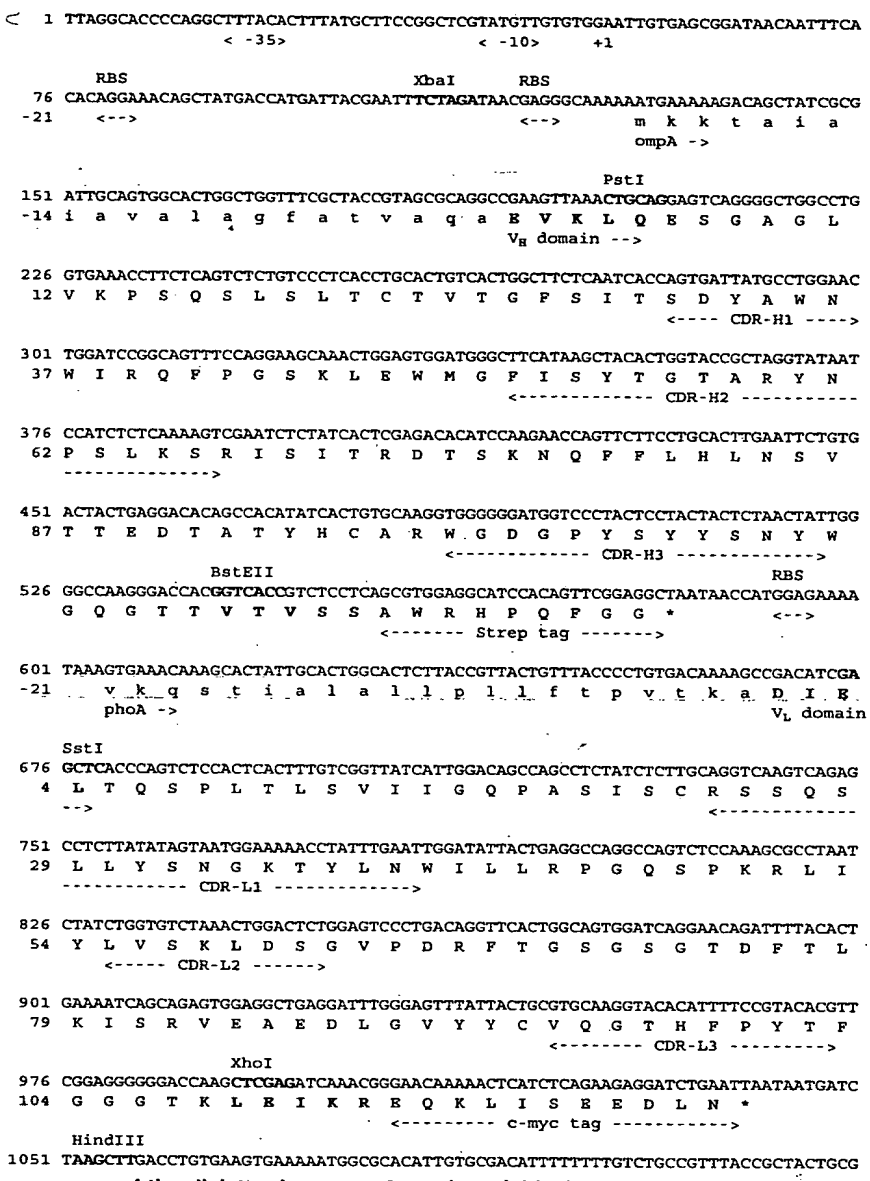

FIGURE 2. Nucleotide sequence of the dicistronic operon for expression of 2D6 Fv fragment in plasmid pASK68. The -10 and -35 consensus sequences of the lac promoter/operator, as well as the transcriptional start point are indicated. The tandem ribosomal binding site (RBS) consists of a short 5′-terminal region from the *lacZ* gene with its RBS, followed by the coding region for the OmpA signal peptide together with its RBS. The Ig variable domain genes (V_H and V_L) of the hybridoma cell line 2D6 were fused in pASK68 via PstI and BstEII restriction sites for V_H and SstI and XhoI for V_L to the signal sequences OmpA and PhoA on their 5′ ends and to the affinity tags *Strep* tag and c-*myc* tag on their 3′sides. The complementary determining region residues according to the hypervariable sequence definition[44] are underlined.

terminus of the V_H domain and the c-*myc* tag[21] at the C-terminus of the V_L domain. pASK68 possesses the regulatory elements of pASK30 (ref. 22) from which it was constructed in several steps via site-directed mutagenesis and PCR following standard methods[23]. The regions encoding the two affinity tags were taken from pASK46-p1II described[20]. Thus pASK68 carries an artificial dicistronic operon for the simultaneous expression of the V_H and V_L chains of the Fv fragment under transcriptional control of the *lac* promoter. Their co-secretion to the periplasm is directed by the bacterial signal sequences of OmpA and PhoA, respectively. Insertion of different variable domain genes is possible via PstI (or NsiI, which yields a compatible sticky end) and BstEII restriction sites for V_H and SstI and XhoI restriction sites for V_L, permitting direct fusion to the signal sequences as well as to the affinity tags (see Fig. 2). In the generic vector pASK68 the variable domain genes were replaced by short cloning sites as described[24].

Cloning and expression of hybridoma-derived antibody V-gene regions. Hybridoma cell lines producing monoclonal antibodies raised against the membrane proteins cytochrome c oxidase and the ubiquinol:cytochrome c oxidoreductase of the bacterium *P. denitrificans* were established according to standard methods[7]. Three hybridoma cell lines were chosen for cloning of the variable regions and production of engineered Fv fragments for immunoaffinity purification experiments. The 7D3 antibody binds to the *Rieske*-type iron sulfur protein sub-

unit and the 2D6 antibody to the cytochrome b subunit of the cytochrome bc_1 complex, while the 7E2 antibody recognizes the native cytochrome c oxidase. Antibody V_H and V_L genes of these hybridoma cell lines were amplified by RT-PCR (reverse transcriptase-polymerase chain reaction) or inverse PCR and cloned into pASK68 using methods described previously[25-28] (see also Experimental Protocol). The RT-PCR approach is pragmatic and fast compared to other methods, however, the original sequence may be modified in those regions where the primers anneal, and the amino acid changes may even lead to altered affinities. Since it was not possible to clone all V-gene regions directly from hybridoma derived first strand cDNA by PCR with published oligonucleotides, we developed a new set of degenerate PCR-primers for the different murine subgroup V-gene regions.

In the presence of pseudogenes or very untypical V(D)J sequences the inverse PCR method was applied[26,28]. One of the most common fusion partners used in hybridoma technology is the nonsecretor myeloma cell line P3-X63-Ag8.653 (ref. 29). This cell line transcribes a nonfunctionally rearranged V_H (GenBank Accession Number X58634) and V_L Kappa gene[30] (GenBank Accession Number X05184, K00888, M35669). In several cases, amplification of these pseudogenes in addition to the functional V_H and V_L antibody genes, could not be prevented.

The synthetic dicistronic operon for expression of 2D6 Fv cDNA in pASK68 is shown in Figure 2. The sequences of 7D3 and 7E2 Fv will be published elsewhere. The Fv fragments were produced in the *E. coli* K12 strain JM83 transformed with the corresponding pASK68 derivatives. The Fv fragments were purified from the periplasmic fractions of induced bacteria by streptavidin affinity chromatography[31]. The spectroscopically[32] determined yields were approximately 0.2 mg (2D6), 0.6 mg (7D3) and 1.0 mg (7E2) Fv fragment from a 1 liter shake flask culture (final $OD_{550} = 1\text{–}1.2$).

Immune complex chromatography. Depending on the stability of the membrane protein and the detergent used, cytochrome c oxidase, cytochrome bc_1 complex, subcomplexes or individual subunits were purified to homogeneity as immune complexes with the corresponding Fv fragments by one-step streptavidin affinity chromatography[31]. For this purpose *P. denitrificans* membranes were combined with the *E. coli* periplasmic fraction containing the appropriate Fv fragments, followed by solubilization and ultracentrifugation (see Experimental Protocol). A typical elution profile of the cytochrome c oxidase / 7E2 Fv complex from the streptavidin column and the corresponding SDS-PAGE gel are shown in Figure 3. In the case of the cytochrome c oxidase the spectroscopically determined yield (ratio of purified co-complex compared to complex initially present in the soluble protein fraction after ultracentrifugation) exceeded 75% and the purification factor was greater than 100. By titrating membranes with increasing amounts of periplasmic fraction, a stoichiometric complex of the cytochrome c oxidase and 7E2 Fv fragment could be directly purified as judged by HPLC gelfiltration removing excess Fv (Fig. 4A). The cytochrome c oxidase in complex with the 7E2 Fv fragment is at least as active[33] with respect to cytochrome c oxidation as native cytochrome c oxidase (Fig. 4B) purified by conventional methods. The typical 3 subunit composition[2] (44, 32, 22 kD) plus a fourth band[34] (≈ 10 kD) for the oxidase was observed by SDS-PAGE (Fig. 3B). When Triton X-100 (TX) was used instead of *n*-dodecyl β-D-maltoside (LM) for solubilization of the cytochrome c oxidase, only two subunits (44 and 32 kDa) were immunopurified (Fig. 5). This is consistent with previous results[2,35] obtained with conventional purification methods using TX or LM as detergents. The cytochrome bc_1 complex was purified as a co-complex with either the 7D3 or the 2D6 Fv fragment by streptavidin affinity chromatography (Fig. 5).

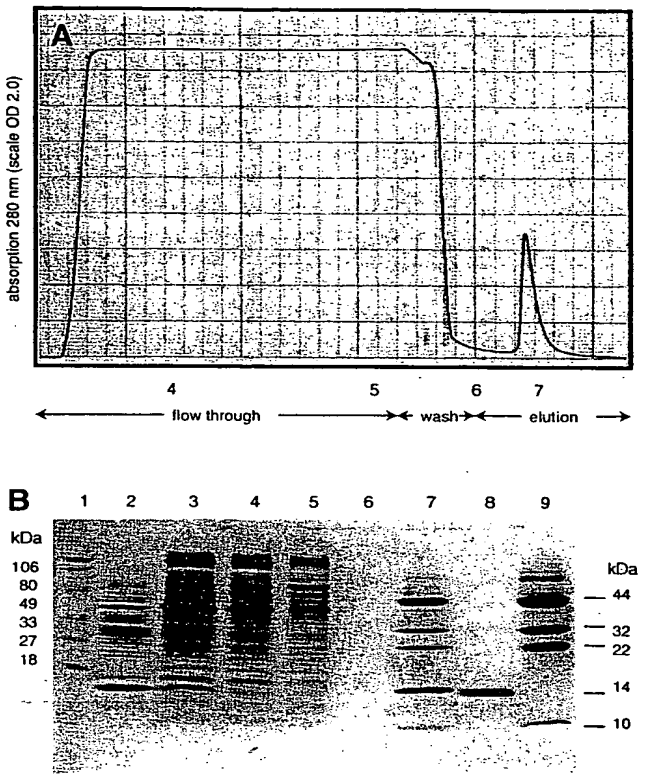

FIGURE 3. Immunoaffinity chromatography of the cytochrome c oxidase complexed with the 7E2 Fv fragment. (A) Elution profile of a typical immune complex chromatography column run. The protein was monitored at 280 nm. Aliquots were taken at the points indicated by the numbers 4–7 (corresponding to the lanes in (B)) and subsequently analyzed by SDS-PAGE. (B) The aliquots from (A) were analyzed by SDS-PAGE[43] (15%) under reducing conditions and stained with Coomassie brilliant blue R250. Periplasm of *E. coli* clone 7E2 Fv (lane 2) was combined with *P. denitrificans* membranes. The supernatant after ultracentrifugation (30 min, 200,000 g) of the solubilized crude protein mixture (lane 3) was subjected to streptavidin affinity chromatography (see (A) and Experimental Protocol). The flow through (lane 4) and subsequent washing steps (lanes 5, 6) show almost complete retardation of the cytochrome c oxidase/7E2 Fv complex. The purified immune complex (lane 7) was eluted with 5 mM diaminobiotin. Streptavidin affinity purified 7E2 Fv fragment (lane 8), conventionally purified cytochrome c oxidase[2] (lane 9) and molecular weight standards (lane 1) are shown for comparison.

However, different ratios of subunit compositions were observed upon prolonged washing with detergent-containing buffer indicating that the bc_1 complex is unstable. Therefore the bc_1 complex was subjected to isoelectric focusing (IEF) and native PAGE according to Schägger and Jagow[36]. In both experiments the bc_1 complex disintegrated almost completely into its individual subunits. This result suggests that the conditions of the immune complex chromatography are milder than those of IEF or native PAGE. Consequently, the obvious disintegration of the bc_1 complex was employed for the purification of its individual subunits (Fig. 5). The cytochrome b subunit was purified with the 2D6 Fv fragment in the presence of *n*-octyl β-D-glucopyranoside (OG), while the *Rieske* type iron sulfur protein was purified with the 7D3 Fv in the presence of either OG or N-

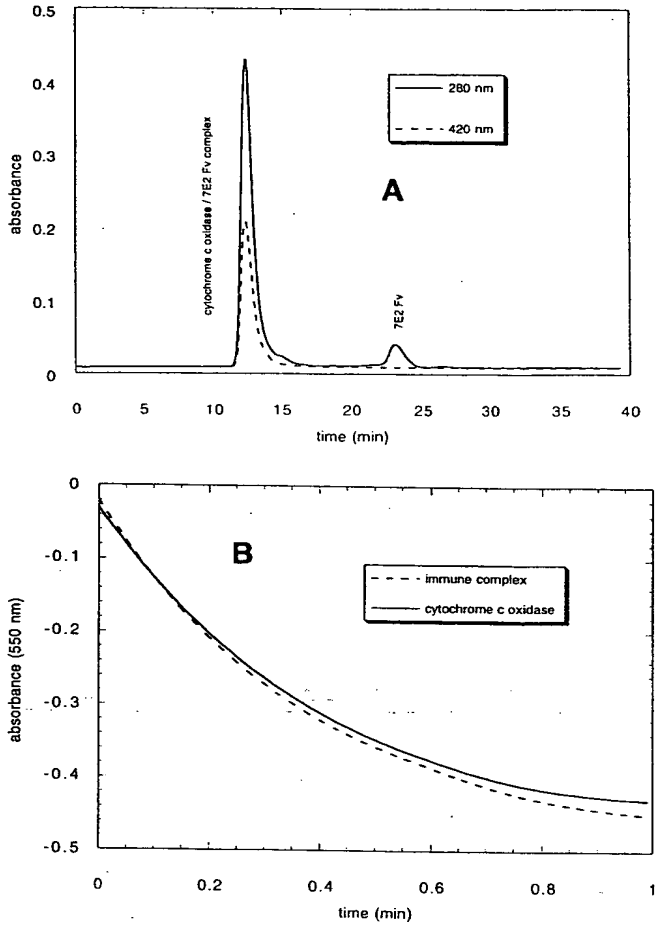

FIGURE 4. (A) 150 µl (≈ 1 mg protein) of the immunopurified cytochrome c oxidase / 7E2 Fv complex (see Fig. 3) was injected to a TSKgel G 3000 SW (7.5 mm ID × 60 cm) HPLC gel filtration column (Toso Haas) equilibrated with PBS (pH 6.8, 0.05% LM) at a flow rate of 1 ml/min. The protein was monitored at 280 nm and 420 nm. The highly active Fv complexed cytochrome c oxidase (Fig. 4B) was eluted after 12.6 min while an excess of the 7E2 Fv fragment was eluted at 23.6 min. (B) Comparison of the enzyme activity[33] (recording of the oxidation of reduced horse cytochrome c at 550 nm) showed that the cytochrome c oxidase complex with the Fv fragment 7E2 (Fig. 3, see Experimental Protocol) was at least as active as conventionally purified cytochrome c oxidase[2].

dodecyl-N,N-dimethylamine-N-oxide (LDAO). The purity and yield of these individual subunits of the bc_1 complex were as good as in the case of the isolated cytochrome c oxidase.

Biochemical and functional characterization of the purified proteins. Fv fragments directly purified by streptavidin affinity chromatography and analyzed by SDS-PAGE under reducing conditions (Fig. 3B) gave rise to a double band of the expected mobility corresponding to the V_H and V_L chains (Mr ≈ 14 kD). The presence of the c-*myc* tag[21] fused to the V_L chain and the *Strep tag*[20] attached to the V_H chain was confirmed by Western blot (data not shown). Crystals of the 7E2 Fv fragment were obtained and diffract X-rays up to 1.28 Å resolution (Ostermeier et al., Proteins: Structure, Function, and Genetics, in press). Preliminary X-ray crystallographic analysis confirmed correct association of the V_L and V_H chain. Binding of the mAb's and Fv fragments to the corresponding antigen (K_d are in the nM range) was analyzed using surface plasmon resonance (data will be published elsewhere), ELISA (data not shown) and HPLC gel filtration (Fig. 4A); calibration with a standard revealed that all Fv fragments investigated eluted as a monomer with an apparent molecular weight of ≈ 28 kD. No dimer formation or aggregation was observed. The complex of 7E2 Fv fragment with the cytochrome c oxidase is at least as active as the native cytochrome c oxidase purified by other methods[2] (Fig. 4B). Thus the bound Fv fragment behaves like an additional inert subunit not influencing the activity of the protein.

Discussion

The novel purification strategy for membrane proteins described here offers several attractive features. It is independent of the choice of the raw material or the expression system overproducing the target molecule (antigen). This is particulary important for the production of membrane proteins, because currently procaryotic, unicellular eucaryotic, multicellular eucaryotic, viral or transgenic animal expression systems are in use or under investigation[37]. Secondly, the use of an Fv fragment, which interacts noncovalently with the affinity matrix as an adapter molecule for the purification of the membrane protein, bypasses several cumbersome aspects of immunoaffinity chromatography[8,11–13,16–17,38]. Since monoclonal antibodies can have extremely high binding constants, the antigens frequently cannot be recovered in their native form. The widespread use of immunoaffinity chromatography is especially limited, if the antigen is an integral multisubunit membrane protein complex. The covalent coupling of monoclonal antibodies[8,12] or their corresponding fragments[11] to chemically activated matrices decreases the capacity of the immunoaffinity column due to potential inactivation of antigen binding sites. In addition, immunoglobulins have to be purified for this purpose. Alternatively, purified antibodies were biotinylated[16] and then bound to the antigen in solution. The antigen-antibody complexes were immobilized on a streptavidin-agarose column[17], and the antigen subsequently eluted. These columns are, however, not reusable. Elution of the antigen-antibody complex via a chemically cleavable connector, thus sacrificing the column[13] is inefficient. Protein A or G matrices bind immunoglobulins or even their fragments with a high binding constant and have therefore become popular for the immunopurification of antigens. However, only in some cases has it been possible to elute antigen or the Ig bound antigen in the native state[38].

In contrast, generally applicable elution protocols exist for competitive displacement of the immunopurified antigen-Fv complexes from the streptavidin column[31]. The *Strep tag* was derived through the random peptide library-assisted engineering of a C-terminal affinity peptide fused to the V_H chain of an Fv fragment[20]. Consequently, the 7E2 Fv fragment was completely adsorbed to the streptavidin column and recovery was nearly 100%. This fact may also be the reason for the reproducibly high yields of the Fv-membrane protein complexes and purification factors achieved in the immune complex chromatography. The preparation of a high capacity streptavidin sepharose affinity column[31] is routine and inexpensive. Due to the extreme stability of the immobilized core streptavidin the column is reusable for several months under continuous operation.

The Fv fragments are globular adapter molecules with the antigen binding site and the *Strep tag* affinity tail on the opposite ends. Thus steric hindrance during binding of the antigen-Fv complex to the streptavidin column is minimized. Furthermore the Fv fragments may stabilize the membrane proteins upon binding. The specificity of the streptavidin column for the engineered Fv fragments and antigen-Fv complexes is excellent[31]. In none of the chromatography experiments was contaminating protein detectable, either on SDS-PAGE gels or during HPLC gel-filtration.

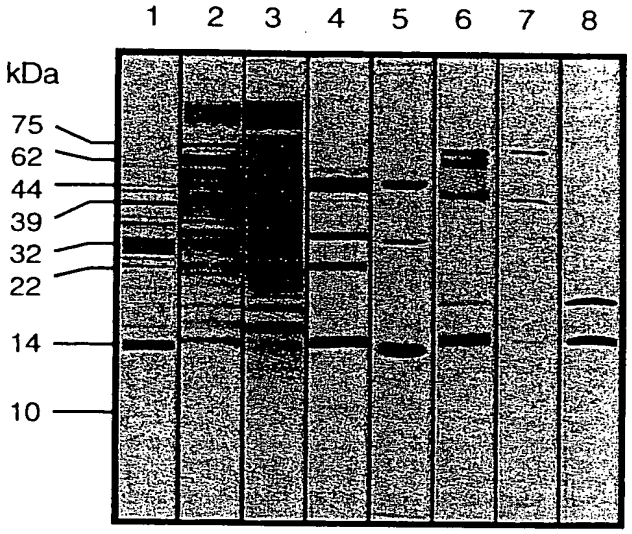

FIGURE 5. Immune complex chromatography of the cytochrome c oxidase, the cytochrome bc$_1$ complex and subcomplexes or individual subunits thereof. After immunoaffinity purification of the antigen-Fv complex from the mixture (lane 2) consisting of periplasm (lane 1) and membrane preparation (lane 3) (see Experimental Protocol) eluted material from several chromatography experiments was analyzed by SDS-PAGE[43] (15%) under reducing conditions and stained with Coomassie brilliant blue (R250). Lane (4) purified cytochrome c oxidase (detergent = LM; subunit I 44, subunit II 32, subunit III 22, additional peptide ≈ 10 kD; 7E2 Fv fragment 14 kD), lane (5) purified cytochrome c oxidase (detergent = TX; subunit I 44, subunit II 32; 7E2 Fv fragment 14 kD), lane (6) purified cytochrome bc$_1$ complex (detergent = LM; complex of cyt b/2D6 Fv fragment 75 kD, cyt c$_1$ 62 kD, cyt b 39 kD, native FeS 20 kD, denatured FeS 22 kD; 2D6 Fv fragment 15 kD), lane (7) purified cytochrome b (detergent = OG; cyt b-2D6 Fv complex 75 kD, cyt b 39 kD; 2D6 Fv 15 kD), lane (8) purified *Rieske*-type iron sulfur protein (detergent = OG or LDAO; FeS Protein 20 kD; 7D3 Fv 14 kD).

Starting from membranes and periplasm the purification procedure can be completed in 4–5 hours. Thus, the one step purification strategy surpasses conventional purification methods by saving time, resources (the Fv fragments need not be purified) and protecting the target molecule from harmful side effects like proteolytic degradation or denaturation during prolonged multiple step purification protocols. In principle, the Fv fragments can be immobilized on the streptavidin column from the periplasmic fraction prior to loading the solubilized crude membrane fraction, or alternatively, purified Fv fragments can be added to the membrane fraction, instead of *E. coli* periplasmic fractions, with no significant difference in performance. However, efficiency and kinetic aspects of complexing the antigen with an Fv fragment in solution favor the experimental approach shown. Detergent exchange or buffer change can be done during the immune complex chromatography. For the purification of individual subunits or subunit compositions of the multimeric membrane protein complexes different detergents, for example, *n*-dodecyl β-D-maltoside (LM), *n*-decyl β-D-maltoside (DM), *n*-nonyl β-D-glucopyranoside (NG), *n*-octyl β-D-glucopyranoside (OG), *n*-octyl β-D-thioglucopyranoside (OTG), Triton X-100 (TX), N-dodecyl-N,N-dimethylamine-N-oxide (LDAO), C_8E_5 (C_xE_y, polyoxyethylenes C_xH_{2x+1}-$(OC_2H_4)_y$-OH), $C_{10}E_6$, $C_{12}E_8$ were all successfully tested in different buffers to at least two times the critical micellar concentration (CMC). Finally, considering that numerous monoclonal antibodies directed against many known proteins are available, this method should be widely applicable and can easily be extended to scFv or Fab fragments.

Because an antigen-Fv complex is purified, the immune-complexed form of the antigen may show a modulated activity. In our experience, however, only 1 in 10 antibodies tested altered the activity of the membrane proteins studied, suggesting that most Fv fragments will behave as inert additional subunits of the target protein or protein complex. To circumvent the problem of those Fv fragments which may influence the activity of the membrane protein, we propose fusing a linear epitope of a well characterized monoclonal antibody to the protein under investigation. In order to remove the Fv fragment from the protein, a proteolytic cleavage site can be incorporated. For this approach, however, a recombinant expression system for the membrane protein would have to be established. Alternatively, competitive displacement with a peptide may be employed. Possible limitations of the Fv adapter molecule purification strategy might depend on the nature of the *Strep tag* fusion peptide sequence. The system is restricted to the neutral or alkaline pH due to potential protonation of histidine in the HPQ core sequence of the *Strep tag* at lower pH values, which reduces the affinity of the tag to the streptavidin column. Because any tag used for purification is exposed to the solvent, it might be accessible to proteinases. So far, proteolytic degradation of the *Strep tag* was not observed.

Since the purification method presented here works well with multimeric integral membrane protein complexes, which are stable only in mild detergents, we expect that it can be and will be used frequently to overcome the limiting problem for structural studies, namely the availability of sufficient amounts of pure material.

Experimental Protocol

Cloning of antibody V-gene regions. Cells (10^6) of the murine hybridoma cell lines were lysed in 1 ml guanidinium thiocyanate buffer (4 M Git, 25 mM NaAc pH 6, 1% mercaptoethanol) and passed several times through a needle (0.4 × 19 mm) to shear chromosomal DNA. Total RNA was pelleted (5h, 259,000g, TLS-55 rotor) through a cesium chloride cushion (5.7 M CsCl, 25 mM NaAc pH 6), solved in DEPC treated water (100 μl) and precipitated with ethanol[23]. First strand cDNA was synthesized in a 20 μl reaction in the presence of oligo(dT) or specific constant region primers according to the manufacturer's instructions (SuperScript Plus RNase H- Reverse Transcriptase, GIBCO BRL). One μl of this solution was used to amplify the V(D)J regions of the antibody V-genes with published primers[25,27] or later with our own primers in a 100 μl standard PCR[39] reaction following the recommendations of the suppliers (Pfu-Polymerase, Stratagene; Taq-Polymerase, Promega). Restriction sites (PstI, BstEII, SstI or XhoI) for cloning in pASK68 were incorporated into the PCR-primers: (V_λ-chain: VLC1T 5′-CAGGCT***GAGCTC***ACTCAGGAATCTGCACTCACC-3′, VLR1T 5′-CCTAGGAC***CTCGAG***(C/T)TTGGTTCC(A/T)CC(A/G)CCGAA-3′; V_κ-chain: VKC1T (subclass 1,2,3,5) 5′-GACATT***GAGCTC***AC(A/C)CAG(A/T)CTCCA(G/T)(C/T)CTCCCTG(G/T)CTG-3′, VKC2T (subclass 4,6) 5′-GACATT***GAGCTC***ACCCAGTCTCCAGCAATCATG(G/T)CTGC-3′, VKR1T (subclass 1–6) 5′-CCGTTTCAG***CTCGAG***CTTGGT(C/G)CC(A/T) (C/G)C(A/T)CCGAACGT-3′; V_H-chain: VHC1T 5′-GAGGT(G/T)(A/C)AG***CTGCAG***(C/G)AGTC(A/T)GGG(C/G)CTGGC(C/T)TGGT-3′, VHR1T 5′-TGAGGAGAC***GGTGACC***GTGGT(C/G)CCTTGGCCCC(A/)-3′). The DNA fragments obtained from PCR were purified from low or high melting point agarose gels, cut with the respective endonucleases and cloned[23] in pASK68 for sequence determination[40] (sequencing primer for pASK68 : primer 1233: 5′-AGCGGATAACAATTTCACACAGGA-3′, primer 3: 5′-TGGGTGAGCTCGATGTC-3′, primer 2a: 5′-CGGTCACCGTCTCCTCA-3′, primer 1: 5′-CGCAGTAGCGGTAAACG-3′), expression and production of Fv fragments. In the presence of pseudogenes or very untypical V(D)J sequences RNA of the hybridoma cells was prepared as described above. 3′-UTR-5′-UTR-$L_1L_2V(D)J\Delta C$ regions (covering the 3′ untranslated region (3′-UTR), the 5′-UTR, L_1 (part of leader sequence encoded by the first exon of Ig genes), L_2VJ or L_2VDJ (exon of Ig genes consisting of rearranged V region of L chain or H chain and part of the first constant domain (ΔC)) of the antibody circular ds-cDNA were amplified by inverse PCR, cloned and sequenced in pBS or Bluescript II KS (Stratagene) as published elsewere[26]. The sequenced regions were amplified in a second

PCR with degenerate primers or special designed primers to conserve authentic V_H and V_L sequences for cloning in pASK68.

Expression of Fv fragments. The Fv fragments encoded by the pASK68-derivatives were produced using *E. coli* K12 strain JM83 (*ara*, Δ(*lac-proAB*), *rpsL*, *φ80lacZΔM15*) (ref. 41). Cells were grown at 22°C in Luria broth (LB)[23] containing 100 μg/ml ampicillin to an A_{550} of 0.5. Expression was induced by adding isopropyl β-D-thiogalactopyranoside (IPTG) to a final concentration of 0.5–1 mM and continued over 3 hours. For preparation of the periplasmic cell fraction, the cells from a 1 L culture were collected by centrifugation, resuspended in 10 ml 50 mM Tris/HCl, pH 8.0, 500 mM sucrose, 1 mM EDTA and kept on ice for 30 min. The spheroplasts were removed by centrifugation and the supernatant passed through a sterile filter (0.2 μm). Avidin was added to a final concentration of 40 μg/ml for the complexation of endogenous biotin groups in order to protect the strepavidin column.

Production of the streptavidin CH sepharose 4B column. Recombinant core streptavidin was prepared exactly following published protocols[31]. The functional tetrameric streptavidin was coupled to activated CH sepharose 4 B (Pharmacia) at 5 mg streptavidin per ml gel according to the manufacturer's instructions.

Membrane protein preparation. For preparation of membranes enriched in cytochrome c oxidase, wild type *P. denitrificans* ATCC 13543 was grown in methanol medium, and membranes for immunoaffinity purification of the bc_1 complex were prepared as previously described[42] from an overproducing strain (deletion strain G440 transformed with plasmid pEG436), which was grown aerobically at 32°C in succinate medium. Membranes were thawed and the protein concentration adjusted to approximately 10 mg/ml in 50 mM Tris/HCl or 50 mM potassium phosphate buffer pH 8.0, 1 mM EDTA, 100 mM NaCl, 100 μM Pefabloc (Merck) and the appropriate volume of the periplasmic fraction from *E. coli* containing equivalent amounts of a corresponding Fv fragment. Solid *n*-dodecyl β-D-maltopyranoside (LM) or *n*-octyl β-D-glucopyranoside (OG) or N-dodecyl-N,N-dimethylamine-N-oxide (LDAO, 30% stock solution) were added to a ratio of 1–1.5 g/g of protein and the mixture was stirred at 4°C for 45 min. After centrifugation at 200,000-g for 30 min, the pellet was discarded and the supernatant was directly subjected to the streptavidin affinity chromatography.

Immunoaffinity chromatography. The crude protein mixture (≈ 100 ml) was loaded on the pre-equilibrated (50 mM Tris/HCl, pH 8, or PBS (4 mM KH_2PO_4, 16 mM Na_2HPO_4, 115 mM NaCl), pH 8, containing 0.025% *n*-dodecyl β-D-maltopyranoside (LM) or 1% *n*-octyl β-D-glucopyranoside (OG) or 0.1% N-dodecyl-N,N-dimethylamine-N-oxide (LDAO) as detergent) streptavidin sepharose column (10 ml, 1.5 cm^2) with a flow rate of 30 ml/h. After washing the column with 25 ml equilibration buffer containing in addition 150 mM NaCl, 2 mM $MgCl_2$ the antigen-Fv complex was eluted with 5 mM diaminobiotin (Sigma) pH 8 or 5 mM Lipoic acid (Merck) pH 6 in equilibration buffer. The chromatography was performed at 4°C.

Isoelectric focusing. The protein sample was desalted on a PD10 column (Pharmacia) equilibrated with 20 mM KPi, pH 8, 0.05% LM and subjected to IEF using the Multiphor II System (Ultrodex, ampholytes 3–10, 0.05% LM, 4 Watt) according to the manufacturers recommendations (Pharmacia).

Acknowledgments

G.K and C.O. are grateful for a Kekule grant and a pre-doctoral fellowship, respectively, of the Fonds der Chemischen Industrie. We thank Kate Pope for technical assistance, Lars-Oliver Essen for discussions and Thomas Schmidt for providing plasmid pSA1 and invaluable advice. This work was supported by the Fonds der Chemischen Industrie, the Deutsche Forschungsgemeinschaft and the Max-Planck-Gesellschaft.

References

1. Yang, X. and Trumpower, B. L. 1986. Purification of a three-subunit ubiquinol-cytochrome c oxidoreductase complex from *Paracoccus denitrificans*. J. Biol. Chem. **261**:12282–12289.
2. Hendler, R. W., Pardhasaradhi, K., Reynafarje, B. and Ludwig, B. 1991. Comparison of energy-transducing capabilities of the two- and three-subunit cytochromes aa_3 from *Paracoccus denitrificans* and the 13-subunit beef heart enzyme. Biophys. J. **60**:415–423.
3. Bill, K., Broger, C. and Azzi, A. 1982. Affinity chromatography purification of cytochrome c oxidase and b-c_1 complex from beef heart mitochondria. Biochim. Biophys. Acta **679**:28–34.
4. Schertler, G. F. X. 1992. Overproduction of membrane proteins. Curr. Opin. Struct. Biol. **2**:534–544.
5. Nygren, P.-Å., Stahl, S. and Uhlén M. 1994. Engineering proteins to facilitate bioprocessing. Trends Biotechnol. **2**:184–188.
6. Cuatrecases, P., Wilchek, M. and Anfinsen, C. B. 1968. Selective enzyme purification by affinity chromatography. Proc. Natl. Acad. Sci. USA **61**:636–643.
7. Köhler, G. and Milstein, C. 1975. Continous cultures of fused cells secreting antibody of predefined specificity. Nature **256**:495–497.
8. Secher, D. S. and Burke, D. C. 1980. A monoclonal antibody for large-scale purification of human leukocyte interferon. Nature **285**:446–450.
9. Campbell, D. H., Luescher, E. and Lerman, L. S. 1951. Immunologic adsorbents. I. Isolation of antibody by means of a cellulose-protein antigen. Proc. Natl. Acad. Sci. **37**:575–578.
10. Gurvich, A. E. and Drizlikh, G. I. 1964. Use of antibodies on an insoluble support for specific detection of radioactive antigens. Nature **203**:648–649.
11. Berry, M. J., Davies, J., Smith, C. G. and Smith, I. 1991. Immobilization of Fv antibody fragments on porous silica and their utility in affinity chromatography. J. Chromatogr. **587**:161–169.
12. Livingstone, D. M. 1974. Immunoaffinity chromatography of proteins. Methods Enzymol. **34**:723–731.
13. Singh, P., Lewis, S. D. and Schafer, J. A. 1979. A support for affinity chromatography that covalently binds amino groups via a cleavable connector arm. Arch. Biochem. Biophys. **193**:284–293.
14. Boyle, M. D. P. (Ed.). 1990. Bacterial Immunoglobulin-Binding Proteins. Academic Press, New York.
15. Derrick, J. P. and Wigley, D. B. 1992. Crystal structure of a streptococcal protein G domain bound to an Fab fragment. Nature **359**:752–754.
16. Hofmann, K., Finn, F. M. and Kiso, Y. 1978. Avidin-biotin affinity columns. General methods for attaching biotin to peptides and proteins. J. Am. Chem. Soc. **100**:3585–3590.
17. Updyke, T. V. and Nicolson, G. L. 1986. Immunoaffinity isolation of membrane antigens with biotinylated monoclonal antibodies and streptavidin-agarose. Methods Enzymol. **121**:717–725.
18. Skerra, A. and Plückthun, A. 1988. Assembly of a functional immunoglobulin Fv fragment in *Escherichia coli*. Science **240**:1038–1041.
19. Skerra, A. 1993. Bacterial expression of immunoglobulin fragments. Curr. Opin. Immunol. **5**:256–262.
20. Schmidt, T. G. M. and Skerra, A. 1993. The random peptide libray-assisted engineering of a carboxy-terminal affinity peptide, useful for the detection and purification of a functional Ig Fv fragment. Protein Eng. **6**:109–122.
21. Munro, S. and Pelham, H. 1986. An Hsp70-like protein in the ER: Identity with the 78 kd glucose-regulated protein and immunoglobulin heavy chain-binding protein. Cell **46**:291–300.
22. Skerra, A., Pfitzinger, I. and Pluckthun, A. 1991. The functional expression of antibody Fv fragments in *Escherichia coli*: Improved vectors and a generally applicable purification technique. Bio/Technology **9**:273–278.
23. Sambrook, T., Fritsch, E. F. and Maniatis, T. 1989. Molecular Cloning: A Laboratory Manual, 2nd ed. Cold Spring Harbour, New York.
24. Skerra, A. 1994. A general vector, pASK84, for cloning, bacterial production, and single-step purification of antibody F_{ab} fragments. Gene **141**:79–84.
25. Orlandi, R., Güssow, D. H., Jones, P. T. and Winter, G. 1989. Cloning immunoglobulin variable domains for expression by the polymerase chain reaction. Proc. Natl. Acad. Sci. USA **86**:3833–3837.
26. Kaluza, B., Betzl, G., Shao, H., Diamantstein, T. and Weidle, U. H. 1992. A general method for chimerization of monoclonal antibodies by inverse polymerase chain reaction which conserves authentic N-terminal sequences. Gene **122**:321–328.
27. Clackson, T., Hoogenboom, H. R., Griffiths, A. D. and Winter, G. 1991. Making antibody fragments using phage display libraries. Nature **352**:624–628.
28. Uematsu, Y. 1991. A novel and rapid cloning method for the T-cell receptor variable region sequences. Immunogenetics **34**:174–178.
29. Kearney, T., Radbruch, A., Liesegang, B. and Rajewsky, K. 1979. A new mouse myeloma cell line that has lost immunoglobulin expression but permits the construction of antibody-secreting hybrid cell lines. J. Immunol. **123**:1548–1558.
30. Strohal, R., Kroemer, G., Wick, G. and Kofler, R. 1987. Complete variable region sequence of a nonfunctionally rearranged kappa light chain transcribed in the nonsecretor P3-X63-Ag8.653 myeloma cell line. Nucl. Acids Res. **15**:2771.
31. Schmidt, T. G. M. and Skerra, A. 1994. One-step affinity purification of bacterially produced proteins by means of the Strep tag and immobilized recombinant core streptavidin. J. Chromatogr. **676**:337–345.
32. Gill, S. C. and Hippel, P. H. 1989. Calculation of protein extinction coefficients from amino acid sequence data. Anal. Biochem. **182**:319–326.
33. Berry, E. A. and Trumpower, B. L. 1985. Isolation of ubiquinol oxidase from *Paracoccus denitrificans* and resolution into cytochrome bc_1 and cytochrome c-aa_3 complexes. J. Biol. Chem. **260**:2458–2467.
34. Haltia, T. 1992. Cytochrome c oxidase: Biochemical, genetic and spectroscopic studies using enzyme from *Paracoccus denitrificans*. Commentationes Physico-Mathematicae et Chemico-Medicae **136**:1–88.
35. Ludwig, B. and Schatz, G. 1980. A two-subunit cytochrome c oxidase (cytochrome aa3) from *Paracoccus denitrificans*. Proc. Natl. Acad. Sci. USA **77**:196–200.
36. Schägger, H. and Jagow, G. 1991. Blue native electrophoresis for isolation of membrane protein complexes in enzymatically active form. Anal. Biochem. **199**:223–231.
37. Hodgson, J. 1993. Expression Systems: A User's Guide. Bio/Technology **11**:887–893.
38. Hauri, H. P., Quaroni, A. and Isselbacher, K. J. 1980. Monoclonal antibodies to sucrase/isomaltase: Probes for the study of postnatal development and biogenesis of the intestinal microvillus membrane. Proc. Natl. Acad. Sci. USA **77**:6629–6633.
39. Saiki, R. K., Gelfand, D. H., Stoffel, S., Scharf, S. J., Higuchi, R., Horn, G. T., Mullis, K. B. and Ehrlich, H. A. 1988. Primer-directed enzymatic amplification of DNA with a thermostable DNA polymerase. Science **239**:487–491.
40. Sanger, F., Nicklen, S. and Coulson, A. R. 1977. DNA sequencing with chain-terminating inhibitors. Proc. Natl. Acad. Sci. USA **74**:5463–5467.
41. Yanish-Peron, C., Viera, J. and Messing, J. 1985. Improved M13 phage cloning vectors and host strains: Nucleotide sequences of the M13mp18 and pUC19 vectors. Gene **33**:103–199.
42. Gerhus, E., Steinrücke, P. and Ludwig, B. 1990. *Paracoccus denitrificans* cytochrome c_1 gene replacement mutants. J. Bacteriol. **172**:2392–2400.
43. Fling, S. P. and Gregerson, D. S. 1986. Peptide and protein molecular weight determination by electrophoresis using a high-molarity buffer system without urea. Anal. Biochem. **155**:83–88.
44. Kabat, E. A., Wu, T. T., Perry, H. M., Gottesman, K. S. and Foeller, C. 1991. Sequences of Proteins of Immunological Interest, 5th ed. U.S. Dept. of Health and Human Services, U.S. Goverment Printing Office, Washington, DC.

PCT WELTORGANISATION FÜR GEISTIGES EIGENTUM
Internationales Büro

INTERNATIONALE ANMELDUNG VERÖFFENTLICHT NACH DEM VERTRAG ÜBER DIE INTERNATIONALE ZUSAMMENARBEIT AUF DEM GEBIET DES PATENTWESENS (PCT)

(51) Internationale Patentklassifikation 6 :		(11) Internationale Veröffentlichungsnummer: **WO 98/29540**
C12N 15/00	A2	(43) Internationales Veröffentlichungsdatum: 9. Juli 1998 (09.07.98)

(21) Internationales Aktenzeichen: PCT/EP98/00009

(22) Internationales Anmeldedatum: 2. Januar 1998 (02.01.98)

(30) Prioritätsdaten:
97100012.0 2. Januar 1997 (02.01.97) EP
(34) Länder für die die regionale oder internationale Anmeldung eingereicht worden ist: DE usw.

(71) Anmelder *(für alle Bestimmungsstaaten ausser US)*: B.R.A.I.N. BIOTECHNOLOGY RESEARCH AND INFORMATION NETWORK GMBH [DE/DE]; Darmstädter Strasse 34, D–64673 Zwingenberg (DE).

(72) Erfinder; und
(75) Erfinder/Anmelder *(nur für US)*: ECK, Jürgen [DE/DE]; Siegfriedstrasse 138, D–64646 Heppenheim (DE). SCHMIDT, Arno [DE/DE]; Unterdorf 36, D–64572 Büttelborn 3 (DE). ZINKE, Holger [DE/DE]; Hartenauer Strasse 49, D–64404 Bickenbach (DE).

(74) Anwalt: VOSSIUS & PARTNER GBR; Siebertstrasse 4, D–81675 München (DE).

(81) Bestimmungsstaaten: AL, AM, AT, AU, AZ, BA, BB, BG, BR, BY, CA, CH, CN, CU, CZ, DE, DK, EE, ES, FI, GB, GE, HU, ID, IL, IS, JP, KE, KG, KP, KR, KZ, LC, LK, LR, LS, LT, LU, LV, MD, MG, MK, MN, MW, MX, NO, NZ, PL, PT, RO, RU, SD, SE, SG, SI, SK, TJ, TM, TR, TT, UA, UG, US, UZ, VN, ARIPO Patent (GH, GM, KE, LS, MW, SD, SZ, UG, ZW), eurasisches Patent (AM, AZ, BY, KG, KZ, MD, RU, TJ, TM), europäisches Patent (AT, BE, CH, DE, DK, ES, FI, FR, GB, GR, IE, IT, LU, MC, NL, PT, SE), OAPI Patent (BF, BJ, CF, CG, CI, CM, GA, GN, ML, MR, NE, SN, TD, TG).

Veröffentlicht
Ohne internationalen Recherchenbericht und erneut zu veröffentlichen nach Erhalt des Berichts.

(54) Title: RECOMBINANT FUSION PROTEINS BASED ON RIBOSOME–INACTIVATING PROTEINS OF EUROPEAN MISTLETOE *VISCUM ALBUM*

(54) Bezeichnung: REKOMBINANTE FUSIONSPROTEINE AUF DER BASIS RIBOSOMEN–INAKTIVIERENDER PROTEINE DER MISTEL *VISCUM ALBUM*

(57) Abstract

Nucleic acid molecules code for fusion proteins which contain at least one effector module, a processing module and a targeting module. The disclosed nucleic acid molecules preferably further contain a modulator module and/or an affinity module. Also disclosed are vectors containing these nucleic acid molecules, hosts transformed by the disclosed vectors, fusion proteins coded by the disclosed nucleic acids or produced by the disclosed hosts, and medicaments which contain the disclosed polypeptides or vectors. These medicaments are particularly significant for the therapy of diseases associated with a pathological reproduction and/or increased activity of cell populations. A temporary, abrupt and strong proliferation, infiltration and immune activity of cells of the immune system is found in auto–immune diseases and allergies, the specificity of these immune cells being due to their reaction to a particular antigen or allergen. These medicaments may also be advantageously used for treating tumours. The disclosed polypeptides and vectors can be used to develop medicaments and to test toxin activity–modulating factors. The invention thus also concerns corresponding processes, uses and kits. The modules, with the exception of the affinity and targeting modules, are preferably coded by nucleic acids extracted or derived from the mistletoe lectin proprotein coding sequence.

(57) Zusammenfassung

Die Erfindung betrifft Nukleinsäuremoleküle, die Fusionsproteine codieren, die als Komponenten mindestens ein Effektormodul, ein Prozessierungsmodul und ein Targetingmodul enthalten. Vorzugsweise codieren die erfindungsgemäßen Nukleinsäuremoleküle ferner ein Modulatormodul und/oder ein Affinitätsmodul. Die Erfindung betrifft ferner Vektoren, die diese Nukleinsäuremoleküle enthalten, Wirte, die mit den erfindungsgemäßen Vektoren transformiert sind, Fusionsproteine, die von den erfindungsgemäßen Nukleinsäuren codiert oder von den erfindungsgemäßen Wirten produziert werden sowie Arzneimittel, die die erfindungsgemäßen Polypeptide oder Vektoren enthalten. Diese Arzneimittel haben besondere Bedeutung bei solchen Erkrankungen, die auf der pathologischen Vermehrung und/oder der erhöhten Aktivität von Zellpopulationen beruhen. Eine vorübergehende, schubartige starke Proliferation, Infiltration und Immunaktivität von Zellen des Immunsystems findet man bei Autoimmunerkrankungen und Allergien, wobei die Spezifität dieser Immunzellen auf der Reaktion auf jeweils bestimmte Antigene bzw. Allergene beruht. Ferner können solche Arzneimittel auch vorteilhaft zur Tumortherapie eingesetzt werden. Die in dieser Erfindung beschriebenen Polypeptide und Vektoren können zur Entwicklung von Arzneimitteln und zur Testung von Toxinaktivität modulierenden Faktoren eingesetzt werden. Somit betrifft die Erfindung ferner entsprechende Verfahren, Verwendungen und Kits. Vorzugsweise werden die Module mit Ausnahme des Affinitäts– und des Targetingmoduls von Nukleinsäuren codiert, die aus der das Mistellektin–Proprotein codierenden Sequenz stammen oder davon abgeleitet sind.

REF. 19

autoreaktiven T-Zellen in der Peripherie oder zum Ort der Autoimmunreaktion gelangt. Bei Bindung geringer Mengen Antigen an T-Zellen findet natürlicherweise eine Proliferation statt. Durch die Kopplung eines Toxins an die spezifische Erkennungssequenz der neuritogenen T-Zellen kann somit eine sichere T-Zell Eliminierung vermittelt werden, ohne die Gefahr eines gegenteiligen stimulatorischen Effektes zu bergen. Auslöser beispielsweise der Multiplen Sklerose ist die Entstehung und Vermehrung von autoreaktiven T-Lymphozyten (Olive, 1995), die ein Abbauprodukt des "myelin-basic-proteins" - in der Mehrzahl der Fälle die Sequenz "VHFFKNIVTPRTP" - erkennen. Dies führt dazu, daß die Nervenzellen des Patienten vom körpereigenen Immunsystem angegriffen werden. Auch hier ist die Verwendung von krankheitsauslösenden Peptiden als Targetingmodul der Schlüssel zur Anwendung einer auf der Erfindung basierenden Therapieform. Eine weitere derartige Erkrankung ist Myasthenia Gravis, bei der es zu einer Autoimmunreaktion gegen Acetylcholinrezeptoren kommt. Ferner kommt eine Behandlung diverser Leukämien oder Neoplasien in Frage.

Somit ist in einer besonders bevorzugten Ausführungsform der Erfindung die Zielzelle eine Zelle des Immunsystems. Dies kann zum einen eine Zelle des unspezifischen Immunsystems wie zum anderen eine Zelle des spezifischen Immunsystems sein. Im letzteren Falle kann es sich um B-Zellen oder T-Zellen, insbesondere T_H2-Zellen handeln. Ferner können auch entartete Zellen des Immunsystems Zielzellen sein. Auch Zellen, insbesondere entartete Zellen des Nervensystems, beispielsweise Nervenzellen, können bei Wahl geeigneter Targeting-Module Zielzellen sein.

In einer weiteren bevorzugten Ausführungsform des erfindungsgemäßen Nukleinsäuremoleküls ist das Affinitätsmodul eine Histidinsequenz, Thioredoxin, Strep-Tag, T7-Tag, FLAG-Tag, Maltose-Bindungs-Protein oder GFP (Green Fluorescent Protein). Das Affinitätsmodul ist hierbei eine Peptidsequenz, die sich durch eine Liganden-Bindungs-Spezifität oder durch das Vorhandensein geeigneter Epitope auszeichnet, die eine selektive Aufreinigung vorzugsweise durch affinitätschromatographische Verfahren, z. B. mittels immobilisierter Liganden oder immobilisierter Antikörper ermöglicht. Derartige Affinitätsmodule haben stets die Eigenschaft, hochspezifisch und mit hohen Bindungskonstanten Liganden zu binden, die ihrerseits als Liganden an

(i) Nukleinsäuremolekülen, die eine Nukleotidsequenz umfassen, die die in Fig. 11.c angegebene Aminosäuresequenz oder ein Fragment davon codiert;

(ii) Nukleinsäuremolekülen, die die in Fig. 11.c angegebene Nukleotidsequenz oder ein Fragment davon umfassen;

(iii) Nukleinsäuremolekülen, die mit einem Nukleinsäuremolekül aus (i) oder (ii) hybridisieren; und

(iv) Nukleinsäuremolekülen, die zu den in (iii) genannten Nukleinsäuremolekülen degeneriert sind.

3. Nukleinsäuremolekül nach Anspruch 1 oder 2, wobei

(a) das Effektormodul die biologische Aktivität der Mistellektin A-Kette besitzt und ein Allel oder Derivat der in Anspruch 2 definierten Mistellektin A-Kette durch Aminosäure-Deletion, Substitution, Insertion, Addition und/oder Austausche umfaßt; und/oder

(b) das Prozessierungsmodul proteolytisch spaltbar ist und ein Allel oder Derivat des in Anspruch 2 definierten Mistellektin-Propeptids durch Aminosäure-Deletion, Substitution, Insertion, Addition und/oder Austausche umfaßt.

4. Nukleinsäuremolekül nach einem der Ansprüche 1 bis 3 wobei das Fusionsprotein ferner die folgende Komponente aufweist:

(d) ein Modulatormodul, das kovalent mit dem Prozessierungsmodul, dem Effektormodul und/oder mit dem Targetingmodul verbunden ist, und das die intrazelluläre toxische Wirkung des Effektormoduls moduliert.

5. Nukleinsäuremolekül nach Anspruch 4, wobei das Modulatormodul von einem Nukleinsäuremolekül codiert wird, ausgewählt aus der Gruppe bestehend aus:

(i) Nukleinsäuremolekülen, die eine Nukleotidsequenz umfassen, die die in Fig. 11.b angegebene Aminosäuresequenz oder ein Fragment davon codiert;

(ii) Nukleinsäuremolekülen, die die in Fig. 11.b angegebene Nukleotidsequenz oder ein Fragment davon umfassen;

IMMUNOLOGY

THIRD EDITION

JANIS KUBY

Professor of Biology
San Francisco State University

Faculty
Joint Medical Programs
University of California at Berkeley

W. H. FREEMAN AND COMPANY
New York

REF. 20

Senior editor:	Deborah Allen
Development editors:	Michelle Russel Julet and Diane Cimino Maass
Project editor:	Diane Cimino Maass
Line editor:	Ruth Steyn
Cover and text designer:	Marsha Cohen/ Parallelogram Graphics
Illustration coordinator:	Susan Wein
Illustration:	Network Graphics
Production coordinator:	Sheila E. Anderson
Composition:	Sheridan Sellers/W. H. Freeman Electronic Publishing Center
Manufacturing:	Von Hoffman Press, Inc.

ABOUT THE COVER AND FRONTISPIECE

Interactions of cell adhesion molecules, with different ones involved at different times, are responsible for recruiting leukocytes to inflammatory sites and for their migration through the vascular endothelium. Slowed by vasodilation, leukocytes drift against vessel walls, where selectins are responsible for a loose adherence known as "rolling." This initial step in leukocyte migration is shown in a false-color scanning electron micrograph. (See Chapter 15 for more information.)

Library of Congress Cataloging-in-Publication Data

Kuby, Janis.
Immunology / Janis Kuby. — 3rd ed.
p. cm.
Includes bibliographical references and index.
ISBN 0-7167-2868-0
1. Immunology. I. Title.
[DNLM: 1. Immune System. 2. Immunity. QW 504 K95i 1997]
QR181.K83 1997
616.07'9 — dc21
DNLM/DLC
for Library of Congress 96-52442
CIP

Printed in the United States of America

First Printing, 1997

CHAPTER 1

OVERVIEW OF THE IMMUNE SYSTEM

The immune system is a remarkably adaptive defense system that has evolved in vertebrates to protect them from invading pathogenic microorganisms and cancer. It is able to generate an enormous variety of cells and molecules capable of specifically recognizing and eliminating an apparently limitless variety of foreign invaders. These cells and molecules act together in an exquisitely adaptable dynamic network whose complexity rivals that of the nervous system.

Functionally, an immune response can be divided into two interrelated activities—**recognition** and **response**. Immune recognition is remarkable for its specificity. The immune system is able to recognize subtle chemical differences that distinguish one foreign pathogen from another. At the same time, the system is able to discriminate between foreign molecules and the body's own cells and proteins. Once a foreign organism is recognized, the immune system enlists the participation of a variety of cells and molecules to mount an appropriate response, known as an **effector response**, to eliminate or neutralize the organism. In this way the system is able to convert the initial recognition event into different effector responses, each uniquely suited to eliminate a particular type of pathogen. Later exposure to the same foreign organism induces a **memory response**, characterized by a heightened immune reactivity, that serves to eliminate the pathogen and prevent disease.

This chapter presents a broad overview of the cells and molecules that compose the immune system and the mechanisms by which they protect the body against foreign invaders. As is always the case with an overview, the details have been simplified to reveal the essential structure of the immune system. Substantive discussions, experimental approaches, and in-depth definitions are left to the chapters that follow.

HISTORICAL PERSPECTIVE

The discipline of immunology grew out of the observation that individuals who had recovered from certain infectious diseases were thereafter protected from the disease. The Latin term *immunis*, meaning "exempt," is the

source of the English word **immunity**, meaning the state of protection from infectious disease.

Perhaps the earliest written reference to the phenomenon of immunity can be traced back to Thucydides, the great historian of the Peloponnesian War. In describing a plague in Athens, he wrote in 430 B.C. that only those who had recovered from the plague could nurse the sick because they would not contract the disease a second time. Although early societies recognized the phenomenon of immunity, almost two thousand years passed before the concept was successfully converted into a medically effective practice.

The first recorded crude attempts to deliberately induce immunity were performed by the Chinese and Turks in the fifteenth century. Various reports suggest that the dried crusts derived from smallpox pustules were either inhaled into the nostrils or inserted into small cuts in the skin (a technique called **variolation**). In 1718 Lady Mary Wortley Montagu, the wife of the British ambassador to Constantinople, observed the positive effects of variolation on the native population and had the technique applied to her own children. The technique was significantly improved by the English physician Edward Jenner in 1798. Intrigued by the fact that milkmaids who contracted cowpox (a mild disease) were subsequently immune to smallpox (a disfiguring and often fatal disease), Jenner reasoned that introducing fluid from a cowpox pustule into people (i.e., inoculating them) might protect them from smallpox. To test this idea, he inoculated an eight-year-old boy with fluid from a cowpox pustule and later intentionally infected the child with smallpox. As predicted, the child did not develop smallpox. Nevertheless, one cannot help but question the ethical implications of such an experiment!

Jenner's technique of inoculating with cowpox to protect against smallpox spread quickly throughout Europe, but it was nearly a hundred years before the technique was applied to other diseases. As so often happens in science, serendipity combined with astute observation led to the next major advance in immunology, the induction of immunity to cholera by Louis Pasteur. Pasteur had succeeded in growing the organism thought to cause fowl cholera in culture and then had shown that chickens injected with the cultured bacterium developed cholera. After returning from a summer vacation, he injected some chickens with an old culture of the bacterium. The chickens became ill, but to Pasteur's surprise they recovered. Pasteur then grew a fresh culture of the bacterium with the intention of injecting it into some fresh chickens. But the story goes, he was low on chickens and therefore used the previously injected chickens. Again to his surprise, the chickens survived and were completely protected from the disease. Pasteur recognized that aging had weakened the virulence of the pathogen and that such an attenuated strain might be administered to protect against the disease. He called this attenuated strain a **vaccine** (from the Latin *vacca*, meaning "cow") in honor of Jenner's work with cowpox inoculation.

Pasteur extended these findings to other diseases, demonstrating that is was possible to **attenuate**, or weaken, a pathogen and administer the attenuated strain as a vaccine. In a now classical experiment at Pouilly-le-Fort in 1881, Pasteur first vaccinated one group of sheep with heat-attenuated anthrax bacillus; he then challenged the vaccinated sheep and some unvaccinated sheep with a virulent culture of *Bacillus anthracis*. All the vaccinated sheep lived, whereas all unvaccinated animals died. These experiments marked the beginnings of the discipline of immunology. In 1885, Pasteur administered the first vaccine to a human, a young boy who had been bitten repeatedly by a rabid dog (Figure 1-1). The boy, Joseph Meister, lived and later became a custodian at the Pasteur Institute. In 1940, during the Nazi occupation of Paris,

FIGURE 1-1

Wood engraving of Louis Pasteur watching Joseph Meister receive the rabies vaccine. [From *Harper's Weekly* 29:836, 1885; courtesy of the National Library of Medicine.]

the Nazis asked Meister to give them the keys to Pasteur's crypt. Rather than surrender the keys to the Nazis, Meister took his own life.

Discovery of Humoral and Cellular Immunity

Although Pasteur proved that **vaccination** worked, he did not understand the mechanisms involved. The experimental work of Emil von Behring and Shibasaburo Kitasato in 1890 provided the first insights into the mechanism of immunity, earning von Behring the Nobel prize in medicine in 1901 (Table 1-1). Von Behring and Kitasato demonstrated that **serum** (the noncellular part of blood) from animals previously immunized to diphtheria could transfer the immune state to unimmunized animals. In search of the protective agent, various researchers during the next decade demonstrated that an active component from immune serum could neutralize toxins, precipitate toxins, rupture (lyse) bacteria, and clump (agglutinate) bacteria. In each case, the active agent was named for the activity it exhibited: antitoxin, precipitin, bacterolysin, and agglutinin, respectively. Initially, a different serum component was thought to be responsible for each activity, but during the 1930s a single substance, called an **antibody**, was shown to be responsible for all of

TABLE 1-1

NOBEL PRIZES FOR IMMUNOLOGIC RESEARCH

YEAR	RECIPIENT	COUNTRY	RESEARCH
1901	Emil von Behring	Germany	Serum antitoxins
1905	Robert Koch	Germany	Cellular immunity to tuberculosis
1908	Elie Metchnikoff Paul Ehrlich	Russia Germany	Role of phagocytosis (Metchnikoff) and antitoxins (Ehrlich) in immunity
1913	Charles Richet	France	Anaphylaxis
1919	Jules Border	Belgium	Complement-mediated bacteriolysis
1930	Karl Landsteiner	U.S.A.	Discovery of human blood groups
1951	Max Theiler	South Africa	Development of yellow fever vaccine
1957	Daniel Bovet	Switzerland	Antihistamines
1960	F. Macfarlane Burnet Peter Medawar	Australia Great Britain	Discovery of acquired immunological tolerance
1972	Rodney R. Porter Gerald M. Edelman	Great Britain U.S.A.	Chemical structure of antibodies
1977	Rosalyn R. Yalow	U.S.A.	Development of radioimmunoassay
1980	George Snell Jean Dausset Baruj Benacerraf	U.S.A. France U.S.A.	Major histocompatibility complex
1984	Cesar Milstein Georges F. Köhler Niels K. Jerne	Great Britain Germany Denmark	Monoclonal antibody Immune regulatory theories
1987	Susumu Tonegawa	Japan	Gene rearrangement in antibody production
1991	E. Donnall Thomas Joseph Murray	U.S.A. U.S.A.	Transplantation immunology
1996	Peter C. Doherty Rolf M. Zinkernagel	Australia Switzerland	The specificity of the cell-mediated immune response

these activities. Because immunity was mediated by antibodies contained in body fluids (known at the time as *humors*), it was called **humoral immunity**.

In 1883, even before the discovery that a serum component could transfer immunity, Elie Metchnikoff demonstrated that cells also contribute to the immune state of an animal. He observed that certain white blood cells, which he termed **phagocytes**, were able to ingest microorganisms and other foreign material. Noting that these phagocytic cells were more active in immunized animals than nonimmunized animals, Metchnikoff hypothesized that cells, rather than serum components, were the major effector of immunity.

In due course, a controversy developed between those who held to the concept of humoral immunity and those who agreed with Metchnikoff's concept of **cell-mediated immunity**. The controversy eventually was resolved when the interrelated roles of humoral and cellular activities were demonstrated and both were shown to be necessary for the immune response. In the 1950s the **lymphocyte** was identified as the cell responsible for both cellular and humoral immunity.

Early Theories of Immunity

One of the greatest enigmas about the antibody molecule facing early immunologists was its specificity for foreign material, or **antigen**. Two major theories were proposed to account for this specificity: the selective theory and the instructional theory.

The earliest conception of the **selective theory** dates to Paul Ehrlich in 1900. In an attempt to explain the origin of serum antibody, Ehrlich proposed that cells expressed a variety of "side-chain" receptors that could react with infectious agents. Binding of an infectious agent to a side-chain receptor was envisioned as a complementary lock-and-key type of interaction. Ehrlich suggested that interaction between an infectious agent and a cell's side-chain receptor would result in release of the side chain and would induce the cell to produce and release more side-chain receptors with the same specificity. According to Ehrlich's theory, the side-chain specificity was determined prior to antigen exposure and antigen selected the appropriate side chain.

In the 1930s and 1940s the selective theory was replaced by various **instructional theories** in which antigen played a central role in determining the specificity of the antibody molecule. According to the instructional theories, a particular antigen would serve as a template around which antibody would fold. The antibody molecule would thereby assume a configuration complementary to that of the antigen template. Such concepts, first postulated by Friedrich Breinl and Felix Haurowitz and later popularized by Linus Pauling, made sense within the limitations of scientific knowledge at that time. But as new information emerged about the structure of DNA, RNA, and protein, the instructional theories were disproved.

In the 1950s, selection theories resurfaced and, through the insights of Niels Jerne, David Talmadge, and F. Macfarlane Burnet, were refined into a theory that came to be known as the **clonal-selection** theory. According to this theory, individual lymphocytes express membrane receptors that are specific for distinct antigens. Each lymphocyte expresses a unique receptor specificity, which is determined prior to antigen exposure. Binding of antigen to a specific receptor activates the cell, resulting in its proliferation into a **clone** of cells, each with the same immunologic specificity as the original parent cell. The clonal-selection theory has been further refined and is now accepted as the underlying paradigm of modern immunology. This theory is examined in more depth later in the chapter.

Components of Immunity

Immunity—the state of protection from infectious disease—has both nonspecific and specific components. **Innate**, or nonspecific, **immunity** refers to the basic resistance to disease that an individual is born with. **Acquired**, or specific, **immunity** requires the activity of a functional immune system, involving cells called lymphocytes and their products. Innate defense mechanisms provide the first line of host defense against invading pathogens until an acquired immune response develops. In general, most of the microorganisms encountered by a healthy individual are readily cleared within a few days by nonspecific defense mechanisms without enlisting a specific immune response. When an invading microorganism eludes the nonspecific host defense mechanisms, a specific immune response then is enlisted. Acquired immunity does not operate independently of innate immunity; rather, the specific immune response supplements and augments the nonspecific defense mechanisms, producing a more effective total response.

INNATE (NONSPECIFIC) IMMUNITY

Innate immunity can be envisioned as comprising four types of defensive barriers: anatomic, physiologic, endocytic and phagocytic, and inflammatory (Table 1-2).

Tissue damage and infection induce leakage of vascular fluid, containing serum proteins with antibacterial activity, and influx of phagocytic cells into the affected area.

Anatomic Barriers

Physical and anatomic barriers that tend to prevent the entry of pathogens are an organism's first line of defense against infection. The **skin** and the surface of **mucous membranes** are included in this category because they provide an effective barrier to the entry of most microorganisms.

The skin consists of two distinct layers: a relatively thin outer layer—the **epidermis**—and a thicker layer—the **dermis**. The epidermis contains several layers of tightly packed epithelial cells. The outer epidermal layer consists of dead cells and is filled with a waterproofing protein called keratin. Old epidermal cells are sloughed from the surface and are replaced by new cells derived from division of cells lying next to the dermis; as a result, the epidermis is completely renewed every 15–30 days. The epidermis does not contain blood vessels, and epidermal cells are instead bathed in nutrients that diffuse from the underlying dermis. The dermis, which is composed of connective tissue, contains blood vessels, hair follicles, sebaceous glands, and sweat glands. The sebaceous glands are associated with the hair follicles and produce an oily secretion called **sebum**. Sebum consists of lactic and fatty acids, maintaining the pH of the skin between 3 and 5, which is inhibitory to the growth of most microorganisms. A few bacteria that metabolize sebum live as commensals on the skin and are responsible for a severe form of acne. One acne drug, isotretinoin (Accutane), is a vitamin A derivative that prevents sebum formation.

Intact skin not only prevents the penetration of most pathogens but also inhibits most bacterial growth due to its low pH. Breaks in the skin, even small ones, resulting from wounds or abrasion are obvious routes of infection. The skin also is penetrated by biting insects (e.g., mosquitoes, mites, ticks, fleas, and sandflies); if these harbor pathogenic organisms, they can introduce the pathogen into the body as they feed. The protozoan that causes malaria, for example, is carried by mosquitoes who deposit it in humans when they take a blood meal. Similarly, bubonic plague is spread by the bite of fleas, and Lyme disease is spread by the bite of ticks.

The conjunctivae and the alimentary, respiratory, and urogenital tracts are lined by mucous membranes, not by the dry, protective skin covering the exterior of the body. These membranes consist of an outer epithelial layer

TABLE 1-2

SUMMARY OF NONSPECIFIC HOST DEFENSES

TYPE	MECHANISM
Atomic barriers	
Skin	Mechanical barrier retards entry of microbes. Acidic environment (pH 3–5) retards growth of microbes.
Mucous membranes	Normal flora compete with microbes for attachment sites and nutrients. Mucus entraps foreign microorganisms. Cilia propel microorganisms out of body.
Physiologic barriers	
Temperature	Body temperature inhibits growth of some pathogens. Fever response inhibits growth of some pathogens.
Low pH	Acidic pH of stomach kills most ingested microorganisms.
Chemical mediators	Lysozyme cleaves bacterial cell wall. Interferon induces antiviral state in uninfected cells. Complement lyses microorganisms or facilitates phagocytosis.
Phagocytic/endocytic barriers	Various cells internalize (endocytose) and break down foreign macromolecules. Specialized cells (blood monocytes, neutrophils, tissue macrophages) internalize (phagocytose), kill, and digest whole microorganisms.
Inflammatory barriers	Tissue damage and infection induce leakage of vascular fluid containing serum proteins with antibacterial activity, and influx of phagocytic cells into the affected area.

and an underlying connective tissue layer. Although most pathogens enter the body by binding to and penetrating mucous membranes, a number of nonspecific defense mechanisms serve to prevent this entry. For example, saliva, tears, and mucous secretions act to wash away potential invaders and also contain antibacterial or antiviral substances. The viscous fluid called **mucus**, which is secreted by epithelial cells of mucous membranes, entraps foreign microorganisms. In the lower respiratory tract and the gastrointestinal tract, the mucous membrane is covered by **cilia**, hairlike processes projecting from the epithelial cells. The synchronous movement of cilia propel mucous-entrapped microorganisms from these tracts. In addition, nonpathogenic organisms tend to colonize the epithelial cells of mucosal surfaces. These **normal flora** generally outcompete pathogens for attachment sites on the epithelial cell surface and for necessary nutrients.

Some organisms have evolved ways to escape this defense mechanism and thus are likely to invade the body through mucous membranes. For example, influenza virus (the agent that causes flu) has a surface molecule that enables it to attach firmly to cells in mucous membranes, preventing the virus from being swept out by the ciliated epithelial cells. Similarly, the organism causing gonorrhea has surface projections that allow it to bind to mucous membrane epithelial cells in the urogenital tract. Adherence of bacteria to mucous membranes involves interactions between hairlike protrusions on a bacterium, called **fimbriae** or **pili**, and certain glycoproteins or glycolipids that are only expressed by some mucous membrane epithelial cells (Figure 1-2). For this reason, some tissues are susceptible to bacterial invasion, whereas others are not.

The importance of anatomic barriers to host defense is vividly illustrated by a group of mice described in a report in *Nature*. These mice appeared to be immune to the parasitic helminth (worm) that causes schistosomiasis, a chronic and debilitating disease affecting more than 300 million people worldwide. After initial infection with this helminth, the mice developed portal hypertension similar to that observed in humans with schistosomiasis. However, when mice were reinfected with the helminth a second time, a very low yield of the helminth was recovered, and the mice appeared to be resistant to the infection. Because the mice had apparently developed immunity to the helminth, they were considered to be a potential animal model for the study of schistosomiasis in humans. After considerable funding was poured into research on this mouse model, the ability to clear the helminth was found to have nothing to do with a specific immune response; instead it resulted from a complex anatomic reorganization in blood vessel architecture that occurred at the time of the second injection. The *Nature* article warned "not to postulate immunological mechanisms where simple anatomical or physiological explanations might suffice."

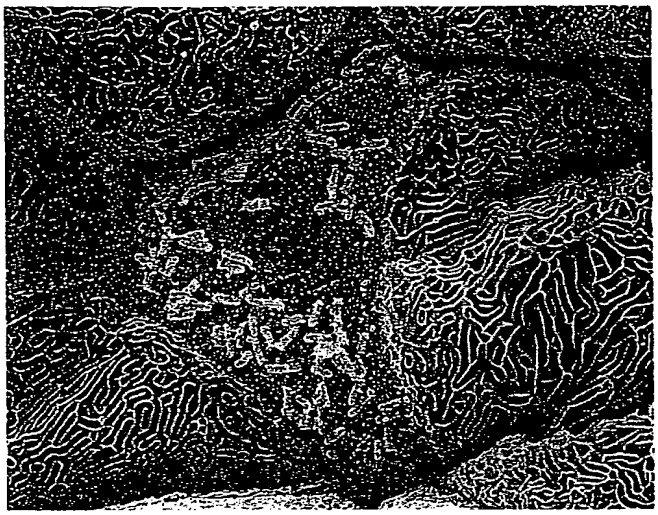

FIGURE 1-2

Electron micrograph of rod-shaped *Escherichia coli* bacteria adhering to surface of epithelial cells of the urinary tract. [From N. Sharon and H. Lis, 1993, *Sci. Am.* 268(1):85.]

Even when a pathogen eludes the anatomic defenses provided by the skin and mucous membranes, it still faces other types of innate defenses including various physiologic, phagocytic, and inflammatory barriers. Only by successfully evading these barriers can a pathogen become established in a host.

Physiologic Barriers

The physiologic barriers that contribute to innate immunity include temperature, pH, oxygen tension, and various soluble factors. Many species are not susceptible to certain diseases simply because their body temperature inhibits pathogen growth. Chickens, for example, display innate immunity to anthrax because their high body temperature inhibits the growth of this pathogen. Gastric acidity also provides an innate physiologic barrier to infection because very few ingested microorganisms can survive the low pH of the stomach. One reason newborns are susceptible to some diseases that do not afflict adults is that their stomach contents are less acid than that of adults.

A variety of soluble factors also contribute to nonspecific immunity. Among these soluble proteins are lysozyme, interferon, and complement. **Lysozyme**, a hydrolytic enzyme found in mucous secretions, is able to cleave the peptidoglycan layer of the bacterial cell wall. **Interferon** comprises a group of proteins produced by virus-infected cells. Among the many functions of the

interferons is the ability to bind to nearby cells and induce a generalized antiviral state. **Complement** is a group of serum proteins that circulate in an inactive proenzyme state. These proteins can be activated by a variety of specific and nonspecific immunologic mechanisms that convert the inactive proenzymes into active enzymes. The activated complement components participate in a controlled enzymatic cascade that results in damage to the membranes of pathogenic organisms, either destroying the pathogens or facilitating their clearance.

Endocytic and Phagocytic Barriers

Another important innate defense mechanism is the ingestion of extracellular macromolecules via **endocytosis** and of particulate material via **phagocytosis**. These two internalization processes not only bring different types of extracellular material into the cell, they also differ in several other ways.

In endocytosis, macromolecules within the extracellular tissue fluid are internalized by cells via the invagination (inward folding) and pinching off of small regions of the plasma membrane. The resultant endocytic vesicles are small, approximately 0.1 μm in diameter. Endocytosis occurs through one of two processes: **pinocytosis** or **receptor-mediated endocytosis** (Figure 1-3). In pinocytosis, nonspecific membrane invagination internalizes macromolecules in proportion to their extracellular concentration. In receptor-mediated endocytosis, macromolecules are selectively internalized after binding to specific membrane receptors.

The endocytic vesicles formed by either process fuse with each other and are delivered to **endosomes**, which are intracellular acidic compartments that serve a sorting function. The acidic interior of endosomes facilitates dissociation of macromolecular ligands from their receptors; the latter are then recycled back to the cell surface. Free macromolecules contained within endosomes fuse with

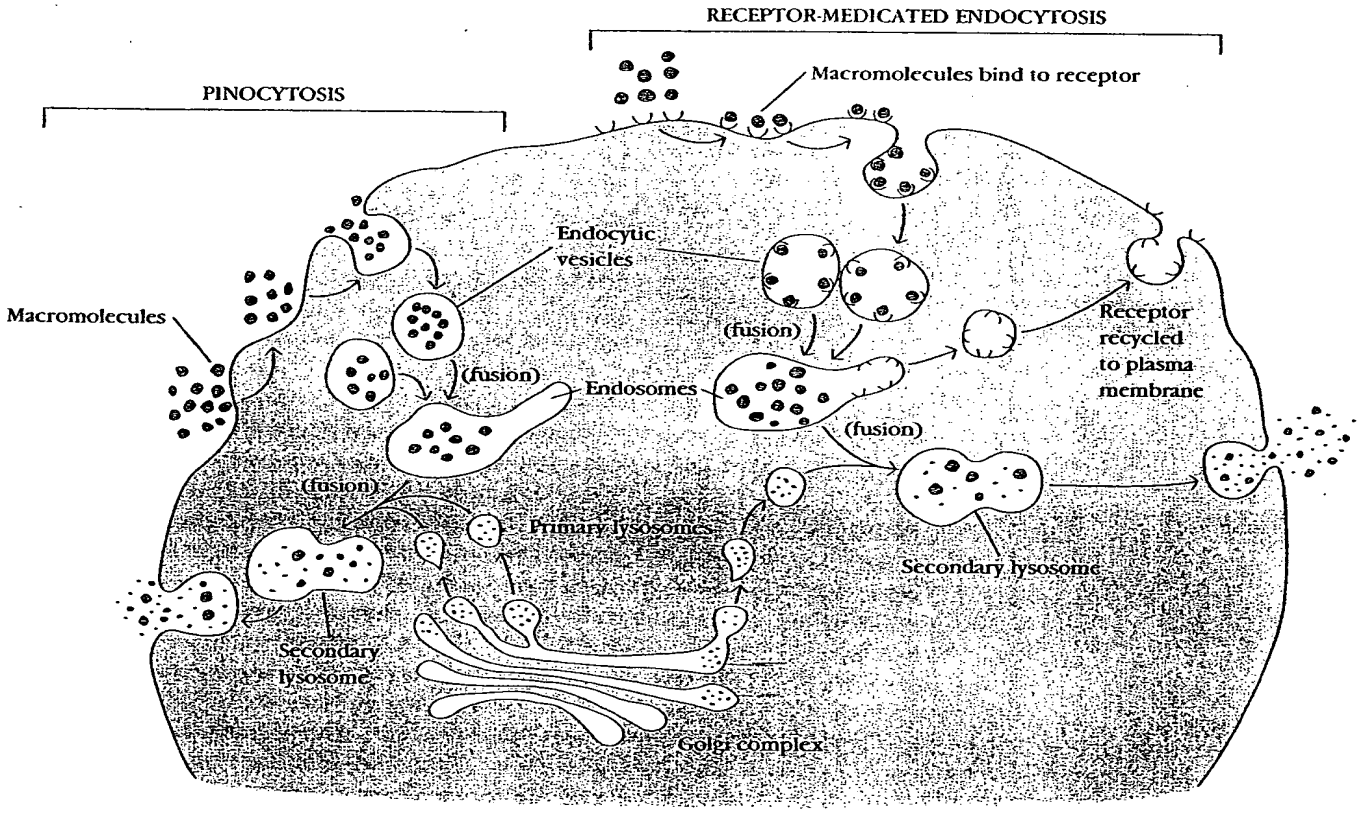

FIGURE 1-3

Endocytosis—the internalization of macromolecules within the extracellular fluid—occurs by pinocytosis or receptor-mediated endocytosis. In both processes, the ingested material is degraded via the endocytic processing pathway.

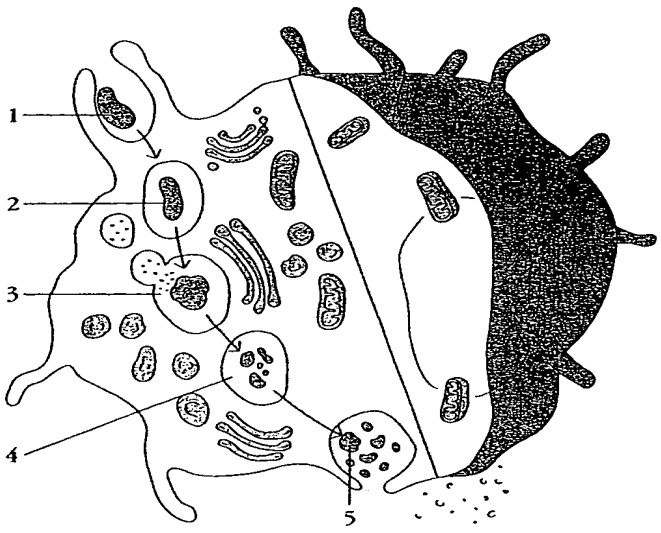

FIGURE 1-4

Phagocytosis of bacteria. Schematic diagram of the steps in phagocytosis: (1) attachment of a bacterium (blue) to long membrane evaginations, called pseudopodia; (2) ingestion of bacterium forming a phagosome, which moves toward a lysosome; (3) fusion of the lysosome and phagosome, releasing lysosomal enzymes into the phagosome; (4) digestion of ingested material; and (5) release of digestion products from the cell.

primary lysosomes to form structures known as **secondary lysosomes**. Primary lysosomes are derived from the Golgi complex and contain large numbers of degradative enzymes, including proteases, nucleases, lipases, and other hydrolytic enzymes. Within secondary lysosomes, the ingested macromolecules are then digested into small breakdown products (e.g., peptides, nucleotides, and sugars), which eventually are eliminated from the cell.

Phagocytosis involves the ingestion of particulate material, including whole pathogenic microorganisms (Figure 1-4). In phagocytosis the plasma membrane expands around the particulate material to form large vesicles called **phagosomes**. These vesicles are roughly 10–20 times larger than endocytic vesicles. The expansion of the membrane in phagocytosis requires participation of microfilaments, which do not take part in endocytosis. Another difference between the two processes is that only specialized cells are capable of phagocytosis, whereas virtually all cells are capable of endocytosis. The specialized phagocytic cells include blood monocytes, neutrophils, and tissue macrophages (see Chapter 3). Once particulate material is ingested into phagosomes, the phagosomes fuse with lysosomes and the ingested material is then digested in the endocytic processing pathway by a process similar to that seen in endocytosis.

Barriers Created by the Inflammatory Response

Tissue damage caused by a wound or by invasion by a pathogenic microorganism induces a complex sequence of events collectively known as the **inflammatory response**. Many of the classic features of the inflammatory response were described as early as 1600 B.C. in Egyptian papyrus writings. In the first century A.D., the Roman physician Celsus described the "four cardinal signs of inflammation" as *rubor* (redness), *tumor* (swelling), *calor* (heat), and *dolor* (pain). In the second century A.D., another physician, Galen, added a fifth sign: *functio laesa* (loss of function).

The cardinal signs of inflammation reflect the three major events that occur during an inflammatory response (Figure 1-5):

1. **Vasodilation**—an increase in the diameter of blood vessels—occurs as the vessels that carry blood away from an affected area constrict, resulting in engorgement of the capillary network. The engorged capillaries are responsible for tissue redness (*erythema*) and an increase in tissue temperature.
2. An **increase in capillary permeability** facilitates an influx of fluid and cells from the engorged capillaries into the tissue. The fluid that accumulates (**exudate**) has a much higher protein content than fluid normally released from the vasculature. Accumulation of exudate contributes to tissue swelling (**edema**).
3. **Influx of phagocytes** from the capillaries into the tissues is facilitated by the increased capillary permeability. The emigration of phagocytes involves a complex series of events including adherence of the cells to the endothelial wall (**margination**) followed by their emigration between the capillary endothelial cells into the tissue (**diapedesis** or **extravasation**) and, finally, their migration through the tissue to the site of the inflammatory response (**chemotaxis**). As phagocytic cells accumulate at the site and begin to phagocytose bacteria, they release lytic enzymes, which can damage nearby healthy cells. The accumulation of dead cells, digested material, and fluid forms a substance called pus.

The events in the inflammatory response are initiated by a complex series of interactions involving a variety of chemical mediators, whose interactions are still only partially understood. Some of these mediators are derived from invading microorganisms, some are released from damaged cells in response to tissue injury, some are generated by several plasma enzyme systems, and some are products of various white blood cells participating in the inflammatory response.

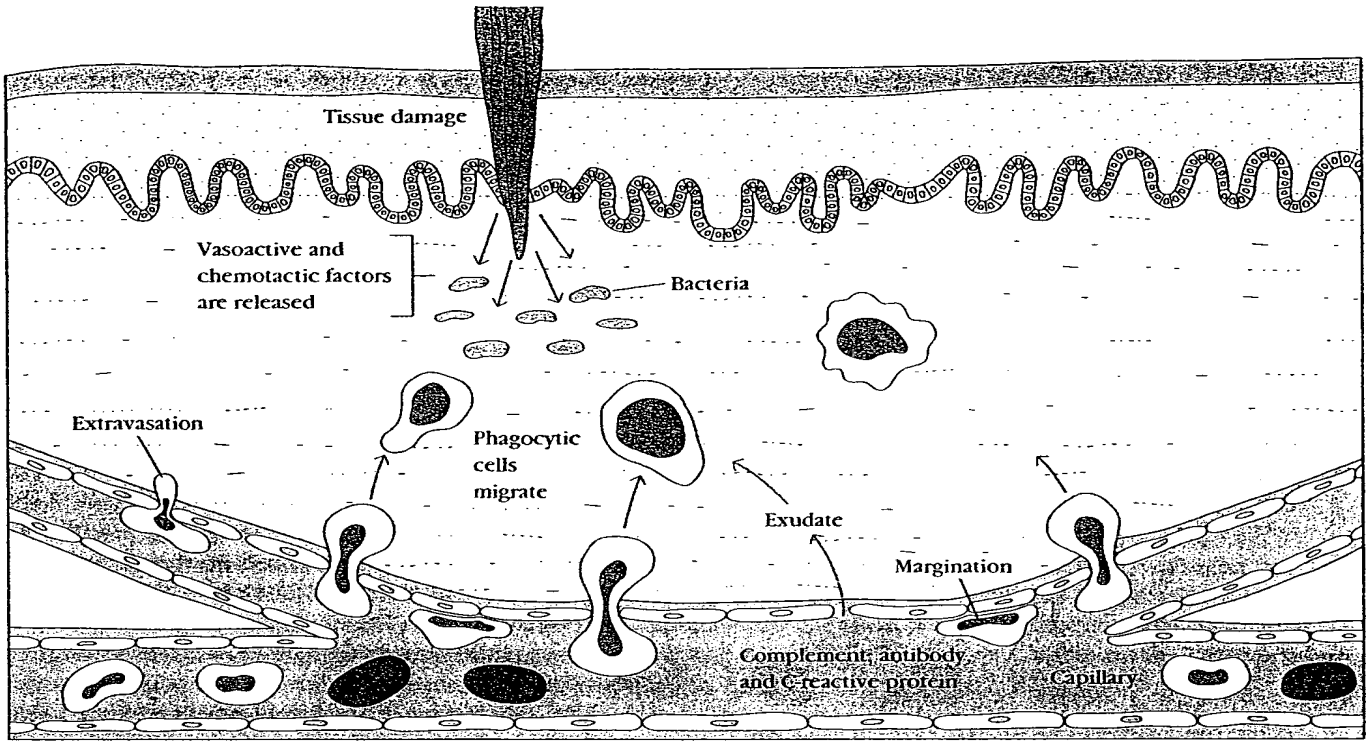

FIGURE 1-5

Major events in the inflammatory response. A bacterial infection causes tissue damage with release of various vasoactive and chemotactic factors. These factors induce increased blood flow to the area, increased capillary permeability, and an influx of white blood cells, including phagocytes and lymphocytes, from the blood into the tissues. The serum proteins contained in the exudate have antibacterial properties, and the phagocytes begin to engulf the bacteria, as illustrated in Figure 1-4.

Among the chemical mediators released in response to tissue damage are various serum proteins called **acute-phase proteins**. The concentrations of these proteins increase dramatically in tissue-damaging infections. C-reactive protein—a major acute-phase protein produced by the liver in response to tissue damage—binds to the C-polysaccharide cell-wall component found on a variety of bacteria and fungi. This binding activates the complement system, resulting in increased clearance of the pathogen either by complement-mediated lysis of the pathogen or by complement-mediated increase in phagocytosis.

One of the principal mediators of the inflammatory response is **histamine**, a chemical released by a variety of cells in response to tissue injury. Histamine binds to receptors on nearby capillaries and venules, causing vasodilation and increased permeability. Another important group of inflammatory mediators, small peptides called **kinins**, are present in an inactive form in blood plasma. Tissue injury induces activation of these peptides, which then cause vasodilation and increased capillary permeability. A particular kinin, called bradykinin, also stimulates pain receptors in the skin. This effect probably serves a protective role because pain normally causes an individual to protect the injured area.

Vasodilation and the increase in capillary permeability that occur in an injured tissue also enable enzymes of the blood-clotting system to enter the tissue. These enzymes activate an enzyme cascade that results in the deposition of insoluble strands of **fibrin**, which are the main component of a blood clot. The fibrin clots wall off the injured area from the rest of the body and serve to prevent the spread of infection.

Once the inflammatory response has subsided and most of the debris has been cleared away by phagocytic cells, tissue repair and regeneration of new tissue occur. Tissue repair begins as capillaries grow into the fibrin of a blood clot. New connective tissue cells, called fibroblasts, replace the fibrin as the clot dissolves. As fibroblasts and capillaries accumulate, scar tissue is formed. The inflammatory response is discussed in more detail in Chapter 15.

ACQUIRED (SPECIFIC) IMMUNITY

Acquired, or specific, immunity reflects the presence of a functional immune system that is capable of specifically recognizing and selectively eliminating foreign microorganisms and molecules (i.e., foreign antigens). Unlike innate immune responses, acquired immune responses are adaptive and display four characteristic attributes:

- Antigenic specificity
- Diversity
- Immunologic memory
- Self/nonself recognition

The **antigenic specificity** of the immune system permits it to distinguish subtle differences among antigens. Antibodies can differentiate between two molecules that differ by only a single amino acid. The immune system is capable of generating tremendous **diversity** in its recognition molecules, allowing it to specifically recognize billions of uniquely different structures on foreign antigens. Once the immune system has recognized and responded to an antigen, it exhibits **immunologic memory**; that is, a second encounter with the same antigen induces a heightened state of immune reactivity. Because of this attribute, the immune system can confer life-long immunity to many infectious agents. Finally, the immune system normally responds only to foreign antigens indicating that it is capable of **self/nonself recognition**. The ability of the immune system to distinguish self from nonself and respond only to nonself-molecules is essential, for the outcome of an inappropriate response to self-molecules can be a fatal autoimmune disease.

As noted already, acquired immunity does not occur independently of innate immunity. The phagocytic cells crucial to nonspecific immune responses are intimately involved in activation of the specific immune response. Conversely, various soluble factors, produced during a specific immune response, have been shown to augment the activity of these phagocytic cells. As an inflammatory response develops, for example, soluble mediators are produced that attract cells of the immune system. The immune response will, in turn, serve to regulate the intensity of the inflammatory response. Through the carefully regulated interplay of acquired and innate immunity, the two systems work together to eliminate a foreign invader.

Cells of the Immune System

Generation of an effective immune response involves two major groups of cells: **lymphocytes** and **antigen-presenting cells**. Lymphocytes are one of many types of white blood cells produced in the bone marrow during the process of hematopoiesis (see Chapter 3). Lymphocytes leave the bone marrow, circulate in the blood and lymph system, and reside in various lymphoid organs. Lymphocytes, which possess antigen-binding cell-surface receptors, mediate the defining immunologic attributes of specificity, diversity, memory, and self/nonself recognition. The two major populations of lymphocytes—**B lymphocytes (B cells)** and **T lymphocytes (T cells)**—are described briefly here and in greater detail in later chapters.

B Lymphocytes

B lymphocytes mature within the bone marrow and leave the marrow expressing a unique antigen-binding receptor on their membrane (Figure 1-6a). The B-cell receptor is a membrane-bound **antibody molecule**. Antibodies are glycoproteins. The basic structure of the antibody molecule consists of two identical heavy polypeptide chains and two identical light polypeptide chains. The chains are held together by disulfide bonds. The amino-terminal ends of each pair of heavy and light chains form a cleft within which antigen binds. When a **naive** B cell, which has not previously encountered antigen, first encounters the antigen for which its membrane-bound antibody is specific, the cell begins to divide rapidly; its progeny differentiate into **memory B cells** and **effector B cells** called **plasma cells**.

Memory B cells have a longer life span and continue to express membrane-bound antibody with the same specificity as the original parent naive B cell. Plasma cells do not express membrane-bound antibody; instead they produce the antibody in a form that can be secreted. Although plasma cells live for only a few days, they secrete enormous amounts of antibody during this time. It has been estimated that a single plasma cell can secrete more than 2000 molecules of antibody per second. Secreted antibodies are the major effector molecule of humoral immunity.

T Lymphocytes

T lymphocytes also arise from hematopoietic stem cells in the bone marrow. Unlike B cells, which mature within the bone marrow, T cells migrate to the thymus gland to mature. During its maturation within the thymus, the T cell comes to express a unique antigen-binding receptor on its membrane, called the **T-cell receptor**. Unlike membrane-bound antibodies on B cells, which can recognize antigen alone, T-cell receptors can only recognize antigen that is associated with cell-membrane proteins known as **major histocompatibility complex (MHC)**

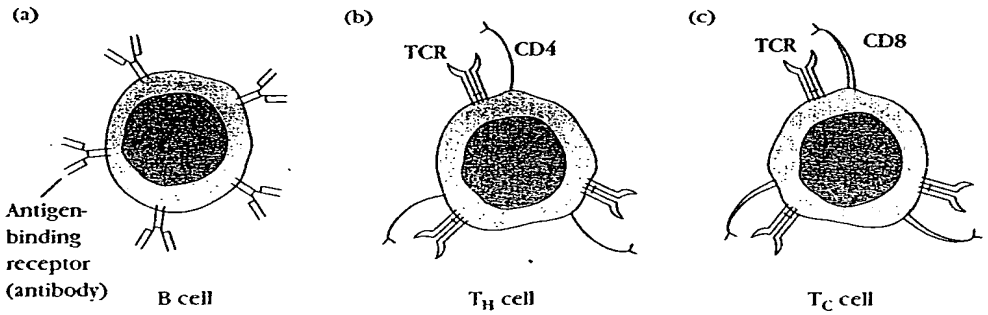

FIGURE 1-6

Distinctive membrane molecules on lymphocytes. (a) B cells have about 10^5 molecules of membrane-bound antibody per cell. All the antibody molecules on a given B cell exhibit the same antigenic specificity and can interact directly with antigen. (b) T cells bearing CD4 only recognize antigen associated with class II MHC molecules. (c) T cells bearing CD8 only recognize antigen associated with class I MHC molecules. In general, $CD4^+$ T cells function as helper cells and $CD8^+$ cells function as cytotoxic cells. Both types of T cells express about 10^5 identical molecules of the antigen-binding T-cell receptor (TCR) per cell, each with the same antigenic specificity.

molecules. When a naive T cell encounters antigen associated with an MHC molecule on a cell, the T cell proliferates and differentiates into memory T cells and various effector T cells.

There are two well-defined subpopulations of T cells: **T helper (T_H)** and **T cytotoxic (T_C) cells**. Although a third type of T cell, called a T suppressor (T_S) cell, has been postulated, recent evidence suggests that it may not be distinct from the T_H and T_C subpopulations. T helper and T cytotoxic cells can be distinguished from one another by the presence of either membrane glycoproteins **CD4** or **CD8** on their surfaces (Figure 1-6b,c). T cells displaying CD4 generally function as T_H cells, whereas those displaying CD8 generally function as T_C cells (see Chapter 3).

After a T_H cell recognizes and interacts with an antigen–MHC II molecule complex, the cell is activated and becomes an effector cell that secretes various growth factors known collectively as **cytokines**. The secreted cytokines play an important role in activating B cells, T_C cells, macrophages, and various other cells that participate in the immune response. Differences in the pattern of cytokines produced by activated T_H cells results in qualitative differences in the type of immune response that develops.

Under the influence of T_H-derived cytokines, a T_C cell that recognizes an antigen–MHC I molecule complex proliferates and differentiates into an effector cell called a **cytotoxic T lymphocyte** (CTL). In contrast to the T_H cell, the CTL generally does not secrete many cytokines and instead exhibits cytotoxic activity. The CTL has a vital function in monitoring the cells of the body and eliminating any that display antigen, such as virus-infected cells, tumor cells, and cells of a foreign tissue graft. Such cells displaying foreign antigen complexed to an MHC molecule are called **altered self-cells**.

Antigen-Presenting Cells

Activation of both the humoral and cell-mediated branches of the immune system requires cytokines produced by T_H cells. It is essential that activation of T_H cells be carefully regulated because an inappropriate T_H-cell response to self-components can have fatal autoimmune consequences. To ensure carefully regulated activation of T_H cells, they only can recognize antigen that is displayed together with class MHC II molecules on the surface of antigen-presenting cells (APCs). These specialized cells, which include macrophages, B lymphocytes, and dendritic cells, are distinguished by two properties: (1) they express class II MHC molecules on their membrane, and (2) they are able to deliver a co-stimulatory signal that is necessary for T_H-cell activation.

Antigen-presenting cells first internalize antigen, either by phagocytosis or by endocytosis, and then re-express a part of that antigen, together with a class II MHC molecule, on their membrane. The T_H cell recognizes and interacts with the antigen–MHC molecule complex on the membrane of the antigen-presenting cell (Figure 1-7). An additional co-stimulatory signal is then provided by the antigen-presenting cell, leading to activation of the T_H cell.

Functions of Humoral and Cell-Mediated Immune Responses

As mentioned earlier, immune responses can be divided into humoral and cell-mediated responses. The term

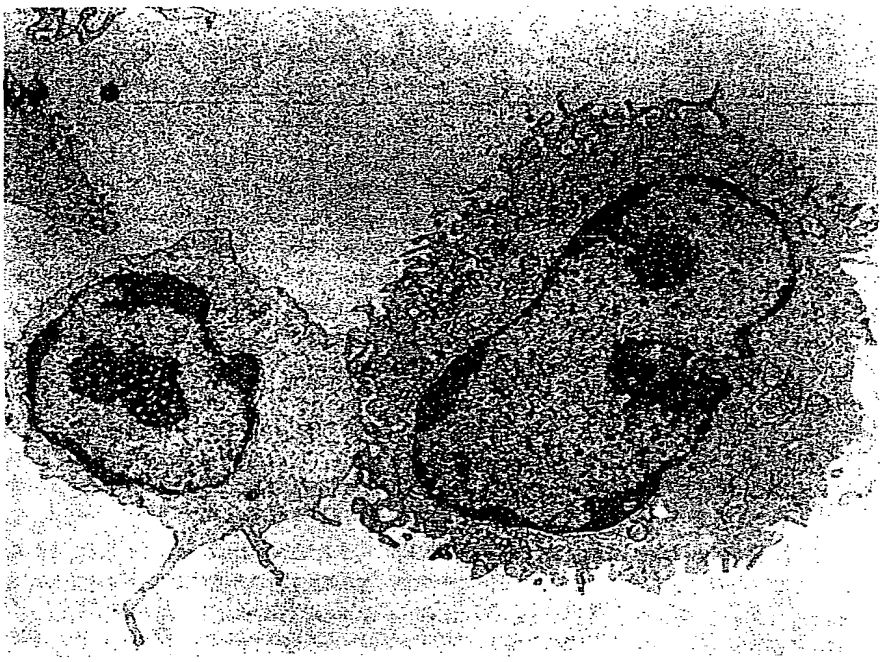

FIGURE 1-7

Electron micrograph of an antigen-presenting macrophage (*right*) associating with a T lymphocyte. [From A. S. Rosenthal et al., 1982, in *Phagocytosis—Past and Future*, Academic Press, p. 239.]

humoral is derived from the Latin *humor*, meaning "body fluid"; thus humoral immunity refers to immunity that can be conferred on a nonimmune individual by administration of serum antibodies from an immune individual. In contrast, cell-mediated immunity can be transferred only by administration of T cells from an immune individual.

The humoral branch of the immune system involves interaction of B cells with antigen and their subsequent proliferation and differentiation into antibody-secreting plasma cells (Figure 1-8). Antibody functions as the effector of the humoral response by binding to antigen and neutralizing it or facilitating its elimination. When an antigen is coated with antibody, it can be eliminated in several ways. For example, antibody can cross-link the antigen, forming clusters that are more readily ingested by phagocytic cells. Binding of antibody to antigen on a microorganism also can activate the complement system, resulting in lysis of the foreign organism. Antibody can also neutralize toxins or viral particles by coating them and preventing their subsequent binding to host cells.

Effector T cells generated in response to antigen are responsible for cell-mediated immunity (see Figure 1-8). Both activated T_H cells and CTLs serve as effector cells in cell-mediated immune reactions. Cytokines secreted by T_H cells can activate various phagocytic cells, enabling them to phagocytose and kill microorganisms more effectively. This type of cell-mediated immune response is especially important in host defense against intracellular bacteria and protozoa. Cytotoxic T lymphocytes (CTLs) participate in cell-mediated immune reactions by killing altered self-cells; they play an important role in the killing of virus-infected cells and tumor cells.

Recognition of Antigen by B and T Lymphocytes

Antigens, which are generally very large and complex, are not recognized in their entirety by lymphocytes. Instead, both B and T lymphocytes recognize discrete sites on the antigen called **antigenic determinants**, or **epitopes**. Epitopes are the immunologically active regions on a complex antigen, the regions that actually bind to B-cell or T-cell receptors.

Although B cells can recognize an epitope alone, T cells can recognize an epitope only when it is associated with an MHC molecule on the surface of a self-cell (either an antigen-presenting cell or altered self-cell). The two branches of the immune system are therefore uniquely suited to recognize antigen in different milieus. The humoral branch (B cells) recognizes an enormous variety of epitopes: those displayed on the surface of bacteria or viral particles, as well as those displayed on soluble proteins, glycoproteins, polysaccharides, or lipopolysaccharides that have been released from invading pathogens. The cell-mediated branch (T cells) recognizes protein epitopes displayed together with MHC molecules on self-cells, including altered self-cells such as virus-infected self-cells and cancerous cells.

Visualizing Concepts

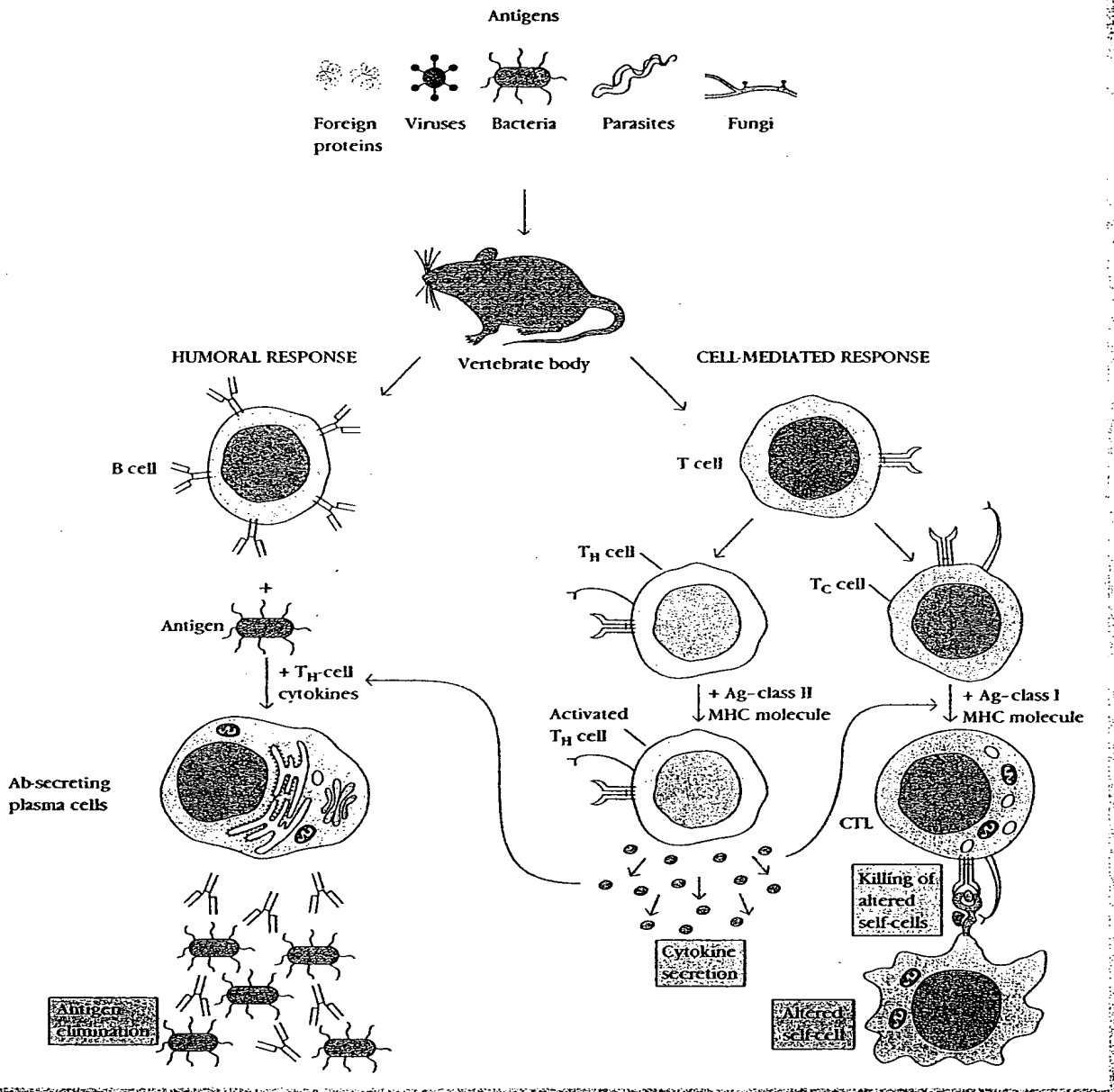

FIGURE 1.8

Overview of the humoral and cell-mediated branches of the immune system. The humoral response involves interaction of B cells with antigen (Ag) and their differentiation into antibody-secreting plasma cells. The secreted antibody (Ab) binds to the antigen and facilitates its clearance from the body. The cell-mediated response involves various subpopulations of T cells that recognize antigen presented on self cells. T_H cells respond to antigen by producing cytokines. T_C cells respond to antigen by developing into cytotoxic T lymphocytes (CTLs), which mediate killing of altered self cells (e.g., virus-infected cells).

Thus, four related but distinct cell-membrane molecules are responsible for antigen recognition by the immune system:

- Membrane-bound antibodies on B cells
- T-cell receptors
- Class I MHC molecules present on all nucleated cells
- Class II MHC molecules present on antigen-presenting cells.

Each of these molecules plays a unique role in antigen recognition, ensuring that the immune system can recognize and respond to the different types of antigen that it encounters.

Generation of Lymphocyte Specificity and Diversity

The antigenic specificity of each B cell is determined by the membrane-bound antigen-binding receptor (i.e., antibody) expressed by the cell. The antibody on a B cell can recognize different epitopes on macromolecules with incredible precision. For example, protein antigens that differ by only a single amino acid often can be discriminated from each other. As a B cell matures in the bone marrow, its specificity is generated by random rearrangements of a series of gene segments encoding the antibody molecule (see Chapter 7). As a result of this process, each mature B cell possesses a single functional gene encoding the antibody heavy chain and a single functional gene encoding the antibody light chain; the cell therefore synthesizes and displays antibody with one specificity on its membrane. All 10^5 antibody molecules on a given B lymphocyte have identical specificity, giving each B lymphocyte, and the clone of daughter cells to which it gives rise, a distinct specificity for antigen. The mature B lymphocyte is therefore said to be **antigenically committed**.

The fine specificity of the antibody molecule is coupled to an enormous diversity. The random gene rearrangements that occur during B-cell maturation in the bone marrow generate an enormous number of different antigenic specificities. The resulting B-cell population, which consists of individual B cells each exhibiting antibody with a distinct specificity, is estimated to collectively exhibit more than 10^8 different antigenic specificities. This enormous diversity in the antigenic specificity of the mature B-cell population is later reduced by a selection process in the bone marrow that eliminates any B cells whose membrane-bound antibody recognizes self-components. This process helps to ensure that self-reactive antibodies (auto-antibodies) are not produced.

The attributes of specificity and diversity also characterize the antigen-binding T-cell receptor (TCR) on T cells. As in B-cell maturation, the process of T-cell maturation involves random rearrangements of a series of gene segments encoding the cell's antigen-binding receptor (see Chapter 11). Each T lymphocyte expresses about 10^5 receptors per cell, and all 10^5 receptors on a cell and its clonal progeny have identical specificity for antigen. The random rearrangement of the TCR genes is capable of generating on the order of 10^{15} unique antigenic specificities. This enormous potential diversity is later diminished through a selection process in the thymus that eliminates any T cell with self-reactive receptors and ensures that only T cells with receptors capable of recognizing antigen associated with MHC molecules will be able to mature (see Chapter 12).

Role of the Major Histocompatibility Complex

The major histocompatibility complex (MHC) is a large genetic complex with multiple loci. The MHC loci encode two major classes of membrane molecules: **class I** and **class II MHC molecules**. As noted previously, T_H cells generally recognize antigen associated with a class II molecule, whereas T_C cells generally recognize antigen associated with class I molecules (Figure 1-9).

Class I MHC molecules are glycoproteins found on the membrane of nearly all nucleated cells, always in association with a small protein called β_2-microglobulin. There are three class I loci in humans (*A*, *B*, and *C*) and two in mice (*K* and *D*). Class II MHC molecules are heterodimeric glycoproteins, consisting of an α and β chain, expressed by the various specialized cells that function as antigen-presenting cells. There are three class II loci in humans (*DR*, *DP*, and *DQ*) and two in mice (*IA* and *IE*). Each class II locus encompasses an α gene and a β gene, which respectively encode the α and β chains of the class II MHC molecule. Both class I and class II MHC genes are highly polymorphic; that is, within a species each gene exists in many different forms, called **alleles**. Because an individual inherits one allele from each parent for each locus, multiple class I MHC molecules are expressed on each nucleated cell in the body; in addition, multiple class II molecules are expressed on antigen-presenting cells.

MHC molecules also function as antigen-recognition molecules, but they do not possess the fine specificity for antigen characteristic of antibodies and T-cell receptors. Rather, individual MHC molecules bind to a spectrum of **antigenic peptides** derived from degradation of antigen molecules. In both class I and class II MHC molecules the distal regions (farthest from the membrane) of different alleles display wide variation in their amino acid sequences. These distal regions form a cleft within which the antigenic peptide sits and is presented to T lympho-

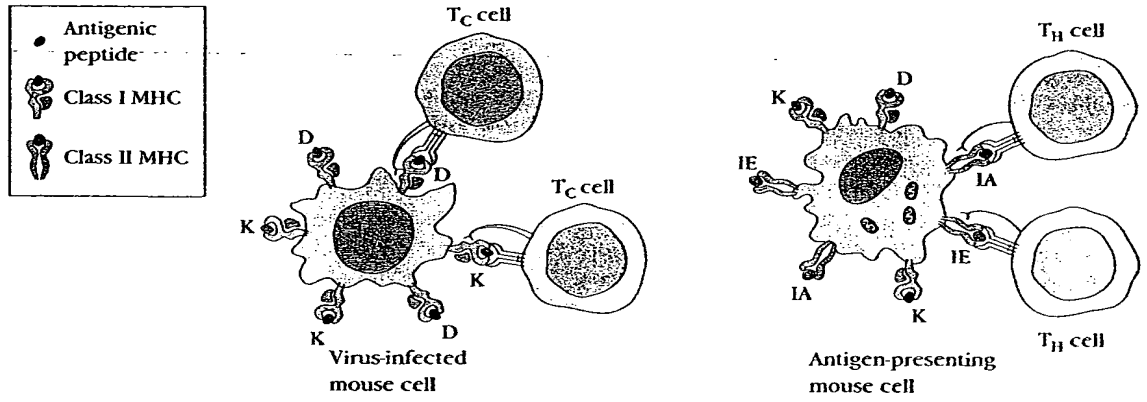

FIGURE 1-9

Role of MHC molecules in antigen recognition by T cells. Class I MHC molecules are encoded by the *K* and *D* loci in mice (*A*, *B*, and *C* loci in humans) and are expressed on nearly all nucleated cells. Class II MHC molecules are encoded by the *IA* and *IE* loci in mice (*DP*, *DQ*, and *DR* loci in humans) and are expressed only on antigen-presenting cells. $CD4^+$ T cells only recognize antigenic peptides displayed with a class II MHC molecule; they generally function as T helper (T_H) cells. $CD8^+$ T cells only recognize antigenic peptides displayed with a class I MHC molecule; they generally function as T cytotoxic (T_C) cells.

cytes (see Figure 1-9). Different allelic forms of the genes encoding class I and class II molecules confer different structures on the antigen-binding cleft with different specificity. Thus the ability to present an antigen to T lymphocytes is influenced by the particular set of alleles that an individual inherits.

Processing and Presentation of Antigens

In order for a foreign protein antigen to be recognized by a T cell it must be degraded into small antigenic peptides that form physical complexes with class I or class II MHC molecules. This conversion of proteins into MHC-associated peptide fragments is called antigen processing and presentation. Whether a particular antigen will be processed and presented together with class I MHC or class II MHC molecules appears to be determined by the route that the antigen takes to enter a cell (Figure 1-10).

Exogenous antigen is produced outside of the host cell and enters the cell by endocytosis or phagocytosis. Antigen-presenting cells (macrophages, dendritic cells, and B cells) degrade ingested exogenous antigen into peptide fragments within the endocytic processing pathway. Experiments suggest that class II MHC molecules are expressed within the endocytic processing pathway and that peptides produced by degradation of antigen in this pathway bind to the cleft within the class II MHC molecules. The MHC molecules bearing the peptide then are exported to the cell surface. Since expression of class II MHC molecules is limited to antigen-presenting cells, presentation of exogenous peptide–class II MHC complexes is limited to these cells. T cells displaying CD4 recognize antigen associated with class II MHC molecules and thus are said to be class II MHC restricted. These cells generally function as T helper cells.

Endogenous antigen is produced within the host cell itself. Two common examples are viral proteins synthesized within virus-infected host cells and unique proteins synthesized by cancerous cells. Endogenous antigens are thought to be degraded into peptide fragments that bind to class I MHC molecules within the endoplasmic reticulum. The peptide–class I MHC complex is then transported to the cell membrane. Since all nucleated cells express class I MHC molecules, all cells producing endogenous antigen use this route to process the antigen. T cells displaying CD8 recognize antigen associated with class I MHC molecules and thus are said to be class I MHC restricted. These cells generally function as T cytotoxic cells.

Clonal Selection of Lymphocytes

A mature immunocompetent animal contains a large number of antigen-reactive clones of T and B lymphocytes; the antigenic specificity of each of these clones is determined by the specificity of the antigen-binding receptor on the membrane of the clone's lymphocytes. As noted earlier, the specificity of each T and B lymphocyte

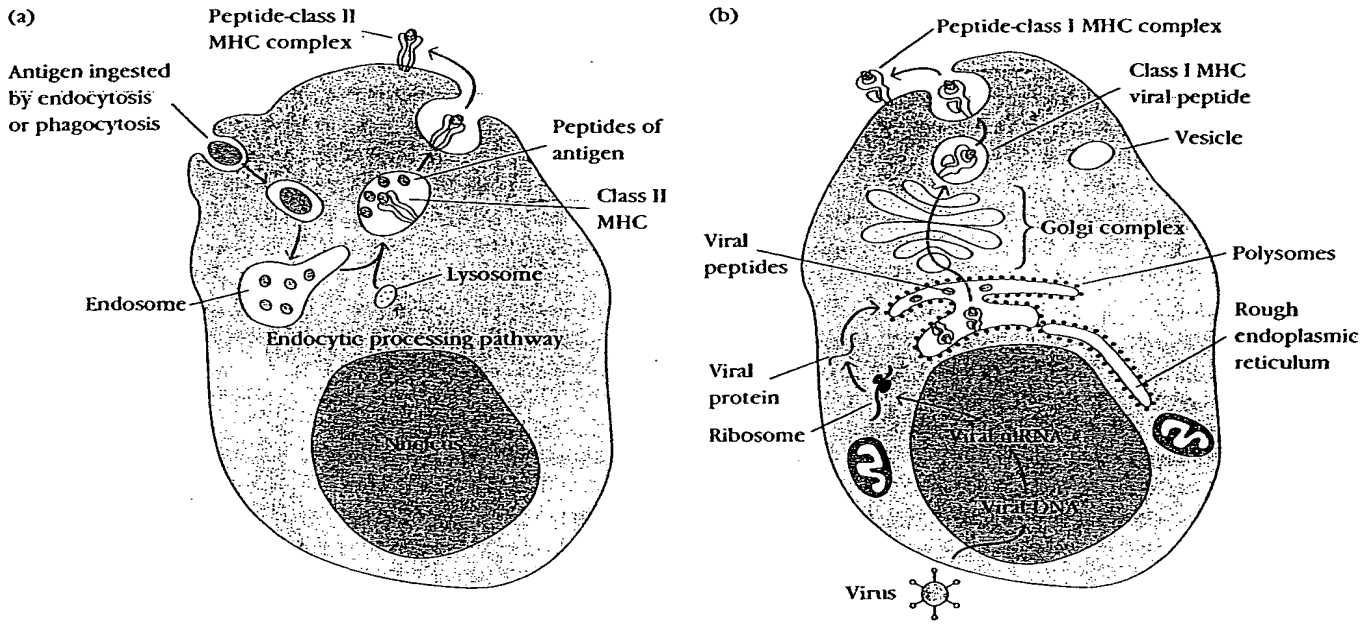

FIGURE 1-10

Processing and presentation of exogenous and endogenous antigens. (a) Exogenous antigen is ingested by endocytosis or phagocytosis and then enters the endocytic processing pathway. Here, within an acidic environment, the antigen is degraded into small peptides, which then are presented with class II MHC molecules on the membrane of the antigen-presenting cell. (b) Endogenous antigen, which is produced within the cell itself (e.g., in a virus-infected cell), is degraded within the cytoplasm into peptides, which move into the endoplasmic reticulum where they bind to class I MHC molecules. The peptide–class I MHC complexes then move via the Golgi complex to the cell surface.

is determined prior to its contact with antigen by random gene rearrangements in the bone marrow or thymus during maturation of lymphocytes.

The role of antigen becomes critical when it interacts with and activates mature, antigenically committed T and B lymphocytes, bringing about expansion of the population of cells with a given antigenic specificity. In this process of **clonal selection**, an antigen binds to and stimulates a particular T or B cell to undergo mitosis and develop into a clone of cells with the same antigenic specificity as the original parent cell (Figure 1-11).

Clonal selection provides a framework for understanding the specificity and self/nonself recognition characteristic of acquired immunity. Specificity is shown because only lymphocytes whose receptors are specific for a given epitope on an antigen will be clonally expanded and thus mobilized for an immune response. Self/nonself discrimination is accomplished by the clonal elimination, during development, of lymphocytes bearing self-reactive receptors or by the functional suppression of these cells in adults.

Immunologic memory also is a consequence of clonal selection. During clonal selection the number of lymphocytes specific for a given antigen is greatly amplified. Moreover, many of these lymphocytes, referred to as memory cells, appear to have a longer life span than the naive lymphocytes from which they arise. The initial encounter of a naive immunocompetent lymphocyte with an antigen induces a **primary response**; a second contact with antigen will induce a more rapid and heightened **secondary response**. The amplified population of memory cells accounts for the more rapid and intense response that characterizes a secondary response and distinguishes it from the initial primary response.

In the humoral branch of the immune system, antigen induces the clonal proliferation of B lymphocytes into antibody-secreting plasma cells and memory B cells. As seen in Figure 1-12a, the initial primary response has a lag of approximately 5–7 days before antibody levels start to rise. This lag is the time required for activation of naive B cells by antigen and T_H cells and for the subsequent proliferation and differentiation of the activated B cells into antibody-secreting plasma cells. Antibody levels peak in the primary response at about day 14 and then begin to drop off as the plasma cells begin to die. In the secondary response the lag is much shorter (only 1–2 days) and antibody levels are much higher and are sustained for a much longer time. The secondary response reflects the response of the clonally expanded population of memory B cells. These memory cells respond to the antigen more rapidly

than the naive B cells; in addition, because there are many more memory cells than naive B cells, larger numbers of plasma cells are generated during the secondary response and antibody levels are consequently 100-fold to 1000-fold higher.

In the cell-mediated branch, the recognition of an antigen-MHC complex by a specific mature T lymphocyte induces clonal proliferation into various T cells with effector functions (e.g., T_H cells and CTLs) and into memory T cells. The cell-mediated response to a skin graft is depicted in Figure 1-12b. When skin from a strain C mouse is grafted onto a strain A mouse, a primary response develops and the graft is rejected in about 10–14 days. If strain C is grafted a second time onto the same mouse, it is rejected much more vigorously and rapidly than the first graft. If a primary graft from a strain B mouse is grafted onto a strain A mouse together with the graft from strain C, the response to strain B is a typical primary response. That is, the graft rejection is a specific immune response. The mouse shows a secondary response to graft C, it gives a primary response to graft B. The increased speed of rejection of graft C reflects the

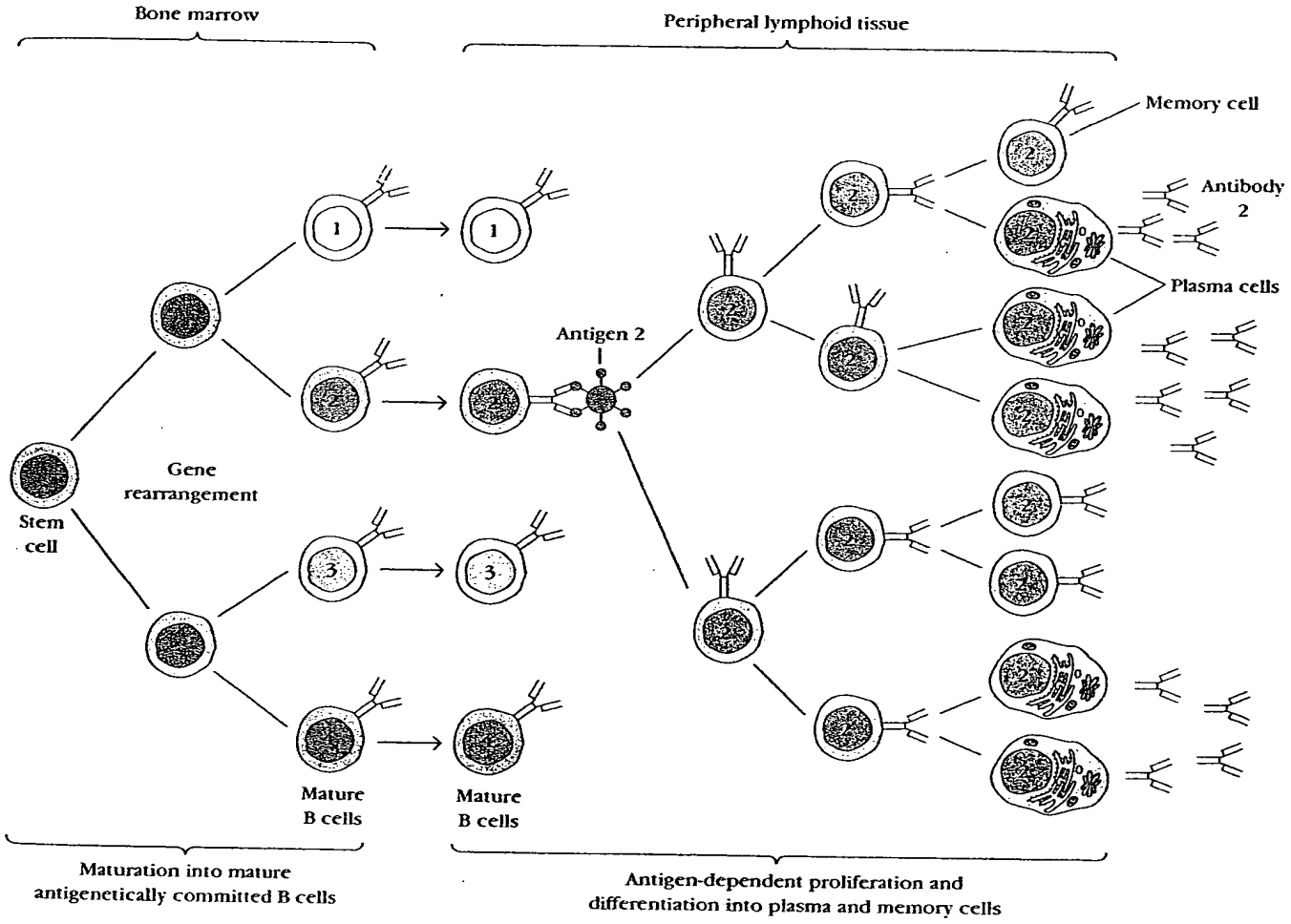

FIGURE 1-11

Maturation and clonal selection of B lymphocytes. Maturation, which occurs in the absence of antigen, produces antigenically committed B cells, each of which expresses antibody with a single antigenic specificity (indicated by 1, 2, 3, and 4). Clonal selection occurs when a given antigen binds to a B cell whose membrane-bound antibody molecules are specific for epitopes on that antigen. Clonal expansion of an antigen-activated B cell (number 2 in this example) leads to a clone of memory B cells and effector B cells, called plasma cells; all cells in the expanded clone are specific for the original antigen. The plasma cells secrete antibody reactive with the activating antigen. Similar processes occur in the T-lymphocyte population resulting in clones of memory T cells and effector T cells; the latter include activated T_H cells, which secrete cytokines, and cytotoxic T lymphocytes (CTLs).

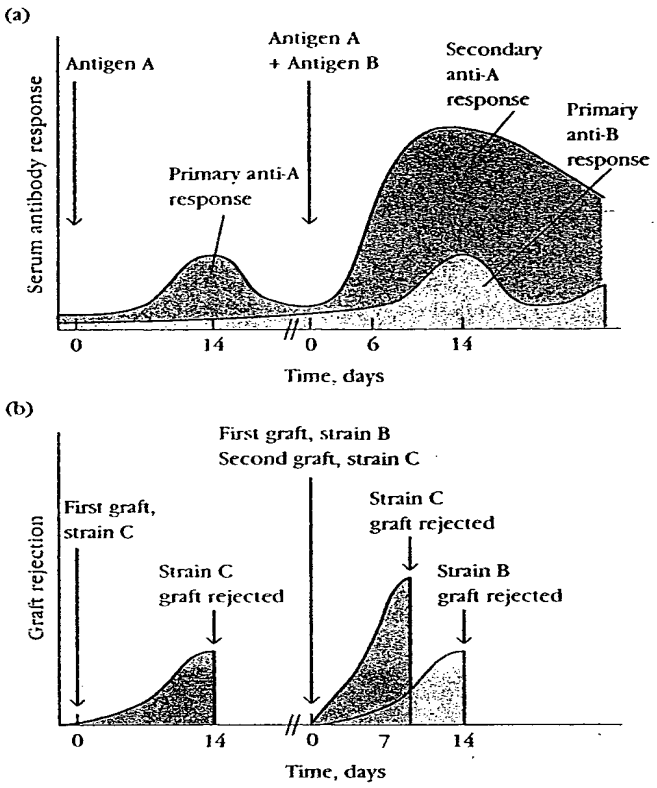

FIGURE 1-12

Differences in the primary and secondary response to injected antigen (humoral response) and to a skin graft (cell-mediated response) reflect the phenomenon of immunologic memory. (a) When an animal is injected with an antigen, it produces a primary serum antibody response of low magnitude and relatively short duration, peaking at about 10–17 days. A second immunization with the same antigen results in a secondary response that is greater in magnitude, peaks in less time (2–7 days), and lasts longer (months to years) than the primary response. (b) When skin from a strain C mouse is grafted onto a strain A mouse, the graft is rejected in about 10–14 days. If a second strain C graft is grafted onto the same mouse, it is rejected much more vigorously and rapidly than the first graft.

presence of a clonally expanded population of memory T_H and T_C cells to the antigens of the foreign graft. This expanded memory population will generate increased numbers of effector cells, resulting in faster graft rejection.

Cellular Interactions Required for Generation of Immune Responses

Both the humoral and the cell-mediated branches of the immune system require interaction among several different types of cells to induce a specific immunologic response. These cells include various antigen-presenting cells, T_H cells, and either B cells for induction of humoral immunity or T_C cells for induction of cell-mediated immunity.

Activation and Proliferation of T Helper Cells

The generation of both humoral and cell-mediated immune responses depends on the activation of T_H cells. This process begins when antigen-binding receptors on T_H cells interact with antigenic peptide–class II MHC complexes on antigen-presenting cells (Figure 1-13). This interaction generates a signal that, together with a necessary co-stimulatory signal, leads to activation and proliferation of the T_H cells (Figure 1-14a). The clonally expanded population of antigen-specific T_H cells can now play a role in the activation of the B and T lymphocytes that generate the humoral and cell-mediated responses, respectively.

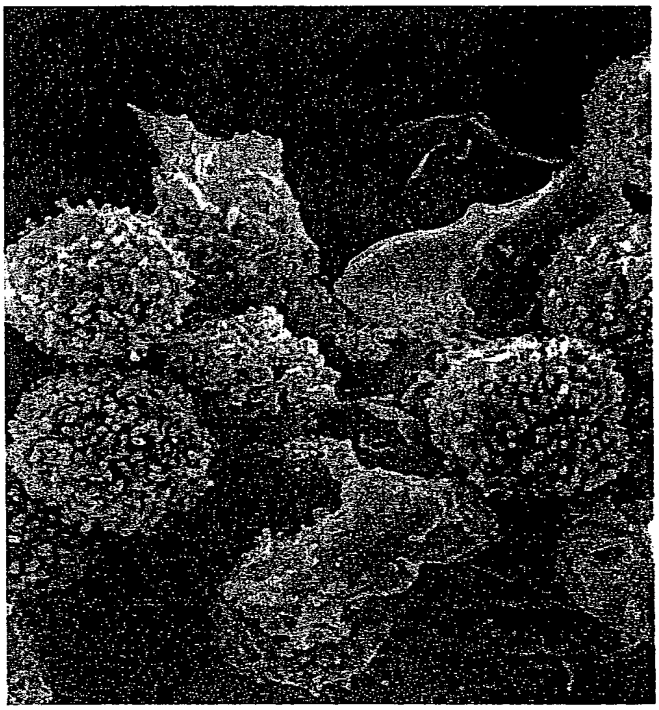

FIGURE 1-13

Scanning electron micrograph reveals numerous T lymphocytes interacting with a single macrophage. The macrophage presents processed antigen associated with class II MHC molecules to the T cells. [From William E. Paul (ed.), 1991, *Immunology: Recognition and Response*, W. H. Freeman and Company, New York; courtesy of Morten H. Nielsen and Ole Werdelin.]

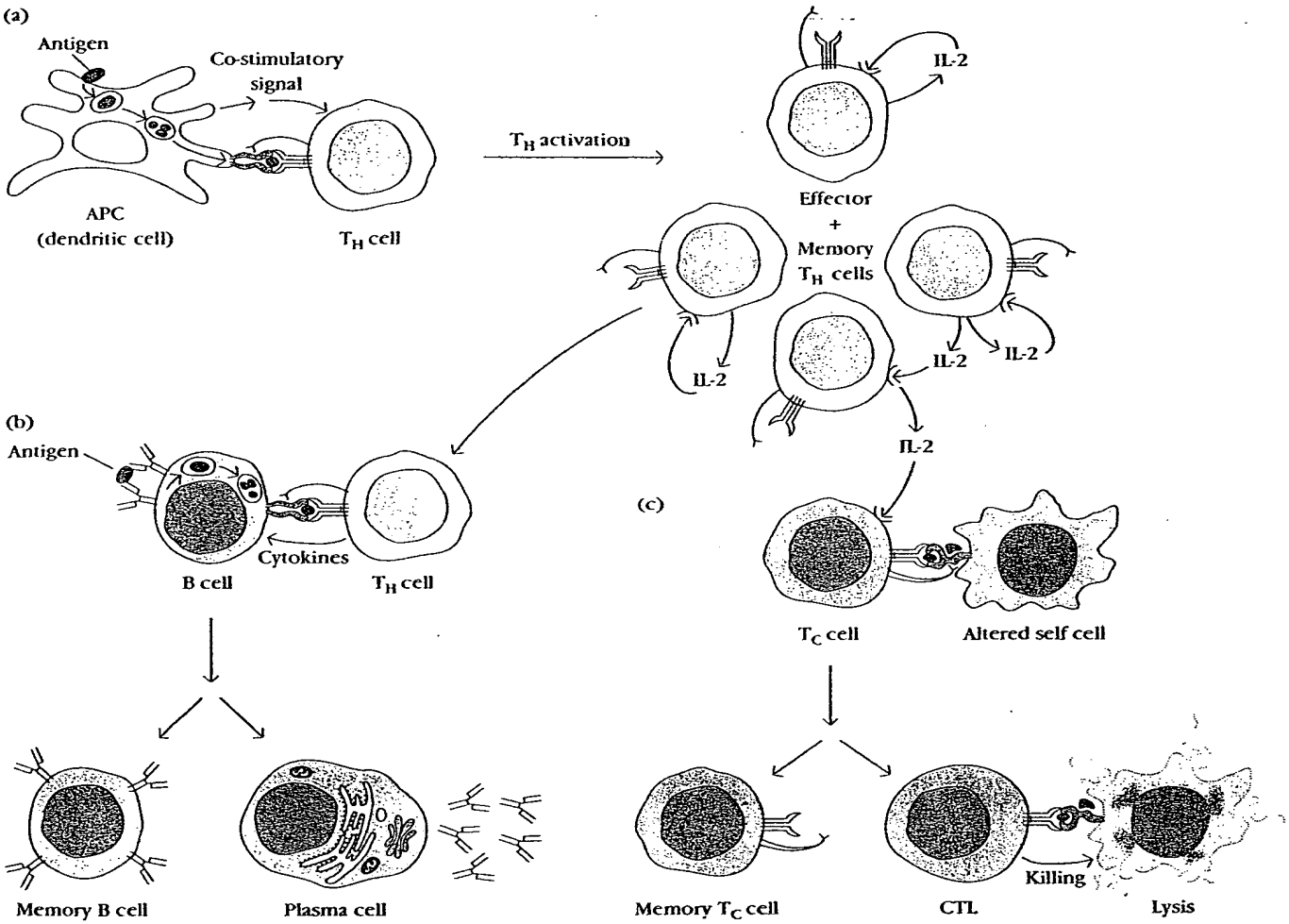

FIGURE 1-14

Cellular interactions involved in induction of immune responses. Activation and proliferation of T_H cells (a) is required for generation of a humoral response (b) and a cell-mediated response to altered self-cells (c). APC = antigen-presenting cell; Ag = antigen. See text for discussion.

Generation of the Humoral Response

Mature antigen-committed B lymphocytes are seeded out from the bone marrow to circulate in the blood or lymph or to reside in various lymphoid organs. Interaction of the mature B cell with antigen triggers its activation and further proliferation and differentiation. This process begins when antigen cross-links membrane-bound antibody molecules on a B cell. Some of the bound antigen is internalized by receptor-mediated endocytosis. After processing the antigen, the B cell presents the resulting antigenic peptides together with a class II MHC molecule on its membrane. A T_H cell specific for the presented antigen-MHC complex then binds to the complex; as a result of this interaction, the T_H cell secretes a number of cytokines that stimulate various stages of B-cell division and differentiation. The activated B cell undergoes a series of cell divisions over approximately a 5-day period differentiating into a population of both antibody-secreting plasma cells and memory cells (Figure 1-14b).

Generation of the Cell-Mediated Response

The cell-mediated response is generated by various subpopulations of T lymphocytes. As in the case of the

humoral response, a clonally expanded population of antigen-specific activated T_H cells is required. Cytokines secreted by these T_H cells help to activate various T effector cells responsible for cell-mediated responses. For example, after a T_C cell binds to processed antigen associated with class I MHC molecules on the membrane of an altered self-cell, IL-2 secreted by T_H cells stimulates proliferation and differentiation of the T_C cell. This process generates cytotoxic T lymphocytes (CTLs), which mediate membrane damage to the altered self-cell leading to cell lysis, as well as populations of memory T_H and T_C cells (Figure 1-14c).

The cytokines secreted by activated T_H cells also regulate the proliferation and differentiation of a number of nonspecific effector cells that play various roles in cell-mediated immune responses. These nonspecific effector cells do not possess the immunologic attributes of specificity and memory; instead, their activity is regulated by cytokines secreted by antigen-specific T_H cells. Among the nonspecific effector cells involved in cell-mediated immunity are natural killer (NK) cells and activated macrophages. These are described in Chapter 3, and their role in cell-mediated immunity is covered in Chapter 16.

SUMMARY

1. Immunity is the state of protection against foreign organisms or substances (antigens). Innate (nonspecific) immune responses include anatomic, physiologic, endocytic and phagocytic, and inflammatory barriers that help prevent the entrance and establishment of infectious agents (see Figures 1-3, 1-4, 1-5). When these nonspecific mechanisms fail to effectively combat an invading pathogen, the body mounts an acquired (specific) immune response.
2. Acquired immune responses exhibit four immunologic attributes: specificity, diversity, memory, and self/nonself recognition. Functionally an immune response involves two interrelated events: recognition of antigen and response to that antigen (i.e., generation of effector cells and molecules). Antigen-presenting cells, B lymphocytes, and T lymphocytes are the primary cells involved in generation of immune responses.
3. Both B and T lymphocytes possess antigen-binding receptors in their membrane. The receptors on B cells are antibody molecules, which can recognize and interact directly with antigen. T-cell receptors, in contrast, only recognize antigen that is associated with either class I or class II MHC molecules on the surface of cells. During maturation of B and T lymphocytes, each cell comes to express receptors that recognize a single antigenic determinant (epitope).
4. The two major subpopulations of T lymphocytes are T helper (T_H) cells and T cytotoxic (T_C) cells. In general, T_H cells express CD4, a membrane glycoprotein, and recognize antigen associated with class II MHC cells, whereas T_C cells express CD8 and recognize antigen associated with class I MHC cells (see Figure 1-9).
5. Exogenous (extracellular) antigens are internalized and degraded by antigen-presenting cells (macrophages, B cells, and dendritic cells); the resulting antigenic peptides complexed with class II MHC molecules then are displayed on the cell surface. Endogenous (intracellular) antigens (e.g., viral and tumor proteins produced in altered self-cells) are degraded in the cytoplasm and then displayed with class I MHC molecules on the cell surface. (See Figure 1-10.)
6. Interaction of a mature, immunocompetent lymphocyte with the antigen it recognizes stimulates the cell to proliferate and differentiate into effector cells and memory cells (see Figure 1-11). Such initial exposure to a particular antigen induces a primary response; the expanded population of memory cells permits a more rapid and intense secondary response following subsequent exposure to the same antigen (see Figure 1-12).
7. The immune system produces both humoral and cell-mediated responses. The humoral response is best-suited for elimination of exogenous antigens; the cell-mediated response, for elimination of endogenous antigens. The effector cells of the humoral response are plasma cells, which secrete soluble antibody. The effector cells of the cell-mediated response are activated T_H cells, which secrete various cytokines, and cytotoxic T lymphocytes (CTLs), which arise from T_C cells and can destroy altered self-cells. T_H-cell activation is required for both types of response. (See Figures 1-8 and 1-14.)

REFERENCES

ADA, G. L., AND G. NOSSAL. 1987. The clonal selection theory. *Sci. Am.* **257**(2):62.

ENGELHARD, V. H. 1994. How cells process antigens. *Sci. Am.* **271** (2):54.

GREY, H. M., A. SETTE, AND S. BUUS. 1989. How T cells see antigen. *Sci. Am.* **261**(5):56.

JOHNSON, H. M., F. W. BAZOR, B. E. SZENTE, AND M. A. JARPE. 1994. How interferons fight disease. *Sci. Am.* **270**(5):68.

Life, Death and the Immune System. 1994. Readings from *Scientific American Magazine.* W. H. Freeman and Company.

SHER, A., AND R. AHMED. 1995. Immunity to infection. *Curr. Opin. Immunol.* 7:471.

STUDY QUESTIONS

1. Indicate to which branch(es) of the immune system the following statements apply, using **H** for the humoral branch and **CM** for the cell-mediated branch. Some statements may apply to both branches.

a. _____ Involves class I MHC molecules
b. _____ Responds to viral infection
c. _____ Involves T helper cells
d. _____ Involves processed antigen
e. _____ Most likely responds following an organ transplant
f. _____ Involves T cytotoxic cells
g. _____ Involves B cells
h. _____ Involves CD8+ T cells
i. _____ Responds to extracellular bacterial infection
j. _____ Involves secreted antibody
k. _____ Kills virus-infected self cells

2. Specific immunity exhibits four characteristic attributes, which are mediated by lymphocytes. List these four attributes and briefly explain how they arise.

3. Name three features of a secondary immune response that distinguish it from a primary immune response.

4. Compare and contrast the four types of antigen-binding molecules utilized by the immune system—antibodies, T-cell receptors, class I MHC molecules, and class II MHC molecules—in terms of the following characteristics:

a. Specificity for antigen
b. Cellular expression
c. Types of antigen recognized

5. Cells can internalize material by endocytosis and phagocytosis. Name four properties that distinguish these two processes.

6. Fill in the blanks in the following statements with the most appropriate terms:

a. _____, _____, and _____ all function as antigen-presenting cells.
b. Antigen-presenting cells deliver a _____ signal to _____ cells.
c. Only antigen-presenting cells express class _____ MHC molecules, whereas nearly all cells express class _____ MHC molecules.
d. _____ antigens are internalized l presenting cells, degraded in the _____ displayed with class _____ MHC on the cell surface.
e. _____ antigens are produced in : cells, degraded in the _____, ar with class _____ MHC molec cell surface.

7. Briefly describe the three major events in matory response.

8. The CD8+ T cell is said to be class I restri does this mean?

9. Match each term related to innate imm with the most appropriate description lis (1–19). Each description may be used once, once, or not at all.

Terms:

a. _____ Fimbriae or pili
b. _____ Exudate
c. _____ Sebum
d. _____ Margination
e. _____ Dermis
f. _____ Lysosome
g. _____ Histamine
h. _____ Macrophage
i. _____ Lysozyme
j. _____ Bradykinin
k. _____ Interferon
l. _____ Edema
m. _____ Complement
n. _____ Extravasation
o. _____ C-reactive protein
p. _____ Phagosome

Descriptions:

1) Thin outer layer of skin
2) Layer of skin containing blood vessels an glands
3) One of several acute-phase proteins
4) Hydrolytic enzyme found in mucous sec
5) Migration of a phagocyte through the wall into the tissues
6) Acidic antibacterial secretion found in th
7) Has antiviral activity
8) Induces vasodilation

9) Accumulation of fluid in intercellular space resulting in swelling
10) Large vesicle containing ingested particulate material
11) Accumulation of dead cells, digested material, and fluid
12) Adherence of phagocytic cells to the endothelial wall
13) Structures involved in microbial adherence to mucous membranes
14) Stimulates pain receptors in the skin
15) Phagocytic cell found in the tissues
16) Phagocytic cell found in the blood
17) Group of serum proteins involved in cell lysis and clearance of antigen
18) Cytoplasmic vesicle containing degradative enzymes
19) Protein-rich fluid that leaks from the capillaries into the tissues

CHAPTER 24

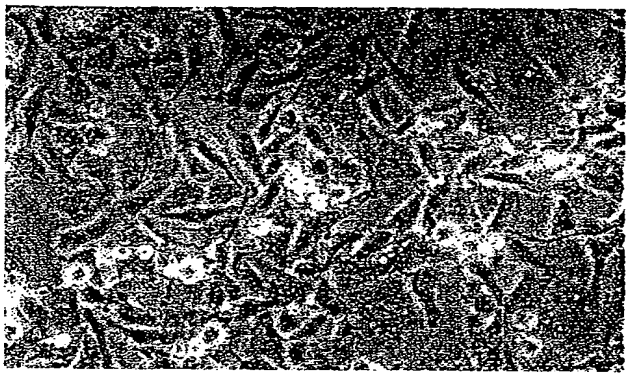

CANCER AND THE IMMUNE SYSTEM

As the death toll from infectious disease has declined in the Western world, cancer has become the second-ranking cause of death, led only by heart disease. Current estimates project that one person in three in the United States will develop cancer, and that one person in five will die from cancer. From an immunologic perspective, cancer cells can be viewed as altered self-cells that have escaped normal growth-regulating mechanisms. This chapter examines the unique properties of cancer cells, paying particular attention to those properties that can be recognized by the immune system. The immune responses that develop to cancer cells, as well as the methods by which cancers manage to evade those responses, are then described. Finally, current clinical and experimental immunotherapies for cancer are discussed.

CANCER: ORIGIN AND TERMINOLOGY

In a mature animal, a balance is usually maintained between cell renewal and cell death in most organs and tissues. The various types of mature cells in the body have a given life span; as these cells die, new cells are generated by the proliferation and differentiation of various types of stem cells. Under normal circumstances, the production of new cells is so regulated that the numbers of any particular type of cell remain constant. Occasionally, though, cells arise that are no longer responsive to normal growth-control mechanisms. These cells give rise to clones of cells that can expand to a considerable size, producing a **tumor**, or **neoplasm**.

A tumor that is not capable of indefinite growth and does not invade the healthy surrounding tissue extensively is **benign**. A tumor that continues to grow and

becomes progressively invasive is **malignant**; the term **cancer** refers specifically to a malignant tumor. In addition to uncontrolled growth, malignant tumors exhibit **metastasis**; in this process, small clusters of cancerous cells dislodge from a tumor, invade the blood or lymphatic vessels, and are carried to other tissues, where they continue to proliferate. In this way a primary tumor at one site can give rise to a secondary tumor at another site (Figure 24-1).

Malignant tumors are classified according to the embryonic origin of the tissue from which the tumor is derived. **Carcinomas** are tumors arising from endodermal or ectodermal tissues such as skin or the epithelial lining of internal organs and glands. **Sarcomas**, which arise less frequently, are derived from mesodermal connective tissues such as bone, fat, and cartilage. The **leukemias** and **lymphomas** are malignant tumors of hematopoietic cells of the bone marrow. Leukemias proliferate as single cells, whereas lymphomas tend to grow as tumor masses.

MALIGNANT TRANSFORMATION OF CELLS

Treatment of normal cultured cells with chemical carcinogens, irradiation, and certain viruses can alter the morphology and growth properties of the cells. In some cases this process, referred to as **transformation**, makes the cells able to induce tumors when they are injected into animals. Such cells are said to have undergone **malignant transformation**, and they often exhibit in vitro culture properties similar to those of cancer cells. For example, they have decreased requirements for growth factors and serum, are no longer anchorage-dependent, and grow in a density-independent fashion. Moreover, both cancer cells and transformed cells can be subcultured indefinitely; that is, they are **immortal**. Because of the similar properties of cancer and transformed cells, the process of malignant transformation has been studied extensively as a model of cancer induction.

Various chemical agents (e.g., DNA-alkylating reagents) and physical agents (e.g., ultraviolet light and ionizing radiation) that cause mutations have been shown to induce transformation. Induction of malignant transformation with such chemical or physical carcinogens appears to involve multiple steps and at least two distinct phases: **initiation** and **promotion**. Initiation involves changes in the genome but does not, in itself, lead to malignant transformation. Following initiation, promoters stimulate cell division and lead to malignant transformation.

The importance of mutagenesis in the induction of cancer is illustrated in certain diseases such as xeroderma pigmentosum. This rare disease in humans is caused by a defect in the gene encoding a DNA-repair enzyme called UV-specific endonuclease. Individuals with this disease are unable to repair UV-induced mutations and consequently develop skin cancers.

A number of DNA and RNA viruses have been shown to induce malignant transformation. Two of the best-studied DNA viruses known to cause malignant transformation are SV40 and polyoma. In both cases the viral genomes, which integrate randomly into the host chromosomal DNA, include several genes that are expressed early in the course of viral replication. SV40 encodes two early proteins called T and t, and polyoma encodes three early proteins called T, mid-T, and t. Each of these proteins plays a role in malignant transformation of virus-infected cells.

Most RNA viruses replicate in the cytoplasm and do not induce malignant transformation. The exceptions are retroviruses, which transcribe their RNA into DNA by means of a reverse transcriptase enzyme and then integrate the DNA transcript into the host's chromosomal DNA. This process is similar in the cytopathic retroviruses such as HIV-1 and HIV-2 and in the transforming retroviruses, which induce changes in the host cell that lead to malignant transformation. In some cases, retrovirus-induced transformation is related to the presence of **oncogenes**, or "cancer genes," carried by the retrovirus.

One of the best-studied transforming retroviruses is the **Rous sarcoma virus**. This virus carries an oncogene called v-*src*, which encodes a 60-kDa protein kinase (v-Src) that catalyzes the addition of phosphate to tyrosine residues on proteins. The first evidence that oncogenes alone could induce malignant transformation came from studies on the v-*src* oncogene from Rous sarcoma virus. When the v-*src* oncogene from Rous sarcoma virus was cloned and transfected into normal cells in culture the cells underwent malignant transformation.

ONCOGENES AND CANCER INDUCTION

In 1971 Howard Temin suggested that oncogenes might not be unique to transforming viruses but might also be found in normal cells; indeed, he proposed that oncogenes might be acquired by a virus from the genome of an infected cell. He called these cellular genes **proto-oncogenes**, or **cellular oncogenes** (c-*onc*), to distinguish them from their viral counterpart (v-*onc*). In the

Visualizing Concepts

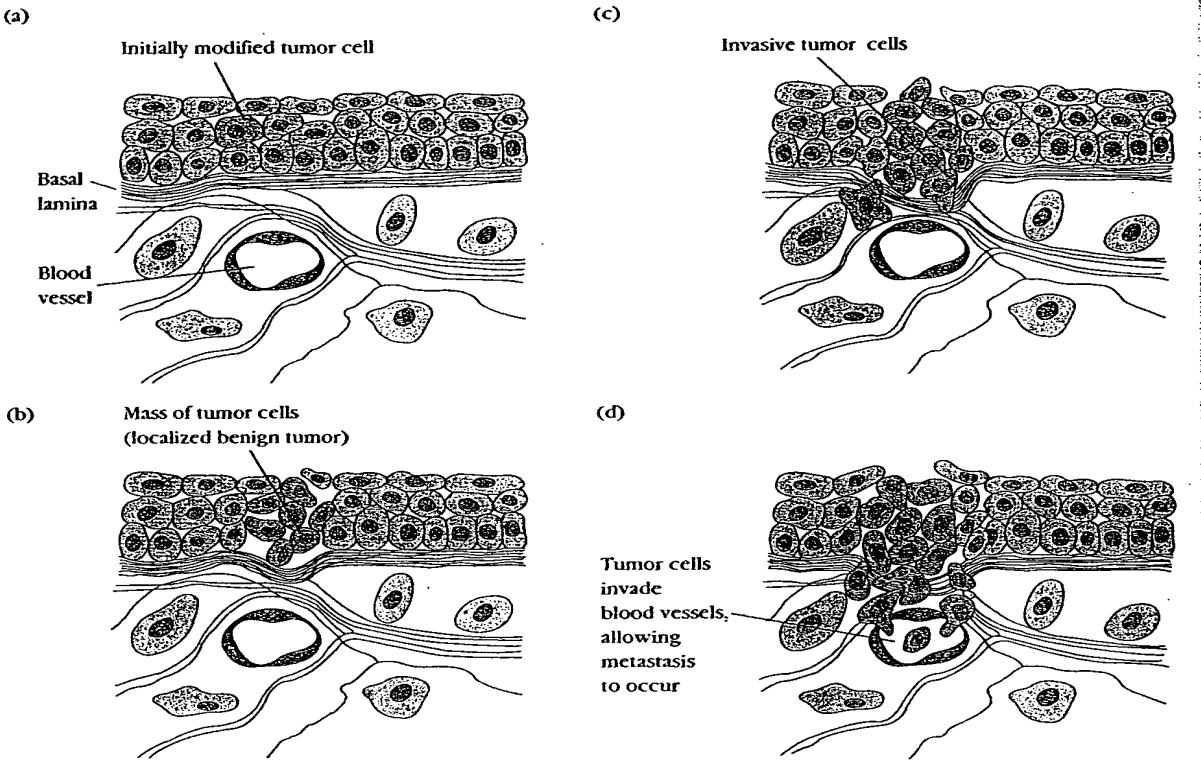

FIGURE 24-1

Tumor growth and metastasis. (a) A single cell develops altered growth properties at a tissue site. (b) The altered cell proliferates, forming a mass of localized tumor cells, or benign tumor. (c) The tumor cells become progressively more invasive, invading the underlying basal lamina. The tumor is now classified as malignant. (d) The malignant tumor metastasizes by generating small clusters of cancer cells that dislodge from the tumor and are carried by the blood or lymph to other sites in the body. [Adapted from J. Darnell et al., 1990, *Molecular Cell Biology*, 2d ed. Scientific American Books.]

mid-1970s J. M. Bishop and H. E. Varmus identified a homologous DNA sequence in normal chicken cells that is homologous to v-*src* from Rous sarcoma virus. This cellular oncogene was designated c-*src*. Since these early discoveries, numerous cellular oncogenes have been identified.

Sequence comparisons of viral and cellular oncogenes reveal that they are highly conserved in evolution. Although most cellular oncogenes consist of a series of exons and introns, their viral counterparts consist of uninterrupted coding sequences, suggesting that the virus might have acquired the oncogene sequence via an intermediate RNA transcript from which the intron sequences were removed during RNA processing. The actual coding sequences of viral oncogenes and the corresponding proto-oncogenes exhibit a high degree of homology; in some cases a single point mutation is all that distinguishes a viral oncogene from the corresponding

TABLE 24-1

FUNCTIONAL CLASSIFICATION OF ONCOGENES

TYPE/ NAME	NATURE OF GENE PRODUCT
CATEGORY I: ONCOGENES THAT INDUCE CELLULAR PROLIFERATION	
Growth factors	
sis	A form of platelet-derived growth factor (PDGF)
Growth-factor receptors	
fms	Receptor for colony-stimulating factor 1 (CSF-1)
erbB	Receptor for epidermal growth factor (EGF)
neu	Protein related to EGF receptor
erbA	Receptor for thyroid hormone
Signal transducers	
src	Tyrosine kinase
abl	Tyrosine kinase
Ha-*ras*	GTP-binding protein with GTPase activity
N-*ras*	GTP-binding protein with GTPase activity
K-*ras*	GTP-binding protein with GTPase activity
Transcription factors	
jun	Component of transcription factor AP1
fos	Component of transcription factor AP1
myc	DNA-binding protein
CATEGORY II: ONCOGENES THAT INHIBIT CELLULAR PROLIFERATION*	
RB	Suppressor of retinoblastoma
p53	Nuclear phosphoprotein that inhibits formation of small-cell lung cancer and colon cancers
DCC	Suppressor of colon carcinoma
APC	Suppressor of adenomatous polyposis
NF1	Suppressor of neurofibromatosis
WT1	Suppressor of Wilm's tumor
CATEGORY III: ONCOGENES THAT REGULATE PROGRAMMED CELL DEATH	
bcl-2	Suppressor of apoptosis

* The activity of the category II oncogene products is not well understood. However, loss or mutation in these oncogenes is associated with development of the indicated cancers.

proto-oncogene. It is now believed that most, if not all, oncogenes (both viral and cellular) are derived from cellular genes that encode various growth-controlling proteins. In addition, the proteins encoded by a particular oncogene and its corresponding proto-oncogene appear to have very similar functions. As discussed below, the conversion of a proto-oncogene into an oncogene appears in many cases to involve a change in the level of expression of a normal growth-controlling protein.

Function of Oncogenes

Homeostasis in normal tissue is maintained by a highly regulated process of cellular proliferation balanced by cell death. If there is an imbalance, either at the level of cellular proliferation or at the level of cell death, then a cancerous state will develop. Oncogenes have been shown to play an important role in this process, either by regulating cellular proliferation or by regulating cell death. Oncogenes can be divided into three categories reflecting these different activities (Table 24-1).

Induction of Cellular Proliferation

One category of oncogenes encodes proteins that induce cellular proliferation. Some of these proteins function as growth factors or growth-factor receptors. Included among these are *sis*, which encodes a form of platelet-derived growth factor, and *fms*, *erbB*, and *neu*, which encode growth-factor receptors. In normal cells the expression of growth factors and their receptors is carefully regulated. Usually, one population of cells secretes a growth factor that acts on another population of cells carrying the receptor for that factor, thus stimulating proliferation of the second population. Inappropriate expression of either a growth factor or its receptor can result in uncontrolled proliferation.

Other oncogenes in this category encode products that function in signal-transduction pathways or as transcription factors. The *src* and *abl* oncogenes encode tyrosine kinases, and the *ras* oncogene encodes a GTP-binding protein. The products of these genes act as signal transducers. The *myc*, *jun*, and *fos* oncogenes encode transcription factors. Overactivity of any of these oncogenes may result in unregulated proliferation.

Inhibition of Cellular Proliferation

A second category of oncogenes—called **tumor-suppressor genes**, or anti-oncogenes—function to inhibit excessive cell proliferation. Inactivation of these

oncogenes abolishes their inhibitory activity, resulting in unregulated proliferation. The prototype of this category of oncogenes is *Rb*, the retinoblastoma gene. Hereditary retinoblastoma is a rare childhood cancer in which tumors develop from neural precursor cells in the immature retina. The affected child inherits a mutated *Rb* allele; somatic inactivation of the remaining *Rb* allele leads to tumor growth. Probably the single most frequent abnormality in human cancer is mutations in *p53*, which encodes a nuclear phosphoprotein. Over 90% of small-cell lung cancer and over 50% of breast and colon cancers have been shown to be associated with mutations in *p53*.

Regulation of Programmed Cell Death

A third category of oncogenes regulates programmed cell death. These genes encode proteins that either block or induce apoptosis. Included in this category of oncogenes is *bcl-2*, an anti-apoptosis gene. This oncogene was originally discovered from a chromosomal translocation associated with B-cell follicular lymphoma. Since its discovery, *bcl-2* has been shown to play an important role in regulating cell survival during hematopoiesis and in survival of selected B cells and T cells during maturation (see Chapters 8 and 12). Interestingly, the Epstein-Barr virus contains a gene that has sequence homology to *bcl-2* and may act in a similar manner to suppress apoptosis.

Conversion of Proto-Oncogenes to Oncogenes

In 1972 R. J. Huebner and G. J. Todaro suggested that mutations or genetic rearrangements of proto-oncogenes by carcinogens or viruses might alter the normal regulated function of these genes, converting them into potent cancer-causing oncogenes (Figure 24-2). Considerable evidence supporting this hypothesis accumulated in subsequent years. For example, some malignantly transformed cells contain multiple copies of cellular oncogenes, resulting in increased production of oncogene products. Such amplification of cellular oncogenes has been observed in cells from various types of human cancers. Several groups have identified c-*myc* oncogenes in homogeneously staining regions (HSRs) of chromosomes from cancer cells; these HSRs represent long tandem arrays of amplified genes.

In addition, some cancer cells exhibit chromosomal translocations, which usually involve movement of a proto-oncogene from one chromosomal site to another (Figure 24-3). In many cases of Burkitt's lymphoma, for example, c-*myc* is moved from its normal position on chromosome 8 to a position near the immunoglobulin heavy-chain enhancer on chromosome 14. As a result of this translocation, synthesis of the c-Myc protein, which functions as a transcription factor, increases.

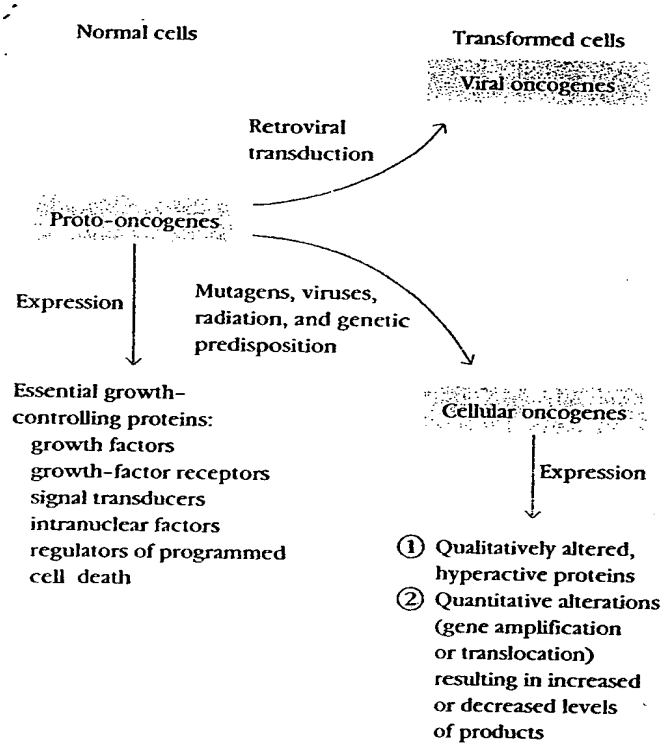

FIGURE 24-2

Conversion of proto-oncogenes into oncogenes can involve mutation, resulting in production of qualitatively different gene products, or DNA amplification or translocation, resulting in increased or decreased expression of gene products.

Mutation in proto-oncogenes has also been associated with cellular transformation and may be a major mechanism by which chemical carcinogens or x-irradiation convert a proto-oncogene into a cancer-inducing oncogene. For instance, a single-point mutation in c-*ras* has been detected in human lung carcinoma, prostate carcinoma, bladder carcinoma, and neuroblastoma. This single mutation appears to reduce the GTPase activity of the Ras protein and may alter its function in the regulation of cellular growth.

Viral integration into the host-cell genome may in itself serve to convert a proto-oncogene into a transforming oncogene. For example, avian leukosis virus (ALV) is a retrovirus that does not carry any viral oncogenes and yet is able to transform B cells into lymphomas. This particular retrovirus has been shown to integrate within the c-*myc* proto-oncogene, which contains three exons.

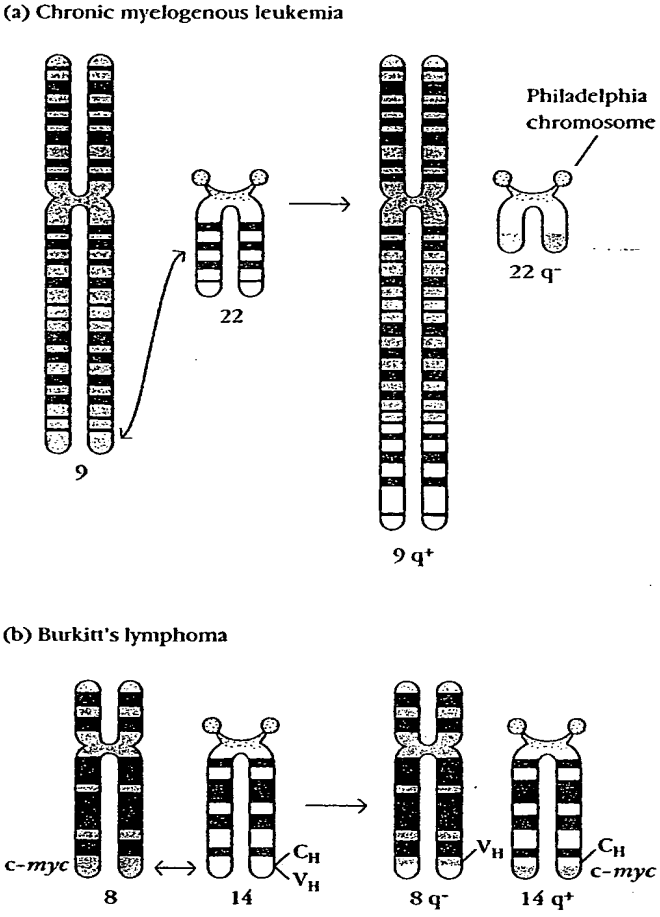

FIGURE 24-3

Chromosomal translocations in (a) chronic myelogenous leukemia (CML) and (b) Burkitt's lymphoma. Leukemic cells from all patients with CML contain the so-called Philadelphia chromosome, which results from a translocation between chromosomes 9 and 22. Cancer cells from some patients with Burkitt's lymphoma exhibit a translocation that moves part of chromosome 8 to chromosome 14. It is now known that this translocation involves c-*myc*, a cellular oncogene. Abnormalities such as these are detected by banding analysis of metaphase chromosomes. Normal chromosomes are shown on the left, and translocated chromosomes on the right.

Exon 1 of c-*myc* has an unknown function; exons 2 and 3 encode the Myc protein. Insertion of AVL between exon 1 and exon 2 has been shown in some cases to allow the provirus promoter to increase transcription of exons 2 and 3, resulting in increased synthesis of c-Myc.

A variety of tumors have been shown to express significantly increased levels of growth factors or growth-factor receptors. In adult T-cell leukemia, T cells infected with the HTLV-1 retrovirus show constitutive expression of IL-2 and the IL-2 receptor, enabling the cells to autostimulate their own proliferation in the absence of antigen activation (see Figure 13-13). Expression of the receptor for epidermal growth factor, which is encoded by c-*erbB*, has also been shown to be amplified in many cancer cells. And in breast cancer, increased synthesis of the growth-factor receptor encoded by *c-neu* has been linked with a poor prognosis.

One of the best examples of the association between increased expression of growth factors and cancer induction involves transforming growth factor (TGF-α). TGF-α, which is secreted by a variety of transformed cells, is similar in both structure and function to epidermal growth factor (EGF), and like EGF it is also able to bind to the EGF receptor on cells. Increased expression of both TGF-α and the EGF receptor have been observed in many cancer cells and in cells that have been transformed with retroviruses, viral oncogenes, and carcinogens.

TGF-α is thought to act as an autocrine activator of the EGF receptor. The effects of TGF-α overproduction have been studied by producing transgenic mice containing a TGF-α transgene linked to a metallothionine promoter. In these mice, the level of TGF-α expression could be controlled by adjusting their zinc intake. Experiments with these mice revealed that when TGF-α expression was high, they developed carcinomas of the liver and breast and also exhibited enlargement of the pancreas; however, when TGF-α expression was low, none of these changes was observed. Thus overexpression of the gene encoding TGF-α enables it to function as an oncogene in this system.

Induction of Cancer: A Multistep Process

The development from a normal cell to a cancerous cell is thought to be a multistep process of clonal evolution driven by a series of somatic mutations that progressively convert the cell from normal growth to a precancerous state and finally into a cancerous state.

The presence of myriad chromosomal abnormalities in precancerous and cancerous cells lends support to the role of multiple mutations in the development of cancer. This has been demonstrated in human colon cancer, which progresses in a series of well-defined morphologic stages (Figure 24-4). Colon cancer begins as small, benign tumors in the colorectal epithelium, called adenomas. These precancerous tumors grow, gradually becoming increasingly disorganized in their intracellular organization until they acquire the malignant phenotype. These well-defined morphologic stages of colon cancer have been correlated with a sequence of gene changes involving inactivation or loss of three anti-oncogenes

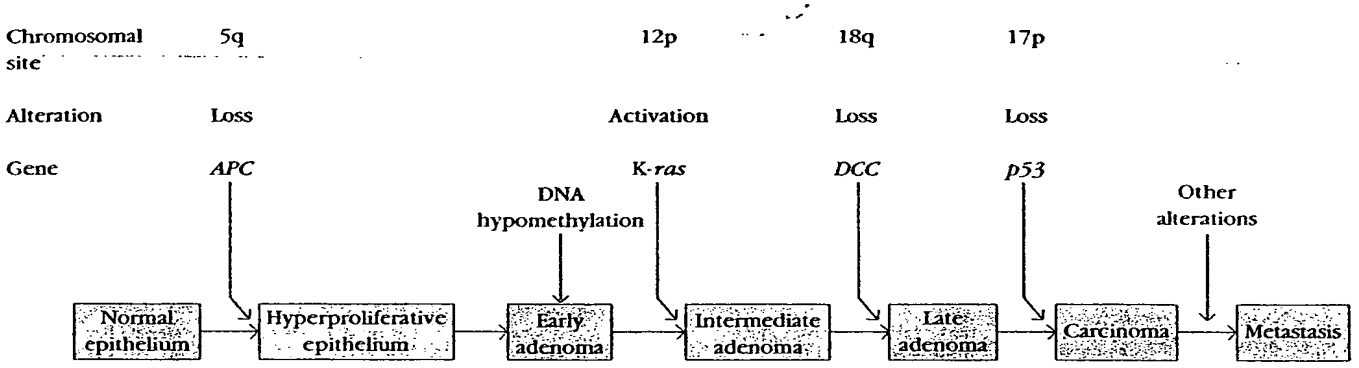

FIGURE 24-4

Model of sequential genetic alterations leading to metastatic colon cancer. Each of the stages indicated at the bottom is morphologically distinct, allowing researchers to determine the sequence of genetic alterations. [Adapted from B. Vogelstein and K. W. Kinzler, 1993, *Trends Genet.* 9:138.]

(*APC*, *DCC*, and *p53*) and activation of one cellular proliferation oncogene (K-*ras*).

Studies with transgenic mice also support the role of multiple steps in the induction of cancer. Transgenic mice expressing high levels of Bcl-2 develop a population of small resting B cells, derived from secondary lymphoid follicles, that have greatly extended life spans. Gradually these transgenic mice develop lymphomas. Analysis of lymphomas in these transgenic mice have shown that approximately half have a c-*myc* translocation to the immunoglobulin H-chain locus. The synergism of Myc and Bcl-2 is highlighted in double-transgenic mice (produced by mating the *bcl-2*$^+$ transgenic mice with *myc*$^+$ transgenic mice). In this case the mice develop a very rapid onset leukemia.

TUMORS OF THE IMMUNE SYSTEM

Tumors of the immune system are classified as lymphomas or leukemias. Lymphomas proliferate as solid tumors within a lymphoid tissue such as the bone marrow, lymph nodes, or thymus; they include Hodgkin's and non-Hodgkin's lymphomas. Leukemias tend to proliferate as single cells and are detected by increased cell numbers in the blood or lymph. Leukemia can develop in lymphoid or myeloid lineages.

Historically the leukemias were classified as acute or chronic according to the clinical progression of the disease. The acute leukemias appeared suddenly and progressed rapidly, whereas the chronic leukemias were much less aggressive and developed slowly as mild, barely symptomatic diseases. These clinical distinctions apply to untreated leukemias; with current treatments the acute leukemias often have a good prognosis, and permanent remission can often be achieved. Now the major distinction between acute and chronic leukemias is the maturity of the cell involved. Acute leukemias tend to arise in less mature cells, whereas chronic leukemias arise in mature cells. The acute leukemias include **acute lymphocytic leukemia** (ALL) and **acute myelogenous leukemia** (AML); these diseases can develop at any age and have a rapid onset. The chronic leukemias include **chronic lymphocytic leukemia** (CLL) and **chronic myelogenous leukemia** (CML); these diseases develop slowly and are seen in adults.

A number of B- and T-cell leukemias and lymphomas have been shown to involve chromosomal translocations in which a proto-oncogene is translocated into the immunoglobulin genes or T-cell-receptor genes. One of the best-characterized involves the translocation of c-*myc* in Burkitt's lymphoma and in mouse plasmacytomas. In 75% of Burkitt's lymphoma patients, c-*myc* is translocated from chromosome 8 to the Ig heavy-chain gene cluster on chromosome 14 (see Figure 24-3b). In the remaining patients, c-*myc* remains on chromosome 8 and the κ or λ light-chain genes are translocated to a region 3′ of c-*myc*. Kappa-gene translocations from chromosome 2 to chromosome 8 occur 9% of the time, and λ-gene translocations from chromosome 22 to chromosome 8 occur 16% of the time.

Translocations of c-*myc* to the Ig heavy-chain gene cluster on chromosome 14 have been analyzed in some detail. In some cases the entire c-*myc* gene is translocated head-to-head to a region near the heavy-chain enhancer. In other cases exons 1, 2, and 3 or exons 2 and

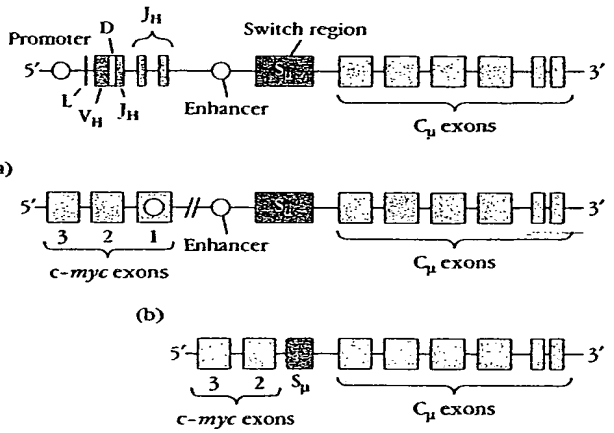

FIGURE 24-5

In many patients with Burkitt's lymphoma, the c-*myc* gene is translocated to the immunoglobulin heavy-chain gene cluster on chromosome 14. In some cases, the entire c-*myc* gene is inserted near the heavy-chain enhancer (a), but in other cases, only the coding exons (2 and 3) of c-*myc* are inserted at the S_m switch site (b). Only exons 2 and 3 of c-*myc* are coding exons. Translocation may lead to overexpression of c-Myc or to changes in the protein due to increased somatic mutation.

3 of c-*myc* are translocated head-to-head to the S_m or S_a switch site (Figure 24–5). In each case the translocation removes the *myc* coding exons from the regulatory mechanisms operating in chromosome 8 and places them in the immunoglobulin-gene region, a very active region that is expressed constitutively in these cells. The consequences of constitutive *myc* expression in lymphoid cells have been investigated in transgenic mice. In one study mice containing a transgene consisting of all three c-*myc* exons and the immunoglobulin heavy-chain enhancer were produced. Of 15 transgenic pups born, 13 developed lymphomas of the B-cell lineage within a few months of birth.

Various hypotheses have been suggested to account for *myc*-related oncogenesis. Some researchers have suggested that the presence of the immunoglobulin enhancer may result in overproduction of the c-Myc. Another hypothesis, based on the unusual level of mutations observed in exon 1 of c-*myc* after translocation, is that somatic mutation within the immunoglobulin V-region genes may induce mutations in the oncogene that lead to faulty regulation through its exon 1 or to changes in the function of its protein product.

TUMOR ANTIGENS

The subdiscipline of tumor immunology involves the study of antigens on tumor cells and the immune response to these antigens. Two types of tumor antigens have been identified on tumor cells: **tumor-specific transplantation antigens** (TSTAs) and **tumor-associated transplantation antigens** (TATAs). Tumor-specific antigens are unique to tumor cells and do not occur on normal cells in the body. They may result from mutations in tumor cells that generate altered cellular proteins; cytosolic processing of these proteins would give rise to novel peptides that are presented with class I MHC molecules, inducing a cell-mediated response by tumor-specific CTLs (Figure 24–6). Tumor-associated antigens, which are not unique to tumor cells, may be proteins that are expressed on normal cells during fetal development when the immune system is immature and unable to respond but that normally are not expressed in the adult. Reactivation of the embryonic genes encoding these proteins in tumor cells results in their expression on the fully differentiated tumor cells. Tumor-associated antigens may also be proteins that are normally expressed at extremely low levels on normal cells but are expressed at much higher levels on tumor cells.

Characterization of tumor transplantation antigens is difficult because they do not generally elicit an antibody response and thus cannot be isolated by immunoprecipitation. Many tumor antigens are cellular proteins that give rise to peptides presented with MHC molecules; typically, these antigens have been identified by their ability to induce antigen-specific CTLs.

Tumor-Specific Antigens

Tumor-specific antigens have been identified on tumors induced with chemical or physical carcinogens and on some virally induced tumors. Demonstrating the presence of tumor-specific antigens on spontaneously occurring tumors is particularly difficult because the immune response to such tumors eliminates all of the tumor cells bearing recognizable antigens and in this way selects for cells bearing lower levels of tumor-specific antigens.

Chemically or Physically Induced Tumor Antigens

Methylcholanthrene and ultraviolet light are two carcinogens that have been used extensively to generate

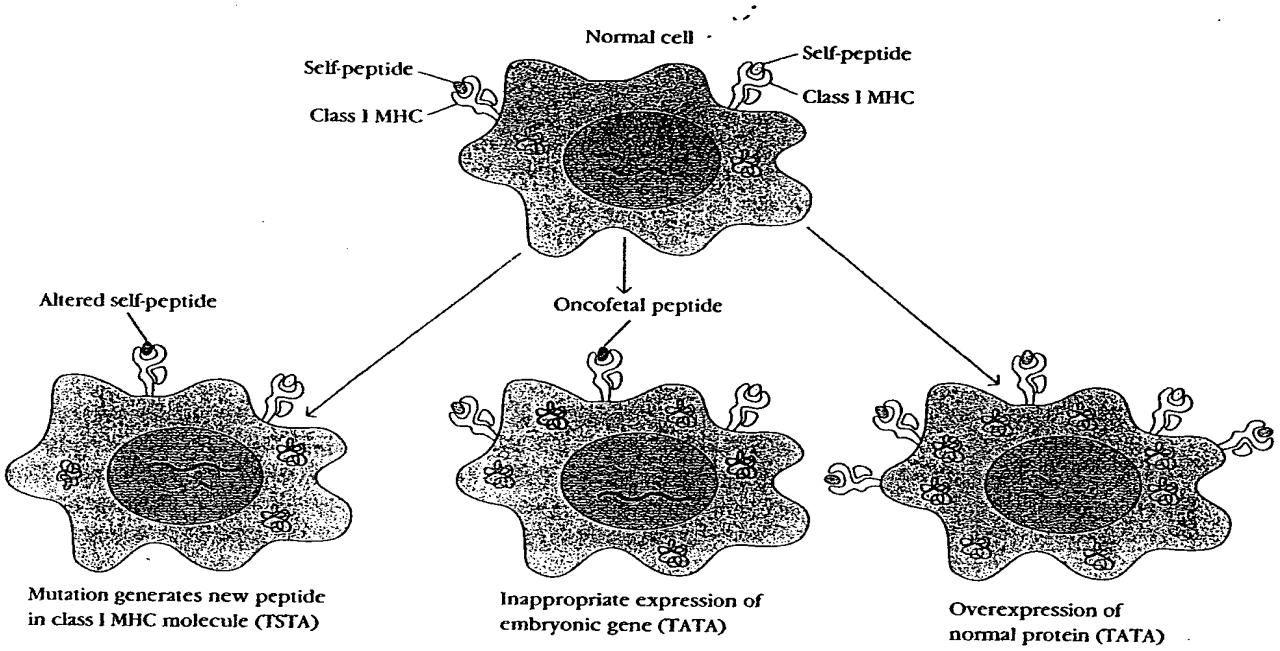

FIGURE 24-6

Different mechanisms generate tumor-specific transplantation antigens (TSTAs) and tumor-associated transplantation antigens (TATAs). The latter are more common.

tumor-cell lines. When syngeneic animals are injected with killed cells from a carcinogen-induced tumor-cell line, the animals develop a specific immunologic response that can protect against later challenge by live cells of the same line but not other tumor-cell lines (Table 24-2). Even when the same chemical carcinogen induces two separate tumors at different sites in the same animal, the tumor antigens are distinct and the immune response to one tumor does not protect against the other tumor.

The tumor-specific transplantation antigens of chemically induced tumors have been difficult to characterize because they cannot be identified by induced antibodies but only by their T-cell–mediated rejection. One experimental approach that has allowed identification of genes encoding some TSTAs is outlined in Figure 24-7. When a mouse tumorigenic cell line (tum^+), which induces progressive tumor growth, is treated in vitro with a chemical mutagen, some cells are mutated so that they no longer are capable of inducing a tumor in syngeneic mice. These mutant tumor cells are designated as tum^- variants. Most tum^- variants have been shown to express TSTAs that are not expressed by the original tum^+ tumor-cell line. When tum^- cells are injected into syngeneic mice, these unique TSTAs that the tum^- cells

TABLE 24-2

IMMUNE RESPONSE TO METHYL-CHOLANANTHRENE (MCA) OR POLYOMA VIRUS (PV)*

TRANSPLANTED KILLED TUMOR CELLS	SOURCE OF LIVE TUMOR CELLS FOR CHALLENGE	TUMOR GROWTH
CHEMICALLY INDUCED		
MCA-induced sarcoma A	MCA-induced sarcoma A	–
MCA-induced sarcoma A	MCA-induced sarcoma B	+
VIRALLY INDUCED		
PV-induced sarcoma A	PV-induced sarcoma A	–
PV-induced sarcoma A	PV-induced sarcoma B	+
PV-induced sarcoma A	SV40-induced sarcoma C	+

* Tumors were induced either with MCA or PV, and killed cells from the induced tumors were injected into syngeneic animals, which were then challenged with live cells from the indicated tumor-cell lines. The absence of tumor growth after live challenge indicates that the immune response induced by tumor antigens on the killed cells provided protection against the live cells.

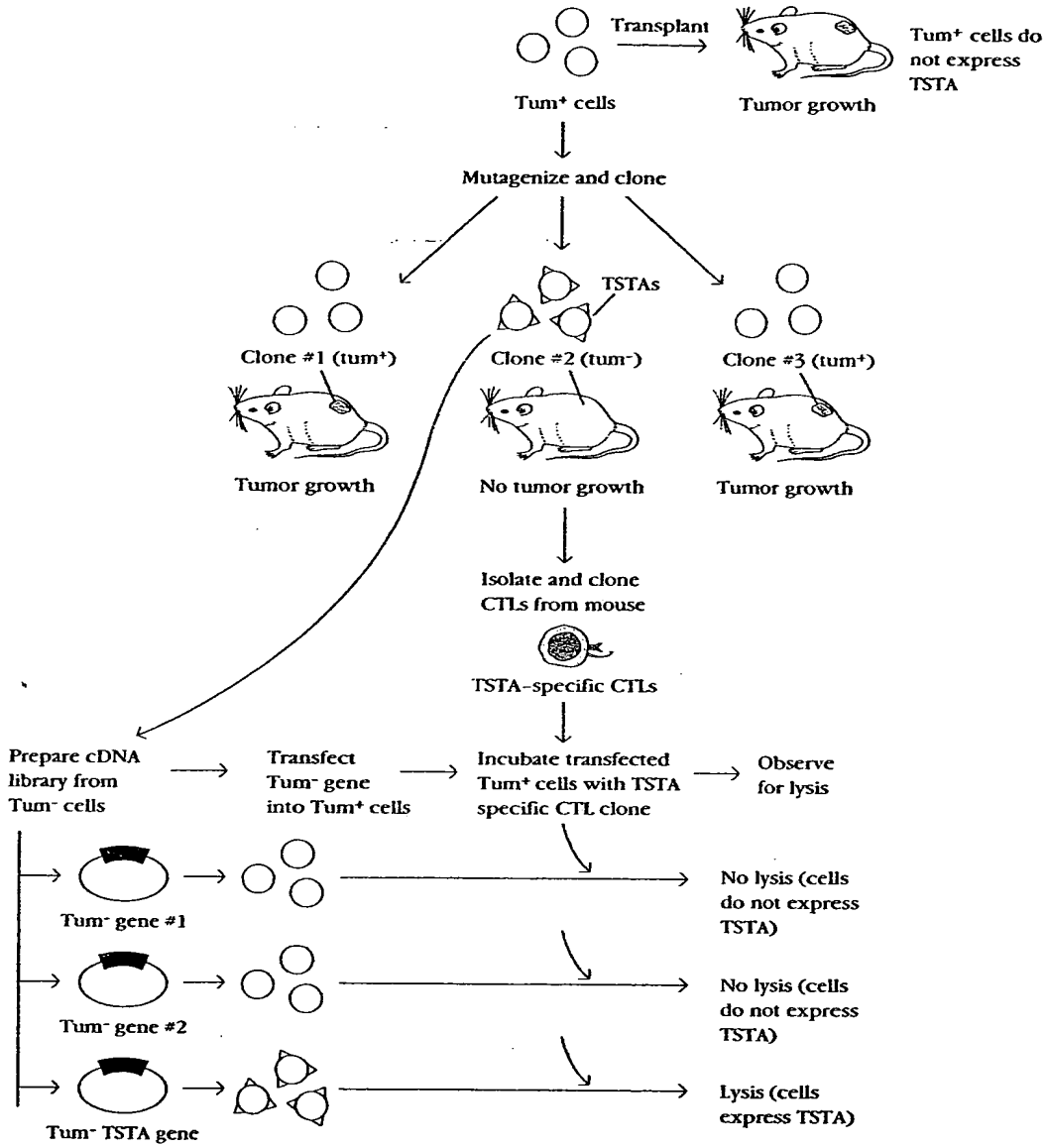

FIGURE 24-7

One procedure for identifying genes encoding tumor-specific transplantation antigens (TSTAs). Most TSTAs can be detected only by the cell-mediated rejection they elicit. In the first part of this procedure, a nontumorigenic (tum^-) cell line is generated; this cell line expresses a TSTA that is recognized by syngeneic mice, which mount a cell-mediated response against it. To isolate the gene encoding the TSTA, a cosmid gene library is prepared from the tum^- cell line, the genes are transfected into tumorigenic tum^+ cells, and the transfected cells are incubated with TSTA-specific CTLs.

express are recognized by specific CTLs. The TSTA-specific CTLs destroy the tum^- tumor cells, thus preventing tumor growth. To identify the genes encoding the TSTAs that are expressed on a tum^- cell line, a cosmid DNA library is prepared from the tum^- cells. Genes from the tum^- cells are transfected into the original tum^+ cells. The transfected tum^+ cells are tested for the expression of the tum^- TSTAs by their ability to activate cloned CTLs specific for the tum^- TSTA. A number of diverse TSTAs have been identified by this method.

In the past few years, two methods have facilitated the characterization of TSTAs (Figure 24-8). In one method peptides bound to class I MHC molecules on the membrane of the tumor cells are eluted with acid and puri-

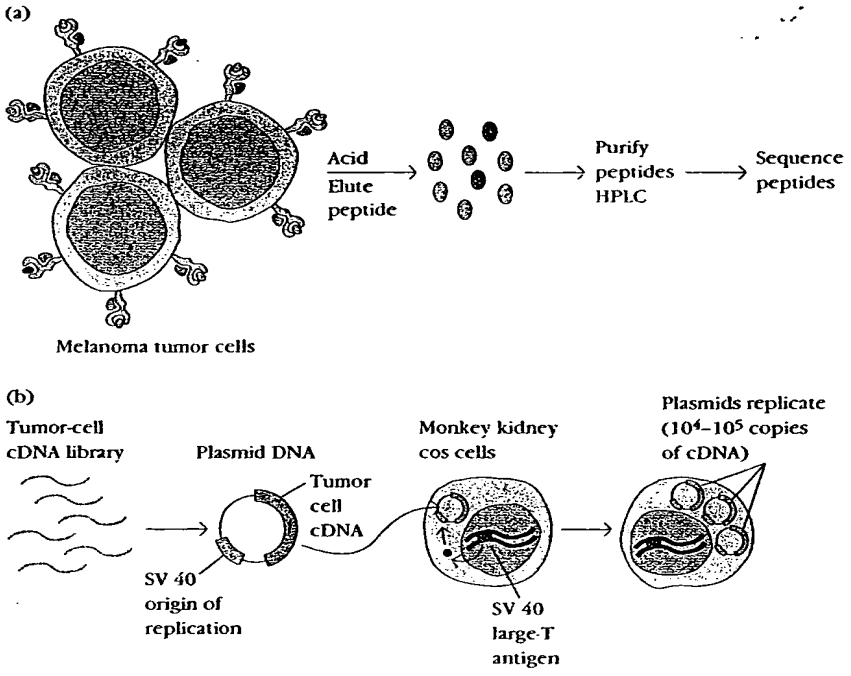

FIGURE 24-8

Two methods used to isolate tumor antigens that induce tumor-specific CTLs. See text for details.

fied by high-pressure liquid chromatography (HPLC). In some cases sufficient peptide is eluted to allow its sequence to be deduced by Edman degradation. In a second approach cDNA libraries are prepared from tumor cells. These cDNA libraries are transfected transiently into COS cells, which are monkey kidney cells transfected with the gene coding for the SV40 large-T antigen. When these cells are later transfected with plasmids containing the tumor-cell cDNA and an SV40 origin of replication, the large-T antigen stimulates plasmid replication, so that up to 10^4–10^5 plasmid copies are produced per cell. This results in high-level expression of the tumor-cell DNA.

The genes encoding some TSTAs have been shown to differ from normal cellular genes by a single-point mutation. Further characterization of TSTAs has demonstrated that many TSTAs are not cell-membrane proteins; rather, as indicated already, they are cytosolic proteins that are processed and presented as short peptides together with class I MHC molecules on the surface of tumor cells where they can be recognized by CTLs as altered self-cells.

Virally Induced Tumor Antigens

In contrast to chemically induced tumors, virally induced tumors express tumor antigens shared by all tumors induced by the same virus. For example, when syngeneic mice are injected with killed cells from a particular polyoma-induced tumor, the recipients are protected against subsequent challenge with live cells from any polyoma-induced tumors (see Table 24–2). Likewise, when lymphocytes are transferred from mice with a virus-induced tumor into normal syngeneic recipients, the recipients reject subsequent transplants of all syngeneic tumors induced by the same virus. In the case of both SV40- and polyoma-induced tumors, the presence of tumor antigens is related to the neoplastic state of the cell. Although virally induced tumor antigens have not yet been established in human cancers, Burkitt's lymphoma cells have been shown to express a nuclear antigen of the Epstein-Barr virus that may indeed be a tumor-specific antigen for this type of tumor.

The potential value of these virally induced tumor antigens can be seen in animal models. In one experiment mice immunized with a preparation of genetically engineered polyoma virus tumor antigen were shown to be immune to subsequent injections of live polyoma-induced tumor cells. In another experiment mice were immunized with a vaccinia virus vaccine engineered with the gene encoding the polyoma tumor antigen. These mice also developed immunity, rejecting later injections of live polyoma-induced tumor cells (Figure 24-9). The first example of a virally induced tumor antigen associated with a human cancer is a peptide from human papilloma virus. This oncoviral peptide may prove useful for immunization of patients carrying virus-associated tumors.

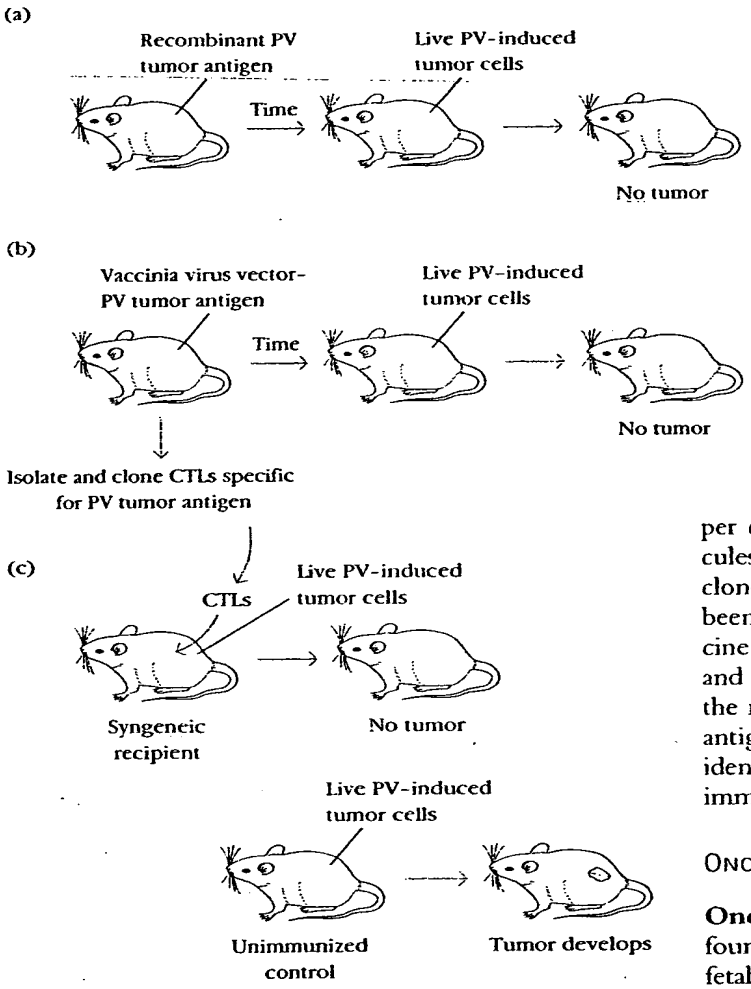

FIGURE 24-9

Experimental induction of immunity against tumor cells induced by polyoma virus (PV) has been achieved by immunizing mice with recombinant polyoma tumor antigen (a), with a vaccinia vector vaccine containing the gene encoding the PV tumor antigen (b), or with CTLs specific for the PV tumor antigen (c). Unimmunized mice (*bottom*) develop tumors when injected with live polyoma-induced tumor cells, whereas the immunized mice do not.

Tumor-Associated Antigens

The majority of tumor antigens are not unique to tumor cells but also are present on normal cells. These tumor-associated transplantation antigens may be proteins usually expressed only on fetal cells but not on normal adult cells, or they may be proteins expressed at low levels by normal cells but at much higher levels by tumor cells. The latter category includes growth factors and growth-factor receptors, as well as oncogene-encoded proteins.

Several growth-factor receptors are expressed at significantly increased levels on tumor cells and can serve as tumor-associated antigens. For instance, a variety of tumor cells express the EGF receptor at levels 100 times greater than that in normal cells. An example of an overexpressed growth factor serving as a tumor-associated antigen is a transferrin growth factor, designated p97, which aids in the transport of iron into cells. Whereas normal cells express less than 8,000 molecules of p97 per cell, melanoma cells express 50,000–500,000 molecules of p97 per cell. The gene encoding p97 has been cloned, and a recombinant vaccinia virus vaccine has been prepared carrying the cloned gene. When this vaccine was injected into mice, it induced both humoral and cell-mediated immune responses, which protected the mice against live melanoma cells expressing the p97 antigen. Results such as this highlight the importance of identifying tumor antigens as potential targets of tumor immunotherapy.

Oncofetal Tumor Antigens

Oncofetal tumor antigens, as the name implies, are found not only on cancerous cells but also on normal fetal cells. These antigens appear early in embryonic development, before the immune system acquires immunocompetence; if these antigens appear later on cancer cells, they are recognized as nonself and induce an immunologic response. Two well-studied oncofetal antigens are **alpha-fetoprotein** (AFP) and **carcinoembryonic antigen** (CEA).

Although the serum concentration of AFP drops from milligram levels in fetal serum to nanogram levels in normal adult serum, elevated AFP levels are found in a majority of patients with liver cancer (Table 24-3). CEA is a membrane glycoprotein found on gastrointestinal and liver cells of 2- to 6-month-old fetuses. Approximately 90% of patients with advanced colorectal cancer, and 50% of patients with early colorectal cancer have increased levels of CEA in their serum; some patients with other types of cancer also exhibit increased CEA levels. However, because AFP and CEA can be found in trace amounts in some normal adults and in some noncancerous disease states, the presence of these oncofetal antigens is not diagnostic of tumors but rather serves to monitor tumor growth. If, for example, a patient has

had surgery to remove a colorectal carcinoma, CEA levels are monitored following surgery. An increase in the CEA level is an indication of resumed tumor growth.

Oncogene Proteins as Tumor Antigens

A number of tumors have been shown to express tumor-associated antigens encoded by cellular oncogenes. These antigens are also present in normal cells encoded by the corresponding proto-oncogene. In many cases there is no qualitative difference between the oncogene and proto-oncogene products; instead, the increased levels of the oncogene product can be recognized by the immune system. For example, as noted earlier, human breast-cancer cells exhibit elevated expression of the oncogene-encoded Neu protein, a growth-factor receptor, whereas normal adult cells express only trace amounts of Neu protein. Because of this difference in the Neu level, anti-Neu monoclonal antibodies can recognize and selectively eliminate breast-cancer cells without damaging normal cells.

A few tumors have been shown to express a proto-oncogene product that is qualitatively different from the normal protein. For example, single-point mutations in the *ras* proto-oncogene have been detected in a number of tumors including 17 out of 17 cases of malignant prostate cancer. If these qualitative changes can be recognized effectively by the immune system as tumor-specific antigens, they will lend themselves to various cancer immunotherapy approaches.

TABLE 24-3

ELEVATION OF ALPHA-FETOPROTEIN (AFP) AND CARCINOEMBRYONIC ANTIGEN (CEA) IN SERUM OF PATIENTS WITH VARIOUS DISEASES

DISEASE	NO. OF PATIENTS TESTED	% OF PATIENTS WITH HIGH AFP OR CEA LEVELS *
	AFP > 400 μg/ml	
Alcoholic cirrhosis	NA	0
Hepatitis	NA	1
Hepatocellular carcinoma	NA	69
Other carcinoma	NA	0
	CEA > 10 ng/ml	
Cancerous		
Breast carcinoma	125	14
Colorectal carcinoma	544	35
Gastric carcinoma	79	19
Noncarcinoma malignancy	228	2
Pancreatic carcinoma	55	35
Pulmonary carcinoma	181	26
Noncancerous		
Alcoholic cirrhosis	120	2
Cholecystitis	39	1
Nonmalignant disease	115	0
Pulmonary emphysema	49	4
Rectal polyps	90	1
Ulcerative colitis	146	5

* Although trace amounts of both AFP and CEA can be found in some healthy adults, none would have levels greater than those indicated in the table.

TATAs on Human Melanomas

Several tumor-associated transplantation antigens have been identified on human melanomas. Five of these—MAGE-1, MAGE-3, BAGE, GAGE-1,2—are oncofetal-type antigens. Each of these antigens is expressed on a significant proportion of human melanoma tumors, as well as on a number of other human tumors, but not on normal differentiated tissues except for the testis where it is expressed on germ-line cells. In addition, a number of differentiation antigens expressed on normal melanocytes—including tyrosinase, gp100, Melan-A or MART-1, and gp75—are overexpressed by melanoma cells, enabling them to function as tumor-associated transplantation antigens.

Several of the human melanoma tumor antigens are shared by a number of other tumors. About 40% of human melanomas are positive for MAGE-1, and about 75% are positive for MAGE-2 or 3. In addition to melanomas, a significant percentage of glioma cell lines, breast tumors, non-small cell lung tumors, and head or neck carcinomas express MAGE-1, 2 or 3. These shared tumor antigens could be exploited for clinical treatment. It might be possible to produce a tumor vaccine expressing the shared antigen for treatment of a number of these tumors, as discussed later in the chapter.

IMMUNE RESPONSE TO TUMORS

In experimental animals tumor antigens can be shown to induce both humoral and cell-mediated immune responses resulting in destruction of the tumor cells. In general, the cell-mediated response appears to play the major role in tumor elimination. A number of tumors have been shown to induce tumor-specific CTLs that recognize tumor antigens presented by class I MHC on the tumor cells. However, as discussed below, expression of class I MHC molecules is decreased in a number of tumors, thereby limiting the role of specific CTLs in destroying tumor cells.

Role of NK Cells and Macrophages

As noted in Chapter 16, recognition of tumor cells by NK cells is not MHC restricted. Thus the activity of these cells is not compromised by the decreased MHC expression exhibited by some tumor cells. In some cases Fc receptors on NK cells can bind to antibody-coated tumor cells leading to ADCC (see Figure 16-12). The importance of NK cells in tumor immunity is suggested by the mutant mouse strain called beige and by **Chediak-Higashi syndrome** in humans. In both cases, a genetic defect causes marked impairment of NK cells and an associated increased incidence of certain types of cancer.

Numerous observations indicate that activated macrophages also play a significant role in the immune response to tumors. For example, macrophages are often observed to cluster around tumors, and their presence is often correlated with tumor regression. Like NK cells, macrophages are not MHC restricted and express Fc receptors, enabling them to bind to antibody on tumor cells and mediate ADCC. The antitumor activity of activated macrophages is probably mediated by lytic enzymes and reactive oxygen and nitrogen intermediates. In addition, activated macrophages secrete a cytokine called tumor necrosis factor (TNF-α) that has potent antitumor activity. When TNF-α is injected into tumor-bearing animals, it has been found to induce hemorrhage and necrosis of the tumor (see Figure 15-14a).

Immune Surveillance Theory

The immune surveillance theory was first conceptualized in the early 1900s by Paul Ehrlich. He suggested that cancer cells frequently arise in the body but are recognized as foreign and eliminated by the immune system. Some 50 years later Lewis Thomas suggested that the cell-mediated branch of the immune system had evolved to patrol the body and eliminate cancer cells. According to these concepts, tumors arise only if cancer cells are able to escape immune surveillance, either by reducing their expression of tumor antigens or by an impairment in the immune response to these cells.

Among the early observations that seemed to support the immune surveillance theory was the increased incidence of cancer in transplantation patients on immunosuppressive drugs. Other findings, however, were difficult to reconcile with this theory. Nude mice, for example, lack a thymus and consequently lack functional T cells. According to the immune surveillance theory, these mice should show an increase in cancer, but instead nude mice are no more susceptible to cancer than other mice. Furthermore, although individuals on immunosuppressive drugs do show an increased incidence of cancers of the immune system, other common cancers (e.g., lung, breast, and colon cancer) are not increased in these individuals, contrary to what the theory predicts. One possible explanation for the selective increase in immune-system cancers is that the immunosuppressive agents themselves may exert a direct carcinogenic effect on immune cells.

Experimental data concerning the effect of tumor-cell dosage on the ability of the immune system to respond also are incompatible with the immune surveillance theory. For example, animals injected with very low or very high doses of tumor cells develop tumors,

whereas those injected with intermediate doses do not. The mechanism by which a low dose of tumor cells "sneaks through" is difficult to reconcile with the immune surveillance theory. Finally, this theory assumes that cancer cells and normal cells exhibit qualitative antigen differences. In fact, as discussed in previous sections, many types of tumors do not express tumor-specific antigens, and any immune response that develops must be induced by quantitative differences in antigen expression by normal cells and tumor cells.

The basic concept of the immune surveillance theory—that malignant tumors arise only if the immune system is somehow impaired or if the tumor cells lose their immunogenicity, enabling them to escape immune surveillance—at this time remains unproved. Nevertheless, it is clear that an immune response can be generated to tumor cells and therapeutic approaches aimed at increasing that response may serve as a defense against malignant cells.

TUMOR EVASION OF THE IMMUNE SYSTEM

Although the immune system clearly can respond to tumor cells, the fact that so many individuals die each year from cancer suggests that the immune response to tumor cells is often ineffective. This section describes several mechanisms by which tumor cells appear to evade the immune system.

Immunologic Enhancement of Tumor Growth

Following the discovery that antibodies could be produced to tumor-specific antigens, attempts were made to protect animals against tumor growth by active immunization with tumor antigens or by passive immunization with antitumor antibodies. Much to the surprise of the researchers, these immunizations did not protect against tumor growth; in many cases they actually enhanced growth of the tumor.

The tumor-enhancing ability of immune sera subsequently was studied in cell-mediated lympholysis (CML) reactions in vitro. Serum taken from animals with progressive tumor growth was found to block the CML reaction, whereas serum taken from animals with regressing tumors had little or no blocking activity. K. E. and I. Hellstrom extended these findings by showing that children with progressive neuroblastoma had high levels of some kind of blocking factor in their sera and that children with regressive neuroblastoma did not have such factors. Since these first reports, blocking factors have been found to be associated with a number of human tumors.

In some cases, antitumor antibody itself acts as a blocking factor. Presumably the antibody binds to tumor-specific antigens and masks the antigens from cytotoxic T cells. In many cases the blocking factors are not antibodies alone but rather antibodies complexed to tumor antigens. Although these immune complexes have been shown to block the CTL response, the mechanism of this inhibition is not known. The complexes also may inhibit ADCC by binding to Fc receptors on NK cells or macrophages and blocking their activity.

Modulation of Tumor Antigens

Certain tumor-specific antigens have been observed to disappear from the surface of tumor cells in the presence of serum antibody and then to reappear after the antibody is no longer present. This phenomenon, called **antigenic modulation**, is readily observed when leukemic T cells are injected into mice previously immunized with a leukemic T-cell antigen (TL antigen). These mice develop high titers of anti-TL antibody, which binds to the TL antigen on the leukemic cells and induces capping, endocytosis, and/or shedding of the antigen-antibody complex. As long as antibody is present, these leukemic T cells fail to display the TL antigen and thus cannot be eliminated.

Reduction in Class I MHC Molecules

Since $CD8^+$ CTLs only recognize antigen associated with class I MHC molecules, any alteration in the expression of class I MHC molecules on tumor cells may exert a profound effect on the CTL-mediated immune response. Malignant transformation of cells is often associated with a reduction (or even a complete loss) of class I MHC molecules, and a number of tumors have been shown to express decreased levels of class I MHC molecules (Table 24-4). In many cases the decrease in class I MHC expression is accompanied by progressive tumor growth, and so the absence of MHC molecules on a tumor is generally an indication of a poor prognosis. As illustrated in Figure 24-10, the immune response itself may play a role in selecting tumor cells with decreased class I MHC expression.

Lack of Co-stimulatory Signal

T-cell activation requires an activating signal, triggered by recognition of a peptide–MHC molecule complex by the T-cell receptor, and a co-stimulatory signal triggered by the interaction of B7 on antigen-presenting cells with CD28 on the T cells (see Figure 12-14). Both signals are needed to induce IL-2 production and proliferation of T cells. The poor immunogenicity of many tumor cells may be due in large part to the lack of the co-stimulatory molecules. Without sufficient numbers of antigen-presenting

TABLE 24-4

SOME TUMORS WITH ALTERED MHC EXPRESSION AND THE BIOLOGICAL CONSEQUENCES

EXPERIMENTAL TUMOR SYSTEMS	ALTERED MHC EXPRESSION	BIOLOGICAL CONSEQUENCES
AKR mouse leukemia	Absence of H-2K	Increased tumorigenicity
Murine D122 Lewis lung carcinoma	Reduced H-2K/H-2D ratio	Increased metastasis
Methylcholanthrene-induced murine T10 sarcoma	Absence of H-2K and increased H-2D	Increased metastasis
SV40-transformed mouse cells	Absence of H-2K	Increased tumorigenicity
Radiation leukemia virus (RadLV)–transformed mouse cells	Absence of class I	Lethal leukemogenesis
Herpes simplex virus type 2 (HSV-2)–infected cells	Reduced class I molecules	Resistance to lysis by CTLs
Human Burkitt's lymphoma	Absence of class I	Resistance to lysis by CTLs
Human urothelial cell line TGr III	Reduced class I	Increased tumorigenicity and invasiveness
Human small-cell lung cancer	Deficient class I	Increased tumorigenicity and early metastisis
Human neuroblastoma	Deficient class I	Increased N-*myc* expression
Human mucinous colorectal carcinoma	Reduced class I	Poor prognosis
Human melanomas	Reduced class I	Increased invasiveness and thicker primary form

SOURCE: From K. M. Hui, 1989, *BioEssays* **11**:23.

cells in the immediate vicinity of a tumor, the T cells will receive only a partial activating signal, which may lead to clonal anergy.

CANCER IMMUNOTHERAPY

Although various immune responses can be generated to tumor cells, the response frequently is not sufficient to prevent tumor growth. One approach to cancer treatment is to augment or supplement these natural defense mechanisms. Several types of cancer immunotherapy in current use or under development are described in this concluding section.

Manipulation of Co-stimulatory Signal

Several research groups have demonstrated that tumor immunity can be enhanced by providing the co-stimulatory signal necessary for activation of CTL precursors (CTL-Ps). When mouse CTL-Ps are incubated with melanoma cells in vitro, antigen recognition occurs, but in the absence of a co-stimulatory signal, the CTL-Ps do not proliferate and differentiate into effector CTLs. However, when the melanoma cells are transfected with the gene encoding the B7 ligand, then the CTL-Ps differentiate into effector CTLs.

These findings offer the possibility that B7-transfected tumor cells might be used to induce a CTL response in vivo. For instance, when P. Linsley, L. Chen, and their colleagues injected melanoma-bearing mice with $B7^+$ melanoma cells, the melanomas completely regressed in more than 40% of the mice. S. Townsend and J. Allison used a similar approach to vaccinate mice against malignant melanoma. Normal mice were first immunized with irradiated, B7-transfected melanoma cells and then challenged with unaltered malignant melanoma cells. The "vaccine" was found to protect a high percentage of the mice (Figure 24-11a). It is hoped that a similar vac-

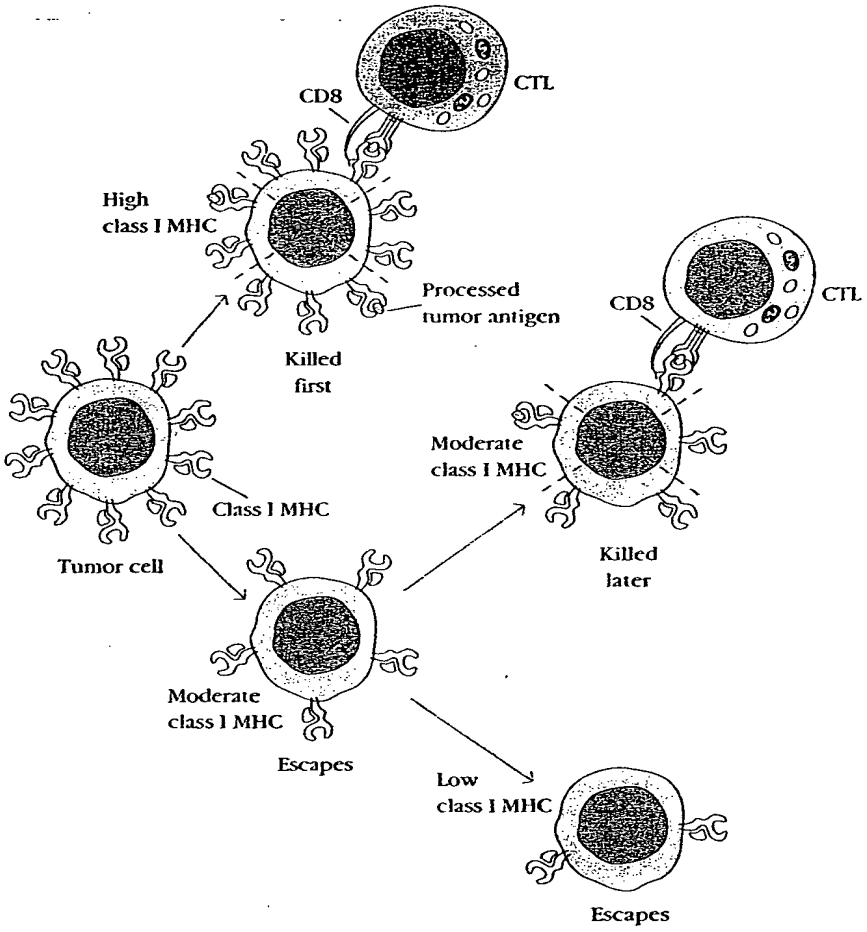

FIGURE 24-10

Down-regulation of class I MHC expression on tumor cells may allow a tumor to escape CTL-mediated recognition. The immune response may play a role in selecting for tumor cells expressing lower levels of class I MHC molecules by preferentially eliminating those cells expressing high levels of class I molecules. With time, malignant tumor cells may express progressively fewer MHC molecules and thus escape CTL-mediated destruction.

cine might prevent metastasis after surgical removal of a primary melanoma in human patients.

Because human melanoma antigens are shared by a number of different human tumors, it might be possible to generate a panel of B7-transfected melanoma cell lines that are typed for tumor antigen expression and for HLA expression. In this approach, the tumor antigen(s) expressed by a patient's tumor would be determined, and then the patient would be vaccinated with an irradiated B7-transfected cell line that expresses a similar tumor antigen(s).

Enhancement of APC Activity

Mouse dendritic cells cultured in GM-CSF and incubated with tumor fragments have been shown to activate both T_H cells and CTLs specific for the tumor antigens. When these mice were subsequently challenged with live tumor cells, they displayed tumor immunity. These experiments have led to a number of approaches aimed at expanding the population of antigen-presenting cells, so that these cells can activate T_H or CTLs specific for tumor antigens.

One approach that has been tried is to transfect tumor cells with the gene encoding GM-CSF. These engineered tumor cells, when reinfused back into the patient, will secrete GM-CSF, enhancing the differentiation and activation of host antigen-presenting cells, especially dendritic cells. As these dendritic cells accumulate around the tumor cells, the GM-CSF secreted by the tumor cells will enhance the presentation of tumor antigens to T_H and CTLs cells by the dendritic cells (Figure 24-11b). Clinical trials using melanoma cells transfected with GM-CSF are currently under way in melanoma patients.

Another way to expand the dendritic cell population is to culture dendritic cells from peripheral-blood progenitor cells in the presence of GM-CSF, TNF-α, and IL-4. These three cytokines allow the generation of large numbers of dendritic cells. If these dendritic cells are

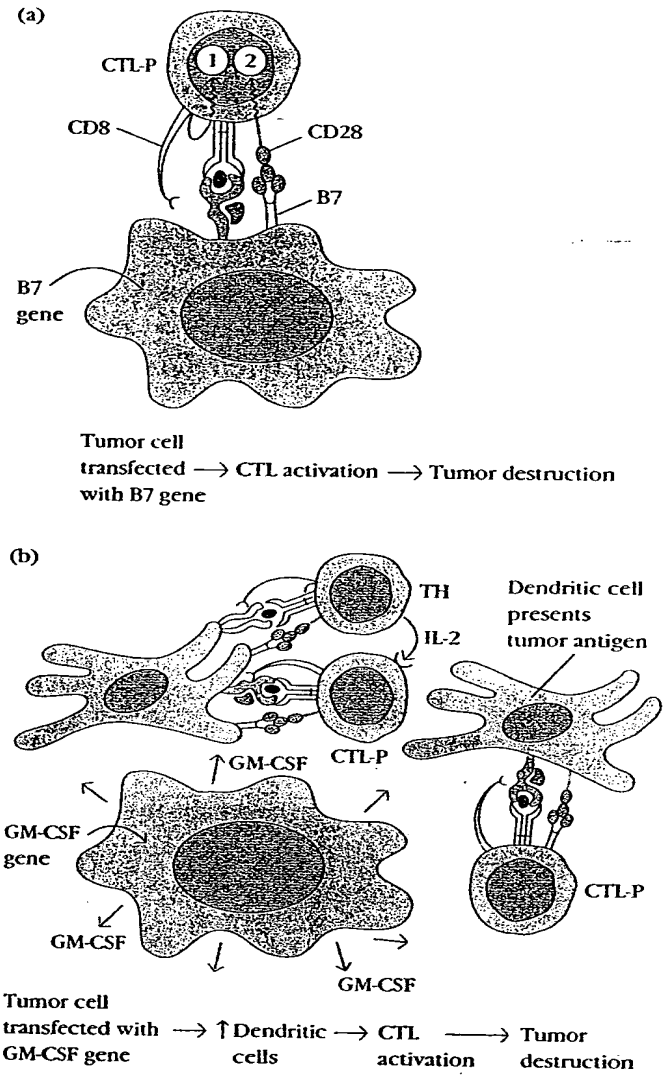

FIGURE 24-11

Use of transfected tumor cells for cancer immunotherapy. (a) Tumor cells transfected with the B7 gene express the co-stimulatory B7 molecule, enabling the tumor cells to provide both activating signal 1 and co-stimulatory signal 2 to CTL-Ps. As a result of the combined signals, the CTL-Ps differentiate into effector CTLs, which can mediate tumor destruction. In effect, the transfected tumor cell acts as an antigen-presenting cell. (b) Transfection of tumor cells with the gene encoding GM-CSF allows the tumor cells to secrete high levels of GM-CSF. This cytokine will activate dendritic cells in the vicinity of the tumor, enabling the dendritic cells to present tumor antigens to both T_H cells and CTL-Ps.

pulsed with tumor fragments and then reintroduced into the patient, they can now activate T_H and T_C cells specific for the tumor antigens.

A number of adjuvants, including the attenuated strain of *Mycobacterium bovis* called bacillus Calmette-Guerin (BCG) and *Corynebacterium parvuum*, have been used to boost tumor immunity. These adjuvants activate macrophages increasing their expression of various cytokines, class II MHC molecules, and the B7 co-stimulatory molecule. These activated macrophages are better activators of T_H cells, resulting in generalized increases in both humoral and cell-mediated responses. Although initially hailed as a "cancer cure," these adjuvants have shown only modest therapeutic results in melanoma patients and on the whole the clinical results with adjuvants have been disappointing.

Cytokine Therapy

The isolation and cloning of the various cytokine genes, mentioned in Chapter 13, has facilitated their large-scale production. A variety of experimental and clinical approaches have been developed to use recombinant cytokines, either singly or in combination, to augment the immune response against cancer. Among the cytokines that have been evaluated in cancer immunotherapy are interferons α, β, and γ, IL-1, IL-2, IL-4, IL-5, and IL-12; GM-CSF and TNF. Although these trials have produced occasional hopeful results, many obstacles remain to the successful use of this type of cancer immunotherapy.

The most notable obstacle is the complexity of the cytokine network itself (see Figure 13-4). This complexity makes it very difficult to know precisely how intervention with a given recombinant cytokine will affect the production of other cytokines. And since some cytokines act antagonistically, it is possible that intervention with a recombinant cytokine, designed to enhance a particular branch of the immune response, may actually lead to suppression. In addition, cytokine immunotherapy is plagued by difficulties with administering the cytokines in a localized fashion. In some cases systemic administration of high levels of a given cytokine has been shown to lead to serious and even life-threatening consequences. Although the results of several experimental and clinical trials of cytokine therapy for cancer are discussed here, it is important to keep in mind that this therapeutic approach is still in its infancy.

Interferons

Large quantities of purified recombinant preparations of the interferons, IFN-α, IFN-β, and IFN-γ, are now available, each of which has shown some promise in the treatment of human cancer. To date, most of the clinical trials have involved IFN-α. Daily injections of recombinant IFN-α have been shown to induce partial or complete

tumor regression in some patients with hematologic malignancies such as leukemias, lymphomas, and myelomas and with solid tumors such as melanoma, Kaposi's sarcoma, renal cancer, and breast cancer.

Interferon-mediated antitumor activity may involve several mechanisms. All three types of interferon have been shown to increase class I MHC expression on tumor cells; IFN-γ has also been shown to increase class II MHC expression on macrophages. Given the evidence for decreased levels of class I MHC molecules on malignant tumors, the interferons may act by restoring MHC expression, thereby increasing CTL activity against tumors. In addition, the interferons have been shown to inhibit cell division of both normal and malignantly transformed cells in vitro. It is possible that some of the antitumor effects of the interferons are related to this ability to directly inhibit tumor-cell proliferation. Finally, IFN-γ increases the activity of T_C cells, macrophages, and NK cells, all of which play a role in the immune response to tumor cells.

Tumor Necrosis Factors

The tumor necrosis factors, TNF-α and TNF-β, have been shown to exhibit direct antitumor activity, killing some tumor cells and reducing the rate of proliferation of others while sparing normal cells (Figure 24-12). In the presence of TNF-α or TNF-β a tumor undergoes visible hemorrhagic necrosis and tumor regression (see Figure 15-14a). TNF-α has also been shown to inhibit tumor-induced vascularization (angiogenesis) by damaging the vascular endothelial cells in the vicinity of a tumor, thereby decreasing the flow of blood and oxygen that is necessary for progressive tumor growth.

Phase I clinical trials of recombinant TNF-α in cancer patients appeared quite promising, and early news stories hailed TNF-α as the "cure for cancer." Further evaluation revealed that although TNF-α holds some promise, it is far from being an antitumor wonder drug. Injection of TNF-α directly into the tumor has led to complete tumor regression in some patients, but not in others.

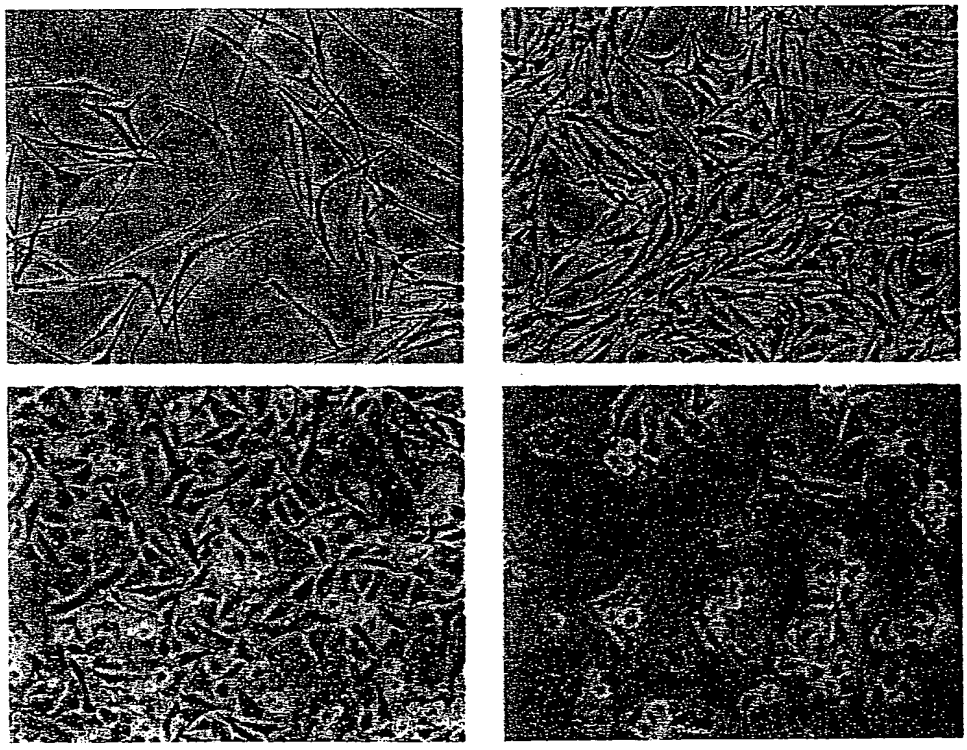

FIGURE 24-12

Photomicrographs of cultured normal melanocytes *(top)* and of cultured cancerous melanoma cells *(bottom)* in the presence and absence of tumor necrosis factor α (TNF-α). Note that in the presence of TNF-α, the cancer cells stop proliferating, whereas TNF-α has no inhibitory effect on proliferation of the normal cells. [From L. J. Old, 1988, *Sci. Am.* 258(5):59.]

TNF-α therapy has several limitations: the short half-life of TNF-α necessitates frequent injections; and its adverse side effects include fever, chills, blood-pressure changes, and decreased counts of white blood cells.

In Vitro–Activated LAK and TIL Cells

Animal studies have shown that lymphocytes can be activated against tumor antigens in vitro by culturing the lymphocytes with x-irradiated tumor cells in the presence of IL-2 and added tumor antigens. These activated lymphocytes mediate more effective tumor destruction than untreated lymphocytes when they are reinjected into the original tumor-bearing animal. It is difficult, however, to activate in vitro enough lymphocytes with antitumor specificity to be useful in cancer therapy.

While sensitizing lymphocytes to tumor antigens by this method, S. Rosenberg discovered that in the presence of high concentrations of cloned IL-2 and without the addition of tumor antigens, large numbers of activated lymphoid cells were generated that could kill fresh tumor cells but not normal cells. He called these cells **lymphokine-activated killer (LAK) cells**. In one study, for example, Rosenberg found that infusion of LAK cells plus recombinant IL-2 into tumor-bearing animals mediated effective tumor-cell destruction (Figure 24-13). LAK cells appear to be a heterogeneous population of lymphoid cells that includes natural killer (NK) cells and natural cytotoxic (NC) cells; the relative numbers of the two cell types depend on the source of the lymphocytes and the conditions of IL-2 activation.

Because large numbers of LAK cells can be generated in vitro and because these cells are active against a wide variety of tumors, their effectiveness in human tumor immunotherapy has been evaluated in several clinical trials. In these trials, peripheral-blood lymphocytes were removed from patients with various advanced metastatic cancers and were activated in vitro to generate LAK cells. Patients were then infused with their autologous LAK cells together with IL-2. A trial with 25 patients in 1985 resulted in cancer regression in some patients. A more extensive trial with 222 patients in 1987 resulted in complete regression in 16 patients. However, a number of undesirable side effects are associated with the high levels of IL-2 required for LAK-cell activity. The most noteworthy is vascular leak syndrome, which involves emigration of lymphoid cells and plasma from the peripheral blood into the tissues, leading to shock.

Tumors contain lymphocytes that have infiltrated the tumor and presumably are taking part in an antitumor response. By taking small biopsy samples of tumors, one can obtain a population of these lymphocytes and expand it in vitro with IL-2. These activated **tumor-infiltrating lymphocytes** are called **TIL cells**. Many

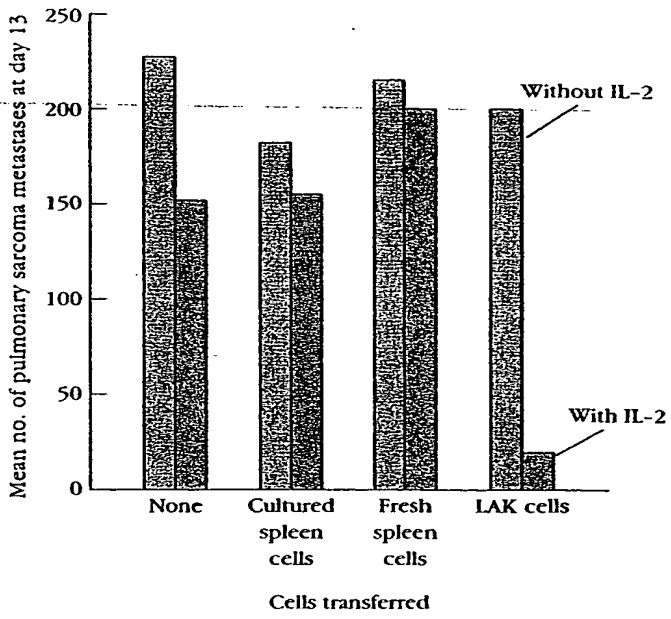

FIGURE 24-13

Experimental demonstration of tumor-destroying activity of LAK cells plus IL-2. Spleen cells or LAK cells, in the presence or absence of recombinant IL-2, were infused into mice with pulmonary sarcoma. The animals were evaluated 13 days later for the number of pulmonary sarcoma metastases. The LAK cells were prepared by isolating lymphocytes from tumor-bearing animals and incubating them in vitro with high concentrations of IL-2. Note that tumor regression occurred only when LAK cells and IL-2 were infused. [Data from S. Rosenberg et al., 1988, *Ann. Int. Med.*, **108**:853.]

TIL cells have a wide range of antitumor activity and appear to be indistinguishable from LAK cells. However, some TIL cells have specific cytolytic activity against their autologous tumor. These tumor-specific TIL cells are of interest because they have increased antitumor activity and require 100-fold lower levels of IL-2 for their activity than do LAK cells. In one study TIL cells were expanded in vitro from biopsy samples taken from patients with malignant melanoma, renal-cell carcinoma, and small-cell lung cancer. The expanded TIL cells were reinjected into autologous patients together with continuous infusions of recombinant IL-2. Renal-cell carcinomas and malignant melanomas showed partial regression in 29% and 23% of the patients, respectively.

Monoclonal Antibodies

Monoclonal antibodies have been used in various ways as experimental immunotherapeutic agents for cancer.

For example, anti-idiotype monoclonal antibodies have been used with some success in treating human B-cell lymphomas and T-cell leukemias. In one remarkable study, R. Levy and his colleagues successfully treated a 64-year-old man with terminal B-cell lymphoma. At the time of treatment the lymphoma had metastasized to the liver, spleen, bone marrow, and peripheral blood. Because this was a B-cell cancer the membrane-bound antibody on all the cancerous cells had the same idiotype. By the procedure outlined in Figure 24-14, these researchers produced mouse monoclonal antibody specific for the B-lymphoma idiotype. When this mouse monoclonal anti-idiotype antibody was injected into the patient, it bound specifically to the B-lymphoma cells because these cells expressed that particular idiotype. Since B-lymphoma cells are susceptible to complement-mediated lysis, the monoclonal antibody activated the complement system and lysed the lymphoma cells without harming other cells. After four injections with this anti-idiotype monoclonal antibody, the tumors began to shrink, and as of the last report this patient has been in complete remission.

Monoclonal antibodies also have been used to prepare tumor-specific **immunotoxins**. These agents consist of the inhibitor chain of a toxin (e.g., diphtheria toxin) linked to an antibody against a tumor-specific or tumor-associated antigen (see Figure 5-23). In vitro studies have demonstrated that these "magic bullets" can kill tumor

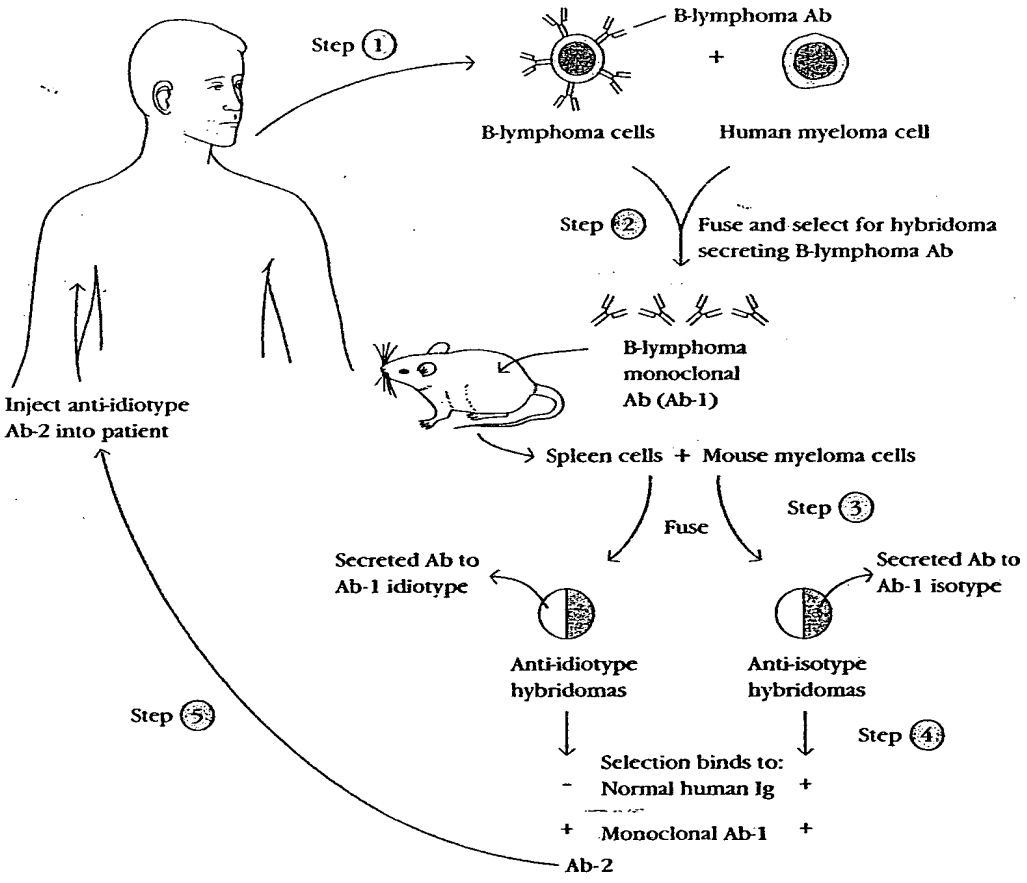

FIGURE 24-14

Treatment of B-cell lymphoma with monoclonal antibody specific for idiotypic determinants on the cancer cells. Because all the lymphoma cells are derived from a single transformed B cell, they all express membrane-bound antibody (Ab-1) with the same idiotype (i.e., the same antigenic specificity). In the procedure illustrated, monoclonal anti-idiotype antibody (Ab-2) against the B-lymphoma membrane-bound antibody was produced (steps 1–4). When this anti-idiotype antibody was injected into the patient (step 5), it bound selectively to B-lymphoma cells, which then were susceptible to complement-plus-antibody lysis.

cells without harming normal cells. Immunotoxins specific for tumor antigens in a variety of cancers (e.g., melanoma, colorectal carcinoma, metastatic breast carcinoma, and various lymphomas and leukemias) have been evaluated in phase I or phase II clinical trials. In eight separate trials, 12%–75% of leukemia and lymphoma patients exhibited partial or complete remission. In contrast, the clinical responses in patients with larger tumor masses were disappointing. In these patients, the tumor mass may render most of the tumor cells inaccessible to the immunotoxin.

Another cancer immunotherapy involves using monoclonal antibodies to bridge activated T cells directly to a tumor. In this approach two different monoclonal antibodies are produced: one specific for a tumor-cell membrane molecule and one specific for the CD3 membrane molecule of the TCR complex. A hybrid monoclonal antibody, or heteroconjugate, is then prepared with specificity for the tumor antigen and for CD3 (see Figure 5-25d). In vitro experiments with these heteroconjugates have revealed that they are able to cross-link and activate T cells directly on the surface of the tumor cell.

The finding that a variety of tumors express significantly increased levels of growth-factor receptors suggests that treatment with monoclonal antibodies against these receptors might inhibit tumor-cell activity. Monoclonal antibodies to the EGF receptor, to the p97 (transferrin) receptor, and to the IL-2 receptor have each been produced. In one study hundreds of mice with a lethal tumor were treated with chemotherapy alone or with chemotherapy plus monoclonal antibody to the EGF receptor. Chemotherapy alone failed to slow tumor growth in these mice, but every mouse that received the combined therapy recovered fully and the tumor did not recur following treatment. In a phase I clinical trial at Memorial Sloan-Kettering Cancer Center, patients with squamous-cell lung carcinoma are being treated with monoclonal antibody to EGF receptor. The results of this trial have not yet been published.

Tumor-Cell Vaccines

In a novel approach to developing tumor vaccines, a patient's own tumor cells are killed by x-irradiation, mixed with BCG, and reinjected into the patient. One woman treated in this way had been diagnosed with advanced malignant melanoma with literally hundreds of tumors on her right leg. Within 7 weeks after receiving this experimental vaccine, the tumors in her leg had disappeared, and the woman was still alive more than 3 years after treatment. Recent reports indicate that about 25% of patients with malignant melanoma have shown complete or partial remission after treatment with killed autologous tumor cells plus BCG.

SUMMARY

1. Tumor cells differ from normal cells in numerous ways. In particular, changes in growth regulation in tumor cells allow them to proliferate indefinitely, then invade the underlying tissue, and eventually metastasize to other tissues (see Figure 24-1). Normal cells can be transformed in vitro by chemical and physical carcinogens and by transforming viruses. Transformed cells exhibit altered growth properties and are sometimes capable of inducing cancer when they are injected into animals.
2. Proto-oncogenes encode proteins involved in control of cellular growth. It seems likely that conversion of a proto-oncogene to an oncogene may be involved in the induction of some kinds of cancer. This conversion may result from mutation in an oncogene, or its translocation or amplification (see Figure 24-2). A study of transformed cells has revealed the important role of cellular and viral oncogenes in the transformation process.
3. A number of B- and T-cell leukemias and lymphomas are associated with translocated proto-oncogenes. In its new site the translocated gene may come under the influence of an enhancer and be transcribed at higher levels than usual, or it may be subject to alteration by somatic mutation.
4. Tumor cells display tumor-specific antigens and the more comon tumor-associated antigens. Among the latter are oncofetal antigens, and increased levels of oncogene products. Several tumor-associated antigens expressed by melanoma cells are shared by other tumors; these common antigens might be useful clinically.
5. The immune response to tumors includes CTL-mediated lysis, NK-cell activity, macrophage-mediated tumor destruction, and destruction mediated by ADCC. Several cytotoxic factors, including TNF-α and TNF-β, help to mediate tumor-cell killing. Tumors may evade the immune response by modulating their tumor antigens, by reducing their expression of class I MHC molecules, and by antibody-mediated or immune-complex–mediated inhibition of CTL activity.
6. Experimental cancer immunotherapy has taken a variety of approaches. Enhancement of the co-stimulatory signal required for T-cell activation and of the activity of antigen-presenting cells has been achieved with transfected melanoma cells, leading to tumor destruction in experimental animals (see Figure 24-11). In some cases, injections of cytokines such as IFN-α and TNF-α have been shown to have beneficial effects. In another approach lymphocytes are activated in vitro

with high concentrations of IL-2, thereby inducing LAK cells or TIL cells with antitumor activity. Infusions of LAK cells plus IL-2 have reduced tumor development in experimental animals (see Figure 24-13). Some promising clinical results have been obtained in treating B-cell lymphomas and T-cell leukemias with monoclonal anti-idiotype antibodies (see Figure 24-14). Monoclonal antibodies specific for tumor antigens also have been used to produce immunotoxins. Vaccines of killed autologous tumor cells mixed with BCG have been somewhat effective in treatment of malignant melanomas.

REFERENCES

AISENBERG, A. C. 1993. Utility of gene rearrangements in lymphoid malignancies. *Annu. Rev. Med.* **44**:75.

ALLISON, J. P., A. A. HURWITZ, AND D. R. LEACH. 1995. Manipulation of costimulatory signals to enhance antitumor T-cell responses. *Curr. Opin. Immunol.* **7**:682.

BOON, T., ET AL. 1994. Tumor antigens recognized by T lymphocytes. *Annu. Rev. Immunol.* **12**:337.

CARBONE, D. P., AND J. D. MINNA. 1993. Antioncogenes and human cancer. *Annu. Rev. Med.* **44**:451.

COHEN, J. J. 1993. Apoptosis. *Immunol. Today* **14**:136.

COULIE, P. G., ET AL. 1994. A new gene coding for a differentiation antigen recognized by autologous cytolytic T lymphocytes on HLA-A2 melanomas. *J. Exp. Med.* **180**: 35.

COURNOYER, D., AND C. T. CASKEY. 1993. Gene therapy of the immune system. *Annu. Rev. Immunol.* **11**:297.

GEORGE, J. T., R. A. SPOONER, AND A. A. EPENETOS. 1994. Applications of monoclonal antibodies in clinical oncology. *Immunol. Today.* **15**:559.

JHAPPAN, C., ET AL. 1990. TGF-α overexpression in transgenic mice induces liver neoplasia and abnormal development of the mammary gland and pancreas. *Cell* **61**:1137.

KRADIN, R. L., ET AL. 1989. Tumor infiltrating lymphocytes and interleukin-2 treatment of advanced cancer. *Lancet* (March 18):577.

LIVINGSTONE, L. R., ET AL. 1992. Altered cell cycle arrest and gene amplification potential accompany loss of wild type *p53*. *Cell* **70**:923.

SUGIMURA, T. 1992. Multistep carcinogenesis: a 1992 perspective. *Science* **258**:603.

TOPALIAN, S. L., D. SOLOMON, AND S. A. ROSENBERG. 1989. Tumor-specific cytolysis by lymphocytes infiltrating human melanomas. *J. Immunol.* **142**:3714.

VAN DEN EYNDE, B., AND V. G. BRICHARD. 1995. New tumor antigens recognized by T cells. *Curr. Opin. Immunol.* **7**:674.

VOGELSTEIN, B., AND K. W. DINZLER. 1993. The multistep nature of cancer. *Trends Genet.* **9**:138.

WILLIAMS, G. T., C. A. SMITH, N. J. MCCARTHY, AND E. A. GRIMES. 1992. Apoptosis: final control point in cell biology. *Trends Cell Biol.* **2**:263.

STUDY QUESTIONS

1. Indicate whether each of the following statements is true or false. If you think a statement is false, explain why.

a. Hereditary retinoblastoma results from overexpression of a cellular oncogene.

b. Translocation of c-*myc* gene is found in many patients with Burkitt's lymphoma.

c. Multiple copies of cellular oncogenes are sometimes observed in cancer cells.

d. Viral integration into the cellular genome may convert a proto-oncogene into a transforming oncogene.

e. All oncogenic retroviruses carry viral oncogenes.

f. The immune response against a virus-induced tumor protects against another tumor induced by the same virus.

g. LAK cells are tumor specific.

2. You are a clinical immunologist studying acute lymphoblastic leukemia (ALL). Leukemic cells from most patients with ALL have the morphology of lymphocytes but do not express cell-surface markers characteristic of mature B or T cells. You have isolated cells from ALL patients that do not express membrane Ig but do react with monoclonal antibody against a normal pre-B cell marker (B-200). You therefore suspect that these leukemic cells are pre-B cells. How would you confirm that the leukemic cells are committed to the B-cell lineage by means of genetic analysis?

3. In a recent experiment melanoma cells were isolated from patients with early or advanced stages of malignant melanoma. At the same time T cells specific for tetanus toxoid antigen were isolated and cloned from each patient.

a. When early-stage melanoma cells were cultured together with tetanus toxoid antigen and the teta-

nus toxoid–specific T-cell clones, the T-cell clones were observed to proliferate. This proliferation was blocked by addition of chloroquine or by addition of monoclonal antibody to HLA-DR. Proliferation was not blocked by addition of monoclonal antibody to HLA-A, -B, -DQ, or -DP. What might these findings indicate about the early-stage melanoma cells in this experimental system?

b. When the same experiment was repeated with advanced-stage melanoma cells, the tetanus toxoid T-cell clones failed to proliferate in response to the tetanus toxoid antigen. What might this indicate about advanced-stage melanoma cells?

c. When early and advanced malignant melanoma cells were fixed with paraformaldehyde and incubated with processed tetanus toxoid, only the early-stage melanoma cells could induce proliferation of the tetanus toxoid T-cell clones. What might this indicate about early-stage melanoma cells?

d. How might you confirm your hypothesis experimentally?

4. What are three likely sources of tumor antigens?

5. Various cytokines have been evaluated for use in tumor immunotherapy. Describe four mechanisms by which cytokines mediate antitumor effects and the cytokines that induce each type of effect.

6. Infusion of transfected melanoma cells into cancer patients is a promising immunotherapy.

a. Which two genes have been transfected into melanoma cells for this purpose? What is the rationale behind use of each of these genes?

b. Why might use of such transfected melanoma cells also be effective in treating other types of cancers?

REVIEW ARTICLE

Leukemia: Management of Relapse After Allogeneic Bone Marrow Transplantation

By Lalit Kumar

Purpose: To review the current state of knowledge regarding the management of leukemic relapse after allogeneic bone marrow transplantation (BMT).

Patients and Methods: The literature was analyzed using MEDLINE (National Library of Medicine, Bethesda, MD) and reports were identified through review of report bibliographies. Pertinent studies were selected and data synthesized into a review format.

Results: Leukemic relapse after allogeneic BMT is an important cause of treatment failure. The risk of leukemic relapse varies from 20% to 60% depending on the diagnosis and phase of disease. Reinduction chemotherapy (CT), second BMT, interferon (IFN) alfa, and donor leukocyte infusions are various options, but none of the approaches is clearly optimal. Approximately 50% of acute myeloid leukemia (AML) and acute lymphoblastic leukemia (ALL) patients achieve remission after standard induction CT. However, most patients finally relapse and die of uncontrolled leukemia. Second BMT is successful in 20% to 25% patients and is a reasonable option in patients who relapse more than 6 months after the initial transplant. Young patients with a good performance status and those in remission from initial transplant relapse have a better outcome after second BMT. Venoocclusive disease (VOD), interstitial pneumonitis (IP), and acute graft-versus-host disease (GVHD) are the main complications. Therapy with IFN alfa results in cytogenetic complete remission (CR) in 10% to 25% patients with chronic myeloid leukemia (CML). The initial results of leukocyte infusions from the original donor are promising. However, acute GVHD and bone marrow aplasia are associated complications. The correct dose and schedule of donor leukocyte infusions need to be determined in future studies to minimize GVHD while maintaining the graft-versus-leukemia (GVL) effect.

Conclusion: Identification of patients at increased risk for relapse and use of biologic response modifiers post-transplant to augment the GVL effect in such patients are possible areas of improvement for future studies.

J Clin Oncol 12:1710-1717.

ALLOGENEIC bone marrow transplantation (BMT) results in long-term disease-free survival (DFS) in patients with chronic myeloid leukemia (CML) in chronic phase, acute myeloid leukemia (AML), and acute lymphoblastic leukemia (ALL). Leukemic relapse after BMT is an important cause of treatment failure. The actuarial probability of relapse varies according to the phase of disease at the time of transplant. In patients transplanted during remission from acute leukemia or during chronic-phase CML, the risk of relapse is less than 30%.[1-3] In contrast, the risk of relapse is high, 40% to 60%, for patients with advanced leukemia or those receiving T-cell–depleted donor marrow transplants.[4] Leukemia recurrence usually occurs within 2 years of BMT.[5] In CML, relapse generally occurs as a second chronic phase. However, an occasional patient may relapse directly into blast crisis without an identifiable period of chronic-phase hematopoiesis.[6]

From the Department of Medical Oncology, Institute Rotary Cancer Hospital, All India Institute of Medical Sciences, New Delhi, India.

Submitted September 13, 1993; accepted April 19, 1994.

Address reprint requests to Lalit Kumar, MD, DM, Assistant Professor of Medical Oncology, Institute Rotary Cancer Hospital, All India Institute of Medical Sciences, New Delhi 110029, India.

0732-183X/94/1208-0022$3.00/0

PATIENTS AND METHODS

Diagnosis

The diagnosis of relapse after BMT is not always straightforward. In some cases, the clinical, hematologic, and cytogenetic features of relapse are obvious. In CML patients, post-BMT cytogenetic studies have shown that the presence of Philadelphia chromosome (Ph)-positive metaphases in a proportion of bone marrow cells are not infrequent.[7] These are usually observed within 100 days of BMT and are considered a residual of mature recipient cells that survived the transplant conditioning regimen. In a small proportion of these patients, the Ph-positive metaphases in the marrow may be detected later. Persistent or increasing proportions of Ph-positive metaphases in serial cytogenetics are associated with an increased risk of relapse. Sporadic Ph-positive metaphases (found in low percentages and not seen in repeated karyotypes) are not related to imminent relapse.[7,8] In a study reported by Offit et al,[9] the presence of more than 25% Ph-positive metaphases and a condition of mixed chimerism was associated with an increased risk of hematologic relapse.

Information regarding the predictive value of post-BMT cytogenetics in acute leukemia is limited. Approximately 10% to 15% of ALL and 25% to 30% of AML patients have a specific chromosome translocation and, in most of these, the precise break points are not yet well characterized.[10]

Recently, the polymerase chain reaction (PCR) technique has been used after BMT/chemotherapy (CT) to detect residual leukemia cells and to predict impending relapse in Ph-positive CML and ALL,[11-13] in B- and T-cell ALL,[14,15] in AML type M2 with t(8;21),[16] in AML type M3 with t(15;17),[17] and in follicular lymphomas with t(14;18).[18] CML has been studied most extensively.[11-12,19] These studies have shown that BCR-ABL fusion messages often persists in CML patients after BMT. The prognostic value of this finding is less clear; only some patients who are PCR-positive after BMT progress to

REF. 21

clinical relapse. It has been suggested that patients with sustained PCR positivity more than 6 months after BMT have a higher probability of relapse than in patients who are PCR-negative.[19] The quantitative PCR assay used more recently aids assessment of the proliferation of residual leukemia cells and may thus allow early detection of impending relapse.[20,21]

Treatment

Treatment of patients who relapse after allogeneic BMT is difficult. Conventional CT, second BMT, interferon (IFN) alfa, and donor leukocyte infusions from original bone marrow donors are various therapeutic options.

CT. In AML patients who relapse after BMT, the standard induction CT with cytarabine and anthracycline results in a complete remission (CR) rate of approximately 35%. Time from BMT to relapse is the most important predictor of response to reinduction CT. Patients who relapse within 100 days of BMT are unlikely to obtain a meaningful remission and have a high treatment-related mortality rate.[22]

Results of reinduction CT in ALL patients have been reported in three studies.[22-24] The CR rate is approximately 50%. However, most patients finally relapse and die of uncontrolled leukemia, with the 3-year DFS rate being less than 10%. Patients with a long interval between BMT and relapse (>1 year) and those with isolated extramedullary relapse have a better outcome.

Radich et al[25] from Seattle have recently updated the results of treatment in 77 patients who relapsed after BMT. Sixty patients received standard CT, which resulted in remission for nine patients with acute leukemia and reinduction to chronic phase in six patients with CML.[25] Frassoni et al[26] for the European Bone Marrow Transplant Group (EBMTG) have reported the results of induction CT in 74 patients with acute leukemia. Thirty-two patients (43%) achieved a CR, with a median DFS duration of 12 months. Four patients (two with AML and two with ALL) were in continuous CR between 27 and 60 months after the relapse at the time of reporting. For patients who achieved remission, the actuarial probability of survival was 12.5% with a 3-year follow-up. This was significantly better than for patients who were not treated or did not achieve remission (8%), $P < .001$.[26]

Second BMT. The results of second BMT have been reported in a number of studies[27-37] (Table 1). Most patients in these studies had received cyclophosphamide and total-body irradiation (Cy-TBI) for preparation and T-cell–depleted donor marrow to prevent acute graft-versus-host disease (GVHD). Various regimens used for preparation before second BMT include the following: busulfan-Cy (Bu-Cy); Cy-TBI; Bu plus etoposide (VP-16) plus Cy; Bu + melphalan, Bu alone, and mitoxantrone plus VP-16 plus total-lymphoid irradiation. The choice of the preparatory regimen thus depends on the agents used before first BMT so as to avoid cumulative toxicity. Therefore, for most patients who have received cyclo-TBI before first transplant, Bu-Cy or Bu plus VP-16 plus Cy have been used and vice versa. Significant toxicity to preparatory regimens has been observed in most of these studies. Recently, it has been suggested that toxicity of the Bu-Cy regimen may be reduced by Cy elimination in selected patients whose lymphocytes are of donor origin.[33,34] Whether such an approach would be without an increased risk of relapse needs confirmation. Cullis et al[33] used high-dose Bu alone for conditioning before second BMT in eight CML patients. Three patients died: two of transplant-related complications and one of relapse. The remaining five patients are alive and disease-free.[33]

RESULTS

Second BMT

More than 200 patients with acute and chronic leukemia have received a second BMT in the past 8 years. Bone marrow from the original donor and acute GVHD prophylaxis similar to first BMT were used in most patients.

The Seattle group recently reported the results of second BMT in 77 patients (CML, n = 28; AML, n = 32; ALL, n = 15; and lymphoma, n = 2). High-dose Bu-Cy or Cy plus carmustine (BCNU) plus VP-16 was used for preparation before second transplant. Engraftment occurred in 74 patients. The estimated DFS rates at 3 years are 8%, 10%, and 25% for ALL, AML, and CML, respectively.[25] The Baltimore group transplanted 23 patients with recurrent leukemia after initial syngeneic (n = 3) or allogeneic (n = 20) BMT. The preparatory regimen before second BMT consisted of Bu-Cy in 14 patients and Cy-TBI in nine. Twelve patients died, eight before day 100. At a median follow-up duration of 2 years after second BMT, the overall survival, leukemia-free survival (LFS), and probability of remaining in remission at 26 months were 47%, 38%, and 76%, respectively. The outcome was better in patients with CML (seven of 12, 58% survivors) compared with acute leukemia patients (four of 11, 36% survivors).[34] Similar results have been reported from Hammersmith Hospital in London. Sixteen CML patients received second BMT following relapse after T-cell–depleted marrow transplant. Eight patients achieved LFS ranging from 158 to 1,789 days (median, 424 d). The actuarial probability of survival and LFS at 4 years are 41% and 49%, respectively. Six patients died of transplant-related complications.[33] The results obtained in these and other single-center studies have been confirmed by two recent multicenter studies.[32,35]

In the EBMTG study, 90 patients with AML (n = 41), ALL (n = 13), and CML (n = 27) received second transplant. Forty-three patients were either in remission from acute leukemia or in the chronic phase of CML, and 47 were in continuing relapse from leukemia or in accelerated-phase/blast crisis of CML at the time of second BMT. Seventy patients died: 37 of early transplant-related toxicity and 23 of relapse or failure to eradicate leukemia. There were 20 survivors. Thus, at a 3-year follow-up duration, the actuarial probabilities of LFS and relapse were 11% and 69%, respectively.[32] Similarly, in the International Bone Marrow Transplant Registry (IBMTR) study, among 114 patients (AML, n = 46, ALL, n = 29; and CML, n = 39) who received second BMT, the 2-year probabilities of LFS and relapse were 21% and 65%, respectively.[35]

Factors That Affect the Outcome of Second Transplant

Interval between first and second transplant. The interval between first and second transplant is an important factor in determining the outcome of a second transplant. In the EBMTG study, the LFS rate was 9% in patients

Table 1. Results of Second BMT

First Author, Year	No of Patients	Leukemia Type	Disease Status at Second BMT (no.)	Outcome	Survival (months)
Atkinson, 1986[28]	9	AML (5)	R (5/5)	CR 3/5,—died 2,	8, 19, 9+ 0.3, 0.6
		ALL (1)	R	CR	33+
		CML (1)	AP	CR	36+
		Ph† AL (1)	R	—died	3
		AM (1)	R	—died	0.5
Barrett, 1991[32]	90	AML (41)	NG	LFS 4/41	29.1-79.9+
		ALL (19)		3/19	27.0-71.2+
		CML (27)		6/27	29.6-49.0+
		MDS (1)			
		Lym (2)			
Cullis, 1992[33]	16	CML (16)	CP (13)	8 (50%)	5.0-59.6+
			AP (3)		
Wagner, 1992[34]	23	CML (12)	CP (6)	7/12 (58%)	3.8-110.5+ M-23.8+
			AP (6)		
		AML (7)	CR (4)	2/7	8.9+, 60.5+
			R (3)	Died 5/7	0.7-16.2, M-1.8
		ALL (4)	CR (3)	2/4	37.6+, 89.5+
			R (1)	Died-2	1, 3
Mrsic, 1992[35]	114	AML (46)	NG	34%*	2%†
		ALL (29)			
		CML (39)	CP (19)	37% at 2 years	
			AP/BC (20)		
Spinolo, 1992[36]	17	AML (5)	CR (1)	LFS 1/5	37+
			R (4)	Died 4/5	1.8-17
					M-7.2
		ALL (8)	CR (7)	2/8	55+, 61.5+
			R (1)	Died 6/8	0.9-14.6
					M-9.9
		CML (3)	CP (1)		
			BC (2)	Died 3/3	0.3, 3.8, 23.7
		Lym (1)	R	Died	4.6
Hashimoto, 1992[37]	8	ALL (3)	NG	3/8	8-27+
		AML (3)		Died 4/8 of VOD	
		CML (1)			
		RAEB (1)			
Radich, 1993[25]	77	CML (28)	CP (6), AP/BC (22)	LFS 7	22-78+ M-35.5
		AML (32)	CR (6), R (26)	4	26-88+ M-51
		ALL (9)	CR (2), R (6)	0	
		ALL (8)	CR (1), R (7)	2	25+, 39+

Abbreviations: CP, chronic phase; AP, accelerated phase; CR, complete remission; R, relapse; LFS, leukemia-free survival; NG, details not given, FU, follow-up; M, median; RAEBT, refractory anemia with excess blasts in transformation; MDS, myelodysplastic syndrome; Ly-Ly, lymphoblastic lymphoma; Lym, lymphoma; AM, acute myelofibrosis; VOD, venoocclusive disease.

*Acute leukemia in remission.

†Acute leukemia not in remission.

with an interval of less than 566 days between first and second transplant, compared with 36% in patients with an interval more than 566 days between first and second BMT.[32] Similarly, in the IBMTR study, the probabilities of LFS and relapse were 7% and 77% in patients who relapsed within 6 months of first BMT compared with 28% and 59% in patients who relapsed more than 6 months after first BMT ($P < .0002$).[35]

Treatment-related mortality is also higher in patients who relapse early posttransplant. For example, in the IBMTR study, it was 90% in patients who relapsed within 6 months of initial BMT. This was significantly less in patients who relapsed within 6 to 12 months (38%) and beyond 12 months (33%) of initial transplant ($P < .001$).[35]

The poor outcome from second BMT in patients who relapse within 6 months of first BMT is possibly due to poor performance status, higher toxicity with venoocclusive disease (VOD), and interstitial pneumonitis (IP; discussed later). Thus, at present, it seems reasonable to

delay second BMT until more than 6 months after the first transplant have elapsed.

Treatment-related toxicity. The risk of preparative regimen-related toxicities, mainly VOD and IP, is higher after the second than after the first transplant.[25,35,36] In a recent study from Seattle, among 77 patients, 64% developed VOD (grade I/II, 36%; III/IV, 26%) after second BMT. None of the patients with severe VOD survived.[25] The management of established severe VOD is largely unsatisfactory. Recent efforts have therefore been directed toward prevention of VOD by using the drugs to interrupt the coagulation cascade or to diminish the influence of factors that favor thrombogenesis. These include prophylactic use of heparin, prostaglandin E_1, and recombinant tissue plasminogen factor (r-TPA), and oral administration pentoxifylline, a tumor necrosis factor-alpha (TNF-a) blocker. The use of pentoxifylline and r-TPA in phase I/II trials has shown promise in lessening VOD.[38,39] Prospective randomized studies are in progress to expand these preliminary results.

Similar to the IBMTR study, the incidence of severe IP in the Seattle study was higher after second than after first BMT: 17% versus 4%. Other pulmonary complications were also more common after second BMT.[25] The prophylactic use of ganciclovir may be a reasonable approach to reduce the risk of IP in such high-risk cytomegalovirus-(CMV)-positive recipients.[40]

Disease status before second transplant. Patients in remission from acute leukemia at the time of second BMT have a better LFS rate compared with those who are not in remission.[26] It has been suggested that CML patients who are in chronic phase before second BMT have a better outcome than patients who are in accelerated phase or blast crisis.[25,26,32] However, in the recent IBMTR study, there was no difference in relapse risk between patients who received second transplant in chronic phase versus accelerated or blastic phase. LFS was also similar whether CML was in chronic, accelerated, or blastic phase before second BMT.[35]

GVHD. The incidence and severity of acute and chronic GVHD after second transplant are generally similar to that seen after first transplant. In the study by the Baltimore group, six of 23 patients with grade I acute GVHD after first BMT also developed acute GVHD after second BMT: grade I in five patients and grade II in one. In the remaining 17 patients, who had no evidence of acute GVHD after first BMT, only one developed grade II GVHD after second BMT.[34] In the IBMTR study, the incidence of acute GVHD after second BMT for the whole group was similar for the patients with or without acute GVHD after first BMT. Chronic GVHD occurred in 20% of patients after first BMT and in 21% patients who survived for longer than 90 days after second BMT.[35]

One approach to GVHD prophylaxis after second BMT may be selective T-cell depletion of donor marrow followed by post-BMT administration of interleukin-2 (IL-2).[41] IL-2 potently activates T lymphocytes and natural-killer cells, both of which are thought to play a role in the graft-versus-leukemia (GVL) effect.[42]

IFN Alfa

The beneficial effects of IFN alfa against the Ph-positive clone have been well documented in chronic-phase CML patients before BMT.[43] A number of studies have reported the use of IFN alfa in CML patients for treatment of post-BMT relapse[44-49] (Table 2). Arcese et al[46] treated 20 CML patients with hematologic or cytogenetic relapse after T-cell–depleted BMT. All five patients with hematologic relapse obtained hematologic remission without reduction of marrow Ph-positive cells. Of 15 patients with cytogenetic relapse, two achieved cytogenetic CR. Both complete cytogenetic responders are alive at 67 and 76+ months from relapse. The Seattle group treated 18 CML patients with hematologic relapse.[48] Six patients (33%) achieved cytogenetic CR. The median time to achieve response was 3 months (range, 1 to 18), and the median duration of response was 13+ months (range, 6+ to 20+). Similar results have been reported recently by the French group.[49] Among 28 CML patients treated for hematologic (n = 19) or cytogenetic (n = 9) relapse, seven (25%) achieved cytogenetic CR (Table 2).

More recently, Arcese et al[50] for the EBMTG have reported the results of IFN alfa treatment for post-BMT relapse. Among 28 patients with hematologic relapse, seven (25%) achieved cytogenetic CR, as compared with four of 24 patients with cytogenetic relapse. IFN therapy significantly delayed the progression toward hematologic relapse. The delayed progression to hematologic disease increased the probability of survival, which was significantly higher at 2 years for patients treated with IFN at the time of cytogenetic relapse than for patients who never received IFN or for those treated at hematologic progression. However, IFN failed to cure the patients. Most later progressed to more advanced disease and died. IFN alfa was administered at doses of 3 to 5 $\times$ 10^6 IU/m^2 daily or on alternate days in these studies[44-47,49]; higher doses were associated with significant toxicity in the Seattle study.[48]

Thus, IFN alfa therapy results in hematologic response in most, and cytogenetic CR in 10% to 25% of CML patients with relapse. However, its impact on long-term survival is not yet known.

The mechanisms by which IFN inhibits leukemic cell growth remain ill-defined. Data suggest that IFN increases the expression of major histocompatibility antigens, which

Table 2. IFN Alfa Therapy for CML Relapse

Author, First Year	No. of Patients	Relapse Type (no.)	Response	Survival (months)
Newland, 1987[44]	1	HR	Ph^-	15+
Borgies, 1989[45]	1	HR	Ph^-	15+
Arcese, 1991[46]	20	HR (5)	5/5 H. remission, Ph^+	
		Cyt. R (15)	2 Ph^-	67 and 76+
			10 HR	
			3 H remission	
Steegmann, 1991[47]	1	HR	Ph^-	14+
Higano, 1992[48]	18	HR	6/18 Ph^-	NG
Pigneux, 1992[49]	28	HR (19)	4/19 Ph^-	
		Cyt. R (9)	3/9 Ph^-	NG

Abbreviations: HR, hematologic relapse; Cyt. R, cytogenetic relapse; NG, not given; H remission, hematologic remission.

may facilitate recognition and suppression of leukemia host cells by donor lymphocytes. Direct cytotoxic effect/differentiation of leukemic cells is another possibility.[51]

Three studies have used IFN therapy prophylactically after allogeneic BMT. Meyers et al[52] from Seattle administered IFN alfa to ALL patients after allogeneic BMT with the intent to decrease the incidence of CMV infection. Although the CMV infection rate was not influenced by IFN, patients in the IFN-treated group had a significantly lower relapse rate (50% *v* 25%). Klingemann et al,[51] in a phase I study, administered IFN alfa-2b to autologous or allogeneic BMT patients once stable engraftment was achieved. The daily tolerated dose of IFN was much lower (1×10^6 IU/m^2/d) compared with earlier studies in relapsed patients. In a recent EBMTG study,[53] IFN alfa-2b was administered to six patients with advanced CML. In four patients, IFN treatment was continued until day 365 after BMT. In two patients, treatment was discontinued because of fever and bone pain. None of six patients developed de novo acute GVHD. Three patients died: two of relapse and one of infection. The results of these preliminary studies confirm the feasibility of IFN alfa treatment as soon as stable engraftment is achieved.

Donor Leukocyte Infusions

Infusion of donor leukocytes has been used previously in leukemia therapy. Sullivan et al[54] transfused donor leukocytes to patients with advanced acute leukemia shortly after BMT in an attempt to reduce the risk of relapse. However, the recipients of this therapy had relapse rates similar to those of controls and had more acute GVHD and reduced survival. Kolb et al[55] in 1990 first reported successful treatment of three CML patients with hematologic relapse using IFN alfa and infusion of viable buffy-coat cells from donor marrow, but no additional CT. All three patients achieved hematologic and cytogenetic CR lasting from 32 to 91 weeks' posttreatment at the time of reporting. Two patients developed grade II GVHD, which resolved with immunosuppressive treatment. Cullis et al[56] treated two patients in cytogenetic relapse after T-cell–depleted allogeneic BMT with infusions of viable donor buffy-coat cells, but without IFN or additional CT. Both patients achieved cytogenetic remission confirmed by PCR studies. Subsequently, more patients have been treated by donor leukocyte infusions (Table 3).[57-63] Bar et al[62] treated five CML patients in hematologic relapse. All five patients achieved cytogenetic CR, with PCR remission in four. A sixth patient in cytogenetic relapse did not respond. Similar results have been reported more recently by Drobyski et al.[63] In this study, eight CML patients received a T-cell dose of 2.5 to 5×10^8/kg for hematologic relapse (six accelerated phase and two blast crisis). Seven patients developed acute GVHD, which was grade I in five patients and grade III/IV in two. Four patients had bone marrow aplasia that required bone marrow boosts from the original donor in three. All six patients in accelerated phase achieved complete Ph negativity, with PCR negativity in five. Both patients in blast crisis died: one of GVHD and one of progressive disease.

Kolb et al[64] for the EBMTG reported the results of donor buffy-coat infusions in 56 patients treated in 18 European centers. Forty patients were treated for recurrent CML and 16 patients for acute leukemia, lymphoma, multiple myeloma, osteomyelofibrosis, and myelodysplastic syndrome. IFN alfa was administered concomitantly to 46 patients. Seventy percent of patients (36 of 56) achieved CR; 30 of 46 patients given IFN alfa responded, as compared with seven of 10 patients not given IFN. Fifty percent of patients (28 of 56) developed clinical signs of GVHD, but pancytopenia was frequent in patients who responded.

How donor leukocyte infusions eradicate the leukemic clone is not entirely clear. It has been suggested that infusion of allogeneic T cells either mediates a direct cytotoxic effect against host hemopoietic cells or indi-

Table 3. Results of Donor Leukocyte Infusions for Leukemia Relapse

First Author, Year	No. of Patients	Leukemia Type (no.)	Relapse Type (no.)	AGVHD	Outcome
Kolb, 1990[55]†	3	CML (3)	HR	2/3 Gr. II	3/3 Ph^-
Cullis, 1992[56]	2	CML (2)	Cyt. R	2/2 Gr. II	2/2 Ph^- (2/2 PCR^-)
Frassoni, 1992[57]†	10	CML (7)	HR	4/7 Gr. I	3 Ph^+, 2 Ph^-
					2 died of BMA
		MM (1)	NG		1 died of BMA
		AML (2)‡			
Lonnqvist, 1992[58]†	4	CML (3)	HR	1/4 Gr. I	2 Ph^-
					1 Ph^+
		PV (1)			NR
Helg, 1992[59]	3	CML (3)	HR (2)	3/3 Gr. NG	3/3 Ph^-
			Cyt. R (1)		
Novotny, 1992[60]†	6	CML (6)	HR	NG	2 Ph^-
					3 died of BMA
Szer, 1993[61]	4	AML	HR	3/4	1CR
				Gr. II 2/4	3 died of leukemia
				1/4 Gr. III	1 NR
Bar, 1993[62]	6	CML (6)	HR (5)	3/6 Gr. III-IV	5/5 Ph^-
					(4/5 PCR^-)
			Cyt. R (1)		1 NR
Drobyski, 1993[63]†	8	CML (8)	HR (8)	5 Gr. I	6 Ph^-
				2 Gr. III-IV	(5/6 PCR^-)
					4 BMA
Total	46	CML (38)	HR (34)		25 Ph^-
			Cyt. R (4)		7 Ph^+
					6 died
		AL (6[4])*	HR (4)		CR (1), NR (3)
		MM (1)			NR
		PV (1)			NR

Abbreviations: HR, hematologic relapse; Cyt. R, cytogenetic relapse; AGVHD, acute graft-versus-host-disease; NG, details not given; AL, acute leukemia; PV, polycythemia vera; RAEBT, refractory anemia with excess blasts; MM, multiple myeloma; Gr., grade; NR, no response; BMA, bone marrow aplasia.

*Figure in brackets represents assessable patients.

†Given IFN alfa in addition.

‡Given prophylactically.

rectly stimulates the GVL effect.[55,56,63] Thus, the results of donor leukocyte infusions with or without IFN alfa in the treatment of recurrent leukemia after BMT are encouraging. Further clinical trials are needed to determine the timing and optimum dose of T cells in various stages of relapse (hematologic/cytogenetic) to reduce toxicity while maintaining the GVL effect.

DISCUSSION

The management of leukemic relapse after allogeneic BMT presents a dilemma to the treating transplant physician. Induction CT, second BMT, IFN alfa, and donor leukocyte infusions are various options. Thirty percent to 55% of patients with acute leukemia achieve remission after induction CT, with a LFS rate of less than 10%. Second transplant results in a LFS rate of 20% to 25% and is a reasonable option for patients who relapse more than 6 months after initial BMT. The increased toxicity associated with the preparatory regimen may possibly be reduced in the future with the use of less intensive preparatory regimens. IFN alfa controls the symptoms in most CML patients, but only 10% to 25% of patients achieve Ph negativity. Encouraging results have been obtained with donor leukocyte infusions in CML patients.

Identification of patients at high risk for relapse post-transplant through quantitative PCR assay and prophylactic use of biologic response modifiers to augment the GVL effect in such patients with minimal residual disease are possible areas of progress in future studies.

REFERENCES

1. Gale RP, Horowitz MM, Biggs JC, et al: Transplant or chemotherapy in acute myelogenous leukaemia. Lancet 1:1119-1122, 1989
2. Barrett AJ, Horowitz MM, Gale RP, et al: Marrow transplantation for acute lymphoblastic leukemia. Factors affecting relapses and survival. Blood 74:862-871, 1989
3. Goldman JM, Apperley JF, Jones L, et al: Bone marrow transplantation for patients with chronic myeloid leukemia. N Engl J Med 314:202-207, 1986
4. Maramont AM, Horowitz MM, Gale RP, et al: T-cell depletion of HLA identical transplants in leukemia. Blood 78:2120-2130, 1991
5. Bortin MM, Ringden O, Horowitz M, et al: Temporal relationships between the major complications of bone marrow transplantation for leukemia. Bone Marrow Transplant 4:339-344, 1989
6. Cullis JO, Marks DI, Schwarer AP, et al: Relapse into blast crisis following bone marrow transplantation for chronic phase chronic myeloid leukaemia. Br J Haematol 81:378-382, 1992
7. Zaccaria A, Rosti G, Testoni N, et al: Cytogenetic events after bone marrow transplantation for Philadelphia chromosome positive chronic myeloid leukaemia. Leuk Res 15:289-296, 1991
8. Bilhou-Nabera C, Bernard P, Marit G, et al: Serial cytogenetic studies in allografted patients with chronic myeloid leukemia. Bone Marrow Transplant 9:263-268, 1992
9. Offit K, Burns JP, Cunningham I, et al: Cytogenetic analysis of chimerism and leukemia relapse in chronic myelogenous leukemia patients after T-cell depleted bone marrow transplantation. Blood 75:1346-1355, 1990
10. van Dongen Jacques JM, Breit TM, Adriaansen HJ, et al: Detection of minimal residual disease in acute leukemia by immunological marker analysis and polymerase chain reaction. Leukemia 6:47-59, 1992 (suppl 1)
11. Hughes TP, Morgan GJ, Martiat P, et al: Detection of residual leukemia after bone marrow transplantation for chronic myeloid leukemia: Role of polymerase chain reaction in predicting relapse. Blood 77:874-878, 1991
12. Roth MS, Antin JH, Ash R, et al: Prognostic significance of Philadelphia chromosome positive cells detected by the polymerase chain reaction after allogeneic bone marrow transplant for chronic myelogenous leukemia. Blood 79:276-282, 1992
13. Miyamura K, Tanimoto M, Morishima Y, et al: Detection of Philadelphia chromosome positive acute lymphoblastic leukemia by polymerase chain reaction: Possible eradication of minimal residual disease by marrow transplantation. Blood 79:1366-1370, 1992
14. Yamada M, Wasserman R, Lange B, et al: Minimal residual disease in childhood B-lineage lymphoblastic leukemia: Persistence of leukemia cells during the first 18 months of treatment. N Engl J Med 323:448-455, 1990
15. Nizet Y, Daele SV, Vaerman LJL, et al: Long term follow up of residual disease in acute lymphoblastic leukemia patients in complete remission using clonogenic IgH probes and polymerase chain reaction. Blood 82:1618-1625, 1993
16. Nacifora G, Larson RA, Rowley JD: Persistence of the 8;21 translocation in patients with acute myeloid leukemia type M2 in long term remission. Blood 82:712-715, 1993
17. Miller WH Jr, Levine K, De Blasio A, et al: Detection of minimal residual disease in acute promyelocytic leukemia by a reverse transcription polymerase chain reaction assay for the PML/RAR-a fusion mRNA. Blood 82:1689-1694, 1993
18. Gribben JG, Neuberg D, Freedman AS, et al: Detection by polymerase chain reaction of residual cells with the *bcl-2* translocation is associated with increased risk of relapse after autologous bone marrow transplantation for B-cell lymphoma. Blood 81:3449-3457, 1993
19. Negrin RS, Blume KG: The use of polymerase chain reaction for the detection of minimal residual malignant disease. Blood 78:255-258, 1991
20. Lion T, Henn T, Gaiger A, et al: Early detection of relapse after bone marrow transplantation in patients with chronic myelogenous leukemia. Lancet 341:275-276, 1993
21. Cross NCP, Feng L, Chase A, et al: Competitive polymerase chain reaction to estimate the number of BCR-ABL transcripts in chronic myeloid leukemia patients after bone marrow transplantation. Blood 82:1929-1936, 1993
22. Mortimer J, Blinder MA, Schulman S, et al: Relapse of acute leukemia after marrow transplantation: Natural history and results of subsequent therapy. J Clin Oncol 7:50-57, 1989
23. Barrett AJ, Joshi R, Tew C: How should acute lymphoblastic leukaemia relapsing after bone marrow transplantation be treated? Lancet 1:1188-1190, 1985
24. Bostrom B, Woods WG, Nesbit ME, et al: Successful reinduction of patients with acute lymphoblastic leukemia who relapse following bone marrow transplantation. J Clin Oncol 5:376-381, 1987
25. Radich JP, Sanders JE, Buckner CD, et al: Second allogeneic marrow transplantation for patients with recurrent leukemia after initial transplant with total body irradiation-containing regimens. J Clin Oncol 11:304-313, 1993
26. Frassoni F, Barrett AJ, Granena A, et al: Relapse after allogeneic bone marrow transplantation for acute leukaemia: A survey by the EBMT of 117 cases. Br J Haematol 70:317-320, 1988
27. Champlin RE, Ho WG, Lenarsky C, et al: Successful second marrow transplants for treatment of acute myelogenous leukemia and acute lymphoblastic leukemia. Transplant Proc 17:496-499, 1985
28. Atkinson K, Biggs J, Concannon A, et al: Second marrow transplants for recurrence of haematological malignancy. Bone Marrow Transplant 1:159-166, 1986
29. Blume KG, Forman SJ. High dose busulphan/etoposide as a preparatory regimen for second bone marrow transplants in haematological malignancies. Blut 55:49-53, 1987
30. Maramont AM, Van Lint MT, Frassoni F, et al: Second marrow transplants for relapsed leukemia after bone marrow transplantation. Bone Marrow Transplant 3:332-333, 1988 (suppl 1)
31. Sanders JE, Buckner CD, Clift RA, et al: Second marrow transplants for patients with hematological malignancy who relapse after first transplant. Blood 74:203a, 1989 (suppl 1, abstr)
32. Barrett AJ, Locatelli F, Treleaven J, et al: Second transplants for leukaemic relapse after bone marrow transplantation; High mortality but favourable effect of chronic GVHD on continued remission. A report by the EBMT Leukaemia Working Party. Br J Haematol 79:567-574, 1991
33. Cullis JO, Schwarer AP, Hughes TP, et al: Second transplants for patients with chronic myeloid leukaemia in relapse after original transplant with T-depleted donor marrow: Feasibility of using busulphan alone for reconditioning. Br J Haematol 80:33-39, 1992
34. Wagner JE, Vogelsang GB, Zehnbauer BA, et al: Relapse of leukemia after bone marrow transplantation: Effect of second myeloablative therapy. Bone Marrow Transplant 9:205-209, 1992
35. Mrsic M, Horowitz MM, Atkinson K, et al: Second HLA-identical sibling transplants for leukemia recurrence. Bone Marrow Transplant 9:269-275, 1992
36. Spinolo JA, Yau JC, Dicke KA, et al: Second bone marrow transplants for relapsed leukemia. Cancer 69:405-409, 1992

37. Hashimoto S, Nakaseko T, Asai T, et al: Second marrow transplantation for hematological malignancies. Exp Hematol 20:715a, 1992 (abstr)

38. Bianco JA, Appelbaum FR, Nemunaitis J, et al: Phase I-II trial of pentoxifylline for the prevention of transplant related toxicities following bone marrow transplantation. Blood 78:1205-1211, 1991

39. Bearman SI, Shuhart MC, Hinds MS, et al: A pilot study of recombinant tissue plasminogen activator (tPA) for the treatment of established severe hepatic venoocclusive disease (VOD) after marrow transplantation. Proc Am Soc Clin Oncol 11:263a, 1992 (abstr)

40. Schmidt GM, Horak DA, Niland JC, et al: A randomized controlled trial of prophylactic ganciclovir for cytomegalovirus pulmonary infection in recipients of allogeneic bone marrow transplantation. N Engl J Med 324:1005-1011, 1991

41. Soiffer RJ, Murray C, Mauch P, et al: Prevention of graft-versus-host disease by selective depletion of CD6-positive T lymphocytes from donor bone marrow. J Clin Oncol 10:1191-1200, 1992

42. Soiffer RJ, Murray C, Cochran K, et al: Clinical and immunologic effects of prolonged infusion of low dose recombinant IL-2 following autologous and T cell depleted allogeneic transplantation. Blood 79:517-526, 1992

43. Kantarjian HM, Deisseroth A, Kurzrock R, et al: Chronic myelogenous leukemia: A concise update. Blood 82:691-703, 1993

44. Newland AC, Jones L, Mir N, et al: Alpha-2 interferon in chronic myeloid leukaemia following relapse post allogeneic transplant. Br J Haematol 66:141-148, 1987

45. Borgies P, Ferrant A, Delannoy A, et al: Interferon-alpha induced and maintained complete remission in chronic granulocytic leukemia in relapse after bone marrow transplantation. Bone Marrow Transplant 4:127-128, 1989

46. Arcese W, Mauro FR, Screnci M, et al: Interferon therapy for Ph positive CML patients relapsing after T-cell depleted allogeneic bone marrow transplantation. Eur J Cancer 27:s28-s30, 1991 (suppl 4)

47. Steegmann JL, Perez M, Vaquez L, et al: Interferon-alpha treatment of accelerated phase chronic myeloid leukemia in relapse after bone marrow transplantation; A case with complete cytogenetic and molecular remission. Bone Marrow Transplant 7:65-67, 1991

48. Higano CS, Raskind WH, Singer JW: Use of α-interferon for the treatment of relapse of chronic myelogenous leukemia in chronic phase after allogeneic bone marrow transplantation. Blood 80:1437-1442, 1992

49. Pigneux A, Reiffers J, Devergie A, et al: Recombinant alpha interferon as treatment for relapse after allogeneic bone marrow transplantation. Presented at the Second International Conference on Chronic Myeloid Leukaemia, Bologna, Italy, October 5-7, 1992 (abstr 275)

50. Arcese W, Goldman JM, D'Arcaugelo E, et al: Outcome for patients who relapse after allogeneic bone marrow transplantation for chronic myeloid leukemia. Blood 82:3211-3219, 1993

51. Klingemann HG, Philips GL: Immunotherapy after bone marrow transplantation. Bone Marrow Transplant 8:73-81, 1991

52. Meyers JD, Flournoy N, Sanders JE, et al: Prophylactic use of human leukocyte interferon after allogeneic marrow transplantation. Ann Intern Med 107:809-816, 1987

53. Niederwieser D, Arcese W, Bandini G, et al: Prophylactic use of interferon alpha after bone marrow transplantation for patients with chronic myelogenous leukemia at high risk of relapse: A pilot study. Semin Hematol 30:40-43, 1993

54. Sullivan KM, Storb R, Buckner CD, et al: Graft versus host disease as adoptive immunotherapy in patients with advanced hematological neoplasms. N Engl J Med 320:828-834, 1989

55. Kolb HJ, Mittermuller J, Clemm C, et al: Donor leukocyte transfusions for treatment of recurrent chronic myelogenous leukemia in marrow transplant patients. Blood 76:2462-2465, 1990

56. Cullis JO, Jiang YZ, Schwarer AP, et al: Donor leukocyte infusions for chronic myeloid leukemia in relapse after allogeneic bone marrow transplantation. Blood 79:1379-1381, 1992

57. Frassoni F, Fagioli F, Sessarego F, et al: The effect of donor leukocyte infusion for CML patients relapsed after allogeneic BMT. Exp Hematol 20:712a, 1992 (abstr)

58. Lonnqvist B, Ljungman P, Carneskog A, et al: Treatment of relapsed myeloproliferative disease after BMT with donor lymphocytes infusions. Presented at the Eighteenth Annual Meeting of the European Group for Bone Marrow Transplantation, Stockholm, Sweden, June 24-27, 1992 (abstr 263)

59. Helg Cl, Soulier Lauper M, Guetty Alberto M, et al: Induction of graft versus leukemia reaction with graft versus host disease for recurrent chronic myelogenous leukaemia after T-cell depleted allogeneic bone marrow transplantation. Presented at the Eighteenth Annual Meeting of the European Group for Bone Marrow Transplantation, Stockholm, Sweden, June 24-27, 1992 (abstr)

60. Novotny J, Hertenstin B, Bunjes D, et al: Patients with relapse of CML after allogeneic bone marrow transplantation receiving interferon-alpha and donor buffy coat transfusions become negative for BCR-ABL transcripts (RT-PCR). Presented at the Second International Conference of Chronic Myeloid Leukaemia, Bologna, Italy, October 5-7, 1992 (abstr 277)

61. Szer J, Grigg AP, Phillips GL, et al: Donor leukocyte infusions after chemotherapy for patients relapsing with acute leukemia following allogeneic BMT. Bone Marrow Transplant 11:109-111, 1993

62. Bar BMAM, Schattenberg A, Mensink EJBM, et al: Donor leukocyte infusions for chronic myeloid leukemia relapsed after allogeneic bone marrow transplantation. J Clin Oncol 11:513-519, 1993

63. Drobyski WR, Keever CA, Roth MS, et al: Salvage immunotherapy using donor leukocyte infusions as treatment for relapsed chronic myelogenous leukemia after allogeneic bone marrow transplantation: Efficacy and toxicity of a defined T-cell dose. Blood 82:2310-2318, 1993

64. Kolb HJ, Mittermuller J, Hertenstein H, et al: High dose therapy and bone marrow transplantation. Adoptive immunotherapy in human and canine chimeras—The role of interferon alpha. Semin Hematol 30:37-39, 1993 (suppl 3)